cuk-H03744-31-P024704

VOLUME 109 — MAY 2000
Number 5, Part 1 (Issued in 3 Parts)

51

— Founded in 1892 —

ANNALS

OF OTOLOGY, RHINOLOGY & LARYNGOLOGY

Official Organ of the
AMERICAN LARYNGOLOGICAL ASSOCIATION
AMERICAN BRONCHO-ESOPHAGOLOGICAL ASSOCIATION

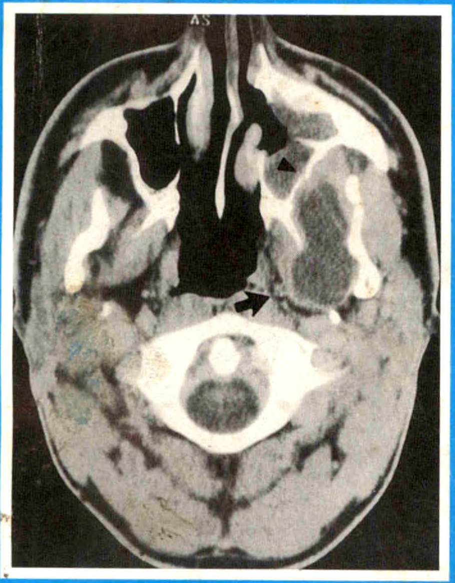

MAKE YOUR DIAGNOSIS. SEE PAGE 523.

ANNALS
PUBLISHING CO.

IMPROVE EAR PROTECTOR EFFECTIVENESS

The majority of Otolaryngologists and Hearing Health Care Professionals in the U.S. believe that patients who wear ear protection, especially custom-molded protectors or preformed rubber ear plugs, should also wear a tight-fitting cap or band for extra protection when swimming or showering.

- PHYSICIANS' CHOICE Head Band improves patient compliance – the stylish PHYSICIANS' CHOICE Head Band is happily worn by boys and girls. The Velcro™ closure allows easy adjustments for a comfortable fit.
- The PHYSICIANS' CHOICE Head Band stays positioned over the ears to help keep water out, and ear protectors in.

PHYSICIANS' CHOICE™ Head Band

You and your patients will appreciate PHYSICIANS' CHOICE Head Band. For more information and to receive a Free PHYSICIANS' CHOICE Head Band sample contact us by phone, mail or fax.

Santa Barbara Medco, Inc.

Our New Website:
www.sbmedco.com
E-mail:
sbmedco@silcom.com

P.O. Box 6843 • Santa Barbara • CA 93160 • FAX 805/683-4864 • PHONE 805/683-1486

ANNALS OF OTOLOGY, RHINOLOGY & LARYNGOLOGY

— Founded in 1892 —

ANNALS
PUBLISHING CO.

EDITOR'S OFFICE

Brian F. McCabe, MD
Department of Otolaryngology – Head & Neck Surgery
University Hospitals & Clinics
Iowa City, IA 52242
(319) 356-2310

BUSINESS OFFICE

Annals Publishing Company
4507 Laclede Avenue
St Louis, MO 63108
(314) 367-4987
Fax (314) 367-4988
E-mail: manager@Annals.com

STAFF

Managing Editor
Michol L. Sheridan

Business Manager
Kenneth A. Cooper, Jr

Chief Copyeditor
Edna Hayes Harrison

Copyeditor
Scott A. Bailey

Circulation Manager
Michelle M. Steuerwald

Editorial Assistant
Nicholas M. Regiacorte

ADVERTISING REPRESENTATIVES

— East & Midwest —
Cunningham Associates
180 Old Tappan Rd
Old Tappan, NJ 07675
(201) 767-4170
Fax (201) 767-8065
JPattis@cunnasso.com

— West —
Charles B. Healy
PO Box 5213
Palm Springs, CA 92263
(760) 320-0118
Fax (760) 325-5473

EDITORIAL CONTENT

The *ANNALS* publishes original manuscripts of clinical and research importance in otolaryngology – head and neck medicine and surgery, bronchoesophagology, head and neck oncology and surgery, plastic and reconstructive surgery, pediatric otolaryngology, audiology, speech pathology, and related specialties. In-depth studies (supplements), papers of historical interest, computer software reviews and applications in otolaryngology are also published, as well as imaging, pathology, and clinicopathology studies, book reviews, and letters to the editor. All papers and supplements are peer-reviewed. The *ANNALS* is the official journal of the American Laryngological Association and the American Broncho-Esophagological Association.

SUBSCRIPTIONS

2000 Annual Subscription Rates	*USA*	*International Surface Mail (All Regions)*
Institution*	$215.00	$240.00
Individual†	150.00	175.00
Resident/Student†	99.00	115.00

*Institutional (multiple-reader) subscription rates apply to public and private libraries, hospitals, and clinics; city, county, state, provincial, and national government bureaus and departments; and commercial and private institutions and organizations.

†Individual, resident, and student subscriptions must be in the individual's name and must be billed to and paid for by the individual.

Airmail rates are available upon request.

Visa, Mastercard, and American Express are accepted as payment.

AVAILABILITY OF CD-ROM

CD-ROMs are available for each volume in March of the following year. The 1998 volume was the first on CD-ROM. Current subscribers can purchase a CD-ROM at $76.00 for an individual and $99.00 for an institution. Orders placed by non-subscribers are $189.00 for an individual and $254.00 for an institution.

CLAIMS & BACK ISSUES

Claims. Claims for missing issues must be received within 60 days of the month of publication for the United States and Canada, and 180 days for other countries. Single copy prices will be charged on missing issues claimed after that time.

Back Issues. A comprehensive inventory of back issues and supplements is available. Prices are furnished on request.

CHANGE OF ADDRESS

Address changes must be received 45 days prior to the effective date so that the subscription will be received without interruption.

MICROFILM

The *ANNALS* is available in microform from University Microfilms International, 300 North Zeeb Road, Ann Arbor, MI 48106.

ANNALS OF OTOLOGY, RHINOLOGY & LARYNGOLOGY (ISSN 0003-4894) is published monthly by Annals Publishing Company, 4507 Laclede Avenue, St Louis, MO 63108. Periodicals postage paid at St Louis, Mo. POSTMASTER: Send address changes to *ANNALS OF OTOLOGY, RHINOLOGY & LARYNGOLOGY*, c/o Annals Publishing Company, 4507 Laclede Avenue, St Louis, MO 63108-2103.

COPYRIGHT© 2000, ANNALS PUBLISHING COMPANY

P24704

Surgeon Controlled™

SuperSoft Silicone™ T-Tubes

*The ideal situation where intubation time is determined by the Otologist, rather than the vagaries of spontaneous extrusion.**

Introduced by Santa Barbara Medco, Inc. The SuperSoft Silicone T-Tube has over 17 years of successful clinical experience as a surgeon controlled ventilation tube. Available in Pretrimmed and Standard sizes.

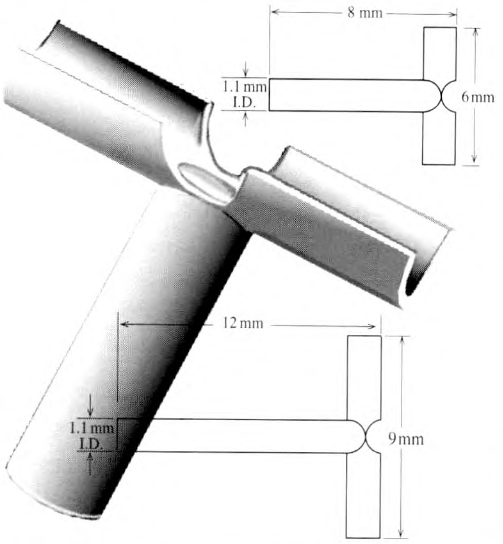

Advantages of the SuperSoft Silicone T-Tube (SSTT):*

- The surgeon controls the intubation period for the large majority of patients.
- Low spontaneous extrusion rate - less than 10% when flanges are trimmed to 3mm.
- Reported lower residual perforations rate (6.7%) than other long-term ventilation tubes.
- Tube removal can be simply and safely performed in the office because of the shortened SuperSoft Silicone flanges.

Please contact us for additional information and an evaluation sample.

Santa Barbara Medco, Inc.
P.O. Box 6843
Santa Barbara, CA 93160
805/683-1486
FAX 805/683-4864

e-mail: sbmedco@silcom.com or
visit us at our website www.sbmedco.com

*"Lowering the Incidence of Perforation following Goode T-Tube Removal", presented at the American Society of Pediatric Otolaryngology Annual Meeting, May 19, 1990, Toronto, Canada, A.F. Inglis, Jr., M.D., M.A. Richardson, M.D., Taya S. Higgins, R.N. - Children's Hospital & Medical Center, 4800 Sandpoint Way, N.E., P.O. Box C5371, Seattle, WA 98105

Physicians' Choice® "Ear Putty"® Ear Plugs provide effective protection against water . . .

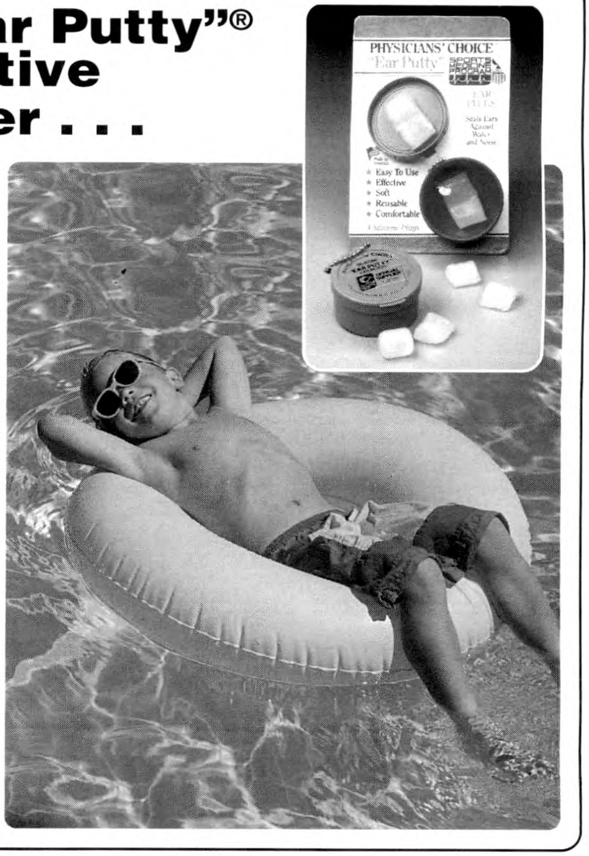

- Prevention -- helps in the prevention of reoccurring ear problems and patient revisits.
- Inexpensive -- costs less than $1.50 per month on average.
- Efficient -- with no fitting required.
- Patient Compliance -- provides a soft and comfortable seal over the ear canal.
- The Physicians' Choice -- "Ear Putty" is the #1 physician recommended ear plugs in the United States.

For a free sample and information on Physicians' Choice "Ear Putty" Ear Plugs please contact us at:

Santa Barbara Medco, Inc.
P.O. Box 6843
Santa Barbara, CA 93160
805/683-1486
FAX 805/683-4864
e-mail: sbmedco@silcom.com

Visit us at our website www.sbmedco.com

ANNALS OF OTOLOGY, RHINOLOGY & LARYNGOLOGY

VOLUME 109 MAY 2000 NUMBER 5

CONTENTS

PART 1

FROM THE AMERICAN LARYNGOLOGICAL ASSOCIATION

Glottal Area Waveform Analysis of Benign Vocal Fold Lesions Before and After Surgery
J. Pieter Noordzij, MD; Peak Woo, MD 441

Laryngeal Adductory Pressure as a Measure of Post-Reinnervation Synkinesis
Randal C. Paniello, MD; Steven E. West, MD 447

Pyriform Sinus Fistula: Management With Chemocauterization of the Internal Opening
Kwang Hyun Kim, MD, PhD; Myung-Whun Sung, MD, PhD; Tae-Yong Koh, MD;
Seung Ha Oh, MD, PhD; In-Sang Kim, MD 452

OTOLOGY

Experimental Autoimmune Inner Ear Disease: An Electrocochleographic and Histophysiologic Study
Henk Bouman, MD, PhD; Sjaak F. L. Klis, PhD; Frits Meeuwsen;
John C. M. J. de Groot, PhD; Guido F. Smoorenburg, PhD; Jan E. Veldman, MD, PhD 457

Cellular Distribution of Mucosa-Associated Lymphoid Tissue With Otitis Media in Children
Masami Kamimura, MD, DMSc; Carey D. Balaban, PhD; Isamu Sando, MD, DMSc;
Tetsuya Ganbo, MD, DMSc; Chiaki Suzuki, MD, DMSc 467

Assessment of Stapes Mobility by Use of a Newly Developed Piezoelectric Ceramic Device. A Preliminary Experiment in Dogs
Kiyofumi Gyo, MD; Hidemitsu Sato, MD; Eiji Yumoto, MD; Naoaki Yanagihara, MD 473

Quantification of the Three-Dimensional Displacement of Normal Facial Movement
Susan E. Coulson, MAppSc; Glen R. Croxson, MBBS, FRACS; Wendy L. Gilleard, MSc 478

RHINOLOGY AND AIRWAY

Effects of Clarithromycin on Rheological Properties of Nasal Mucus in Patients With Chronic Sinusitis
Chae-Seo Rhee, MD; Yuichi Majima, MD; Shinobu Arima, MD; Ha-Won Jung, MD;
Tae-Hoon Jinn, MD; Yang-Gi Min, MD; Yasuo Sakakura, MD 484

Human Uvula: Characterization of Resident Leukocytes and Local Cytokine Production
Katarina Olofsson, MD; Sten Hellström, MD, PhD; Marie-Louise Hammarström, PhD 488

Congenital Defects of the Vomer
Mitsuhiro Mohri, MD; Mutsuo Amatsu, MD 497

LARYNGOLOGY

Estimated Subglottic Pressure in Normal and Dysphonic Subjects
Antoine Giovanni, MD; Corinne Heim, MD; Didier Demolin, PhD; Jean-Michel Triglia, MD 500

Three-Dimensional Anatomic Characterization of the Canine Laryngeal Abductor and Adductor Musculature
Corey W. Mineck, MD; Niro Tayama, MD; Roger Chan, PhD; Ingo R. Titze, PhD 505

Prevention of Pharyngoesophageal Spasm After Laryngectomy With a Half-Muscle Closure Technique
Daniel G. Deschler, MD; E. Thomas Doherty, PhD; Charles G. Reed, PhD;
Richard E. Hayden, MD; Mark I. Singer, MD 514

Pneumomediastinum Due to Venturi Jet Ventilation Used During Microlaryngeal Surgery in a Previously Neck-Irradiated Patient
Luis A. Gaitini, MD; Milo Fradis, MD; Sonia J. Vaida, MD; Mostafa Somri, MD;
Shelton H. Malatskey, MD; Avishai Golz, MD 519

IMAGING CASE STUDY OF THE MONTH

Mucocele of the Infratemporal Fossa as an Unusual Complication of Midfacial Fracture
Evan R. Reiter, MD; Mark A. Varvares, MD; Meredith August, MD, DMD;
Hugh D. Curtin, MD 522

MISCELLANEOUS

Book Reviews 526

Information for Subscribers 1a

Instructions to Authors 6a

Index to Advertisers 9a

PART 2

Temporal Bone Studies of the Human Peripheral Vestibular System
Saumil N. Merchant, MD; Luis Velázquez-Villaseñor, MD; Kojiro Tsuji, MD;
Robert J. Glynn, ScD; Conrad Wall III, PhD; Steven D. Rauch, MD .... Supplement 181

PART 3

Medical Management of Acute Bacterial Sinusitis. Recommendations of a Clinical Advisory Committee on Pediatric and Adult Sinusitis
Itzhak Brook, MD, MSc; W. Manford Gooch III, MD; Stephen G. Jenkins, PhD;
Michael E. Pichichero, MD; Seth A. Reiner, MD; Lawrence Sher, MD;
Terry Yamauchi, MD .... Supplement 182

ANNALS OF OTOLOGY, RHINOLOGY & LARYNGOLOGY

VOLUME 109 JUNE 2000 NUMBER 6

CONTENTS

OTOLOGY

Idiopathic Sudden Sensorineural Hearing Loss: Temporal Bone Histopathologic Study
Juha-Pekka Vasama, MD; Fred H. Linthicum, Jr, MD 527

Mathematical Model Explaining the Sources of Error in Certain Estimates of the Gas Exchange Constants for the Middle Ear
William J. Doyle, PhD 533

Length of the Eustachian Tube and Its Postnatal Development: Computer-Aided Three-Dimensional Reconstruction and Measurement Study
Ken Ishijima, MD; Isamu Sando, MD, DMSc; Carey Balaban, PhD;
Chiaki Suzuki, MD, DMSc; Kenji Takasaki, MD 542

Effect of WEB 2170 BS, Platelet Activating Factor Receptor Inhibitor, in the Guinea Pig Model of Middle Ear Inflammation
R. Murat Karasen, MD; Yavuz Sutbeyaz, MD; Bulent Aktan, MD;
Hasan Ozdemir, PhD; Cemal Gundogdu, MD 549

LARYNGOLOGY

Laryngeal Radionecrosis and Hyperbaric Oxygen Therapy: Report of 18 Cases and Review of the Literature
George A. Filntisis, MD, PhD; Richard E. Moon, MD; Kevin L. Kraft, RN;
Joseph C. Farmer, MD; Richard L. Scher, MD; Claude A. Piantadosi, MD 554

Airway Flow Dynamics and Voice Acoustics After Autologous Fascia Augmentation of Paralyzed Vocal Fold
Antti Saarinen, MD; Heikki Rihkanen, MD, PhD; Sari Lehikoinen-Söderlund, MSc;
Anssi R. A. Sovijärvi, MD, PhD 563

Effects of Dehydration on Phonation in Excised Canine Larynges
Jack Jiang, MD, PhD; Katherine Verdolini, PhD; Ben Aquino, MS;
Jennie Ng; David Hanson, MD 568

Laryngeal Reflexomyographic Responses in Rabbits: A Neurolaryngological Study of Glottal Movement
Shengguang Yin, MD; William W. Qiu, MD, MA; Fred J. Stucker, MD 576

PHARYNGOLOGY

Site of Airway Collapse in Obstructive Sleep Apnea After Uvulopalatopharyngoplasty
LTC Wayne C. Farmer, MC, USA; LT Stanley C. Giudici, MC, USN 581

Pharyngeal Pressure Analysis by the Finite Element Method During Liquid Bolus Swallow
Sung Min Kim, PhD; Timothy M. McCulloch, MD; Kwan Rim, PhD 585

Carcinoma of the Hypopharynx and Cervical Esophagus in Young Adults
Patrick R. Axon, FRCS (ORL); Ricard Simo, FRCS (ORL); Neil Fergie, FRCS; Robert H. Temple, FRCS; W. Trevor Farrington, FRCS 590

RHINOLOGY

Secretory Differentiation of Serially Passaged Normal Human Nasal Epithelial Cells by Retinoic Acid: Expression of Mucin and Lysozyme
Joo-Heon Yoon, MD; Kyung-Su Kim, MD; Sung-Shik Kim, MD; Jeung-Gweon Lee, MD; In Yong Park, MD 594

CLINICAL NOTES

Laryngeal Diversion and Tracheotracheal Speech Fistula for Chronic Aspiration
Desheng Wang, MD; Pavel Dulguerov, MD 602

Actinomycosis Imitating Nasopharyngeal Carcinoma
Ching-Wen Chiang, MD; Yih-Leong Chang, MD; Pei-Jen Lou, MD 605

IMAGING CASE STUDY OF THE MONTH

Sphenoethmoidal Mucocele Presenting With Bilateral Visual Compromise
Todd A. Loehrl, MD; Donald A. Leopold, MD 608

CLINICOPATHOLOGICAL CONSULTATION

Herpes Simplex Viral Laryngitis
Jeffrey T. Vrabec, MD; Claudia P. Molina, MD; Brian West, MD 611

MISCELLANEOUS

Information for Subscribers 3a

Instructions to Authors 4a

Index to Advertisers 8a

ANNALS OF OTOLOGY, RHINOLOGY & LARYNGOLOGY

VOLUME 109 JULY 2000 NUMBER 7

CONTENTS

EAR

Basilar Artery and Vertigo
Louis W. Welsh, MD; John J. Welsh, MD; Bernard Lewin, MD 615

Surgical Management of Uncomplicated Otitis Media in a Pediatric Medicaid Population
Stephen Berman, MD; Jessica Bondy, MHA; Patricia J. Byrns, MD; Dennis Lezotte, PhD 623

Effect of a Beta-Stimulant on the Inner Ear Stria Vascularis
Kosuke Ishii, MD; Wei Gang Zhai, MD; Masumi Akita, MD 628

NOSE, PHARYNX, AND TRACHEA

Comparison of Functional Endonasal Sinus Surgery With and Without Partial Middle Turbinate Resection
Thomas E. Havas, FRACS; David S. G. Lowinger, MB BS 634

Combination of Angiogenesis Inhibitor TNP-470 With Cytotoxic Drugs in Experimental Therapy of Nasopharyngeal Carcinoma
Chao-Nan Qian, MD, PhD; Hua-Qing Min, MD; Han-Liang Lin, MD; Ming-Huang Hong, MD 641

Lack of Predictive Value of the Epworth Sleepiness Scale in Patients After Uvulopalatopharyngoplasty
Stanley Giudici, MD; Wayne Farmer, DO; Anthony Dollinger, MS; Timothy Andrada, MS; Kenneth Torrington, MD; Krishnan Rajagopal, MD 646

LARYNX

Ultrastructure of the Vocal Process of the Arytenoid Cartilage
Kiminori Sato, MD, PhD; Minoru Hirano, MD; Tadashi Nakashima, MD 650

Recurrent Laryngeal Nerve Monitoring During Cricotracheal Resection
Kevin Cavanaugh, MD; Albert H. Park, MD 654

Influence of Phonation on Basement Membrane Zone Recovery After Phonomicrosurgery: A Canine Model
Seung-Ho Cho, MD; Hyung-Tae Kim, MD; In-Ja Lee, MD; Min-Sik Kim, MD; Han-Jong Park, MD 658

HEAD AND NECK

Vascular and Epidermal Effects of Fibroblast Growth Factor on Irradiated and Nonirradiated Skin Flaps
David B. Hom, MD; Tim C. Simplot, MD; Kerri J. Pernell, MS; J. Carlos Manivel, MD; Chang W. Song, PhD 667

Cervical Versus Thoracic Epidural Morphine for the Treatment of Head and Neck Cancer Pain
Loucas Georgiou, MD, PhD; Antonios Louizos, MD; Christina Sklavou, MD; Leonidas Manolopoulos, MD, PhD; Ioannis Yiotakis, MD, PhD; Georgios Adamopoulos, MD, PhD 676

CLINICAL NOTES

Cat-Scratch Disease of the Parotid Gland: An Often-Misdiagnosed Entity
Shelton Malatskey, MD; Milo Fradis, MD; Jacob Ben-David, MD; Ludwig Podoshin, MD 679

Liposarcoma of the Tongue: Case Report and Literature Update
Yorihisa Orita, MD; Kazunori Nishizaki, MD; Toshiaki Ogawara, MD; Ichiro Yamadori, MD; Satoshi Yorizane, MD; Hirofumi Akagi, MD; Yu Masuda, MD 683

Airway Burns and Atelectasis in an Adolescent Following Aspiration of Molten Wax
Sharon Einav, MD; Itzhak Braverman, MD; Ido Yatsiv, MD; Avraham Avital, MD; Moshe Rothschild, MD 687

IMAGING CASE STUDY OF THE MONTH

Internal Carotid Artery Aneurysm Presenting as a Large Pharyngeal Mass
Tomokazu Yoshizaki, MD; Shigekazu Teranishi, MD; Osamu Matsui, MD; Mitsuru Furukawa, MD 690

CLINICOPATHOLOGICAL CONSULTATION

Burkitt's Lymphoma: Historical Background and Recent Insights Into Classification and Pathogenesis
Antonino Carbone, MD; Vincenzo Canzonieri, MD; Annunziata Gloghini, PhD; Alessandra Rinaldo, MD; Gianluca Gaidano, MD, PhD; Alfio Ferlito, MD 693

MISCELLANEOUS

Information for Subscribers 2a

Index to Advertisers 7a

ANNALS OF OTOLOGY, RHINOLOGY & LARYNGOLOGY

VOLUME 109 AUGUST 2000 NUMBER 8

CONTENTS

PART 1

OTOLOGY

Morphological and Functional Study of Regenerated Chorda Tympani Nerves in Humans
Takehisa Saito, MD; Yoshiyuki Shibamori, MD; Yasuhiro Manabe, MD; Takahiro Yamagishi, MD; Takehito Yamamoto, MD; Toshio Ohtsubo, MD; Hitoshi Saito, MD 703

Use of Methotrexate for Autoimmune Hearing Loss
Eric L. Matteson, MD, MPH; Oltita Tirzman, MD; George W. Facer, MD; David A. Fabry, PhD; Jan Kasperbauer, MD; Charles W. Beatty, MD; Thomas J. McDonald, MD 710

Effect of 7-Nitroindazole Upon Cochlear Dysfunction Induced by Transient Local Anoxia
Keiji Tabuchi, MD; Zenya Ito, MD; Tetsuro Wada, MD; Kazuhiko Takahashi, MD; Akira Hara, MD; Jun Kusakari, MD 715

NOSE AND PARANASAL SINUSES

Olfactory Mucosal Findings in Patients With Persistent Anosmia After Endoscopic Sinus Surgery
Sang Hag Lee, MD; Hyun Ho Lim, MD; Heung Man Lee, MD; Hyo Jin Park, MD; Jong Ouck Choi, MD 720

Ultrastructural Changes in Platelet Activating Factor–Induced Epithelial Damage in Rabbit Maxillary Sinus Mucosa
Sea-Yuong Jeon, MD; Pil-Seub Jeong, MD; Chung-Ku Rhee, MD; Yang-Gi Min, MD 726

LARYNGOLOGY

Acquired Tracheoesophageal Fistula in Critically Ill Patients
Michael Wolf, MD; Alon Yellin, MD; Yoav P. Talmi, MD; Eran Segal, MD; Meir Faibel, MD; Jona Kronenberg, MD 731

Postintubation Interarytenoid Adhesion
Xavier Carrat, MD; Jacques Verhulst, MD; Stephane Duroux, MD; Pierre Pescio, MD; François Devars, MD; Louis Traissac, MD 736

Perceptual Characteristics of Adductor Spasmodic Dysphonia
Ton P. M. Langeveld, MD; Harm A. Drost, PhD; Johan H. M. Frijns, MD, PhD; Aeilko H. Zwinderman, PhD; Robert J. Baatenburg de Jong, MD, PhD 741

HEAD AND NECK CANCER

CD34+ Immune Suppressive Cells in the Peripheral Blood of Patients With Head and Neck Cancer
Rajiv Pandit, MD; Deanne M. R. Lathers, PhD; Nicole M. Beal; Thomas Garrity, MD; M. Rita I. Young, PhD 749

Use of a Coincidence Gamma Camera to Detect Primary Tumor With ^{18}Fluoro-2-Deoxy-Glucose in Cervical Lymph Node Metastases From an Unknown Origin
Sophie Périé, MD; Jean-Noël Talbot, MD; Guy Monceaux, MD; Dany Grahek, MD; Khaldoun Kerrou, MD; Françoise Montravers, MD; Jean Lacau St Guily, MD 755

Objective Comparison of Shoulder Dysfunction After Three Neck Dissection Techniques
Pao-Tsai Cheng, MD; Sheng-Po Hao, MD; Yang-Hua Lin, MS; Albert Re-Ming Yeh, MD 761

Timing of Swallowing Events After Single-Modality Treatment of Head and Neck Carcinomas With Radiotherapy
Katherine A. Kendall, MD; Susan W. McKenzie, MS; Rebecca J. Leonard, PhD; Christopher U. Jones, MD 767

CLINICAL NOTES

Massive Epistaxis After Rupture of Intracavernous Carotid Artery Aneurysm. Case Report
Holger Sudhoff, MD; Thomas Stark, MD; Siegfried Knorz, MD; Horst Luckhaupt, MD; Gerd Borkowski, MD 776

Epiglottic Hypoplasia Associated With Lacrimo-Auriculo-Dental-Digital Syndrome
Taraneh Azar, MD; Jennifer A. Scott, MS; James E. Arnold, MD; Nathaniel H. Robin, MD 779

IMAGING CASE STUDIES OF THE MONTH

Paraclinoid Internal Carotid Artery Aneurysm Presenting as Massive Epistaxis
Ju Y. Kim, MD; Jeffrey Farkas, MD; Christopher M. Putman, MD; Mark Varvares, MD 782

Scintigraphic Monitoring of Swallowing Rehabilitation After Horizontal Supraglottic Laryngectomy
Jacopo Galli, MD; Venanzio Valenza, MD; Lucia D'Alatri, MD; Francesca Reale, MD; Giovanni Almadori, MD; Gaetano Paludetti, MD 787

MISCELLANEOUS

Information for Subscribers 3a

Instructions to Authors 4a

Index to Advertisers 8a

PART 2

Controversies in the Medical Management of Persistent and Recurrent Acute Otitis Media. Recommendations of a Clinical Advisory Committee
Michael E. Pichichero, MD; Seth A. Reiner, MD; Itzhak Brook, MD, MSc; W. Manford Gooch III, MD; Terry Yamauchi, MD; Stephen G. Jenkins, PhD; Lawrence Sher, MD .... Supplement 183

This publication is available in microform.

University Microfilms International reproduces this publication in microform: microfiche and 16mm or 35mm film. For information about this publication or any of the more than 13,000 titles we offer, complete and mail the coupon to: University Microfilms International, 300 N. Zeeb Road, Ann Arbor, MI 48106. Call us toll-free for an immediate response: 800-521-3044. Or call collect in Michigan, Alaska and Hawaii: 313-761-4700.

☐ Please send information about these titles:

____

____

Name ____________________________________

Company/Institution __________________________

____

Address ___________________________________

City ______________________________________

State __________________ Zip _________________

Phone ( ) _________________________________

University
Microfilms
International

Courses on the Lateral Approaches to the Skull Base
(In English)

Course Director:
Mario Sanna, MD

This cadaver hands-on workshop provides the individual opportunity to participate in:

- Video presentation of techniques and clinical cases
- Didactic presentations
- Performing the surgical procedures on specially prepared bones and half-heads
- Discussions

For additional information, contact:

Secretary Gruppo Otologico
Via Emmanueli n.42
29100 Piacenza - Italy
telephone: 0523/754362
fax: 0523/453708
E-mail: Corsi.Sanna@otologicgr.inet.it

A161

THIRD MULTI-DISCIPLINARY INTERNATIONAL SYMPOSIUM ON SUPRAESOPHAGEAL COMPLICATIONS OF REFLUX DISEASE

Dates:	August 10-12, 2000
Location:	Westin Copley Place Boston, Massachusetts
Course Director:	Reza Shaker, MD
Accreditation:	AMA Category 1 (17.5 hrs)
Fees:	$495.00 Physicians $350.00 Allied Health Professionals $250.00 Residents, Students

Contact:

Lynne K. Tiras, CMP
International Meeting Managers, Inc
4550 Post Oak Place, Suite 342
Houston, TX 77027
Telephone: (713) 965-0566
Fax: (713) 960-0488
E-mail: imm@insync.net

A178

INSTRUCTIONS TO AUTHORS

SUBMISSION

Send manuscripts to Editor Brian F. McCabe, MD, Department of Otolaryngology–Head and Neck Surgery, The University of Iowa Hospitals and Clinics, Iowa City, IA 52242. Original manuscripts dealing with clinical and scientific aspects of otolaryngology, bronchoesophagology, head and neck medicine and surgery, maxillofacial and plastic surgery, audiology, speech pathology, and related specialties are considered for publication. All materials submitted for publication undergo peer review. All manuscripts must be accompanied by a signed copyright transfer (see "Copyright," below). Include a self-addressed, stamped envelope for notification of receipt of manuscript.

Written permission from both senior author and publisher must be provided to the *Annals* in order to republish tables or illustrations copyrighted elsewhere. Submit this permission with the manuscript.

Papers are scheduled for publication in chronological order of acceptance. Manuscripts received in improper form require longer production time. Manuscripts are edited in accordance with the *AMA Manual of Style*, 9th edition (1998), and with the *Uniform Requirements for Manuscripts Submitted to Biomedical Journals* (*Ann Intern Med* 1988;108:258-65).

MANUSCRIPT PREPARATION

Limit papers to a size that will make up to no more than six printed pages, figuring three double-spaced typewritten pages of text to one typeset page; see the journal for estimating space required for references, illustrations, and tables. If a manuscript of greater length is accepted for publication by the Editor, all typeset pages over six are charged to the author at the publisher's cost of $150 per page. Submit an original and two copies of the manuscript, typed on white bond paper with margins of at least 25 mm (1 in), double-spaced throughout, including abstract, references, tables, and legends. Use a type size no smaller than 10 points, preferably 12. Begin each component on a new page in the following sequence: title page, abstract, text, acknowledgments, references, tables, and figure legends. Number pages consecutively in the upper right corner, beginning with the title page. Avoid the use of staples.

The author is responsible for all statements in the paper, as approved on the copyedited galley proofs. Alterations made by the author after the paper has been typeset are charged to the author.

Use standard abbreviations given in *Uniform Requirements*. Express all measurements in metric terms; if original measurements were made in another system, include these parenthetically. Plot audiograms according to ISO standards. Use generic names whenever possible.

Title page must include 1) a concise but informative title, worded to facilitate indexing; 2) an abbreviated form of the title to be used as a running head; 3) authors' full names (no more than seven authors are permitted) and no more than two academic degrees per author; 4) department(s) and institution(s) to which the work is attributed, with authors' present affiliations and addresses, if different, separately noted; 5) statement of grant or other support; 6) name and address of author to whom reprint requests should be sent; and 7) name, address, telephone and fax numbers, and, if possible, e-mail address of corresponding author. Manuscripts that report animal research performed in the United States must carry the following statement on the title page: "This study was performed in accordance with the PHS Policy on Humane Care and Use of Laboratory Animals, the NIH *Guide for the Care and Use of Laboratory Animals*, and the Animal Welfare Act (7 U.S.C. et seq.); the animal use protocol was approved by the Institutional Animal Care and Use Committee (IACUC) of __________ University (or institution)."

Abstracts contain no more than 150 words and state the goal of the study, primary procedures, main findings, and principal conclusions.

Key Words, chosen as far as possible from the National Library of Medicine *Medical Subject Headings*, are listed after the abstract.

References, double-spaced, are numbered consecutively in the order in which they are cited in the text. Primary references should be used whenever possible. The author is charged $1.50 for each reference over 30. Use the style of references given in *Uniform Requirements* or a current issue of the *Annals*. Include the names of all authors and the inclusive page numbers of an article. If a manuscript accepted but not yet published is included in the reference list, give the accepting journal's name, followed by "in press." Manuscripts still in review or not yet accepted formally are cited within the text as "unpublished observations." A reference to a personal communication is also placed in the text, accompanied by a date (year). Papers presented at scholarly meetings but not published are considered "unpublished observations." Papers published only in abstract form are listed as references with "[Abstract]" after the title.

Tables should be on separate sheets, numbered consecutively and headed by a concise title. Put explanatory matter in footnotes. Tables are adjuncts to the text and should not repeat material presented therein. The cost of typesetting tables is billed to the author.

Illustrations must be submitted in three complete sets, unmounted. Only professional-quality glossy photographs and black-and-white line drawings are acceptable. Computer-generated graphs are acceptable only if they are clear and will reproduce well. Letters, numbers, and symbols should be clear and of uniform size throughout, large enough that each item is legible when reduced for publication. Put legends (detailed explanations) to the photographs on a separate page in the manuscript. Affix a label to the reverse side of each illustration indicating figure number, first author's name, and top of the figure. For radiographs, photomicrographs, CT scans, etc, give indications for maximum cropping and labeling on an overlay or photocopy. Cite each figure in the text in consecutive order. Written permission from identifiable subjects is required. The cost of preparing illustrations for publication (sizing to fit journal, and preparation of negatives for printing) is charged to the author without exception. Color illustrations are accepted; cost estimates for color separations and printing are provided on an individual basis. Illustrations should enhance, not repeat, material presented in the manuscript, and should be kept to a minimum.

REVIEWS OF SOFTWARE AND COMPUTER APPLICATIONS

Programs submitted for review must be compatible with an IBM or Macintosh computer, and the author must specify hardware and system requirements. The following operating systems will be supported: MS-DOS; MS-DOS with Windows; and MAC-OS. Submit the software on either a 3.5" or 5.25" disk. If the program is a template, submit also a runtime version of the source program. Software considered for review includes educational software, artificial intelligence software to aid in the diagnosis of otolaryngic disorders, software for logging operations, software to aid in research, and software that addresses specific problems in otolaryngology. Also, manuscripts reviewing software and computer applications relating directly to otolaryngology are considered for publication. See *Ann Otol Rhinol Laryngol* 1991; 100:876 for specific instructions.

SUPPLEMENTS

A manuscript too long for inclusion in the *Annals* (over 12 typeset pages) may be published as a supplement if approved by the Editor. All costs are borne by the author and estimates are provided upon request. Supplements have the advantages of separate identification and rapid publication, but undergo the same critical review as journal articles.

REPRINTS

Rates are quoted when galley proofs are sent to the author. Orders are signed by the author and returned with the proofs.

COPYRIGHT

The following statements should accompany the manuscript, signed by all authors (only original signatures are acceptable): 1) "This paper has not been published or submitted for publication elsewhere." 2) [*For papers with more than one author*] "I have contributed substantively to the development of the content of this paper and have agreed to have my name listed as an author in the final, revised version." 3) "In consideration of the *Annals of Otology, Rhinology & Laryngology* taking action in reviewing and editing my (our) submission, I hereby transfer, assign, or otherwise convey all copyright ownership to Annals Publishing Company in the event such work is published in the *Annals of Otology, Rhinology & Laryngology*."

ANNALS OF OTOLOGY, RHINOLOGY & LARYNGOLOGY

— Founded in 1892 —

Editor

BRIAN F. McCABE, MD
Iowa City, Iowa

Associate Editors

CHARLES D. BLUESTONE, MD
Pittsburgh, Pa
GEORGE A. GATES, MD
Seattle, Wash
LAWRENCE W. DeSANTO, MD
Scottsdale, Ariz
OLLIVIER LACCOURREYE, MD
Paris, France

Board of Editors

JOHN G. BATSAKIS, MD	Houston, Tex; Kalkaska, Mich
JOEL M. BERNSTEIN, MD, PhD	Buffalo, NY
ANDREW BLITZER, MD, DDS	New York, NY
DERALD E. BRACKMANN, MD	Los Angeles, Calif
POUL BRETLAU, MD, DMSc	Copenhagen, Denmark
ITZHAK BROOK, MD	Washington, DC
RICHARD A. BUCKINGHAM, MD	Park Ridge, Ill
RICHARD A. CHOLE, MD, PhD	St. Louis, Mo
ALFIO FERLITO, MD	Udine, Italy
UGO FISCH, MD	Zurich, Switzerland
IMRE FRIEDMANN, MD, ScD	Middlesex, England
BRUCE GANTZ, MD	Iowa City, Iowa
LEE A. HARKER, MD	Omaha, Neb
JEFFREY P. HARRIS, MD, PhD	San Diego, Calif
GERALD B. HEALY, MD	Boston, Mass
WILLIAM F. HOUSE, MD	Los Angeles, Calif
STEVEN K. JUHN, MD	Minneapolis, Minn
TIMOTHY T. K. JUNG, MD, PhD	Loma Linda, Calif
DAVID W. KENNEDY, MD	Philadelphia, Pa
FRANK E. LUCENTE, MD	New York, NY
WILLIAM L. MEYERHOFF, MD, PhD	Dallas, Tex
JOSEF MILLER, PhD	Ann Arbor, Mich
AAGE R. MØLLER, PhD	Dallas, Tex
WILLIAM W. MONTGOMERY, MD	Boston, Mass
EUGENE N. MYERS, MD	Pittsburgh, Pa
JOSEPH B. NADOL, Jr, MD	Boston, Mass
YASUYA NOMURA, MD	Tokyo, Japan
LORNE S. PARNES, MD	London, Canada
JAI H. RYU, PhD	Winston-Salem, NC
JACOB SADÉ, MD	Tel Aviv, Israel
ISAMU SANDO, MD	Pittsburgh, Pa
CLARENCE T. SASAKI, MD	New Haven, Conn
ROBERT T. SATALOFF, MD, DMA	Philadelphia, Pa
RICHARD J. H. SMITH, MD	Iowa City, Iowa
HEINZ R. STAMMBERGER, MD	Graz, Austria
DEAN M. TORIUMI, MD	Chicago, Ill
JAN E. VELDMAN, MD, PhD	Utrecht, The Netherlands
BRUCE M. WENIG, MD	Bronx, NY
T. J. YOO, MD, PhD	Memphis, Tenn

Software Review and Computer Applications Editor

KEVIN T. KAVANAGH, MS, MD	Somerset, Ky

Imaging Editor

YUTAKA SATO, MD	Iowa City, Iowa

Book Review Editor

DENNIS G. PAPPAS, MD	Birmingham, Ala

Emeritus Board Members

WESLEY H. BRADLEY, MD	Albany, NY
JACK D. CLEMIS, MD	Chicago, Ill
SEYMOUR COHEN, MD	Los Angeles, Calif
CHARLES W. CUMMINGS, MD	Baltimore, Md
PATRICK J. DOYLE, MD	Vancouver, Canada
ARNDT J. DUVALL III, MD	Minneapolis, Minn
JOHN M. FREDRICKSON, MD	St Louis, Mo
RICHARD R. GACEK, MD	Syracuse, NY
JEROME C. GOLDSTEIN, MD	Alexandria, Va
SIR DONALD F. N. HARRISON, MD PhD	London, England
SAM E. KINNEY, MD	Cleveland, Ohio
JOHN A. KIRCHNER, MD	New Haven, Conn
DAVID J. LIM, MD	Los Angeles, Calif
FRED H. LINTHICUM, Jr, MD	Los Angeles, Calif
MICHEL PORTMANN, MD	Bordeaux, France
LORING W. PRATT, MD	Waterville, Me
FRANK N. RITTER, MD	Ann Arbor, Mich
ROBERT J. RUBEN, MD	Bronx, NY
WILLIAM H. SAUNDERS, MD	Columbus, Ohio
RUEDIGER THALMANN, MD	St Louis, Mo
LESTER D. R. THOMPSON, MD	Washington, DC
HARVEY M. TUCKER, MD	Cleveland, Ohio
PAUL H. WARD, MD	Los Angeles, Calif

Ann Otol Rhinol Laryngol 109:2000

GLOTTAL AREA WAVEFORM ANALYSIS OF BENIGN VOCAL FOLD LESIONS BEFORE AND AFTER SURGERY

J. PIETER NOORDZIJ, MD
CHARLOTTESVILLE, VIRGINIA

PEAK WOO, MD
NEW YORK, NEW YORK

Glottal area waveform (GAW) is the plot of relative glottal area versus time through 1 representative glottal cycle. It is derived from the quantitative analysis of the videostroboscopic image. A GAW analysis was performed on 24 patients before and after microlaryngeal phonosurgery. Patients with vocal fold polyps, polypoid degeneration, cysts, sulcus vocalis, and Reinke's edema were included. From each GAW, 5 parameters were determined and compared: maximum normalized glottal area, maximum opening rate, maximum closing rate, percent open time at 50% glottal opening, and glottal gap size. Statistically significant differences in postoperative states included an increased maximum glottal area, an increased maximum opening rate, and an increased maximum closing rate. Glottal opening and closing rate are objective measures of vocal fold pliability that have clinical relevance. The GAW may be used to quantitate vocal fold vibratory capability.

KEY WORDS — benign vocal fold lesions, glottal area waveform, vocal fold cyst, vocal fold nodule, vocal fold polyp.

INTRODUCTION

Benign vocal fold lesions (BVFLs) represent a significant problem for otolaryngologists. When these lesions are not responsive to medical and/or speech therapy, excision by microlaryngeal surgery is the next option. The goal of surgery may be to improve phonatory function or to obtain a biopsy specimen to establish the diagnosis.[1]

Aside from the subjective impressions of the patient and voice therapist, there are objective measures available to aid in the assessment of laryngeal function before and after surgery. Acoustic, phonatory airflow, and qualitative stroboscopic measurements have been used to analyze the results of microlaryngeal surgery on BVFLs.[1] These studies are valuable, but give little objective information on vocal fold physiology.

Affordable techniques that quantitatively assess the vibratory patterns of the vocal folds before and after surgery have not been available until recently. High-speed photography was first used to make direct observations of the vocal fold vibratory function in 1937.[2] Unfortunately, it was too expensive and cumbersome to be used in the clinical setting. Nonetheless, quantitative analysis of vocal fold vibratory function during phonation began with measurements from these recordings. Glottal area waveform (GAW) analysis was introduced in 1958 by Timcke et al.[3] From high-speed films, these investigators traced the GAW as representations of the glottal area change during the glottal cycle. Features of the glottal cycle were measured and found to vary with intensity and frequency variations.

Several recent advances now make it possible to analyze the GAW of a patient's vocal folds in the clinical setting. With the advent of videostrobolaryngoscopy (VSL) and video-digitizing personal computers, GAW analysis is now available to practicing otolaryngologists.

In 1996, Woo[4] used computer analysis of the stroboscopic images and described how the GAW varies in normal men and women. By examining 32 men and 33 women, Woo showed significant differences between the sexes in GAW and a number of GAW-related parameters. These measures provide normative data against which similar measures of dysphonic larynges can be compared.

Clinical software has been developed based on image analysis of the stroboscopic image (KSIP, Kay Stroboscopy Image Processing software, Kay Elemetrics, Lincoln Park, NJ). One application of this software is to analyze differences in vocal fold vibratory function as measured before and after phonomicrosurgery. Because restoration of vibratory function and removal of lesions of the vocal folds are primary goals of surgery, quantification of such results may allow the surgeon to better understand and compare results.

From the Department of Otolaryngology–Head and Neck Surgery, Tufts University School of Medicine, New England Medical Center, Boston, Massachusetts. Dr Noordzij is currently in the Department of Otolaryngology–Head and Neck Surgery, University of Virginia Health Sciences Center, Charlottesville, Virginia.

Presented at the meeting of the American Laryngological Association, Scottsdale, Arizona; May 10-11, 1997.

CORRESPONDENCE — Peak Woo, MD, Dept of Otolaryngology–Head and Neck Surgery, Mount Sinai School of Medicine, Box 1189, One Gustave L. Levy Pl, New York, NY 10029-6574.

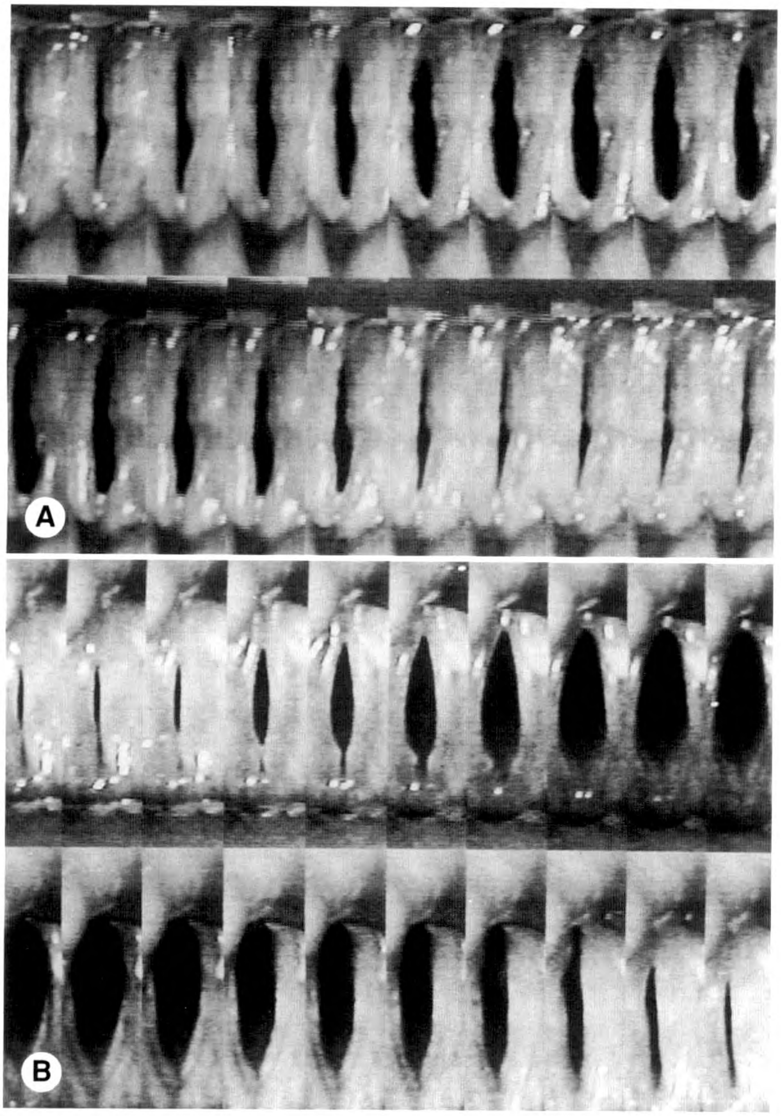

Fig 1. Images of glottal cycle for woman A) with vocal fold polyp and B) after polyp was excised.

The purpose of this study was to measure the GAW before and after microlaryngeal surgery for BVFLs and to analyze these waveforms and their dependent characteristics for significant differences. The GAW parameters analyzed were maximum normalized glottal area, maximum opening rate, maximum closing rate, percent open time at 50% glottal opening (OT-50), and baseline offset (glottal gap). By comparing the GAWs measured before and after microlaryngeal surgery, we hope to define more accurately the effect of surgical excision on vocal fold vibratory patterns and resultant vocal function. Further, by defining important features that change with microlaryngeal surgery, improved assessment and quality control techniques can be used as feedback to the surgeon. Such data could help guide the development of improved phonosurgical techniques.

MATERIAL AND METHODS

Subjects. Twenty-four subjects (7 male and 17 female) were recruited for this study. All subjects had diagnoses of a BVFL. There were 13 patients with polyps, 5 with cysts, 3 with polypoid degeneration, 2 with sulcus vocalis, and 1 with Reinke's edema. All BVFLs were excised by microlaryngeal surgery by the senior surgeon (P.W.). All subjects underwent preoperative and postoperative examinations. The postoperative examinations were performed 4 to 6 weeks after surgery, at which point the voice had stabilized. Visibility of the full length of the vocal folds was required for this study. Patients who had a BVFL and another, concurrent laryngeal disease such as cancer, reflux laryngitis, or paralysis were excluded.

VSL Recording and Setup. Instructions for the VSL phonatory conditions were given by 1 person. The subjects were seated for the VSL examination. Oral cavity and pharyngeal anesthesia was not used. A rigid 70° endoscope (Kay RLS 9100 Rhino-Laryngeal Stroboscope, Kay Elemetrics) was used exclusively because of its superior image quality compared

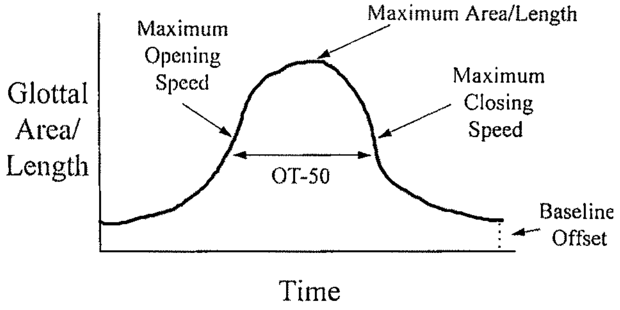

Fig 2. Sample glottal area waveform (GAW) displaying parameters related to GAW analysis. OT-50 — percent open time at 50% glottal opening.

to flexible endoscopes. Each subject was asked to sustain the vowel "ee" at a steady, comfortable pitch and loudness (modal phonation). The subjects were given time to practice and achieve 5 seconds of sustained phonation at a steady frequency and decibel output. The protocol for these recordings has been published previously.[4]

To maintain consistency, we used the frequency and decibel output as visual feedback. The electroglottal signal and the superimposed strobe flash signal were also being recorded for later visual verification of the periodicity of the output.

Image Capture and Analysis. With the strobe flash tracking at 1.5 Hz above the fundamental frequency of vocal fold vibration (F0), there were 20 video frames in 1 vibratory cycle. A unit composed of a strobolaryngoscope, a video recorder, and a personal computer (Kay RLS 9100 Rhino-Laryngeal Stroboscope) was used to digitize sequential video images of the glottal cycle. Starting from a frame of the vocal folds at their most closed position, we captured 20 sequential video frames frame-by-frame and saved them on the computer. The vocal fold area of interest was defined and clipped for further digital image manipulation and analysis with commercially available image analysis software. Figure 1A shows a preoperative example of a 20-frame sequence of glottal areas for a woman with a vocal fold polyp. Figure 1B shows a postoperative example for the same woman.

Kay Stroboscopy Image Processing software (KSIP, Kay Elemetrics) was used to perform automated extraction of the glottal area. For each digitized image, an algorithm detected the edges of the glottis by means of maximum gradient shift between the glottal area (dark) and the vocal folds (white). The program then "marked in" the glottal area based on this contrast. Once the glottal area marking was completed, it was verified by visual inspection. For some images, it was occasionally necessary to selectively "touch up" areas of mucous stranding so as to obtain a true value of glottal area, requiring, of course, operator intervention and judgment. In most cases, the automatic detection was adequate.

Glottal area was calculated by computing the number of pixels composing the detected glottis in each image. Because glottal area can vary depending on the size of the patient and the distance of the laryngoscope from the vocal folds, comparison of the glottal images and areas across subjects was not possible without an internal reference point for each calibration. Therefore, the internal laryngeal landmarks of the anterior commissure and the vocal process were selected as reference points for each subject. The distance between these points was measured with the computer cursor to define the glottal length. To normalize the glottal area between samples, we divided the absolute glottal area in pixels by the glottal length and defined this as the normalized glottal area. The normalized glottal area for the 20 frames of the glottal cycle was then plotted versus time (frame number divided by F0) to produce the GAW.

Analysis of Glottal Area Waveform. A sample waveform tracing is shown in Fig 2. The following key features of the waveform were calculated for each patient's preoperative and postoperative GAWs.

1. The maximum glottal area, ie, the largest area value achieved during the glottal open phase.
2. The maximum opening rate of the waveform, ie, the maximum slope during vocal fold opening.
3. The maximum closing rate of the waveform, ie, the maximum slope during vocal fold closing.
4. The OT-50 (normalized open time at 50%), ie,

   $$\text{OT-50} = \frac{(\text{TMC} - \text{TMO})}{\text{TGCD}} \times 100\%$$

   where TMC is time at midglottal closing, TMO is time at midglottal opening, and TGCD is total glottal cycle duration.
5. The baseline offset, ie, the lowest glottal area value reached during the closed phase.

The rationale for these measures is based on previous studies of the glottal cycle using high-speed photography.[3]

Statistics. All the dependent variable data (maximum glottal area, maximum opening rate, maximum closing rate, OT-50, and baseline offset) were found to be nonparametric. Thus, the Wilcoxon signed rank test was used to determine whether the differences between the dependent variables, preoperative versus postoperative, were significant. The Mann-Whitney U test was used to test the differences between

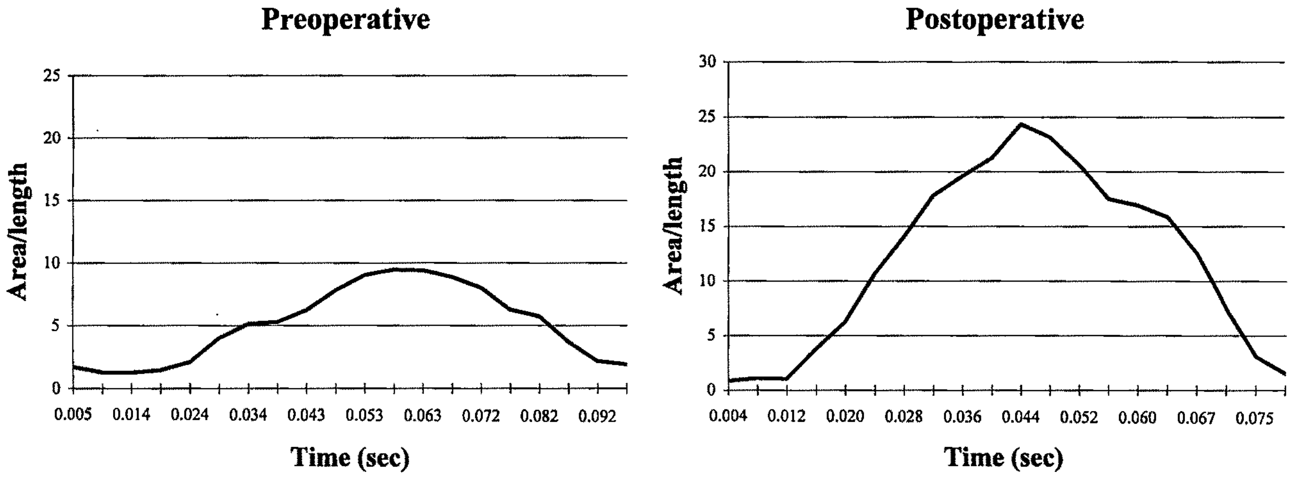

Fig 3. Preoperative and postoperative GAWs corresponding to glottal images of Fig 1A and Fig 1B, respectively.

men and women. A p value of less than .05 was considered significant.

RESULTS

Figure 1 shows sample preoperative and postoperative VSL images of a female patient with a vocal fold polyp. Comparison of these images shows that after the polyp is excised, the vibratory cycle gains amplitude. The glottis also appears to open and close more rapidly after the polyp has been removed. Figure 3 shows the GAWs corresponding to this patient's preoperative and postoperative VSL examinations. The maximum postoperative area improved from 9 to 24 (pixel area divided by glottal length). The postoperative GAW has a steeper ascent and descent, signifying faster opening and closing rates.

Table 1 lists the mean and standard error for each of the GAW parameters found before and after surgery for all 24 patients. The maximum glottal area increased significantly after surgery (by an average of 42%). The maximum opening and closing rates increased significantly after surgery (by 84% and 48%, respectively). There was a nonsignificant trend toward a smaller OT-50 and a smaller baseline offset after the BVFLs were removed.

The mean GAW parameters for the 13 cases involving polyps are shown in Table 2. After polyp excision, there was a nonsignificant trend toward an increased maximum glottal area. The maximum opening and closing rates increased significantly after polypectomy. There was a nonsignificant trend toward a smaller OT-50 and a smaller baseline offset after the polyps were removed.

Analysis of GAW data for the other types of BVFLs (cysts, polypoid degeneration, sulcus vocalis, and Reinke's edema) was not performed, because there were too few cases to make the results meaningful.

Table 3 shows the preoperative and postoperative GAW values for men versus women. The postoperative maximum opening rate was significantly greater in men compared to women. There was a trend toward a greater postoperative maximum glottal area

TABLE 1. GLOTTAL AREA WAVEFORM PARAMETERS BEFORE AND AFTER SURGERY FOR ALL PATIENTS (N = 24)

Glottal Parameter	*Mean ± SE*	*p**
Pre maximum area/length	8.6 ± 0.9	.02
Post maximum area/length	12.3 ± 1.2	
Pre maximum opening rate	262.3 ± 33.3	.03
Post maximum opening rate	483.8 ± 60.3	
Pre maximum closing rate	–323.3 ± 43.5	.01
Post maximum closing rate	–477.3 ± 51.6	
Pre OT-50	0.47 ± 0.03	.15
Post OT-50	0.41 ± 0.02	
Pre baseline offset	1.6 ± 0.2	.20
Post baseline offset	1.2 ± 0.3	

OT-50 — percent open time at 50% glottal opening.

*Derived from Wilcoxon signed rank test comparing "pre" versus "post" parameter values.

TABLE 2. GLOTTAL AREA WAVEFORM PARAMETERS BEFORE AND AFTER SURGERY FOR PATIENTS WITH POLYPS (N = 13)

Glottal Parameter	*Mean ± SE*	*p**
Pre maximum area/length	8.8 ± 1.3	.13
Post maximum area/length	13.0 ± 1.9	
Pre maximum opening rate	273.9 ± 49.5	.05
Post maximum opening rate	501.2 ± 96.2	
Pre maximum closing rate	–318.8 ± 66.3	.05
Post maximum closing rate	–499.4 ± 86.3	
Pre OT-50	0.48 ± 0.05	.31
Post OT-50	0.41 ± 0.02	
Pre baseline offset	1.8 ± 0.4	.39
Post baseline offset	1.4 ± 0.5	

*Derived from Wilcoxon signed rank test comparing "pre" versus "post" parameter values.

TABLE 3. GLOTTAL AREA WAVEFORM PARAMETERS FOR MEN (N = 7) AND WOMEN (N = 17) BEFORE AND AFTER SURGERY

	Mean ± SE		
Glottal Parameter	*Men*	*Women*	*p**
Pre maximum area/ length	7.7 ± 1.8	9.0 ± 1.0	.46
Post maximum area/ length	16.2 ± 2.8	10.7 ± 1.0	.08
Pre maximum opening rate	267.8 ± 77.1	260.1 ± 36.7	.87
Post maximum opening rate	708.9 ± 139.1	391.1 ± 50.6	.02
Pre maximum closing rate	−331.0 ± 86.4	−320.2 ± 51.9	.97
Post maximum closing rate	−647.5 ± 130.3	−407.2 ± 41.8	.09
Pre OT-50	0.45 ± 0.09	0.48 ± 0.02	.01
Post OT-50	0.38 ± 0.04	0.43 ± 0.02	.35
Pre baseline offset	0.6 ± 0.3	2.0 ± 0.3	.02
Post baseline offset	0.8 ± 0.4	1.4 ± 0.4	.42

*Derived from Mann-Whitney U test comparing male and female parameter values.

and a greater postoperative maximum closing rate for men compared to women.

DISCUSSION

Objective measures used to assess postoperative vibratory function after microlaryngeal surgery have been studied previously. Results of electroglottographic measurements, acoustic analysis, and aerodynamic studies have each been shown to change after microlaryngeal surgery.[1,5,6] Although valuable, these studies assess vocal fold vibratory function indirectly and have not become clinically popular. Videostrobolaryngoscopy stands out among the objective measures as the only test that allows visualization of the vocal folds and their vibratory function.

Benign vocal fold lesions may disrupt vocal fold vibratory patterns in a variety of manners. A mass located on the medial edge of the vocal fold can interfere with the modulation of airflow and decrease glottal efficiency. Such a mass would inhibit proper vocal fold contact and be detrimental to the generation of subglottic pressure. In the case of cysts or sulcus vocalis, a tethering of the epithelium to the vocal ligament can occur. The excessive mass seen in polypoid degeneration results in a loss of pitch control and a rough voice. The common pathway by which these lesions affect the voice is disruption of the mucosal vibratory function.[1]

Disordered voices due to BVFLs are associated with stroboscopic findings of decreased amplitude, poor vocal fold closure, and a reduced mucosal wave of the affected vocal fold. In contrast, improved voices after removal of BVFLs are associated with improved vibratory function, improved amplitude, and restoration of vocal fold pliability.[1]

The ability of pliable vocal folds to oscillate and modulate the airflow is an important goal in restoration of vocal fold function via phonomicrosurgery. If the primary goal of phonosurgery is restoration of vibratory capability, then we would expect the peak glottal area to increase as the vocal folds become more pliable. Similarly, we would anticipate that the more pliable vocal folds would oscillate more readily and that this would be indicated by faster rates of glottal area change during the opening and closing phases of the glottal cycle. This indeed was demonstrated.

The rationale for objective image analysis is not trivial. Although vocal fold vibratory behavior is a rich source for research investigations, many clinicians do not have the time and experience to systematically rate the multiple variables of vocal fold vibration. Subjective ratings of amplitude, opening and closing rate, mucosal wave, and other features require experience and a critical eye. Previous work has shown that a few selected measures of the vibratory pattern are clinically relevant and quantifiable.[4] This is the rationale for GAW analysis and measuring GAW parameters.

This study showed statistically significant changes in several of the GAW parameters tested before and after the excision of BVFLs. For the 24 patients tested, the maximum glottal area, maximum opening rate, and maximum closing rate each increased significantly after the BVFL was removed. When the vocal folds are able to achieve larger glottal areas after surgery with the same F0, then the maximum opening and closing rates must be greater. The correlate of this objective measure increase is the visual observation of increased vocal fold pliability on VSL. A decrease in OT-50 and baseline offset would be expected after BVFL excision, and there were nonsignificant trends in this study to verify these expectations. Perhaps a few selective measures from the GAW may be adequate to indicate restoration of vibratory function. This remains to be tested.

When the data were analyzed for polyps, the overall results were similar. In the case of polyps, the trend for each parameter was similar to that for the overall data group. Statistically significant increases in postoperative opening and closing rates occurred with polyps.

Analysis of the results based on gender reveals an affirmation of the normative database created earlier.[4] The maximum glottal area increased after surgery for both sexes. However, the postoperative peak glottal area for men was greater than that for women (p = .08). In normals, maximum glottal area is significantly greater in men compared to women in 4 different modes of phonation.[4] The other GAW parameter known to vary significantly between the sexes is baseline offset. For all phonation modes, the incidence and size of a posterior glottal gap are higher in women than in men. In this study, the postoperative baseline offset for women was greater than that for men (nonsignificant trend). The other GAW parameters analyzed in this study did not vary significantly between the sexes.[4]

The limitations of using objective image analysis for assessment of vocal fold vibratory function must be acknowledged. Because phonation is inherently task-specific, comparisons between the preoperative and postoperative stroboscopic results will only be relevant if the operator controls rigorously the token to be analyzed. Comparison of phonation at the same frequency and amplitude before and after surgery would be ideal, but cannot always be done. In using rigid videoendoscopic examination to obtain the stroboscopic image for analysis, we must recognize the inherent problems of the stroboscopic examination and limit the examinations to periodic oscillatory samples. Thus, aphonic and aperiodic voices may be difficult to compare before surgery versus after surgery. The need to have a complete view of the glottis will mean that some patients with large obstructive lesions and difficult-to-visualize larynges will not be suited to image analysis.

The above limitations should not detract from the information gained from this study. In this study, we have demonstrated 1) that objective evaluation of stroboscopic images is possible, 2) that the GAW, the normalized maximum glottal area, and the maximum rate of glottal area change during opening and closing were significantly altered in patients before and after phonosurgery, and 3) that restoration of vibratory function in phonomicrosurgery may now be measured by some of the techniques discussed in this paper. Further investigation on vocal fold vibratory function in health and disease associated with dysphonia appears warranted.

CONCLUSION

Glottal area waveform analysis was performed on 24 patients before and after microlaryngeal phonosurgery. Patients with vocal fold polyps, cysts, polypoid degeneration, sulcus vocalis, and Reinke's edema were included. Statistically significant differences in postoperative states included an increased maximum glottal area, an increased maximum opening rate, and an increased maximum closing rate. This study demonstrates the importance of restoration of vocal fold vibratory function as a critical factor in the evaluation of phonomicrosurgical results. The parameters of opening and closing rates are objective measures of vocal fold pliability that have clinical relevance.

REFERENCES

1. Woo P, Casper J, Colton R, Brewer D. Aerodynamic and stroboscopic findings before and after microlaryngeal phonosurgery. J Voice 1994;8:186-94.
2. Farnsworth DW. High speed motion pictures of human vocal cords. Bell Lab Rec 1940;18:574-9.
3. Timcke R, Von Leden H, Moore P. Laryngeal vibrations: measurements of the glottic wave. Arch Otolaryngol 1958;68:1-19.
4. Woo P. Quantification of videostrobolaryngoscopic findings — measurements of the normal glottal cycle. Laryngoscope 1996;106:1-27.
5. Berke GS, Gerratt BR, Hanson DG. An acoustic analysis of effects of surgical therapy on voice quality. Otolaryngol Head Neck Surg 1983;91:502-8.
6. Hanson DG, Gerratt BR, Ward PH. Glottographic measurement of vocal dysfunction. A preliminary report. Ann Otol Rhinol Laryngol 1983;92:413-20.

Ann Otol Rhinol Laryngol 109:2000

LARYNGEAL ADDUCTORY PRESSURE AS A MEASURE OF POST-REINNERVATION SYNKINESIS

RANDAL C. PANIELLO, MD   STEVEN E. WEST, MD
ST LOUIS, MISSOURI

Laryngeal adductory pressure (LAP) is the pressure induced as the vocal folds squeeze on a balloon while the recurrent laryngeal nerve (RLN) is stimulated. The LAP has been shown to vary with the frequency of stimulation, with a characteristic slope. The RLN was divided and reanastomosed 4 different ways in 12 canine hemilaryngeal preparations; the 4 subgroups represented a range of expected post-reinnervation synkinesis recovery patterns. The LAP frequency-response curve was measured before surgery and at monthly intervals for 6 months after surgery. In the "best-case" group (RLN adductor and abductor trunks each divided and reanastomosed), the slope was found to return to normal. The 2 whole RLN division–reanastomosis groups (precise realignment or 180° rotation) both gave results similar to those of the "worst-case" group (RLN adductor and abductor trunks divided and transposed); these 3 subgroups were all significantly different from baseline. The slope of the LAP frequency-response curve may be a useful means of indirectly quantifying laryngeal synkinesis.

KEY WORDS — dog, laryngeal synkinesis, recurrent laryngeal nerve.

INTRODUCTION

Many investigators have studied laryngeal reinnervation. Although sporadic reports of success in restoring motion have been given, most instances of primary nerve anastomosis or grafting in humans have resulted in little or no vocal fold motion.[1-3] Four scenarios of recovery from recurrent laryngeal nerve (RLN) paralysis have been described: 1) complete regeneration with synkinesis, 2) partial regeneration with synkinesis, 3) mixed injury, and 4) total paralysis. Crumley[4] has concluded that any innervation, even with synkinesis, is better than complete paralysis, because of the avoidance of denervation atrophy. Additionally, it is thought that some degree of synkinesis is unavoidable with RLN injury, because of changes at the nucleus ambiguus.[5]

Laryngeal synkinesis occurs after RLN transection and repair as nerve fibers that were originally innervating the adductor muscles are misdirected and subsequently innervate the abductor muscle. The reverse also occurs as abductory fibers innervate the adductor muscle group. Normally, approximately 20% to 25% of the 1,000 axons of the RLN innervate the posterior cricoarytenoid (PCA) muscle, with the remaining 75% to 80% supplying the adductor muscles.[1] The aberrant reinnervation pattern occurs because the abductor and adductor fibers are intermixed within the nerve and may regenerate to innervate the "wrong" muscle.[5-8]

A relationship between laryngeal adductory pressure (LAP) and the frequency of stimulation has been found in the canine larynx (Paniello, unpublished observations). At a constant intensity, the slow-twitch PCA muscle shows increased contractility at lower frequencies of stimulation (20 to 30 Hz). At this stimulation frequency, the LAP measured in the larynx is at its minimum as the abductor muscle is maximally stimulated. The adductor muscles, primarily fast-twitch, exert their maximum force at stimulation frequencies of 70 Hz and higher. A linear relationship exists between the frequency of stimulation and the LAP in the transition zone of 30 to 70 Hz (Paniello, unpublished observations).

With reinnervation and misdirection of fibers within the RLN, one would expect a number of observations. First, the slope of the LAP–frequency of stimulation curve should become smaller as the adductor muscles begin responding to lower frequencies and the abductor remains active at higher frequencies. Second, with maximal misdirection of fibers (ie, transposing abductor and adductor branches of the RLN), the relationship of the LAP–frequency of stimulation curve could be reversed from normal. This should occur as the PCA muscle becomes more of a fast-twitch muscle with maximal stimulation at high frequencies and the lateral cricoarytenoid, interary-

---

From the Department of Otolaryngology–Head and Neck Surgery, Washington University School of Medicine, and the Department of Veterans Affairs Medical Center, St Louis, Missouri. Supported by a grant from the National Institutes of Health/National Institute on Deafness and Other Communication Disorders (DC 03859-01). This study was performed in accordance with the PHS Policy on Humane Care and Use of Laboratory Animals, the NIH *Guide for the Care and Use of Laboratory Animals*, and the Animal Welfare Act (7 U.S.C. et seq.); the animal use protocol was approved by the Institutional Animal Care and Use Committee (IACUC) of the Department of Veterans Affairs Medical Center, St Louis, Missouri.

Presented at the meeting of the American Laryngological Association, Palm Desert, California, April 24-25, 1999.

CORRESPONDENCE — Randal C. Paniello, MD, Dept of Otolaryngology–Head and Neck Surgery, Washington University, 517 S Euclid Ave, Box 8115, St Louis, MO 63110.

tenoid, and thyroarytenoid (TA) muscles acquire slow-twitch characteristics and are stimulated at lower frequencies. Some evidence for this phenomenon has been reported by Baldissera et al,[9] who showed a reduction in the contraction of the canine PCA muscle after successful reinnervation of the larynx with the slow phrenic nerve. Likewise, Sato and Hisa[10] have shown fast-to-slow transformation of the TA muscle after transplantation with a pedicled nerve-muscle graft from the cricothyroid muscle. This same transformation of the TA muscle has occurred after its reinnervation by the slower ansa cervicalis nerve.[11] Slow-to-fast transformation was observed in the PCA muscle after reinnervation by the fast hypoglossal nerve.[12]

Because there is no topographic orientation within most of the RLN, complete transection and repair is expected to result in random matching of the proximal axon stumps with the distal axonal tubules. Because the adductor fibers outnumber the PCA fibers by about 3 to 1, a random reinnervation process would be expected to result in both the PCA muscle's and the adductor group's being reinnervated 25% by fibers originally going to the PCA muscle, and 75% by original adductor fibers. To have all of the fibers line up perfectly ("best-case" scenario) would be very unlikely, as would the converse ("worst-case" scenario). The distal RLN does organize and divide into adductor and abductor trunks as it enters the larynx. In this study, these major RLN divisions were divided and reanastomosed in their original alignment or in reverse alignment to simulate these 2 extreme scenarios. The whole RLNs were then divided and repaired precisely or with 180° rotation to give results expected to fall between the 2 extremes.

METHODS AND MATERIALS

Twelve hemilaryngeal preparations were performed in 6 purpose-bred, conditioned, female mongrel dogs. The dogs were housed in a facility approved by the American Association for the Accreditation of Laboratory Animal Care, and National Institutes of Health guidelines for animal care were followed strictly. The Animal Care Committee of the Department of Veterans Affairs Medical Center, St Louis, approved the experimental protocol. After arrival at our laboratory, the dogs were acclimated to the new environment for approximately 2 weeks. A tracheostomy was performed in the manner previously described by Dahm and Paniello.[13]

The LAP was measured with an endotracheal tube connected to a pressure transducer with a balloon inserted between the vocal folds. Anesthesia was induced with 2.5% thiopental sodium (0.5 mL/kg), and general anesthesia was accomplished with 2% halothane. After supine positioning, an endotracheal tube was placed in the tracheal stoma. A laryngoscope was inserted and suspended. By a pertracheal technique (Paniello and Lee, report in review), a needle electrode was placed through the peristomal skin into the region of the RLN to be stimulated. The electrode was connected to a custom RLN constant-current stimulator (WR Medical Electronics) with separate controls for modulating current and frequency (range, 10 to 110 Hz). A grounding wire was placed subcutaneously in the animal's chest region. The position of the electrode was checked by viewing the canine larynx with a 0° telescope (Karl Storz) placed through the laryngoscope. Electrode placement was confirmed by observing ipsilateral adduction of the vocal fold with stimulation; the telescope and laryngoscope were then removed. A 7.0 Sheridan cuffed endotracheal tube was then placed through the stoma and glottis with the balloon part of the tube coming to rest in the supraglottis. The rostral end of the endotracheal tube was tied with a long silk suture, which was used to pull the tube through the glottis during subsequent measurements. The cuff was inflated with 10 mL of air, and the tube pilot was connected to a pressure transducer. A baseline measurement was taken by pulling the balloon cuff through the glottis with the stimulator off. A measurement cycle consisted of passing the balloon from the supraglottis to the subglottis and trachea in an anterograde fashion, followed by a subsequent and immediate retrograde pulling of the balloon from the subglottic-tracheal region to the supraglottis. The actual mechanics of the pull are accomplished by a push-pull using the silk tether at one end and the proximal end of the endotracheal tube. The nerve stimulator was turned on immediately before the measurements and turned off immediately after 3 cycles were completed. Measurements were made at different intensities to generate an adductory pressure-intensity plot. After the maximal adductory force was determined, a supramaximal stimulus (current) was used with frequencies ranging from 10 to 110 Hz (at intervals of 10 Hz) to generate a force-frequency graph. The frequencies were tested in random order.

Four groups of 3 dogs each were used in the experiment (Fig 1). The groups were as follows:

1. Group 1 had transection and reanastomosis of the RLN branches ("best case"): abductor to abductor trunk, and adductor to adductor trunk.
2. Group 2 had transection and transposition of the RLN branches ("worst case"): abductor to adductor trunk, and adductor to abductor trunk.
3. Group 3 had transection and reanastomosis of

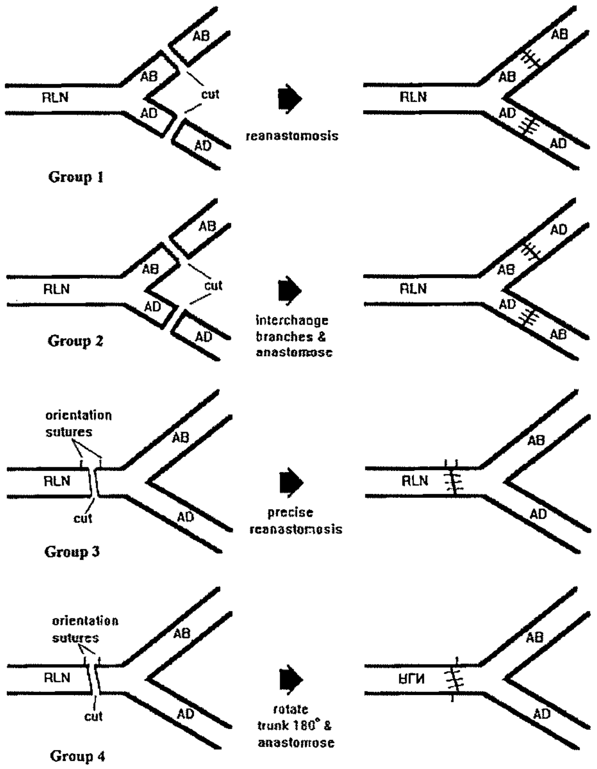

Fig 1. Schematic of 4 experimental groups. RLN — recurrent laryngeal nerve, AB — abductor trunk, AD — adductor trunk.

the RLN with precise realignment.

4. Group 4 had transection and reanastomosis of the RLN with 180° rotation alignment.

"Best" and "worst" cases are felt to represent the extremes of random fiber matching in the repaired RLN.

The nerve procedures were performed under sterile conditions via the same anesthesia method previously described for the tracheostomy. Each RLN was identified and randomly assigned to 1 of the 4 groups. By means of microscopic techniques, the nerve (or appropriate trunk) was then divided and repaired with 8-0 monofilament suture.

Infraglottic examinations were performed at 1-month intervals starting 3 months after nerve injury and repair. The examination consisted of placing a 0° telescope (Karl Storz) through the stoma and viewing the glottis from the subglottis. This was performed with the dog fully awake. The motion of the vocal folds was recorded on videotape. In addition to spontaneous movement, the motion of the vocal folds during swallowing was examined. Swallowing was induced by injecting water into the animal's mouth via a syringe.

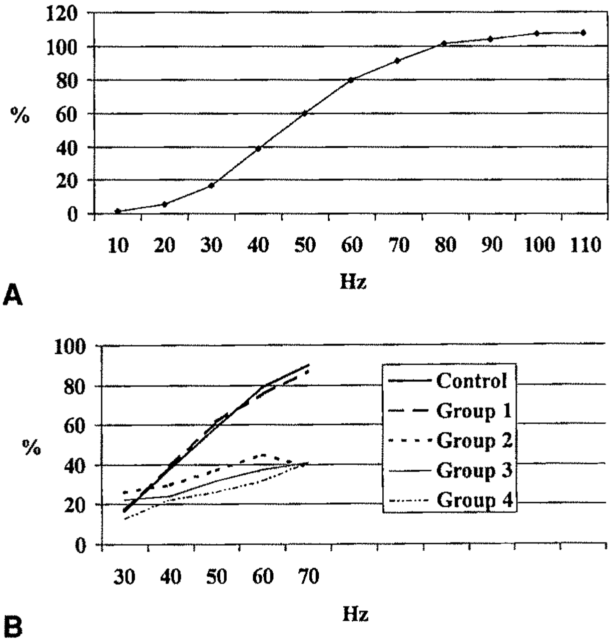

Fig 2. Laryngeal adductory pressure response curves. Pressure at each frequency is expressed as percentage of reference pressure obtained at 80 Hz. Stimulus intensity is supramaximal. A) Preoperative response curve (pooled data; N = 36). B) Responses between 30 and 70 Hz for control group (preoperative) and for 4 experimental groups (postoperative; see Fig 1 and text).

RESULTS

All 12 nerve procedures were successfully performed. Complications from either the tracheostomy or the nerve procedure were minor and consisted of crusting, tracheostomal stenosis requiring stomaplasty (N = 2), and hematoma requiring aspiration (N = 1). Pooled preoperative data (N = 36 trials) gave the characteristic relationship between the LAP (expressed as a percentage of stimulation at 80 Hz) and the stimulation frequency in hertz (Fig 2A). This relationship is linear between 30 and 70 Hz. Figure 2B shows a comparison of this relationship in each of the 4 experimental groups. Student's *t*-tests ($df = 4$) were used to compare the difference in the slope between the preoperative controls and each of the 4 experimental groups. Additionally, a comparison among the 4 groups was performed. A significant difference in the slope was noted between the control group and group 2 ($p < .01$), group 3 ($p < .01$), and group 4 ($p < .01$). No significant difference was noted between group 1 and the controls. Additionally, the intragroup comparison revealed a significant difference between group 1 and group 2 ($p < .05$), group 3 ($p < .05$), and group 4 ($p < .05$). No difference was seen in comparisons of the slopes of groups 2, 3, and 4.

Measurements were compared for each animal at 4, 5, and 6 months. No significant differences were seen in the slope of the LAP response curve in any group during this time interval (ie, no further recovery was seen beyond 4 months).

The infraglottic examinations revealed some characteristic trends among the groups. Group 1 had return of function, with normal movement of the vocal folds noted. In the other 3 groups, the adduction was abnormal, with an anterior and mid–vocal fold bulge. Also, a posterior glottic chink was present after surgery in all the larynges in groups 2 through 4.

DISCUSSION

It is felt that some degree of synkinesis is inevitable after RLN injury, even if an immediate and precise repair is performed. Our data support this assertion for injury involving the entire RLN. Synkinesis, as determined by the slope of the LAP frequency-response curve, was similar in groups with "precise" repair of the whole RLN, "imprecise" repair of the whole RLN (nerve transected and distal end rotated 180° before repair), and maximal misdirection of fibers (abductor and adductor branches divided and switched). This is in marked contrast to the return to normal function of the optimal repair group (abductor and adductor branches divided and sutured exactly together). Thus, in our model, precisely aligning a whole nerve transection resulted in no better results than in maximally misdirecting the fibers.

The LAP response curve reflects a measure of the amount of adductor pressure generated per frequency of stimulation. Characteristically, fast-twitch muscle is maximally stimulated at higher frequencies, whereas slow-twitch muscle shows a greater strength of contraction at lower frequencies. The adductor muscles of the larynx are predominantly fast-twitch muscles, whereas the sole abductor, the PCA muscle, is slow-twitch.[14-16] In the pretreatment control curve, increasing the frequency of stimulation at a constant supramaximal current resulted in an increase in the LAP. Presumably, this occurs as more fast-twitch adductor fibers are recruited. Nerve transections and reanastomosis resulted in a reduced slope of the LAP response curve. This most likely is a result of misdirected fibers in the RLN. Because the RLN lacks topographical organization, the regenerating fibers may innervate either the abductor or adductor fibers.[8]

Group 2 requires some explanation. Hypothetically, reversing the adductor and abductor trunks should result, at low frequency, in maximum adduction, which tapers in a linear manner with increasing frequency as the PCA muscle is activated. The LAP frequency-response curve would be expected to be downsloping. As seen in Fig 2B, a gentle upslope was actually found. One possible explanation for this finding would be related to the uneven number of axons in the 2 trunks. When the larger, adductor trunk was anastomosed into the smaller, abductor distal stump, perhaps as many as two thirds of the axons would remain "unmatched"; similarly, the abductor-into-adductor anastomosis might leave two thirds of the distal axonal tubes "unfilled." These 2 anastomoses, by necessity, were very close together (approximately 2 to 3 mm) at the time of the neurorrhaphy. It is possible that some of the unmatched adductory axons grew into the opposite anastomosis to fill some of the original unfilled adductor tubules. If enough of this crossover occurred, the ratio of abductor and adductor axons reinnervating the adductor muscles might be similar to the random levels predicted in groups 3 and 4, leading to the similar LAP responses seen in Fig 2B. At the time of sacrifice, the nerves were explored, and both neurorrhaphies were found scarred together in one large neuroma, supporting this hypothesis.

In a classic set of experiments, Buller et al[17] showed that a muscle's type was determined by its innervation. Specifically, the normally slow-twitch soleus muscle of the cat was transformed into a predominantly fast-twitch muscle when the muscle was reinnervated with the nerve to the flexor digitorum longus, a fast-twitch muscle. We would expect that this same process is occurring within the intrinsic muscles of the larynx innervated by the RLN. After nerve injury and repair, axons within the RLN originally innervating the fast-twitch adductor muscles may innervate the normally slow-twitch PCA muscle. Obviously, the reverse also occurs. The muscles' assumption of the characteristics of the nerves innervating them would result in an increase in the number of slow-twitch fibers among the adductor muscles. The implications of this transformation are seen in the LAP response curve: at lower frequencies, the LAP is increased, as more adductor muscles have taken on the characteristics of slow-twitch muscles; at higher frequencies, the LAP is decreased for the same reason. Not only does the slope of the LAP response curve decrease when regeneration of fibers is either maximally misdirected or allowed to randomly regenerate, but it also remains normal when direction is given to regeneration (group 1).

More work is needed to determine the histochemistry of the reinnervated laryngeal muscle. More specifically, does fast-to-slow transformation of the adductor muscles occur on a biochemical level? Additionally, research is needed to investigate methods of directing regenerating fibers into "best-case" patterns of recovery.

CONCLUSIONS

Laryngeal adductory pressure can be used to evaluate post-reinnervation synkinesis. In this study, 2 patterns of recovery were seen. The "best-case" recovery group showed normal post-injury recovery of function. The other 3 groups showed similar recovery despite different experimental designs. More work is needed in this area and in efforts to control the misdirection of regenerating RLN fibers after injury.

REFERENCES

1. Crumley RL. Laryngeal synkinesis: its significance to the laryngologist. Ann Otol Rhinol Laryngol 1989;98:87-92.

2. Benninger MS, Crumley RL, Ford CN, et al. Evaluation and treatment of the unilateral paralyzed vocal fold. Otolaryngol Head Neck Surg 1994;111:497-508.

3. Green DC, Berke GS, Graves MC, Natividad M. Physiologic motion after vocal cord reinnervation: a preliminary study. Laryngoscope 1992;102:14-22.

4. Crumley RL. Unilateral recurrent laryngeal nerve paralysis. J Voice 1994;8:79-83.

5. Flint PW, Downs DH, Coltrera MD. Laryngeal synkinesis following reinnervation in the rat. Neuroanatomic and physiologic study using retrograde fluorescent tracers and electromyography. Ann Otol Rhinol Laryngol 1991;100:797-806.

6. Nahm I, Shin T, Watanabe H, Maeyama T. Misdirected regeneration of injured recurrent nerve in the cat. Am J Otolaryngol 1993;14:43-8.

7. Nahm I, Shin T, Chiba T. Regeneration of the recurrent nerve in the guinea pig: reorganization of motorneurons after freezing injury. Am J Otolaryngol 1990;11:90-8.

8. Gacek RR, Malmgren LT, Lyon MJ. Localization of adductor and abductor motor nerve fibers to the larynx. Ann Otol Rhinol Laryngol 1977;86:770-6.

9. Baldissera F, Tredici G, Marini G, et al. Innervation of the paralyzed laryngeal muscles by phrenic motoneurons. A quantitative study by light and electron microscopy. Laryngoscope 1992;102:907-16.

10. Sato F, Hisa Y. Contraction properties and histochemical study of cross-innervated intrinsic laryngeal muscles. In: Hirano M, Kirchner JA, Bless DM, eds. Neurolaryngology: recent advances. San Diego, Calif: Singular Publishing, 1987:120-9.

11. Rice DH, Cooper DS. Contractile properties of canine thyroarytenoid muscle reinnervated from the ansa cervicalis. Ann Otol Rhinol Laryngol 1989;98:153-6.

12. Paniello RC, Lee P, West SE. Laryngeal reinnervation with the hypoglossal nerve. Laryngoscope (in press).

13. Dahm JD, Paniello RC. Tracheostomy for long-term laryngeal experimentation. Otolaryngol Head Neck Surg 1998; 118:376-80.

14. Rosenfield DB, Miller RH, Sessions RB, Patten BM. Morphologic and histochemical characteristics of laryngeal muscle. Arch Otolaryngol 1982;108:662-6.

15. Happak W, Zrunek M, Pechmann U, Streinzer W. Comparative histochemistry of human and sheep laryngeal muscles. Acta Otolaryngol (Stockh) 1989;197:283-8.

16. Brondbo K, Hall C, Dahl HA, Teig E, Gujord KM. A histochemical evaluation of experimentally reinnervated canine laryngeal muscles. J Otolaryngol 1986;15:265-72.

17. Buller AJ, Eccles JC, Eccles RM. Interaction between motoneurons and muscles in respect of the characteristic speed of their responses. J Physiol 1960;150:417-39.

≈

EUROPEAN ACADEMY OF FACIAL PLASTIC SURGERY

The annual meeting of the European Academy of Facial Plastic Surgery will be held September 15-17, 2000, in Thessaloniki, Greece. For information, contact Prof Dr J. Daniilidis, ENT Dept, Aristotelian University of Thessaloniki–AHEPA Hospital, 540 06 Thessaloniki, Greece; telephone 0030/31/994.761-2; fax 0030/31/994.916.

Ann Otol Rhinol Laryngol 109:2000

PYRIFORM SINUS FISTULA: MANAGEMENT WITH CHEMOCAUTERIZATION OF THE INTERNAL OPENING

KWANG HYUN KIM, MD, PHD
MYUNG-WHUN SUNG, MD, PHD
SEUNG HA OH, MD, PHD
TAE-YONG KOH, MD
IN-SANG KIM, MD
SEOUL, KOREA

A branchial remnant originating in the pyriform sinus causes a recurrent fistula or abscess in the neck. In spite of excision, recurrence may result from inadequate removal of the fistula tract. We attempted chemocauterization of the internal opening of the fistula tract with trichloroacetic acid (TCA) on direct endoscopy. This is a 6-year review of 18 patients with pyriform sinus fistula. Medical history, barium esophagography, computed tomography scans, operative findings, and treatment results were analyzed. By direct endoscopy, all patients were found to have a fistula opening in the pyriform sinus, exclusively on the left side. In only 9 patients, the fistula tract was identified by barium esophagography before operation. Computed tomography revealed a suspicious fistula tract originating from the pyriform sinus in 8 of 10 patients. Sixteen patients were initially managed by TCA chemocauterization. There were no serious intraoperative or postoperative complications. Four patients had recurrent masses, which were managed by simple excision in 2 patients and repeated TCA cauterization in the other 2 patients with unobliterated internal openings. We recommend barium swallow study and direct endoscopy for all patients presenting with a recurrent lateral neck abscess, especially on the left side. Our results suggest that initial chemocauterization of the internal opening can be a reasonable alternative procedure for the management of pyriform sinus fistula.

KEY WORDS — chemocauterization, pyriform sinus fistula.

INTRODUCTION

A branchial pouch anomaly originating from the pyriform sinus is uncommon and is typically manifested by recurrent neck abscess.[1-3] Partly due to its rarity, the patients usually do not receive a definite diagnosis until long after the initial symptoms have occurred.[4,5] Although most surgeons agree that complete resection of the fistula tract is the best treatment for the prevention of recurrence, it is sometimes very difficult to excise the whole fistula tract.[1,3,4] It requires a wide neck exploration, and there is a high risk of injury to the important nerves or vessels adjacent to the tract. Risk factors include repeated infections and previous multiple surgical procedures such as drainage or incomplete, previous attempts at excision of the fistula tract.

Since 1993, when we first tried to obliterate the internal opening of the pyriform sinus fistula only by circumferential chemocauterization using trichloroacetic acid (TCA) in a patient with recurrent neck abscess, we have applied this procedure to all patients with pyriform sinus fistula as the first-line treatment. Trichloroacetic acid is a potent cauterizing agent that has been used for chemical peel and treatment of papillomas.[6] It is neutralized by the serum and is systemically nontoxic. In this article, we report the results of this method for the management of pyriform sinus fistula.

MATERIALS AND METHODS

The medical records of 18 patients who were managed under the diagnosis of pyriform sinus fistula at the Department of Otolaryngology–Head and Neck Surgery, Seoul National University Hospital, Seoul, Korea, from 1993 through 1998 were retrospectively reviewed (see Table). Past medical history, clinical manifestations, barium esophagography, computed tomography (CT) scans, endoscopic findings, and treatment results were analyzed.

The age of patients showed a wide range, from 3 to 49 years (mean, 17 years), and there was a slight female preponderance (male to female ratio, 7:11). The patients have been followed up for 1 to 70 months (mean, 23.1 months).

Chemocauterization was performed by suspension laryngoscopy under general anesthesia. The internal opening of the pyriform sinus fistula was cauterized in a circumferential fashion with TCA (10% to 40%) with or without simultaneous drainage of the external abscess. The cauterized wound was allowed to

---

From the Department of Otolaryngology–Head and Neck Surgery, Seoul National University College of Medicine, Seoul, Korea.

Presented at the meeting of the American Laryngological Association, Palm Desert, California, April 24-25, 1999.

CORRESPONDENCE — Kwang Hyun Kim, MD, PhD, Dept of Otolaryngology–Head and Neck Surgery, Seoul National University College of Medicine, 28 Yongon-Dong, Chongno-Gu, Seoul, Korea, 110-744.

SUMMARY OF PATIENTS WITH PYRIFORM SINUS FISTULA

Case No.	*Sex*	*Age (y)*	*Side*	*Preoperative Esophagography*	*Age of Onset (y)*	*Interval to Diagnosis**	*Previous Surgical Procedures*	*Treatment*	*Recurrence*	*Follow-up (mo)*
1	F	3	L	–	3	3 mo	1	TCA	–	13
2	F	4	L	–	3	1 y	2	TCA	+	12
3	F	6	L	–	5	1 y	3	TCA	–	12
4	F	6	L	–	6	10 mo	1	TCA	–	13
5	F	8	L	–	8	1 y	3	TCA	–	8
6	F	8	L	+	5	3 y	1	TCA	+	6
7	F	9	L	–	1	8 y	5	TCA	–	54
8	F	9	L	–	8	10 mo	1	TCA	+	16
9	F	11	L	–	11	1 y	0	TCA	+	8
10	M	13	L	+	5	8 y	2	TCA	–	18
11	F	14	L	–	12	2 y	1	TCA	–	3
12	M	21	L	+	21	2 mo	0	TCA	–	1
13	M	23	L	+	12	11 y	7	TCA	–	70
14	M	24	L	+	23	8 mo	0	TCA	–	21
15	M	32	L	+	4	28 y	3	Excision	–	56
16	M	32	L	+	7	25 y	3	No surgery	–	60
17	M	33	L	+	4	29 y	5	TCA	–	18
18	F	49	L	+	12	37 y	2	TCA	–	68

TCA — trichloroacetic acid.

*From initial presenting symptom to final diagnosis.

heal by secondary intention. In the first 2 cases, 10% TCA was applied, and oral feeding was withheld until the seventh postoperative day, on which the closure of the internal opening was confirmed by direct endoscopy. But 10% TCA seemed too weak, and afterward, 20% or 40% TCA was used and oral feeding was started on the second postoperative day.

RESULTS

The most common presenting manifestation was recurrent neck abscess. The average duration between the initial manifestation and the final diagnosis was 8.8 years. In all but 1 patient, multiple surgical procedures had been repeatedly attempted (average 2.1 times) under the impression of nonspecific neck abscess, tuberculous lymphadenopathy, or suppurative thyroiditis.

When a patient had an abscess in the left side of the neck, esophagography was obtained as an initial workup procedure. However, only 9 of the 18 fistula tracts showed up on esophagography (Fig 1A). Ten patients had CT scans at the time of abscess in the neck, and suspicious fistula tracts were found in the left pyriform sinus leading to the lateral neck or thyroid gland in 8 patients (Fig 1B).

Antibiotics were given intravenously for the initial control of the infection in most of the cases. After the acute infection was controlled, the pyriform sinus was endoscopically examined in all but 1 patient, who refused operation. In these patients, direct endoscopy revealed the internal opening of the fistula tract in the pyriform sinus, exclusively on the left side (Fig 2). There was no bilateral case. Two patients (cases 1 and 9) had the opening in the lateral aspect, and the others, at the apex of the pyriform sinus.

Treatment results are summarized in Fig 3. Sixteen of the 17 patients who underwent endoscopic examination were treated with TCA chemocauterization, and in 1 patient, primary excision was attempted. Four patients had a recurrent mass or abscess (cases 2, 6, 8, and 9). All recurrences occurred within 1 year. Excisions were performed on these recurrent noninfected cystic masses (cases 8 and 9), or incision and drainage was repeated (cases 2 and 6). In the latter 2 patients, the internal openings were found to be open in spite of previous TCA cauterizations, and these openings were cauterized with TCA again. In 2 other patients who were endoscopically reexamined, the internal openings were found to be obliterated. In 5 patients, the follow-up duration is less than 1 year, but they have been followed-up at regular intervals.

DISCUSSION

A branchial pouch anomaly is embryologically defined by its origin and clinically classified by the lo-

P24704

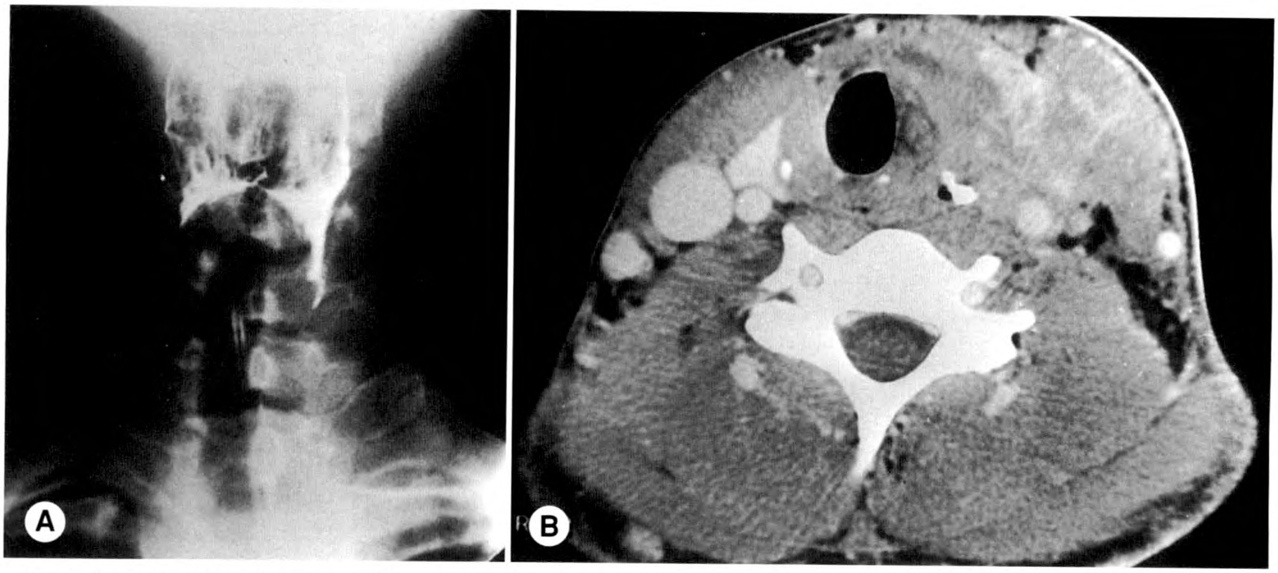

Fig 1. Typical images of patients with recurrent neck abscesses. A) Leakage of barium from left pyriform sinus apex can be seen on barium esophagography. B) Neck computed tomography scan shows suspicious fistula tract originating from pyriform sinus and deep neck abscess.

cation of its internal opening.[7] The embryological precursor of pyriform sinus fistula remains controversial. Much confusion persists in differentiating the diagnosis of third and fourth pouch anomalies because they both arise in the pyriform sinus. There are convincing arguments for considering it either a third or fourth pouch remnant. After Tucker and Skolnick[8] first described a case of a possible remnant of the fourth branchial apparatus, many authors reported similar cases suspected to be of fourth branchial pouch origin.[2,3,9-12] However, a complete fistula of the fourth branchial cleft and pouch is theoretically possible, though it has never been demonstrated.

Differentiation between the third and fourth branchial pouch anomalies can only be made by surgical confirmation of their course. Liston[7] has theorized that the pharyngeal opening of a fourth branchial anomaly should be near the apex of the pyriform sinus, as opposed to that of a third branchial anomaly, which would be in the upper portion of the pyriform sinus, at the level of the thyrohyoid membrane. When we classified our cases according to Liston, 2 cases were considered to be third branchial remnants. The fistula tracts emerged from the lateral aspect of the pyriform sinus, and the external masses were located just below the hyoid bone. But the theoretical intrathoracic tract described by Liston could not be entirely demonstrated in our cases.

Because the discrimination between the third and fourth branchial pouch origins was not only ambigu-

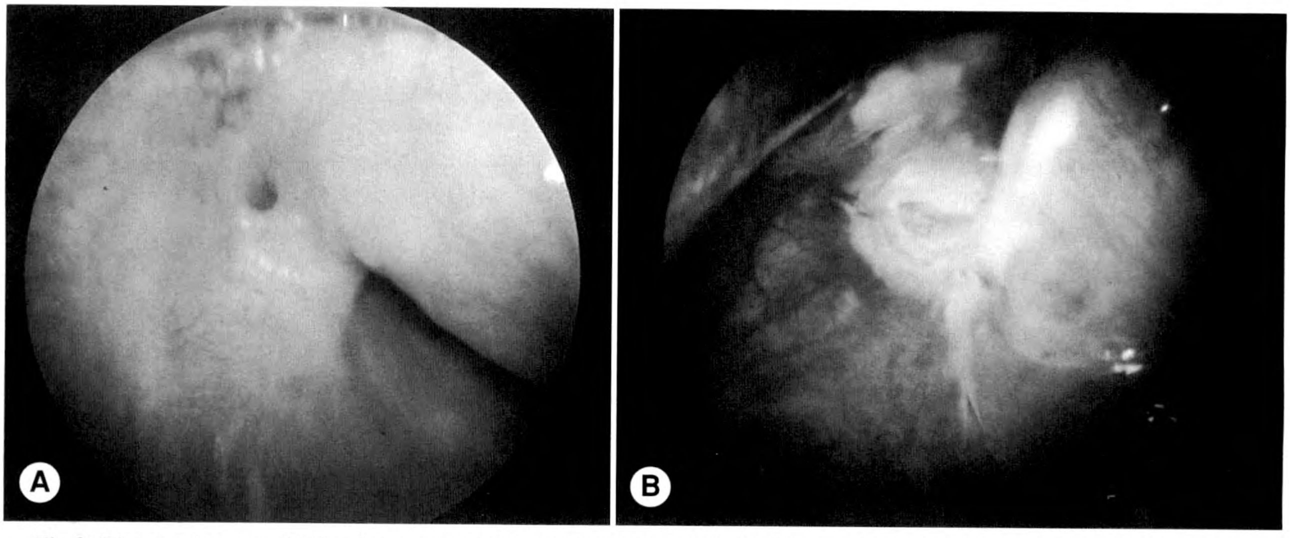

Fig 2. Direct endoscopy. A) Fistula opening at left pyriform sinus apex. B) Same patient, after internal opening of fistula has been circumferentially chemocauterized.

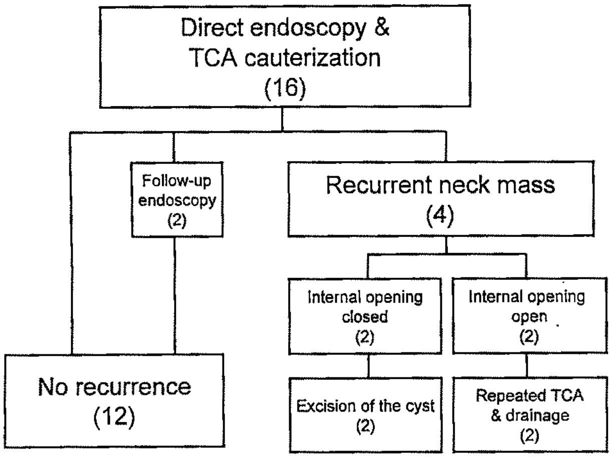
Direct endoscopy & TCA cauterization (16)
Follow-up endoscopy (2)
Recurrent neck mass (4)
Internal opening closed (2)
Internal opening open (2)
No recurrence (12)
Excision of the cyst (2)
Repeated TCA & drainage (2)

Fig 3. Overview of treatment results in patients with pyriform sinus fistula who received chemocauterization with trichloroacetic acid (TCA).

ous in most of the cases but also meaningless in terms of treatment, we used the term "pyriform sinus fistula." Pyriform sinus fistula has been reported to occur in the left side of the neck in over 90% of cases and often presents with repeated neck swelling, suppurative thyroiditis, or, on rare occasions, retropharyngeal abscess.[2,3,8,9,13-16] All of our cases were left-sided, and most of them manifested as repeated neck swelling.

The incidence of pyriform sinus fistula may have been underestimated.[1] Our experience — 18 cases during 6 years at 1 institution — suggests that pyriform sinus fistula may be more common than has been estimated, and that some of the cases might have been misdiagnosed as isolated neck abscesses.

The fistula can be identified with barium esophagography. However, only 50% of our cases had the fistula tract from the pyriform sinus identified on preoperative esophagograms. In pediatric patients, the rate of visualization was lower than in adults. Therefore, otolaryngologists should have a high index of suspicion and positively search for the internal opening by direct endoscopy, regardless of the findings of esophagography, if pyriform sinus fistula is clinically suspected. In our series, CT scans suggested a fistula tract originating from the pyriform sinus, as well as an infectious process, in the lateral neck in 8 of 9 patients; hence, CT might be a useful tool for diagnosing pyriform sinus fistula.

It has been agreed that the entire tract of the pyriform sinus fistula must be completely excised for definitive cure, sometimes after medical therapy or drainage for the control of infection.[1-4,8,11,13] However, repeated infection and previous surgery made complete dissection of the tract hazardous, and impossible in some cases. In most of our cases, recurrent neck abscess followed upper respiratory tract infections, a finding that suggests that contamination from the pharyngeal secretions might be the direct cause of the abscess. To circumvent these problems, we tried to obliterate the internal opening from the inside with chemocauterization as a first-line treatment. In the first 2 cases, we used 10% TCA and placed the patient on nasogastric tube feeding for at least 7 days. The internal openings were found to be obliterated on follow-up endoscopy in these patients. Since then, we have used 20% or 40% TCA, and early oral feeding has been started from the second postoperative day without a nasogastric tube. Among 16 patients treated with chemocauterization, only 2 patients had a persistent internal opening and were recauterized. In the other 2 patients who had a recurrent mass in the lateral neck, the internal openings were found to be obliterated and the excision of the isolated cyst was uncomplicated.

Our experience suggests that when the internal opening and the proximal part of the tract are closed from the inside, the remaining infected fistula tract might obliterate itself in most cases.[3] A persisting tract could be cauterized again, as seen in our cases. In addition, a recurrent mass can be easily excised, when these recurrent masses might present as an isolated cyst without communication to the pyriform sinus. Other advantages of endoscopic chemocauterization include no external scar, shorter general anesthesia, and earlier discharge from the hospital with little morbidity. Even when this procedure fails, there still remains the opportunity of total excision.

Recently, Jordan et al[3] suggested electrical cauterization of the internal opening. We believe that our method has the advantage of obliterating the tract as well as the opening by migration of TCA down into the tract.

Although the follow-up period is not long in some cases and there still remains a risk of recurrence, our experience suggests that endoscopic circumferential chemocauterization of the internal opening in the pyriform sinus can be a relatively safe and simple first-line treatment of pyriform sinus fistula.

CONCLUSION

Because pyriform sinus fistula may be less uncommon than has been previously estimated, left-sided neck abscesses developing after upper respiratory tract infections in healthy young persons should be vigorously investigated by barium esophagography, CT scan, and direct endoscopy. The TCA chemocauterization of the internal opening is a useful alternative mode of therapy that can be successfully used in most patients.

REFERENCES

1. Edmonds JL, Girod DA, Woodroof JM, Bruegger DE. Third branchial anomalies. Avoiding recurrences. Arch Otolaryngol Head Neck Surg 1997;123:438-41.

2. Rosenfeld RM, Biller HF. Fourth branchial pouch sinus: diagnosis and treatment. Otolaryngol Head Neck Surg 1991;105: 44-50.

3. Jordan JA, Graves JE, Manning SC, McClay JE, Biavati MJ. Endoscopic cauterization for treatment of fourth branchial cleft sinuses. Arch Otolaryngol Head Neck Surg 1998;124:1021-4.

4. Chandler JR, Mitchell B. Branchial cleft cysts, sinuses, fistulas. Otolaryngol Clin North Am 1981;14:175-86.

5. Hashizume K, Kawarasaki H, Iwanaka T, et al. A new operational approach for the pyriform sinus fistula. Surg Today 1993;23:293-7.

6. Resnik SS. Chemical peeling with trichloroacetic acid. J Dermatol Surg Oncol 1984;10:549-50.

7. Liston SL. Fourth branchial fistula. Otolaryngol Head Neck Surg 1981;89:520-2.

8. Tucker HM, Skolnick ML. Fourth branchial cleft (pharyngeal pouch) remnant. Trans Am Acad Ophthalmol Otolaryngol 1973;77:368-71.

9. Ostfeld E, Segal J, Auslander L, Rabinson S. Fourth pharyngeal pouch sinus. Laryngoscope 1985;95:1114-7.

10. Ford GR, Balakrishnan A, Evans JNG, Bailey CM. Branchial cleft and pouch anomalies. J Laryngol Otol 1992;106:137-43.

11. Godin MS, Kearns DB, Pransky SM, Seid AB, Wilson DB. Fourth branchial pouch sinus: principles of diagnosis and management. Laryngoscope 1990;100:174-8.

12. Nonomura N, Ikarahi F, Fujisaki T, Nakano Y. Surgical approach to pyriform sinus fistula. Am J Otolaryngol 1993;14: 111-5.

13. DeLozier HL, Sofferman RA. Pyriform sinus fistula: an unusual cause of recurrent retropharyngeal abscess and cellulitis. Ann Otol Rhinol Laryngol 1986;95:377-82.

14. Miyauchi A, Matsuzuka F, Kuma K, Takai SI. Pyriform sinus fistula: an underlying abnormality common in patients with acute suppurative thyroiditis. World J Surg 1990;14:400-5.

15. Doi BO, Hutson JM, Myers NA, McKelvie PA. Branchial remnants: a review of 58 cases. J Pediatr Surg 1988;23:789-92.

16. Taylor WE, Myer CM, Hays L, Cotton RT. Acute suppurative thyroiditis in children. Laryngoscope 1982;92:1269-73.

≈

SAN FRANCISCO OTOLOGY & NEUROTOLOGY UPDATE 2000

The San Francisco Otology & Neurotology Update 2000 will be held October 26-28, 2000, in San Francisco, California. For information, contact University of California, San Francisco, Office of Continuing Medical Education, Room LH-450, San Francisco, CA 94143-0742; telephone (415) 476-4251; fax (415) 476-0318; e-mail: palmerk@ocme.ucsf.edu.

Ann Otol Rhinol Laryngol 109:2000

EXPERIMENTAL AUTOIMMUNE INNER EAR DISEASE: AN ELECTROCOCHLEOGRAPHIC AND HISTOPHYSIOLOGIC STUDY

HENK BOUMAN, MD, PHD SJAAK F. L. KLIS, PHD FRITS MEEUWSEN
JOHN C. M. J. DE GROOT, PHD GUIDO F. SMOORENBURG, PHD JAN E. VELDMAN, MD, PHD
UTRECHT, THE NETHERLANDS

Systemic immunization with swine inner ear antigens in complete Freund's adjuvant induces functional disturbances in the cochlea. Morphometric data indicate that an endolymphatic hydrops develops within 2 weeks. It diminishes 6 weeks after immunization. A progressive decrease in the compound action potential amplitude is observed from 2 to 6 weeks after immunization. Enhancement of the amplitude of the summating potential is present without a clear overall correlation to the presence of endolymphatic hydrops. The amplitude of the cochlear microphonics shows no significant changes after immunization. Western blot analysis of the sera performed 2 and 6 weeks after immunization shows enhanced reactivity at 68, 50, 45, and 27 kd molecular weights, as compared to controls. The same spectrum of cross-reacting antibodies is believed to be instrumental in immune-mediated sensorineural hearing loss in patients. Apparently, cross-reacting antibodies and released mediators disturb cochlear homeostasis, resulting in the observed changes in the electrophysiological responses. However, these changes are not clearly related to structural changes at the light and electron microscopic levels.

KEY WORDS — electrocochleography, experimental autoimmune inner ear disease, histopathology, immune-mediated endolymphatic hydrops, morphometry.

INTRODUCTION

Some forms of sensorineural hearing loss (SNHL) are suspected to have an immunologic (possibly autoimmune) origin. Their onset is often sudden, their course is usually rapid and progressive, and the hearing loss may eventually develop — if not recognized and treated — into profound unilateral or bilateral deafness.[1] The proposed immunologic mechanisms remain controversial. This type of SNHL has clinically been assessed by different immunoassays.[1-5] Western blot analysis of patients' sera has gained wide application and is gradually becoming the standard technique for identifying patients who may respond to immunosuppressive therapy.[5-8] Positive banding has been identified against inner ear antigens with molecular weights of 27-35, 45-50, 60, 65-68, 80, and 220 kd.

Most of our knowledge about inner ear immunology originates from animal studies, because it is difficult to study the human inner ear by standard clinical immunologic methods. Since the early 1960s, audiovestibular dysfunction as a result of immunization with isogeneic or xenogeneic cochlear tissue has been reported in the literature.[9,10] Histologic evidence of immune-mediated inner ear injury, such as loss of cochlear neurons, a perivascular mononuclear cell infiltrate with extravasated red blood cells and perivascular edema in the modiolus, and IgG depositions at various sites throughout the cochlea, has been reported.[9-13] Endolymphatic hydrops is a frequent finding in these immunization experiments. Antibodies to inner ear antigens have been detected. The observed effects of immunization, however, seem to vary considerably, not only between different research laboratories, but also within animal groups.

In experimental immunologic studies of the inner ear, hearing thresholds have been measured mainly by auditory brain stem responses. The hearing loss after injection of isogeneic or xenogeneic cochlear tissue was a unilateral or bilateral deficit ranging from 20 to 50 dB sound pressure level in 20% to 88% of the animals.[12,13] However, detailed electrophysiological data on the compound action potential (CAP), the summating potential (SP), and cochlear microphonics (CM), as described in experimental hydrops studies,[14,15] are not available in immunologic studies of the inner ear. Such data could give more insight into the way an immune response against the inner ear might affect inner ear function.

In this study, therefore, we addressed the following questions: 1) which cells or cell systems in the cochlea are affected? 2) are these cells or cell systems incapacitated or destroyed through a local immune response? and 3) is endolymphatic hydrops a significant aspect of the immune response? Further, we address the question of whether endolymphatic hy-

---

From the Hearing Research Laboratories, Department of Otorhinolaryngology, University Medical Center Utrecht, Utrecht, the Netherlands. Supported by a grant from the Heinsius-Houbolt Foundation, the Netherlands.

CORRESPONDENCE — Jan E. Veldman, MD, PhD, Dept of Otorhinolaryngology, University Medical Center Utrecht, Heidelberglaan 100, 3584 CX Utrecht, the Netherlands.

drops, viewed as an imbalance in endolymph homeostasis, plays a key role in the initial structural and/or functional changes found in the inner ear. These questions were experimentally approached by immunizing guinea pigs subcutaneously with crude swine membranous-labyrinthine tissue extracts ("inner ear antigen") in complete Freund's adjuvant (CFA). Two and six weeks after antigen administration, sera from these animals were tested for the presence of cross-reacting antibodies against swine inner ear antigen through a Western blot assay. Electrophysiological and histophysiologic studies were subsequently performed at the same time intervals after the single inner ear antigen injection. Animals who received only extracting buffer in CFA, without inner ear antigen, served as controls.

MATERIALS AND METHODS

Animals. Twenty-two female albino guinea pigs (Dunkin Hartley, weighing 200 to 300 g) with a positive Preyer's reflex were used. The animals were housed under standard laboratory conditions. The care and use of animals reported in this study were approved by the Animal Care and Use Committee of the School of Medicine, Utrecht University, the Netherlands (DEK-GNK 89055).

Antigen Preparation. Fresh swine temporal bones were obtained from a local slaughterhouse and frozen immediately on dry ice (–80°C). After thawing on ice, surgical dissection of the membranous part of the cochlea was carried out under a binocular microscope. The tissues were stored on ice. Subsequently, proteins were extracted by sonification on ice in 5.75 volumes (wt/vol) of phosphate-buffered saline solution (PBS; pH 7.4) containing 1% Triton X-100, 0.5 mmol/L phenylmethylsulfonyl fluoride (PMFS), 20 μg/mL aprotinin, 0.3 mg/mL ethylenediaminetetraacetic acid (disodium salt; EDTA.2Na), 0.5 μg/mL leupeptin, and 0.7 μg/mL pepstatin. After centrifugation (25 minutes; 20,000 rpm), the supernatant was stored at –80°C. It contained 2.3 mg/mL protein (BCA Protein Assay, Pierce) and was used as the crude inner ear antigen (CAg) for immunization of the guinea pigs.

Immunization Protocols. Animals were divided into 3 groups. The first group (N = 10) received a subcutaneous injection of 0.5 mL of an emulsion containing equal parts of CAg and CFA in the nuchal area. Effects were evaluated after 2 weeks (CAg2 group). The second group (N = 6) received the same subcutaneous injection as described for the first group, but the effects were evaluated after 6 weeks (CAg6 group). The third group (N = 6) served as the control group. The animals of this group were injected once subcutaneously with 0.5 mL of an emulsion of equal amounts of the extraction buffer and CFA without inner ear antigen. For the control group, the effects were evaluated only after 2 weeks.

Immunoblotting. Swine inner ear antigens were prepared as described above, except that sonification was carried out in 10 volumes (wt/vol) of 10 mmol/L Tris–hydrochloric acid (Tris-HCl; pH 7.2) containing 1% sodium dodecylsulfate (SDS), 1 mmol/L iodoacetamide, 0.5 mmol/L PMFS, 20 μg/mL aprotinin, 0.3 mg/mL EDTA.2Na, and 0.5 μg/mL leupeptin. The tissue extract was mixed with an equal volume of 125 mmol/L Tris-HCl (pH 6.8) sample buffer containing 4% SDS, 20% glycerol, and bromophenol blue to the desired color, and SDS–polyacrylamide gel electrophoresis was performed in an 11% polyacrylamide gel with prestained molecular weight markers (Biorad, Richmond, Calif).

Proteins were transferred onto PVDF membranes (Immobilon-P, Millipore Corp, Bedford, Calif) by semidry electroblotting (0.8 mA/cm^2 for 1 hour) with a Transblot cell (Biorad). The transfer buffer (48 mmol/L Tris-HCl [pH 9.2], 39 mmol/L glycine, 20% methanol) was prepared according to Bjerrum and Schafer-Nielsen with 1.3 mmol/L SDS.[16]

After drying, the membranes were cut into strips and incubated under constant agitation in blocking buffer (5% nonfat dry milk, 0.2% Tween-20 [Sigma, St Louis, Mo], 0.01% antifoam-A emulsion [Sigma], 0.02% sodium azide in PBS, pH 7.4) for 1 hour at room temperature in order to prevent nonspecific binding. The membranes were then incubated with guinea pig serum from every individual animal of the 2 experimental groups and the control group (diluted 1:100 in blocking buffer) at room temperature for 2 hours, followed by washing 3 times in blocking buffer and incubation with the alkaline-phosphatase–conjugated secondary antibody (anti–guinea pig Ig, Sigma Immunochemicals, St Louis, Mo; diluted 1:30,000 in blocking buffer) for 1 hour at room temperature. After washing in TBS (20 mmol/L Tris-HCl [pH 7.5], 500 mmol/L sodium chloride), the strips were developed in 5-bromo-4-chloro-3-indolyl phosphate/nitroblue tetrazolium (BCIP-NBT) substrate. The staining reaction was stopped by placing the strips in 20 mmol/L EDTA.2Na in PBS (pH 7.4).

Electrocochleography. Animals were anesthetized with Thalamonal (a mixture of 2.5 mg/mL droperidol and 0.05 mg/mL fentanyl) administered intramuscularly at a dose of 1.8 mL/kg body weight. Artificial ventilation with a gas mixture containing 33% oxygen, 66% nitrous oxide, and 1% halothane was provided through a tracheal cannula. The heart rate was monitored continuously, and the rectal temperature was maintained at 38°C with a heating pad. Both auditory bullae were exposed through a ventrolateral surgical approach. Electrophysiological responses (CAP, CM, and SP) of the cochlea were recorded with a silver ball electrode at the apex. At this location, the amplitudes of the CAP and SP are maximal in the guinea pig. Moreover, the SP measured at the apex is a particularly sensitive indicator for endolymphatic hydrops.[15] The reference electrode was placed in the neck muscles. Stimulus generation and data acquisition were controlled by computer using a CED 1401-plus laboratory interface. Tone burst waveforms were calculated and stored in a revolving memory consisting of 2,500 points with 12-bit resolution. Tone bursts of 2, 4, and 8 kHz were used. Rise and fall envelopes of the tone bursts were cosine-shaped (1 ms each) and were separated by a plateau of 6 ms. The stimuli were led to a Beyer DT48 dynamic transducer, which was connected to a hollow ear bar fitted into the exposed outer ear canal. Calibration was performed with a Brüel and Kjaer 4134 microphone by the substitution method. The inter-burst interval was 99 ms. Consecutive tone bursts were presented with alternating polarity. The responses were amplified (5,000 or 10,000 times), bandpass-filtered (12 dB per octave, –3 dB at 1 Hz and 10 kHz), analog-to-digital converted, averaged (maximum 500 times), and stored on disk for offline analysis. The averaged responses to the tone bursts of opposite polarity were stored separately. The CAP and SP were obtained by addition of the responses to the stimuli of opposite polarity, and the CM by subtraction. The SP measurement was based on the DC level measured approximately 6 ms after the start of the 8-ms tone burst. The CAP amplitude was defined as the distance between the first negative peak (N_1) and the steady-state level of the SP, because in principle, the CAP is superimposed on the SP. The CM was measured as the peak-to-peak value halfway through the sinusoidal response.

Light and Electron Microscopy. After electrocochleography, the animals were painlessly decapitated and the temporal bones containing the bullae, including the dura mater covering the posterior cranial fossa, were excised in toto from the skull. Next, the bullae were opened and the cochleas were immediately fixed by intralabyrinthine perfusion with a trialdehyde fixative and immersed in the same fixative overnight at 4°C. The fixative consisted of 3% glutaraldehyde, 2% formaldehyde, 1% acrolein, 2.5% dimethylsulfoxide in 0.08 mol/L sodium cacodylate buffer, pH 7.4. Subsequently, the temporal bones were rinsed in 0.1 mol/L sodium cacodylate buffer (pH 7.4) for 2 × 15 minutes, decalcified in 10% EDTA.2Na (pH 7.4) for 10 days under constant agitation at room temperature, and rinsed again in the same buffer (2 × 15 minutes). At this time, each temporal bone was divided with a sharp razor blade into the cochlear partition and another part containing the endolymphatic duct and sac. Both parts were post-fixed in 1% osmium tetroxide in 0.1 mol/L sodium cacodylate buffer (pH 7.4) containing 1% potassium rutheniumcyanide for 2 hours at 4°C, and then submitted to several washes in distilled water. Dehydration was performed in a graded ethanol, 2,2-dimethoxypropane, propylene oxide series. The cochleas and the parts containing the endolymphatic duct and sac were embedded in toto in Spurr's low-viscosity resin containing 1% silicone DC 200 fluid (Polaron Equipment Ltd, Biorad Laboratories, Watford, United Kingdom).

Subsequently, the cochleas were divided along a midmodiolar plane and re-embedded. Semithin sections (1 μm) were cut with glass knives on a Reichert-Jung 2050 microtome and stained with methylene blue and azure B in borax for light microscopic evaluation of the organ of Corti, stria vascularis, spiral ganglion, and Reissner's membrane. The endolymphatic sac of every individual animal was further evaluated at both the light and electron microscopic levels.

Ultrathin sections were cut with a diamond knife on an LKB ultratome Nova and collected on Pioloform-coated single-slot copper grids. The sections were contrast-stained with 7% uranyl acetate in 70% methanol and Reynolds' lead citrate, and examined in a JEOL 1200 EX transmission electron microscope operating at 80 kV.

Morphometry. Endolymphatic hydrops was measured objectively by using the "l_R/d ratio" method.[17] The l_R/d ratio is a simple method to express the degree of endolymphatic hydrops; it gives the actual length of Reissner's membrane, l_R, with respect to the straight distance between the points of attachment of Reissner's membrane, d (Fig 1). This ratio will exceed 1.0 when Reissner's membrane bulges into the scala vestibuli in a case of endolymphatic hydrops.

To quantify the length parameters in each individual half-turn of a semithin midmodiolar section of the cochlea, we used the VIDAS image analysis system (Kontron/Zeiss, Eching, Germany). The measurement error of this procedure is less than 5%. Sections were scanned with a Sony black-and-white CCD camera, type XC-77CE, attached to the microscope. The frame size of the camera was 768 × 512 pixels at 256 gray levels. Subsequently, the length of Reissner's membrane and the length between the medial and lateral attachment points of Reissner's membrane were measured. This procedure was per-

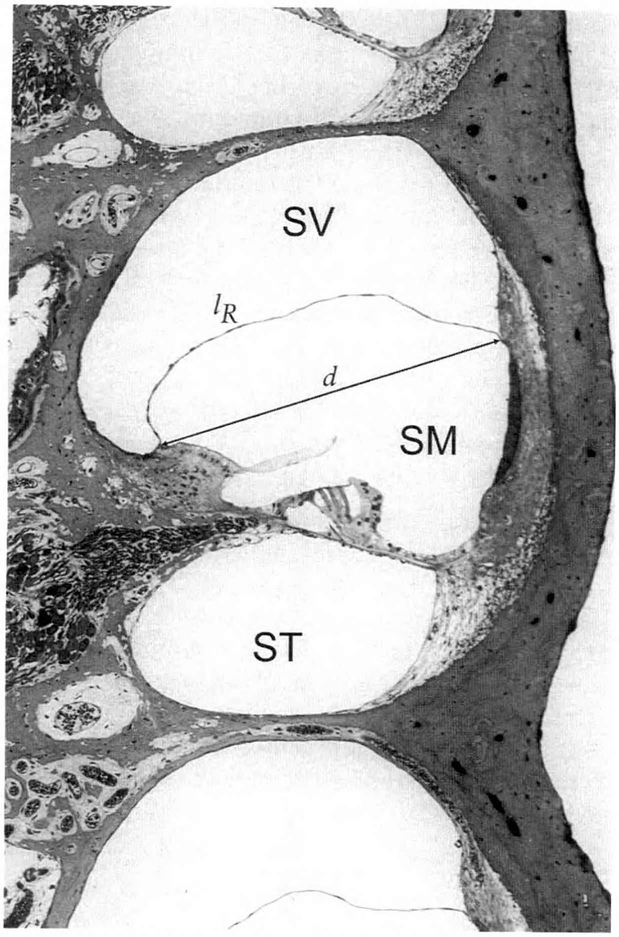

Fig 1. Light microscopic section of cochlear turn with moderate endolymphatic hydrops. There is evident bulging of Reissner's membrane into scala media (SM). SV — scala vestibuli, ST — scala tympani, *l*R — length of Reissner's membrane, *d* — distance between medial and lateral attachment points of Reissner's membrane.

formed on each individual cochlear half-turn and on 2 sections per ear. Thus, for each ear, we had 4 measurements per turn, and the average of these measurements was calculated.

Statistical Analysis. Both the morphometric and the electrocochleographic data were statistically analyzed by analysis of variance (ANOVA). Between-subject tests were performed on the 3 experimental groups. Within-subject variables were right versus left ears and, for electrocochleography, frequency and level of stimulation. The CAP and CM data were logarithmically transformed before analysis in order to improve the homogeneity of variance required by the ANOVA. Statistica software was used in all analyses.

RESULTS

Light Microscopy. Upon light microscopic examination, there was evidence of a frequently occurring mild-to-moderate bilateral endolymphatic hydrops in both experimental animal groups, CAg2 and CAg6 (Fig 1). It was predominantly present in the basal and middle turns of the cochlea. The organ of Corti had a normal appearance, and no outer or inner hair cell loss was noticed. One animal in the CAg6 group showed loss of spiral ganglion cells in the apical portion of the right cochlea. Other structural changes, such as edema, hemorrhage, or a perivascular mononuclear cell infiltrate, were not observed in the scala tympani or in the scala vestibuli. Reissner's membrane — distended in hydropic cochleas — had a normal appearance throughout the cochlea. The same holds true for the stria vascularis in both experimental groups. Light microscopic evaluation of the endolymphatic sac and its direct vicinity did not reveal any differences between the controls and the CAg2 and CAg6 animals. The endolymphatic sac lumen of each animal was filled with its normal contents: a colloid precipitate with some macrophages and leukocytes.

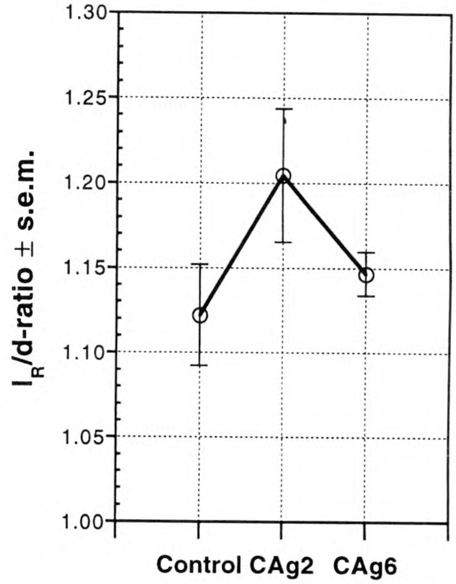

Fig 2. Ratio *l*R/*d*, indicative of size of hydrops, for experimental groups CAg2 and CAg6 (crude inner ear antigen groups, evaluated at 2 weeks and 6 weeks, respectively) and control group averaged over first and second cochlear turns.

Morphometry. The morphometric data of the right and left ears have been analyzed for the 2 basal half-turns and the next 2 half-turns of the first middle cochlear turn. Subjective evaluation of the onset of endolymphatic hydrops corresponds to about *l*R/*d* = 1.15 when considering this basal part of the cochlea. The ANOVA showed no significant differences between the right and left ears. The mean *l*R/*d* values and standard errors of the mean (SEM) of the 2 experimental groups (CAg2 and CAg6) and the control group are presented in Fig 2. Analysis of the *l*R/*d* data shows a p level of only .08 for the treatment

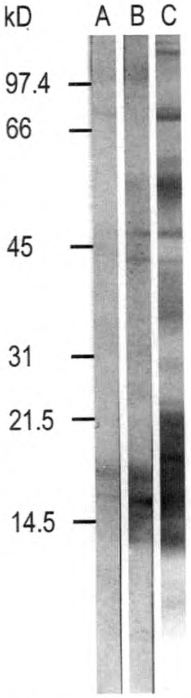

Fig 3. Western blot profile of sera 2 weeks (CAg2 group, lanes A and B) and 6 weeks (CAg6 group, lane C) after systemic immunization with swine inner ear proteins in complete Freund's adjuvant. Numbers on left side represent positions of protein molecular weight standards.

effect. Nevertheless, the results in Fig 2 suggest that systemic immunization with pig inner ear antigen may evoke a hydrops after 2 weeks, whereas the degree of hydrops seems to diminish 6 weeks after immunization.

Immunoblotting. Two weeks after immunization (CAg2 group), Western blot analysis of the serum of every individual animal showed a weak pattern of positive bands. These bands included those with molecular weights of 68, 50, and 45 kd. The 27 kd band was not apparent. Six weeks after antigen administration (CAg6 group), several strongly positive bands were seen. These included the 68, 50, 45, and 27 kd molecular weights (Fig 3). All animals of the control group had a negative immunoassay.

Electrocochleography. The mean CAP amplitude and SEM as a function of stimulus level and frequency for both the CAg2 group and CAg6 group are shown in Fig 4. In each panel the results for the CAg2 and CAg6 groups are compared to the results for the same control group. The CAP amplitude is suppressed at all stimulus frequencies and levels in both experimental groups. However, the effect is more pronounced at the lower stimulus levels. The ANOVA shows a significant interaction between the main effects of immunization and stimulus level when all stimulus levels are included in the analysis. The larger effect at low stimulus levels reflected in the statistical interaction resembles the psychophysically defined phenomenon of "recruitment." Because of the interaction, the significance of CAP amplitude suppression has been tested exclusively for the lower 5 stimulus levels. The significance level is indicated in each panel. Comparison of the results of the 2- and 6-week groups indicates progression of the suppressing effect of immunization on the CAP. In the 6-week group, the main effect of immunization proves to be significant at all 3 frequencies, while this is the case at 2 and 8 kHz only in the 2-week group. The results of tests on possible differences between the right and left ears, which was one of the within-subject variables in the ANOVA, are all negative.

Figure 5 depicts the SP results. The mean SP is always negative at the stimulus frequencies applied, as is typical for measurements of the SP at the apex of the cochlea. The SP in the immunized animals tends to be larger at all frequencies, especially at the higher stimulus levels. Indeed, the ANOVA shows a significant interaction between the effects of immunization and stimulus level at both posttreatment intervals and the 3 stimulus frequencies. Therefore, the statistical significance of SP enhancement has been assessed for the highest 5 stimulus levels. The SP enhancement is significant, except for the 2-kHz data measured 2 weeks after immunization ($p = .30$) and for the 8-kHz data measured 6 weeks after immunization ($p = .09$). The effect of immunization on the SP evoked by 2-kHz stimuli may have increased during the study period from 2 to 6 weeks, suggesting progression of the effect. There are no significant differences between the right and left ears. As to CM, there are no significant differences between immunized and control animals.

Relationship Between Morphometry and Electrocochleography. In order to further examine the relation between endolymphatic hydrops and changes in the SP, we present scatter plots of the SP amplitudes and the morphometric *l*R/*d* values in Fig 6 for the experimental and control ears. The SP data relate to the 4-kHz stimulus (the frequency at which we found the largest effects) and are values averaged over the highest 5 levels. As before, the *l*R/*d* ratio relates to the values averaged over the basal cochlear turn and the basal part of the middle cochlear turn. For the control ears, Fig 6B shows that almost all data lie evenly scattered within the region bordered by *l*R/*d* = 1.15 and SP = −100 μV. For the experimental ears, Fig 6A shows only a few scattered data lying in the region bordered by *l*R/*d* = 1.15 and SP = −100 μV and a greater number of outliers. The data of Fig 6A show no obvious overall correlation between endolymphatic hydrops (high *l*R/*d* values) and SP en-

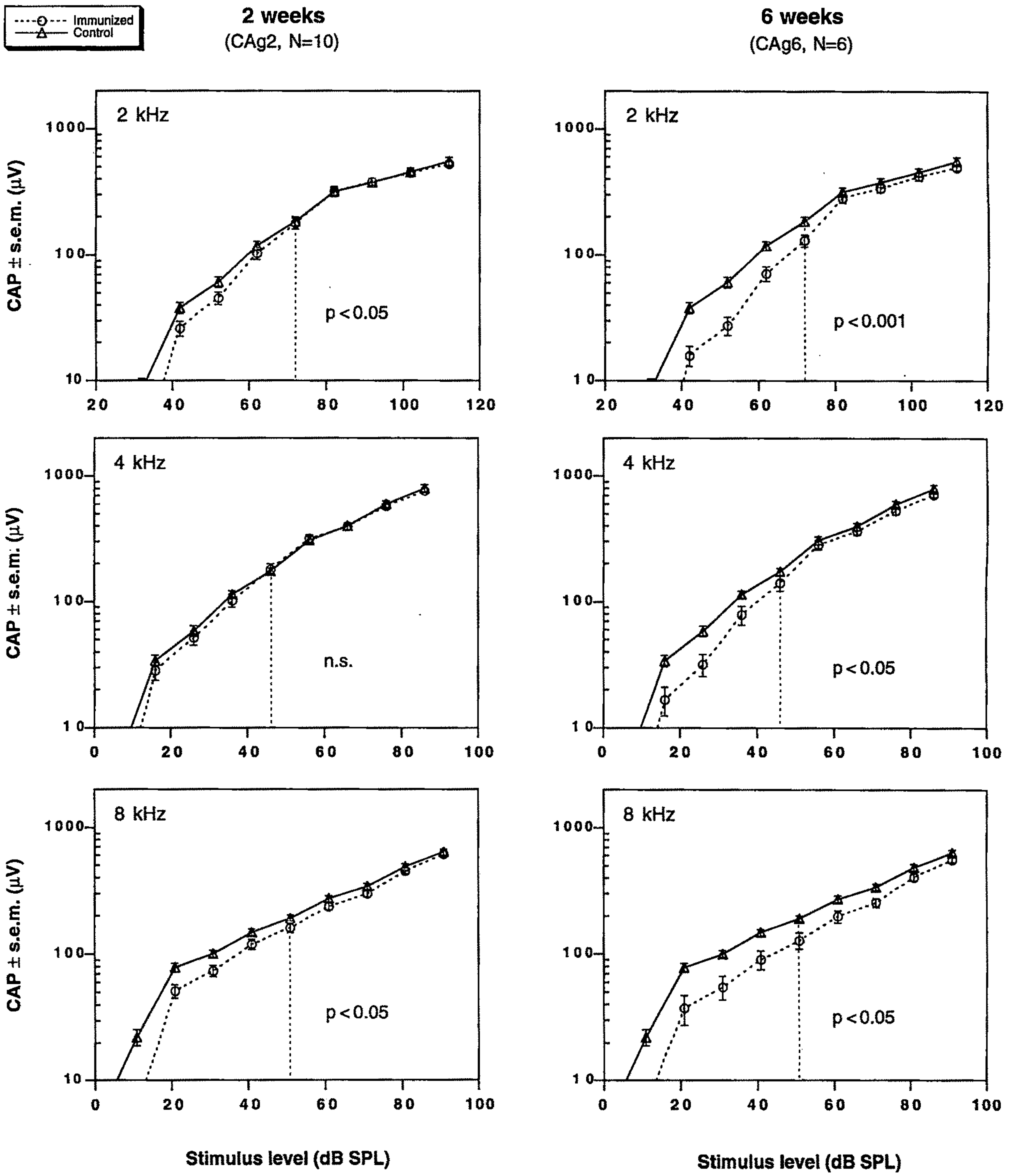

Fig 4. Compound action potential (CAP) input-output curves for 2-, 4-, and 8-kHz probe tone bursts 2 and 6 weeks after systemic immunization with swine inner ear antigen in complete Freund's adjuvant. Mean and standard error of mean (s.e.m.) are shown at each level of stimulation. Circles and dashed lines represent left and right ears of immunized animals (N = 10 and 6 animals, respectively). Triangles and solid lines represent left and right ears of control animals (N = 6 animals).

hancement (r = .33). However, this correlation is higher if we look at only the CAg2 data (r = .58), and it disappears completely 6 weeks after the immunization (CAg6, r = .08). As mentioned earlier, it seems that the degree of endolymphatic hydrops 6 weeks after immunization (CAg6 group) is somewhat less than that 2 weeks after immunization (CAg2 group). There are no obvious differences in SP at 4 kHz between the 2 groups CAg2 and CAg6.

Electron Microscopy. For ultrastructural evaluation, a selected group of experimental animals was

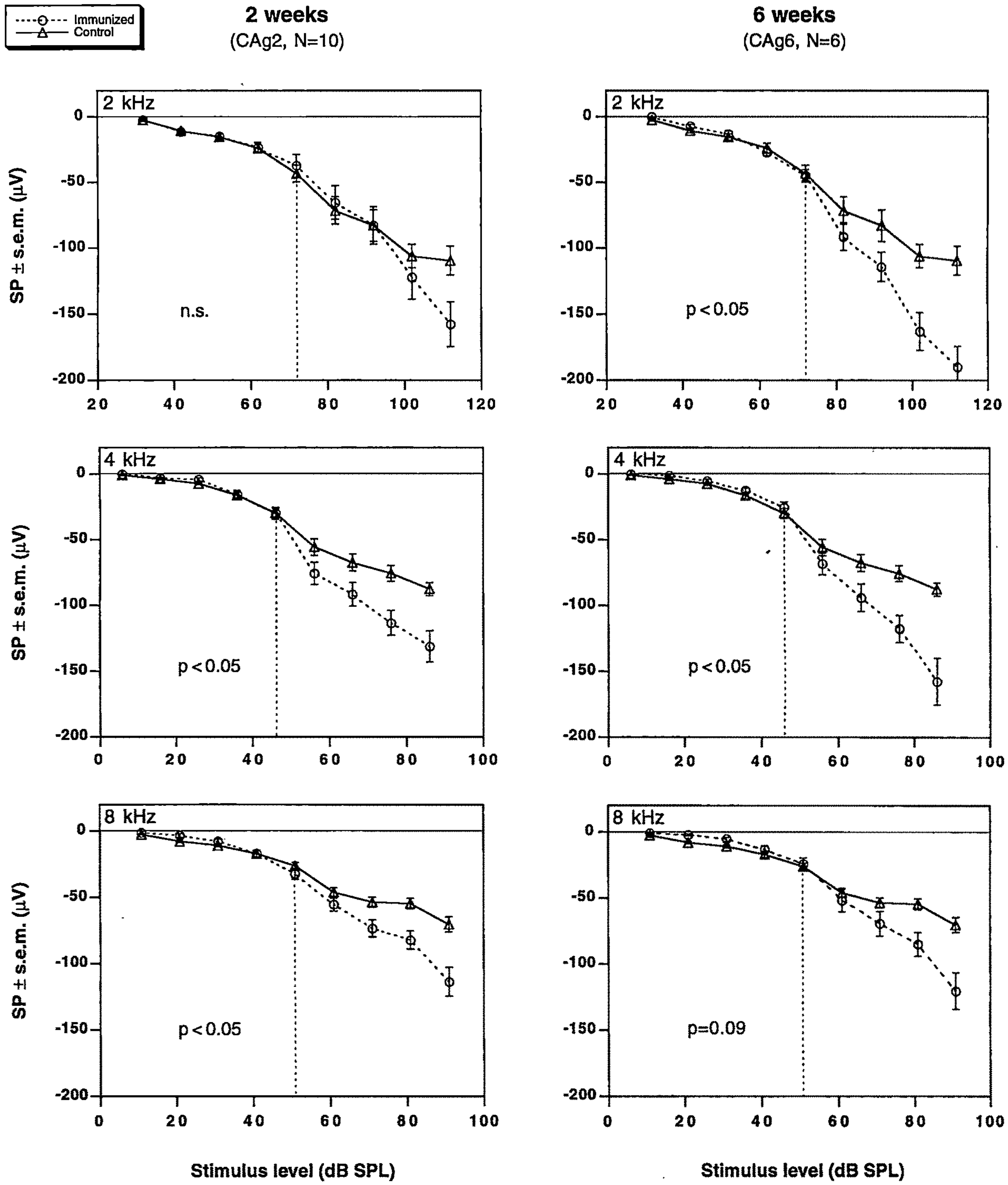

Fig 5. Summating potential (SP) input-output curves for 2-, 4-, and 8-kHz probe tone bursts 2 and 6 weeks after systemic immunization with swine inner ear antigen in complete Freund's adjuvant. Mean and s.e.m. are shown at each level of stimulation. Circles and dashed lines represent left and right ears of immunized animals (N = 10 and 6 animals, respectively). Triangles and solid lines represent left and right ears of control animals (N = 6 animals).

used in such a way that they included all 4 possible combinations of presence or absence of endolymphatic hydrops and presence or absence of an enhanced negative SP. Electron microscopic assessment was performed in a blind fashion with no information as to the electrophysiological or histophysiologic status of the individual animal. All animals showed a normal ultrastructure of the organ of Corti (Fig 7) and the spiral ganglion. There were no signs of electron-dense perivascular depositions (which might indicate deposition of immune complexes or immunoglobulins) in the stria vascularis (Fig 8). Cellular infiltrates were never observed in the cochlea. No morphological differences were obvious between the hy-

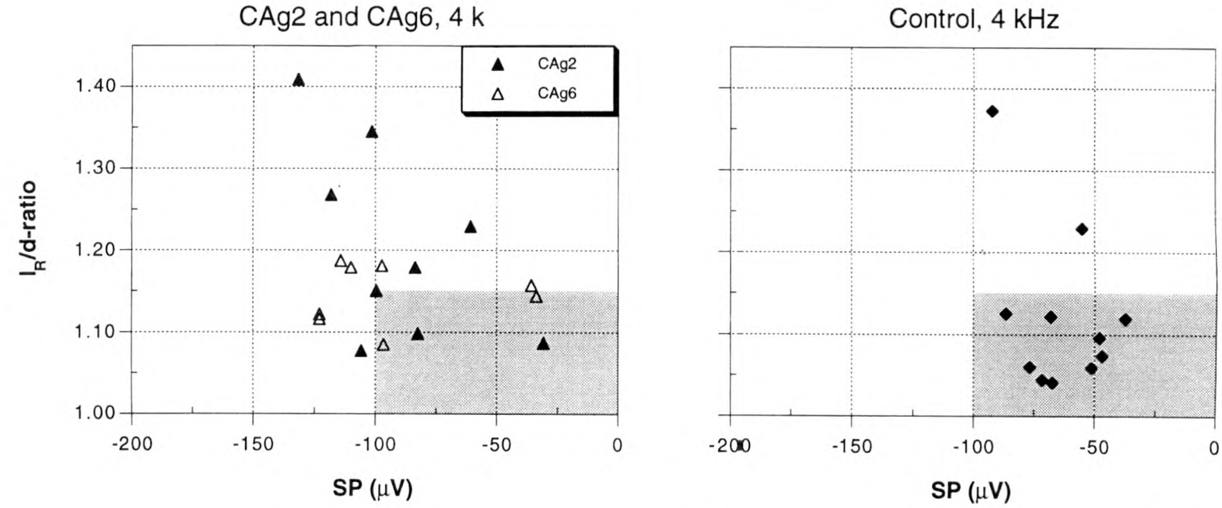

Fig 6. A) Scatter plot of mean amplitude of negative SP for highest 5 stimulus levels at 4-kHz probe tone bursts and calculated mean *I*R/*d* ratio of basal and first middle cochlear turns in each individual animal 2 and 6 weeks after systemic immunization with swine inner ear antigen in complete Freund's adjuvant. B) Control animals. Right and left ears are pooled; shadowed area represents "normal" area.

dropic and nonhydropic ears 2 and 6 weeks after subcutaneous injection of the antigen, irrespective of whether they showed concomitant changes in the SP.

The ultrastructural morphology of the endolymphatic sac and its direct vicinity was not different from that of control animals, either 2 or 6 weeks after treatment. There were no electron-dense depositions in the subepithelial stroma or epithelial lining of the endolymphatic sac (Fig 9), nor was an increase observed in the number of lymphocytes, macrophages, or plasma cells — usually found in this area.

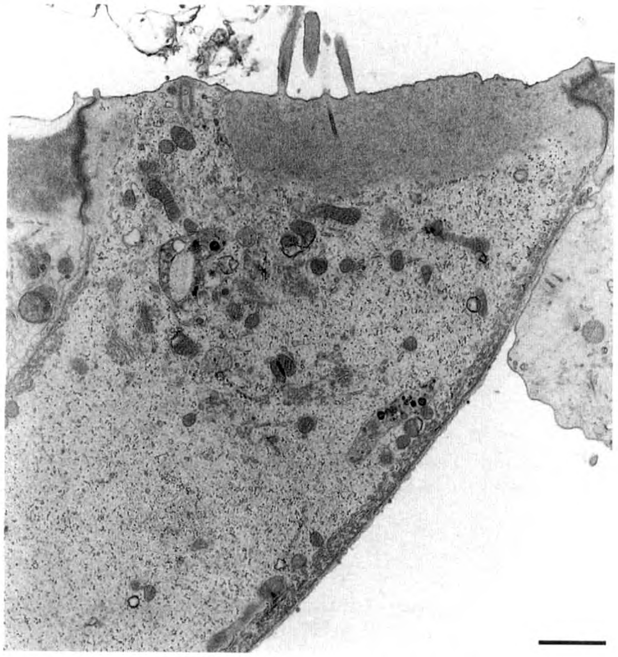

Fig 7. Electron micrograph of outer hair cell from cochlea systemically immunized with swine inner ear antigens. Outer hair cell has normal appearance. Bar — 1 μm.

DISCUSSION

Although not statistically significant at the 5% level, the data suggest that a single injection with swine inner ear antigen in CFA may evoke a hydrops after 2 weeks, whereas the degree of hydrops seems to diminish 6 weeks after immunization. Western blot analyses showed a strongly positive banding at molecular weights of 68, 50, 45, and 27 kd after 6 weeks.

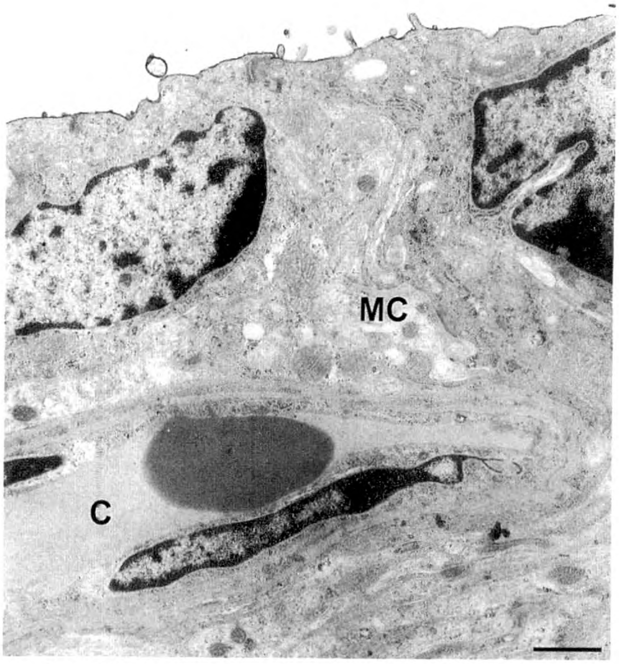

Fig 8. Electron micrographic detail of stria vascularis after systemic immunization with swine inner ear antigen. Marginal cells (MC) have normal appearance, and capillary vessels (C) do not demonstrate any signs of deposits or thickening of basement membrane. Bar — 1 μm.

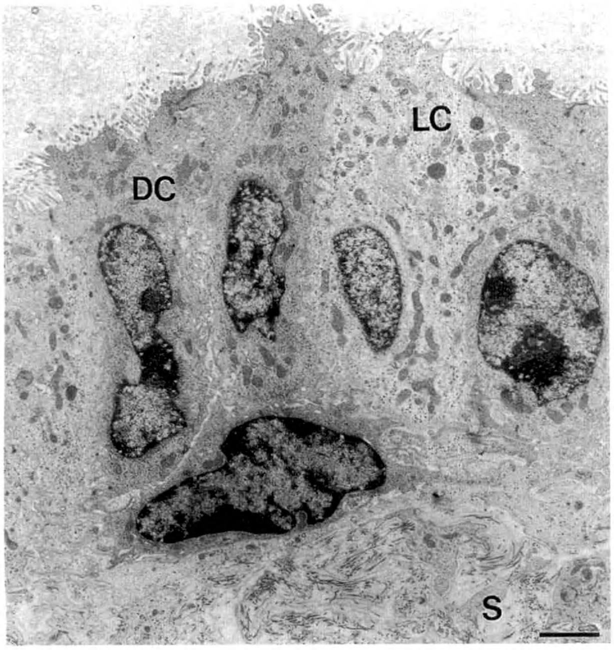

Fig 9. Electron micrographic view of epithelial lining containing light cells (LC) and dark cells (DC) and subepithelial stroma (S) of intermediate part of endolymphatic sac after systemic immunization. Bar — 2 µm.

This is the same spectrum of cross-reacting antibodies thought to be instrumental in immune-mediated SNHL in patients.[5,8] Tissue injury, mediated through a humoral autoimmune response, expresses itself by the effect of activation of the complement cascade, which may lead to direct cytolysis of cellular constituents and the production of biologically active fragments capable of enhancing vascular permeability and attraction of mononuclear and polynuclear cell infiltrates. The same holds for certain forms of autoimmune SNHL in humans.[4] In this experimental autoimmune model, neither a vasculitis nor a mononuclear or polynuclear cell infiltrate was observed in the inner ear. Further, the endolymphatic sac, considered to play a key role in the local inner ear immune defense system, had a normal appearance. Thus, the sequelae in this systemic immunization experiment are not expressed in obvious structural lesions of the inner ear, at least within the observation period of 6 weeks.

However, the electrophysiological changes are quite evident. They are 1) a relatively early and progressive suppression of the CAP at all tested frequencies at the lower stimulus levels; 2) an enhancement of the negative SP at all tested frequencies; and 3) an absence of any significant effect upon the CM. This latter observation is in agreement with the histologic observation that outer hair cell loss is not present up to 6 weeks after treatment. Augmentation of the immune response by boosting the animals with antigen in incomplete Freund's adjuvant only slightly potentiates the observed enhancement of the negative SP (additional experiment, data not shown). The observed CAP and SP may change under various experimental conditions. In the classic "obstruction of endolymph resorption" model (obliteration of the endolymphatic sac and obstruction of the endolymphatic duct in the guinea pig), the time and frequency dependences of the electrophysiological changes during development of endolymphatic hydrops have been inexplicably variable.[14,15,18] The observed electrophysiological changes are generally assumed to be directly related to endolymphatic hydrops and the initial structural changes in the inner ear sensory epithelia. We suggest that pressure buildup in the endolymphatic compartment, in particular, is the determining factor for the observed early electrophysiological changes. It is thought to lead to a deviant operating point of the cochlear mechanoelectrical transduction system, resulting in displacement of the basilar membrane toward the scala tympani. The correlation between an increase in SP and displacement of the basilar membrane toward the scala tympani has been well documented.[19,20]

In recent inner ear immune response models, large threshold elevations of the CAP and CM recorded at the round window (40 to 60 dB in all tested animals; 2 to 4 weeks after perilymphatic antigen rechallenge with keyhole limpet hemocyanin) appeared to be directly related to the extent of immune-mediated cochlear injury, without evidence of endolymphatic hydrops.[21] Less-dramatic threshold elevations of the CAP without CM threshold shifts (20 to 60 dB in 32% of the tested animals; recorded at the round window 2 to 3 months after repeated systemic immunization with bovine inner ear antigens), however, did not clearly show a correlation to the extent of cochlear disease. The organ of Corti and stria vascularis appeared normal. Also, endolymphatic hydrops was not observed.[12] A slight mean threshold elevation of auditory brain stem recordings, already present at day 7 after a single immunization with bovine inner ear antigen in CFA (maximum 9.7 ± 6.4 dB; day 14), was mainly reflected by a cellular infiltrate in the scala tympani at days 7 to 14, together with occasional scattered spiral ganglion cell degeneration.[22] Four weeks after antigen challenge, the cellular infiltrate resolved, but the hearing threshold did not completely recover. Endolymphatic hydrops was, again, not observed.

Our recent experiments demonstrate that a nonspecific cellular infiltrate in the perisaccular region, elicited through deposition of sepharose beads with or without immune complexes,[17] and a specific experimental autoimmune antibody response against swine inner ear antigen can both induce slight electrophysiological changes, comparable to those found in the early stages of the classic "obstruction of endolymph resorption" model. However, we have not found an evident correlation between observed SP changes and the presence of endolymphatic hydrops (Fig 6A). Also, there are no obvious cochlear disorders observed at either a light or an electron microscopic level. Apparently, specific cell-mediated immunity is not instrumental in this animal model. Application of a single injection of a mixture of swine inner ear proteins with CFA certainly induces both a humoral and a cellular immune response. Because cytolytic effects on cochlear epithelia are not seen, it is possible that both cross-reacting antibodies directed against certain epitopes of the inner ear and/or release of biochemical mediators disturb the cochlear biochemical homeostasis, subsequently leading to the measured CAP and SP changes with or without the development of an endolymphatic hydrops. Alternatively, according to the basilar membrane displacement theory, in cases in which hydrops is present without enhancement of the negative SP, it is possible that a new cochlear homeostasis has already been established, in which the basilar membrane has returned to its original position. In this way, enhancement of the negative SP without endolymphatic hydrops would indicate that endolymphatic pressure builds up before distention of Reissner's membrane is histologically obvious. Both mechanisms might operate simultaneously. The present observations indicate that early identification of immune-mediated SNHL, that is, before actual (subcellular) degeneration of cochlear epithelia starts, is critical in order to preserve or restore inner ear function in these patients through immunosuppressive therapy. It remains to be determined at which level the homeostasis is disturbed in the cochlea and which one or more of the antibodies and/or biochemical mediators are responsible for the observed functional changes.

REFERENCES

1. Veldman JE. Review. Immune-mediated sensorineural hearing loss. Auris Nasus Larynx 1998;25:309-17.
2. Hughes GB, Barna BP, Kinney SE, Calabrese LH, Nalepa NJ. Clinical diagnosis of immune inner-ear disease. Laryngoscope 1988;98:251-3.
3. Harris JP, Sharp PA. Inner ear autoantibodies in patients with rapidly progressive sensorineural hearing loss. Laryngoscope 1990;100:516-24.
4. Veldman JE. Pharmacological treatment of immune-mediated inner ear disorders. A clinical immunology and audiology survey. Scand Audiol Suppl 1986(suppl 26):21-6.
5. Veldman JE, Hanada T, Meeuwsen F. Diagnostic and therapeutic dilemmas in rapidly progressive sensorineural hearing loss and sudden deafness. Acta Otolaryngol (Stockh) 1993; 113:303-6.
6. Yamanobe S, Harris JP. Inner ear–specific autoantibodies. Laryngoscope 1993;103:319-25.
7. Mosciscki RA, San Martin JE, Quintero C, Rauch SD, Nadol JB, Bloch KJ. Serum antibody to inner ear proteins in patients with progressive hearing loss. JAMA 1994;272:611-6.
8. Cao MY, Deggouj N, Gersdorff M, Tomasi J-P. Guinea pig inner ear antigens: extraction and application to the study of human autoimmune inner ear disease. Laryngoscope 1996; 106:207-12.
9. Beickert P. Zur Frage der Empfindungsschwerhörigkeit und Autoallergie. Z Laryngol 1961;54:837-42.
10. Terrayama Y, Sasaki Y. Studies on experimental allergic (isoimmune) labyrinthitis in guinea pig. Acta Otolaryngol (Stockh) 1963;58:49-64.
11. Harada T, Matsunaga T, Hong K, Inoue K. Endolymphatic hydrops and type III allergic reaction. Acta Otolaryngol (Stockh) 1984;97:450-9.
12. Harris JP. Experimental autoimmune sensorineural hearing loss. Laryngoscope 1987;97:63-76.
13. Orozco CR, Niparko JK, Richardson BC, Dolan DF, Ptok MU, Altschuler RA. Experimental model of immune-mediated hearing loss using cross-species immunization. Laryngoscope 1990;100:941-7.
14. Horner KC, Cazals Y. Rapidly fluctuating thresholds at the onset of experimentally-induced hydrops in the guinea pig. Hear Res 1986;26:319-25.
15. Van Deelen GW, Ruding PRJW, Veldman JE, Huizing EH, Smoorenburg GF. Electrocochleographic study of experimentally induced endolymphatic hydrops. Arch Otorhinolaryngol 1987;244:167-73.
16. Bjerrum OJ, Schafer-Nielsen C. Buffer systems and transfer parameters for semi-dry electroblotting with a horizontal apparatus. In: Dunn MJ, ed. Electrophoresis '86. Weinheim, Germany: VCH, 1986:315-27.
17. Bouman H, Klis SFL, De Groot JCMJ, Smoorenburg GF, Huizing EH, Veldman JE. Induction of an immune-mediated endolymphatic hydrops by perisaccular deposition of sepharose beads with and without immune complexes. Hear Res 1998;117: 119-30.
18. Kumagami H, Miyazaki M. Chronological changes of electrocochleogram in experimental endolymphatic hydrops. ORL 1983;45:143-53.
19. Durrant JD, Dallos P. Modification of DIF-summating potential components by stimulus biasing. J Acoust Soc Am 1974;56:562-70.
20. Klis JFL, Smoorenburg GF. Modulation at the guinea pig round window of summating potentials and compound action potentials by low-frequency sound. Hear Res 1985;20:15-23.
21. Woolf NK, Harris JP. Cochlear pathophysiology associated with inner ear immune responses. Acta Otolaryngol (Stockh) 1986;102:353-64.
22. Yamanobe S, Harris JP. Spontaneous remission in experimental autoimmune labyrinthitis. Ann Otol Rhinol Laryngol 1992;101:1007-14.

CELLULAR DISTRIBUTION OF MUCOSA-ASSOCIATED LYMPHOID TISSUE WITH OTITIS MEDIA IN CHILDREN

MASAMI KAMIMURA, MD, DMSC
SAPPORO, JAPAN

CAREY D. BALABAN, PHD
PITTSBURGH, PENNSYLVANIA

ISAMU SANDO, MD, DMSC
PITTSBURGH, PENNSYLVANIA

TETSUYA GANBO, MD, DMSC
TOKYO, JAPAN

CHIAKI SUZUKI, MD, DMSC
FUKUSHIMA, JAPAN

This study examined mucosa-associated lymphoid tissue (MALT) in the eustachian tube (ET), middle ear (ME), and mastoid antrum (MA) in 163 celloidin-embedded temporal bones from children with or without otitis media. Otitis media was defined by the presence of histopathologically identified inflammatory cell infiltration in the mucosa or cavity of the ME. We found MALT in the ET in 30 cases (46.2%), in the ME in 19 cases (29.2%), and in the MA in 4 cases (6.2%) out of 65 cases of otitis media, and in the ET in 7 (7.1%), in the ME in 0, and in the MA in 0 out of 98 specimens without otitis media. No MALT appeared in any children under the age of 1 month. Immunohistochemical methods were used to investigate MALT in 12 horizontally cut temporal bones with OM. The follicular area contained OPD4-positive (helper-inducer T) cells and a few CD8-positive (cytotoxic and suppressor T) cells, whereas the parafollicular area contained OPD4-positive and CD8-positive T cells. CD57-positive (natural killer) cells were confined to the germinal center. CD30-positive (activated T and B) cells were observed throughout the follicles. A few CD15-positive (granulocyte, monocyte) cells were found in the follicles. Histopathologic and immunohistochemical findings were indistinguishable for MALT in the ET, ME, and MA. Our results suggest that MALT may be a mechanism for producing a rapid and massive local immune reaction to repeated bacterial infections via the ET.

KEY WORDS — immunohistochemistry, mucosa-associated lymphoid tissue, otitis media, temporal bone.

INTRODUCTION

In patients with otitis media (OM), inflammatory cells are observed in the mucosa and the fluid in the lumen of the middle ear (ME). Further, it is known that mucosa-associated lymphoid tissue (MALT) is present in the ME mucosa of children with OM.[1,2] For example, van der Baan et al[2] reported that MALT was found in 18 of 21 (86%) biopsy cases of ME mucosa of children with OM, and Matsune et al[1] found that MALT was present in the eustachian tube (ET) in 9 (64%) and in the ME in 3 of 14 (21%) children with OM.

Mucosa-associated lymphoid tissue has been reported in a variety of tissues.[1-8] It is characterized histologically by rounded aggregations of lymphocytes in the lamina propria, usually with a germinal center. The number and size of lymphoid follicles vary among tissues. These follicles are divided typically into 3 regions in hematoxylin and eosin (H & E)–stained sections: follicular area, parafollicular area, and germinal center (if present). The follicular area is defined as a darkly staining region of densely packed lymphocytes. The parafollicular area surrounds the follicular area; it contains many endothelial cells from venules. The germinal center is defined as the lightly stained center of the lymphoid follicle. Immunohistochemical studies have examined lymphocyte subsets in MALT from nasal,[3] bronchial,[4,5] gut,[6,7] and laryngeal tissues.[8] These studies all found a similar distribution of lymphocyte subsets. The follicular area consisted of B cells and a few T cells. The parafollicular area consisted of cytotoxic-suppressor T cells, helper-inducer T cells, and a few B cells. The germinal center consisted of B cells and helper-inducer T cells. However, relatively little is known about the structure and cellular distribution of different lymphocyte subsets in MALT within the ET, ME, and mastoid antrum (MA).

This study is a histopathologic and immunohistochemical investigation of the presence and morphology of MALT in the submucosa of the ET, ME, and MA in children who have OM. This is the first study

---

From the Elizabeth McCullough Knowles Otopathology Laboratory, Division of Otopathology, Department of Otolaryngology, University of Pittsburgh School of Medicine, Pittsburgh, Pennsylvania. Dr Kamimura is currently in the Department of Otolaryngology, Sapporo Medical University, Sapporo, Japan. This study was supported by National Institutes of Health Research Grant 2R01DC00123-19A2 from the National Institute on Deafness and Other Communication Disorders.

Presented at the Association for Research in Otolaryngology Midwinter Research Meeting, St Petersburg, Florida, February 14-19, 1998.

CORRESPONDENCE — Isamu Sando, MD, DMSc, Division of Otopathology, Dept of Otolaryngology, University of Pittsburgh School of Medicine, Eye and Ear Institute Building, Suite 153, 203 Lothrop St, Pittsburgh, PA 15213.

TABLE 1. PRIMARY MONOCLONAL ANTIBODIES USED IN IMMUNOHISTOCHEMISTRY

Monoclonal Antibody	*Specificity*	*Dilution*	*Source*	*Clone*
CD8	Cytotoxic-suppressor T cells	1:50	Dako, Carpinteria, Calif	C8/144B
OPD4	Helper-inducer T cells	1:35	Dako, Carpinteria, Calif	OPD4
CD57	Natural killer (NK) cells	1:50	Zymed, South San Francisco, Calif	NK-1
CD30	Activated T and B cells	1:50	Pharmingen, San Diego, Calif	BerH8
CD15	Granulocytes and monocytes	1:50	Pharmingen, San Diego, Calif	HI98

to investigate the subsets of lymphocytes, monocytes, granulocytes, and natural killer cells in the various subdivisions of MALT by means of celloidin-embedded temporal bone sections.

MATERIALS AND METHODS

Temporal Bone Sections. The presence of MALT in the ET, ME, and MA was investigated with 163 (95 horizontally cut, 68 vertically cut) celloidin-embedded temporal bone–ET specimens obtained from children ranging in age from 1 day to 12 years (mean, 2.3 years). Evidence of OM was defined as the presence of histopathologically confirmed inflammatory cell infiltration into the ME mucosa or ME cavity. This histopathologic definition of OM clearly includes cases of clinically diagnosed OM.[2,9] It also includes cases of "silent OM," which have histopathologic evidence of ME inflammation but no clinical signs such as otorrhea or perforation.[10] It excludes cases with evidence of inflammation of the ET mucosa, but no inflammation of the ME or MA mucosa. We defined normal (non-OM) cases by the absence of histopathologically identified inflammatory cell infiltration in the ME mucosa and ME cavity. For example, a specimen with inflammation of the ET only would be a normal (non-OM) case. Clinical records were consistent with the assumption that these normal (non-OM) cases did not have a history of recurrent OM. Thirty temporal bone–ET specimens obtained from cases with OM and MALT were investigated histopathologically for the presence of MALT in the ET, ME, and MA. Twelve horizontally sectioned specimens were selected for immunostaining so that the distribution of immunopositive cells in MALT from the ET, ME, and MA could be compared in the same section. Specimens obtained at autopsy were fixed in 10% formalin, decalcified by 5% trichloroacetic acid, and embedded in celloidin. Sections of 30-μm thickness were prepared from tissue blocks. Every 10th or 20th section was stained routinely with H & E[11] for histopathologic analysis. Some of the remaining unstained sections were stained through the ET, ME, and MA for immunohistochemical analysis. These sections were preserved in 80% ethanol for 5 to 29 years previous to our immunohistochemical study.

Immunohistochemistry. Immunohistochemical methods were used to investigate the 12 horizontally sectioned cases with OM and MALT (6 male and 6 female cases, ranging in age from 2 months to 72 months with a mean of 14.9 months). Unstained temporal bone–ET sections were soaked in distilled water for 60 minutes and then mounted on gelatin-coated slide glasses. A few drops of poly-L-lysine (Sigma, St Louis, Mo) were placed on the slide, and the sections were dried. The sections were then soaked in the antigen retrieval solution — saturated sodium hydroxide (NaOH)–methanol (75 g NaOH dissolved in 500 mL of methanol in a brown glass bottle for 1 to 2 weeks) in methanol at a ratio of 1:3 — for 30 minutes.[12] The sections were rinsed twice in 100% methanol, 70% methanol, and phosphate buffered saline (PBS), respectively. Microwave antigen recovery incubation with 10-mmol/L sodium citrate (Sigma) buffer (pH 6.0) was also performed for 5 minutes at 60°C for OPD4 (helper-inducer T cells), CD8 (cytotoxic-suppressor T cells), CD15 (granulocytes, monocytes), and CD57 (natural killer cells). The primary antibodies are listed in Table 1. These antibodies are all directed against epitopes that are resistant to 10% formalin fixation and are used in clinical laboratories for pathological studies of paraffin-embedded human tissues. Other studies[12,13] have shown that 10% formalin fixation does not preclude immunohistochemical analysis of decalcified, celloidin-embedded sections of human tissues.

For CD57 immunohistochemical analysis, sections were also treated with 0.1% trypsin solution (pH 7.8, Sigma) in 0.1% calcium chloride (Sigma) for 5 minutes at 37°C.[13] Endogenous peroxidase was blocked by incubation with 3% hydrogen peroxide for 10 minutes, and nonspecific binding was also inhibited by incubation with a blocking solution containing 2% nonfat dry milk, 2% normal goat serum, and 0.5% Triton X-100 (Sigma) for 10 minutes. The sections were first incubated with the primary antibody overnight. Primary antibodies were diluted with PBS including 1% bovine serum albumin (BSA) and 0.5% Triton X-100. Secondary biotinylated antibodies (goat anti-mouse IgG and IgM; heavy and light chains, Jackson ImmunoResearch Laboratories, Inc, West Grove, Pa) were applied to the sections for 1.5 hours.

TABLE 2. CO-OCCURRENCE OF MALT AND OTITIS MEDIA IN CHILDREN

	MALT in ET	*MALT in ME*	*MALT in MA*
OM (ME inflammation)	30/65 (46.2%)*[a]	19/65 (29.2%)*[b]	4/65 (6.2%)
Non-OM (no ME inflammation)	7/98 (7.1%)	0/98 (0%)	0/98 (0%)

MALT — mucosa-associated lymphoid tissue, ET — eustachian tube, ME — middle ear, MA — mastoid antrum, OM — otitis media.

*p < .01 versus non-OM (Fisher's exact test); a versus b, p < .05 (Fisher's exact test).

Sections were then processed with the avidin-biotin-peroxidase complex technique (ABC; Vector Laboratories Inc, Burlingame, Calif) for 1 hour. The color was developed with 0.05% 3,3'diaminobenzidine tetrahydrochloride in 4% sodium acetate, plus 0.03% hydrogen peroxide. Sections were dehydrated through a graded series of ethanol (70%, 80%, 95%, and 100%), then immersed in xylene and coverslipped with Permount (Fisher Scientific, Fair Lawn, NJ).

We used "Negative Control Sera/Immunoglobulins" (BioGenex, San Ramon, Calif) instead of primary antibodies as negative controls. Formalin-fixed, paraffin-embedded tonsil sections (BioGenex) served as positive controls. These paraffin-embedded tonsil sections were deparaffinized, treated with the citrate buffer antigen retrieval method (see below), and stained immunohistochemically with standard ABC methods (see below).

The presence of a single MALT in a series of every 10th or 20th section was scored as positive in each region. The differences in the presence of MALT in control versus OM specimens and with age were analyzed with Fisher's exact test.

RESULTS

Histopathologic Findings. The presence of MALT in the submucosa of the ET, ME, and MA was assessed in every 10th or 20th section, depending upon the staining performed originally on the archival series. The presence of MALT was more frequent in children with OM (Table 2). We found MALT in the ET in 30 (46.2%), in the ME in 19 (29.2%), and in the MA in 4 (6.2%) of 65 cases with OM and in the ET in 7 (7.1%), in the ME in 0, and in the MA in 0 of 98 specimens without OM. The presence of MALT was significantly more frequent in the ET and ME submucosae of specimens from children with OM than in non-OM specimens (Fisher's exact test, p < .01). There was also a spatial gradient in the frequency of observing MALT. In the cases with OM, there was a significantly greater frequency of occurrence of MALT in the ET than in the ME submucosa (Fisher's exact test, p < .05). All cases with MALT in the ME also showed MALT in the ET, and the 4 cases with MALT in the MA also displayed MALT in both the ME and ET (Table 3). The presence of MALT as a function of age at death is shown in Table 4; MALT did not appear in any children under the age of 1 month. The presence of MALT was significantly greater in children with OM at ages 1 to 2 years than those with OM at 1 to 12 months (Fisher's exact test,

TABLE 3. PRESENCE OF MALT IN 30 CASES WITH OM

Case	*Age*	*Sex*	*ET*	*ME*	*MA*
1	4 mo	M	*	*	*
2	5 mo	M	*	*	*
3	7 mo	M	*	*	*
4	1 mo	F	*	*	*
5	1 mo	F	*	*	
6	2 mo	M	*	*	
7	6 mo	F	*	*	
8	7 mo	F	*	*	
9	10 mo	F	*	*	
10	1 y	F	*	*	
11	1 y	F	*	*	
12	1 y	F	*	*	
13	1 y	F	*	*	
14	1 y	M	*	*	
15	2 y	F	*	*	
16	2 y	F	*	*	
17	2 y	F	*	*	
18	2 y	M	*	*	
19	6 y	M	*	*	
20	4 mo	M	*		
21	5 mo	M	*		
22	8 mo	F	*		
23	9 mo	M	*		
24	1 y	F	*		
25	1 y	F	*		
26	1 y	M	*		
27	2 y	M	*		
28	3 y	M	*		
29	5 y	F	*		
30	10 y	M	*		

*Presence of MALT.

TABLE 4. PRESENCE OF MALT IN ET AS FUNCTION OF AGE

	0-1 mo	*1-12 mo*	*1-2 y*	*3-6 y*	*7-12 y*
OM	0/8 (0%)	13/29 (44.8%)[a]	13/16 (81.3%)[b]	3/7 (42.9%)	1/5 (20.0%)
Non-OM	0/30 (0%)	2/20 (10.0%)	2/9 (22.2%)	2/22 (9.1%)	1/17 (5.9%)

a versus b, p < .01 (Fisher's exact test).

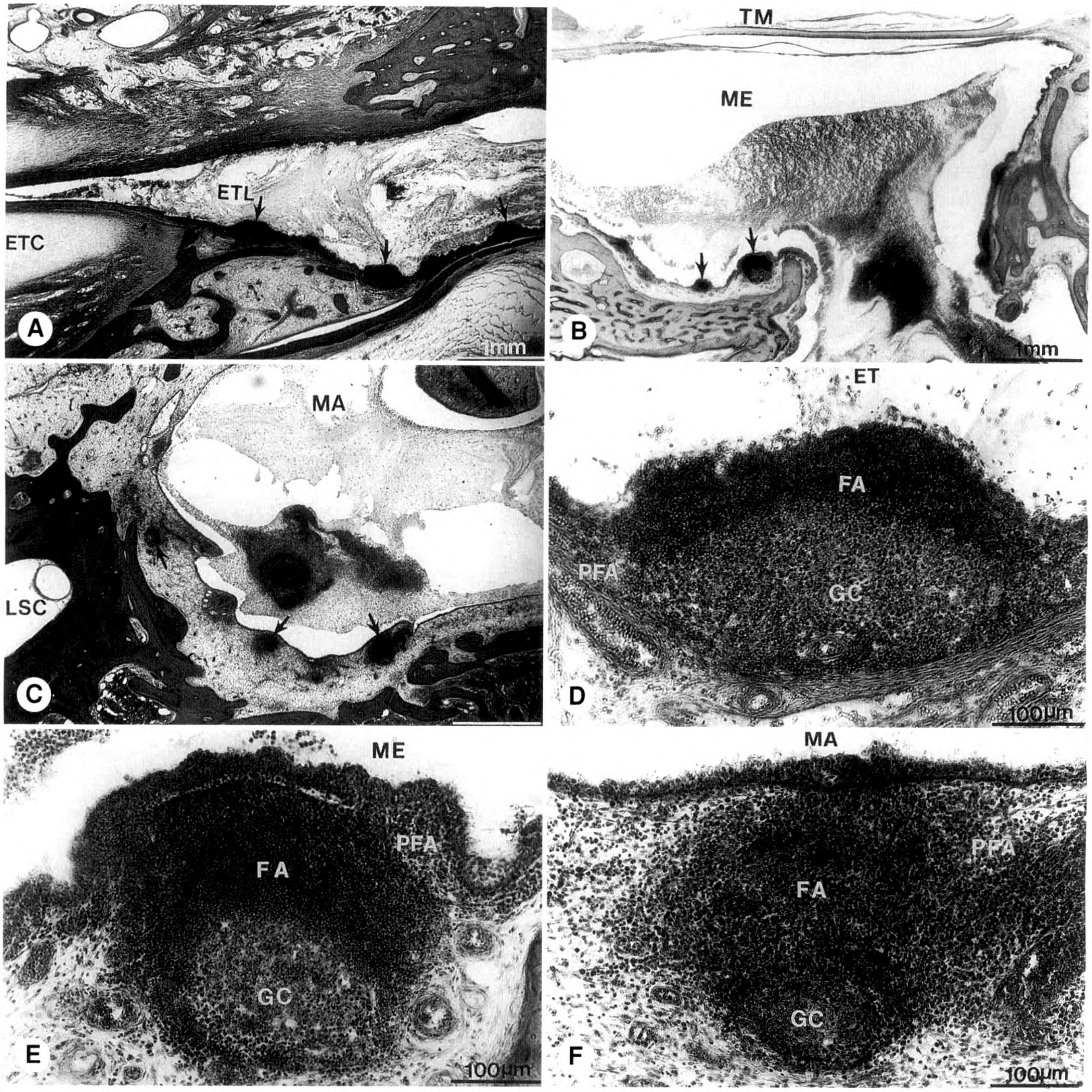

Fig 1. MALT follicles (arrows) in A) eustachian tube, B) middle ear, and C) mastoid air cells (H & E). D-F) High-power views of MALT shown in A-C. ET — eustachian tube; ETC — eustachian tube cartilage; ETL — eustachian tube lumen; FA — follicular area; GC — germinal center; LSC — lateral semicircular canal; MA — mastoid antrum; ME — middle ear cavity; PFA — parafollicular area; TM — tympanic membrane.

$p < .01$). Thereafter, the presence of MALT declined with age.

Distribution of Leukocytes in MALT. Many MALTs were observed in the ET, ME, and MA mucosae of H & E–stained sections (Fig 1A-C). Histopathologic and immunohistochemical findings were indistinguishable for MALT in the ET, ME, and MA. Three distinct cellular areas can be distinguished in MALT from H & E–stained sections: the follicular area, the germinal center, and the parafollicular area (Fig 1D-F). All MALTs, regardless of location, contained characteristic lymphocyte subsets. CD8-positive (cytotoxic-suppressor T) cells were associated predominantly in the parafollicular area and scattered in the follicular area, but were scarce in the germinal center (Fig 2A). OPD4-positive (helper-inducer T) cells were associated predominantly in the parafollicular area and scattered in the follicular area and the germinal center. By contrast, CD57-positive (natural killer) cells were confined to the germinal center (Fig 2B). CD30-positive (activated T and B) cells were observed throughout the follicular and parafollicular areas and germinal center (Fig 2C). CD15-positive

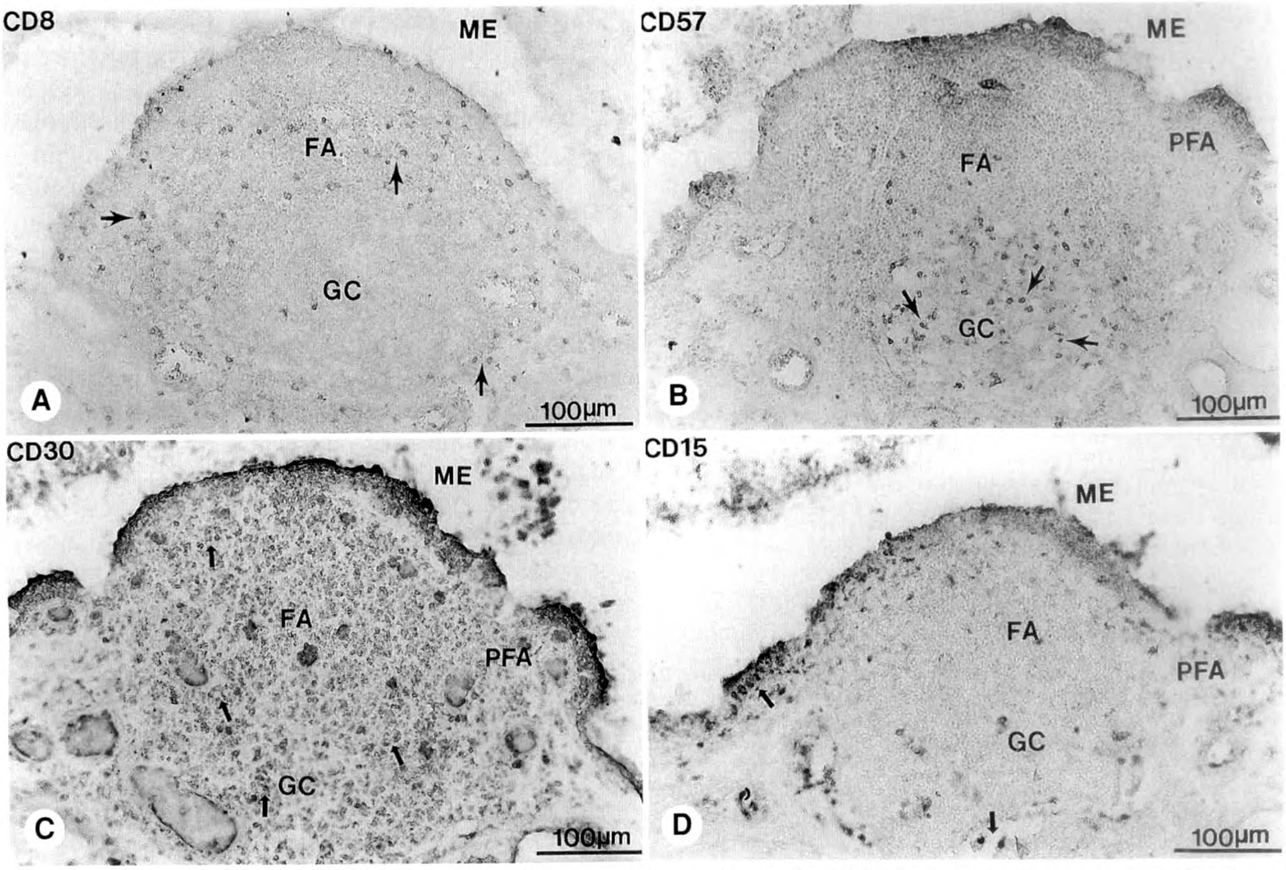

Fig 2. Immunohistochemically stained MALT follicles in middle ear (H & E). A) CD8-positive (cytotoxic-suppressor T) cells. B) CD57-positive (natural killer) cells. C) CD30-positive (activated T and B) cells. D) CD15-positive (granulocyte, monocyte) cells. Arrows — positive cells; FA — follicular area; GC — germinal center; ME — middle ear cavity; PFA — parafollicular area.

(granulocyte and monocyte) cells were absent in the lymphoid follicles, but were scattered within the mucosa in the parafollicular area (Fig 2D).

DISCUSSION

The location of MALT within the ET and ME in our 30 cases with OM confirmed findings of Matsune et al[1] from a smaller series of cases. Specifically, we confirmed that there is a significant association of MALT with OM in children and that MALT is present most frequently in the ET, less frequently in the ME, and rarely in the MA. All of our specimens with MALT in the ME had histopathologically defined OM, but only 19 of 65 cases with ME inflammation had MALT in the ME. All cases with MALT in the ME also displayed MALT in the ET (and 4 cases with MALT in the MA also had MALT in the ET and ME). As reported by Matsune et al,[1] the data suggest that MALT may form initially at the pharyngeal aspect of the ET. However, the origins of this lymphoid tissue, the factors influencing its initial formation, and the cellular processes that produce a widespread presence in the ME are unknown.

The presence of MALT in the ET varied with age. No MALT was observed in cases from the first postnatal month. The presence of MALT was high in cases with OM at ages 1 to 2 years, then declined with age. This peak in the presence of MALT corresponds with the time period when approximately 50% of infants have ME effusion lasting at least 4 weeks.[14] However, the frequency of observing MALT is reduced markedly after 7 years of age, when the incidence of OM is reduced.[15] These data, then, suggest that MALT proliferates in response to chronic ET and ME inflammation, then regresses.

It is assumed that a major function of MALT is closely associated with immunologic defense mechanisms. MALT appears to supply cells committed to the production of IgA.[5] The antigens that enter the MALT through the M cells are recognized by antigen-presenting cells in the lymphoepithelium, the germinal center, and the follicular area. After B cells recognize this antigen, B cells differentiate into surface IgA-expressing B cells. These cells leave the MALT through the surrounding lymph vessels and return to the MALT (homing) via the high endothelial venules from the systemic circulation. These cells then differentiate into antibody-producing cells under the control of helper or suppressor T cells.

Our study showed that the follicular area contained a few cytotoxic-suppressor T cells and helper-inducer T cells and that the parafollicular area contained cytotoxic-suppressor T cells and helper-inducer T cells. This distribution of lymphocyte subsets resembles that of MALT in sinus mucosa,[3] bronchus-associated lymphoid tissue (BALT),[4,5] gut-associated lymphoid tissue (GALT),[6,7] and larynx-associated lymphoid tissue (LALT).[8] It seems that there may be 2 different kinds of MALT. BALT,[16] LALT,[8] and MALT in the ET, ME, and MA are well developed in young children and regress later. In this group, respiratory infections are frequent and MALT is needed in the respiratory tract until mucosal immunity has been established there. On the other hand, GALT[6] is present well before birth and does not regress in later life.

Both the high frequency and occurrence of MALT in the ET and the similarities of lymphocyte populations in MALT and BALT are consistent with the role of the ET as a respiratory mucosa. The presence of MALT in the ET of infants also tends to be associated with rich mucosal folds of the ET[17] that strongly resemble bronchial mucosal folds and are thought to be important for clearance of the ET.[18,19] Two features of the presence of MALT in the ET, though, are potentially important. First, MALT is present most commonly in the pharyngeal half of the ET.[1] Second, all cases with MALT in the ME also have MALT in the ET. These findings indicate that MALT is associated with regions of the ET that 1) are encountered initially by bacteria entering the ET-ME space from the nasopharynx (and hence receive a relatively high exposure to these organisms) and 2) are exposed to cleared bacteria and bacterial debris in mucus moving toward the pharyngeal orifice. Hence, MALT may be a mechanism for producing a rapid and massive local immune reaction to repeated bacterial infections via the ET.

ACKNOWLEDGMENTS — The authors express deep gratitude to Eugene N. Myers, MD, Professor and Chairman of the Department of Otolaryngology, University of Pittsburgh School of Medicine, and Charles D. Bluestone, MD, Professor of Otolaryngology, University of Pittsburgh School of Medicine, and Director, Department of Pediatric Otolaryngology, Children's Hospital of Pittsburgh, for their encouragement to study this subject. We also thank Gloria J. Limetti, technician, for cutting celloidin sections and performing hematoxylin and eosin staining.

REFERENCES

1. Matsune S, Takahashi H, Sando I. Mucosa-associated lymphoid tissue in middle ear and eustachian tube in children. Int J Pediatr Otorhinolaryngol 1996;34:229-36.

2. van der Baan S, Seldenrijk CA, Henzen-Logmans SC, Drexhage HA. Serous otitis media and immunological reactions in the middle ear mucosa. Acta Otolaryngol (Stockh) 1988;106:428-34.

3. Tsurumaru H. Lymphoid follicle formation in sinus mucosa of chronic sinusitis. Nippon Jibiinkoka Gakkai Kaiho 1996;99:1662-75.

4. Sato A, Hayakawa H, Uchiyama H, Chida K. Cellular distribution of bronchus-associated lymphoid tissue in rheumatoid arthritis. Am J Respir Crit Care Med 1996;154:1903-7.

5. Sato A, Chida K, Iwata M, Hayakawa H. Study of bronchus-associated lymphoid tissue in patients with diffuse panbronchiolitis. Am Rev Respir Dis 1992;146:473-8.

6. Pabst R. The anatomical basis for the immune function of the gut. Anat Embryol (Berl) 1987;176:135-44.

7. Spencer JT, Finn T, Issacson PG. Gut associated lymphoid tissue: a morphological and immunocytochemical study of the human appendix. Gut 1985;26:672-9.

8. Kracke A, Hiller AS, Tschernig T, et al. Larynx-associated lymphoid tissue (LALT) in young children. Anat Rec 1997;248:413-20.

9. Palva T, Taskinen E. Inflammatory cells in chronic middle ear disease. Acta Otolaryngol (Stockh) 1990;109:124-9.

10. Paparella MM, Meyerhoff WL, Goycoolea MV. Silent otitis media. Laryngoscope 1980;90:1089-98.

11. Sando I, Doyle WJ, Okuno H, Takahara T, Kitajiri M, Coury WJ III. A method for the histopathological analysis of the temporal bone and the eustachian tube and its accessory structures. Ann Otol Rhinol Laryngol 1986;95:267-74.

12. Shi S, Cote C, Kalra KL, Taylor CR, Tandon AK. A technique for retrieving antigens in formalin-fixed, routinely acid-decalcified, celloidin-embedded human temporal bone sections for immunohistochemistry. J Histochem Cytochem 1992;40:787-92.

13. Ganbo T, Sando I, Balaban CD, Suzuki C, Sudo M. Immunohistochemistry of lymphocytes and macrophages in human celloidin-embedded temporal bone sections with acute otitis media. Ann Otol Rhinol Laryngol 1997;106:662-8.

14. Shurin PA, Pelton SI, Donner A, Klein JO. Persistence of middle-ear effusion after otitis media in children. N Engl J Med 1979;300:1121-3.

15. Bluestone CD, Klein JO. Otitis media, atelectasis, and eustachian tube dysfunction. In: Bluestone CD, Stool SE, Kenna MA, eds. Pediatric otolaryngology. 3rd ed. Philadelphia, Pa: WB Saunders, 1996:388-582.

16. Emery JL, Dinsdale F. The postnatal development of lymphoreticular aggregates and lymph-nodes in infants' lungs. J Clin Pathol 1973;26:539-45.

17. Sudo M, Sando I. Developmental changes in folding of the human eustachian tube. Acta Otolaryngol (Stockh) 1996;116:307-11.

18. Aoki H, Sando I, Takahashi H. Mucosal folds of eustachian tube in young children. Auris Nasus Larynx 1993;20:125-30.

19. Sando I, Takahashi H, Aoki H, Matsune S. Mucosal folds in human eustachian tube: a hypothesis regarding functional localization in the tube. Ann Otol Rhinol Laryngol 1993;102:47-51.

ASSESSMENT OF STAPES MOBILITY BY USE OF A NEWLY DEVELOPED PIEZOELECTRIC CERAMIC DEVICE

A PRELIMINARY EXPERIMENT IN DOGS

KIYOFUMI GYO, MD
HIDEMITSU SATO, MD
EIJI YUMOTO, MD
NAOAKI YANAGIHARA, MD

EHIME, JAPAN

A piezoelectric device was developed for assessment of stapes mobility during middle ear surgery. The device comprises a pair of ceramic bimorph elements: one for activation of the stapes and the other to pick up the vibration as an electric output, which varies in accordance with the stapes mobility, ie, the inverse of the cochlear input impedance (Z_{SC}). The device is compact and easily manipulated even in the narrow surgical field of the ear. However, the measuring range is restricted to between 1 and 10 kHz. Measurement of Z_{SC} was conducted with this device in 5 ears of 5 dogs. The mean magnitude of Z_{SC} increased with frequency in the range from 1 to 10 kHz: 0.95 megohm at 1 kHz and 8.8 megohms at 10 kHz. After fixation of the stapes with dental cement, the magnitude increased to more than 10 megohms, except at 1 kHz. The results suggest that the device is useful in detecting decreases in stapes mobility in patients with chronic otitis media.

KEY WORDS — cochlear impedance, piezoelectric element, stapes fixation.

INTRODUCTION

The success of tympanoplasty depends on a variety of factors, such as the severity of the middle ear disease, the type of ossicular reconstruction, and the surgeon's proficiency; however, the mobility of the stapes is considered the most critical factor affecting postoperative hearing. Otologic surgeons usually determine stapes mobility by carefully placing an ear pick on the stapes and assessing mobility with the fingers. This maneuver provides only a rough estimate, and the results are subjective. The test is more difficult and even less informative when the superstructure of the stapes is missing.

We developed a piezoelectric ceramic device for the measurement of stapes mobility during middle ear surgery. The device enabled objective assessment of stapes mobility in the form of cochlear input impedance (Z_{SC}), which is composed of the impedances of the stapes–annular ligament and the cochlea. Before actual application in human subjects, the device was tested in dogs. This paper introduces the design and principles of the device, and reports on the changes in magnitude of Z_{SC} after fixation of the stapes with dental cement.

MEASURING DEVICE

The sensor probe of the device comprises a pair of piezoelectric ceramic elements (Fig 1). The elements are made of lead titanate zirconate coated with a resin layer for insulation. The dimensions of each element are 7 mm in length, 1.2 mm in width, and 0.6 mm in thickness. The lower element is for activation of the stapes via a tip made of hydroxyapatite, and the upper element is for picking up the vibrations as an electrical output, which varies in accordance with the stapes mobility, ie, the inverse of Z_{SC}. The measurement is carried out by placing the tip of the probe on the head or footplate of the stapes. The magnitude and angle of Z_{SC} are calculated by the formulas described in Fig 2.

For calibration of the probe, the vibration amplitude at the tip was measured with a laser-Doppler

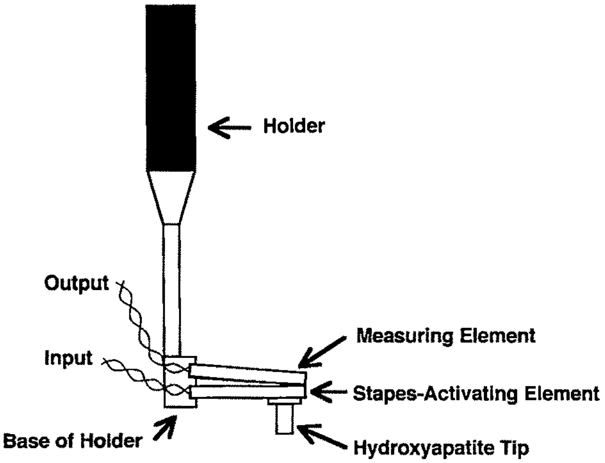

Fig 1. Structure of piezoelectric device.

From the Department of Otolaryngology, Ehime University School of Medicine, Ehime, Japan.

CORRESPONDENCE — Kiyofumi Gyo, MD, Dept of Otolaryngology, Ehime University School of Medicine, Shigenobu-cho, Ehime, 791-02, Japan.

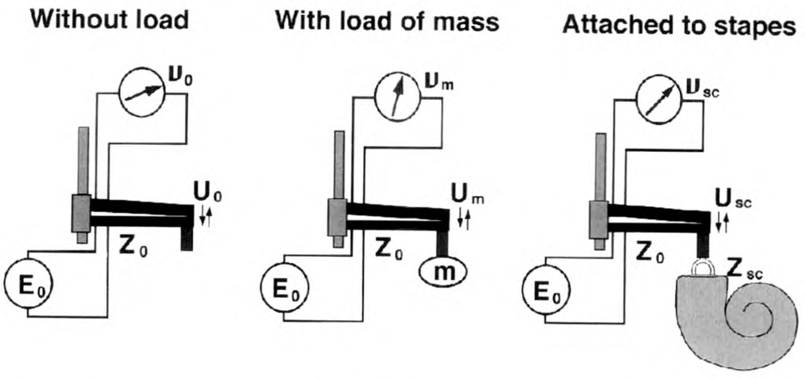

$$U_0 = a\frac{E_0}{Z_0} \qquad U_0 = a\frac{E_0}{Z_0 + jm\omega} \qquad U_0 = a\frac{E_0}{Z_0 + Z_{sc}}$$

$$U_0 = b\,\upsilon_0\, e^{j(\omega t + A_0)} \qquad U_0 = b\,\upsilon_m\, e^{j(\omega t + A_m)} \qquad U_0 = b\,\upsilon_{sc}\, e^{j(\omega t + A_{sc})}$$

Fig 2. Mechanical analog of measurements and formulas for calculating magnitude and angle of stapes-cochlea impedance (Z_{sc}). Alternating current, E_0, applied to piezoelectric element with mechanical impedance of Z_0, elicits vibration of probe with velocity of U_0 at tip. Relationship is linear, with constant of "a," due to linear input-output function of piezoelectric element. Velocity can be monitored electrically by connecting another piezoelectric element to former element at free end. Output voltage from pickup element, μ_0, is proportional to velocity of probe with constant of b. When probe is loaded with mass (m) or with Z_{sc}, vibration of probe and output voltage are U_m and μ_m, or U_{sc} and μ_{sc}, respectively. From 3 stages of single measurement, Z_{sc} in each frequency f can be calculated by following formulas.

$$\text{Magnitude of } Z_{sc} = \frac{2\pi\, mf}{S^2} \cdot \frac{V_m}{V_s} \cdot \frac{Q}{P}$$

$$\text{Angle of } Z_{sc} = \frac{\pi}{2} + (A_m - A_{sc}) + (A_p - A_q)$$

$$P = \sqrt{\left(1 - \frac{V_m}{V_0}\cos(A_m - A_0)\right)^2 + \left(-\frac{V_m}{V_0}\sin(A_m - A_0)\right)^2}$$

$$Q = \sqrt{\left(1 - \frac{V_{sc}}{V_0}\cos(A_{sc} - A_0)\right)^2 + \left(-\frac{V_{sc}}{V_0}\sin(A_{sc} - A_0)\right)^2}$$

$$A_p = \tan^{-1}\left(\frac{-\dfrac{V_m}{V_0}\sin(A_m - A_0)}{1 - \dfrac{V_m}{V_0}\cos(A_m - A_0)}\right)$$

$$A_q = \tan^{-1}\left(\frac{-\dfrac{V_{sc}}{V_0}\sin(A_{sc} - A_0)}{1 - \dfrac{V_{sc}}{V_0}\cos(A_{sc} - A_0)}\right)$$

where V_0, V_m, V_{sc}, and A_0, A_m, A_{sc} indicate ratio of output voltage to loading voltage and phase angle in 3 conditions: without load, with load of mass, and with load of stapes-cochlea impedance, respectively. Therefore, $V_0 = \mu_0/E_0$, $V_m = \mu_m/E_0$, and $V_{sc} = \mu_{sc}/E_0$.

vibrometer (Polytek OFV3000, Waldbronn, Germany). When an alternating current of 10 V peak to peak was applied to the probe free of load, the amplitude was approximately 0.01 µm at 1 kHz, which corresponded to the amplitude of the stapes vibration evoked by the sound stimulus of 74 dB sound pressure level at the tympanic membrane.[1] The vibration-frequency curve was almost flat between 0.1 and 8 kHz, represented a resonant peak of 16 dB at 9 kHz, and declined over 10 kHz. When a weight of 100 mg was glued to the tip, the vibration-frequency curve was almost flat between 0.1 and 12 kHz.

MATERIALS AND METHODS

Five dogs weighing 8 to 11 kg were subjected to this study, which followed our institution's ethical guidelines for animal experiments. The dogs were anesthetized with sodium pentobarbital (30 mg/kg) and fixed on a surgical table. A cannula was inserted into the trachea and the animal was ventilated with a

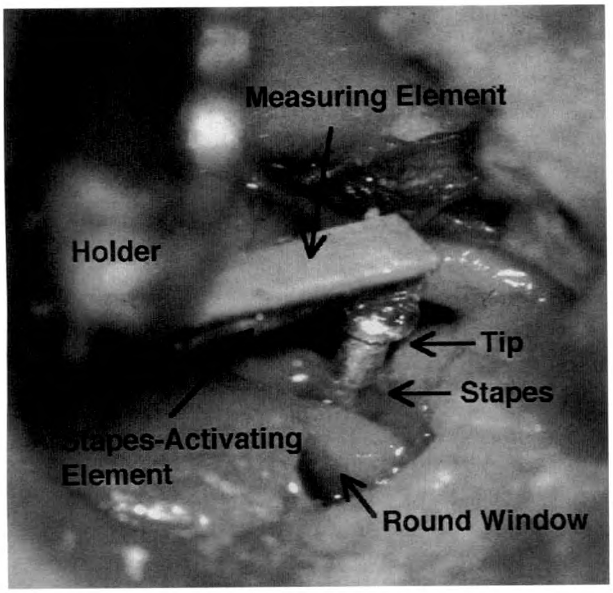

Fig 3. Piezoelectric device placed on head of stapes.

respirator after administration of pancuronium bromide for immobilization. After a local injection of a mixture of lidocaine hydrochloride and adrenaline, a retroauricular skin incision was made and the otic bulla was opened. Under an operating microscope, the incudostapedial joint was dislodged, and the tympanic membrane, incus, and malleus were removed. The ear canal, tympanic ring, and bulla wall were removed to allow easy access to the stapes. Hemostasis was completed before the measurement.

The probe was mounted on a micromanipulator, the position of which was adjustable in 3 dimensions, and advanced until the tip made contact with the head of the stapes (Fig 3). The loading voltage to the probe was adjusted to 2 V peak to peak at all the test frequencies. The ratio of output voltage to loading voltage, and the phase angle between voltages, were measured by a spectrum analyzer (Hewlett-Packard 3582A, Palo Alto, Calif). The data were averaged 16 times. One trial took 8 seconds. Recordings were repeated 3 times by changing the position of the tip, and the measurement that represented the lowest impedance at 2 kHz was adopted for further analysis. The trial difference was narrow, usually within 3 dB, in output voltage.

After completion of the measurements, the stapes was fixed with dental cement and the recordings were repeated. Then, the stapes was removed and its size measured for calculation of the Zsc. The area of the footplate was computed with an image analyzer (Nireco Luzex-FS, Tokyo, Japan). A mean of 1.7 mm^2 was obtained with a range of 1.5 to 2.0 mm^2 and a standard deviation of 0.28 mm^2 (N = 5).

RESULTS

Figure 4 shows the individual magnitudes and phase angles of Zsc in the 5 dogs. As the coherence of the measuring system was poor below 0.8 kHz due to the stiffness of the vibrator, the data were analyzed in this study between 1 and 10 kHz, with an interval of 1 kHz. Considerable individual variation between the animals was noted. On average, the magnitude of Zsc was 0.95 megohm at 1 kHz, which increased gradually at higher frequencies. The maximum value was 8.8 megohms at 10 kHz. The angle was close to 0° below 3 kHz, and approached +90° at higher frequencies.

Fixation of the stapes increased the magnitude of Zsc in all test frequencies, as shown in Fig 5. The increase was more remarkable at lower frequencies than at higher frequencies. The maximal change was 22 dB at 2 kHz and the minimum was 9 dB at 9 kHz.

DISCUSSION

Measurements of Zsc have been conducted with a

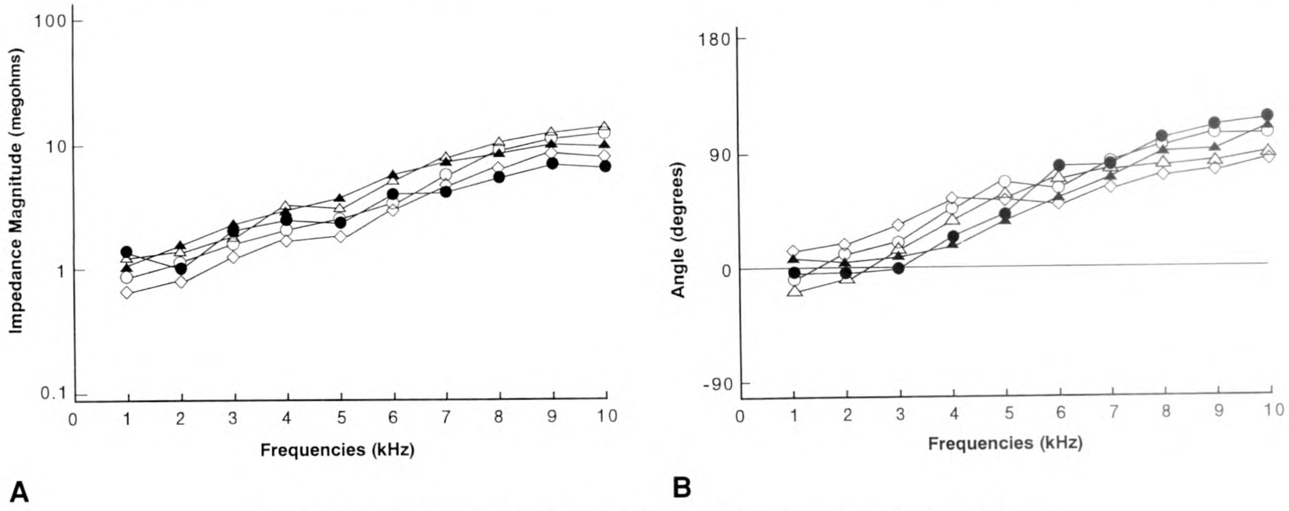

Fig 4. Magnitude (A) and phase angle (B) of cochlear input impedance in 5 dogs.

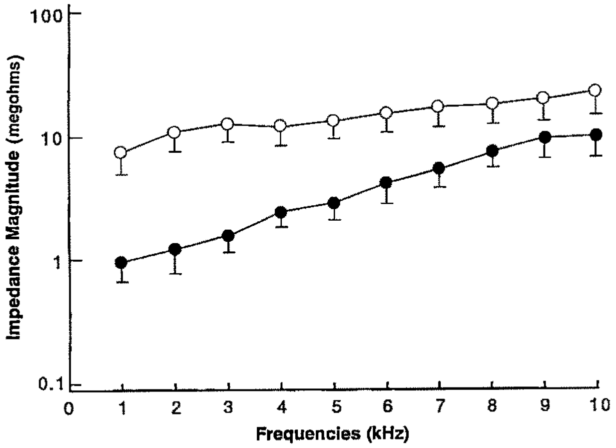

Fig 5. Mean magnitude of Zsc before (closed circle) and after (open circle) fixation of stapes. Vertical bar — 1 SD.

variety of methods, such as a capacitive probe,[2] time-averaged holography,[3] a microscope with stroboscope illumination,[4] a pressure transducer,[5] a laser-Doppler vibrometer,[6] and a gamma ray counter.[7,8] These methods are, however, not applicable to human subjects, due to technical difficulties and safety problems. In 1963 Lau et al[9] developed an ossicular mobility checker, but the device did not become popular because the clinical significance of the device was not fully recognized at that time. As far as we know, no further attempt has been made to measure the Zsc in human subjects. Previously, we attempted to measure vibrator-induced hearing in patients with chronic otitis media during tympanoplasty by temporarily attaching a ceramic vibrator on the stapes and activating it with an electrical current.[10] This test, however, necessitated the patient's voluntary response as in pure tone audiometry, and therefore the results were subjective. The present device represents an improvement by incorporating a pickup element for objective assessment. Further, the present device does not need a sound delivery system for stimulation. We believe that measurements can be conducted relatively safely because the device is designed to anchor the base of the holder first and then to place the tip on the stapes as a second step, thus enabling gentle application. One major drawback is that the range of measurement is restricted to frequencies above 1 kHz because of the stiffness of the ceramic element. The accuracy of the recordings was poor at low frequencies.

The impedance of the cochlea was proved to be a function of frequency. According to experimental studies in cats,[2-4,7] chinchillas,[8] and guinea pigs,[5] the impedance-frequency curve had a negative slope at low frequencies, represented a minimum value between 0.2 and 2 kHz, and increased slightly at higher frequencies. The magnitude of Zsc varies according to the animal species: at 1 kHz, it was 0.8 to 3.3 megohms in cats,[2-4,7] 0.65 megohm in chinchillas,[8] and 0.5 megohm in guinea pigs.[5] The value in dogs was 0.95 megohm in the present study. At present, data from human subjects are not available. These findings suggest that the magnitude of Zsc is larger in big animals, corresponding to the mass of the stapes and the fluid in the cochlea, which provide resistance. Lynch et al[7] suggested that the high impedance at low frequencies was due to the stiffness of the stapes–annular ligament, whereas the impedance at middle and high frequencies was controlled mainly by the mass of the cochlea.

As a preliminary study, the effect of stapedial fixation was investigated by cementing the stapes to the surrounding bone. As shown in Fig 5, the experimental fixation caused an increase in Zsc magnitude from 9 to 22 dB. These values are rather small compared to the conductive hearing loss of 40 to 60 dB often seen in patients with otosclerosis. We ascribed this difference to the laxity of the connection between the probe tip and the stapes.

Mobility of the stapes is important in reconstruction of the sound transmission apparatus of the middle ear. During surgery for chronic otitis media, the mobility of the stapes is often found to be disturbed as a consequence of inflammation, and there is an air-bone gap on the postoperative audiogram. In such cases, simple reconstruction of the ossicular chain is insufficient, and either stapedotomy or stapedectomy may be indicated in order to obtain good hearing. Although further studies (including clinical trials) will be necessary, we believe that the present device is useful in detecting a decrease in stapes mobility in patients with chronic otitis media.

REFERENCES

1. Gyo K, Goode RL, Miller C. Experimental study of stapes vibration produced by the output transducer of an implantable hearing aid. Arch Otolaryngol Head Neck Surg 1987;113:1078-81.

2. Tonndorf J, Khanna SM, Fingerhood BJ. The input impedance of the inner ear in cats. Ann Otol Rhinol Laryngol 1966; 75:752-63.

3. Khanna SM, Tonndorf J. The vibratory pattern of the round window in cats. J Acoust Soc Am 1971;50:1475-83.

4. Guinan JJ, Peake WT. Middle-ear characteristics of anesthetized cats. J Acoust Soc Am 1967;41:1237-61.

5. Dancer A, Franke R. Intracochlear sound pressure measurements in guinea pigs. Hear Res 1980;2:191-205.

6. Kurokawa H, Goode RL. Sound pressure gain produced by the human middle ear. Otolaryngol Head Neck Surg 1995; 113:349-55.

7. Lynch TJ, Nedzelnitsky V, Peake WT. Input impedance of the cochlea in cat. J Acoust Soc Am 1982;72:108-30.

8. Ruggero MA, Rick NC, Robles RL, Shivapuja BG. Middle ear response in the chinchilla and its relationship to mechanics at the base of the cochlea. J Acoust Soc Am 1990;87:1612-29.

9. Lau HH, Michler H, Zoellner F. Versuch einer technischen Verbesserung der Schallsonde. Acta Otolaryngol (Stockh) 1963; 56:421-7.

10. Gyo K, Yanagihara N. Clinical assessment of ossicular mobility by use of a ceramic vibrator designed for implantable hearing aids. Ann Otol Rhinol Laryngol 1986;95:323-6.

≈

CALL FOR PAPERS

Pediatric Diabetes (Mark A. Sperling, MD, Editor-in-Chief; masp+@pitt.edu) is pleased to solicit manuscripts for publication in forthcoming issues and will consider full-length papers, preliminary communications with important new information, clinical reports, and reviews of major topics. Invited editorials and perspectives will be a regular feature. Full-length papers and reviews of major topics should generally not exceed a total of 5,000 words (approximately 20 double-spaced typewritten pages) for the text, references, tables, figures, and figure legends, excluding running title page, title page, and abstract. Preliminary communications with important new information, clinical reports, invited editorials, and perspectives should generally not exceed 2,000 words. For more information, please contact our web site at: www.munksgaard.dk, go to Scientific Journals, and click on the mock-up of the journal cover. Also, you can contact the Editorial Office at: Editorial Assistant, Sandra K. Arjona, MLS, arjonas@chplink.chp.edu, Children's Hospital of Pittsburgh, 3705 Fifth Ave, Pittsburgh, PA 15213; telephone (412) 692-7765; fax (412) 692-7813. Manuscripts can be submitted electronically as an e-mail attachment, or as hard print copy sent in quadruplicate to the above address.

Ann Otol Rhinol Laryngol 109:2000

QUANTIFICATION OF THE THREE-DIMENSIONAL DISPLACEMENT OF NORMAL FACIAL MOVEMENT

SUSAN E. COULSON, MAPPSC
EASTWOOD, AUSTRALIA

GLEN R. CROXSON, MBBS, FRACS
CAMPERDOWN, AUSTRALIA

WENDY L. GILLEARD, MSC
LIDCOMBE, AUSTRALIA

This study was undertaken to quantify 3-dimensional (3-D) facial movement in normal subjects, and to identify the individual axes in which this movement occurred. Displacement data on 42 subjects were collected and analyzed with the Expert Vision Motion Analysis System. The 3-D displacement was calculated by vectorially subtracting maximum marker movement from previously identified reference marker points. The 3-D range of normal facial movement was quantified, with the greatest displacement occurring during maximum smile. When the individual axes were examined, we found that most movement occurred in the vertical axes for the majority of expressions, followed by the anterior-posterior axis. These results may create an objective baseline from which disorders of the facial nerve, and hence, medical, surgical, and physiotherapy treatment interventions, can be analyzed in the future.

KEY WORDS — facial expression, facial nerve, facial paralysis, movement, reference values, three-dimensional analysis.

INTRODUCTION

The measurement of normal facial motion in an objective, quantifiable way is essential if scientific scrutiny is to be applied to the treatment of disorders of facial movement. Currently, the methods used to examine facial motion in a clinical setting are subjective, and they usually are 2-dimensional (2-D). The most commonly used subjective method is the House-Brackmann system.[1] This system, and other grading methods reviewed by House,[2] are based upon the degree of dysfunction and have a low interobserver reliability.[3] The House-Brackmann system was also the only nonsignificant testing factor in a study assessing the effects of physiotherapy intervention on patients after facial nerve paralysis.[4]

Two-dimensional facial measurement techniques have included photographic methods,[5-8] as well as capture onto videotape.[9] Videotaping of movement with 1 camera only allows for a selection of single frames to be analyzed,[10,11] or variations in light reflected by surface deformation to be measured.[9] The majority of measurements are taken from the front and so do not account for all 3 axes of facial motion.

When 3-dimensional (3-D) motion analysis techniques are used to quantify facial movement, measurements are done in the sagittal and frontal planes; however, there are few studies in this area, and they typically have a smaller number of subjects.[12,13] The dynamic nature of expression is measured, and head movements may be automatically accounted for, thereby decreasing measurement error.

This current study has 2 main aims: 1) quantification of the 3-D displacement of normal facial movement and 2) investigation of the 3-D axes in which normal facial movement occurs.

METHOD

The study group comprised 42 normal subjects, 21 men and 21 women, with no past history of facial nerve paralysis. The mean age was 32.33 years, with the age range between 19 and 44 years. The study was approved by the University of Sydney Ethics Committee, and all subjects were volunteers. Data collection was done by the first author at the School of Exercise and Sports Science, The University of Sydney, New South Wales, Australia.

Subjects had 19 spherical retroreflective markers, approximately 7 mm in size, placed on specific facial points that were chosen from a review of the literature.[5,7,14,15] Markers were placed both on places on the face that were thought not to move during facial expression (facial reference points[16]) and on points that show maximal excursion[17] during facial movement, as shown in Fig 1 and Table 1. To investigate movement around the eye and the nose, 2 sets of marker placements were used to ascertain which markers gave more information about both eye closure and nose wrinkle. The attachment of the mark-

---

From the Department of Otorhinolaryngology, Royal Prince Alfred Hospital, Camperdown (Croxson), and the Faculty of Health Sciences, School of Exercise and Sports Science, The University of Sydney, Lidcombe (Gilleard), Australia. Supported by a Grant in Aid from the Garnett Passe and Rodney Williams Memorial Foundation.

CORRESPONDENCE — Susan E. Coulson, MAppSc, Physiotherapist, Suite 5, 35 Fourth Ave, Eastwood, NSW 2122, Australia.

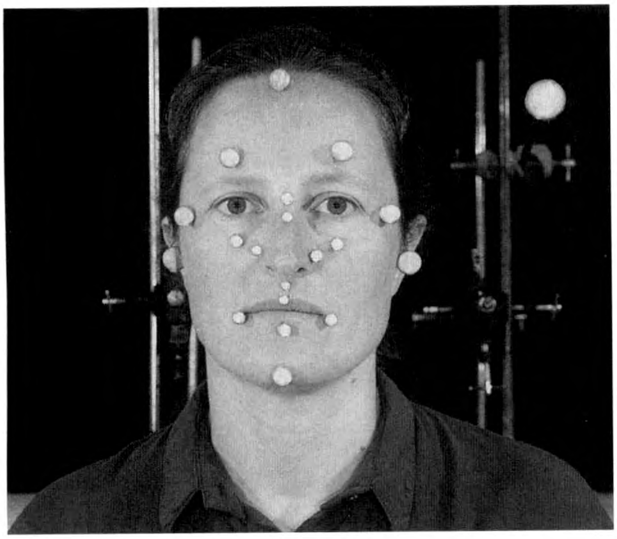

Fig 1. Facial marker points used in this study.

ers was done with Scotch Double Stick Tape (3M). The protocol of facial expressions, also used in previous studies,[16,17] was thought to reflect movement in the branches of the facial nerve. These were designated as rest, forehead raise, eye closure, nose wrinkle, maximum smile, pout, and lips pulled down. Each movement was done 3 times in succession, maximally, over an 8-second period, with the subject relaxing after each attempt. Subjects spent about 45 minutes having the facial markers applied and removed and participating in the data collection.

The marker positions were recorded by 4 NEC TI23A video cameras with an electronic shutter speed of 0.001 second and a filming frequency of 60 Hz. Two cameras were placed at 30°, and 2 at 70°, on either side of the subject's face, at a distance of 1.2 m in an "umbrella configuration."[18] Four 75-W spotlights were mounted on the camera tripods in line with the optical axis of the cameras. To collect data after video capture, and to allow computerized analysis of the 3-D coordinates of the centroids of the retroreflective markers, we used the Expert Vision Motion Analysis System[17] (Motion Analysis Corporation, Santa Rosa, Calif).

The 3-D area in which data were collected was defined by a calibration frame that comprised 16 spheres hung in 4 strings in a cubic arrangement. To allow direct linear transformation of the coordinate points using an 11-parameter calculation,[19] a minimum of 6 markers on the frame must be viewed by at least 2 cameras at all times. The horizontal (x) axis, the vertical (y) axis, and the anterior-posterior (z) axis were defined as shown in Fig 2, with the vertical axis being true vertical. The expected accuracy of the data collected in the area defined by the calibration frame would be approximately 1 part in 1,500, or >0.07%.[20]

After data collection, each frame of data was viewed to label the marker positions and ensure continuity of the marker trajectories. The data were then smoothed at 5 Hz, which was determined by using the residual analysis and curve-fitting techniques described by Winter.[21] The individual x, y, and z axis displacements of the moving markers dur-

TABLE 1. DISPLACEMENT OF FACIAL MOVEMENT MARKERS

			Individual Axes of Movement (mm)		
Expression	*Facial Marker*	*R (mm)*	*x*	*y*	*z*
FR	3 cm superior right pupil	12.43 ± 3.28	2.31 ± 1.73	11.39 ± 2.91	3.55 ± 2.48
FR	3 cm superior left pupil	12.77 ± 3.17	2.83 ± 1.85	11.60 ± 2.92	3.71 ± 2.26
EC	2 cm inferior right pupil	8.83 ± 3.24	4.31 ± 2.24	6.22 ± 2.91	3.06 ± 2.93
EC	2 cm inferior left pupil	7.77 ± 3.01	3.59 ± 2.37	5.76 ± 2.55	2.48 ± 2.30
EC	2 cm right lateral canthus	9.87 ± 3.00	4.78 ± 2.18	2.62 ± 2.58	7.50 ± 3.20
EC	2 cm left lateral canthus	10.41 ± 3.23	4.86 ± 2.16	2.84 ± 2.83	7.92 ± 3.40
NW	2 cm inferior right pupil	8.23 ± 3.22	2.92 ± 1.78	6.45 ± 3.54	2.54 ± 2.58
NW	2 cm inferior left pupil	10.11 ± 2.60	2.77 ± 1.95	8.69 ± 2.96	2.92 ± 2.46
NW	Right alar	7.50 ± 3.14	1.62 ± 1.46	5.52 ± 3.36	3.59 ± 2.68
NW	Left alar	8.53 ± 2.65	1.41 ± 1.10	6.80 ± 2.97	3.59 ± 2.57
MS	Right commissure	13.10 ± 4.24	5.11 ± 3.54	7.83 ± 4.71	6.83 ± 3.76
MS	Left commissure	14.13 ± 4.23	4.77 ± 2.70	8.86 ± 3.86	8.63 ± 4.49
PO	Right commissure	10.71 ± 3.77	3.54 ± 2.71	4.67 ± 2.61	8.40 ± 3.83
PO	Left commissure	11.15 ± 3.12	3.28 ± 1.99	4.53 ± 2.59	9.05 ± 2.94
LD	Right commissure	11.04 ± 4.16	4.53 ± 2.82	4.99 ± 2.76	7.45 ± 4.81
LD	Left commissure	10.26 ± 4.12	3.91 ± 2.81	5.08 ± 3.03	6.66 ± 4.43

Data are mean ± SD.

$R = \sqrt{(x^2 + y^2 + z^2)}$.

x — horizontal; y — vertical; z — anterior-posterior; FR — forehead raise; EC — tight eye closure; NW — nose wrinkle; MS — maximum smile; PO — pout; LD — lips pulled down.

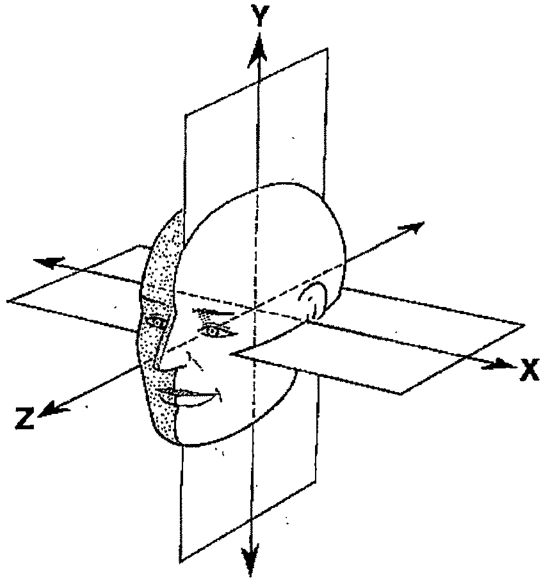

Fig 2. Three-dimensional axes of facial movement.

ing facial expression were calculated by examining the displacement of the moving marker with relation to the reference marker[16] for each movement. The displacement was calculated by vectorially subtracting the reference marker coordinates from the moving marker coordinates for the individual axes at the maximum and minimum displacement frames for each trial, as outlined in equation 1. The maximum displacement for each axis was then recorded, and the principal movement axis for each movement was thereby determined.

$$\text{(1)}\quad \text{Maximum Displacement} = (\text{Moving}^{max} - \text{Reference}^{max}) - (\text{Moving}^{min} - \text{Reference}^{min})$$

To determine the resultant 3-D displacement (R) of the facial movements, the maximum displacements of the individual axes of movement (x, y, and z) were used in equation 2.

$$\text{(2)}\quad R = \sqrt{(x^2 + y^2 + z^2)}$$

Repeated-measures analysis of variance (ANOVA) techniques were used to analyze differences between axis displacements.[22] The level of significance was set at $p < .05$. To analyze nonorthogonal repeated measures contrasts, post hoc tests of significance with a higher Bonferroni critical F were also used.[23,24] To automate this process, we used Miniplan statistical software and Microsoft Excel 5.0 software.

The repeatability, or test-retest reliability, of this study was examined for 6 subjects (3 men and 3 women) by use of intraclass correlation coefficients (ICCs).[25] The ICC (2,1) was chosen for this study because 1 investigator analyzed all the displacement scores, and so a 2-way ANOVA was performed.[25] Because ICCs are sensitive to outliers, a count-based technique, the percentage close agreement (PCA), was used to obtain an agreement index over repeated measures.[26]

TABLE 2. REPEATED MEASURES ANOVA OF COMBINED DISPLACEMENTS FOR VARIATIONS IN MARKER PLACEMENTS DURING TIGHT EYE CLOSURE AND NOSE WRINKLE

Comparison	*df*	*F Value*	*F Critical*
Eye closed inferior versus eyes closed lateral	(1,40)	15.10	4.08
Nose wrinkle inferior versus nose wrinkle alar	(1,40)	5.649	4.08

RESULTS

Combined Three-dimensional Displacements (R). The mean R displacements ranged from 7.5 mm for the right alar marker during nose wrinkle to 14.13 mm for the left commissure marker during maximum smile. The superior 3-cm right and left pupil markers measuring forehead raise had similar mean 3-D displacements of 12.43 mm on the right side and 12.77 mm on the left side (Table 1).

During tight eye closure, 2 different marker placements were used. The 2-cm lateral eye markers had mean 3-D displacements of the right = 9.87 mm and the left = 10.41 mm, whereas the 2-cm inferior eye markers were right = 8.83 mm and left = 7.77 mm. The other movement that used 2 different marker configurations was the nose wrinkle. The 2-cm inferior pupil marker had mean displacements of 8.23 mm on the right and 10.11 mm on the left, whereas the alar markers had 7.50 mm on the right and 8.53 mm on the left (Table 1). These markers were examined to determine whether there was significantly greater movement of either marker placement (Table 2). The 2-cm lateral canthus markers had significantly greater displacement than the 2-cm inferior pupil markers during tight eye closure (F = 15.102), and the inferior pupil markers had significantly greater displacement than the alar markers during nose wrinkle (F = 5.649).

Displacement of Individual Axes of Facial Movement. The mean individual horizontal, vertical, and anterior-posterior axis displacements of facial movement were measured for the protocol of facial expressions and markers and are shown in Table 1. The individual axis displacements ranged from 11.6 mm for the left 3-cm inferior pupil marker in the vertical axis during forehead raise, to 1.41 mm for the left alar marker in the horizontal axis during nose wrinkle.

The individual axes of facial movement were examined to determine whether there was significantly more horizontal, vertical, or anterior-posterior axis displacement in the whole face, and the results are shown in Table 3. There was significantly more ver-

TABLE 3. REPEATED MEASURES ANOVA FOR INDIVIDUAL AXES OVER WHOLE FACE

Comparison	*df*	*F Value*	*F Critical*
(x and z) versus y	(1,40)	113.314	4.08
x versus z	(1,40)	50.660	4.08

tical than horizontal and anterior-posterior axis displacement [(x and z versus y)] across the whole face (F = 113.314), as shown in Table 3. There was also significantly more anterior-posterior axis displacement than horizontal displacement (z versus x) across the whole face (F = 50.660).

The protocol of facial movements was examined, by use of post hoc contrasts, for significant differences in the displacement of the individual 3-D axes, as shown in Table 4. In 3 of the 6 facial expressions, the vertical component of the movement was significantly greater than the horizontal or anterior-posterior displacement of that movement. As shown in Table 4, the vertical axis was strongly significant as the predominant axis of movement for forehead raise (F = 226.521), and the 2-cm inferior pupil markers were predominant during nose wrinkle (F = 100.287). The vertical axis also had significantly greater displacement for the 2-cm inferior pupil markers during tight eye closure (F = 37.897), and for the alar markers during nose wrinkle (F = 45.783).

TABLE 4. POST HOC CONTRASTS FOR INDIVIDUAL AXES

Comparison	*df*	*F Value*	*F Critical*
Forehead raise			
(x or z) vs y	(1,40)	226.521	12.06
x vs z	(1,40)	2.791	12.06
Eyes closed inferior			
(x or z) vs y	(1,40)	37.897	12.06
x vs z	(1,40)	9.554	12.06
Eyes closed lateral			
(x or y) vs z	(1,40)	50.597	12.06
x vs z	(1,40)	8.164	12.06
Nose wrinkle inferior			
(x or z) vs y	(1,40)	100.287	12.06
x vs z	(1,40)	1.952	12.06
Nose wrinkle alar			
(x or z) vs y	(1,40)	45.783	12.06
x vs z	(1,40)	16.784	12.06
Maximum smile			
(x or z) vs y	(1,40)	9.586	12.06
x vs z	(1,40)	20.147	12.06
Pout			
(x or y) vs z	(1,40)	64.910	12.06
x vs y	(1,40)	8.819	12.06
Lips pulled down			
(x or z) vs y	(1,40)	0.351	12.06
x vs z	(1,40)	14.366	12.06

TABLE 5. MAXIMUM MEAN INDIVIDUAL AXIS DISPLACEMENTS ACROSS WHOLE FACE

	Horizontal	*Vertical*	*Anterior-Posterior*
Mean right displacement	3.64	6.21	5.37
Mean left displacement	3.43	6.76	5.62
Mean overall displacement	3.53	6.49	5.49

Data are in millimeters.

The maximum mean vertical displacement was 6.49 mm overall, comprising 6.21 mm on the right and 6.76 mm on the left (Table 5). As shown in Table 1, the maximum mean vertical axis displacements ranged from 11.39 mm for the 3-cm superior pupil marker during forehead raise to 2.6 mm for the 2-cm right lateral canthus marker during tight eye closure.

As shown in Table 4, the anterior-posterior axis during pout was the predominant axis of movement, having a strongly significant difference from the other 2 axes (F = 64.910). For 3 other movements — maximum smile (F = 20.147), lips pulled down (F = 14.366), and the alar markers during nose wrinkle (F = 16.784) — the anterior-posterior axis had significantly more movement than the horizontal axis (Table 4). The maximum mean anterior-posterior axis displacement across the whole face was 5.49 mm, as compared to a maximum mean horizontal axis displacement of 3.53 mm (Table 5). The maximum mean anterior-posterior axis displacements ranged from 9.05 mm for the left commissure during pout to 2.48 mm for the left 2-cm inferior pupil marker during tight eye closure (Table 1).

The mean maximum overall facial horizontal axis displacement was the lowest of the 3 axes at 3.53 mm (Table 5). The horizontal axis displacements for the alar markers during nose wrinkle were lower (right = 1.62 mm and left = 1.41 mm) than was the marker placement for any other axis (Table 1). The highest mean maximum horizontal axis displacement occurred for the right commissure marker during maximum smile (5.11 mm).

Test-Retest Reliability. Forehead raise had high test-retest reliability, demonstrated by high ICCs and PCAs for all displacements except the anterior-posterior axis displacement ICC. All tight eye closure ICC displacements were low; however, 11 of the 16 pre-to-post displacements were within 66.7% PCA at 3 mm between occasions. High test-retest reliability was recorded for nose wrinkle in the 3-D displacement ICCs, and 80% of all markers except 1 were within 80% PCA at 3 mm between occasions. Maximum smile recorded a variable test-retest reliability with a large range of ICCs and PCAs. During the pout expression, the 3-D displacement ICC of the right and left commissure markers had a high test-retest reliability, whereas the individual movement axes displacements had low ICCs.

DISCUSSION

The amount of displacement during facial expression in each axis was tested to examine in which direction most facial movement occurred. There was significantly more vertical than horizontal or anterior-posterior axis displacement across the whole face. There was also significantly more anterior-posterior axis displacement than horizontal displacement across the whole face. The maximum mean axis displacements also reflect this trend, with the highest being in the vertical axis, followed by the anterior-posterior axis, and the lowest being in the horizontal axis. The 2 axes in which most of the reference marker movement occurred were the vertical and anterior-posterior axes.[16] The results from this study therefore indicate that most movement occurred in a vertical direction on the face, followed by an anterior-posterior direction, with the least movement occurring in a horizontal direction. As there are no 3-D benchmarks to compare these displacements to, we hope that further comparative studies may increase the understanding of normal facial movement.

The 3-D results in this current study question the validity of quantifying facial movement via 2-D frontal photographic measures[5-7] and 2-D frontal video analysis,[9,10] and question the conclusions drawn from those studies. Two-dimensional frontal photographs[5-7] and 2-D frontal video analysis[9,10] do not take into account anterior-posterior axis displacement that occurs on the face, as only the horizontal and vertical components are accounted for. This factor is more critical for certain movements for which anterior-posterior axis displacement plays a significant role, for example, a pout, during which the lips are pushed as far forward as possible. During the pout, there is significantly more anterior-posterior axis displacement than vertical and horizontal axis displacement of the commissure markers.

Three movements on the face have significantly more anterior-posterior axis than horizontal axis displacement. These movements are maximum smile, lips pulled down, and movements of alar markers during nose wrinkle. The maximum smile is a movement that is commonly measured in the 2-D frontal plane.[10,11] The vertical and horizontal components are accounted for; however, no anterior-posterior axis movement is recorded in that situation. For a more accurate representation of the displacement of facial movement for the smile, as well as for other movements, 2-D studies need to take profile as well as frontal views of the face, as done in some studies.[7,27] Three-dimensional movement analysis provides a tool that allows the displacement of the 3 axes of facial movement to be simultaneously measured,[16,17] thereby overcoming the problem of the loss of the anterior-posterior axis in the frontal plane.

Marker placements for this study were derived from static 2-D photographic studies[5,7,14,15] and 2-D digitization of single video frames.[10] It was found that the 2-cm inferior pupil markers had significantly greater displacement than the alar markers during nose wrinkle. Future studies may choose both these marker placements. The alar markers are attached to the nose itself, however, and hence directly reflect the movement of the alar portion of the nose. With tight eye closure, the 2-cm lateral canthus markers had significantly greater displacement than the 2-cm inferior pupil markers. This may mean that the 2-cm lateral canthus markers give better information about maximum displacement during tight eye closure than do the 2-cm inferior pupil markers.

A wide range of test-retest reliability was recorded, with forehead raise having the highest reliability and the movements around the mouth and eyes having lower reliability. The lower third of the face has the added movement from the temporomandibular joint, which may contribute to this decreased reliability. As the reliability of measurements of these facial movements with 3-D procedures has not been previously reported, comparisons cannot be made between studies. Future investigation of movements in the lower third of the face, however, must account for this decreased reliability. Instructions to the patient during the test procedure may have affected reliability, as emotional response was not controlled, and data collection procedures may have accounted for further reliability limitations.

CONCLUSIONS

1. The 3-D displacement of normal facial movement was quantified. This ranged from 7.5 mm during nose wrinkle to 14.13 mm during maximum smile.

2. The individual axes of facial movement were quantified. There was significantly more vertical (y) axis facial displacement than horizontal (x) or anterior-posterior axis (z) displacement [y > (x or z)] across the whole face.

3. The anterior-posterior axis displacement was significantly greater than the horizontal axis displacement.

These 3-D displacement results, indicating that the vertical axis is the predominant axis of movement, followed by the anterior-posterior axis, with the least movement occurring in the horizontal axis, question the validity of 2-D frontal facial measures. Profile as well as frontal views of the face should be taken in 2-D photographic studies to account for the significant amount of anterior-posterior axis displacement that occurs during facial movement. Future studies may use 3-D movement analysis, as this provides a tool that allows the displacements of the 3 axes of facial movement to be simultaneously measured, thereby overcoming the problem of the loss of the anterior-posterior axis in the frontal plane.

ACKNOWLEDGMENTS — The authors thank the staff, particularly Ray Patton, of the School of Exercise and Sports Science, Faculty of Health Science, The University of Sydney, for their scientific and technical support.

REFERENCES

1. House JW, Brackmann DE. Facial nerve grading system. Otolaryngol Head Neck Surg 1985;93:146-7.

2. House JW. Facial nerve grading systems. Laryngoscope 1983;93:1056-69.

3. Croxson GR, May M, Mester SJ. Grading facial nerve function. House-Brackmann versus Burres-Fisch methods. Am J Otol 1990;11:240-6.

4. Coulson SE, Croxson GR. Assessing physiotherapy rehabilitation outcomes following facial nerve paralysis. Aust J Otolaryngol 1995;2:20-4.

5. Larrabee WF, Maupin G, Sutton D. Profile analysis in facial plastic surgery. Arch Otolaryngol 1985;111:682-7.

6. Coughlan BA, Mathews B, Pigott RW. A method for measuring facial asymmetry. J Physiol (Lond) 1985;364:20P.

7. Farkas LG, Bryson W, Klotz J. Is photogrammetry of the face reliable? Plast Reconstr Surg 1980;66:346-55.

8. Hilger PA, Webster RC, Hilger JA, Smith RA. A computerized nasal analysis system. Arch Otolaryngol 1983;109:653-62.

9. Neely JG, Cheung JY, Wood MW, Byer SJ, Rogerson A. Computerized quantitative dynamic analysis of facial motion in the paralyzed and synkinetic face. Am J Otol 1992;13:97-107.

10. Wylie DR, Goodale MA. Left-sided oral asymmetries in spontaneous but not posed smiles. Neuropsychologia 1988;26:823-32.

11. Katsikitis M, Pilowsky I. A study of facial expression in Parkinson's disease using a novel microcomputer based method. J Neurol Neurosurg Psychiatry 1988;51:362-6.

12. Redolfi M, Reffigno G, Pedotti A. Multiparametric analysis of lips and jaw kinematics in normal and stuttering subjects. In: Shiavi R, Wolf S, eds. Abstract book: Tenth Congress of the International Society of Electrophysiology and Kinesiology. Charleston, SC, 1994:70-1.

13. Stussi E, Handshin S, Frey M. Quantification of facial asymmetries. A method of objectifying motor impairments following facial nerve injuries: pilot study. Biomed Tech (Berlin) 1992;37:14-9.

14. Ferrario VF, Sforza C, Miani A, Tartaglia G. Craniofacial morphometry by photographic evaluations. Am J Orthod Dentofacial Orthop 1993;103:327-37.

15. Peckitt NS, Walker RV, Barker GR. The facial nerve function coefficient: analysis of 100 subjects. J Oral Maxillofac Surg 1992;50:338-9.

16. Coulson SE, Croxson GR, Gilleard WL. Three-dimensional quantification of "still" points during normal facial movement. Ann Otol Rhinol Laryngol 1999;108:265-8.

17. Coulson SE, Croxson GR, Gilleard WL. Quantification of the three dimensional displacement of normal facial movement. A pilot study. Aust J Otolaryngol 1996;2:344-8.

18. Nigg BM, Herzog W. Biomechanics of the musculoskeletal system. New York, NY: John Wiley & Sons, 1994.

19. Expert Vision Reference Manual. Santa Rosa, Calif: Motion Analysis Corporation, 1989.

20. Walton JS. The accuracy and precision of a video-based motion analysis system. In: Proceedings of the 30th International Technical Symposium of Optical Optoelectronic Applied Science Engineering, High Speed Photography, and Videography Photonics. San Diego, Calif, 1986:17-22.

21. Winter DA. Biomechanics and motor control of human movement. 2nd ed. New York, NY: John Wiley & Sons, 1990:36-43.

22. Tabachnick BG, Fidel LS. Using multivariate statistics. 2nd ed. New York, NY: Harper Collins, 1989.

23. Harris RJ. A primer of multivariate statistics. New York, NY: Academic Press, 1975.

24. Thomas JR, Nelson JK. Research methods in physical activity. Champaign, Ill: Human Kinetics, 1990.

25. Shrout PE, Fleiss JL. Intraclass correlations: uses in assessing interrater reliability. Psychol Bull 1979;86:420-8.

26. Rey JM, Plapp JM, Stewart G, Richards I, Bashir M. Reliability of the psychosocial axes of DSM-III in an adolescent population. Br J Psychiatry 1987;150:228-34.

27. Burton AM, Bruce V, Dench N. What's the difference between men and women? Evidence from facial measurement. Perception 1993;22:153-76.

Ann Otol Rhinol Laryngol 109:2000

EFFECTS OF CLARITHROMYCIN ON RHEOLOGICAL PROPERTIES OF NASAL MUCUS IN PATIENTS WITH CHRONIC SINUSITIS

CHAE-SEO RHEE, MD
SEOUL, KOREA
YUICHI MAJIMA, MD
TSU, JAPAN
SHINOBU ARIMA, MD
TSU, JAPAN
HA-WON JUNG, MD
SEOUL, KOREA
TAE-HOON JINN, MD
SEOUL, KOREA
YANG-GI MIN, MD
SEOUL, KOREA
YASUO SAKAKURA, MD
TSU, JAPAN

Macrolide antibiotics have a variety of actions along with antimicrobial action. To determine the effects of oral administration of clarithromycin (CAM) on rheological properties, we measured the spinability, dynamic viscoelasticity, and solid composition of human nasal mucus from 18 patients with chronic sinusitis before and after administration of CAM for 4 weeks. After administration of CAM, the spinability and percent solid composition of nasal mucus increased from 26.5 ± 12.2 mm to 40.2 ± 18.7 mm and 7.86% ± 3.47% to 13.90% ± 3.67% ($p < .05$), respectively, whereas the ratio of the viscosity to the elasticity (η'/G') of nasal mucus after the administration of CAM decreased in all of the mucus samples. These results suggest that treatment with CAM may modulate the rheological properties of nasal mucus in patients with chronic sinusitis.

KEY WORDS — chronic sinusitis, clarithromycin, elasticity, nasal mucus, spinability, viscosity.

INTRODUCTION

Macrolide antibiotics are widely used for the treatment and prevention of airway infection. There is also increasing evidence that macrolide antibiotics are effective in the treatment of chronic sinusitis.[1] Some reports demonstrated a reduction in the amounts of sputum or nasal secretion during macrolide use.[2,3] It is also reported that erythromycin inhibits respiratory glycoconjugate secretion from human airways in vitro.[4] The clinical effects of macrolide antibiotics may depend on their anti-inflammatory and antisecretory actions, as well as their antimicrobial properties. It has been suggested that oral macrolides affect the rheological properties of sputum in chronic lower airway infections.[2] However, no studies have been previously reported on the rheological properties of nasal mucus from patients with chronic sinusitis after oral administration of macrolides. The purpose of this study was to investigate the effects of a newly developed oral macrolide, clarithromycin (CAM), on the rheological properties, including spinability and viscoelasticity, and the solid composition of human nasal mucus in patients with chronic sinusitis.

MATERIALS AND METHODS

Chronic sinusitis included in this study was defined as disease with persistent symptoms and signs for 8 weeks or repeating acute sinusitis of at least 4 episodes per year, each lasting at least 10 days, in association with persistent changes on computed tomography 4 weeks after medical therapy without intervening acute infection.[5] The patients ranged in age from 16 to 58 years, with a mean of 30.2 years. Seven were female, and 11 were male. They had no history of allergy and showed negative reactions to both a skin test and a radioallergosorbent test to house dust mites. Patients who had undergone nasal surgery or were on topical or oral antiallergic drug therapy were excluded from this study. Clarithromycin was administered orally at a dose of 500 mg/d for 4 weeks. No patients received any other medication during the period of CAM administration. Nasal mucus from 18 patients with chronic sinusitis was collected separately from each nasal cavity before and after administration of CAM by aspiration with a Juhn Tym Tap (Xomed, Jacksonville, Fla). Care was taken not to stimulate the nasal mucosa during the collection. A quantity sufficient for rheological measurement was collected both before and after CAM administration from the same nasal cavity of 18 patients, from 36 nasal cavities before administration, and from 34 after administration. The collected samples were frozen at −70°C and preserved for rheological measurement. Bacteriologic examination was not performed. This study was performed from November 1996 through February 1997.

From the Department of Otorhinolaryngology–Head and Neck Surgery, Seoul National University College of Medicine, Seoul, Korea (Rhee, Jung, Jinn, Min), and the Department of Otorhinolaryngology, Mie University School of Medicine, Tsu, Japan (Majima, Arima, Sakakura). This research was supported by a Grant-in-Aid for General Scientific Research from the Ministry of Education of Japan (No. 07457398,10470355).

CORRESPONDENCE — Yuichi Majima, MD, Dept of Otorhinolaryngology, Mie University School of Medicine, 2-174 Edobashi, Tsu, Mie 514, Japan.

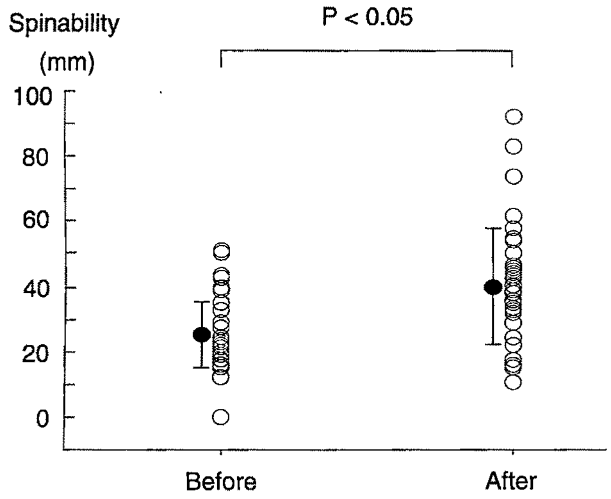

Fig 1. Spinability of nasal mucus before and after administration of clarithromycin (CAM). Posttreatment values are significantly higher than pretreatment values ($p < .05$; $n = 34$).

Spinability was measured with a Filancemeter (Sefam, Vandoeuvre-Les-Nancy, France). Because the reproducibility of measurement is better for larger volumes of sample,[6] the measurement was performed with a 15-µL mucus sample at a distraction velocity of 10 mm/s. An electrical signal through the mucus was interrupted at the point at which the stretched mucus thread was broken, permitting the reading of a spinability measurement. Measurements were repeated until there were 3 readings within 15% of each other. The value of spinability was defined as the average of these 3 measurements in each sample. Spinability was determined at a temperature of 22°C to 25°C and a humidity of 30% to 33% throughout the measurements.

Viscoelastic properties were measured with a controlled shear rate rheometer (Nippon Rheology Equipment Inc, Chiba, Japan). This was generally based on deformation in the cone and plate geometry. The angle between the cone and plate was 1°. Approximately 0.3 mL of nasal mucus was placed on the plate. The cone contacting the plate oscillated or vibrated with an angle speed v (radians per second; 1 rad/s = 0.16 Hz), and the rotation torque was set to M(N•m). The dynamic viscosity (η') and elasticity (G') of the nasal mucus were calculated according to the following formulas: Dynamic viscosity (η') = $3Mf/2\pi R^3 v$ and Elastic modulus (G') = $2F/\pi R^2$ where R is the radius (in centimeters) of the cone, f is the angle between the cone and the plate (in radians), and F is the thrust load force (in pascals). G' is indicative of the elastic behavior of the specimen, and η' is a measure of viscous behavior. Both G' and η' were determined at a constant temperature of 25°C.

We used a microbalance to calculate the wet and dry weights of samples of mucus larger than 20 mg, in order to calculate the percent solid composition (%SC).[7] The mucus sample was weighed in a microbalance on a previously weighed glass slide. The slide was then dried in an oven at 45°C overnight. The dried sample was reweighed, and the %SC was calculated from the ratio of wet weight to dry weight of the mucus.

All data are expressed as mean ± 1 standard deviation. A Wilcoxon signed-rank test was used for statistical analysis of the results. The value of $p < .05$ was considered as statistically significant.

RESULTS

The spinability of nasal mucus from both right and left nasal cavities was measured before CAM administration in 18 patients with chronic sinusitis. The mean values of spinability of nasal mucus samples from the right and left nasal cavities were 24.6 ± 10.1 mm and 28.6 ± 14.2 mm, respectively. Administration of CAM for 4 weeks significantly increased the spinability of both right and left nasal mucus samples, to 42.7 ± 20.9 mm and 37.4 ± 16.0 mm, respectively ($p < .05$; $n = 18$, 16 in right and left nasal cavities, respectively). The spinability of 34 nasal mucus samples from both sides of the nasal cavity increased significantly after administration of CAM for 4 weeks, from 26.5 ± 12.2 mm to 40.2 ± 18.7 mm ($p < .05$; Fig 1).

The viscoelastic properties were only studied for 5 patients because the volume of mucus after administration of CAM was too small to measure viscoelasticity. All of the mucus samples decreased in ratio of viscosity to elasticity (η'/G' at 1 Hz) after the administration of CAM, from 0.035 ± 0.005 to 0.029 ± 0.006, although a statistical analysis was not performed (Fig 2).

The %SC of mucus collected from each nasal cavity before and after CAM administration ranged from 1.89% to 13.79% and from 7.79% to 22.22%, respectively. Administration of CAM led to a significant increase in %SC, from 7.86% ± 3.47% to 13.90% ± 3.67% (Fig 3).

DISCUSSION

Spinability is the thread-forming capacity of mucus under the influence of large-amplitude elastic deformation. The spinability gives information about the internal cohesion forces of the mucus. The concentration of mucous glycoproteins (MGPs), the degree of intermolecular and intramolecular cross-linkings, and the hydration of mucus are factors that control mucus spinability.[7-9] The measurement of spin-

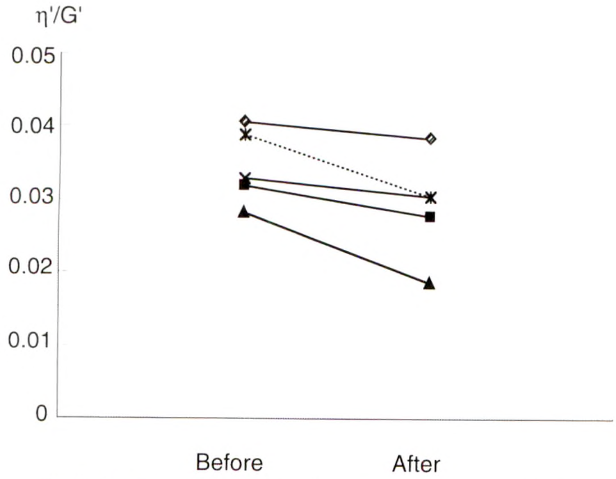

Fig 2. Ratio of viscosity to elasticity (η'/G') of nasal mucus before and after administration of CAM. After administration of CAM, ratio η'/G' decreased in all samples.

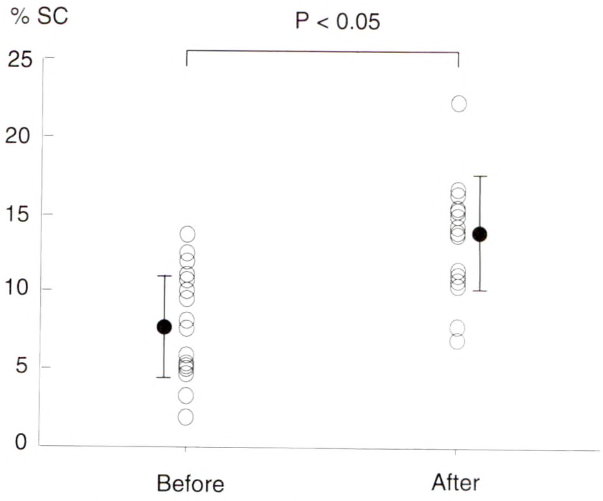

Fig 3. Percent solid composition (%SC) of nasal mucus before and after administration of CAM. Posttreatment values are significantly higher than pretreatment values ($p < .05$; $n = 18$).

ability is relatively quick and simple. However, because the spinability showed a large variation within the individual samples, reflecting the inhomogeneity of nasal mucus, we measured repeatedly until 3 readings were within 15% of each other. This usually required about 5 measurements. The value of spinability was defined as the average of these 3 measurements in each sample. Because room humidity may also affect the spinability of mucus,[7,9] the temperature and humidity were maintained throughout the measurements at 22°C to 25°C and 30% to 33%, respectively.

Insufficiently polymerized mucus, as in bronchorrhea or, on the other hand, a very highly cross-linked mucus, as in purulent sputum, will exhibit a low spinability.[8] The value of spinability in frog mucus, a model of normal respiratory mucus, is 57.3 ± 17.1 mm.[8] In the present study, the spinability was 26.5 ± 12.2 mm in mucus samples from chronic sinusitis. The mean value of mucus spinability in chronic sinusitis was lower than that in normal mucus. This kind of measurement has never been reported previously. Our data on spinability in chronic sinusitis are higher than recently reported values of spinability of nasal mucus in patients with chronic purulent rhinitis, in which the spinability was distributed from 5 to 15 mm.[10] This may be due to the different rheological properties between sinusitis and rhinitis or different mucus characteristics, because most of our patients produced a mucoid or mucopurulent nasal mucus, not a purulent one.

It is reported that a spinability equal to or higher than 50 mm at a distraction velocity of 10 mm/s should be the best rheological characteristic for optimal mechanical coupling between the mucus and cilia.[8] Moreover, in chronic obstructive lung diseases, the mucociliary transport velocity of sputum on mucus-depleted frog palate was positively correlated to the spinability of the same sputum samples.[8] In the present study, orally administered CAM significantly increased the spinability and brought it closer to the optimal value for mucociliary clearance. This effect of treatment with macrolide antibiotics has not been previously reported in either upper or lower respiratory tract diseases. Deceleration of nasal mucociliary clearance has been reported in patients with chronic sinusitis.[11] This reduction of mucociliary clearance may be due to an impairment of interaction between the mucus and ciliary activity.[12] Rheological abnormalities of nasal mucus are also considered one of the causes of slowing of nasal mucociliary clearance.[13] Our results suggest that the increase in spinability of nasal mucus CAM administration could contribute to the improvement of reduced nasal mucociliary clearance in chronic sinusitis. Nishi et al[3] reported that by the end of 4 weeks of treatment with oral CAM, reduced nasal mucociliary clearance improved significantly in patients with sinobronchial syndrome. Our and their findings suggest that CAM could be clinically useful in correcting abnormal nasal mucociliary clearance in patients with sinobronchial syndrome or chronic sinusitis. The effect of oral CAM on the reduced nasal mucociliary clearance of chronic sinusitis must be clarified in a further study.

The viscoelastic properties of mucus are highly dependent on the rate of shear applied to the sample. Thus, the controlled shear rate rheometer used in this study has a clear advantage in that the shear rate in the test mucus is defined and uniform. The dynamic viscoelastic properties measured in this study showed a decrease in viscosity and an increase in elasticity with increasing oscillatory frequency (data not shown). These curves are the reflection of the gel-like nature of respiratory mucus such as tracheobronchial[14] or nasal mucus.[15] Ciliary beat is a cyclic pattern, with a fast effective stroke and a slow recovery stroke, at about 10 Hz in the nasal cavity. On the other hand, the effective shear rate applied to mucus by cilia may be 1 to 3 Hz in vivo.[16] Thus, to examine the rheological properties of mucus in relation to the mucociliary clearance, the viscoelasticity was determined at a frequency of 1 Hz in the present study. The viscoelastic properties of nasal mucus were determined both before and after administration of CAM in only 5 subjects. This is because the amount of mucus collected after administration of the drug was not sufficient for rheological measurement in our rheometer. Although statistical analysis was not performed, all of the mucus samples decreased in ratio of viscosity to elasticity (η'/G') of the nasal mucus after the administration of CAM (Fig 2). The ratio η'/G' can be interpreted as a "relaxation time" or tangent δ.[14] Because an inverse correlation between η'/G' value and mucociliary transport velocity has been reported,[14] our results suggest that after administration of CAM, the nasal mucus could be transported more effectively by the cilia. Our rheological data obtained from the measurement of both spinability and viscoelasticity clearly showed that systemically administered CAM could change the abnormal rheological properties of nasal mucus to more optimal properties for mucociliary transport in chronic sinusitis patients.

The increase in %SC of nasal mucus after the administration of CAM may be due to a decrease in water production and/or an increase in MGP secretion. Oral CAM may reduce the sputum volume in association with symptom improvement in patients with sinobronchial syndrome.[3] It has been also reported that macrolide inhibits respiratory glycoconjugate secretion from human airways in vitro.[4] Further, others reported that macrolides inhibit water secretion across the mucosa toward the respiratory lumen.[17] These reports and the present study imply that an increase in %SC after administration of CAM may result from reduced water production, rather than increased secretion of MGP.

In conclusion, CAM, orally administered to patients with chronic sinusitis, led to an increase in %SC and spinability of nasal mucus. Moreover, after administration of CAM, the nasal mucus had a decrease in the ratio η'/G'. These rheological alterations following administration of CAM could contribute to changing the abnormal rheological properties of nasal mucus to more optimal conditions and thereby improve mucociliary clearance in patients with chronic sinusitis.

REFERENCES

1. Ichimura K, Shimazaki Y, Ishibashi T, Higo R. Effect of new macrolide roxithromycin upon nasal polyps associated with chronic sinusitis. Auris Nasus Larynx 1996;23:48-56.

2. Tamaoki J, Takeyama K, Tagaya E, Konno K. Effect of clarithromycin on sputum production and its rheologic properties in chronic respiratory tract infections. Antimicrob Agents Chemother 1995;39:1668-90.

3. Nishi K, Mizuguchi M, Tachibana H, et al. Effect of clarithromycin on symptoms and mucociliary transport in patients with sino-bronchial syndrome. Nippon Kyobu Shikkan Gakkai Zasshi 1995;33:1392-400.

4. Goswami SK, Kivity S, Marom Z. Erythromycin inhibits respiratory glycoconjugate secretion from human airways in vivo. Am Rev Respir Dis 1990;141:72-8.

5. Lund VJ, Kennedy DW, eds. Quantification for staging sinusitis. Ann Otol Rhinol Laryngol Suppl 1995;104(suppl 167):17-20.

6. Zahm JM, Puchelle E, Duvivier C, Didelon J. Spinability of respiratory mucous. Validation of a new apparatus: the Filancemeter. Bull Eur Physiopathol Respir 1986;22:609-13.

7. Rubin BK, Ramirez O, Zayas JG, Finegan B, King M. Collection and analysis of respiratory mucus from subjects without lung disease. Am Rev Respir Dis 1990;141:1040-3.

8. Puchelle E, Zahm JM, Duvivier C. Spinability of bronchial mucus. Relationship with viscoelasticity and mucous transport properties. Biorheology 1983;20:239-49.

9. Puchelle E, Zahm JM, Jacquot J, Pierrot D. Effect of airway humidity on spinability and transport capacity of canine airway secretions. Biorheology 1989;26:315-22.

10. Passàli D, Bellussi L, Lauriello M. The rheological characteristics of nasal mucus in patients with rhinitis. Eur Arch Otorhinolaryngol 1995;252:348-52.

11. Sakakura Y, Ukai K, Majima Y, Murai S, Harada T, Miyoshi Y. Nasal mucociliary clearance under various conditions. Acta Otolaryngol (Stockh) 1983;96:167-73.

12. Majima Y, Sakakura Y, Matsubara T, Miyoshi Y. Possible mechanism of reduction of nasal mucociliary clearance in chronic sinusitis. Clin Otolaryngol 1986;11:55-60.

13. Majima Y, Hirata K, Tacheuchi K, Hattori M, Sakakura Y. Effects of orally administrated drugs on dynamic viscoelasticity of human nasal mucus. Am Rev Respir Dis 1990;141:79-83.

14. King M. Interaction between mechanical properties of mucus and mucociliary transport: effect of pharmacologic interactions. Biorheology 1979;16:57-6.

15. Majima Y, Sakakura Y, Hattori M, Hirata K. Rheologic properties of nasal mucus from patients with chronic sinusitis. Am J Rhinol 1993;7:217-21.

16. Widdicombe JG, Wells UM. Airway secretions. In: Proctor FD, Andersen IB, eds. The nose: upper airway physiology and the atmospheric environment. Amsterdam, the Netherlands: Elsevier Biomedical Press, 1982:215-44.

17. Tamaoki J, Isono K, Sakai N, Kanemura T, Konno K. Erythromycin inhibits Cl secretion across canine tracheal epithelial cells. Eur Respir J 1992;5:234-8.

Ann Otol Rhinol Laryngol 109:2000

HUMAN UVULA: CHARACTERIZATION OF RESIDENT LEUKOCYTES AND LOCAL CYTOKINE PRODUCTION

KATARINA OLOFSSON, MD
STEN HELLSTRÖM, MD, PHD
MARIE-LOUISE HAMMARSTRÖM, PHD
UMEÅ, SWEDEN

Upper airway infections often lead to macroscopic changes in the architecture of the uvula. Using immunomorphometric analysis, we investigated the frequency and distribution of immune cells and of cytokine-producing cells in uvular samples. Tissue macrophages, αβ T cells, γδ T cells, and B cells were, in declining order, the main cell populations. γδ T cells and B cells exhibited reciprocal localization, with almost all γδ T cells residing in the vicinity of the epithelium, and all B cells in the glandular area. The presence of cells expressing the suppressor phenotype $CD8^+CD28^-$ αβ T cells is suggested. Fifteen to twenty-five percent of the immune cells expressed the down-regulatory cytokine tumor growth factor β. Most macrophages were located subepithelially, in the vicinity of the basal lamina. The composition and cytokine profile of leukocytes in the tissue suggest that the uvula may be a site, additional to the jejunal mucosa, for induction of mucosal tolerance to inhaled and ingested antigens. Concomitantly, the uvula appears to be protected from invasion of microbial pathogens by a subepithelial barrier of macrophages and γδ T cells.

KEY WORDS — gamma delta T cells, human uvula, immunomorphometry, intraepithelial lymphocytes.

INTRODUCTION

The uvula has been assigned several functions, eg, articulator in speech development,[1] protecting the orifices of the eustachian tubes,[2] moisturizing the oral cavity,[3] and simplifying drinking and swallowing.[4] Upper airway infections often lead to macroscopic changes in the appearance of the uvula, and it may therefore play a role in mucosal immune reactions. Surgical intervention for snoring and obstructive sleep apnea often includes resection of the uvula.[5]

Almost nothing is known about immune cells in the uvula. Along the alimentary tract, the mucosal surface has to be protected from infections, and at the same time, the immune system must tolerate components that are beneficial for the individual, eg, food constituents and the commensal microflora. Induction of tolerance to orally administered antigens is believed to take place in the jejunal mucosa.[6] T cells possessing the capability of immune suppression exert their function mainly by secreting down-regulatory cytokines, preferentially, tumor growth factor β (TGF-β) and interleukin (IL) 10.[7,8]

Secretory IgA plays a major role in the humoral immune defense of the mucosa. Induction sites are characterized by the presence of follicles with germinal centers. Cell-mediated mucosal immune protection is provided by intraepithelial lymphocytes and macrophages. Intraepithelial lymphocytes have been demonstrated in the intestinal epithelium,[9,10] the gingival epithelium,[11] and the epithelia of the nasopharyngeal and palatine tonsils.[12,13] A significant proportion of intraepithelial lymphocytes are γδ T cells. In gut and gingiva, γδ T cells are essentially localized to the epithelium,[14] whereas in palatine tonsils, γδ T cells are also found in the lamina propria.[13] Intraepithelial γδ T cells have been suggested to scan the epithelium for stressed cells and/or to regulate epithelial cell proliferation and differentiation.[15] Most γδ T cells recognize antigens in a major histocompatibility complex–unrestricted fashion,[16-18] and certain γδ T cell clones are effective killers of epithelial tumor cells[19] and cells expressing stress-induced major histocompatibility class I–related molecules.[20] The uvula is incessantly exposed to airborne and alimentary antigens and may therefore play some role in the local immune protection and in mucosal tolerance. To investigate these possibilities, we have performed a detailed analysis of the distribution and frequencies of different leukocyte types, as well as of cytokine-producing cells, in human uvula tissue.

MATERIALS AND METHODS

Tissues. Uvula tissue was obtained from 9 patients characterized as social obstructive snorers with an apnea-hypopnea index (AHI) of ≤ 5 ($n = 5$) and from patients with mildly obstructive sleep apnea with an AHI between 6 and 16 ($n = 4$; Table 1). The two diagnostic groups were regarded as a single group, because no major differences in distribution and frequency of immune cells or cytokine-producing cells were noted (data not shown). Preoperative evalua-

---

From the Department of Otorhinolaryngology, Umeå University Hospital (Olofsson, Hellström), and the Department of Immunology, University of Umeå (Olofsson, Hammarström), Umeå, Sweden. This work was supported by grants from the Swedish Natural Science Research Council (grant B-AA/BU 11234-300 to M.-L.H.) and the Swedish Medical Research Council (grant 06578 to S.H.).

CORRESPONDENCE — Marie-Louise Hammarström, PhD, Dept of Immunology, University of Umeå, SE-901 85 Umeå, Sweden.

TABLE 1. CLINICAL CHARACTERISTICS OF PATIENTS INCLUDED IN THIS STUDY

Sex	*Age (y)*	*AHI*	*Diagnosis*
M	44	10	SAS
F	53	6	SAS
M	51	4	SOS
M	61	10	SAS
M	61	1	SOS
F	63	3	SOS
M	51	16	SAS
M	40	12	SAS
M	44	2	SOS

AHI — apnea-hypopnea index (number of apnea [cessation of airflow for at least 10 seconds] and hypopnea [50% decrease in thermistor tracing compared with baseline in combination with oxygen desaturation] events per hour of sleep); SAS — sleep apnea syndrome (patients with mild obstructive sleep apnea with AHI between 6 and 16); SOS — social obstructive snorers (patients with AHI of 5 or less).

tion was based on overnight recordings of nasal and oral air, finger oximetry, body posture, and respiratory and body movements. The duration of sleep was estimated from a pressure-sensitive bed recording. We would have preferred to analyze uvula tissue from healthy persons as a control material, but such samples cannot be obtained, for ethical reasons. Moreover, we consider postmortem material to be an unsuitable alternative, because of possible autolytic changes occurring after death (and in certain cases even before death, eg, in artificially ventilated patients).

Tissue samples were taken after uvulopalatoplasty or uvulopharyngopalatoplasty. Surgery was performed with a scalpel or laser under general or local anesthesia. Approximately 2 mL of a local anesthetic, 0.5% Citanest, with 4 µg of adrenaline per milliliter, was injected just inferior to the uvular base. The uvula was resected about 10 mm from its basal flexure along the midline. The excised uvula was flattened on a cork-plate, with its nasal surface facing downward and its oral surface upward. The part of the uvula facing the soft palate was termed the proximal or superior part, whereas the other end was called the distal or inferior part (Fig 1). We then divided the uvula in the midline from the basal flexure to the most inferior part, thus preparing right and left halves. One half was immediately immersed in isopentane precooled in liquid nitrogen and stored at –70°C until use, and the other half was paraffin-embedded.

Antibodies. Characteristics of the antibodies used are listed in Table 2.

Histologic Analysis. Fresh tissue samples were transferred to saline solution and within 30 minutes placed in 0.1-mol/L phosphate buffer (pH 7.0) containing 2% formaldehyde and 0.5% glutaraldehyde. The tissue was then fixed in a microwave oven set at 45°C and 600 W. After a quick rinse in 0.1-mol/L phosphate buffer, specimens were dehydrated in a graded series of ethanol and embedded in paraffin wax. The tissue was cut into 5-µm sections and stained with toluidine blue.

Immunohistochemical Staining. Immunoperoxidase and immunofluorescence staining of frozen tissue was performed as described earlier.[12,13] Staining for cytokines and immunoglobulins was performed by immunoperoxidase staining with the modification that 0.0005% saponin was present during incubation with the monoclonal antibody (mAb) and conjugate. A mixture of mAbs αFi and βF1 was used for detection of TcR-$\alpha\beta^+$ cells, and a mixture of mAbs L-26 and 4KB128 for detection of B cells. Frequencies of TcR-$\gamma\delta^+$ cells were determined in sections stained by indirect immunofluorescence, which, in our experience, is a more sensitive method than the

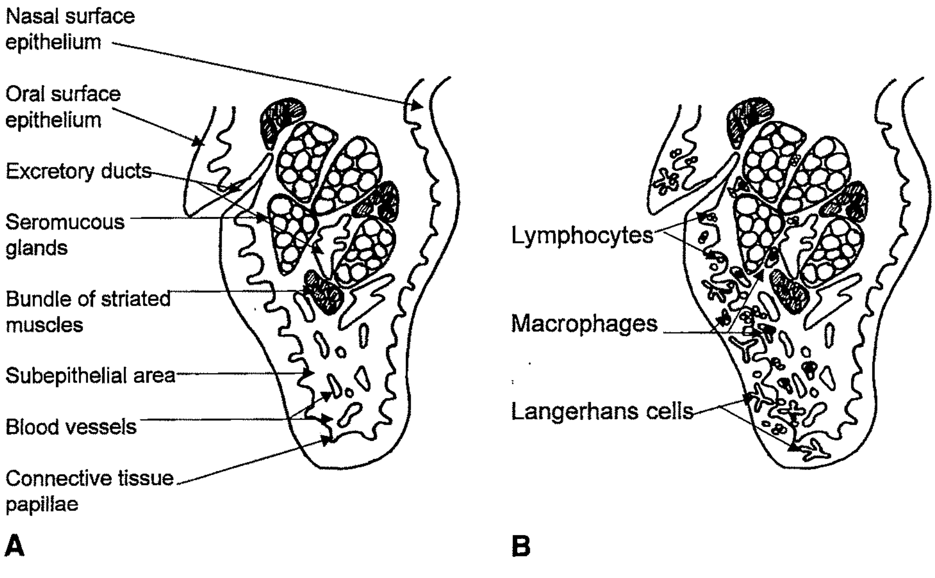

Fig 1. Schematic drawings of human uvula (top is proximal; bottom is distal), summarizing localization of immune cells in relation to structures of uvula. Lymphocytes that are intraepithelial and subepithelial are mainly T cells. Both compartments comprise TcR-$\alpha\beta^+$ and TcR-$\gamma\delta^+$ cells. A) Three main compartments. B) Major localization trends of immune cells.

TABLE 2. ANTIBODIES USED IN THIS STUDY

		Isotype	*mAb/Clone*	*Source*
Marker and main reactivity				
CD3	T cells, subset of thymocytes	IgG1	T3-4B5	Dakopatts, Glostrup, Denmark
TcR-γδ	Monomorphic determinant of δ-chain of γδ TcR	IgG1	TCRδ1	T cell Diagnostics, Cambridge, Mass
TcR-αβ	Monomorphic determinant of β-chain of αβ TcR	IgG1	βF1/8A3	T cell Diagnostics
TcR-αβ	Monomorphic determinant of α-chain of αβ TcR	IgG2a	αF1/3A8	T cell Diagnostics
CD4	MHC class II restricted T cells	IgG1	MT310	Dakopatts
CD8	MHC class I restricted T cells	IgG1	DK25	Dakopatts
CD154/ CD40L	Activated CD4$^+$ T cells	IgG1	M90	Serotec, Oxford, England
CD152/ CTLA-4	Activated T cells	IgG2a	BN13	Becton-Dickinson, Mountain View, Calif
CD28	Subpopulations of T cells and plasma cells	IgG1	CD28.2	Immunotech, Marseille, France
CD20	B cells	IgG2a	L-26	Dakopatts
CD22	B cells	IgG2b	4KB128	Dakopatts
IgA	Human IgA, both subclasses	IgG1	6E2C1	Dakopatts
IgG	Human IgG, all 4 subclasses	IgG1	TM15	The Binding Site, Birmingham, England
IgM	Human IgM	IgG1	R1/69	Dakopatts
CD40	Mature B cells, but is absent from plasma cells	IgG1	EA5	Serotec
CD68	Macrophages and/or monocytes, cytotoxic lymphocytes	IgG1	EBM11	Dakopatts
CD15	Granulocytes	IgM	C3D-1	Dakopatts
CD1a	Langerhans' cells, thymocytes	IgG2a	NA1/34	Dakopatts
HLA DR	Antigen-presenting cells, B cells, activated T cells	IgG2a	DK22	Dakopatts
CD80/ B7.1	Antigen-presenting cells, macrophages and/or monocytes, B cells	IgM	BB-1	Serotec
CD45	Leukocytes	IgG1	2B11 and PD7/26	Dakopatts
Epithelial antigen	Human epithelial cells	IgG1	BerEP4	Dakopatts
Cytokine and main producer cell				
IL-2	T cells	IgG1	80-3418-01	Genzyme, Cambridge, Mass
IL-6	Macrophages and/or monocytes, T cells	IgG1	18871A	Becton-Dickinson
IL-10	T cells, macrophages and/or monocytes	IgG1	9D7	Mabtech, Nacka, Sweden
IFN-γ	T cells, NK cells	IgG1	1-D1K	Mabtech
TNF-α	Macrophages, T cells, NK cells	IgG1	301	Endogen, Cambridge, Mass
TGF-β	Many cell types, including T cells	IgG	Polyclonal, rabbit	RD Systems, Abingdon, England
Negative control and specificity				
Negative control	*Aspergillus niger* glucose oxidase	IgG1	DAK-G01	Dakopatts
Negative control	*Aspergillus niger* glucose oxidase	IgG2a	DAK-G05	Dakopatts
Negative control	*Aspergillus niger* glucose oxidase	IgM	DAK-G08	Dakopatts

immunoperoxidase method for revelation of γδ T cells in frozen tissue sections.[10,11] For comparison, parallel sections were also stained with anti-TcR-αβ mAb by immunofluorescence. A neutralizing preparation of rabbit anti–TGF-β in combination with horseradish peroxidase–conjugated donkey anti-rabbit immunoglobulin (Amersham International) was used for detection of TGF-β.

Uvula sections incubated with isotype-matched mAbs specific for a fungal antigen and normal rabbit IgG, respectively, served as negative controls. Palatine tonsils served as positive controls.

Morphometry. Quantitation of immunohistochem-

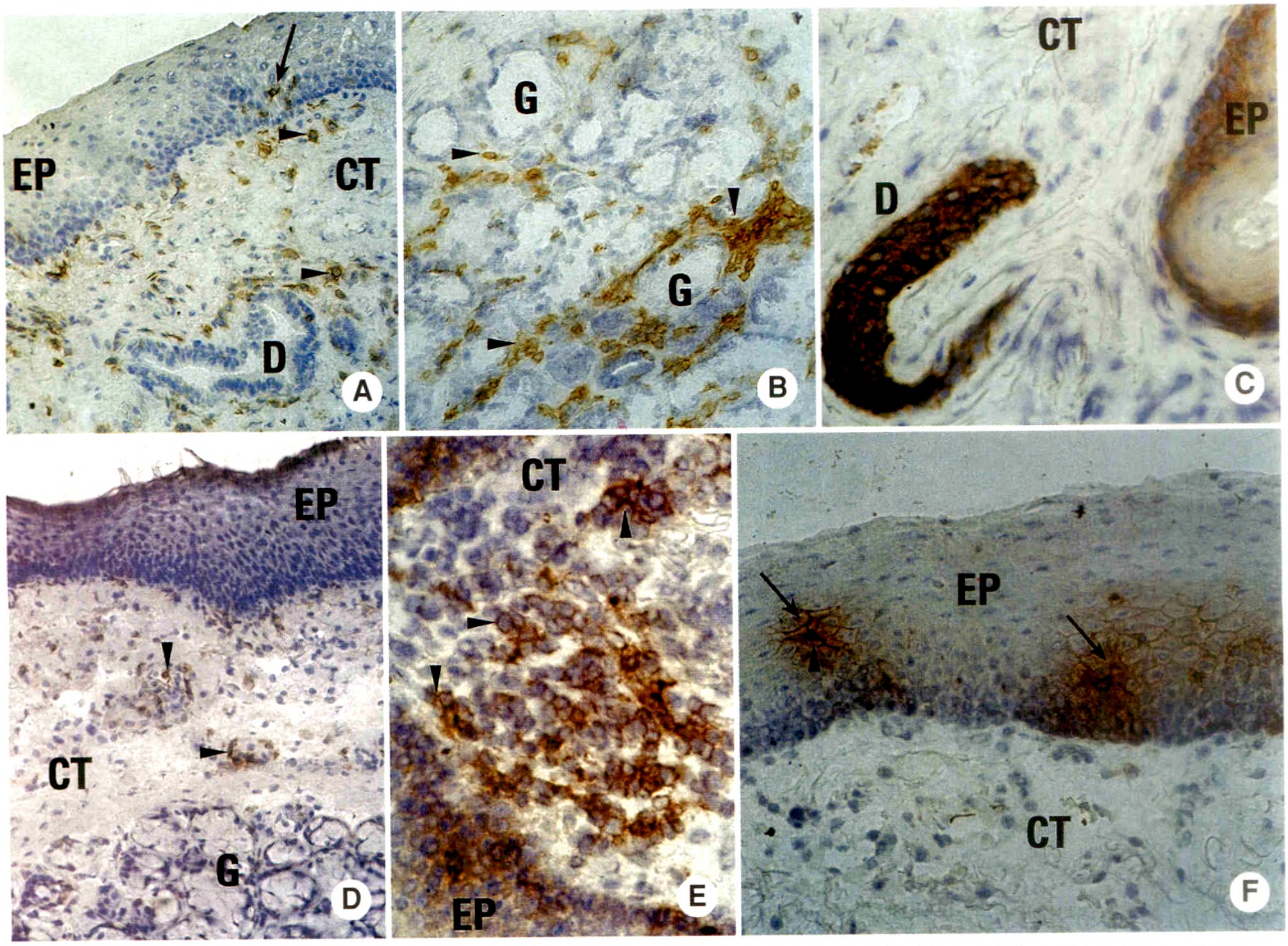

Fig 2. Immunohistochemical staining of cryosections from uvula tissue. A) Immunoperoxidase staining with mixture of anti-CD45 mAbs 2B11 and PD7/26 (original ×32). $CD45^+$ cells (arrow) can be seen in surface epithelium (EP) and in subepithelial connective tissue (CT). Arrowheads — subepithelial $CD45^+$ cells; D — glandular ducts. B) Immunoperoxidase staining with anti-CD45 mAbs 2B11 and PD7/26 (original ×64). Arrowheads — single and conglomerate $CD45^+$ cells in connective tissue septa, embracing glands (G). C) Immunoperoxidase staining with antiepithelial mAb BerEP4 (original ×64). Basal cells in squamous surface epithelium (EP) were intensely stained, whereas middle and upper parts were devoid of staining. Epithelial cells lining glandular ducts (D) are stained with BerEP4 mAb. CT — subepithelial connective tissue of lamina propria. D) Immunoperoxidase staining with anti-CD68 mAb EBM 11 (original ×32). $CD68^+$ cells (arrowheads) were mainly detected in subepithelial connective tissue (CT) of lamina propria. G — glands; EP — surface epithelium. E) Immunoperoxidase staining with anti-CD1a mAb Na1/34 (original ×128). $CD1a^+$ cells with lymphocyte morphology (arrowheads) in subepithelial connective tissue (CT) of lamina propria. EP — surface epithelium. F) Immunoperoxidase staining with anti-CD1a mAb Na1/34 (original ×64). Intraepithelial $CD1a^+$ cells with typical dendritic morphology (arrowhead) and its associated network (arrows). EP — surface epithelium; CT — connective tissue of lamina propria.

ically stained cells was carried out with Weibel's point-counting technique.[12,13,21]

Statistical Analysis. Comparison between the epithelial and subepithelial compartments was performed with the 2-tailed Student's *t*-test for paired samples. A p value of ≤.01 was regarded as significant.

RESULTS

General Characterization of Uvula Tissue. The schematic drawing in Fig 1A shows that the uvula consists of 3 main compartments: 1) the surface epithelium, 2) the subepithelial area, and 3) the area of the glands. The surface epithelium is a keratinized or parakeratinized stratified squamous epithelium, 15 to 20 cell layers thick, resting on a prominent basal lamina. Fingerlike connective tissue papillae of the lamina propria penetrate the epithelium in a saw-toothed pattern. The lamina propria is sporadically perforated by openings of excretory ducts carrying secretion from glands onto the epithelial surface. The mixed seromucous glands are situated in the mid-central and proximal regions of the tissue and embedded in a network of striated muscle bundles and adipose cells.

Leukocytes, defined as $CD45^+$ cells, were present as scattered individual cells in the epithelium, in the subepithelial areas, and in the connective tissue septa between the glands (Fig 2A,B). Follicles were not seen. Occasionally, the surface epithelium was covered by exudates, mainly of T cells ($CD3^+$ cells) and

TABLE 3. FREQUENCY OF DIFFERENT TYPES OF IMMUNE CELLS IN SURFACE EPITHELIUM, SUBEPITHELIAL AREA, AND GLANDULAR AREA OF HUMAN UVULA AS DETERMINED BY IMMUNOMORPHOMETRY

	% Positive Cells			*Frequency of Positive Cells*	
Marker	*Surface Epithelium*	*Subepithelial Area*	*Significance*[a]	*Glandular Area*	*n*[b]
CD3	2.9 ± 1.8[c]	4.2 ± 1.4	NS	++[d]	9
TcR-αβ	1.9 ± 0.7	2.3 ± 1.2	NS	++	8
TcR-γδ	0.7 ± 0.5	1.6 ± 0.8	**	–	9
CD4	1.2 ± 0.7	1.7 ± 1.2	NS	+	8
CD8	2.8 ± 1.3	3.8 ± 1.8	NS	++	8
CD28	0.2 ± 0.3	0.2 ± 0.2	NS	+	4
CD152/CTLA-4	<0.2	<0.2		–	4
CD154/CD40L	<0.2	<0.2		±	4
CD20 and CD22	<0.2	<0.2		++	9
CD40	0.1 ± 0.1	1.0 ± 0.4	NS	±	4
CD68	1.2 ± 0.7	3.2 ± 1.1	***	+++	9
CD80/B7.1	<0.2	0.5 ± 0.2	NS	±	4
CD1a	2.7 ± 1.4	1.2 ± 1.3	NS	±	9
HLA DR	2.4 ± 1.4	1.2 ± 1.1	NS	+++	9
CD15	<0.2	0.4 ± 0.8	NS	±	9

[a] Statistical analysis comparing frequencies of cells in epithelium and subepithelial area was performed with Student's paired *t*-test. *** — $p \leq .001$; ** — $p = .002$ to .01; NS — not significant ($p > .01$).

[b] Number of patients analyzed.

[c] Numbers indicate percentage of marker-positive cells in total number of cells (mean ± 1 SD) as determined by morphometric analysis according to Weibel of immunohistochemically stained cryosections.

[d] In glandular areas, frequency of stained cells located in connective tissue surrounding seromucous glands was scored from – to +++: – — no positive cells detected; ± — 0% to 5% positive cells; + — 5% to 30% positive cells; ++ — 30% to 65% positive cells; +++ — >65% positive cells.

granulocytes ($CD15^+$ cells).

Immune Cells in Surface Epithelium and Excretory Duct Epithelium. Figure 1B is a simplified outline demonstrating the major localization trends of lymphocytes and macrophages in the uvula. The majority of leukocytes were T cells, as defined by CD3 expression (Table 3). Both αβ T cells and γδ T cells were present throughout the epithelium. However, the cells tended to preferentially localize in the vicinity of the basal lamina (Fig 3A,C). αβ T cells predominated over γδ T cells, with a TcR-$\alpha\beta^+$/TcR-$\gamma\delta^+$ ratio of 2.5 ± 1.6 (n = 7). Further, $CD8^+$ cells were frequent and predominated over $CD4^+$ cells (Fig 3B and Table 3), with an average CD4/CD8 ratio of 0.4. The sum of $CD8^+$ cells and $CD4^+$ cells often exceeded the number of T cells in the individual samples. Virtually no cells expressing the coreceptors CD28, CD152/CTLA-4, or CD154/CD40L or the B cell markers CD20 and CD22 were detected within the epithelium (Table 3).

Intraepithelial tissue macrophages, defined as $CD68^+$ cells, were present in all samples and were preferentially located adjacent to the basal lamina. Because it has been shown that macrophages can express CD4,[22] it is possible that some of the $CD4^+$ cells are indeed macrophages rather than T cells (see above).

The proportion of cells expressing the Langerhans' cell marker CD1a and HLA-DR was almost 3% of all cells in the epithelium. The $CD1a^+$ cells were spread, singly or in small clusters, in different parts of the epithelium. In all samples, $CD1a^+$ cells with epithelial morphology were seen in the vicinity of $CD1a^+$ cells with typical dendritic morphology (Fig 2F). This staining pattern could be due either to an extended dendritic network or to an ectopic induction of CD1a on adjacent epithelial cells.[11,23]

$CD3^+$ and $CD8^+$ cells were also present between the epithelial cells lining the glandular ducts, whereas no $CD4^+$ or TcR-$\gamma\delta^+$ cells were detected at this location. In contrast to the surface epithelium, the ductal epithelium harbored B cells; however, they did not express the B cell coreceptor CD40. The ductal epithelium also contained $CD80^+$ and $CD68^+$ cells.

Immune Cells in Subepithelial Area. T cells ($CD3^+$ cells) predominated also in the subepithelial area, with αβ T cells being present at a higher frequency than γδ T cells (TcR-$\alpha\beta^+$/TcR-$\gamma\delta^+$ ratio of 1.4 ± 0.7; n = 9; Table 3). The frequency of γδ T cells was significantly higher in the subepithelial area than in the epithelium ($p < .01$; Table 3). $CD8^+$ cells predomi-

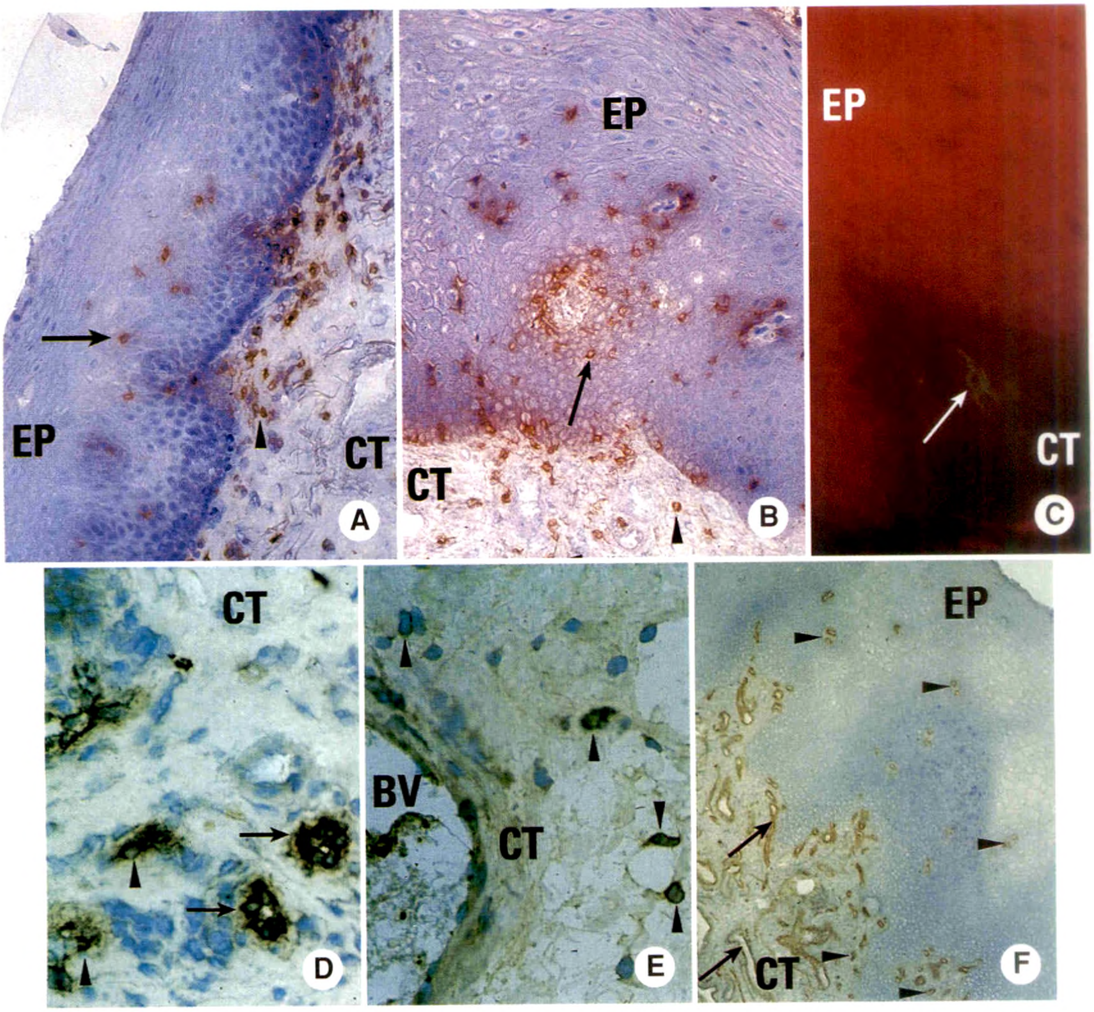

Fig 3. Immunohistochemical staining of cryosections from uvula tissue. A) Immunoperoxidase staining with anti-CD3 mAb T3-4B5 (original ×64). CD3$^+$ cells can be seen in surface epithelium (EP) and in subepithelial connective tissue (CT). Arrow — intraepithelial CD3$^+$ cell; arrowhead — subepithelial CD3$^+$ cells. B) Immunoperoxidase staining with anti-CD8 mAb DK 25 (original ×64). CD8$^+$ cells can be seen in surface epithelium (EP) and in subepithelial connective tissue (CT). Arrow — intraepithelial CD8$^+$ cell; arrowhead — subepithelial CD8$^+$ cell. C) Immunofluorescence staining with anti–TcR-$\gamma\delta$ mAb TCRδ1 (original ×160). Counterstained with Evans blue. Subepithelial $\gamma\delta$ T cells (arrow) in connective tissue (CT) of lamina propria. EP — surface epithelium. D) Immunoperoxidase staining with anti–TNF-α mAb 301 (original ×128). Single TNF-α–positive cells (arrowheads) can be seen in connective tissue (CT) of lamina propria. Endothelial cells in blood vessels (arrows) showed intense membrane staining with anti–TNF-α mAb. E) Immunoperoxidase staining with anti–TGF-β specific antibodies (original ×128). Single TGF-β–positive cells (arrowheads) were detected in connective tissue (CT) of lamina propria. BV — blood vessel. F) Immunoperoxidase staining with IL-6 mAb 18871A (original ×16). Scattered single cells with immune cell morphology were seen (arrowheads). In addition, endothelial cells within subepithelial blood vessels showed intense staining (arrows). EP — surface epithelium; CT — connective tissue of lamina propria.

nated over CD4$^+$ cells, with an average CD4/CD8 ratio of 0.4. The sum of CD4$^+$ and CD8$^+$ cells was higher than the number of CD3$^+$ cells. T cells expressing the coreceptor CD28 were uncommon, and the few CD28$^+$ cells detected were located in close contact with the basal lamina.

Tissue macrophages (CD68$^+$ cells) constituted the second largest immune cell population in the subepithelial area and were more frequent than in the epithelium (Table 3). They were distributed throughout the compartment, but were concentrated in the vicinity of the basal lamina (Fig 2D). CD1a$^+$ cells equaled the number of HLA DR$^+$ cells, but were fewer than the CD68$^+$ cells — findings that suggest that both activated and resting macrophages are present. Indeed, the presence of CD80/B7.1$^+$ cells suggests the presence of functional antigen-presenting cells (Table 3). The majority of CD1a$^+$ cells had the morphology of dendritic cells, but a few cells in conglomerates had a lymphocyte appearance (Fig 2E).

There were no B cells, as defined by CD20, CD22, and/or CD40 expression, in the subepithelial com-

TABLE 4. FREQUENCY OF CYTOKINE-PRODUCING IMMUNE CELLS IN HUMAN UVULA AS DETERMINED BY IMMUNOMORPHOMETRY

	% Positive Cells					Frequency of Positive Cells	
Cytokine	*Surface Epithelium*	*n*[a]	*Subepithelial Area*	*n*	*Significance*[b]	*Glandular Area*	*n*
TGF-β	1.1 ± 0.3[c]	9	1.1 ± 0.5	9	NS	±[d]	9
IL-10	0.3 ± 0.3	9	0.3 ± 0.2	9	NS	+	9
IFN-γ	0.5 ± 0.2	9	0.3 ± 0.2	9	NS	±	9
IL-2	0.4 ± 0.1	4	0.2 ± 0.2	4	NS	–	4
TNF-α	0.2 ± 0.2	9	2.0 ± 1.1	9	***	+	9
IL-6	0.1 ± 0.1	6	0.5 ± 0.3	9	NS	+	9

[a] Number of patients analyzed.

[b] Statistical analysis comparing frequencies of cells in epithelium and subepithelial area was performed with Student's paired *t*-test. *** — $p \leq .001$; NS — not significant ($p > .01$).

[c] Numbers indicate percentage of cells stained by different mAbs of total number of cells (mean ± 1 SD) as determined by morphometric analysis according to Weibel's point-counting technique of immunohistochemically stained cryosections.

[d] In glandular areas, relative frequencies of positive cells were scored: – — not detected; ± — present but infrequent; + — present in significant numbers (3% to 15%).

partment, nor could any cells expressing IgA, IgG, or IgM be detected in this area.

Granulocytes (CD15$^+$ cells) were seen in 6 of 9 samples. They were located in small aggregates in the lamina propria and at the luminal side of the endothelial cells in blood vessels.

Immune Cells in Glandular Area. Leukocytes (CD45$^+$ cells) were present in the narrow connective tissue septa embracing the seromucous glands (Fig 2B). The microanatomical structure of the glandular area made it impossible to apply the point-counting technique of Weibel; therefore, the frequency was estimated semiquantitatively (Table 3). Tissue macrophages (CD68$^+$ cells) predominated and displayed the same distribution pattern as HLA DR$^+$ cells (Fig 2D). Further, based on location, it appears as if CD1a$^+$ cells and CD80$^+$ cells were subpopulations of CD68$^+$ cells.

The majority of lymphocytes were TcR-αβ$^+$ and CD8$^+$ cells. T cells expressing the coreceptors CD28 and CD154/CD40L were rare, and CD152/CTLA-4$^+$ cells were not detected. The glandular area was devoid of γδ T cells. B cells (CD20/CD22$^+$ cells) were as frequent as CD8-expressing cells. The distribution of the IgA-, IgG-, and IgM-positive cells coincided with the distribution of B cells, and the sum of immunoglobulin-positive cells equaled the number of B cells; these findings suggest that plasma cells are absent, because they lack the B cell markers used here. Granulocytes (CD15$^+$) were infrequent and unevenly distributed as single cells or in small cell aggregates adjacent to the glands.

Cytokine Expression of Immune Cells in Uvula Tissue. Uvula tissue was analyzed for the presence of cells producing 1) the regulatory cytokines TGF-β and IL-10, 2) the cell-mediated immunity–associated cytokines IFN-γ and IL-2, and 3) the proinflammatory cytokines TNF-α and IL-6.

On average, 1% of all cells within the surface epithelium and in the subepithelial area were stained with anti–TGF-β antibodies (Table 4 and Fig 3E). These cells were often located in the connective tissue close to the basal lamina. Only occasional TGF-β$^+$ cells were detected in the glandular area and the ductal epithelium. IL-10$^+$ cells were present at very low frequency in all 3 compartments (Table 4).

A small fraction of cells were stained by anti–IL-2 and anti–IFN-γ mAbs and preferentially located in the basal part of the surface epithelium (Table 4). The IL-2$^+$ and IFN-γ$^+$ cells in the subepithelial area were often seen in close contact with endothelial cells of blood vessels. No IL-2$^+$ cells and only occasional IFN-γ$^+$ cells were detected in the glandular area.

TNF-α$^+$ cells were present throughout the uvula tissue, but were most prominent in the subepithelial area, in which they constituted approximately 2% of the cells (Table 4). IL-6$^+$ cells displayed the same distribution pattern as TNF-α$^+$ cells, but were present at a lower frequency. In addition to single cells, the endothelial cells delineating blood vessels in the subepithelial area were stained with the anti–TNF-α and anti–IL-6 mAbs (Fig 3D,F). In the glandular area, intensely stained TNF-α$^+$ and IL-6$^+$ cells, enclosing the glands like baskets, were seen.

Phenotype of Epithelial Cells in Surface Epithelium, and Epithelium of Glands and Glandular Ducts. All epithelial cells in the basal layers of the surface epithelium, and cells in the single-layered epithelium lining the ducts and on the basolateral side of the glands, expressed the epithelial antigen detected by mAb BerEP4 (Fig 2C).

DISCUSSION

This is, to the best of our knowledge, the first investigation characterizing the leukocyte population and the local cytokine production in the uvula. The study material consisted of uvula tissue from patients with mild sleep disorders. The fact that no differences in immune cell composition, distribution, or frequency were noted between the 2 patient groups — ie, social obstructive snorers with apnea-hypopnea indexes of 1 to 4 and patients with sleep apnea syndrome and apnea-hypopnea indexes between 6 and 16 — suggests that the results reflect the immune status in normal uvula tissue. Tissue macrophages, $\alpha\beta$ T cells, $\gamma\delta$ T cells, and B cells were, in declining order of frequency, the main immune cell populations. They showed distinct distribution patterns in the 3 compartments of the uvula. Almost all $\gamma\delta$ T cells resided in the vicinity of and within the epithelium, whereas all B cells were found between the glands and in glandular ducts. $\alpha\beta$ T cells were present at all 3 microanatomical sites. Tissue macrophages, although present throughout the tissue, preferentially homed to the subepithelial and glandular areas. The frequencies of T cells in the epithelium and the subepithelial area of the uvula were similar to the frequencies of T cells in the corresponding compartments of palatine tonsils.[13]

The intraepithelial and subepithelial connective tissue $\alpha\beta$ T cells seem to comprise the same T cell subtypes. In these 2 areas there was a marked predominance of $CD8^+$ cells over $CD4^+$ cells. Because the sum of $CD8^+$ and $CD4^+$ cells exceeded the number of T cells ($CD3^+$ and TcR^+) in most samples and it has been shown that macrophages can express CD4,[22] it is possible that some of the $CD4^+$ cells are macrophages rather than T cells. That cells expressing the costimulatory receptor CD28 were generally not detected implies that most $\alpha\beta$ T cells in the uvula are not conventional T helper cells ($CD4^+CD28^+$ and $TcR\text{-}\alpha\beta^+$) or cytotoxic T cells ($CD8^+CD28^+$ and $TcR\text{-}\alpha\beta^+$), but rather, that they may have suppressive functions. Indeed, 15% to 25% of the leukocytes in these 2 compartments produced the down-regulatory cytokine TGF-β. These cells were localized in the lower third of the epithelium and juxtaposed to the basal lamina on the subepithelial side. In human jejunum, a suggested site for induction of oral tolerance,[6] the quantitatively dominating $CD8^+CD28^-TcR\text{-}\alpha\beta^+$ cell population[10] is considered to be involved in the oral tolerance phenomenon. Moreover, jejunal intraepithelial lymphocytes can be induced to express TGF-β1 upon in vitro activation.[24] Although the uvula only transiently encounters inhaled and ingested antigens, it might serve as an additional site for induction of mucosal tolerance.

The epithelium and the subepithelial area also harbored $\gamma\delta$ T cells. However, in contrast to the intestinal,[10] gingival,[11] and nasal mucosae,[25] the frequency of $\gamma\delta$ T cells was significantly higher in the subepithelial area compared to the epithelium. McMenamin et al[26,27] have shown that $\gamma\delta$ T cells specifically down-regulate IgE production against inhaled protein antigens. $\gamma\delta$ T cells have been attributed an essential role in local tissue defense accomplished by stimulating macrophages to TNF-α production.[28] In the uvula, TNF-α–producing cells show the same tissue distribution as macrophages ($CD68^+$ cells), and this finding suggests that the majority of TNF-α^+ cells are indeed macrophages. Interestingly, cells producing IFN-γ, which activates macrophages, were detected in proximity to the basal lamina and the TNF-α^+ cells. We have previously shown that activated $\gamma\delta$ T cells in chronically inflamed periodontitis gingiva produce IFN-γ.[23] It is possible that at least some IFN-γ–producing cells in the uvula are indeed $\gamma\delta$ T cells.

Tissue macrophages ($CD68^+$ cells) constituted the major subepithelial immune cell population and showed a similar location to that of TNF-α– and IL-6–producing cells — a finding suggesting that they are activated cytokine-secreting cells. Most macrophages were situated juxtaposed to the surface epithelium. In analogy, tissue macrophages in human colonic mucosa are located in the lamina propria adjacent to the basal lamina of the luminal epithelium.[29] These observations indicate that tissue macrophages in the uvula and in the intestine form a secondary defense barrier with the possible function of eliminating pathogenic microorganisms that have penetrated through the epithelium.

B cells, as defined by CD20/CD22 expression, were present in moderate numbers in the connective tissue septa enclosing the seromucous acini and muscle fibers. However, no typical antibody-secreting plasma cells were detected, nor were the glandular epithelial cells stained by anti-IgA antibodies. Thus, so far, there is no evidence that the uvula contributes to the humoral defense of the oral cavity.

Taken together, the results suggest that the uvula may be an additional site for induction and/or maintenance of mucosal tolerance. Concomitantly, the uvula appears to be protected from invasion by pathogens by a line of tissue macrophages and $\gamma\delta$ T cells adjacent to the surface epithelium.

ACKNOWLEDGMENTS — The skillful technical assistance of A.-L. Grehn is gratefully acknowledged. We also wish to express our sincere gratitude to Prof S. Hammarström for stimulating discussions and constructive criticism throughout the work.

REFERENCES

1. Fritzell B. The velopharyngeal muscle in speech. An electromyographic and cineradiographic study. Acta Otolaryngol [Suppl] (Stockh) 1969(suppl 250).

2. Ettema SL, Kuehn DP. A quantitative histologic study of the normal human adult soft palate. J Speech Hear Res 1994;37: 303-13.

3. Kuehn DP, Kahane JC. Histologic study of the normal human adult soft palate. Cleft Palate J 1990;27:26-34.

4. Finkelstein Y, Talmi YP, Zohar Y. Readaptation of the velopharyngeal valve following uvulopalatopharyngoplasty. Plast Reconstr Surg 1988;82:20-7.

5. Hester TO, Phillips B, Archer SM. Surgery for obstructive sleep apnea, effects on sleep, breathing and oxygenation. South Med J 1995;88:907-10.

6. Weiner HL. Oral tolerance: immune mechanisms and treatment of autoimmune diseases. Immunol Today 1997;18: 335-43.

7. Friedman A, al-Sabbaga A, Santos LM, et al. Oral tolerance: a biologically relevant pathway to generate peripheral tolerance against external self antigens. Chem Immunol 1994;58: 259-90.

8. Groux H, O'Garra A, Bigler M, et al. A CD4$^+$ T cell subset inhibits antigen-specific T cell responses and prevents colitis. Nature 1997;389:737-42.

9. Trejdosiewicz LK, Smart CJ, Oakes DJ, et al. Expression of T cell receptors TcR1 (γ/δ) and TcR2 (α/β) in the human intestinal mucosa. Immunology 1989;68:7-12.

10. Lundqvist C, Baranov V, Hammarström S, Athlin L, Hammarström M-L. Intra-epithelial lymphocytes. Evidence for regional specialization and extrathymic T cell maturation in the human gut epithelium. Int Immunol 1995;7:1473-87.

11. Lundqvist C, Hammarström M-L. T-cell receptor $\gamma\delta$–expressing intraepithelial lymphocytes are present in normal and chronically inflamed human gingiva. Immunology 1993;79:38-45.

12. Olofsson K, Hellström S, Hammarström M-L. Abundance of intraepithelial $\gamma\delta$ T cells in hypertrophic obstructive but not in chronically infected adenoids. Clin Exp Immunol 1996;106: 396-403.

13. Olofsson K, Hellström S, Hammarström M-L. The surface epithelium of recurrent infected palatine tonsils is rich in $\gamma\delta$ T cells. Clin Exp Immunol 1998;111:36-47.

14. Söderström K, Bucht A, Halapi E, et al. High expression of Vγ8 is a shared feature of human $\gamma\delta$ T cells in the epithelium of the gut and in the inflamed synovial tissue. J Immunol 1994; 152:6017-27.

15. Komano H, Fujiura Y, Kawaguchi M, et al. Homeostatic regulation of intestinal epithelial γ-δ T cells. Proc Natl Acad Sci U S A 1995;92:6147-51.

16. Constant P, Davodeau F, Peyrat MA, et al. Stimulation of human $\gamma\delta$ T cells by nonpolypeptidic mycobacterial ligands. Science 1994;264:267-70.

17. Chien YH, Jores R, Crowley MP. Recognition by $\gamma\delta$ T cells. Annu Rev Immunol 1996;14:511-32.

18. Kaufmann SH. γ/δ And other unconventional T lymphocytes: what do they see and what do they do? Proc Natl Acad Sci U S A 1996;93:2272-9.

19. Maeurer MJ, Martin D, Walter W, et al. Human intestinal Vδ1$^+$ lymphocytes recognize tumor cells of epithelial origin. J Exp Med 1996;183:681-96.

20. Groh V, Steinle A, Bauer S, Spies T. Recognition of stress-induced MHC molecules by intestinal epithelial $\gamma\delta$ T cells. Science 1998;279:1737-40.

21. Weibel ER, Kistler GS, Scherle WF. Practical stereological methods for morphometric cytology. J Cell Biol 1966;30:23-38.

22. Parnes JR. Molecular biology of CD4 and CD8. Adv Immunol 1989;44:265-311.

23. Lundqvist C, Baranov V, Teglund S, Hammarström S, Hammarström M-L. Cytokine profile and ultrastructure of intraepithelial $\gamma\delta$ T cells in chronically inflamed human gingiva suggest a cytotoxic effector function. J Immunol 1994;153:2302-12.

24. Lundqvist C, Melgar S, Yeung MM-W, Hammarström S, Hammarström M-L. Intraepithelial lymphocytes in human gut have lytic potential and a cytokine profile that suggest T helper 1 and cytotoxic functions. J Immunol 1996;157:1926-34.

25. Pawankar RU, Okuda M, Suzuki K, Okumura K, Ra C. Phenotypic and molecular characteristics of nasal mucosal $\gamma\delta$ T cells in allergic and infectious rhinitis. Am J Respir Crit Care Med 1996;153:1655-65.

26. McMenamin C, Pimm C, McKersey M, Holt PG. Regulation of IgE responses to inhaled antigen in mice by antigen-specific $\gamma\delta$ T cells. Science 1994;265:1869-71.

27. McMenamin C, McKersey M, Kuhnlein P, Hunig T, Holt PG. Gamma delta T cells down-regulate primary IgE responses in rats to inhaled soluble protein antigens. J Immunol 1995;154: 4390-4.

28. Nishimura H, Emoto M, Hiromatsu K, et al. The role of $\gamma\delta$ T cells in priming macrophages to produce tumor necrosis factor–α. Eur J Immunol 1995;25:1465-8.

29. Nagashima R, Maeda K, Imai Y, Takahashi T. Lamina propria macrophages in the human gastrointestinal mucosa: their distribution, immunological phenotype and function. J Histochem Cytochem 1996;44:721-31.

Ann Otol Rhinol Laryngol 109:2000

CONGENITAL DEFECTS OF THE VOMER

MITSUHIRO MOHRI, MD MUTSUO AMATSU, MD

KOBE, JAPAN

Six cases of congenital defect of the vomer, a rare nasal anomaly, are reported. All 6 patients visited Kobe University Hospital with other complaints, and the anomaly was incidentally detected. In all cases, the nasal septum showed a defect at the posteroinferior portion that appeared to coincide with the location of the vomer. None of the patients had a past history of nasal trauma, nasal surgery, drug abuse, or infectious disease. This anomaly may be attributable to an embryological disorder based on an immature ossification center of the vomer.

KEY WORDS — congenital defect, embryology, nasal septum, ossification, vomer.

INTRODUCTION

Among a variety of local and systemic causative factors of nasal septal defects, the most frequent cause is iatrogenic perforation subsequent to bilateral mucosal tears without underlying cartilage or bone during septal surgery. The perforation is usually located at the anterior half of the nasal septum regardless of the etiologic factors. On the other hand, nasal septal defects located at the posterior half are seldom encountered in daily practice. We have encountered 6 such cases. None of these patients had undergone nasal surgery or experienced any trauma to the region. The common and single local finding was a defect of the posteroinferior half of the nasal septum that coincided with the location of the vomer. No deformity was detected in other parts of the body or in the adjacent head and neck region. We present these cases and discuss the possible etiologic factors.

CASE REPORTS

Six patients visited our department at Kobe University Hospital with a variety of complaints unrelated to a nasal or paranasal pathogenesis. Four were male, and 2 were female. Their ages ranged from 4 to 61 years, with a mean age of 38 years. The patient profiles are listed in the Table. None of the patients had a history of nasal or paranasal surgery, cauterization, tuberculosis, syphilis, or drug abuse. Their external noses appeared symmetric and without evidence of deformity or trauma. Flexible fiberoptic examination was carried out transnasally in all 6 patients to examine the nasal cavity and the epipharynx. In each case, the anomaly was detected incidentally. These patients were found to have a posteroinferior defect of the nasal septum that coincided with the location of the vomer (Fig 1A). The margin of the defect was smooth and lined with normal epithelia. The defects showed a slight variety in size and shape. For example, they were wedge-shaped in 2 cases, and oval in 4 cases (Fig 1B). The structure of the nasal cavity and epipharynx was otherwise unremarkable in all cases. A careful examination of the palate also revealed no abnormalities in any of the cases. Computed tomography revealed a defect of the posterior part of the nasal septum (Fig 2).

DISCUSSION

The nasal septum consists of the septal cartilage anteriorly, the perpendicular plate of the ethmoid bone superiorly, and the vomer posteroinferiorly. The vomer is a wedge-shaped bone that connects the hard palate and the superior part of the nasal septum.

Defects of the septum tend to occur in the anteroinferior region, with typical causes being septoplasty, cauterization for epistaxis, drug abuse, and accidental injury.[1] Such defects are usually detected because of symptoms such as nasal crusting and whistling.[2] Closure of the defect is an important goal for rhinologists. To the best of our knowledge, our 6 cases are the first reported defects of the vomer region of the septum. Due to the lack of previous history or associated symptoms, the defects are believed to be

PATIENT PROFILES

Case No.	*Sex*	*Age*	*Disease*
1	F	44	Chronic otitis media
2	M	55	Laryngeal polyp
3	M	61	Acute otitis media
4	M	4	Otitis media with effusion
5	M	39	Pituitary adenoma
6	F	24	Cholesteatoma

From the Department of Otorhinolaryngology–Head and Neck Surgery, Kobe University School of Medicine, Kobe, Japan.

CORRESPONDENCE — Mitsuhiro Mohri, MD, Dept of Otorhinolaryngology–Head and Neck Surgery, Kobe University School of Medicine, 7-5-2 Kusunoki-cho, Chuo-ku, Kobe 650-0017, Japan.

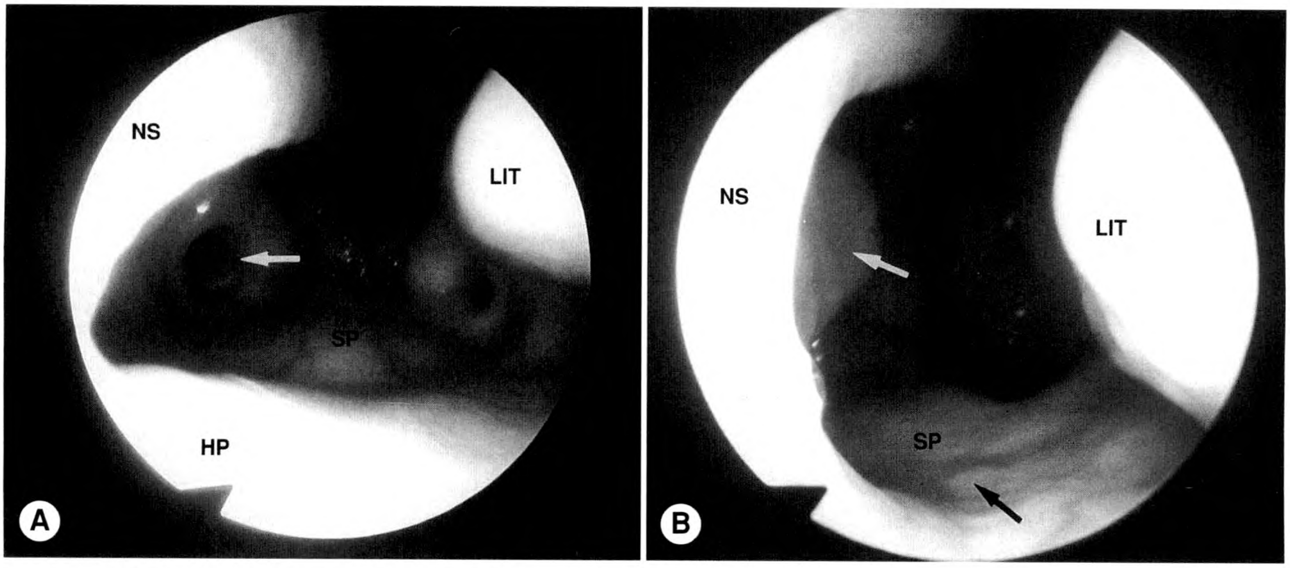

Fig 1. Endoscopic views of congenital defects of vomer through left nasal cavities. NS — nasal septum, LIT — left inferior turbinate. A) (Case 1) Note wedge-shaped defect between posterior end of NS and normal hard palate (HP). Right tubal orifice (arrow), as well as wide nasopharynx, is visible through defect. SP — soft palate, elevated during phonation. B) (Case 6) Note oval defect between NS and posterior end of normal hard palate (black arrow). Right inferior turbinate (white arrow) is visible through defect. SP — soft palate.

congenital.

In human embryological development of the nasal septum and palate, the bilateral primitive nasal cavities are separated by the nasomedial processes, which develop into the primary nasal septum.[3] The mesenchymal cells of primordial tissue, which form the primary nasal septum, gradually extend posteriorly and later grow downward into the oral cavity. About the middle of the second month, shelflike outgrowths of the maxillary processes, referred to as palatal shelves, arise on either side and grow toward the midline. Further growth brings the nasal septum and bilateral palatal shelves into contact with each other and ultimately causes their complete fusion. Thus, the 3 processes fuse at the same time to divide the oral cavity and the nasal cavity. The nasal septum becomes fused to the cephalic face of the palate.

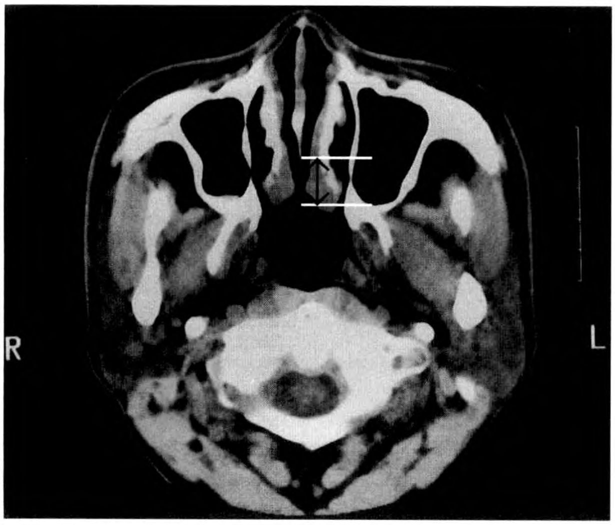

Fig 2. (Case 2) Axial computed tomography of congenital defect of vomer. Note short septum due to defect (arrow).

The vomeral bone develops in 3 steps during the prenatal stage.[4] The earliest appearance of the vomeral bone in the human fetus is at the 8th week of gestation,[5] at which time it appears bilaterally at the posteroinferior end of the cartilaginous nasal septum.[4] These paired vomeral bones fuse to each other in the midline caudal to the nasal septum to form a U-shaped bone in the coronal plane at the 17th gestational week. The base of the U-shaped bony structure is altered by apposition in the median plane during development. The vomeral bone thus appears as a Y-shaped bony structure in the coronal plane.

Based on embryological development, 2 plausible causes can be proposed. The "immature ossification center" theory suggests the presence of an incomplete or immature ossification center that could lead to incomplete development and/or later absorption of the posterior part of the vomer. Accordingly, the degree of maturity of the ossification center can account for the variety in size and shape of the defect. A larger defect may indicate a lower degree of maturation.

The "incomplete downward growth" theory suggests that the posterior extension and downward growth of the primary nasal septum may be stunted, so that the caudal part of the septum cannot reach the palate when the bilateral palatal shelves fuse completely. Even though the ossification center is mature, incomplete downward growth may lead to a defect of the caudal end of the septum. However, such incomplete downward growth may itself be due to immaturity of ossification.

Although none of the patients complained of a nasal disorder, 4 of the 6 presented with bilateral ear diseases, including otitis media with effusion, acute otitis media, chronic otitis media, and cholesteatoma. The pharyngeal orifice of the auditory tube, the hard palate, and the mobility of the soft palate were all macroscopically normal. Although the direct influence of this anomaly on ear diseases is not clear, some kind of relationship may exist.

Because this anomaly is not associated with any nasal disorders, otolaryngologists may easily overlook the posterior end of the nasal septum. Without a flexible endoscope, it is difficult to observe the posteroinferior part of the septum to identify this anomaly, but it should be kept in mind that this anomaly may be encountered during routine clinical examinations.

REFERENCES

1. Seeley RC. Repair of septal perforation, a rhinological problem. A rhinoplastic approach (author's technique). Laryngoscope 1949;59:130-46.
2. Mohammed Y-M. Repair of nasal septal perforation. Am J Rhinol 1997;11:35-40.
3. Patten BM. The normal development of the facial region. In: Pluzansky S, ed. Congenital anomalies of the face and associated structures. Springfield, Ill: Charles C Thomas, 1961:11-45.
4. Sandikcioglu M, Molsted K, Kjaer I. The prenatal development of the human nasal and vomeral bones. J Craniofac Genet Dev Biol 1994;14:124-34.
5. Williams PL, Warwick R, Dyson M, Bannister LH, eds. Gray's anatomy. 37th ed. London, England: Churchill Livingstone, 1989:386.

≈

EUROPEAN SOCIETY OF PEDIATRIC ORL

The Vth International Conference of the European Society of Pediatric ORL will be held July 9-13, 2000, in Graz, Austria. For more information, contact Claire Zwerina, Secretary to Prof Stammberger, ENT-Department, University Hospital, Auenbruggerplatz 20, A-8036 Graz, Austria; fax ++43/316/385/3425.

Ann Otol Rhinol Laryngol 109:2000

ESTIMATED SUBGLOTTIC PRESSURE IN NORMAL AND DYSPHONIC SUBJECTS

ANTOINE GIOVANNI, MD
MARSEILLE, FRANCE

CORINNE HEIM, MD
MARSEILLE, FRANCE

DIDIER DEMOLIN, PHD
BRUSSELS, BELGIUM

JEAN-MICHEL TRIGLIA, MD
MARSEILLE, FRANCE

The objective of this report was to study the clinical interest of estimated subglottic pressure (ESGP) with measurements of intraoral pressure according to the "airway interrupted method." Twenty healthy female subjects and 27 dysphonic female patients were included and asked to produce sounds under different conditions of pitch and intensity. The ESGP increased with intensity and slightly with pitch in both patients and controls. A comparison between patients and controls showed significantly higher values of ESGP in patients under all conditions of intensity and pitch. For normal intensity and usual pitch, ESGP has been found to be 6.1 hectopascals (hPa) in control subjects and 8.25 hPa in patients ($p = .002$). Discriminant analysis of all the measured data showed that data recorded for low intensity (lowest possible intensity without whispering) and high pitch (9 semitones above the usual pitch) were the most discriminant. The authors concluded that ESGP allows good discrimination between dysphonic patients and control subjects and might be included in the basic clinical set of objective parameters.

KEY WORDS — dysphonia, estimated subglottic pressure, objective measurements.

INTRODUCTION

One of the basic assumptions in most studies concerning objective voice analysis for dysphonic patients has been that dysfunction is due to vibratory abnormalities and glottal leakage. Accordingly, most protocols of objective voice analysis have measured either jitter and shimmer, which depend on vibration, or acoustic and aerodynamic parameters, which depend on airflow.[1] Comparisons with perceptual voice analysis confirm that these data are well correlated with roughness and breathiness,[2] which correspond to the R and B factors of the GRBAS (grade, rough, breathy, asthenic, strained) score described by Hirano.[3] However, these correlations are imperfect, and more research is needed to improve the clinical reliability of measurement techniques.

One aerodynamic parameter that has been proposed for voice evaluation is subglottic pressure (SGP).[4] Several physiological studies in normal subjects have shown that SGP increases with the intensity of the voice[4,5] and, to a lesser extent, with pitch.[4,6] It has been shown to be statistically higher in dysphonic patients than in healthy subjects.[7] In dysphonic patients, the abnormal increase of SGP has been attributed to phonatory strain, which corresponds to the increase in both laryngeal resistance and aerodynamic forces.[8]

Several methods have been proposed for measurement of SGP. The direct method consists of placing a pressure transducer either in the subglottal region through the cricothyroid membrane or between the anesthetized vocal cords. Indirect estimation of SGP can be obtained from esophageal pressure measured by means of an intraesophageal catheter when lung pressure is constant.[4] These methods are all relatively invasive and difficult to use in a clinical setting.

Smitheran and Hixon[9] have developed a noninvasive technique of indirect estimation of SGP during a rapid succession of /pi/ sounds. This method is called the "airway interrupted method" (AIM). During production of the /i/ sound, the vocal cords are vibrating, the lips are open, and intraoral pressure (IOP) is equal to atmospheric pressure. Conversely, just before the explosive nonvocal phoneme /p/, the lips are closed, the vocal cords are open and still, and SGP is the same as IOP (Fig 1). Thus, assuming that SGP is constant, IOP just before the explosive /p/ sound should be the same as SGP. The IOP can be measured with a pressure sensor placed in the mouth. Interpolation of IOP during the lip closure phase allows an estimated SGP (ESGP) to be made during the closure phase.

Löfqvist et al[10] confirmed the reliability of the AIM by comparing ESGP and transtracheal measurements

---

From the Laboratoire d'Audio-Phonologie, Université de la Méditerranée, Marseille, France (Giovanni, Heim, Triglia), and the Laboratoire de Phonologie, Université Libre de Bruxelles, Brussels, Belgium (Demolin). This work was supported by a grant from the Assistance Publique Hôpitaux de Marseille (PRA 1050).

CORRESPONDENCE — Antoine Giovanni, MD, Laboratoire d'Audio-Phonologie Clinique, Fédération ORL, CHU Timone, 13385 Marseille Cedex 5, France.

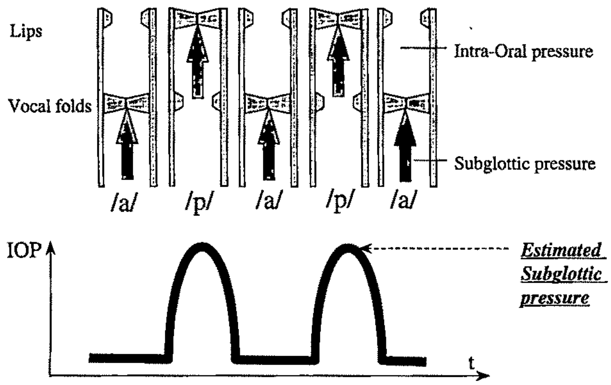

Fig 1. Estimation of subglottic pressure from intraoral pressure (IOP).

made simultaneously. The common variance between the 2 measurements (determination coefficient r^2) was 0.92. The AIM has already been used in the assessment of dysphonia,[1] but further study is necessary to define optimal conditions of pitch and intensity for recording ESGP. Further study is also needed to clarify previous data concerning the differences between men and women. Holmberg et al[5] and Sawashima et al[6] reported no significant difference between the sexes with regard to SGP, whereas Iwata[7] reported that SGP was higher in men than in women at the same intensity.

The twofold purpose of this study was 1) to assess the value of ESGP as a marker of dysphonia by comparing ESGP values in dysphonic patients and controls and 2) to ascertain optimal pitch and intensity conditions for objective voice evaluation in women.

PATIENTS AND METHODS

The voices of 27 women consulting for dysphonia were recorded. The cause of dysphonia was nodules in 12 cases, Reinke's edema in 6 cases, postoperative vocal cord lesions in 3 cases, sulcus glottidis in 3 cases, angiomatous polyp in 1 case, epidermoid cyst in 1 case, and bilateral leukoplakia in 1 case. The mean patient age was 40 years (range, 13 to 69). Recordings were also made in 20 female controls with no history of voice disorder. The mean age of the controls was 27 years (range, 21 to 45).

TABLE 1. ESTIMATED SUBGLOTTIC PRESSURE VALUES MEASURED IN CONTROLS UNDER DIFFERENT CONDITIONS

Conditions	*Mean*	*Standard Deviation*	*95% Confidence Interval (Upper Limit)*
Fu and LI	3.89	1.21	4.45
Fu and MLI	4.89	0.96	5.33
Fu and NI	6.10	1.19	6.66
Fu and MHI	7.79	1.26	8.43
Fu and HI	9.89	2.39	11.01
Fu+3 and NI	6.91	1.14	7.45
Fu+6 and NI	7.26	1.36	7.89
Fu+9 and NI	8.30	1.46	8.99

Fu — normal pitch; LI — lowest possible intensity without whispering; MLI — middle low intensity (between LI and NI); NI — normal intensity; MHI — middle high intensity (between NI and HI); HI — highest possible intensity; Fu+3 — normal pitch plus 3 semitones (etc).

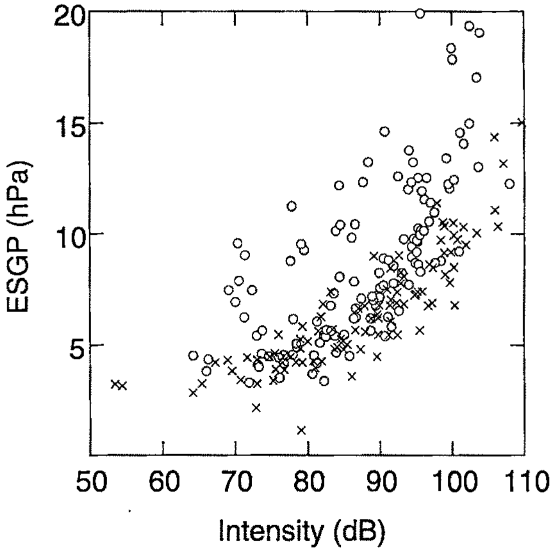

Fig 2. Estimated subglottic pressure (ESGP) values as function of intensity. Crosses — controls; circles — patients; hPa — hectopascals.

Data acquisition and processing were performed with the EVA system, which allows simultaneous measurement of acoustic and aerodynamic dimensions of the voice.[2] Measuring devices including a pressure sensor are arranged in a specially designed mouthpiece. The IOP for calculation of ESGP is measured with a suction catheter (Vygon No. 12, diameter 4 mm) with 2 small side holes in the tip to prevent obstruction by saliva. Acoustic signals are recorded by means of a coaxial AKG C409 microphone located 5 cm from the mouth, behind the buffer screen of the pneumotachograph.

In the pretest phase of the recording session, the examiner determined the normal pitch (Fu) of the subject with reference to musical notes played on a keyboard. The subject was asked to say a sentence with no plosive consonants (in French: *Mélanie a mis l'eau au moulin, elle a mal aux mains*). During test recording, "normal pitch" was used to give keyboard cues in 3-semitone increments, ie, Fu, Fu+3, Fu+6, and Fu+9. Regarding intensity, the subject was instructed to speak at her usual, comfortable level for normal intensity (NI), at the lowest possible level without whispering for low intensity (LI), at the highest possible level for high intensity (HI), at a level between NI and LI for middle low intensity (MLI), and at a level between NI and HI for middle high

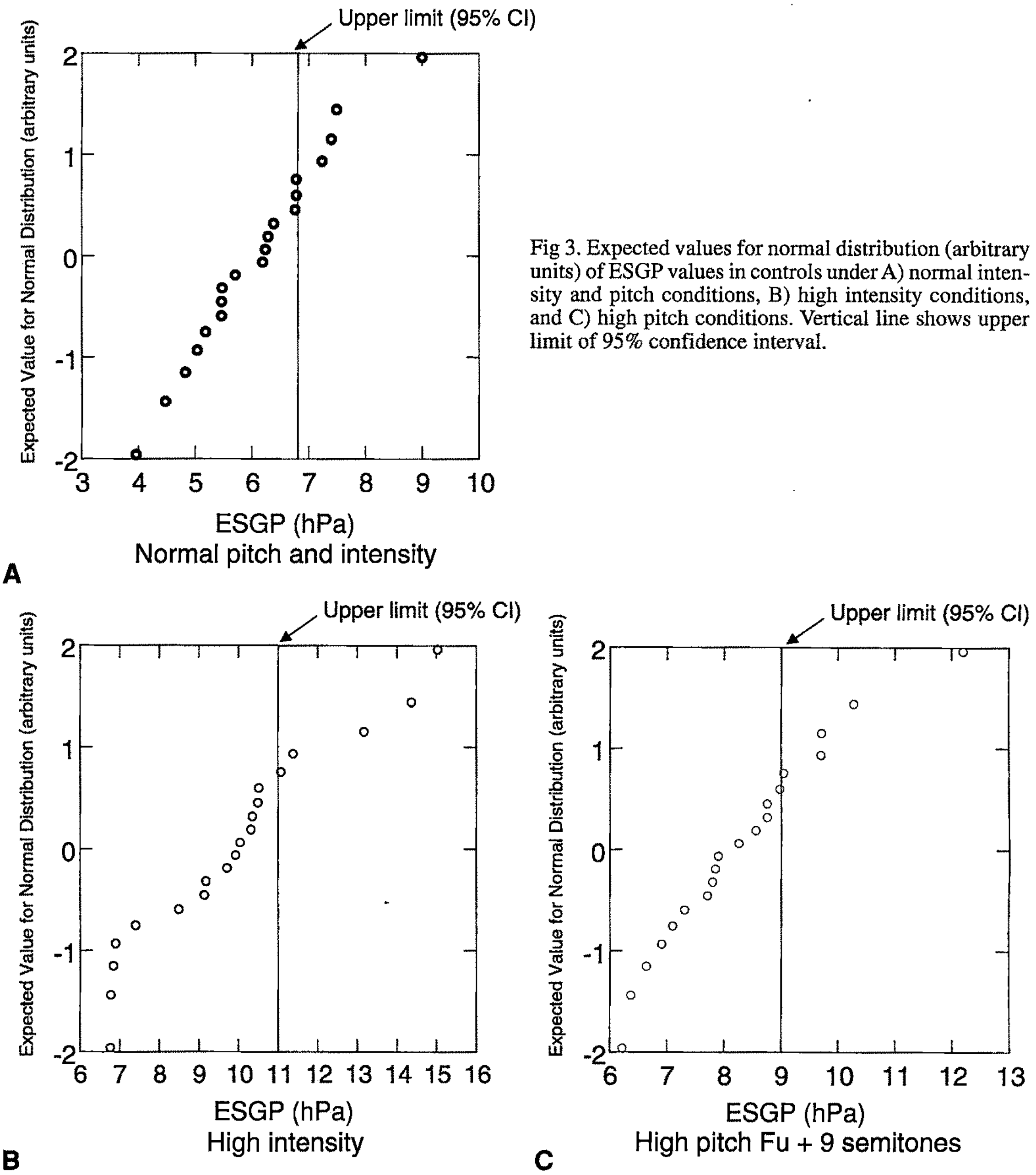

Fig 3. Expected values for normal distribution (arbitrary units) of ESGP values in controls under A) normal intensity and pitch conditions, B) high intensity conditions, and C) high pitch conditions. Vertical line shows upper limit of 95% confidence interval.

intensity (MHI). The judgment of an experienced examiner was crucial in ensuring good compliance with instructions.

During the test phase, subjects pronounced 8 series of 10 /pa/ sounds with an interval of approximately 1 second between each /pa/. Each series was recorded under different pitch and intensity conditions as follows: 1) Fu and NI, 2) Fu and LI, 3) Fu and MLI, 4) Fu and HI, 5) Fu and MHI, 6) Fu+3 and NI, 7) Fu+6 and NI, and 8) Fu+9 and NI. One or more trials were made at each combination of pitch

TABLE 2. ESTIMATED SUBGLOTTIC PRESSURE VALUES MEASURED IN PATIENTS AND CONTROLS AT DIFFERENT INTENSITY LEVELS

	LI	*MLI*	*NI*	*MHI*	*HI*	$ESGP^{DI}$
Controls (n = 20)	3.89 ± 1.21	4.89 ± 0.96	6.10 ± 1.19	7.79 ± 1.26	9.89 ± 2.39	0.66 ± 0.46
Patients (n = 27)	5.87 ± 2.14	6.81 ± 2.59	8.25 ± 2.94	9.90 ± 3.15	12.31 ± 3.69	0.58 ± 0.48
p	<.001	.001	.002	.004	.011	.362*

Data are mean ± SD.

$ESGP^{DI}$ — difference between estimated subglottic pressure at NI and estimated subglottic pressure at HI.

*Not significant.

TABLE 3. ESTIMATED SUBGLOTTIC PRESSURE VALUES MEASURED IN PATIENTS AND CONTROLS AT DIFFERENT PITCH LEVELS

	Fu	*Fu+3*	*Fu+6*	*Fu+9*	*$ESGP^{DF}$*
Controls (n = 20)	6.10 ± 1.19	6.91 ± 1.14	7.26 ± 1.36	8.30 ± 1.46	0.19 ± 0.20
Patients (n = 27)	8.25 ± 2.94	9.93 ± 3.32	11.38 ± 4.98	11.44 ± 3.16	0.42 ± 0.52
p	.002	<.001	<.001	<.001	.156*

Data are mean ± SD.

$ESGP^{DF}$ — difference between ESGP at Fu and ESGP at Fu+9.

*Not significant.

and intensity. The examination lasted approximately 20 minutes.

The difference between ESGP at Fu and ESGP at Fu+6 was calculated as follows: $ESGP^{DF} = (ESGP^{FU+6} - ESGP^{FU})/ESGP^{FU}$. The difference between ESGP at NI and ESGP at HI was calculated as follows: $ESGP^{DI} = (ESGP^{HI} - ESGP^{NI})/ESGP^{NI}$.

Data were analyzed with Systat software. The 2 groups were compared at each combination of pitch and intensity by the nonparametric Mann-Whitney test. The limit for rejection of the null hypothesis was $p < .05$. Discriminant factor analysis was performed with the principal component analysis technique.

RESULTS

Under normal pitch and intensity conditions, the mean ESGP in the control group was 6.10 hectopascals (hPa) with an upper limit of the 95% confidence interval of 6.66. As shown in Table 1, ESGP increased sharply with intensity (mean 9.89 hPa for high intensity) and only slightly with pitch (mean 8.30 hPa at FU+9 semitones). As shown in Figs 2 and 3A,B, the value distribution was approximately normal.

As in controls, ESGP in patients increased sharply with intensity and only slightly with pitch (Tables 2 and 3). However, ESGP was significantly higher in patients than controls under all conditions of intensity and pitch. There was no significant difference between controls and patients with regard to either $ESGP^{DF}$ or $ESGP^{DI}$. Discriminant analysis using data obtained at each intensity allowed discrimination of controls and patients in 74% of cases (Wilks λ =

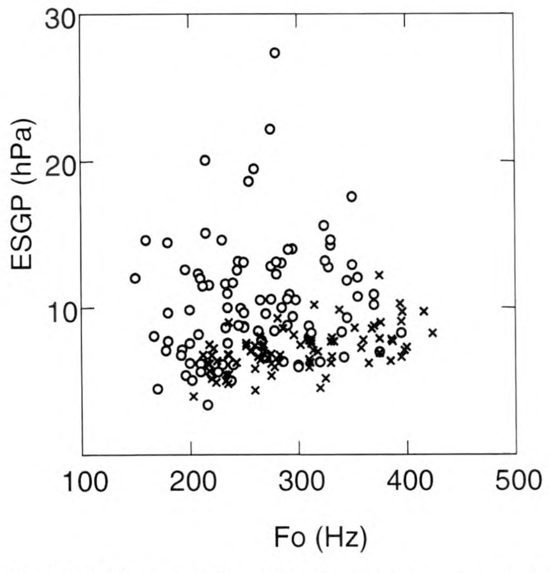

Fig 4. ESGP as function of pitch. Crosses — controls; circles — patients; Fo — fundamental frequency.

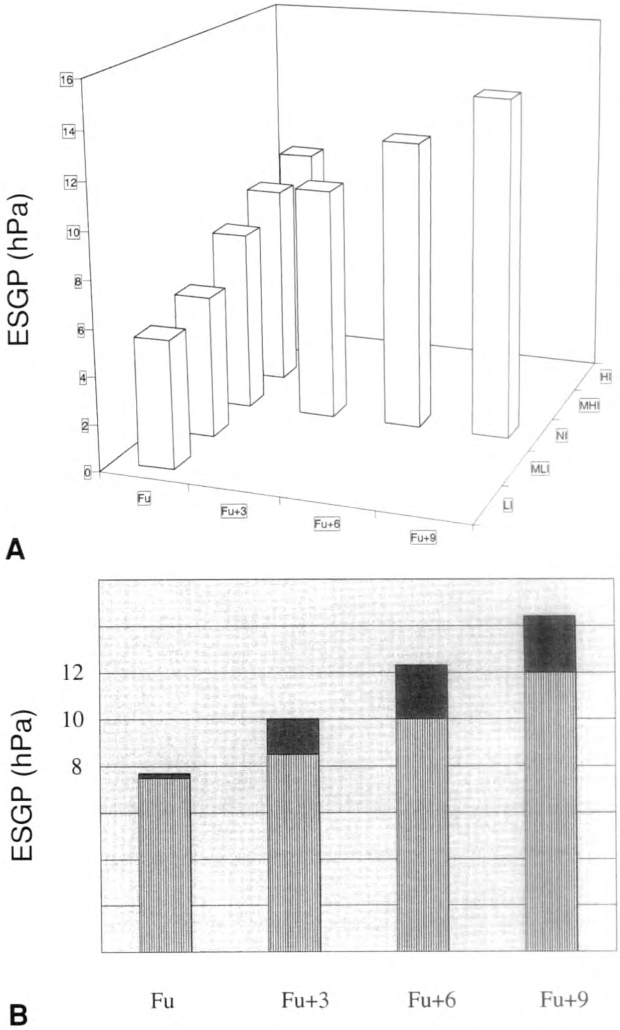

Fig 5. Data from 49-year-old female patient presenting bilateral nodules. A) Three-dimensional "phonetogram-like" representation of ESGP as function of pitch and intensity. x-axis — pitch; y-axis — ESGP; z-axis — intensity. B) Bar graph comparing her ESGP with mean ESGP in controls. Dark gray zones indicate elevated ESGP.

0.021). Discriminant analysis using data obtained at each pitch allowed discrimination of controls and patients in 83% of cases (Wilks $\lambda = 0.016$). Analysis of canonical coefficients confirmed that values measured at low intensity and at high pitch were the most discriminant (Fu, 0.036; Fu+3, 0.044; Fu+6, 0.230; Fu+9, 0.254; LI, 0.489; MLI, 0.293; NI, 0.304; MHI, 0.050; and HI, 0.002). The graphs in Figs 3C and 4 illustrate the difference between the 2 groups.

Figure 5A shows a graph plotted with data obtained in a 49-year-old female patient with nodules. At normal pitch, ESGP was slightly higher than the upper limit of 95% CI (7.7 versus 6.66 hPa). At high pitch FU+9), ESGP was almost twofold higher (14 hPa), and significantly higher than the upper limit of 95% CI (8.99 hPa). Figure 5B compares values collected in the same patient with the mean normal value for each level of pitch.

DISCUSSION

The results of this study confirm that ESGP is always higher in dysphonic female patients than in healthy female controls, regardless of pitch and intensity.[11] Although clinical findings remain the mainstay of diagnosis, this finding suggests that measurement of ESGP should be included in patient workup. More generally, our findings indicate that ESGP is a robust indicator for objective voice analysis to distinguish between normal and dysphonic subjects. However, data must be interpreted as a function of sample recording conditions. In our study, the upper limit of the 95% confidence interval was 6.66 hPa under normal conditions, 9.89 for high intensity, and 8.30 for loud voice.

Unlike previous authors, we did not take into account the position of the catheter in the mouth. Baken[1] stated that catheter placement was a key issue in reliable measurement of ESGP and developed a system using an impression of the canine teeth to hold the catheter in place. We encountered no problems related to catheter position, probably because our catheter was rigid enough to resist compression by the teeth and featured several side holes to prevent obstruction by saliva.

The results of discriminant analysis and analysis of canonical coefficients confirmed that values measured at low intensity and values measured at high pitch were the most discriminant. At low intensity, dysphonic patients always required higher ESGP than normal subjects to initiate vocal fold vibration. This difference could result from excessive stiffness due to vocal fold lesions or abnormal muscle tension. As described by Titze,[12] phonation threshold pressure could be a useful clinical parameter. At high pitch, the difference between control subjects and patients is even more marked, because of the stiffening of the vocal fold necessary to increase pitch.

On the basis of this study, we conclude that ESGP allows discrimination between dysphonic patients and control subjects and could be included in the basic clinical set of objective parameters. Our findings further suggest that sensitivity could be optimized by making test recordings at the lowest intensity and highest pitch. A possible format for presentation of ESGP would be a 3-dimensional phonetogram-like graph showing the intensity-pitch relationship as shown in Fig 5A. However, further study will be necessary to correlate ESGP results with those obtained by perceptual voice analysis.

REFERENCES

1. Baken RJ. Clinical measurement of speech and voice. Boston, Mass: Little, Brown, 1987.

2. Giovanni A, Robert D, Estublier N, Teston B, Zanaret M, Cannoni M. Objective evaluation of dysphonia: preliminary results of a device allowing simultaneous acoustic and aerodynamic measurements. Folia Phoniatr Logop 1996;48:175-85.

3. Hirano M. Objective evaluation of the human voice, clinical aspects. Folia Phoniatr (Basel) 1989;41:69-144.

4. Schutte HK. The efficiency of voice production. Groningen, the Netherlands: Kemper, 1980.

5. Holmberg EB, Hillman RE, Perkell JS. Glottal airflow and transglottal air pressure measurements for male and female speakers in soft, normal and loud voice. J Acoust Soc Am 1988; 60:511-28.

6. Sawashima M, Niimi S, Horiguchi S, Yamaguchi H. Expiratory lung pressure, airflow rate, and vocal intensity: data on normal subjects. In: Fujimura O, ed. Vocal physiology: voice production, mechanisms and functions. New York, NY: Raven Press, 1988:415-22.

7. Iwata S. Aerodynamic aspects for phonation in normal and pathologic larynges. In: Fujimura O, ed. Vocal physiology: voice production, mechanisms and functions. New York, NY: Raven Press, 1988:423-31.

8. Le Huche F, Allali A. La voix, pathologies vocales. Paris, France: Masson, 1990.

9. Smitheran JR, Hixon T. A clinical method for estimating laryngeal airway resistance during vowel production. J Speech Hear Disord 1981;46:138-46.

10. Löfqvist A, Carlborg B, Kitzing P. Initial validation of an indirect measure of subglottal pressure during vowels. J Acoust Soc Am 1982;72:633-5.

11. Piccirillo JF, Painter C, Fuller D, Haiduk A, Fredrickson JM. Assessment of two objective voice function indices. Ann Otol Rhinol Laryngol 1998;107:396-400.

12. Titze IR. Phonation threshold pressure: a missing link in glottal aerodynamics. J Acoust Soc Am 1992;91:2926-35.

Ann Otol Rhinol Laryngol 109:2000

THREE-DIMENSIONAL ANATOMIC CHARACTERIZATION OF THE CANINE LARYNGEAL ABDUCTOR AND ADDUCTOR MUSCULATURE

COREY W. MINECK, MD
MEMPHIS, TENNESSEE
ROGER CHAN, PHD
IOWA CITY, IOWA
NIRO TAYAMA, MD
TOKYO, JAPAN
INGO R. TITZE, PHD
IOWA CITY, IOWA

The biomechanics of vocal fold abduction and adduction during phonation, respiration, and airway protection are not completely understood. Specifically, the rotational and translational forces on the arytenoid cartilages that result from intrinsic laryngeal muscle contraction have not been fully described. Anatomic data on the lines of action and moment arms for the intrinsic laryngeal muscles are also lacking. This study was conducted to quantify the 3-dimensional orientations and the relative cross-sectional areas of the intrinsic abductor and adductor musculature of the canine larynx. Eight canine larynges were used to evaluate the 3 muscles primarily responsible for vocal fold abduction and adduction: the posterior cricoarytenoid, the lateral cricoarytenoid, and the interarytenoid muscles. Each muscle was exposed and divided into discrete fiber bundles whose coordinate positions were digitized in 3-dimensional space. The mass, length, relative cross-sectional area, and angle of orientation for each muscle bundle were obtained to allow for the calculations of average lines of action and moment arms for each muscle. This mapping of the canine laryngeal abductor and adductor musculature provides important anatomic data for use in laryngeal biomechanical modeling. These data may also be useful in surgical procedures such as arytenoid adduction.

KEY WORDS — abduction, adduction, arytenoid cartilage, laryngeal anatomy, laryngeal muscle, vocal fold.

INTRODUCTION

The physiology and biomechanics of vocal fold abduction and adduction during phonation, respiration, and airway protection (eg, in swallowing) are beginning to be understood on a quantitative level. Traditionally, it has been assumed that each laryngeal muscle functions as a unit, with a single direction of action. However, recent research has demonstrated that at least some of the intrinsic laryngeal muscles are composed of different compartments that may function independently. For example, Sanders et al[1-4] showed that the posterior cricoarytenoid (PCA) muscle has 2 or 3 separate bellies that may each function as an independent unit during different types of abduction. Sanders et al[3,4] also showed that the innervation of the human PCA muscle stems from 2 separate nerve branches to supply 2 different compartments, further lending support to independent function. Therefore, it was the purpose of this study to characterize the 3-dimensional (3-D) orientations and relative cross-sectional areas of the laryngeal abductor and adductor muscles for the purpose of biomechanical modeling. The canine larynx was chosen because the active contractile properties of some canine laryngeal muscles had previously been measured.[5-7] Because it is practically difficult to measure the active properties of viable human laryngeal muscles (the tissue must be removed before death), an animal model is desirable, and dogs offer a model similar to the human larynx in laryngeal muscle morphology, anatomy, and possibly function.

The motion of the arytenoid cartilage on the cricoarytenoid joint (CAJ) is complex and has been examined extensively.[8-14] Classically, arytenoid motion on the CAJ has been described as a rotation around a "vertical" axis.[15] However, many anatomic and vocal fold kinematic studies have suggested that the 2 major arytenoid motions are 1) rocking around the longitudinal axis of the CAJ facet in a somewhat anterior-posterior direction and 2) sliding along this axis in a somewhat medial-lateral direction.[8,10,11,13,14] Selbie et al[14] showed that the rocking axis could be congruent with the classic "vertical" axis, such that the rocking motion is often perceived as a rotation under the perspective of an endoscope. Current beliefs suggest that the arytenoid motion is critically determined by several major factors, including the geometry of the CAJ facets, the anatomy of the fibro-

---

From the National Center for Voice and Speech, Department of Speech Pathology and Audiology, University of Iowa, Iowa City, Iowa (all authors), and the Department of Otolaryngology, University of Tokyo, Tokyo, Japan (Tayama). Dr Mineck is currently in the Department of Otolaryngology–Head and Neck Surgery, University of Tennessee, Memphis, Tennessee. This work was supported by grant P60 DC00976 from the National Institutes of Health/National Institute on Deafness and Other Communication Disorders. This study was performed in accordance with the PHS Policy on Humane Care and Use of Laboratory Animals, the NIH *Guide for the Care and Use of Laboratory Animals*, and the Animal Welfare Act (7 U.S.C. et seq.); the animal use protocol was approved by the Institutional Animal Care and Use Committee (IACUC) of the University of Iowa.

CORRESPONDENCE — Roger Chan, PhD, National Center for Voice and Speech, Dept of Speech Pathology and Audiology, 330 WJSHC, University of Iowa, Iowa City, IA 52242.

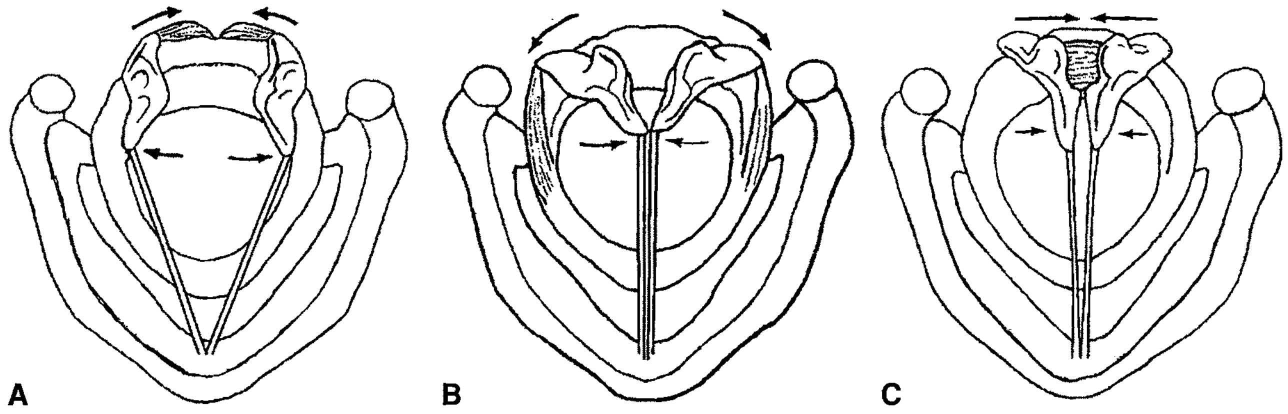

Fig 1. Classic descriptions of arytenoid motion and vocal fold abduction and adduction associated with contraction of A) posterior cricoarytenoid (PCA) muscle, B) lateral cricoarytenoid (LCA) muscle, and C) interarytenoid (IA) muscle. (Copyright 1989. Novartis. Reprinted with permission from the *Atlas of Human Anatomy*, illustrated by Frank H. Netter, MD. All rights reserved.)

elastic connective tissues in the synovial joint, and the actions of the laryngeal abductor and adductor muscles.[16]

The laryngeal abductor and adductor muscles are believed to have rapid contraction rates, especially the lateral cricoarytenoid (LCA) muscle.[17] The isotonic twitch contraction time of the canine LCA muscle has been estimated to be on the order of 10 ms, whereas for the PCA muscle, it was around 30 ms.[17] With such rapid contraction times, these muscles play a primary role in the rapid opening of the glottis during inspiration and in rapid closure of the glottis for protection against foreign body inhalation (eg, during swallowing).

The PCA muscle originates at the posterior surface of the lamina of the cricoid cartilage and converges on the laterally directed muscular process of the arytenoid cartilage. This muscle has been described as having 3 parts in dogs and either 2 or 3 parts in humans. For the canine PCA muscle, a horizontal belly, a vertical belly, and an oblique belly have been described by Sanders et al.[1,2] For the human PCA muscle, Bryant et al[18] described a medial and a lateral belly, but Sanders et al[4] divided this muscle again into horizontal, vertical, and oblique portions. The PCA muscle rocks the arytenoid posteriorly so that the vocal process swings laterally, superiorly, and posteriorly, abducting the vocal fold (Fig 1A).

The LCA muscle originates on the superior border of the anterior arch of the cricoid cartilage and courses posteriorly to the muscular process of the arytenoid cartilage. The LCA muscle is believed to adduct the vocal fold by rocking the arytenoid cartilage anteriorly such that the vocal process moves medially, inferiorly, and anteriorly[19] (Fig 1B).

The interarytenoid (IA) muscle is composed of a transverse portion and an oblique portion. The oblique portion originates on the superior aspect of the arytenoid cartilage, crosses the midline, and inserts into the muscular process of the contralateral arytenoid cartilage. The transverse portion connects the lateral borders of the 2 arytenoid cartilages together. Thus, during IA contraction, the arytenoid cartilages are drawn together, adducting the vocal folds (Fig 1C).

This study was conducted to characterize the 3-D orientations and the cross-sectional areas of the intrinsic abductor and adductor musculature of the canine larynx. Data acquired through this study should be useful in establishing a database for 3-D biomechanical modeling of vocal fold posturing. Specifically, they should allow for calculation of the lines of action and moment arms for the intrinsic laryngeal muscles during vocal fold abduction and adduction.

METHODS

Larynges from 4 female and 4 male dogs were excised postmortem after the dogs underwent cardiovascular experimentation in accordance with the Institutional Animal Care and Use Committee of the University of Iowa. No dogs had evidence of trauma or head and neck disease (Table 1). After harvest, the larynges were either slowly or quickly frozen (with

TABLE 1. SUBJECT INFORMATION

Dog	*Sex*	*Weight (kg)*
1	F	20
2	M	25
3	M	27
4	F	26
5	M	20
6	F	22
7	M	20
8	F	20

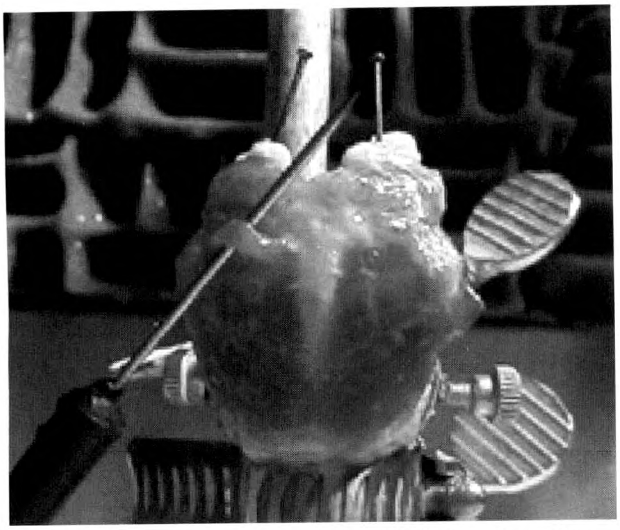

Fig 2. Posterior view of mounted canine larynx shows dissection (isolation) of muscle bundle of left PCA muscle.

liquid nitrogen) and were stored at −20°C. Before dissection, each larynx was thawed overnight in a 4°C refrigerator. Immediately before dissection, larynges were further thawed in physiological saline solution (0.9%).

Each canine larynx was first dissected by means of a blunt instrument technique to expose the PCA, LCA, and IA muscles. Any excess fat or fascial tissue was removed in preparation for mounting and muscle bundle dissection.

The larynx was mounted on a laboratory bench by securing the trachea over a piece of polyvinylchloride tubing with an O-clamp around the first and second tracheal rings. Pincer clamps were used to secure the cricoid cartilage in the anatomic position. The arytenoid cartilages were firmly fixed in the cadaveric position with straight pins such that any rotation or translation of the arytenoid cartilages was eliminated. The larynx was then positioned such that the posterior ridge of the cricoid lamina (the cricoid prominence) between the PCA muscles was vertical (Fig 2).

Once the larynx was mounted, 3-D spatial coordinates for the cricoid cartilage, the arytenoid cartilages, and the laryngeal abductors and adductors were obtained with a MicroScribe-3DX digitizer (Immersion Corp, Salt Lake City, Utah) with HyperSpace Modeler software (Mira Imaging, Salt Lake City). The spatial resolution or accuracy of the system was 0.2 mm. In an effort to normalize the orientation across larynges, the origin for each larynx was defined as the most superior and anterior aspect of the cricoid ring in the midsagittal plane. After origin definition, the coordinates of the most posterior point on the cricoid prominence (between the right and left PCA muscles) were acquired. This point was used as a reference to the origin to establish the y-axis by a translation in the negative y direction with respect to the x direction; changes in the z direction were ignored. The z-axis was established by acquiring a number of points along the cricoid prominence. The x-axis was then empirically established by its orthogonal relationships with the y- and z-axes.

By means of blunt dissection instruments, an individual muscle bundle was carefully isolated and partially separated from the rest of the muscle. Next, its points of origin and insertion were visually identified (Fig 2). In all cases, the geometric center of the point of muscle bundle attachment was used as an estimate of the insertion or origin for that bundle. The coordinates of origin and insertion of each bundle were digitized before the bundle was removed with tissue forceps and iris scissors. The mass of each muscle bundle was measured with a Mettler AE100 laboratory balance with a measurement reliability of 0.1 mg (Mettler Instruments, Hightstown, NJ). Throughout the dissection, saline solution was periodically applied to the larynx to keep the tissues from drying.

The muscles of interest were organized into the following groups: left and right PCAs (further separated into oblique and vertical portions); left and right LCAs; and left and right IAs (further separated into superior and inferior portions).

Geometric Descriptions of Muscles. For each muscle bundle, 6 points were recorded (3 for origin, 3 for insertion). The mean x, y, and z coordinates for each of the 3 samples were calculated to yield an average origin or insertion for each muscle bundle. The length l of each muscle bundle was then calculated from the Pythagorean theorem:

$$l = \sqrt{(x2 - x1)^2 + (y2 - y1)^2 + (z2 - z1)^2} \quad (1)$$

where $x1$, $y1$, and $z1$ are the coordinates of the origin and $x2$, $y2$, and $z2$ are those of the insertion. An orientation vector **r** was defined for each muscle bundle as

$$\mathbf{r} = \mathbf{r}x\mathbf{i} + \mathbf{r}y\mathbf{j} + \mathbf{r}z\mathbf{k} \quad (2)$$

where **i**, **j**, and **k** are unit vectors along the orthogonal axes, and that

$$\mathbf{r}x = x2 - x1 \quad (3)$$

$$\mathbf{r}y = y2 - y1 \quad (4)$$

$$\mathbf{r}z = z2 - z1 \quad (5)$$

As the mass m of each bundle was measured and the length was calculated, the cross-sectional area A was determined by

$$A = \frac{m}{\rho l} \quad (6)$$

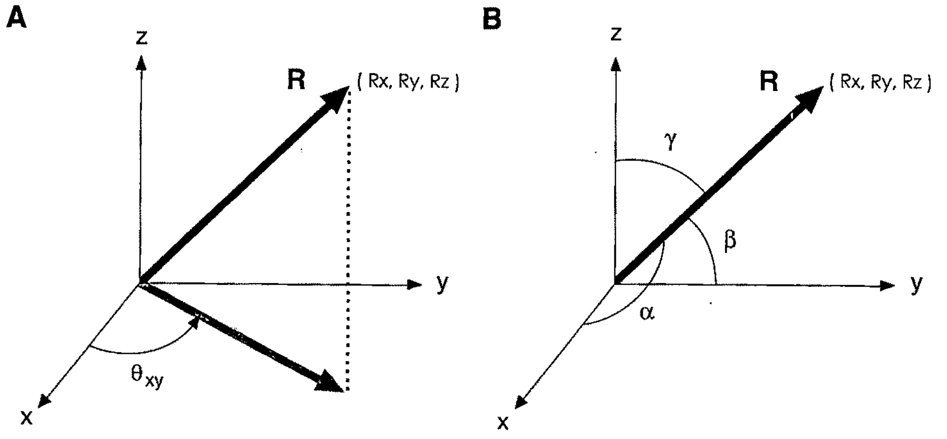

Fig 3. Three-dimensional illustration of A) 2-dimensional projection angle θ_{xy} of vector **R**, and B) angles α, β, and γ of vector **R**.

where ρ is the density of canine laryngeal muscle obtained previously (0.001043 g/mm^2).[20] The assumption here was that the muscle bundle has a uniform cross-sectional area along its entire course.

Resultant Vectors for Muscle Bundle Groups. The relative contribution of each muscle bundle to the total action of a muscle was estimated from cross-sectional area data. The orientation vector **r** for each bundle was multiplied by that bundle's cross-sectional area A. This product was defined as the scaled force vector $\mathbf{r}A$. The assumption here was that all muscle fibers have equal contractile force per unit cross-sectional area. The scaled force vectors were summed and divided by the total cross-sectional area for that grouping of muscle bundles to yield an average *resultant* force vector **R**,

$$\mathbf{R} \equiv \mathbf{R}_x\mathbf{i} + \mathbf{R}_y\mathbf{j} + \mathbf{R}_z\mathbf{k} = \frac{\sum\limits_{i=1}^{n} riAi}{\sum\limits_{i=1}^{n} Ai} \tag{7}$$

A resultant force vector was calculated for each of the following muscle bundle groups, or *muscle portions*: 1) left PCA, oblique portion (L PCA o); 2) left PCA, vertical portion (L PCA v); 3) right PCA, oblique portion (R PCA o); 4) right PCA, vertical portion (R PCA v); 5) left LCA (L LCA); 6) right LCA (R LCA); 7) left IA, inferior portion (L IA inf); 8) left IA, superior portion (L IA sup); 9) right IA, inferior portion (R IA inf); and 10) right IA, superior portion (R IA sup).

Data on the superior portion of the IA muscle are not reported, because its anatomy was found to be grossly different from that of humans. Our observations showed that it did not connect the 2 arytenoid cartilages together. Rather, both its origin and insertion appeared to originate from the same side in the canine larynx.

Planar Projection Angle Calculations. For 2-dimensional (2-D) planar analysis, the resultant force vector **R** for each muscle portion was used to calculate the projection angle in each of the 3 orthogonal planes. The projection angle in the xy plane was calculated from the formula (Fig 3A)

$$\theta_{xy} = \tan^{-1}\frac{\mathbf{R}_y}{\mathbf{R}_x} \tag{8}$$

The positive x direction was medial-to-lateral on the right side, and the positive y direction was posterior-to-anterior. Angles were reported in standard fashion, with positive rotation defined as counterclockwise from the x-axis toward the y-axis.

Projection angles in the yz and xz planes were similarly calculated for each muscle portion:

$$\theta_{yz} = \tan^{-1}\frac{\mathbf{R}_z}{\mathbf{R}_y} \tag{9}$$

$$\theta_{zx} = \tan^{-1}\frac{\mathbf{R}_x}{\mathbf{R}_z} \tag{10}$$

Thus, the xy plane was horizontal, the yz plane sagittal, and the xz plane coronal.

Direction Cosines. For the purpose of 3-D modeling, the direction cosines were also calculated. The direction cosines were defined as the cosine of the angle between a given resultant force vector **R** and each of the 3 axes (Fig 3B),

$$\cos\alpha = \frac{\mathbf{R}_x}{\|\mathbf{R}\|} \qquad \cos\beta = \frac{\mathbf{R}_y}{\|\mathbf{R}\|} \qquad \cos\gamma = \frac{\mathbf{R}_z}{\|\mathbf{R}\|} \tag{11}$$

where $\|\mathbf{R}\|$ is the magnitude or length of the resultant force vector.

RESULTS AND DISCUSSION

Measurement Reliability. During the data acquisition process, there were 2 major sources of experimental and measurement errors. First, muscles and other soft tissues of the larynx sometimes showed

TABLE 2. MAGNITUDE OF MEASUREMENT ERRORS BY MUSCLE PORTION

	Length (mm)	*Cross-sectional Area (mm²)*	θ_{xy} (°)	θ_{yz} (°)	θ_{zx} (°)
L PCA o	0.772 (5.20%)	0.207 (0.81%)	2.97 (1.65%)	2.42 (1.35%)	4.50 (2.78%)
L PCA v	1.277 (8.81%)	0.525 (4.99%)	6.03 (3.35%)	4.34 (2.41%)	3.90 (2.16%)
L PCA (total)	0.916 (6.22%)	0.298 (0.83%)	3.79 (2.10%)	2.94 (1.63%)	4.70 (2.61%)
R PCA o	0.755 (4.99%)	0.238 (1.07%)	2.41 (1.34%)	2.77 (1.54%)	4.86 (2.70%)
R PCA v	0.767 (5.05%)	0.271 (2.55%)	3.60 (2.00%)	2.29 (1.27%)	3.66 (2.03%)
R PCA (total)	0.759 (5.01%)	0.249 (0.76%)	2.80 (1.56%)	2.61 (1.45%)	4.46 (2.48%)
L LCA	0.791 (5.47%)	0.355 (1.65%)	2.18 (1.21%)	4.56 (2.53%)	14.18 (7.88%)
R LCA	0.850 (5.91%)	0.350 (1.68%)	3.15 (1.75%)	5.66 (3.15%)	9.42 (5.23%)
L IA inf	0.718 (8.02%)	0.746 (6.60%)	4.23 (2.35%)	3.81 (2.12%)	7.44 (4.13%)
R IA inf	0.714 (7.42%)	0.919 (7.06%)	4.82 (2.68%)	5.10 (2.83%)	8.49 (4.72%)
Mean error	0.792 (6.21%)	0.486 (2.80%)	3.49 (1.94%)	4.11 (2.28%)	8.11 (4.51%)
SD	0.168 (1.41%)	0.240 (2.47%)	1.18 (0.65%)	1.21 (0.67%)	3.32 (1.85%)

See text for abbreviations.

slight movement and deformation under the pressure of the digitizer probe. Second, external forces applied on the larynx during muscle bundle dissection sometimes also caused slight tissue movement and deformation. Because of these errors, there was some variability in the measured coordinates across different sampled points of the same muscle bundle insertion or origin.

Experimental error or variability of the data was quantified for dog 7, which was chosen because there were a large number of muscle bundles in each of its different muscle portions. Error in length measurement was estimated by first finding the maximum length possible based on the 3 origin data points and the 3 insertion data points for each muscle bundle. The maximum lengths were then averaged across bundles for each muscle portion. Table 2 shows the deviations between the maximum lengths and the average lengths for the 8 different muscle portions, and their percentage errors. As shown in Table 2, the mean error for all muscles was 6.2%.

The maximum possible cross-sectional area for each bundle of dog 7 was calculated from equation 6 on the basis of the measured mass, the balance reliability (0.1 mg), and the average length data. The minimum possible cross-sectional area was calculated similarly, but it was based on the maximum calculated length for each bundle. The difference between the maximum and the minimum for each bundle was obtained, and an average was calculated for each muscle portion. Table 2 shows that the error ranged from about 1% to 7%. The maximum and minimum orientation angles (2-D projection angles) were calculated from the 3 origin points and the 3 insertion points for each bundle to estimate the error in vector calculations. The difference between these angles was obtained for each bundle, and an average error was computed for each muscle portion. Table 2 shows that the percentage error values, reported with respect to 180°, ranged from about 1% to 8%, with most of them smaller than 3%.

Muscle Mass, Length, Cross-Sectional Area, and Orientation. Table 3 shows the mass of each muscle portion for all subjects and their averages. It can be

TABLE 3. MASS OF CANINE LARYNGEAL ABDUCTOR AND ADDUCTOR MUSCLES

	Dog 1	*Dog 2*	*Dog 3*	*Dog 4*	*Dog 5*	*Dog 6*	*Dog 7*	*Dog 8*	*Mean*	*SD*
L PCA o	0.429	0.580	0.480	0.580	0.210	0.359	0.300	0.305	0.405	0.136
L PCA v	0.161	0.168	0.206	0.137	0.148	0.136	0.169	0.121	0.155	0.027
L PCA (total)	0.590	0.748	0.686	0.716	0.358	0.495	0.469	0.449	0.564	0.142
R PCA o	0.337	0.511	0.353	0.529	0.213	0.301	0.273	0.266	0.348	0.115
R PCA v	0.171	0.143	0.263	0.135	0.118	0.201	0.191	0.181	0.175	0.046
R PCA (total)	0.507	0.655	0.616	0.664	0.331	0.502	0.464	0.447	0.523	0.115
L LCA	0.273	0.351	0.402	0.466	0.184	0.346	0.268	0.269	0.320	0.089
R LCA	0.269	0.304	0.357	0.448	0.182	0.358	0.276	0.270	0.308	0.080
L IA inf	0.123	0.068	0.139	0.130	0.082	0.128	0.106	0.112	0.111	0.025
R IA inf	0.154	0.095	0.152	0.182	0.073	0.143	0.112	0.139	0.131	0.036
Total	1.916	2.221	2.351	2.607	1.210	1.972	1.695	1.686	1.957	0.439

Data are mass in grams.

TABLE 4. LENGTH OF CANINE LARYNGEAL ABDUCTOR AND ADDUCTOR MUSCLES

	Dog 1	*Dog 2*	*Dog 3*	*Dog 4*	*Dog 5*	*Dog 6*	*Dog 7*	*Dog 8*	*Mean*	*SD*
L PCA o	14.527	14.199	16.142	15.911	14.161	15.261	13.096	15.081	14.797	1.005
L PCA v	11.899	15.082	15.634	16.029	14.885	14.568	13.310	14.540	14.493	1.325
L PCA (total)	13.943	14.396	16.029	15.933	14.342	15.113	13.149	14.965	14.734	0.979
R PCA o	14.287	14.486	15.378	16.763	14.827	15.322	13.441	14.948	14.932	0.967
R PCA v	14.509	15.373	17.008	18.892	15.732	16.600	14.940	13.852	15.863	1.604
R PCA (total)	14.342	14.683	15.786	17.150	15.128	15.748	13.903	14.583	15.165	1.036
L LCA	13.259	14.993	14.768	14.918	13.913	15.394	14.431	13.976	14.457	0.701
R LCA	14.407	15.006	13.954	16.152	12.803	13.982	15.442	15.276	14.394	1.210
L IA inf	9.412	7.834	9.210	9.744	8.897	8.887	8.945	8.920	8.951	0.527
R IA inf	10.054	8.728	14.280	10.489	8.048	8.622	7.761	9.807	9.626	1.969

Data are in millimeters.

seen that the PCA muscle was always the most massive, whereas the IA muscle had the smallest mass, and the LCA muscle was in between. The oblique portion of the PCA muscle was consistently more massive than the vertical portion, in many cases by 2 to 3 times. The data also showed that muscles of the right and the left sides were basically symmetric to each other in terms of mass. These results were consistent with previous classic anatomic descriptions of the laryngeal abductor and adductor muscles.

Table 4 shows the lengths of the muscle portions, which were averages of individual muscle bundle lengths. Note that the lengths of the PCA muscle were not simple averages of those of the oblique and vertical portions, because there was always a larger number of muscle bundles in the oblique portion, as evidenced by its larger mass (Table 3). Nonetheless, the data showed that their lengths were quite similar to one another (mean differences <1 mm). The lengths of the LCA muscle were also close to those of the PCA muscle, whereas the IA muscle was about 30% to 50% shorter.

The cross-sectional area for each muscle bundle was estimated from the measured mass and the calculated length. The average cross-sectional area for each muscle portion was calculated, and the results are shown in Table 5. Similar to the mass data, the PCA muscle was consistently the largest in cross-sectional area, whereas the LCA muscle was often about 40% smaller and the IA muscle was about 60% smaller. Also, the oblique portion of the PCA muscle was again about 2 to 3 times larger than the vertical portion.

Table 6 shows the average projection angles and direction cosines of the 8 muscle portions. The angles of orientation were averaged across all subjects. They were oriented such that the muscular process of the arytenoid cartilage was the geometric origin, and a positive angle was defined as rotating in a counterclockwise direction from x to y, y to z, or z to x.

Figure 4 illustrates the angles of the 2 portions of the PCA muscle on the xy, yz, and xz planes. The orientation angles of the arrows represent the lines of action of the muscle portions, whereas the lengths of the arrows are indications of their relative force magnitudes as they were scaled according to the muscle cross-sectional areas. Hence, the arrows represent projections of the resultant force vectors of the 2 PCA portions onto the 3 orthogonal planes. Not surprisingly, the oblique portion was always at a more

TABLE 5. CROSS-SECTIONAL AREA OF CANINE LARYNGEAL ABDUCTOR AND ADDUCTOR MUSCLES

	Dog 1	*Dog 2*	*Dog 3*	*Dog 4*	*Dog 5*	*Dog 6*	*Dog 7*	*Dog 8*	*Mean*	*SD*
L PCA o	27.20	38.10	27.95	33.46	14.03	22.13	21.44	19.04	25.42	7.86
L PCA v	13.02	10.42	12.96	8.12	9.54	8.89	12.03	9.21	10.52	1.91
L PCA (total)	40.22	48.52	40.91	41.58	23.57	31.02	33.47	28.25	35.94	8.24
R PCA o	22.84	33.32	21.73	29.89	14.29	18.99	19.47	17.34	22.23	6.41
R PCA v	11.26	8.92	14.82	6.87	7.16	11.47	12.18	12.46	10.64	2.77
R PCA (total)	34.10	42.25	36.55	36.76	21.44	30.46	31.65	29.80	32.88	6.16
L LCA	19.48	23.03	25.83	31.78	13.11	22.16	17.79	19.37	21.57	5.61
R LCA	17.82	19.60	23.91	26.63	14.05	25.12	17.55	17.61	20.80	4.41
L IA inf	12.81	8.34	14.44	12.83	8.94	13.73	11.34	12.01	11.30	2.54
R IA inf	14.71	10.47	14.41	16.55	8.84	15.77	13.88	13.73	13.02	2.90
Total	140.14	154.20	159.05	170.13	95.96	145.26	133.68	129.73	141.02	22.60

Data are in square millimeters as computed from muscle mass, length, and density (see equation 6 in text).

TABLE 6. MEAN PROJECTION ANGLES AND DIRECTION COSINES OF CANINE LARYNGEAL ABDUCTOR AND ADDUCTOR MUSCLES

	2-D Projection Angles (°)			*3-D Direction Cosines*		
	θ_{xy}	θ_{yz}	θ_{zx}	$\cos\alpha$	$\cos\beta$	$\cos\gamma$
L PCA o	−22.3	−115.5	130.7	0.739	−0.293	−0.607
L PCA v	−17.0	−97.2	157.6	0.372	−0.119	−0.920
L PCA (total)	−21.1	−108.6	139.0	0.647	−0.247	−0.721
R PCA o	−158.6	−117.6	−126.9	−0.759	−0.298	−0.579
R PCA v	−169.8	−94.3	−157.4	−0.413	−0.063	−0.909
R PCA (total)	−161.2	−107.4	−137.3	−0.666	−0.228	−0.710
L LCA	75.0	−25.6	150.9	0.238	0.869	−0.433
R LCA	99.7	−23.6	−158.6	−0.158	0.902	−0.403
L IA inf	−43.0	157.5	68.9	0.701	−0.660	0.269
R IA inf	−137.7	152.1	−64.3	−0.692	−0.627	0.358

oblique orientation than the vertical portion. It was also always stronger, especially its component on the xy plane.

Figure 5 summarizes the resultant force vectors of all 3 abductor and adductor muscles, namely, the LCA, PCA (the resultant of the 2 portions), and IA (the inferior portion). Again, the orientation angles represent their lines of action, whereas the lengths are estimations of the relative magnitudes of their forces projected onto the 3 planes. In terms of the orientation angles, the data were qualitatively consistent with classic descriptions of the muscles. The lines of action as shown in Fig 5 suggested that the LCA tends to pull the muscular process of the arytenoid cartilage anteriorly, inferiorly, and medially, thereby moving the vocal process medially and adducting the vocal fold. The PCA muscle, on the other hand, tends to move the muscular process posteriorly, inferiorly, and medially, abducting the vocal fold. Interestingly, the IA muscle seems to be somewhat of an antagonist of the LCA muscle on the basis of their orientation angles on the xy and yz planes. Nonetheless, its superior-medial direction of action as shown on the xz plane suggested that it might move the arytenoid toward the midline, thereby adducting the vocal fold. These data on the average lines of action of the abductor and adductor muscles may be useful clinically for certain phonosurgical procedures. For example, data on the orientation angles of the LCA muscle may serve as quantitative guidelines for clinicians to establish a more physiological direction of the sutures used in arytenoid adduction.

In terms of the relative force magnitudes, the data suggested that the PCA muscle was always stronger than the LCA and IA muscles, especially on the xz plane, where it was 3 to 4 times stronger. The LCA muscle was slightly weaker than the PCA muscle on the xy and yz planes, but the difference was much larger on the xz plane. The IA muscle was always the weakest, especially on the yz plane, where it was 2 to 3 times weaker than the other two. These findings were consistent with the cross-sectional area data, as the muscle's resultant force vectors were computed partly on the basis of their cross-sectional areas. The assumption was that the maximum active stress was similar for the 3 different muscles, such that the relative magnitude of force generated by a muscle is proportional to its cross-sectional area.

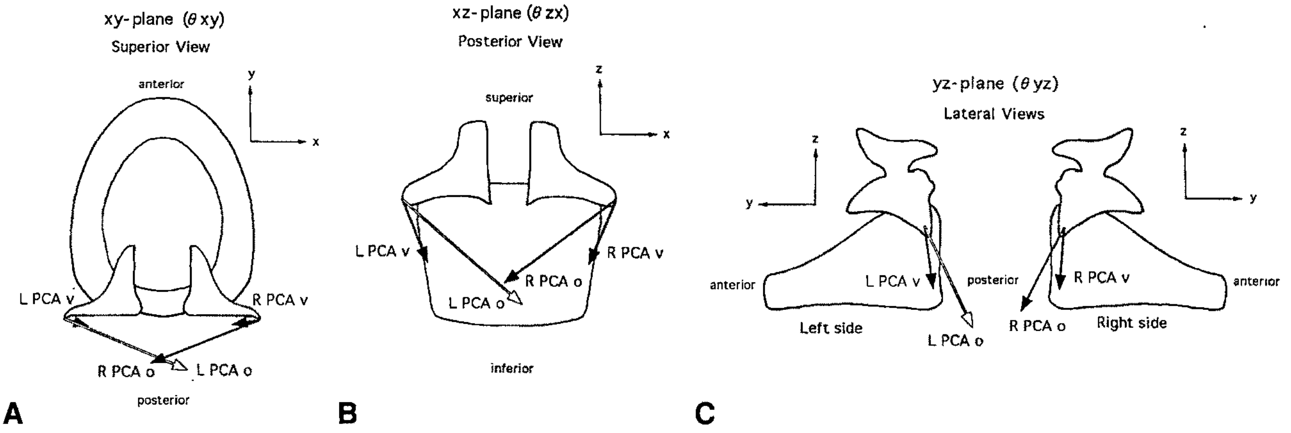

Fig 4. Resultant force vectors of oblique and vertical portions of PCA muscle. A) Superior view; vectors projected onto xy plane. B) Posterior view; vectors projected onto xz plane. C) Lateral views; vectors projected onto yz plane.

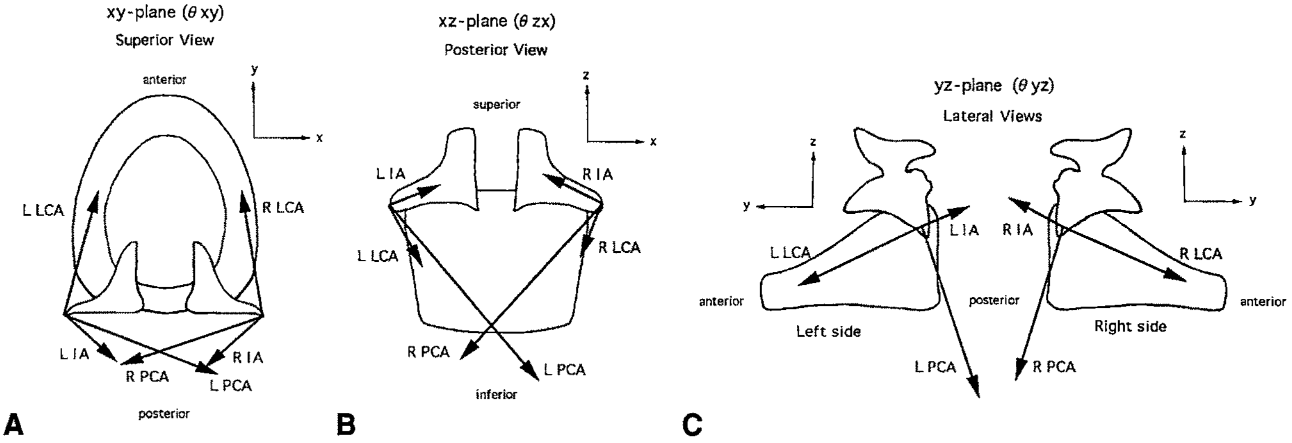

Fig 5. Resultant force vectors of PCA, LCA, and IA muscles. A) Superior view; vectors projected onto xy plane. B) Posterior view; vectors projected onto xz plane. C) Lateral views; vectors projected onto yz plane.

Limitations and Suggestions for Further Studies. One limitation of the present study was that the calculations of muscle lengths and orientation angles were made by assuming that the muscle bundles form a straight line between the origin and insertion points. However, this was not always the case, especially for the PCA, in which muscle fibers often were seen to course around the curved laryngeal cartilage surfaces. Also, the fiber bundles on a muscle's surface were often more curved than the internal bundles. Such errors likely led to underestimations of length, overestimations of cross-sectional area, and discrepancies in estimations of the effective line of action in some of the muscles. In future experiments, increasing the number of sampling points for each bundle might help to reduce such errors. For example, by taking an extra data point at the midpoint of each muscle bundle, one can establish more accurate estimations of the muscle bundle length and its effective orientation angle on the basis of the best-fit curve for the 3 data points (origin, insertion, and midpoint).

During data collection, the cricoid and the arytenoid cartilages were securely fixed in the cadaveric position to minimize specimen movement and to ensure accurate measurements of the 3-D coordinates. However, slight movements of the cricoid and the arytenoid cartilages were still sometimes observed during muscle bundle resection and data acquisition. Such movements likely introduced random errors into the 3-D coordinate data sampled by the digitizer. In future experiments, extra pins or other devices should be used to more securely fix the cartilages so as to eliminate these errors.

Anatomic differences between the canine and human larynges must be acknowledged when canine data are used for modeling of the human larynx. The canine larynx is similar to the human larynx in terms of size, morphological features, and basic vocal fold anatomy, but there are also some significant differences. The human IA muscle consists of a transverse portion and an oblique portion, both of which clearly and consistently cross the midline. For the canine IA muscle, however, our observations showed that it can be divided into a superior portion and an inferior portion. The inferior portion was distinctly separated into left and right halves joined by a sheet of tendon-like connective tissue at the midline, whereas the superior portion stayed on the same arytenoid cartilage and extended anteriorly to insert into the structures above the arytenoid cartilage (the cuneiform and corniculate processes). Further, the arytenoid cartilages of dogs are proportionately larger than those of humans.

Considering such anatomic differences between the canine larynx and the human larynx, the 3-D characterization of the canine laryngeal muscles may only represent a rough approximation of the human muscles. However, the two species exhibit sufficient similarities in basic laryngeal anatomy that the canine model remains a valuable approximation of the human larynx.

CONCLUSIONS

The PCA, LCA, and IA muscles are important in the control of vocal fold abduction and adduction. These muscles function in a well-coordinated manner during phonation, respiration, and airway protection to allow for various adjustments of the anatomic orientations of the vocal folds. This study quantified the mass, length, relative cross-sectional area, and angle of orientation in 3-D space of these abductor and adductor muscles in 8 canine larynges. This 3-D anatomic characterization allowed for the calculations of average lines of action and moment arms for the muscles, providing important data for biomechanical modeling of vocal fold posturing. These data may also be useful in devising clinical guidelines for certain phonosurgical procedures such as arytenoid adduction.

REFERENCES

1. Sanders I, Jacobs I, Wu B-L, Biller HF. The three bellies of the canine posterior cricoarytenoid muscle: implications for understanding laryngeal function. Laryngoscope 1993;103:171-7.

2. Sanders I, Rao F, Biller HF. Arytenoid motion evoked by regional electrical stimulation of the canine posterior cricoarytenoid muscle. Laryngoscope 1994;104:456-62.

3. Sanders I, Wu B-L, Mu L, Li Y, Biller HF. The innervation of the human larynx. Arch Otolaryngol Head Neck Surg 1993;119:934-9.

4. Sanders I, Wu B-L, Mu L, Biller HF. The innervation of the human posterior cricoarytenoid muscle: evidence for at least two neuromuscular compartments. Laryngoscope 1994;104: 880-4.

5. Alipour-Haghighi F, Titze IR, Perlman AL. Tetanic contraction in vocal fold muscle. J Speech Hear Res 1989;32:226-31.

6. Alipour-Haghighi F, Perlman AL, Titze IR. Tetanic response of the cricothyroid muscle. Ann Otol Rhinol Laryngol 1991;100:626-31.

7. Alipour F, Titze I. Active and passive characteristics of the canine cricothyroid muscles. J Voice 1999;13:1-10.

8. Sonesson B. Die funktionelle Anatomie des Cricoarytenoid Gelenkes. Z Anat Entwicklungsgesch 1959;121:292-303.

9. Frable MA. Computation of motion at the cricoarytenoid joint. Arch Otolaryngol 1961;73:551-6.

10. von Leden H, Moore P. The mechanics of the cricoarytenoid joint. Arch Otolaryngol 1961;73:541-50.

11. Ardran GM, Kemp FH. The mechanism of the larynx: Part I. The movement of the arytenoid and cricoid cartilages. Br J Radiol 1966;39:641-54.

12. Sellars IE, Sellars S. Cricoarytenoid joint structure and function. J Laryngol Otol 1983;97:1027-34.

13. Neuman TR, Hengesteg A, Lepage RP, Kaufman KR, Woodson GE. Three-dimensional motion of the arytenoid adduction procedure in cadaver larynges. Ann Otol Rhinol Laryngol 1994;103:265-70.

14. Selbie WS, Zhang L, Levine WS, Ludlow CL. Using joint geometry to determine the motion of the cricoarytenoid joint. J Acoust Soc Am 1998;103:1115-27.

15. Williams PL, Warwick R, eds. Gray's anatomy. 36th ed. New York, NY: Churchill Livingstone, 1980.

16. Kahane J. The cricoarytenoid joint: perspectives gained since von Leden and Moore (1961). J Voice (in press).

17. Martensson A, Skoglund CR. Contraction properties of intrinsic laryngeal muscles. Acta Physiol Scand 1964;60:318-36.

18. Bryant NJ, Woodson GE, Kaufman K, et al. Human posterior cricoarytenoid muscle compartments, anatomy and mechanics. Arch Otolaryngol Head Neck Surg 1996;122:1331-6.

19. Sanders I, Mu L, Wu B-L, Biller HF. The intramuscular nerve supply of the human lateral cricoarytenoid muscle. Acta Otolaryngol (Stockh) 1993;113:679-82.

20. Perlman AL, Titze IR. Development of an in vitro technique for measuring the elastic properties of vocal fold tissue. J Speech Hear Res 1988;31:288-98.

Ann Otol Rhinol Laryngol 109:2000

PREVENTION OF PHARYNGOESOPHAGEAL SPASM AFTER LARYNGECTOMY WITH A HALF-MUSCLE CLOSURE TECHNIQUE

DANIEL G. DESCHLER, MD
BOSTON, MASSACHUSETTS

E. THOMAS DOHERTY, PHD
SAN FRANCISCO, CALIFORNIA

CHARLES G. REED, PHD
SAN FRANCISCO, CALIFORNIA

RICHARD E. HAYDEN, MD
PHILADELPHIA, PENNSYLVANIA

MARK I. SINGER, MD
SAN FRANCISCO, CALIFORNIA

Because pharyngoesophageal spasm can limit successful voice restoration after total laryngectomy, 24 patients underwent a modified pharyngeal closure in an effort to avoid this problem. All patients underwent total laryngectomy with appropriate neck dissections and pharyngeal closure with a half-muscle closure technique in which only one side of the remnant constrictor muscles was used to reinforce the primary closure. Twenty-three patients underwent voice restoration. Twenty-two (96%) had a functional voice, and 1 patient (4%) had pharyngoesophageal spasm that required a secondary myotomy. One fistula (4%) occurred and resolved with conservative measures. Quantitative voice analysis demonstrated no significant differences between half-closure patients and control patients for fundamental frequency (96 Hz versus 101 Hz) or intensity (57 dB versus 64 dB). Extensive qualitative analysis by trained and naive listeners revealed no differences. This preliminary report indicates the half-muscle closure modification of the pharyngeal closure at primary laryngectomy may provide a simple and effective means of avoiding pharyngoesophageal spasm and maintaining an effective voice without increased complications.

KEY WORDS — half-muscle closure, laryngectomy, pharyngoesophageal spasm, tracheoesophageal puncture.

INTRODUCTION

The tracheoesophageal puncture (TEP) technique for voice restoration, introduced by Singer and Blom in 1980,[1] is a highly successful means of providing functional voice rehabilitation after total laryngectomy. As experience evolved with the procedure, it became evident that voice restoration with this technique could be limited by pharyngeal constrictor muscle spasm induced by the insufflation of air into the esophagus and neopharynx.[2] The incidence of voice-limiting pharyngeal constrictor muscle spasm in the postlaryngectomy population ranges from 10% to 40%.[2,3] It was found that selective constrictor myotomy completed secondarily could alleviate the problem,[2,4] but subsequent efforts centered on technique modifications and adjuvant procedures performed in the primary setting to prevent voice-limiting spasm. Primary constrictor myotomy successfully decreased the incidence of spasm, but was associated with higher postlaryngectomy fistula rates.[3,5] Pharyngeal plexus neurectomy was later introduced, but it could be technically challenging.[3] Both procedures demonstrated decreased spasm rates ranging from 10% to 16%,[3,6] but were not without drawbacks.

We began using a half-muscle pharyngeal closure technique at primary laryngectomy to prophylactically address the issue of potential voice-limiting spasm while maintaining the use of the highly vascular constrictor muscles to reinforce the layered pharyngeal closure. The technique is described, and preliminary results in 24 patients are presented.

MATERIALS AND METHODS

Surgical Technique. Patients are staged before operation and identified as candidates for treatment of stage III and IV disease with total laryngectomy. Informed consent is obtained, and total laryngectomy with appropriate neck dissections is completed in the standard fashion. As the constrictor muscles are released from the oblique line at the thyroid lamina, care is taken to preserve the muscles. The degree to which the constrictor can be preserved is solely dependent on the tumor extent, and the oncological goals of the procedure must not be compromised. With the larynx removed and the margins identified as clear, the pharynx is closed in a 2-layered fashion that approximates the mucosal edges and reinforces this layer with a second layer of submucosal tissue.

From the Department of Otolaryngology–Head and Neck Surgery, MCP-Hahnemann University, Philadelphia, Pennsylvania (Deschler, Hayden), and the Department of Speech and Audiology, San Francisco Veterans Hospital (Doherty, Reed), and the Department of Otolaryngology–Head and Neck Surgery, University of California (Singer), San Francisco, California. This research was supported in part by the Veterans Administration Research and Development Service.

CORRESPONDENCE — Daniel G. Deschler, MD, Dept of Otolaryngology–Head and Neck Surgery, Massachusetts Eye and Ear Infirmary, 243 Charles St, Boston, MA 02114.

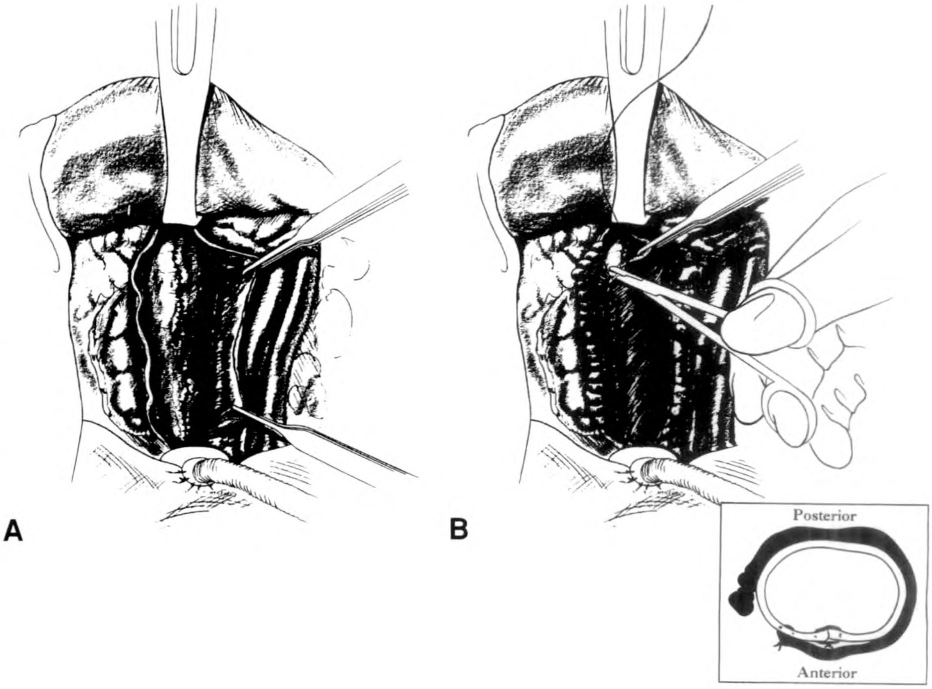

Fig 1. Left constrictor muscle is A) identified and mobilized for coverage of layered pharyngeal closure at midline and B) sutured over midline pharyngeal closure with right constrictor muscles oversewn. Inset) Constrictor muscles overlap pharyngeal mucosal closure by 8 to 10 mm.

An I- or T-shaped closure may be used, depending on anatomy and surgeon preference. No muscle is used in the second layer.

The constrictor muscle remnants are identified bilaterally (Fig 1A). The muscles may be freed from medial and lateral attachments to increase mobility, but care is taken not to compromise the vascular integrity of the muscle flaps. Each flap is mobilized over the midline closure, and the side with the least restriction and the best vascularity is chosen for the half-muscle closure. The remaining side is lateralized and oversewn with a running, locking 3-0 chromic gut suture (Fig 1B). This prevents these muscles from migrating medially and healing to the half-muscle closure.

The other muscle flap is now mobilized over the midline closure and sutured to the submucosal connective tissue of the pharynx with interrupted 3-0 absorbable sutures. The flap should overlap the midline closure by 8 to 10 mm and extend from the tongue base to the esophageal entry (Fig 1B). The half-muscle closure with the constrictor muscle flap provides a vascular reinforcement to the layered pharyngeal closure and provides muscular tone to the neopharyngeal segment while eliminating a circumferential muscular ring, which may be predisposed to spasm. Drains are placed, the stoma is formalized, and closure is completed in the standard fashion. The TEP may be completed in the primary or secondary setting as determined by the surgeon. An oral diet is begun between postoperative days 7 and 10. Placement of the TEP prosthesis is completed, and speech therapy is begun.

Patient Testing. Twenty-four patients presented with stage III or IV laryngeal, hypopharyngeal, or other carcinoma involving the larynx and were amenable to surgical therapy. Informed consent was obtained, and all patients underwent total laryngectomy with appropriate neck dissection and had the pharyngeal closure completed with the half-muscle closure technique. Twenty-three patients underwent voice restoration with the TEP technique as described by Singer and Blom.[1] Patients' records were reviewed for complications, including pharyngocutaneous fistula formation, preoperative and postoperative radiotherapy, success of voice restoration, occurrence of voice-limiting pharyngeal constrictor spasm, and need for a secondary selective myotomy.

Available patients from the half-muscle closure group completed voice recordings, which underwent quantitative and qualitative voice analysis by means of our previously described protocol.[7,8] To compare tracheoesophageal voice in these 2 patient groups, we used standardized vocal tasks of sustained phonation and speech. The tasks selected permit both quantitative and qualitative measures of acoustic characteristics such as loudness and pitch, as well as psychoacoustic judgments of pleasantness and intelligibility.

Four half-closure patients and 12 control laryngectomy patients completed this portion of the study. Patients were asked to produce a sustained /a/. This was done at both soft and loud intensities. Subjects were also asked to attempt high and low pitches for each loudness level. These utterances were used to establish each patient's dynamic range and estimates of the jitter in the vocalizations. A 1-second sample from the middle of the phonation was analyzed for these calculations. For this specific study, the utterances at high pitch–loud level were used, because these represent a maximum effort and tend toward more stable vibratory segments. The patients were then asked to read 2 standard passages. The "Rainbow Passage" allows listeners to rate the pleasantness of the patient's voice. The "Grandfather Passage" provides a means to rate the patient's intelligibility and the listener's ability to evaluate the content of the speaker's message. Finally, the patients read 50 words from 1 of 4 standardized lists. These are sets of single-syllable words that are phonetically balanced. Each list contains a distribution of phonemes that is in proportion to their occurrence in the English language. Each word was placed within the carrier phrase "Say (*word*) again" to allow fluency of speech.

Signal recordings were done with patients seated in an audiology booth while they produced speech samples. A Bruel and Kjaer (B&K) 1-inch condenser microphone, cartridge type 4132, was positioned approximately 30 cm from the speaker's mouth. The signal was fed to a B&K microphone amplifier type 2603. The acoustic signals were processed by a pulse code modulator and a Sony PCM-501ES digital audio processor, and were stored on a Panasonic AG-1900 videocassette recorder. This technique records signals in a digital form that is virtually identical to that of compact disc recordings. Data acquisition was performed with the analog-to-digital converter (ADC) of a Creative Technology Ltd Sound Blaster 16 ASP analog and digital input-output system in a Vanguard 486/33 personal computer. The ADC has a resolution of 16 bits, which is accurate to within ±0.0015% of the full-scale reading. All signals were sampled at 44.1 kHz.

Voice samples were analyzed for amplitude and fundamental frequency. The range and mean of each parameter were calculated for the 2 groups.

Two groups of listeners were selected to evaluate voice quality. One group consisted of 6 trained listeners who were formally trained and licensed in speech pathology. Six naive listeners constituted the second group and had no formal speech training or consistent contact with tracheoesophageal speakers. The listeners evaluated each patient's voice quality from a recording and were blinded to the patient's operative history. The "Rainbow" and "Grandfather" passages were used to evaluate 9 qualitative voice parameters: intelligibility, communicative effectiveness, effective use of pitch, effective use of intensity, speaking rate, pleasantness, wetness, fluency, and extraneous speech noise. Listeners rated patients from 1 to 10 on a 10-cm line. Scores were measured from 1 to 100 with a millimeter ruler. Listeners then evaluated the word list. Scores were rated as the absolute number correct out of 50 words. The half-muscle closure patients were compared with 12 accomplished TEP speakers who had total laryngectomy and traditional pharyngeal closures, who were evaluated with the same protocol. The small sample size in this study precluded meaningful statistical analysis.

RESULTS

Twenty-four patients were in the study group and underwent total laryngectomy with a half-muscle pharyngeal closure within a 2-year period. Twenty-two patients underwent preoperative radiotherapy; 20 of these patients had a primary laryngeal malignancy. One patient underwent full-course radiotherapy for a tonsillar carcinoma and developed a second primary tumor in the larynx 4 years later. Another patient underwent radiotherapy for advanced nasopharyngeal carcinoma 9 years earlier and presented with carcinoma within a thyroglossal duct cyst involving the larynx. This lesion was irradiated after initial resection, but it recurred, necessitating surgical salvage. The remaining 2 patients completed postoperative radiotherapy for advanced primary laryngeal lesions. Two patients required pectoralis major myocutaneous flap reconstructions of anterior cervical skin resected with the primary tumor.

The immediate postoperative course in all patients was uncomplicated. They began an oral diet between postoperative days 7 and 10 and were discharged within 2 weeks of surgery. The patient with the recurrent carcinoma within the thyroglossal duct cyst who had undergone repeated radiotherapy returned 10 days after discharge with a pharyngocutaneous fistula at the superior portion of the pectoralis major flap anterior neck reconstruction. Conservative management with nasogastric tube feedings and antibiotics was instituted, and the fistula resolved 3 weeks later with no further complications.

Twenty-three patients underwent TEP at the time of laryngectomy; prosthesis placement and speech therapy began 10 to 14 days later. One patient was scheduled for secondary TEP that was later deferred. Of the 23 patients who underwent TEP, 22 (96%) achieved satisfactory voice rehabilitation. One patient had pharyngoesophageal spasm that prevented adequate airflow. He underwent an uncomplicated selective constrictor myotomy as a secondary procedure, which resulted in a good voice. This patient was early in the series, and in all subsequent cases

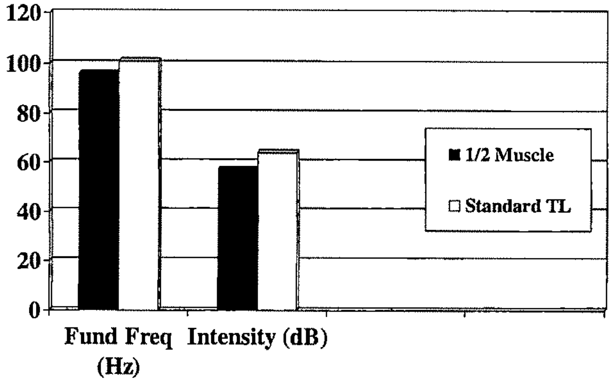

Fig 2. Comparison of fundamental frequency in hertz and intensity in decibels between half-muscle closure and standard total laryngectomy (TL) groups.

the contralateral constrictor muscle flap that was not used for the half-muscle closure was formally oversewn.

Four half-muscle closure patients were available for formal voice recording and analysis. These results were compared with those of 12 similar control patients who underwent laryngectomy with traditional closure techniques. Quantitative analysis of fundamental frequency (pitch) in hertz yielded a mean of 96 Hz (range, 78 to 127 Hz) for the half-muscle closure patients, compared with 101 Hz (range, 57 to 244 Hz) for the control patients. The mean intensity (sound pressure level) measured in decibels was 57 dB (range, 53 to 65 dB) for the half-closure patients and 64 dB (range, 53 to 69 dB) for the control patients (Fig 2).

Six naive and 6 trained listeners evaluated the patients' voice quality over the 10 parameters of intelligibility, communicative effectiveness, effective use of pitch, effective use of intensity, speaking rate, pleasantness, wetness, fluency, extraneous speech noise, and word list scores. There were no marked differences noted between the 2 listener groups for the 10 parameters. Likewise, no differences were demonstrated between the patient groups for any of the 10 parameters, but meaningful statistical analysis of these perceptual data is limited by the small sample size.

DISCUSSION

Voice restoration with the TEP technique and the Blom-Singer prosthesis is a highly successful means of voice rehabilitation for patients who undergo laryngectomy. The TEP method is simple, reproducible, and translatable throughout otolaryngology practice.[1,2,9-15] Limitations can result from spasm within the pharyngoesophageal segment during air insufflation, which prevents voice production.[4] Modifications in laryngectomy technique and adjuvant procedures such as primary myotomy[5] and pharyngeal plexus neurectomy[3] were introduced in an effort to prevent voice-limiting pharyngoesophageal spasm. The half-muscle closure technique is the result of similar efforts.

Blom et al[6] reviewed 29 patients who underwent total laryngectomy and voice restoration and were randomized into 3 study groups: primary pharyngeal constrictor myotomy, unilateral pharyngeal plexus neurectomy, or unilateral pharyngeal plexus neurectomy with a cricopharyngeal drainage myotomy. One patient in each group demonstrated voice-limiting pharyngoesophageal spasm, for a 90% success rate in each group. Acoustic analysis of available patients from each group demonstrated significantly higher fundamental frequencies in the patients who underwent neurectomy only than in those who underwent pharyngeal constrictor myotomy or neurectomy with drainage myotomy. The authors concluded that residual resting tone in the patients who underwent unilateral neurectomy could contribute favorably to fundamental frequency in tracheoesophageal speakers. No qualitative analysis was completed with this study, and the postoperative fistula rates were not discussed.

The half-muscle variation on pharyngeal closure attempts to provide the benefits of the 2 existing methods for addressing potential voice-limiting pharyngoesophageal spasm at the time of laryngectomy while limiting the drawbacks of each. One constrictor muscle flap provides a vascular reinforcing layer for the pharyngeal closure, as is available with the constrictor myotomy. The fistula rate for the half-muscle closure group was acceptably low at 4%. Because no further incisions or risks to mucosal integrity are needed as with the primary myotomy procedure, the risk of fistula for the half-muscle closure group may be less than with primary myotomy. Because only 1 constrictor muscle flap is used for pharyngeal closure reinforcement, a circumferential muscular ring that may go into spasm is not created. Twenty-two of 23 patients were able to achieve a functional voice, for a 96% success rate. This compares favorably with the 84% to 90% success rates reported with the primary myotomy and plexus neurectomy techniques.[3,5,6] The 1 failure in the half-muscle closure group occurred early in the series, with the fourth patient, before the contralateral constrictor muscle flap was routinely oversewn. In this case, the constrictor muscles that were not used in the closure likely migrated toward the midline and healed in continuity with the constrictor muscle flap used for the half-muscle closure, creating a circumferential muscle ring that allowed spasm. A good voice resulted after the constrictor muscles were formally divided during an uncomplicated secondary myotomy.

In a manner similar to the plexus neurectomy, tone-providing muscle remains intimately related to the neopharyngeal conduit, which allows acceptable fundamental frequency levels that are acoustically similar to those of control patients. A completely patulous conduit was also avoided, as can occur when no muscle closure is used at all. A degree of flaccidity may be possible and could account for the slightly lowered intensity levels in the half-closure patients compared with controls, but further study is needed to explore this finding. Unlike the plexus neurectomy, the half-muscle closure procedure is technically straightforward, does not add significant time to the ablative surgery, and is easily learned.

The qualitative review of the available half-closure patients revealed no significant differences for any of the 10 parameters tested: intelligibility, communicative effectiveness, effective use of pitch, effective use of intensity, speaking rate, pleasantness, wetness, fluency, extraneous speech noise, and word list scores. Again, the small sample size in this preliminary report does not allow meaningful statistical analysis at this point.

In conclusion, control of voice-limiting pharyngoesophageal spasm remains an important challenge in postlaryngectomy voice rehabilitation. The results demonstrated with the half-muscle closure technique indicate the value of this method for prophylactically addressing potential pharyngoesophageal spasm at the time of the primary surgery. Voice-limiting spasm only occurred in 1 of 23 patients treated with this closure method, for a 4% failure rate. The fistula rate was also low at 4%. The voice achieved with the half-muscle closure technique was comparable with that of control tracheoesophageal speakers with no spasm. Finally, the half-muscle closure technique is a simple and straightforward variation on the traditional pharyngeal closure technique for laryngectomy that is easily adopted and demonstrates marked success in allowing successful voice rehabilitation with the TEP technique.

REFERENCES

1. Singer MI, Blom ED. An endoscopic technique for restoration of voice after laryngectomy. Ann Otol Rhinol Laryngol 1980;89:529-33.

2. Singer MI, Blom ED, Hamaker RC. Further experience with voice restoration after total laryngectomy. Ann Otol Rhinol Laryngol 1981;90:498-502.

3. Singer MI, Blom ED, Hamaker RC. Pharyngeal plexus neurectomy for alaryngeal speech rehabilitation. Laryngoscope 1986;96:50-4.

4. Singer MI, Blom ED. Selective myotomy for voice restoration after total laryngectomy. Arch Otolaryngol 1981;107: 670-3.

5. Hamaker RC, Singer MI, Blom ED, Daniels HA. Primary voice restoration at laryngectomy. Arch Otolaryngol 1985; 111:182-6.

6. Blom ED, Pauloski BR, Hamaker RC. Functional outcome after surgery for prevention of pharyngospasms in tracheoesophageal speakers. Part I. Speech characteristics. Laryngoscope 1995;105:1093-103.

7. Deschler DG, Doherty ET, Reed CG, Anthony JP, Singer MI. Tracheoesophageal voice following tubed free radial forearm flap reconstruction of the neopharynx. Ann Otol Rhinol Laryngol 1994;103:929-36.

8. Deschler DG, Doherty ET, Reed CG, Singer MI. Quantitative and qualitative analysis of tracheoesophageal voice after pectoralis major flap reconstruction of the neopharynx. Otolaryngol Head Neck Surg 1998;118:771-6.

9. Wilson SE, Watson JB. Differences in speaking proficiencies in three laryngectomee groups. Arch Otolaryngol 1985; 111:216-9.

10. Lopez MJ, Kraybill W, McElroy TH, Guerra O. Voice rehabilitation practices among head and neck surgeons. Ann Otol Rhinol Laryngol 1987;96:261-3.

11. Robbins J, Fisher HB, Blom EC, Singer MI. A comparative acoustic study of normal, esophageal and tracheoesophageal speech production. J Speech Hear Disord 1984;49:202-10.

12. Yoshida GY, Hamaker RC, Singer MI, Blom ED, Charles GA. Primary voice restoration at laryngectomy: 1989 update. Laryngoscope 1989;99:1093-5.

13. Recher G, Pesavento G, Cristoferi V, Ferlito A. Italian experience of voice restoration after laryngectomy with tracheoesophageal puncture. Ann Otol Rhinol Laryngol 1991;100:206-10.

14. Morris HL, Smith AE, Van Demark DR, Maves MD. Communication status following laryngectomy: the Iowa experience 1984-1987. Ann Otol Rhinol Laryngol 1992;101:503-10.

15. Lacau St Guily J, Angelard B, El-Bez M, et al. Postlaryngectomy voice restoration: a prospective study in 83 patients. Arch Otolaryngol Head Neck Surg 1992;118:252-5.

Ann Otol Rhinol Laryngol 109:2000

PNEUMOMEDIASTINUM DUE TO VENTURI JET VENTILATION USED DURING MICROLARYNGEAL SURGERY IN A PREVIOUSLY NECK-IRRADIATED PATIENT

LUIS A. GAITINI, MD MILO FRADIS, MD SONIA J. VAIDA, MD
MOSTAFA SOMRI, MD SHELTON H. MALATSKEY, MD AVISHAI GOLZ, MD
HAIFA, ISRAEL

Serious complications secondary to Venturi jet ventilation used during microlaryngoscopy are rare, but when they occur, they may pose a life-threatening emergency. We report the case of a 45-year-old woman, previously treated with 70 Gy of irradiation for a T1 laryngeal carcinoma, who developed pneumomediastinum and subcutaneous emphysema after the use of Venturi jet ventilation. Keeping in mind the histologic changes to the irradiated structures, we suggest more caution when using Venturi jet ventilation in patients who have recently undergone neck irradiation therapy.

KEY WORDS — pneumomediastinum, Venturi jet ventilation.

INTRODUCTION

Direct microlaryngoscopy is a common procedure for the diagnosis and treatment of laryngeal diseases and is usually performed under general anesthesia.[1-3] Ventilation during microlaryngoscopy is most commonly accomplished with high-pressure jet ventilation.[2,4] Suspension microlaryngoscopy with Venturi jet ventilation via the laryngoscope is a relatively safe and well-established technique.[3,5,6] Although it was originally described in conjunction with laser surgery, we have found it to be perfectly adaptable for conventional microsurgery, allowing very wide visualization of the surgical field.[3]

At our hospital, Venturi jet ventilation is performed by the insertion of the jet injector into the laryngoscope. The jet needle is constructed by shaping and cutting a 16F needle and placing it in the channel provided in the laryngoscope. The oxygen source from the central supply at 40 psi is connected to a Penlonn time-cycled ventilator.[3] High-pressure plastic tubing connects this to the jet needle by means of a Luer lock connection.[3]

Although it is a relatively safe procedure and we have used this technique in 1,230 cases, rare complications may occur suddenly and present the surgeon with a life-threatening emergency. We report a case of pneumomediastinum and subcutaneous emphysema after the use of Venturi jet ventilation in a patient who was previously treated with radiotherapy for T1 carcinoma of the larynx. The patient recovered spontaneously, and no active measures were taken.

CASE REPORT

A 45-year-old woman was admitted to the Bnai Zion Medical Center for hoarseness. On examination, an irregularity of the anterior third of the right vocal cord was found. She underwent, under general anesthesia, suspension laryngoscopy with Venturi jet ventilation via the laryngoscope, and a biopsy of the right vocal cord was performed.

The histologic examination showed a well-differentiated squamous cell carcinoma, and the patient was treated with radiotherapy, receiving a total of 70 Gy of irradiation to the larynx and both sides of the neck. At follow-up 2 months later, a small area of erythroplakia was found on the anterior third of the right vocal cord, and it was decided to take another biopsy specimen from this area. The patient underwent suspension laryngoscopy with Venturi jet ventilation, performed by the same anesthesiologist and otolaryngologist who performed the former laryngoscopy. At the end of the procedure, the oxygen saturation decreased to 79%, and crepitations were felt on both sides of the neck. A chest radiograph showed pneumomediastinum and subcutaneous emphysema (see Figure).

The patient was treated with oxygen by mask and 24,000,000 IU of penicillin G intravenously, and the dyspnea and subcutaneous emphysema gradually subsided. The histologic examination of the biopsy ma-

---

From the Departments of Anesthesiology (Gaitini, Vaida, Somri) and Otolaryngology–Head and Neck Surgery (Fradis, Malatskey), Bnai Zion Medical Center; the Bruce Rappaport Faculty of Medicine, Technion-Israel Institute of Technology (Fradis, Golz); and the Department of Otolaryngology–Head and Neck Surgery, Rambam Medical Center (Golz); Haifa, Israel.

CORRESPONDENCE — Milo Fradis, MD, Dept of Otolaryngology–Head and Neck Surgery, Bnai Zion Medical Center, PO Box 4940, 31048 Haifa, Israel.

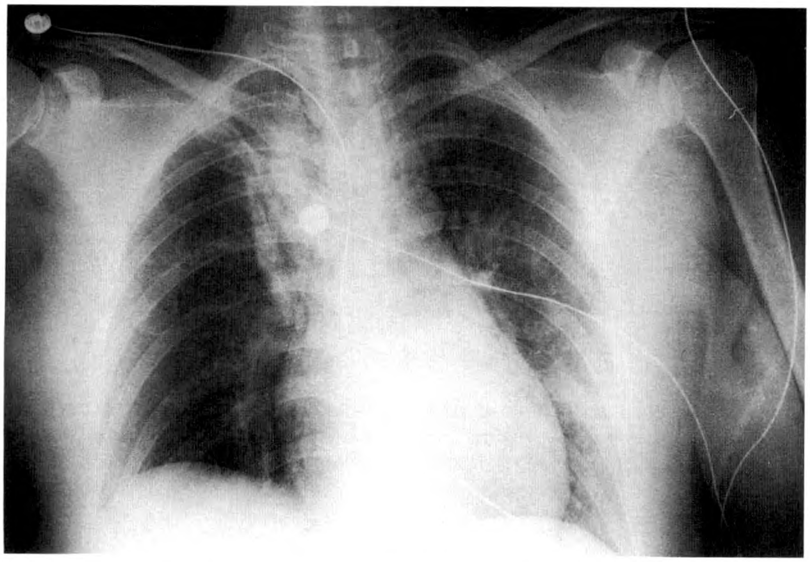

Chest radiograph showing pneumomediastinum and subcutaneous emphysema.

terial showed no signs of malignancy. The patient was followed-up for 2 years and showed no signs of recurrence of the disease.

DISCUSSION

During suspension laryngoscopy, an excellent visualization of the vocal cords can be obtained by the Venturi technique.[3-6] Complications of Venturi jet ventilation are uncommon, but pneumothorax,[4,7,8] pneumomediastinum,[6,8] hypoventilation,[1] and severe abdominal distention[1,8] have been described.

The hazards of excessive airway pressure occurring during anesthesia are well recognized.[9] Interruption of the mucosal integrity of the pharynx and tracheobronchial tree may result in the leakage of gas into the surrounding tissues, and as a consequence, interstitial emphysema may occur.[2,9] During Venturi jet ventilation, excessive airway pressure may be caused by the supply of excessive pressure to the trachea or by an insufficient expiration time.[2,10] The pressure supplied to the trachea depends on the setting of the pressure regulator, the diameter of the jet used, and the cross-sectional diameter of the trachea.[2,10,11] In our department, we use only the supraglottic setting during microlaryngeal surgery, which is a relatively safe procedure, and complications are very rare.[1] Out of 1,230 cases, we have had 4 previous respiratory complications (3 cases of subcutaneous emphysema and 1 case of pneumomediastinum with subcutaneous emphysema). All of the abovementioned cases were in patients who had not previously undergone irradiation, but all of them had short, stiff necks, making the placement of the laryngoscope difficult, and we assume that a tear in the pharyngeal or laryngeal mucosa occurred during the placement of the laryngoscope. The present case was in a 45-year-old woman with a slender neck, and the placement of the laryngoscope was not traumatic in either the first or the second procedure. The precise cause of the pneumomediastinum in this case is not clear, but we assume that the short time (2 months) between the irradiation and the second procedure was responsible for the occurrence of the pneumomediastinum, as the tissues were still edematous and fragile. Edema of the larynx and the surrounding tissues is a well-known complication occurring in the early months after irradiation; it is related to the dose of irradiation and may require 6 to 12 months to subside.[12]

The complications of the Venturi jet ventilation technique have been described by O'Sullivan and Healy,[2] who discussed several factors that could cause glottic obstruction with subsequent impairment of expiration and could precipitate pneumomediastinum or subcutaneous emphysema. Paratracheal fascial plane dissection with resultant pneumomediastinum or pneumothorax may occur with excessive air pressure. Once air has entered the tissues, the development of tissue emphysema, pneumomediastinum, or pneumothorax may occur suddenly. Therefore, most authors caution against placing the jet tip against the mucosa or below the vocal cords.[1,2,6] In our department, now, when performing microlaryngeal surgery on irradiated patients, we usually use an orotracheal intubation in order to avoid prolonged instrumentation of the glottis and ensuing glottic obstruction.[2]

In the past, we have performed microlaryngeal surgery for squamous cell carcinoma on 22 irradiated patients using Venturi jet ventilation without complications. A retrospective analysis of those cases revealed that all of the patients underwent microlaryngoscopy at least 6 months after the radiotherapy.

Although serious complications secondary to Venturi jet ventilation during microlaryngoscopy are uncommon, if they occur, they may pose a life-threatening emergency. We suggest that one be very cautious when using Venturi jet ventilation a short time after neck irradiation therapy.

REFERENCES

1. Braverman I, Sichel J-Y, Halimi P, Goldsher M, Kadari A. Complication of jet ventilation during microlaryngeal surgery. Ann Otol Rhinol Laryngol 1994;103:624-7.
2. O'Sullivan TJ, Healy GB. Complications of Venturi jet ventilation during microlaryngeal surgery. Arch Otolaryngol 1985;111:127-31.
3. Collins GI, Podoshin L, Fradis M, Schor G, Backner D. Automatic ventilation for suspension laryngoscopy. Laryngoscope 1983;93:374-5.
4. Spoerel WE, Greenway RE. Technique of ventilation during endolaryngeal surgery under general anaesthesia. Can Anaesth Soc J 1973;20:369-77.
5. Norton ML, Strong MS, Vaughan CW, Snow JC, Kripke BJ. Endotracheal intubation and Venturi (jet) ventilation for laser microsurgery of the larynx. Ann Otol Rhinol Laryngol 1976;85:656-63.
6. Rontal M, Rontal E, Wenokur M. Jet insufflation anesthesia for endolaryngeal surgery. Laryngoscope 1980;90:1162-8.
7. Chang J-L, Bleyaert A, Bedger R. Unilateral pneumothorax following jet ventilation during general anesthesia. Anesthesiology 1980;53:244-6.
8. Chang J-L, Meeuwis H, Bleyaert A, Babinski M, Petruscak J. Severe abdominal distention following jet ventilation during general anesthesia. Anesthesiology 1978;49:216-7.
9. Newton NI, Adams AP. Excessive airway pressure during anaesthesia. Hazards, effects and prevention. Anaesthesia 1978;33:689-99.
10. Woo P, Eurenius S. Dynamics of Venturi jet ventilation through the operating laryngoscope. Ann Otol Rhinol Laryngol 1982;91:615-21.
11. Spoerel WE, Grant PA. Ventilation during bronchoscopy. Can Anaesth Soc J 1971;18:178-88.
12. Fajardo LF. Morphology of radiation effects on normal tissues. In: Perez CA, Brady LW, eds. Principles and practice of radiation oncology. Philadelphia, Pa: JB Lippincott, 1992:759-68.

≈

FIFTH INTERNATIONAL CONFERENCE ON HEAD AND NECK CANCER

The Fifth International Conference on Head and Neck Cancer will be held July 29–August 2, 2000, in San Francisco, California. For information, contact Concepts in Meetings & Events, Robin L. Wagner, President, 7819 Lloyd Ave, Pittsburgh, PA 15218-1941; telephone (412) 243-5156; fax (412) 243-5160; e-mail: rlwa@med.pitt.edu.

Ann Otol Rhinol Laryngol 109:2000

IMAGING CASE STUDY OF THE MONTH

MUCOCELE OF THE INFRATEMPORAL FOSSA AS AN UNUSUAL COMPLICATION OF MIDFACIAL FRACTURE

EVAN R. REITER, MD
RICHMOND, VIRGINIA
MEREDITH AUGUST, MD, DMD
BOSTON, MASSACHUSETTS
MARK A. VARVARES, MD
BOSTON, MASSACHUSETTS
HUGH D. CURTIN, MD
BOSTON, MASSACHUSETTS

INTRODUCTION

Complications of midfacial fractures may arise either at the time of the initial trauma or as sequelae of surgical repair even years later.[1-5] Most complications involve functional or cosmetic deficits of the globe and orbit, such as diplopia, enophthalmos, exophthalmos, or ptosis,[2,5] injury to the infraorbital nerve,[3,4] or cosmetic deformity resulting from improper fragment alignment.[1,3,4] Depending on the extent of fracture and the approach used in reduction, complications may arise relating to neighboring structures, including the paranasal sinuses.[1,3-5] These typically include sinusitis or oroantral fistulas.[1,3,4,6] Mucocele formation, not uncommon as a late complication of frontoethmoid fractures,[7] is rarely reported after zygomaticomaxillary complex (ZMC)[8] or orbital floor fractures.[5,9]

Here we describe a rare late complication of a midfacial fracture, a mucocele of the infratemporal fossa. We discuss the pathogenesis of posttraumatic mucoceles in this region, and our treatment of this challenging problem.

CASE REPORT

A 31-year-old man presented to an outside physician with a cystic lesion of the left cheek. Twelve years earlier, during an altercation, the patient had suffered what was diagnosed as an orbital blow-out fracture. This was repaired with an antral pack placed via a Caldwell-Luc approach, with no subsequent ophthalmologic or sinus symptoms. Computed tomography (CT) scanning showed a low-density, rim-enhancing mass anteroinferior to the zygoma, extending into the infratemporal fossa. The maxillary sinus was clear. Bone algorithm scans showed an abnormality of the anterior wall of the maxillary sinus, consistent with the patient's previous trauma and surgical repair. There was a second abnormality of the posterior wall of the sinus, suggesting that the previously diagnosed orbital floor fracture was actually a ZMC fracture. An attempt at cyst removal was made via a sublabial approach. Pathology revealed a stratified squamous epithelium with focal lymphocytic infiltration consistent with an epidermal inclusion cyst.

The patient returned with recurrence of the lesion 6 months later. The CT at that time showed irregularity of the anterior and posterior walls of the maxillary sinus consistent with a ZMC fracture (see Figure, A). There was partial opacification of the maxillary sinus. A low-density abnormality filled much of the infratemporal fossa and masticator space. The abnormality deviated the medial pterygoid muscle posteriorly, impinging on the parapharyngeal fat. More inferiorly, a rounded abnormality of similarly low density was seen just lateral to the buccinator muscle in the buccal fat pad (see Figure, B). The patient was referred to our service at this time for treatment of this recurrent lesion. Findings on physical examination were normal with the exception of a nontender cystic mass of the left malar region, extending posteriorly, inferior to the zygoma. There was hypesthesia in the distribution of the infraorbital nerve. The patient was taken to the operating room and underwent a transantral drainage of the infratemporal fossa portion of the cyst. The posterior wall of the antrum was removed and wide marsupialization of the cyst was achieved in an effort to allow continued drainage of the cyst contents. Pathological findings were consistent with sinonasal respiratory epithelium with chronic inflammation. However, upon 1-month follow-up, the cyst had clearly recurred.

The patient was returned to the operating room

From the Departments of Otology and Laryngology (Reiter, Varvares) and Radiology (Curtin), Massachusetts Eye and Ear Infirmary, and the Department of Oral and Maxillofacial Surgery, Massachusetts General Hospital (August), Harvard Medical School, Boston, Massachusetts. Dr Reiter is currently in the Department of Otolaryngology–Head and Neck Surgery, Virginia Commonwealth University, Richmond, Virginia.

CORRESPONDENCE — Mark A. Varvares, MD, Division of Head and Neck Surgery, Dept of Otology and Laryngology, Massachusetts Eye and Ear Infirmary, 243 Charles St, Boston, MA 02114.

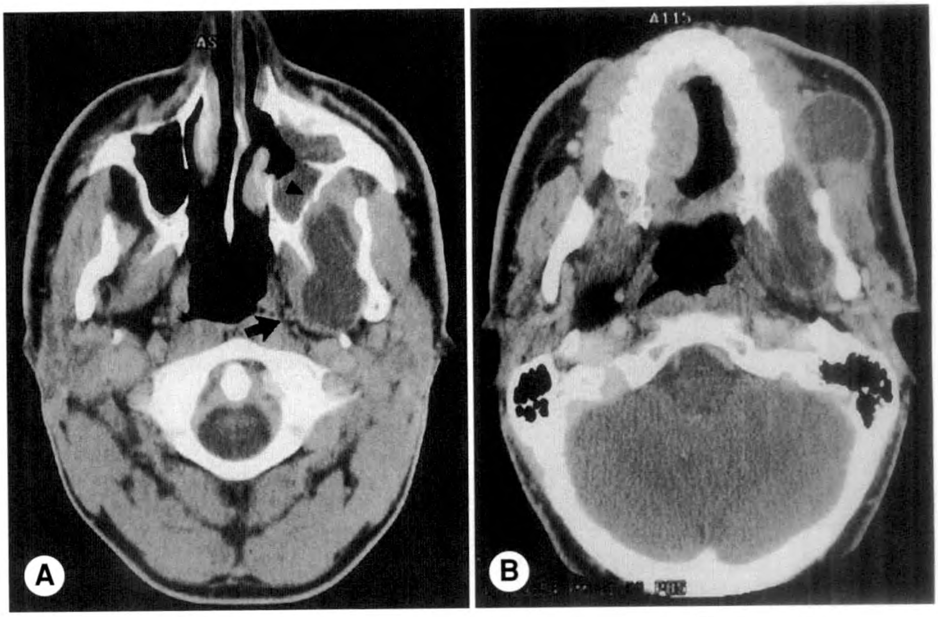

Contrast-enhanced computed tomography scan in axial plane. A) Showing low-density mass of infratemporal fossa and masticator space, with posterior deviation of parapharyngeal fat (arrow). Note fracture of posterior wall of maxillary sinus (arrowhead) immediately adjacent to lesion. B) Lower cut showing infratemporal fossa component of lesion, and second low-density lesion anterior within buccal space.

shortly thereafter and underwent complete excision of the cyst via a modified facial translocation approach. A lateral rhinotomy incision was made with a subciliary and lateral canthal extension, and a facial flap was then elevated in the subperiosteal plane. A cystic mass was immediately encountered along the lateral aspect of the maxilla, extending beneath the zygoma. The anterior maxilla and zygoma were then mobilized as a unit, leaving the palate and orbital floor intact. The cyst was bluntly dissected free from the facial soft tissues anteriorly and from the infratemporal and masticator spaces posteriorly. The cyst was filled with thick, yellow mucoid fluid. Pathological evaluation of the cyst wall revealed respiratory epithelium with chronic inflammation. Six months after operation, there is no evidence of cyst recurrence.

COMMENT

Mucoceles are commonly encountered epithelium-lined, cystic, expansile masses of the paranasal sinuses. They are most frequently encountered in the frontal and ethmoid sinuses, and less commonly in the sphenoid and maxillary sinuses.[10] Mucoceles have the potential for bone erosion. They expand the osseous wall of the involved sinus, and have been found to extend beyond the paranasal sinuses to the orbit,[7,9] to the facial soft tissues,[11] or intracranially.[12]

Central to the formation of mucoceles is sequestration of viable sinus mucosa without an adequate pathway for mucus drainage, from either obstruction of the sinus ostium or entrapment of mucosa in an ectopic location.[10,11] The most frequent cause of mucosal entrapment is trauma, whether surgical or otherwise, although other sinonasal disorders such as tumors, inflammatory polyps, and septal deviation are implicated.[10] A vast experience with postoperative mucoceles of the maxillary sinus has been reported in Japan. Although the pathogenesis is likely multifactorial, one reason for the high prevalence in this population was felt to be the high incidence of sinusitis and low availability of antibiotics in post–World War II Japan, leading to a large number of Caldwell-Luc procedures performed.[11] Kaneshiro et al[11] reported 71 patients as having postoperative maxillary cysts that arose 10 to 20 years after the Caldwell-Luc procedure. Roughly 75% of these patients presented with pain or swelling of the cheek, while less common presentations included purulent intraoral discharge (9%), toothache (9%), and paresthesias (1%).

The development of posttraumatic mucoceles in the maxillary sinus was noted by Kreidler and Koch,[8] who endoscopically examined the maxillary sinuses of 25 asymptomatic patients an average of 7 years after midfacial trauma. One or more mucoceles were found in 4 patients, and significant mucosal synechiae in 6. There are, however, only a few reports in the literature of mucoceles occurring as sequelae of orbital floor fractures.[5,9] Several large series looking at repair of orbital floor[6] and midfacial fractures[3] did not report mucoceles among their complications. It is possible that posttraumatic mucoceles noted within the maxillary sinus endoscopically[8] seldom manifest clinically and are thus not recognized or reported as complications of midfacial fractures. Alternately, the discrepancy may arise from selection bias, as ophthalmologic or maxillofacial surgeons treating orbital floor or midfacial fractures might not be aware of a patient's subsequently presenting to an otolaryngologist with a postoperative mucocele.

The case presented here is to our knowledge the first case reported in the English-language literature of a mucocele of the infratemporal fossa arising as a sequela of a midfacial fracture. The fracture was originally diagnosed and treated as an isolated orbital floor fracture. However, the patient's initial CT scan on presentation to our service showed a fracture of the posterior wall of the maxillary sinus (see Figure, A) in addition to the diagnosed orbital floor fracture. An orbital floor fracture may extend posteriorly through the inferior orbital fissure and then inferiorly along the posterolateral wall of the maxilla in the infratemporal and pterygopalatine fossae. This fracture plane is considered part of the "classic" tripod fracture; thus, the patient's injury is more appropriately classified as a ZMC fracture. As the posterior sinus wall is cosmetically invisible and non–load-bearing, it is seldom considered in reduction of midfacial fractures. In the case presented, the posterior sinus wall fracture or its reduction with antral packing likely led to mucosal entrapment in the infratemporal fossa and considerable morbidity secondary to mucocele formation. This is supported by the proximity of the posterior wall fracture to the mucocele (see Figure, A) and the absence of maxillary sinus opacification seen in the patient's original CT scans.

The concept of mucosal entrapment leading to mucocele formation is supported by rare reports of mucoceles arising completely external to the paranasal sinuses. Stewart et al[5] reported a case of intraorbital mucocele after repair of an orbital floor fracture. Stack and Klotch[13] described a mucocele of the pterygomaxillary space that arose after transantral ligation of the internal maxillary artery. Both groups of authors hypothesized that the fracture or operative trauma led to sequestration of antral mucosa that initiated formation of the cyst. A third report, by Weiss,[14] described 2 cases of abscess formation in the infratemporal fossa after midfacial fractures. These may also represent posttraumatic mucoceles arising from mucosal entrapment in the infratemporal fossa that subsequently became infected.

The implication of this case for facial trauma lies in what we may term "mucosal reduction" in addition to fracture reduction. Certainly, the apparent rarity of this complication does not justify the added morbidity of routine exploration of every posterior wall maxillary sinus fracture identified by CT in patients with facial trauma. However, in cases in which access to a sinus cavity has been provided by the trauma itself, or achieved for fracture reduction, we suggest careful examination of exposed fracture lines for mucosal entrapment. This includes functionally and cosmetically "silent" areas such as the posterior wall of the maxillary sinus, in which fractures are typically not reduced. For example, in the case presented here, the posterior maxillary sinus wall might have been inspected via the Caldwell-Luc approach used to reduce the orbital floor fracture without added time or morbidity. In addition, the case of Stewart et al[5] raises the possibility of mucosal entrapment occurring at a site of fracture reduction. This might also have occurred in our patient, as the transantral reduction of the orbital floor fracture, rather than the posterior wall maxillary sinus fracture itself, might have actually led to mucosal entrapment in the infratemporal fossa. These cases illustrate how a brief search for and reduction of entrapped sinus mucosa at the time of fracture repair might obviate the need for further surgery and subsequent morbidity.

Treatment of mucoceles ideally involves complete removal of the cyst lining. This has traditionally been accomplished via a Caldwell-Luc approach.[11,13] Larger cysts may be treated with wide marsupialization to allow for continued drainage, as complete excision might otherwise be difficult or lead to significant morbidity. This may be achieved endoscopically,[15,16] transfacially,[16] or sublabially with a Caldwell-Luc approach.[11] We first attempted marsupialization of the mucocele in our patient, as complete extirpation of this extensive cyst, as well as control of major vessel bleeding if encountered, would have been difficult by a transantral approach. After recurrence following this more conservative treatment, we chose a more aggressive approach that would allow relatively safe and wide exposure for complete extirpation of the cyst. Janecka et al[17,18] have popularized the concept of "modular craniofacial disassembly" for access to tumors of the skull base. Borrowing from this principle, we mobilized the anterior aspect of the maxilla and zygoma to achieve direct exposure to the buccal space, infratemporal fossa, and masticator space. After complete cyst excision, fixation of the mobilized bone with miniplates provided for an excellent cosmetic result 6 months after operation.

ACKNOWLEDGMENT — The authors thank Richard Cortese for his assistance with the Figure.

REFERENCES

1. Finlay PM, Ward-Booth RP, Moos KF. Morbidity associated with the use of antral packs and external pins in the treatment of the unstable fracture of the zygomatic complex. Br J Oral Maxillofac Surg 1984;22:18-23.
2. Mauriello JA. Complications of orbital trauma surgery. Adv Ophthalmic Plast Reconstr Surg 1988;7:99-115.
3. Souyris F, Klersy F, Jammet P, Payrot C. Malar bone fractures and their sequelae: a statistical study of 1393 cases covering a period of 20 years. J Craniomaxillofac Surg 1989;17:64-8.

4. Zingg M, Laedrach K, Chen J, et al. Classification and treatment of zygomatic fractures: a review of 1,025 cases. J Oral Maxillofac Surg 1992;50:778-90.

5. Stewart MG, Patrinely JR, Appling WD, Jordan DR. Late proptosis following orbital floor fracture repair. Arch Otolaryngol Head Neck Surg 1995;121:649-52.

6. Goldman RJ, Hessburg PC. Appraisal of surgical correction in 130 cases of orbital floor fracture. Am J Ophthalmol 1973;76:152-5.

7. Larson CH, Adkins WY, Osguthorpe JD. Posttraumatic frontal and frontoethmoid mucoceles causing reversible visual loss. Otolaryngol Head Neck Surg 1983;91:691-4.

8. Kreidler JF, Koch H. Endoscopic findings of maxillary sinus after middle face fractures. J Oral Maxillofac Surg 1975;3:10-4.

9. Kaltreider SA, Dortzbach RK. Destructive cysts of the maxillary sinus affecting the orbit. Arch Ophthalmol 1988;106:1398-402.

10. Zizmor J, Noyek AM. Cysts, benign tumors and malignant tumors of the paranasal sinuses. Otolaryngol Clin North Am 1973;6:487-508.

11. Kaneshiro S, Nakajima T, Yoshikawa Y, Iwasaki H, Tokiwa N. The postoperative maxillary cyst: report of 71 cases. J Oral Surg 1981;39:191-8.

12. Schaefer SD, Close LG, Mickey BE. The surgical management of epidural mucoceles. Laryngoscope 1988;98:14-7.

13. Stack BC Jr, Klotch DW. Mucocele of the pterygomaxillary space. Ann Otol Rhinol Laryngol 1995;104:246-7.

14. Weiss BR. Infratemporal fossa abscess: unusual complication of maxillary sinus fracture. Laryngoscope 1977;87:1130-3.

15. Kennedy DW, Josephson JS, Zinreich SJ, Mattox DE, Goldsmith MM. Endoscopic sinus surgery for mucoceles: a viable alternative. Laryngoscope 1989;99:885-95.

16. Marks SC, Latoni JD, Mathog RH. Mucoceles of the maxillary sinus. Otolaryngol Head Neck Surg 1997;117:18-21.

17. Janecka IP, Sen CN, Sekhar LN, Arriaga M. Facial translocation: a new approach to the cranial base. Otolaryngol Head Neck Surg 1990;103:413-9.

18. Janecka IP. Classification of facial translocation approach to the skull base. Otolaryngol Head Neck Surg 1995;112:579-85.

≈

INTERNATIONAL CONFERENCE ON NEWBORN HEARING SCREENING DIAGNOSIS AND INTERVENTION

The International Conference on Newborn Hearing Screening Diagnosis and Intervention will be held in Milan, Italy, October 12-14, 2000. In Europe, contact Dr Ferdinando Grandori, Center of Biomedical Engineering, Polytechnic of Milan, piazza Leonardo da Vinci 32, I-20133 Milan, Italy; fax +39.02.2399.3360; e-mail NHS2000@biomed.polimi.it. In the United States, contact Dr Deborah Hayes, The Children's Hospital, 1056 E 19th Ave, B030, Denver, CO 80218; telephone (303) 861-6424; fax (303) 764-8220; e-mail: Hayes.deborah@tchden.org.

BOOK REVIEWS

Headache and Facial Pain

Franco Mongini. Hard cover, illustrated, indexed, 284 pages, 1999. Thieme, Stuttgart, Germany, $99.

Purpose: The author wishes to convey that there are multiple factors that complicate the assessment and management of different types of headaches and facial pain. Various local and systemic etiologic factors can be present in the same disorder, and disorders of different types can be superimposed in the same patient. The author feels that patients can receive a diagnosis and treatment that take into account only certain aspects of the problem, depending on the specialist that is involved. Further, he is convinced that there is the necessity for a common approach to both groups of disorders: headache and facial pain.

Contents: The book is divided into 4 parts: classification and pathophysiology, general clinical aspects, diagnosis and therapy of headache, and diagnosis and therapy of facial pain.

Attributes: There is considerable interplay among the various disorders, such as myogenic facial pain and myogenic craniocervical pain, cluster headaches and chronic paraxial hemicrania, and, of course, migraine itself. Added to this are headache variants — obviously a very complex problem. It is no wonder that psychological concerns become so important. The author makes a strong thrust toward conveying the idea that typically there are 2 or more causes of a pain disorder and that the physician needs to recognize this. The book is not overweighted with migraine headaches or any other neurologic disorder. Rather, there are data generally and generously cited of mechanisms relevant to the clinical problems for each disorder.

Limitations: The book as a whole is greater than any of its parts. In other words, the condition of otalgia is not mentioned, and one would have to grasp the entire book to get general and specific information about the causes and diagnosis.

Applicability: The book is written by a neurologist, but written for other interested specialties (otolaryngologists, dentists, neurosurgeons). There is not an overplay of specific neurologic disorders. It adds tremendously to the physician's repertoire of knowledge on the subject of headaches.

DENNIS G. PAPPAS, MD
Birmingham, Alabama

Molecular Medicine: Novel Findings of Gene Diagnosis, Regulation of Gene Expression, and Gene Therapy

Isao Hashimoto, Hideichi Shinkawa, Toshihiro Suda, Shigeki Tsuchida, and Sorokuyagihashi Jouniuitto, editors. Hard cover, illustrated, indexed, 222 pages, 1999. Elsevier, New York, NY, $139.50.

Purpose: To publish all presented papers for the symposium held in Hirosaki, Japan, in July 1998, which primarily focused on the fields of gene diagnosis, regulation of gene expression, and gene therapy. All presented papers in the symposium were collected and published within this book. It was felt by the editors that the scientists provided in-depth information on recent research work and an overview of their specific subjects.

Contents: Three sections that include gene diagnosis (10 papers), regulation of gene expression (14 papers), and gene therapy (3 papers). Presenters of these papers are from different fields such as biochemistry, internal medicine, dermatology, and otology.

Attributes: Someday, DNA (deoxyribonucleic acid) tests may provide instant diagnosis of future ailments and life expectancy, though they do not as yet. Genes for approximately 1,200 disorders have been identified. Most people carry a few defective genes with no signs of disease, and many genes only contribute to susceptibility. This book conveys chemical studies that show DNA alterations as the cause or pathogenesis of many diseases. Of exceptional value is the portion on otolaryngology, mainly that of hereditary sensorineural hearing loss, in which the overview is comprehensive, concise, and informative. The use of molecular techniques in the diagnosis of hearing impairment is not as yet in effect. However, the information is becoming more available, and it is considerable, as found in this book. Typically, the otolaryngologist will use molecular information to accurately diagnose different types of hearing impairment.

Limitations: Only 2 chapters of this book are referable to the otolaryngologist.

Applicability: It is worth the time of every otolaryngologist to read at least the 2 chapters referable to the specialty contained in this book. I strongly recommend it.

DENNIS G. PAPPAS, MD
Birmingham, Alabama

Atlas of Head and Neck Surgery

Carl E. Silver and John S. Rubin. Second edition. Hard cover, illustrated, indexed, 348 pages, 1999. Churchill Livingstone, New York, NY, $195.

Purpose: To demonstrate the commonly performed major operative procedures for management of neoplasms of the head and neck.

Contents: There are 11 chapters, which include applications of free tissue transfer for reconstruction, approaches to the cranial base, both anterior and lateral, laryngeal conservation surgery, cysts and primary tumors of the neck, tumors of the lip and parapharyngeal space, and management of mediastinal goiter and parathyroid glands.

Attributes and Limitations: The authors (and contributors) give a clear, representative illustration of the important steps of each operation in a prolific and productive manner. Their ability to discuss each operation in a comprehensive manner is done with maximum impact and shows skillful execution. Likewise, the magnificent drawings give fine support to the text. Actually, for an atlas, there is ample description of the procedural techniques. Though it is all done in black-and-white, without any color, the drawings are very clear-cut and descriptive.

Applicability: This text is a valuable reference to all otolaryngologists, because there is involvement of all aspects of the otolaryngological specialties.

DENNIS G. PAPPAS, MD
Birmingham, Alabama

Ann Otol Rhinol Laryngol 109:2000

IDIOPATHIC SUDDEN SENSORINEURAL HEARING LOSS: TEMPORAL BONE HISTOPATHOLOGIC STUDY

JUHA-PEKKA VASAMA, MD
HELSINKI, FINLAND

FRED H. LINTHICUM, JR, MD
LOS ANGELES, CALIFORNIA

We microscopically examined the temporal bones of 12 ears with idiopathic sudden sensorineural hearing loss (iSSNHL), 10 ears with presbycusis, 11 ears with normal hearing, and 8 unaffected contralateral ears of patients with iSSNHL. The degeneration of the spiral ligament, vascular stria, hair cells, dendrites, and apical spiral ganglion cells was greater in ears with iSSNHL than in the other groups. The apical ganglion cells were significantly more affected than the basal ganglion cells, and the spiral ganglion cell loss increased as a function of duration of iSSNHL. Cochlear ossification was found in 1 ear with iSSNHL, and hydrops in 2. These findings suggest a viral rather than a vascular or ruptured inner ear membrane origin for iSSNHL.

KEY WORDS — ganglion cells, histopathology, idiopathic sensorineural hearing loss, sensorineural hearing loss, sudden sensorineural hearing loss, temporal bone.

INTRODUCTION

Idiopathic sudden sensorineural hearing loss (iSSNHL) occurs abruptly or develops over several days. The hearing loss is usually unilateral and varies in severity from a mild loss to profound deafness. About 25% of patients have spontaneous recovery, 50% have partial return of hearing, and 25% have no recovery of hearing.[1] The cause of this disorder is not known, but histopathologic studies of human temporal bones have suggested viral,[2-6] vascular,[7,8] and immunologic[9] causes and a theory of ruptured inner ear membranes.[10,11]

The histopathologic evidence to support the vascular theory is not very convincing. For example, experimentally induced hearing loss of vascular origin causes extensive cochlear fibrosis and ossification in the inner ears of dogs and guinea pigs.[12,13] However, similar changes have not been found in humans with iSSNHL in histopathologic or radiologic studies.[2,14]

The clinical and histopathologic evidence from animal and human studies favors a viral cause for iSSNHL. For example, changes in inner ear structures and progressive or abrupt hearing loss have been found in guinea pigs after experimentally induced cytomegaloviral and herpetic viral labyrinthitis.[15,16] In humans, a clear association of herpes viruses to iSSNHL has been documented, and other neurotropic viruses like mumps and measles might account for severe neuronal atrophy in ears with iSSNHL as a result of postnatal presumptive viral labyrinthitis.[17,18] Interestingly, human temporal bone histopathologic findings have been quite similar both in ears with known viral labyrinthitis and in ears with iSSNHL.[2,3,19,20] In clinical work, one can quite frequently see iSSNHL occur after upper respiratory tract infection.

To our knowledge, no attempts have been made to evaluate how iSSNHL affects the neuronal population in different segments of the spiral ganglion in the cochlea. Therefore, we studied histopathologic changes in ears with iSSNHL and compared the findings with those in presbycusis, in normal hearing, and in the ear contralateral to ears with iSSNHL. A preliminary evaluation had suggested a greater decrease in the number of apical neurons than in other types of sensorineural hearing loss.

MATERIALS AND METHODS

All specimens that fulfilled the diagnostic criteria of iSSNHL, presbycusis, and normal hearing in the House Ear Institute's collection of 1,362 temporal bones were included in the study. There were temporal bones from 12 ears with iSSNHL (7 female, 5 male; age, 42 to 95 years; mean age, 74 years), 10 ears with presbycusis (7 female, 3 male; age, 76 to 92 years; mean age, 84 years), 11 ears with normal hearing (7 female, 4 male; age, 44 to 82 years; mean age, 66 years), and the unaffected ears contralateral to 8 ears with iSSNHL. The ears with iSSNHL were from patients with abrupt unilateral partial or profound sensorineural hearing loss without a cause. The criteria for presbycusis were based on the clinical diagnosis made in the clinic before the patient's death. The diagnosis was made in middle-aged and elderly

---

From the House Ear Institute, Los Angeles, California. Supported by the Finnish Cultural Foundation and the Del E. Webb Foundation.

CORRESPONDENCE — Juha-Pekka Vasama, MD, Dept of Otolaryngology, Helsinki University Central Hospital, Haartmaninkatu 4 E 00290 Helsinki, Finland.

TABLE 1. MEAN PERCENT OF NORMAL FOR STRUCTURES IN CASES OF IDIOPATHIC SUDDEN SENSORINEURAL HEARING LOSS

Pt No.	*Age (y)*	*PTA (dB)*	*Duration (y)*	*Spiral Ligament*	*Vascular Stria*	*Hair Cells*	*Dendrites*	*Basal Ganglion Cells*	*Apical Ganglion Cells*
1	79	48	0.1	100	15	90	75	100	100
2	77	63	1.7	100	20	70	88	100	100
3	61	90	0.5	100	15	20	5	100	14
4	76	37	0.3	100	50	75	85	98	33
5	75	B	47	100	15	0	0	17	5
6	94	B	3	5	5	0	5	88	23
7	65	B	28	100	50	65	70	78	100
8	77	93	50	100	55	5	20	62	37
9	71	B	15.5	100	90	70	50	100	100
10	95	110	28	100	20	5	45	95	72
11	42	B	1.3	80	45	30	65	100	46
12	75	50	14	UD	40	75	65	98	73

PTA — pure tone average; B — beyond output of audiometer; UD — undetermined.

individuals with high-tone hearing losses of various degrees with no history (including family) or physical finding to account for the loss. The normal-hearing ears were from patients with a unilateral problem (vestibular schwannoma or other tumor, or chronic otitis) who had an auditory threshold averaging less than 25 dB in the speech frequencies in their healthy ear.

The pure tone average (the mean of the thresholds at the frequencies 0.5, 1, and 2 kHz) was 57 dB in ears with iSSNHL, 52 dB in ears with presbycusis, 11 dB in normal hearing ears, and 26 dB in the unaffected ears of iSSNHL patients. Five patients with iSSNHL (Nos. 5, 6, 7, 9, and 11) had profound hearing loss, and the threshold in the affected ear was beyond the output of the audiometer. One patient (No. 12) had had a respiratory tract infection, and 5 patients (Nos. 2, 3, 6, 8, and 11) had had vertigo at the time of the onset of their hearing loss. The time interval from the onset of iSSNHL to death ranged from 1 month to 50 years (mean, 16 years). Table 1 shows the characteristics of the 12 patients with iSSNHL.

All temporal bones were fixed in 10% formalin, decalcified in ethylenediaminetetraacetic acid, embedded in celloidin, and cut horizontally at a thickness of 20 μm. Every 10th section was stained with hematoxylin and eosin and mounted on a glass slide. Histopathologic changes were examined under a light microscope. The measurements of the cochlear structures were made at the midmodiolar and perimodiolar slides of each bone to avoid the distortion of tangential cuts. The amounts of intact spiral ligament, vascular stria, hair cells, and dendrites (peripheral processes) were determined in the $2^1/_2$ turns of the cochlea that comprise the basal, middle, and apical turns by means of the methods described by Schuknecht[1] and Guild.[21] The measurements of the cochlear structures in ears with iSSNHL, presbycusis, and normal hearing and in the unaffected ears of patients with iSSNHL were compared with those from child and young adult bones that had 100% of all structures. The hair cell counts are accurate when only the midmodiolar and perimodiolar sections are examined, for none of the organ of Corti is cut on the bias, and the 4 rows of hair cells stand out clearly. In slides above or below this level, the organ of Corti is cut on the bias, and in sections 20 μm thick, as ours are, the various rows of hair cells overlap and a clear count cannot be made. In this study, the percentage of hair cell survival denotes outer hair cells and includes inner hair cells only if the survival percentage is zero.

The cell population in the $1^1/_2$ turns of the spiral ganglion was determined with the method described by Otte et al.[22] According to this method, the spiral ganglion was descriptively divided into 4 segments by the vertical midmodiolar line. The ganglion cells in each segment were counted with 200× magnification and with the aid of an ocular grid. The total of neurons was summed for all 4 segments of the cochlea. The ganglion cell population for the whole cochlea was determined by multiplying their summed counts by 10 to account for the unmounted section and again by a factor of 0.9 to account for cells that would be counted twice due to their location at the interface between sections.[23] In every individual ear, the neuronal count in each segment was age-matched to that of the mean value of 100 cochleas without known cochlear neuronal disease taken from the study by Otte et al.[22] This allowed the age-related neuronal loss to be taken into consideration. In our study, basal ganglion cells represent Otte's segments 1 to 3, and apical ganglion cells represent segment 4

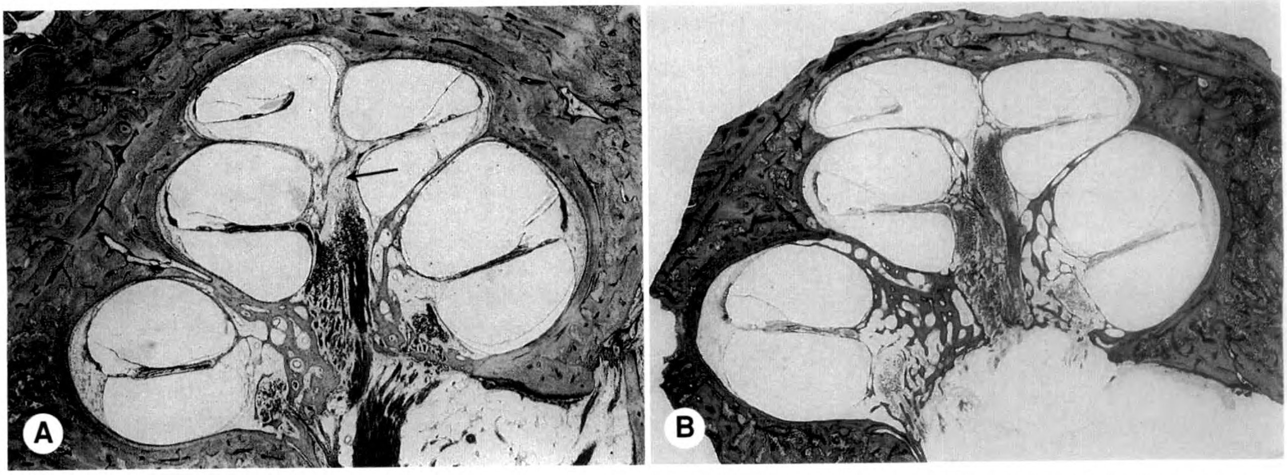

Fig 1. Photomicrographs of cochleas (H & E, original ×5.3). A) Cochlea from patient with idiopathic sudden sensorineural hearing loss with decrease in spiral ganglion cells more pronounced in apical spiral ganglion (arrow). B) Normal cochlea.

(Fig 1). Differences between the groups were evaluated by unpaired *t*-tests, differences in basal and apical ganglion cells within the group were evaluated by paired *t*-tests, and Pearson product moment correlations were calculated. The criterion for statistical significance was set at $p < .05$ (2-tailed).

RESULTS

Table 1 shows the percentage of normal for the intact spiral ligament, vascular stria, hair cells, dendrites, and apical and basal spiral ganglion cells for the 12 ears with iSSNHL. The spiral ligament volume was reduced in only 2 ears and was undetermined in 1 ear. The volume of vascular stria was less than 55% of normal in 11 ears. The amount of hair cells and dendrites was reduced in every ear, and in 6 ears it was less than 50% of normal. Five ears had a normal basal ganglion cell count, and 4 ears had a normal apical ganglion cell count. Eight ears had a greater loss of apical ganglion cells than basal ganglion cells. In ears with a normal apical ganglion cell count, the hair cells and dendrites were less affected; the amount was between 50% and 90% of normal.

Table 2 shows the mean (±SD) percent of normal for the intact spiral ligament, vascular stria, hair cells, dendrites, and apical and basal spiral ganglion cells for each of the 4 groups. The spiral ligament volume was not significantly different in ears with iSSNHL than those in the other groups. The volume of the vascular stria was significantly smaller in the iSSNHL group than in the normal hearing group, but did not differ significantly from the volumes in ears with presbycusis or unaffected ears of patients with iSSNHL. The number of hair cells was, on average, 55% lower in ears with iSSNHL than in the other groups, and the differences were all statistically significant. The number of dendrites was also lower in ears with iSSNHL than in the other groups, and these differences were significant for normal-hearing and unaffected ears.

There were no statistically significant differences between the groups in basal ganglion cell counts. However, the apical ganglion cell count was significantly lower in ears with iSSNHL than in other groups, and in the iSSNHL group the difference between apical and basal ganglion cells was significant ($p < .05$). Cochlear ossification was present in only 1 ear with iSSNHL (patient 11). Cochlear hydrops was present in 2 ears with iSSNHL (patients 4 and 9) and in 1 ear with presbycusis. Cochlear vascularity was equivalent in ears with iSSNHL and normal hearing (Table 2).

TABLE 2. MEAN PERCENT OF NORMAL FOR STRUCTURES BY GROUP

Group	*No. of Ears*	*Age (y)*		*PTA (dB)*	*Spiral Ligament*	*Vascular Stria*	*Hair Cells*	*Dendrites*	*Basal Ganglion Cells*	*Apical Ganglion Cells*	*Cochlear Ossification*	*Cochlear Hydrops*
		Mean	*Range*									
iSSNHL	12	74	42-95	57 ± 25	91 ± 27	34 ± 26	40 ± 35	44 ± 32	86 ± 25	59 ± 36	1	2
iSSNHL, unaffected ear	8	75	61-95	26 ± 18	100 ± 0	49 ± 28	96 ± 5[c]	81 ± 16[a]	90 ± 18	87 ± 24[a]		
Presbycusis	10	84	76-92	52 ± 22	100 ± 0	48 ± 12	76 ± 17[b]	69 ± 21	81 ± 26	86 ± 17[a]		1
Normal hearing	11	66	44-82	11 ± 6	100 ± 0	77 ± 17[c]	93 ± 8[c]	91 ± 4[d]	98 ± 6	92 ± 14[b]		

iSSNHL — idiopathic sudden sensorineural hearing loss.

[a] $p < .05$ in 2-tailed *t*-test compared with iSSNHL; [b] $p < .01$; [c] $p < .001$; [d] $p < .0001$.

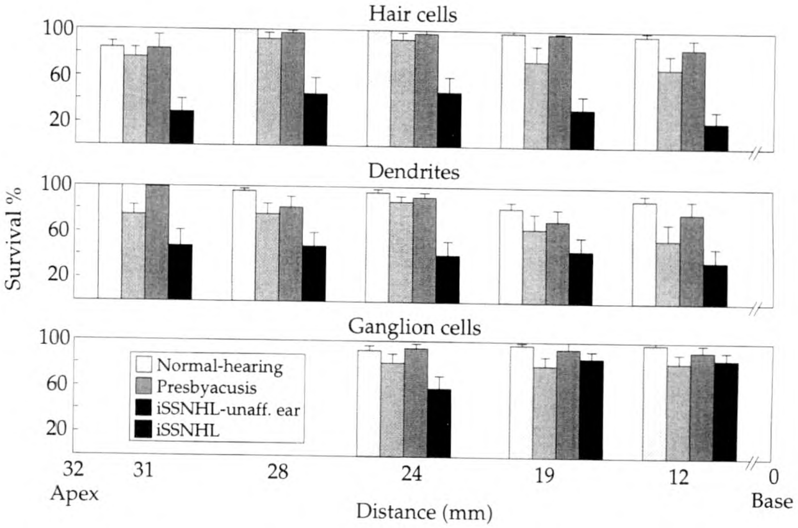

Fig 2. Composite cochleograms (±SEM) of 4 groups studied, illustrating percent of surviving structures in various parts of cochlea. Only structures in midmodiolar and perimodiolar areas were recorded to avoid distortion in tangential sections of sensory structures. Ganglion cell cochleogram, which included all slides with spiral ganglion, does not relate spatially to that of rest of cochlea, because it has only 1.5 turns, versus 2.5 turns for entire cochlea. Apical spiral ganglion receives nerve fibers from apical, as well as middle, turn of cochlea. Hook area is omitted from cochleogram, because its 90° rotation from rest of cochlea makes evaluation of hair cells and dendrites impossible by light microscope. Distance axis is not to scale.

Figure 2 illustrates the mean (±SEM) survival percentage of hair cells and dendrites from the basal (12 and 19 mm), middle (24 and 28 mm), and apical (31 mm) cochlear turns and the basal (10.5 and 18.5 mm) and apical (25 mm) ganglion cell counts from all groups. On average, the hair cell survival rate was greatest in the middle turn and least in the basal turn of the cochlea in all groups. The dendrite survival rate was, on average, largest in the apical turn and smallest in the basal turn of the cochlea in all groups. Hair cell and dendritic degeneration was evident in ears with iSSNHL and with presbycusis. The correlation between the degeneration of hair cells and that of dendrites within the groups was obvious. The mean apical ganglion cell count was slightly smaller than the basal ganglion cell count in all groups except that with presbycusis. However, the loss of apical ganglion cells was remarkable in ears with iSSNHL, and only in this group was the difference between basal and apical ganglion cell counts statistically significant.

There was a statistically significant correlation between the duration of iSSNHL and the total ganglion cell survival rate ($r = -.682$; $p < .05$) and between the pure tone average and the hair cell survival rate ($r = -.966$; $p < .001$). Although there was a tendency for the hair cells and dendrites to decrease as a function of the duration of iSSNHL and for the ganglion cells and dendrites to decrease as a function of the pure tone average, the correlations did not achieve statistical significance.

DISCUSSION

Our study shows that ears with iSSNHL have more severe histopathologic changes in the cochlea than ears with presbycusis or normal hearing or the unaffected ears contralateral to ears with iSSNHL. The degeneration of the spiral ligament, vascular stria, hair cells, dendrites, and apical spiral ganglion cells is greater in ears with iSSNHL than in the other groups. Our findings further demonstrate that in ears with iSSNHL the apical ganglion cells are significantly more affected than the basal ganglion cells, and that the degeneration of apical ganglion cells is not associated with the loss of hair cells or dendrites in the middle and apical turns of the cochlea.

In humans, severe ganglion cell loss has been reported in patients with iSSNHL after respiratory tract infection.[1,24] Moreover, Khetarpal et al[18] speculated that neurotropic viruses like herpes, mumps, and measles might account for severe neuronal atrophy. They found that the spiral ganglion cell count was markedly smaller in human ears with iSSNHL caused by postnatal presumptive viral labyrinthitis than in ears with iSSNHL that had no history of an upper respiratory tract infection. Isolated neuronal atrophy in the cochlea has been shown to indicate a possible viral neuropathy, and viruses that attack the inner ear may have specific cell type preferences.[2] It may be that apical ganglion cells in humans are less resistant to neurotropic viruses than basal ganglion cells.

Fibrosis and ossification of the cochlea have been reported as typical temporal bone findings in iSSNHL with a vascular origin.[2,25] However, no fibrous or osseous obliteration of the intralabyrinthine fluid spaces was observed with 3-dimensional magnetic resonance imaging in inner ears of patients with iSSNHL.[14] In our study, ossification of the cochlea was seen in only 1 of 12 ears with iSSNHL, and every ear had normal cochlear vascularity consistent with the study by Schuknecht.[1] In view of the extensive arterial blood supply and the venous drainage of the human inner ear, we would have expected a clear correlation between the degeneration of apical ganglion cells and the hair cells and dendrites in the middle and apical cochlear turns. In fact, the lack of such a correlation suggests that the apical ganglion cells were the primary target and that their degeneration was not secondary to that of hair cells, supporting cells, and dendrites. Therefore, isolated apical ganglion cell loss does not fit well with a vascular ischemic theory.

Simmons[26] has suggested a double membrane break theory for iSSNHL. A rupture in an oval or round window might lead to a subsequent rupture of Reissner's membrane through a pressure change between the endolymph and perilymph compartments. In our study, endolymphatic hydrops was observed in 2 ears with iSSNHL. However, neither of these 2 patients had symptoms of Meniere's disease or showed any histopathologic evidence of membrane ruptures or fistulas. This agrees with the finding by Schuknecht and Donovan,[2] who reported no histologic evidence of breaks in the windows or in Reissner's membrane or the basilar membrane of the cochlear duct in patients with iSSNHL.

Four patients with iSSNHL had a normal apical ganglion cell count, and 3 of them had a normal basal ganglion cell count, as well. These patients differed from others with iSSNHL, in that all 3 had a much greater survival percentage of hair cells and dendrites. It is possible that in these cases, factors other than the suggested viral origin contributed to hearing loss. For example, sudden hearing loss has been described as a first presenting symptom of Meniere's disease, and endolymphatic hydrops has been documented in the human inner ear after known viral infection.[19,27] One of our patients with iSSNHL and normal ganglion cell counts had cochlear hydrops without any symptoms of Meniere's disease. The endolymphatic hydrops in this patient probably was not severe enough to cause any significant histopathologic changes. Interestingly, greater apical than basal ganglion cell loss has been found in patients with far-advanced Meniere's disease.[28]

Although iSSNHL can result from a variety of causes, the presently available evidence seems to indicate that viral infection is one of the most common etiologic factors. Speculation about the cause has led to the use of diagnostic tools like laser Doppler flowmetry[29] and a variety of treatments like vasodilation, which, based on the recent research findings, seems questionable. However, vasodilators are still widely used among practitioners to treat iSSNHL. In this study, the greater loss of neurons in the apical spiral ganglion, without a corresponding loss of sensory structures, suggests a viral origin, because most other conditions that affect the cochlea, such as prenatal hypoxia, acoustic trauma, presbycusis, ototoxicity, congenital defects, and hereditary factors, produce a majority of their changes in structures in the base of the cochlea.

ACKNOWLEDGMENT — We thank Karen Berliner, PhD, for making valuable comments on the manuscript.

REFERENCES

1. Schuknecht HF. Pathology of the ear. Philadelphia, Pa: Lea & Febiger Press, 1993.
2. Schuknecht HF, Donovan ED. The pathology of idiopathic sudden sensorineural hearing loss. Arch Otorhinolaryngol 1986;243:1-15.
3. Sando I, Harada T, Loehr A, Sobel JH. Sudden deafness: histopathologic correlation in temporal bone. Ann Otol Rhinol Laryngol 1977;86:269-79.
4. Bordley JE, Kapur YP. Histopathologic changes in the temporal bone resulting from measles infection. Arch Otolaryngol 1977;103:162-8.
5. Zajtchuk JT, Matz GJ, Lindsay JR. Temporal bone pathology in herpes oticus. Ann Otol Rhinol Laryngol 1972;81:331-8.
6. Lindsay JR, Davey PR, Ward PH. Inner ear pathology in deafness due to mumps. Ann Otol Rhinol Laryngol 1960;69:918-35.
7. Gussen R. Sudden deafness of vascular origin: a human temporal bone study. Ann Otol Rhinol Laryngol 1976;85:94-100.
8. Belal A Jr. Pathology of vascular sensorineural hearing impairment. Laryngoscope 1980;90:1831-9.
9. Hoistad DL, Schachern PA, Paparella MM. Autoimmune sensorineural hearing loss: a human temporal bone study. Am J Otolaryngol 1998;19:33-9.
10. Gussen R. Sudden hearing loss associated with cochlear membrane rupture: two human temporal bone reports. Arch Otolaryngol 1981;107:598-600.
11. Gussen R. Sudden deafness associated with bilateral Reissner's membrane ruptures. Am J Otolaryngol 1983;4:27-32.
12. Igarashi M, Alford BR. Functional and histopathological correlations after microembolism of the peripheral labyrinthine artery in the dog. Laryngoscope 1969;79:603-23.
13. Suga F, Preston J, Snow JB. Experimental microembolism of cochlear vessels. Arch Otolaryngol 1970;92:213-20.
14. Albers FW, Demuynck KM, Casselman JW. Three-dimensional magnetic resonance imaging of the inner ear in idiopathic sudden sensorineural hearing loss. J Otorhinolaryngol Relat Spec 1994;56:1-4.
15. Woolf NK, Harris JP, Ryan AF, Butler DM, Richman DD. Hearing loss in experimental cytomegalovirus infection of the guinea pig inner ear: prevention by systemic immunity. Ann Otol Rhinol Laryngol 1985;94:350-6.
16. Stokroos JS, Albers FWJ, Schirm J. The etiology of idiopathic sudden sensorineural hearing loss: experimental herpes simplex virus infection of the inner ear. Am J Otol 1998;19:447-52.

17. Wilson WR. The relationship of the herpesvirus family to sudden hearing loss: a prospective clinical study and literature review. Laryngoscope 1986;96:870-7.

18. Khetarpal U, Nadol JB, Glynn RJ. Idiopathic sudden sensorineural hearing loss and postnatal viral labyrinthitis: a statistical comparison of temporal bone findings. Ann Otol Rhinol Laryngol 1990;99:969-76.

19. Yoon TH, Paparella MM, Schachern PA, Alleva M. Histopathology of sudden hearing loss. Laryngoscope 1990;100: 707-15.

20. Schuknecht HF, Kimura RS, Naufal PM. The pathology of sudden deafness. Acta Otolaryngol (Stockh) 1973;76:76-97.

21. Guild SR. A graphic reconstruction method for the study of the organ of Corti. Anat Rec 1921;22:141-57.

22. Otte J, Schuknecht HF, Kerr AG. Ganglion cell populations in normal and pathological human cochlea: implications for cochlear implantation. Laryngoscope 1978;88:1231-46.

23. Konigsmark BW. Methods for the counting of neurons. In: Nauta WJH, Ebbeson SOE, eds. Contemporary research methods in neuroanatomy. Berlin, Germany: Springer-Verlag, 1970:315-40.

24. Ishii T, Toriyama M. Sudden deafness with severe loss of cochlear neurons. Ann Otol Rhinol Laryngol 1977;86:541-7.

25. Belal A Jr. The effects of vascular occlusion on the inner ear. J Laryngol Otol 1979;93:955-68.

26. Simmons FB. The double membrane break syndrome in sudden hearing loss. Laryngoscope 1979;89:59-66.

27. Byl FM Jr. Sudden hearing loss: eight years' experience and suggested prognostic table. Laryngoscope 1984;94:647-61.

28. Vasama J-P, Linthicum FH Jr. Ménière's disease and endolymphatic hydrops without Ménière's symptoms: temporal bone histopathology. Acta Otolaryngol (Stockh) 1999;119:297-301.

29. Miller JM, Ren T-Y, Nuttall AL. Studies of inner ear blood flow in animals and human beings. Otolaryngol Head Neck Surg 1995;112:101-13.

* * *

CALL FOR PAPERS

Pediatric Diabetes (Mark A. Sperling, MD, Editor-in-Chief; masp+@pitt.edu) is pleased to solicit manuscripts for publication in forthcoming issues and will consider full-length papers, preliminary communications with important new information, clinical reports, and reviews of major topics. Invited editorials and perspectives will be a regular feature. Full-length papers and reviews of major topics should generally not exceed a total of 5,000 words (approximately 20 double-spaced typewritten pages) for the text, references, tables, figures, and figure legends, excluding running title page, title page, and abstract. Preliminary communications with important new information, clinical reports, invited editorials, and perspectives should generally not exceed 2,000 words. For more information, please contact our web site at: www.munksgaard.dk, go to Scientific Journals, and click on the mock-up of the journal cover. Also, you can contact the Editorial Office at: Editorial Assistant. Sandra K. Arjona, MLS, arjonas@chplink.chp.edu, Children's Hospital of Pittsburgh, 3705 Fifth Ave, Pittsburgh, PA 15213; telephone (412) 692-7765; fax (412) 692-7813. Manuscripts can be submitted electronically as an e-mail attachment, or as hard print copy sent in quadruplicate to the above address.

Ann Otol Rhinol Laryngol 109:2000

MATHEMATICAL MODEL EXPLAINING THE SOURCES OF ERROR IN CERTAIN ESTIMATES OF THE GAS EXCHANGE CONSTANTS FOR THE MIDDLE EAR

WILLIAM J. DOYLE, PHD
PITTSBURGH, PENNSYLVANIA

Mover-Lev and colleagues reported a carbon dioxide–oxygen time-constant ratio of 3.9 for transmucosal gas exchange in guinea pigs under conditions of a large positive oxygen pressure gradient and a negative carbon dioxide gradient. That ratio is much less than the value of 19 reported previously for monkeys and used in predictive models of middle ear pressure regulation. In this report, the mathematics that underlie models of transmucosal gas exchange are developed and the conditions that allow accurate estimation of time constants are defined. The results demonstrate that the experimental and analytic methods used by Mover-Lev et al do not control for certain confounding effects or concurrently measure all required system parameters. Under the most realistic conditions, their ratio of 3.9 represents a significant underestimation of a true value on the order of 10. Also, their expectation of nonvarying, transmucosal time constant ratios for pairings that include reactive gases is simplistic and true only for identical experimental contexts.

KEY WORDS — gas exchange, middle ear pressure, modeling.

INTRODUCTION

The normal middle ear (ME) can be considered to be a relatively rigid, nonventilated, intermittently open gas pocket. For proper function, that gas pocket must be maintained at near-ambient pressure, and the mechanism(s) for regulating ME pressure is fundamental to our understanding of ME physiology and pathophysiology.[1-6] To describe ME pressure regulation, the relative rates of gas exchange between the ME and 4 adjacent compartments need to be defined. These include the diffusion-limited exchanges of gas with the environment via the tympanic membrane[6-8] and with the inner ear via the round window membrane[9,10]; the perfusion-diffusion–limited exchange of gas with the ME mucosa[11,12]; and the gradient-driven bolus exchange of gas with the nasopharynx during transient opening of the eustachian tube.[13]

Mathematical models describing gas exchange between the ME and blood have been published.[10,14,15] The use of these models to describe ME pressure regulation requires accurate estimates of their free parameters, which include, for the most simple situations, the gas-specific time constants and the extant partial pressure gradients that drive the exchange. In that regard, experimental results showed that certain assumptions previously included in calculating the theoretical values of the time constants for different gases were in error and that empirical estimates derived from direct measurement greatly improve the explanatory power of the models.[14-18] For example, in monkeys, the rate of ME pressure change following the establishment of relatively small positive ME-blood partial pressure gradients for different gases was studied. Those experiments reported a relative ratio of 698:37:1 for the carbon dioxide–oxygen–nitrogen (CO_2:O_2:N_2) time constants, which is different from the ratio of approximately 38:2:1 predicted for perfusion-limited gas exchange.[11,12] These data were interpreted as evidencing a primarily diffusion-limited ME-blood exchange of O_2 and CO_2, and a perfusion-limited exchange of N_2 and other inert gases. From these experimentally derived values, simple 2-compartment mathematical models accurately predict ME gas composition, the change in ME pressure during periods of eustachian tube obstruction, and the counterintuitive ME pressure response to certain maneuvers that affect ME gas composition.[16-18]

More recently, Mover-Lev et al[19] studied transmucosal gas exchange in guinea pigs under conditions of a positive ME-to-blood O_2 pressure gradient and a negative CO_2 gradient. They reported a ratio for the measured CO_2-to-O_2 time constants on the order of 3.9 and argued that the respective constants (ie, CO_2:O_2 ratio of around 19) reported for the monkey experiments were in error. In the present report, the experimental and analytic methods used by Mover-Lev et al are shown to calculate inaccurate estimates of the time constants for transmucosal gas exchange because of a failure to control for certain confound-

---

From the Department of Otolaryngology, Children's Hospital of Pittsburgh and the University of Pittsburgh School of Medicine, Pittsburgh, Pennsylvania. Supported in part by a grant from the National Institutes of Health (DC01620).

CORRESPONDENCE — William J. Doyle, PhD, Dept of Pediatric Otolaryngology, One Children's Place, 3705 Fifth Ave at DeSoto St, Pittsburgh, PA 15213-2583.

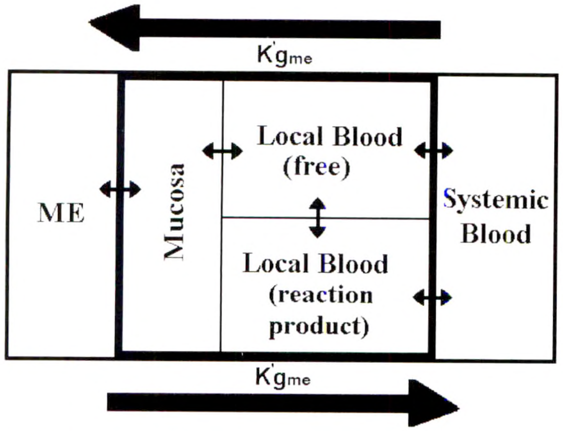

Fig 1. Diagram depicts subcompartments and related pathways for transmucosal exchange of gas between middle ear (ME) and systemic blood. For certain limiting conditions, details of subcompartment exchanges can be treated as black box, and exchange can be modeled as gas transfer from middle ear to systemic blood. (See text for details.)

ing effects and to concurrently measure all required system parameters. Because of the importance of estimating the time constants for transmucosal gas exchange to realistic descriptions of ME pressure behavior, the theory underlying the experimental measurement of those constants is presented as a mathematical model, and its implications with respect to experimental design are discussed.

METHODS

Figure 1 is a diagram of the pathways for gas exchange between the ME and systemic blood. There, gradient-driven gas exchange occurs between sequential compartments; ie, the ME air space exchanges gas with the mucosa, the mucosa exchanges gas with the local blood, the local blood exchanges gas with blood components (for reactive gases), and the local blood and blood components exchange gas with the systemic blood by volume transfers. For most experimental situations, information is unavailable for the exchange parameters that govern intercompartmental transfers. Therefore, subcompartmental exchanges are treated usually as a black box, with the measurable system parameters consisting of the ME and systemic blood gas partial pressures and the rate of change in ME pressure.

The general behavior of ME pressure in this compartmental system is quite complex and can be nonlinear. However, under certain conditions, that description reduces to a set of linear equations that relate the rates of change in gas partial pressures to the product of a multicomponent, gas-specific time constant and the extant partial pressure gradient between ME and systemic blood. This can be appreciated by considering the electrical circuit presented in Fig 2A, which is analogous to the exchange pathways represented in Fig 1. In the electrical analogy, the gas partial pressure (Pgi) of compartment i is represented by a voltage, the exchange volumes (number of moles of gas g exchanged per unit time = $Ng/\delta t$) by current flows, barriers to exchange by resistors, and the effective compartment volumes by capacitors. Specifically, in the Figure, gas partial pressures in the ME, mucosa, and local blood (both as molecular gas and as reaction product) are represented as the voltage measured by voltmeters labeled ME, M, B, and P, respectively, while that of the systemic blood is represented as the ground state. Effective ME (Vme), mucosal ($Vgm = VmSgm$, where Sgm is the solubility of gas g in the mucosa), and local blood volumes ($Vgb = VbSgb$) are represented by the capacitors labeled C1, C2g, and C3g, respectively, and the volume of gas potentially stored as a reaction product is represented by the capacitor labeled C4g. The resistors labeled R1g and R2g, which limit intercompartmental gas flow between the ME, mucosa, and local blood, are valued (1/conductance) as the inverse of the respective time constants (Kig) for intercompartmental gas (g) transfers. The resistor (R3g) between the capacitors representing local blood (C3g) and reaction product (C4g) is valued as the inverse of the time constant for the specific chemical reaction (which for reactive gases can be assumed to approach 0; ie, $K3g >>> K1g, K2g$), and the resistors between the capacitors representing the 2 local blood compartments (C3g, C4g) and the ground are valued as functions of the inverse of the volume blood flow rate (1/Q). For this system, the rate of change in the voltage at C1 (ME partial pressure) depends on the total potential (ref. ground), and on the relative scaling of the 5 resistances and of the 4 capacitances; and the rate of change in total ME pressure is the sum of the

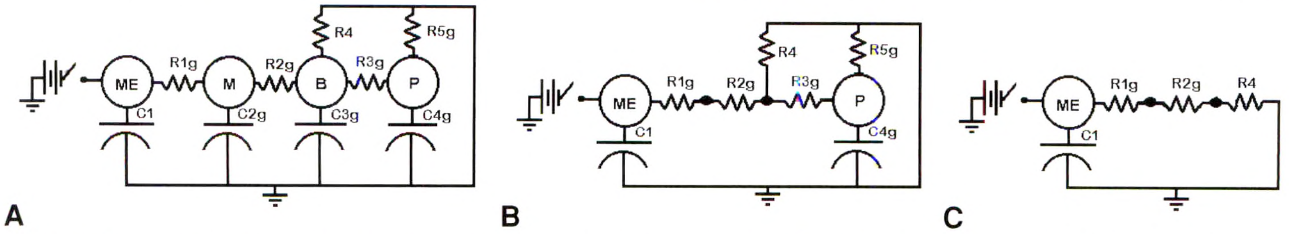

Fig 2. Representation of pathways for gas exchange between middle ear and systemic blood as electrical circuit (A) and simplifications of that circuit under certain limiting conditions applicable to middle ear (B,C). (See text for details.)

voltage changes for all component gases.

For the normal ME, the volume of the air space is much greater than the effective volume of the mucosa, which in turn is greater than that of the local blood, or in the electrical analogy, $C1 >>> C2g > C3g$. Allowing the capacitance of C2g and C3g to approach 0 simplifies the electrical circuit to that shown in Fig 2B. There, 2 competing subcircuits (exchange pathways) with different relative conductances are in evidence. The first consists of flow across R1g, R2g, R3g, and R5g, while the second consists of the flow across the serial resistors R1g, R2g, and R4. Because flow will be distributed over the 2 pathways in direct relation to the inverse of their respective resistances, pathway 1 will become flow-limiting if $C4g >> 0$ and $R4g >> R3$, and pathway 2 will become flow-limiting when $C4g = 0$ ($\Rightarrow R3g = \infty$) or $R3g >> R4$.

For inert gas exchange, the second set of conditions is strictly applicable (no conversion of molecular gas to reaction products; $C4g = 0$, $R3g = \infty$) and the circuit further simplifies to the configuration shown in Fig 2C. There, the serial resistances of R1g, R2g, and R4 are additive, such that

(1) $$1/Rtg = 1/R1g + 1/R2g + 1/R4 = K'g$$

where K'g is the measured pathway conductance for gas g. From Ohm's law, the value of K'g is equal to the flow divided by the voltage or

(2) $$K'g = (Ng/\delta t)/(Pgme - PgB)$$

where Pgme is the partial pressure of gas g in the ME, PgB the partial pressure of gas g in the systemic blood, and gas flow ($Ng/\delta t$) can be measured as the rate of change in the number of moles of gas g within the ME: $\delta Ngme/\delta t = Ngme(t) - Ngme(t - \delta t)$. From the general gas law, $Ngme = PmeVme/Rt$ (where R is the gas constant and T the system temperature) and equation 2 can be rewritten as

(3) $$K'gme = RTK'g/Vme = (Pgme(t) - Pgme(t - \delta t))/(Pgme(t - \delta t) - PgB)$$

Equation 3 shows that for constant ME volume and temperature, an ME- and gas-specific time constant (K'gme) for the exchange pathway can be estimated by the slope of the linear function relating the change in ME gas partial pressure during a short time interval ($Pgme(t) - Pgme(t - \delta t)$) to the difference between the time-averaged ME gas partial pressure for the interval and the ME-blood differential partial pressure ($Pgme(t - \delta t) - PgB$), with more exact solutions obtained as $\delta t \rightarrow 0$.

As discussed above, equation 3 estimates an ME- and gas-specific time constant for reactive gases under the additional condition that either $C4g = 0$ or $K3g >> K4g$, which causes gas flow to be limited to pathway 2. For the other limiting case (flow exclusively over pathway 1), a time constant for reactive gas exchange can be estimated by equation 3, though the linearity of the function is only maintained for time periods where $C4g > 0$. There, total pathway resistance is given by $1/Rtg = 1/R1g + 1/R2g + 1/R3g + 1/R5g = 1/R1g + 1R2g = K'g$ (when R1g and $R2g >>> R3g \rightarrow 0$, and $C4g > 0$). Under other conditions, reactive gas exchange is distributed over the 2 pathways and the time constant calculated by equation 3 represents a weighted average of the exchange constants for each of the 2 pathways. Also note that if the blood flow per unit time is small (R5g is large), gas transfers to reaction product can saturate that compartment ($Pgp = 0$), causing a time-dependent redistribution of flow to pathway 2. This invalidates the linear form of equation 3 that is prerequisite for the calculation of a time constant by these methods.

The experiment reported by Mover-Lev et al[19] was designed to provide estimates of the CO2:O2 time constant (K'gme) ratio. The measured parameters in their experiment were the system temperature (T), which was considered to be a constant, the average steady-state ME partial pressures of gases in anesthetized guinea pigs, which were assumed to be equal to the respective gas partial pressures in blood (because $\delta Ngme/dt = 0$ when $Pgme = Pgb$), and the fractional pressure (Fg) contributed by each gas as measured by mass spectrometry. The latter can be written as

(4) $$Fg = Ngme/(N_{O2}me + N_{CO2}me + N_{N2}me)$$

which, for a fixed-volume, temperature-stable cavity, is equal to

(5) $$Fg = Pgme/(P_{O2}me + P_{CO2}me + P_{N2}me)$$

For each gas, the investigators calculated an exchange constant based on the rate of change in fractional pressure (their page 195) and used these estimates to define the ratio for the CO2:O2 time constants, ie, the relative exchange rates at identical partial pressure. However, this calculation can be shown to be in error by substituting the expression for Pgme that includes the Fg from equation 5 into equation 3, or

(6) $$K'gme = ((Pme(t) - 47)Fg(t) - (Pme(t - \delta t) - 47)Fg(t - \delta t)/((Pme(t - \delta t) - 47)Fg(t - \delta t) - PgB))$$

where

(7) $$Pme = P_{O2}me + P_{N2}me + P_{CO2}me + P_{H2O}me$$

and

(8) $$\delta Pme/\delta t = (\delta P_{O2}me + \delta P_{N2}me + \delta P_{CO2}me + \delta P_{H2O}me)/\delta t$$

In equation 6, the value of 47 represents the unmeasured contribution of water (H_2O) to the total ME pressure (assumed to be constant and equal to that for saturation at body temperature) and Fg is the measured fractional pressure of gas g ignoring water vapor. Critical to the evaluation of equation 6 is the knowledge of the total ME pressure (Pme; see equation 7) and the gas partial pressure in the systemic blood (PgB), neither of which was measured in the experiment. Moreover, equation 8 shows that Pme varies in a complicated way over time, as the partial pressures of the different physiological gases change at a rate determined by their respective time constants and extant partial pressure gradients. Because Fg is not linearly related to Pgme over the course of an experiment, estimates of both the numerator and denominator of equation 3 using uncorrected, fractional pressures are inaccurate. Also, for experimental designs that fail to anticipate the temporal pattern of ME change, the assumption of a closed ME required for estimating time constants may be violated. This possibility is realized if, at any time during the course of the experiment, the total ME pressure exceeds the opening pressure of the eustachian tube. This will cause gas transfers to the environment over a pathway not represented in the mathematical description, and will introduce errors into the estimated time constant of magnitude order proportional to the representation of the specific gas in the ME.

To illustrate the sources and magnitudes of the errors in the calculation of time constants based on fractional pressures, equations 6 and 7 were combined to form the model equation

$$(9)\ \mathrm{Pme}(t) = \mathrm{E}((\mathrm{Pme}(t - \delta t) - \mathrm{P}_{H_2O}\mathrm{me})\mathrm{Fg}(t - \delta t) - \mathrm{K'gme}((\mathrm{Pme}(t - \delta t) - \mathrm{P}_{H_2O})\mathrm{Fg}(t - \delta t) - \mathrm{PgB}))$$

which relates the total ME pressure at time t (Pme(t)) to the sum (E) across component gases (O_2, CO_2, N_2, H_2O) of the sum of the partial pressure of each gas at time t − δt and the product of the scaled time constant for the gas and the extant pressure differential between ME and blood. In simulations using this model, the partial pressures of O_2 and CO_2 in blood were taken from the data reported in the article by Mover-Lev et al[19] for the steady-state ME pressure of those gases in anesthetized guinea pigs, while those for N_2 and H_2O were taken from a handbook of physiology.[20] As a first approximation, all blood gas partial pressures were assumed to be constant over the time period modeled. Because the Mover-Lev et al experiment followed the change in fractional pressures over time after exposing the ME to air, the total pressure at time t = 0 was taken as atmospheric (760 mm Hg), and the fractional pressures at that time were assigned values approximately equal to those of air ($N_2 = 0.79$, $O_2 = 0.21$, $CO_2 = 0$, $H_2O = 0$). The relative scaling of the time constants for the gases was taken from data published for experiments in monkeys (CO_2:O_2:N_2 = 698:37:1). This was converted to estimates of K'gme for each gas by multiplying the relative values by a constant chosen by trial and error to reproduce the experimental results for the fractional CO_2 pressure change.[12] Using these initial conditions, I iterated equation 9 through a total of 240 iterations with the time interval between solutions set equal to 1 minute. For each iteration, the partial pressure of all gases, their fractional pressures, and the total ME pressure were calculated, and these values were used to construct pressure-versus-time functions for the different model conditions. Time constants were calculated for O_2 and CO_2 from the fractional gas pressures by the methods described by Mover-Lev et al, and these were compared to the fixed values of those parameters used in the model.

Initial simulations were run under the assumption that the ME is a closed gas pocket. However, those results showed that total ME pressure is expected to increase far in excess of the opening pressures of the eustachian tube measured for humans and animals.[2,13,21,22] Consequently, to account for the expected venting of gases at total ME pressures greater than the tubal opening pressure, the simulations were repeated with a conditional modification of equation 9. There, partial pressures of all gases within the ME were adjusted before each iteration by an amount equal to the product of their extant fractional ME pressure and the difference between total ME pressure and the tubal opening pressure (Po) or

$$(10)\qquad \mathrm{Pgme}(t + 0.5\delta t) = \mathrm{Pgme}(t) - X$$

where $X = \mathrm{Fg}(\mathrm{Pme}(t) - \mathrm{P}_{H_2O}(t) - \mathrm{Po})$ for $\mathrm{Po} < \mathrm{Pme}(t)$ or $X = 0$ for $\mathrm{Po} \geq \mathrm{Pme}(t)$. This modification vents ME pressure in excess of the tubal opening pressure at a composition distributed among component gases according to their fractional representation within the ME space.

RESULTS

The results of the model simulations document 3 major sources of error in the estimates of the time constants for transmucosal gas exchange presented by Mover-Lev et al.[19] The first is a systematic error introduced by the design of the experiment. There, the assumption of a closed ME volume is not consistent with the predicted venting, via the eustachian tube, of gas at total ME pressures in excess of the tubal opening pressure. The other errors are associated with the incomplete characterization in the experiment of the 2 free parameters of the mathemati-

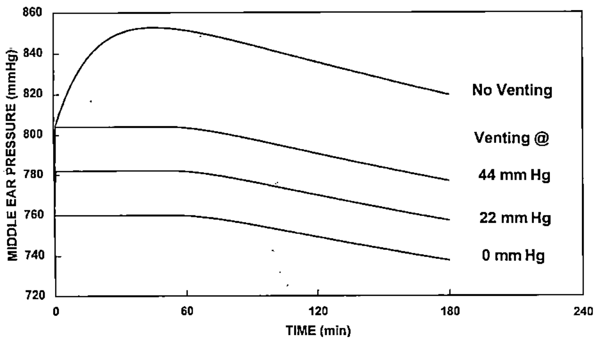

Fig 3. Model simulation of middle ear pressure-time function for Mover-Lev et al[19] experiment under conditions of middle ear closed to environment or middle ear that vents gas through eustachian tube at ambient pressure (760 mm Hg) plus 44, 22, and 0 mm Hg.

cal model that are required to estimate the time constant, ie, the ME partial pressure and the ME-blood partial pressure gradient. Specifically, accurate representation of gas partial pressure by fractional pressure requires concurrent measurement of total ME pressure, and accurate determination of the ME-blood partial pressure gradient requires concurrent measurements of the partial pressure of the gas in both the ME and the blood. The predicted effect of these 3 sources of error on the estimation of the transmucosal exchange constants is described below.

Middle Ear as Closed Cavity. The equations developed in the previous section to estimate the time constants assume that the ME is a closed cavity and that the dominant pathway for ME gas transfer (ie, the only pathway for gas transfers that affect the ME pressure during the course of the experiment) is across the mucosa. However, past studies show that the eustachian tube acts as a directional pressure valve and that it will passively open and vent gases at total, greater-than-ambient ME pressures of from 0 to approximately 50 mm Hg for different animal species.[13,21,22] Such venting will not only decrease the total ME pressure, but will also decrease the partial pressures of all component gases by an amount proportional to their fractional representation in the ME. Experiments designed to measure time constants for transmucosal exchange must control for this possible effect by limiting the total ME pressure generated over the course of the experiment to values less than the tubal opening pressure. The model simulation of the experiment shows that this condition most probably was not satisfied for the experiment reported by Mover-Lev et al.[19]

Figure 3 shows the simulated total ME pressure-versus-time function for the experiment reported by Mover-Lev et al.[19] The ambient pressure was assumed to be 760 mm Hg for all simulations (though this is arbitrary and does not affect the results), and the curves were generated under the assumptions that either the ME behaves as a closed cavity, or that the eustachian tube vents at ambient pressure plus 0, 22, and 44 mm Hg (typical range of eustachian tube opening pressures for different animals). From the data presented in the Figure, greater-than-ambient ME pressure is expected to be generated in this experimental setting. This is caused by the underlying experimental conditions, which create, at the onset of the data collection period, large blood-ME gradients for the fast-exchange gases, CO_2 (approximately 75 mm Hg) and H_2O (approximately 47 mm Hg). These gradients, in turn, drive the increase in pressure as the ME air space is rapidly resaturated with H_2O and equilibrated with the CO_2 partial pressure of blood.

TIME CONSTANTS AND CARBON DIOXIDE–OXYGEN RATIO INPUTTED INTO MODEL AND CALCULATED VALUES

	CO_2	*O_2*	*N_2*	*CO_2:O_2*
True value	0.0523	0.0027	0.0005	19.1
Partial pressure				
No venting	0.0523 (1.00)	0.0027 (1.00)	0.0005 (1.00)	9.1
Venting at				
44 mm Hg	0.0511 (1.00)	0.0089 (0.69)	0.0555 (0.79)	5.7
22 mm Hg	0.0509 (1.00)	0.0135 (0.29)	0.1034 (0.50)	3.8
0 mm Hg	0.0507 (1.00)	0.0192 (0.17)	0.1550 (0.42)	2.6
Fractional pressure				
No venting	0.0511 (0.99)	0.0105 (0.72)	0.0293 (0.17)	4.8
Venting at 0 mm Hg	0.0488 (1.00)	0.0116 (0.76)	0.0417 (0.32)	4.2

Time constants are per minute. Values in parentheses are fraction of variance explained.

From equation 6, a time constant can be calculated by regressing the change in ME gas partial pressure over an interval on the average ME-blood partial pressure differential for the interval. Using the partial pressure data available from the model simulation and an interval defined by the 1-minute period between iterations, I determined the time constants presented in the Table. Also reported for each time constant is the square of the Pearson product moment correlation coefficient (R^2) that estimates the fraction of variance in the time constant that is explained by the linear relationship. As expected, under conditions of a closed ME (no venting), the calculated time constants for all 3 gases were identical to the values used as parameters in the model. However, while the calculated CO_2 time constant was relatively stable over all venting conditions, the inclusion of venting caused a significant overestimation

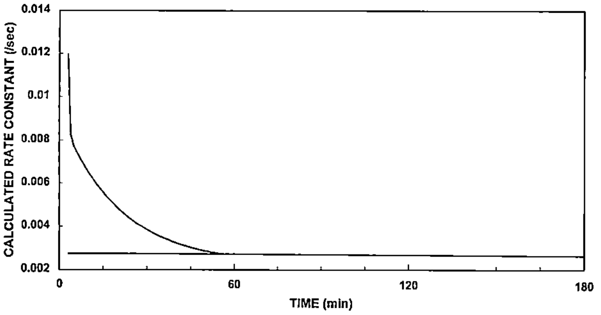

Fig 4. Model simulation of change with time in oxygen (O_2) time constant calculated by using partial pressures under conditions of closed middle ear (straight line) and of middle ear that vents pressures in excess of ambient (curvilinear function). Time-invariant O_2 exchange constant used as model parameter was valued at 0.003/min.

of the time constants for both N_2 and O_2 and an underestimation of the CO_2:O_2 time constant ratio. Figure 4 shows the calculated O_2 time constant as a function of time for a closed ME and for an ME that vents at ambient pressure. Because of the linear form of equation 6, the constant to be estimated is independent of time, as was true for the nonventing ME. However, the solution to the equation for the venting condition is time-dependent and shows a decay to a constant value (equal to the time constant) by approximately 40 minutes. A similar though more pronounced effect can be demonstrated for N_2. This nonlinear behavior results from the fact that the magnitude of the decrease in ME partial pressure during eustachian tube venting is directly related to the fractional representation of the gas in the ME ($N_2 >> O_2 > CO_2$, early in the experiment). Because the calculation of time constants assumes a closed ME, the model equation attributes the decrease in gas partial pressure caused by venting to transmucosal transfers, thereby artificially inflating the estimated value of the time constants of gases in decreasing magnitude from the most representative to the least representative species. Consequently, experiments that fail to control for this effect will generate downwardly biased estimates of the CO_2:N_2 and CO_2:O_2 time-constant ratios (as was reported by Mover-Lev et al,[19] in comparison to the values reported for monkey experiments) and of the N_2:O_2 time constant ratios (not reported, but consistent with the data presented in the Figure).

Representation of Partial Pressures by Fractional Pressures. Because total ME pressure is not constant during the course of the experiment (as demonstrated in the simulated results reported above), gas partial pressure ($((P_{me} - P_{H_2O})F_g))$) becomes a nonlinear function of the fractional gas pressure (F_g). Consequently, mathematical operations that use the latter as a measure of the former produce erroneous results. Moreover, in a closed cavity, the measured fractional pressure (but not the true partial pressure) of a more slowly exchanged gas will be increased or decreased by the relative enrichment (blood-ME transfers) or depletion (ME-blood transfers) within the cavity of a more rapidly exchanged gas. This phenomenon is directly applicable to the experiment of Mover-Lev et al,[19] in which, early in the course of the experiment, H_2O and CO_2 diffused into the ME, causing an increase in the total ME pressure and stable O_2 and N_2 partial pressures, but a decrease in the O_2 and N_2 fractional pressures. As with the effect of venting, the apparent but unreal decrease in O_2 and N_2 pressures when measured as fractional pressures is attributed by the assumptions inherent in the equations to transmucosal gas transfer, thereby inflating the measured time constants for those gases.

The Table reports the time constants for CO_2, O_2, and N_2 calculated by using their fractional pressures under the conditions of the Mover-Lev et al[19] experiment and assuming that the eustachian tube does (at ambient pressure) or does not vent gas. Under both conditions of venting, the estimated CO_2 time constant is little affected by the error introduced from using fractional pressures, but those for O_2 and N_2 are increased relative to their true value. Consequently, the value of the ratio for the CO_2:O_2 exchange constants reported by Mover-Lev et al (approximately 3.9) and calculated by using fractional pressures is erroneous and represents an underestimation of the true value of the ratio.

Figure 5 shows the fractional pressure–versus–time functions for CO_2 and O_2 generated by using the model under conditions of nonventing and venting. The only condition that varied in the 2 simulations was the inputted O_2 exchange constant (and thus the CO_2:O_2 time constant ratio). For both gases, the simulated functions are quite similar to those presented in the published Figure from the Mover-Lev et al[19] experiment. There, the functions for CO_2 and O_2 intersected at approximately 160 minutes, which from the simulation corresponds to a true time constant ratio of approximately 10:1. These results show that the methods used by Mover-Lev et al result in significant lower biasing of the estimated exchange constants for more slowly exchanged gases when measured in experiments that include multiple gas exchanges.

Assumption of Constant Blood Gas Partial Pressures. For inert gases, it is reasonable to assume that the systemic gas partial pressure is time-invariant for periods of stable atmospheric pressure. However, this is not true of reactive gas species, in which the systemic gas partial pressure is determined by a num-

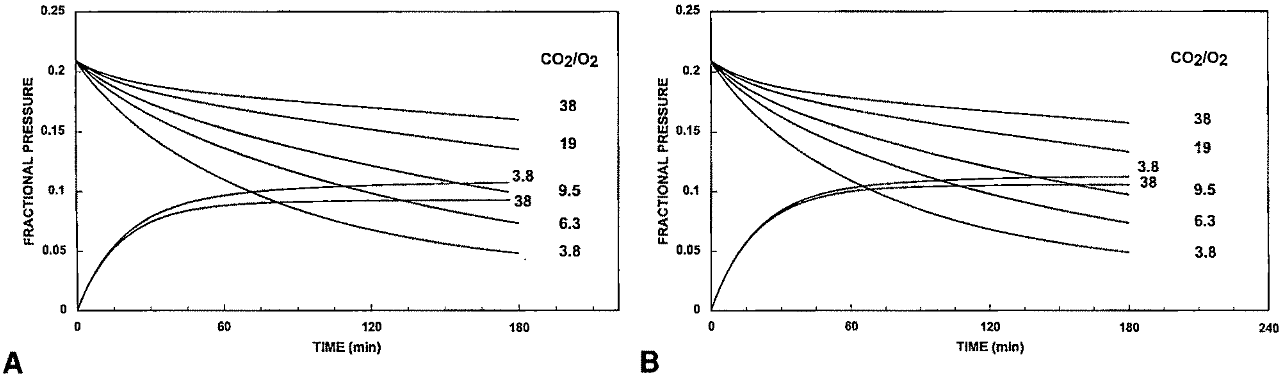

Fig 5. Model simulation of fractional pressure of O_2 (descending curves) and of carbon dioxide (CO_2; ascending curves) as function of time for A) nonventing and B) venting middle ears under conditions of changing model parameter related to O_2 exchange constant from value that yielded CO_2:O_2 exchange constant ratio of 38 to one that yielded ratio of 3.8.

ber of factors (eg, tidal volume, respiration rate, blood pH, etc) that change during sleep or with depth of anesthesia. For example, during sleep, the blood partial pressure of CO_2 shows a cyclic pattern of increase, whereas that of O_2 decreases. Equation 6 shows that for conditions of changing systemic blood gas pressures, the methods used to calculate time constants are not strictly applicable, because they generate a variable that is a nonlinear function of time. Consequently, without concurrent measurement of the blood gas partial pressure–versus–time function, the model parameters are incomplete, and there is no definable, functional relationship between the estimates calculated by the methods described by Mover-Lev et al[19] and the respective true time constants for different gases.

Also of interest is the fact that for different constant systemic blood gas partial pressures, the methods of Mover-Lev et al[19] produce different estimates of the true exchange constants and highly variable CO_2:O_2 time constant ratios. For example, the model simulations reported above used constant systemic blood gas partial pressures for O_2 and CO_2 that were equal to their respective average values reported for steady-state ME pressures in anesthetized guinea pigs. However, the reported values for CO_2 of 75.3 ± 13.2 mm Hg and for O_2 of 23.5 ± 12.5 mm Hg are associated with large standard deviations, possibly attributable to sampling at different times after induction of anesthesia (ie, temporal variability). For conditions of pressure venting and true CO_2 and O_2 time constants of 0.052/min and 0.003/min (ratio = 19), estimates for those constants based on fractional pressures at constant average systemic blood gas partial pressures of +2, +1, +0, and −1 standard deviations were 0.0496 and 0.0101 (ratio = 4.9), 0.0492 and 0.0109 (ratio = 4.5), 0.0488 and 0.0117 (ratio = 4.2), and 0.0484 and 0.0121 per minute (ratio = 4.0), respectively. Note that the calculated ratios approach the average ratio of 3.91 reported by Mover-Lev et al, despite the underlying true ratio of 19. Thus, without a concurrent measurement of the blood gas partial pressures, the data from the guinea pig experiment are not interpretable, but, contrary to the statement by Mover-Lev et al, they do not exclude the CO_2:O_2 time constant ratio of 19:1 reported for monkeys.

DISCUSSION

The mechanism of ME pressure regulation remains an aspect of physiology that is poorly understood. Because the ME is a relatively noncollapsible, temperature-stable gas pocket, its pressure is affected by mechanisms that alter the contained volume of gases. Two primary mechanisms have been demonstrated to change the ME gas volume: 1) the pressure gradient–driven bolus exchange of mixed gases between the nasopharynx and the ME during eustachian tube opening, and 2) the gradient-driven diffusive exchange of gases between the ME and the blood.[1-5] More recently, the ME and mastoid mucosa have been suggested to regulate and stabilize ME pressure in the absence of a well-functioning eustachian tube.[23-31] However, experimental evidence supporting this hypothesis is derived from the short-term observation of increasing ME pressure in response to certain preconditions that without exception disturb the preexisting equilibria between the ME and blood in the partial pressures of fast-exchange gases such as CO_2 and O_2.[23,24] Therefore, these counterintuitive observations are explainable in terms of passive, gradient-driven diffusion.[18]

Rarely have experimental studies of ME pressure regulation been formulated as falsifiable tests of hypotheses. There, an experiment would be designed specifically to evaluate the compatibility of the observed system behavior with the predictions of the 2 well-established gas exchange mechanisms outlined above (ie, gas transfers via the eustachian tube, and across the ME mucosa). Previously, such an approach was compromised by the lack of a well-formulated mathematical description of transmucosal gas exchange from which such predictions could be developed. However, with the early work on models of ME gas exchange by Ranade et al,[10] and the more recent contributions by Ostfeld and Silberberg[14,15] and others,[16-18] this limitation has been removed. In that regard, it is essential that experimental determinations of the fixed parameters of the various models yield accurate results, because, for example, overestimation or underestimation of time constants for different gases would produce unrealistic predictions of system behavior. This, in turn, could serve to advance ill-conceived pressure-regulating mechanisms that, by default, better explain an experimental result than the standard model.

Unfortunately, procedures for estimating the fixed model parameters for transmucosal gas exchange in other biological systems are not strictly applicable to the ME. Passive gas exchange is most well characterized for open, ventilated gas pockets such as the lung, which, unlike the noncollapsible, intermittently open gas pocket of the ME, maintain local alveolar pressure at close to ambient values so that the fractional gas pressures are directly proportional to the gas partial pressures. A failure to make this distinction between closed and open gas pockets underlies one of the more important sources of error in the calculation of time constants by Mover-Lev et al.[19]

In the previous sections, a mathematical model of ME transmucosal gas exchange was developed, and the specified conditions that allow for measurement of the model parameters were outlined. The equations show that under conditions of a stable systemic blood gas partial pressure and an ME closed to other routes of gas exchange, a gas-specific time constant can be calculated for inert gases as the ratio of the change in gas partial pressure per unit time to the average partial pressure gradient for the time interval. A simple test of the agreement between experimental conditions and model requirements, and thus of the applicability of this mathematical relationship to the experimental data, is the demonstration of the expected time-invariance of the measured exchange constant. Alternatively, functions that vary with time demonstrate that an assumption inherent in the model was violated by the experimental protocol, and that the time constant is inaccurate.

The time constant for transmucosal exchange of reactive gases can also be calculated by using this relationship under a defined set of restrictive conditions that essentially force gas exchange exclusively over 1 of 2 possible pathways (Fig 2). However, for more generalized conditions, the calculated value of the time constant for reactive gases is context-specific and represents a weighted average (based upon extant, relative pathway conductances) of the time constants for exclusive gas transfers across each of the 2 competing pathways. Therefore, in presenting the results for estimates of the time constants for reactive gas exchange by using the methods outlined here, the prevailing conditions must also be specified. Moreover, because the dynamics of intercompartmental gas exchange alter the extant conditions (eg, saturation of reaction product, intercompartmental gradients), the relative volumes of reactive gas exchanged over each pathway can change during the course of an experiment, and the calculated time constant can vary with time. For these reasons, the time constant ratios that include reactive gases can take on a wide range of values both between experiments and within a given experiment, and comparisons of such ratios without reference to prevailing conditions, as were made by Mover-Lev et al,[19] are not valid.

REFERENCES

1. Ingelstedt S, Jonson B. Mechanisms of the gas exchange in the normal human ME. Acta Otolaryngol [Suppl] (Stockh) 1967(suppl 224):452-61.

2. Bluestone CD, Doyle WJ. Anatomy and physiology of the eustachian tube and middle ear related to otitis media. J Allergy Clin Immunol 1988;81:997-1003.

3. Magnuson B, Falk B. Physiology of the eustachian tube and ME pressure regulation. In: Jahn AF, Santos-Sacchi J, eds. Physiology of the ear. New York, NY: Raven Press, 1988:81-101.

4. Swarts JD, Alper CM, Seroky JT, Chan KH, Doyle WJ. In vivo observation with magnetic resonance imaging of middle ear effusion in response to experimental underpressures. Ann Otol Rhinol Laryngol 1995;104:522-8.

5. Alper CM, Tabari R, Seroky JT, Doyle WJ. Magnetic resonance imaging of the development of otitis media with effusion caused by functional obstruction of the eustachian tube. Ann Otol Rhinol Laryngol 1997;106:422-31.

6. Riu R, Flottes L, Bouche J, Le Den R. La physiologie de la trompe d'Eustache. Paris, France: Librairie Arnette, 1966.

7. Elner A. Gas diffusion through the tympanic membrane. Acta Otolaryngol (Stockh) 1970;69:185-91.

8. Doyle WJ, Alper CM, Seroky JT, Karnavas WJ. Exchange rates of gases across the tympanic membrane in rhesus monkeys. Acta Otolaryngol (Stockh) 1998;118:567-73.

9. Morgenstern C. Oxygen supply of middle ear mucosa under normal conditions and after eustachian tube occlusion. Ann Otol Rhinol Laryngol [Suppl] 1980;89(suppl 68):76-8.

10. Ranade A, Lambertsen CJ, Noordergraff A. Inert gas exchange in the ME. Acta Otolaryngol [Suppl] (Stockh) 1980 (suppl 371).

11. Doyle WJ, Seroky JT. Middle ear gas exchange in rhesus monkeys. Ann Otol Rhinol Laryngol 1994;103:636-45.

12. Doyle WJ, Seroky JT, Alper CM. Gas exchange across the middle ear mucosa in monkeys: estimation of exchange rates.

Arch Otolaryngol Head Neck Surg 1995;121:887-92.

13. Cantekin EI, Bluestone CD, Saez CA, Doyle WJ, Phillips DC. Normal and abnormal middle ear ventilation. Ann Otol Rhinol Laryngol [Suppl] 1977;86(suppl 41):1-15.

14. Ostfeld E, Silberberg A. Transient pressure change in the middle ear. Arch Otolaryngol Head Neck Surg 1991;117:1390-4.

15. Ostfeld EJ, Silberberg A. Theoretic analysis of middle ear gas composition under conditions of nonphysiologic ventilation. Ann Otol Rhinol Laryngol 1992;101:445-51.

16. Hergils L, Magnuson B. Middle ear gas composition in humans: experimental findings and theoretical model of gas diffusion. In: Lim DJ, Bluestone CD, Casselbrant M, Klein JO, Ogra PL, eds. Proceedings of the Sixth International Symposium on Recent Advances in Otitis Media. Hamilton, Canada: BC Decker, 1996:106-9.

17. Alper CM, Karnavas WJ, Swarts JD, Tabari R, Seroky JT, Doyle WJ. Middle ear gas composition of cynomolgus monkeys: prediction and measurement. In: Lim DJ, Bluestone CD, Casselbrant M, Klein JO, Ogra PL, eds. Proceedings of the Sixth International Symposium on Recent Advances in Otitis Media. Hamilton, Canada: BC Decker, 1996:116-9.

18. Doyle WJ. Increases in middle ear pressure resulting from counter-diffusion of oxygen and carbon dioxide into the middle ear of monkeys. Acta Otolaryngol (Stockh) 1997;117:708-13.

19. Mover-Lev H, Sadé J, Ar A. Rate of gas exchange in the middle ear of guinea pigs. Ann Otol Rhinol Laryngol 1998;107:194-8.

20. Loring SH, Butler JP. Gas exchange in body cavities. In: Tenney SK, Farhi LE, eds. The respiratory system. Gas exchange. Bethesda, Md: American Physiological Society, 1987:283-96. (Handbook of physiology; vol 4).

21. Doyle WJ. Eustachian tube function in the chinchilla. Arch Otolaryngol 1985;111:305-8.

22. Buchman CA, Doyle WJ, Swarts JD. Eustachian tube function in the ferret. Acta Otolaryngol (Stockh) 1993;113:5-80.

23. Felding JU, Rasmussen JB, Lildholdt T. Gas composition of the normal and the ventilated ME cavity. Scand J Clin Lab Invest [Suppl] 1987;47(suppl 186):31-41.

24. Hergils L, Magnuson B. Human middle ear gas composition studied by mass spectrometry. Acta Otolaryngol (Stockh) 1990;110:92-9.

25. Buckingham R, Stuart DR, Girgis SJ. Experimental evidence against middle ear oxygen absorption. Laryngoscope 1985;95:437-42.

26. Hergils L, Magnuson B. Morning pressure in the middle ear. Arch Otolaryngol 1985;111:86-9.

27. Bylander AKH, Ivarsson A, Tjernstrom O, Andreasson L. Middle ear pressure variations during 24 hours in children. Ann Otol Rhinol Laryngol [Suppl] 1985;94(suppl 120):33-5.

28. Hergils L, Magnuson B. Middle-ear pressure under basal conditions. Arch Otolaryngol Head Neck Surg 1987;113:829-32.

29. Hergils L, Magnuson B. Regulation of negative middle ear pressure without tubal opening. Arch Otolaryngol Head Neck Surg 1988;114:1442-4.

30. Buckingham RA. Patent eustachian tube in the underaerated middle ear: a paradox. Ann Otol Rhinol Laryngol 1988;97:219-21.

31. Miura M, Takahashi H, Honjo I, Hasebe S, Tanabe M. Influence of the gas exchange function through the middle ear mucosa on the development of sniff-induced middle ear disease. Laryngoscope 1998;108:683-6.

≈

EUROPEAN SOCIETY OF PEDIATRIC ORL

The Vth International Conference of the European Society of Pediatric ORL will be held July 9-13, 2000, in Graz, Austria. For more information, contact Claire Zwerina, Secretary to Prof Stammberger, ENT-Department, University Hospital, Auenbruggerplatz 20, A-8036 Graz, Austria; fax ++43/316/385/3425.

Ann Otol Rhinol Laryngol 109:2000

LENGTH OF THE EUSTACHIAN TUBE AND ITS POSTNATAL DEVELOPMENT: COMPUTER-AIDED THREE-DIMENSIONAL RECONSTRUCTION AND MEASUREMENT STUDY

KEN ISHIJIMA, MD
HAMAMATSU, JAPAN

ISAMU SANDO, MD, DMSC
PITTSBURGH, PENNSYLVANIA

CAREY BALABAN, PHD
PITTSBURGH, PENNSYLVANIA

CHIAKI SUZUKI, MD, DMSC
FUKUSHIMA, JAPAN

KENJI TAKASAKI, MD
NAGASAKI, JAPAN

Eleven normal human temporal bone–eustachian tube (ET) specimens obtained from 11 individuals whose ages were 3 months to 88 years were studied to investigate the path length along the ET lumen and its postnatal development by means of a computer-aided 3-dimensional reconstruction and measurement method. The path length of the ET lumen of the 3-month-old infant was 21.2 mm, and its growth was in correlation with age to attain its adult length (average, 37.00 ± 4.16 mm). The ratio of the length of the cartilaginous portion together with the junctional portion to the length of the bony portion was 8:1 in an infant at the age of 3 months and 4:1 in adults. That the bony portion of the ET develops relatively more than the cartilaginous and junctional portions may cause this finding. In addition, there is a developmental shift in the orientation of the cartilaginous portion with respect to the bony portion of the ET. In children, the cartilaginous and bony portions are both aligned with the line that connects the pharyngeal orifice and the tympanic orifice. In adults, however, the cartilaginous portion is angled inferiorly and laterally from the bony portion. This change may reflect the relative growth of the face.

KEY WORDS — computer-aided three-dimensional reconstruction, eustachian tube, postnatal development.

INTRODUCTION

Immaturity of the eustachian tube (ET) has been implicated as an explanation for the high prevalence of otitis media with effusion in children.[1] In a recent study, we reported that the shape of the lumen of the cartilaginous portion of the ET changes markedly during adolescence, from a flattened tube to a flattened funnel opening widely at the pharyngeal orifice.[2] However, to investigate the morphological difference between the ET in adults and that in children, we also must analyze the postnatal development of the path length of the ET.

There have been a number of previous studies that measured the length of the ET as the linear distance between the pharyngeal and tympanic orifices.[3-10] However, because the course of the ET clearly is curved in adults,[11] the pharyngeal orifice–tympanic orifice distance is not the actual length. Further, the calculated 2:1 ratio between the length of the cartilaginous portion and that of the bony portion of the ET[10,12] may be underestimated because of the curvature of the ET lumen in 3 dimensions.

This postnatal developmental study used computer-assisted 3-dimensional (3-D) reconstruction methods to analyze developmental changes in the path length of the ET lumen, defined as the curve that connects the midpoints of the lumen in virtual sections.

METHODS

The materials used for this study were 11 temporal bone–ET specimens obtained from 11 individuals whose ages were 3, 8, and 16 months and 4, 17, 28, 38, 70, 70, 71, and 88 years at death. None of the individuals had any known congenital anomaly or either a clinical history or histologic evidence of ear disease. We separated them into 2 groups: the child group (4 cases, ranging from 3 months to 4 years of age) and the adult group (7 cases, ranging from 17 to 88 years of age; mean age, 54.6 years). The specimens were fixed in 10% formalin, decalcified in 5% trichloroacetic acid, dehydrated in graded concentrations of ethanol, and embedded in celloidin.[13] After reference marks had been made in the celloidin blocks for 3-D reconstruction, the blocks were sectioned at

---

From the Elizabeth McCullough Knowles Otopathology Laboratory, Division of Otopathology, Department of Otolaryngology, University of Pittsburgh School of Medicine, Pittsburgh, Pennsylvania. Dr Ishijima is currently in the Department of Otolaryngology, Hamamatsu Rosai Hospital, Hamamatsu, Japan. Supported by research grant 2R01DC00123-21A2 from the National Institutes of Health/National Institute on Deafness and Other Communication Disorders.

CORRESPONDENCE — Isamu Sando, MD, DMSc, Division of Otopathology, Dept of Otolaryngology, University of Pittsburgh School of Medicine, Suite 153, Eye and Ear Institute Building, 203 Lothrop St, Pittsburgh, PA 15213.

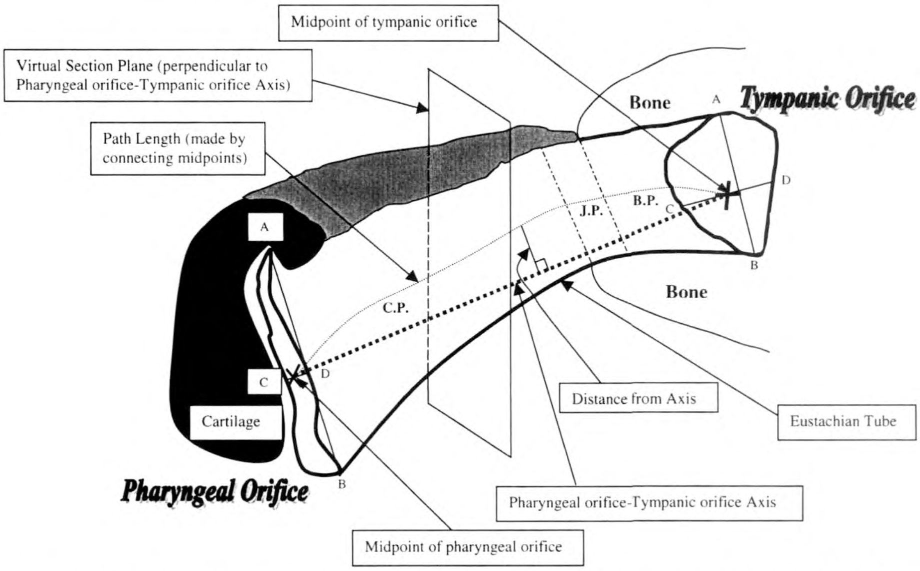
Midpoint of tympanic orifice
Virtual Section Plane (perpendicular to Pharyngeal orifice-Tympanic orifice Axis)
Path Length (made by connecting midpoints)
Bone
A
Tympanic Orifice
D
J.P.
B.P.
C
B
A
Bone
C.P.
C
D
Cartilage
Distance from Axis
Eustachian Tube
Pharyngeal Orifice
B
Pharyngeal orifice-Tympanic orifice Axis
Midpoint of pharyngeal orifice

Fig 1. Schematic drawing of left eustachian tube (ET) viewed from anterosuperolateral direction. Line AB — long axis of "virtual cross sections" of ET lumen at pharyngeal and tympanic orifices. Virtual cross sections are made from reconstruction in plane perpendicular to pharyngeal orifice–tympanic orifice axis of ET. Line CD — line perpendicular to and bisecting line AB. Midpoints (X) of line CD are seen as centers in each orifice of ET lumen. Midpoints (small dots) in approximately 200 virtual cross sections of ET lumen located between pharyngeal and tympanic orifices are seen also as center of lumen along ET. Path length of ET is defined as curve connecting midpoints of lumen in virtual sections. Anterior and posterior parts of ET lumen are covered by cartilage and bone, and are called cartilaginous portion (C.P.) and bony portion (B.P.), respectively. Intermediate region, junctional portion (J.P.), is covered partly by bone inferiorly and cartilage superiorly.

30 μm in thickness, as close to perpendicular to the axis of the ET as possible. Every 40th section was stained with hematoxylin and eosin and prepared for light microscopic study. Additional section slides besides every 40th section were made for the part of the ET between the anterior margin of its junctional portion and the posterior margin of the bony portion to determine the exact location of both the junctional and bony portions along the entire ET. These histologic slides were then used for computer-aided 3-D reconstruction. The equipment used for reconstruction consisted of a personal computer (NEC PC-9801RL), a frame buffer (Sapience HyperFrame+) for full-color images, a digitizer (Hitachi HDG-1515; resolution, 0.1 mm), and a printer. With the software developed by Takagi and Sando,[14] modified by Fujita and Sando,[15] and revised by Sudo et al,[16] accurate reconstruction and measurement could be made of the ET in 3-D fashion. A detailed explanation of the reconstruction and measurement follows (Fig 1).

The ET lumen, the ET cartilage, and the temporal and sphenoid bones bordering the ET were reconstructed for each specimen. The initial step in the analysis of measuring ET length was identification of a line connecting the centers of the pharyngeal and tympanic orifices. The pharyngeal orifice was defined as the anteriormost section that contained a complete cross section of the mucosal lining of the ET; the tympanic orifice was defined similarly with respect to the anterior-superior margin of the tympanic annulus. The center of each orifice was defined as the midpoint of a line perpendicular to the line connecting the superior and inferior margins of the lumen. This pharyngeal orifice–tympanic orifice line provides a standard axis for creating virtual sections through the reconstructed images and a head-based coordinate frame for analyzing changes in shape and orientation during development. The length of this line is defined as the pharyngeal orifice–tympanic orifice distance. The path length of the ET lumen was measured from a series of approximately 200 computer-generated virtual cross sections of the lumen ("virtual cuts") in a plane perpendicular to the pharyngeal orifice–tympanic orifice line. In virtual cross sections, we again defined the pharyngeal and tympanic orifices in the same manner as mentioned above. We defined the line between the centers of the pharyngeal and the tympanic orifices as the pharyngeal orifice–tympanic orifice distance of the ET. Then, the coordinates of the center of the lumen in each virtual cut, determined in the same manner as described above, were used to calculate the path length of the ET by applying the standard linear distance formula to successive points and summing these distances across the reconstruction.

With virtually cut cross sections, we performed reconstruction and measurement of the ET in its 3 portions: the cartilaginous portion, the bony portion, and the junctional portion,[16] which is located between the bony and cartilaginous portions and is surrounded

MEASUREMENTS OF EUSTACHIAN TUBE

Age	*Distance Between Pharyngeal and and Tympanic Orifices (mm)*	*Length of Entire ET (mm)*	*Length of Cartilaginous and Junctional Portions (mm)*	*Length of Bony Portion (mm)*	*Ratio of Cartilaginous and Junctional Portions to Bony Portion*
Child group					
3 mo	20.60	21.23	18.89	2.33	8.1:1
8 mo	24.30	25.82	21.94	3.87	5.7:1
1 y 4 mo	27.49	28.73	24.42	4.31	5.7:1
4 y	30.46	32.10	26.64	5.46	4.9:1
17 y*	33.86	36.12	28.54	7.59	3.8:1
Adult group (n = 7)†					
Mean 54.57 y	33.43 ± 4.03	37.00 ± 4.16	29.60 ± 3.37	7.40 ± 0.89	(4.01 ± 0.26):1

Ratio of path length to distance is 1.048 ± 0.014 in 4 children, and 1.108 ± 0.029 in 7 adults (mean ± SD).

*To compare data of youngest adult case with cases of child group, case of 17-year-old is also listed.

†Measurements are mean ± SD.

in part by bone and in part by cartilage. However, those measurements were made in 2 parts — the cartilaginous portion together with the junctional portion as one part, and the bony portion as another — because the ET cartilage surrounding the junctional portion of the ET is a part of the lateral lamina. As it is known that the lateral lamina is attached by the tensor veli palatini muscle (TVPM) and is believed to move away from the medial lamina of the ET cartilage to open the ET lumen when the TVPM constricts with deglutition or yawning, the lumen of the ET in the junctional portion may be opened also by the TVPM. One could regard the junctional portion, therefore, as a part of the cartilaginous portion from the viewpoint of ET ventilatory function.

RESULTS

The pharyngeal orifice–tympanic orifice distance and the path length of the ET lumen of the reconstructed specimens are summarized in the Table. The pharyngeal orifice–tympanic orifice distance of the ET, the path of the entire ET, the cartilaginous and junctional portions of the ET, and the bony portion of the ET had all reached adult length by 17 years of age. The changes in distance and length between 3 months of age and the youngest case in the adult group — 17 years of age — are plotted: Fig 2A for the pharyngeal orifice–tympanic orifice distance; Fig 2B for the path length of the entire ET; Fig 2C for the length of the cartilaginous and junctional ET; and Fig 2D for the length of the bony ET. Nonlinear regression analysis of data from all cases indicated that the growth of the ET follows an exponential association function of the form $L = A + B(1 - e^{-t/C})$, where L is the length in millimeters, A represents neonatal length in millimeters, B is a magnitude parameter in millimeters, and C represents a rate constant for growth in years. For the bony ET, $L = 2.54 + 4.58(1 - e^{-t/3.05})$, with a mean corrected r = .94, whereas for the cartilaginous and junctional ET, $L = 18.6 + 11.2(1 - e^{-t/2.42})$, with a corrected r = .81. The rate constants for the two regions did not differ significantly, indicating that they grow at the same rate. However, a comparison of the neonatal length estimates (parameter A) and the growth magnitude parameters (parameter B) shows that the bony portion of the ET roughly triples in length during development, whereas the cartilaginous and junctional portions grow only to about 160% of neonatal length. The net result of this difference in relative growth magnitude is an age-related decrease in the ratio of the length of the cartilaginous and junctional portions to the length of the bony portion. That is, it changes from a ratio of 8:1 in infants to an adult ratio of 4:1 by 17 years of age (see Table and Fig 3).

Nonlinear regression analysis also revealed that the pharyngeal orifice–tympanic orifice distance increases with age according to the relationship $L = 19.6 + 13.9(1 - e^{-t/1.88})$, with a corrected r = .82. The corresponding relationship for the total length of the ET lumen was $L = 21.2 + 15.7(1 - e^{-t/2.63})$, with a corrected r = .86. Although the magnitude parameters indicate similar relative magnitudes of growth for the pharyngeal orifice–tympanic orifice distance (71%) and the ET lumen path length (74%), the difference in rate constants indicates that the ET lumen continues to grow after the completion of growth of the pharyngeal orifice–tympanic orifice distance, which achieves its adult range at the age of 4 years. (The distance seems to grow gradually in Fig 2A, but statistical examination revealed that there is no significant growth in pharyngeal orifice–tympanic orifice distance after the age of 4 years.) As a result, the ratio of the path length to the pharyngeal orifice–tympanic orifice distance of the ET is greater in adults than in children ($p < .01$; see Table and *t*-

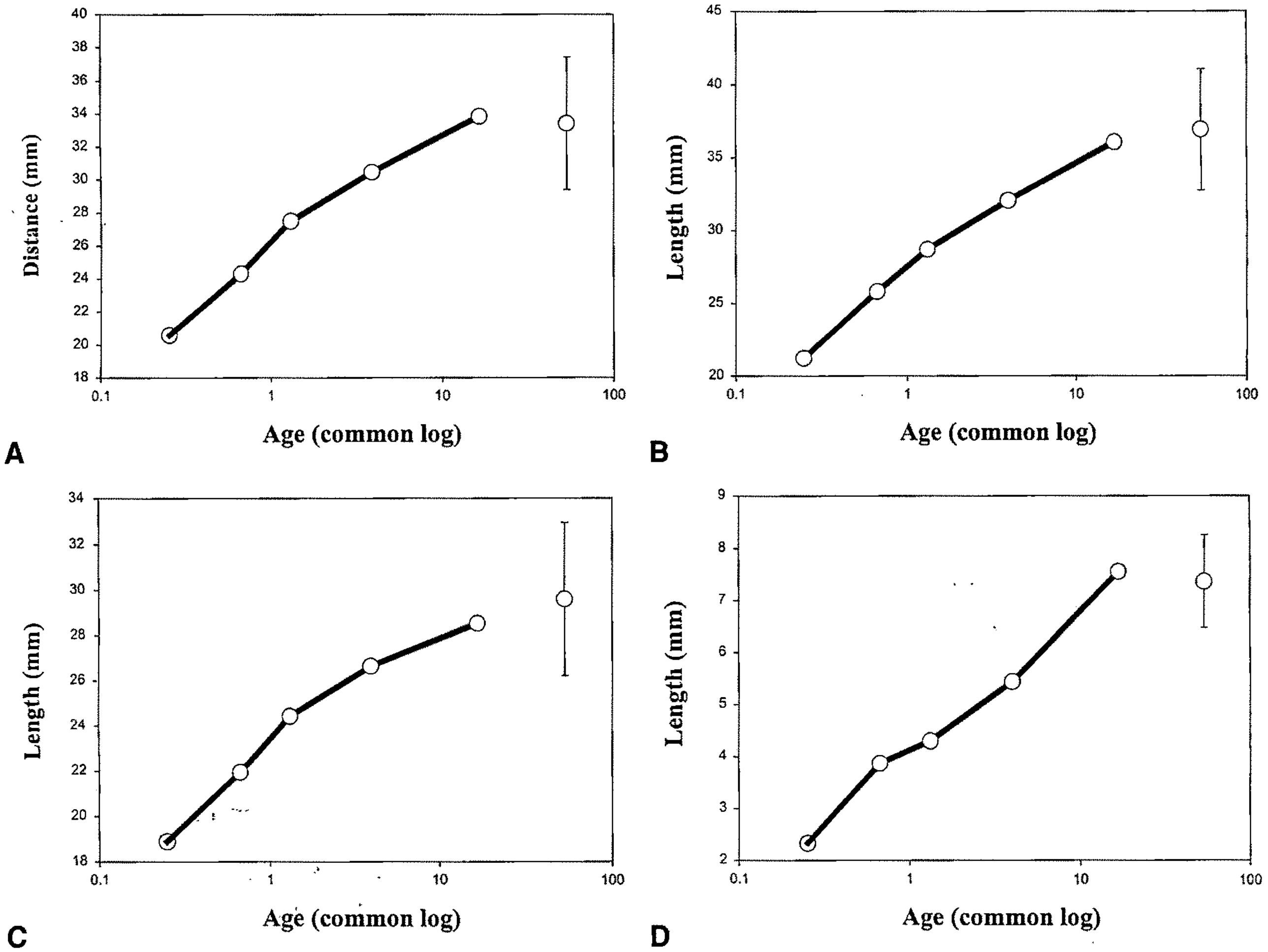

Fig 2. Graph shows postnatal development of ET characteristics. A) Pharyngeal orifice–tympanic orifice distance, B) overall path length, C) path length of cartilaginous portion with junctional portion, and D) path length of bony portion are shown for each of 4 children, youngest case (17 years old) of adult group, and average of adult group. Error bar in A-D indicates standard deviation of adults.

test for difference between path length and pharyngeal orifice–tympanic orifice distance). In other words, the ET lumen shows a greater deviation from the pharyngeal orifice–tympanic orifice axis in adults than in children.

The distance from the center of the ET lumen to the pharyngeal orifice–tympanic orifice axis is plotted in Fig 4 for both child and adult groups. Repeated-measures analysis of variance (between-groups factor, age [adult versus child], within-groups factor, percent distance from pharyngeal orifice) was performed on the measurements of every fourth virtual section from the series of 100 normalized sections. The analysis revealed significant main effects of both age (F[1,8] = 12.10; $p < .01$) and distance from the pharyngeal orifice (F[24,192] = 9.65; $p < .01$), and a significant 2-way interaction effect (F[24,192] = 1.99; $p < .01$). The main effect of age indicated that on average, the center of the ET lumen in adults is further from the pharyngeal orifice–tympanic orifice axis than in children. The main effect of the position of the section along the pharyngeal orifice–tympanic orifice axis (percent distance from the pharyngeal orifice) was also present when data from adults (F[24,120] = 9.49; $p < .01$) and children (F[24,72] = 2.98; $p < .01$) were analyzed separately, indicating that the distance of the center of the lumen from the pharyngeal orifice–tympanic orifice axis varied along the path length of the ET. In both children and adults, the most remarkable deviation was seen in the most posterior part of the cartilaginous portion of the ET.

DISCUSSION

This study, to our knowledge, provides the first quantitative assessment of the postnatal development of ET path length. Three-dimensional reconstruction methods illustrated several basic features of ET development. The postnatal growth of the pharyngeal orifice–tympanic orifice distance, the path length of the entire ET, the path length of the lumen of the cartilaginous and junctional ET segments, and the path length of the lumen of the bony ET segment

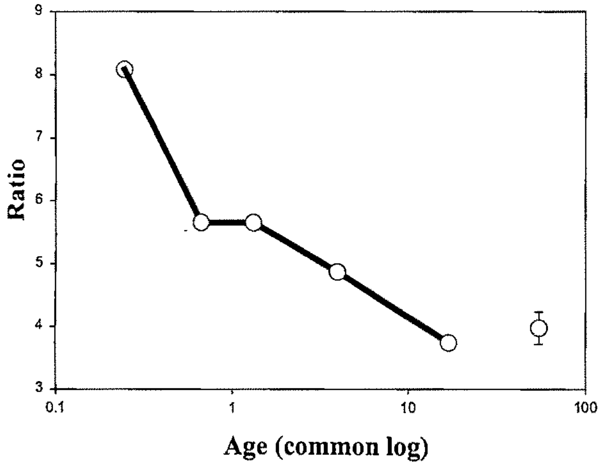

Fig 3. Graph shows postnatal change in ratio of cartilaginous portion and junctional portion to bony portion. Ratio is shown for each of 4 children, youngest case (17 years old) of adult group, and average of adult group. Error bar indicates standard deviation of adults.

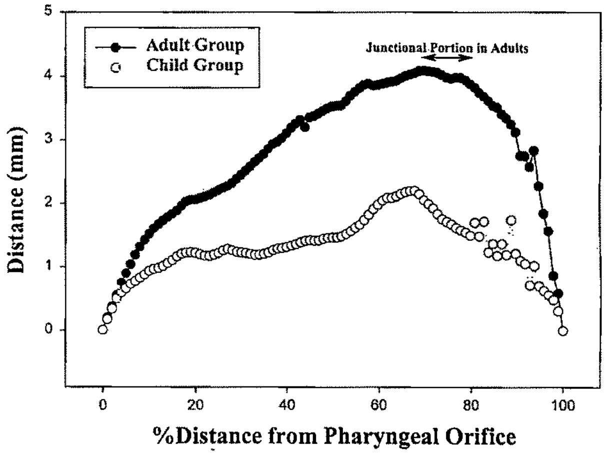

Fig 4. Mean deviation of ET from its pharyngeal orifice–tympanic orifice axis in both children and adults.

could all be characterized by a similar exponential association relationship, $L = A + B(1 - e^{-t/C})$, with A representing the neonatal length, B indicating the magnitude of growth, and C representing the rate constant. The rate constant for growth of the pharyngeal orifice–tympanic orifice distance was less than 2 years; the rate constant for the growth in the path length of the ET lumen segments was 2.5 to 3 years. Hence, the pharyngeal orifice–tympanic orifice distance reaches its adult dimensions earlier than the path length. That the pharyngeal orifice–tympanic orifice distance (axis) reaches the adult size range by 4 years of age correlates with the fact that the head circumference almost reaches its adult dimensions in the same time frame.[17] Because this finding simply indicates that the distance between the fixed end points of the ET is defined by skull growth, it is likely that the most important factor for the ET function is not the pharyngeal orifice–tympanic orifice distance, but the path length.

The growth curve in Fig 2C for the cartilaginous and junctional regions of the ET indicates that the path length reaches approximately 98% of its adult length by 7 years of age. This finding is consistent with the previous report by Sadler-Kimes et al[18] that growth of the cartilaginous ET is negligible after 7 years of age. The same relationship holds for both the path length of the bony ET and the total path length of the ET. These findings indicate that major changes in the length of the ET are completed before a major remodeling of the cartilaginous portion of the ET after 10 years of age[2] that results in an increased height, width, and cross-sectional area of the ET lumen. Hence, ET development can be divided into 2 phases. The first phase (infancy to 10 years) is characterized by elongation of the ET but maintenance of a flattened tube lumen of the cartilaginous ET. In the second phase (10 to 17 years),

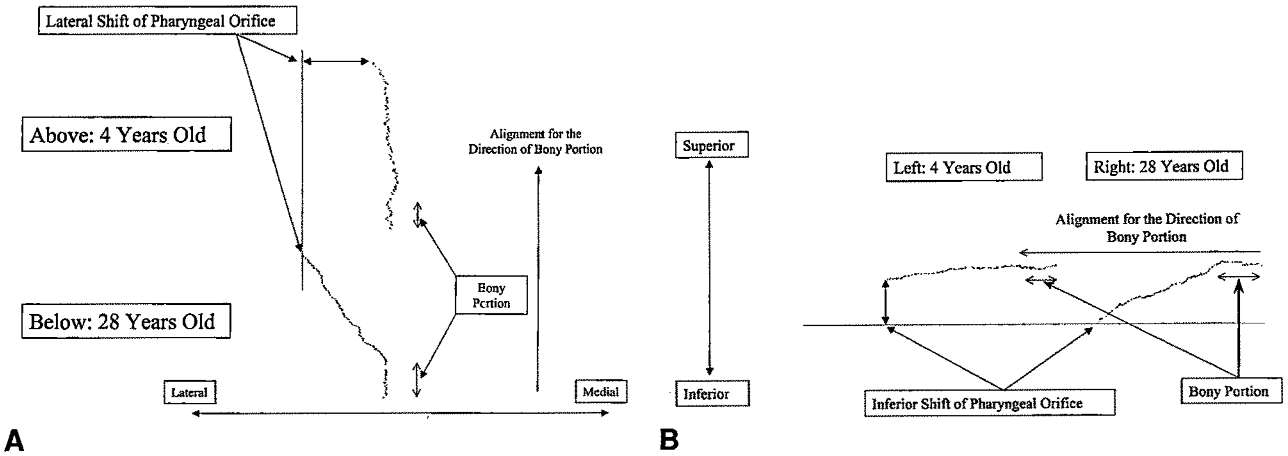
Lateral Shift of Pharyngeal Orifice
Above: 4 Years Old
Alignment for the Direction of Bony Portion
Bony Portion
Below: 28 Years Old
Lateral
Medial
A
Superior
Inferior
Left: 4 Years Old
Right: 28 Years Old
Alignment for the Direction of Bony Portion
Inferior Shift of Pharyngeal Orifice
Bony Portion
B

Fig 5. Views of ET illustrate its course and show midpoints of cross-sectional areas of ET lumen of both 4-year-old case and 28-year-old case with bony portions aligned. A) Left ET viewed from top. In comparing 2 cases, lateral shift of location of pharyngeal orifice is seen in adult. B) Left ET tube viewed from anterolateral direction. In comparing 2 cases, inferior shift of location of pharyngeal orifice is seen in adult.

the lumen of the cartilaginous ET is remodeled to resemble a flattened funnel that opens into the pharyngeal orifice.

The relative magnitude of the growth of the bony portion of the ET lumen was greater than the relative magnitude of growth of the cartilaginous and junctional portions. Whereas the bony portion triples in length during development, the cartilaginous and junctional portions only increase by a factor of approximately 1.6. As a result, there is a marked decrease in the ratio of the length of the cartilaginous and junctional portions of the ET to the length of the bony portion of the ET during development, from a ratio of 8:1 in infants to a ratio of 4:1 in adults. Previous researchers who reported the findings that the ratio of the cartilaginous portion to the bony portion is 2:1[10,12] might have included the junctional portion along with the bony portion, because the junctional portion of the ET is partly surrounded by bone. We found in this study that the junctional portion occupies approximately 7% of the path length of the ET, and when it was included with the bony portion, the ratio was 2.8:1 in adults.

The orientation of the reconstruction of the ET lumen in each specimen is normalized to an internal axis defined by the centers of the tympanic and pharyngeal orifices. It is not possible to reference these reconstructions to sagittal and horizontal planes of the head, because landmarks are not available in the specimens. However, assuming that the petrous apex that contains the bony portion of the ET exists on an approximately horizontal plane, an approximation of developmental changes in the location of the pharyngeal orifice can be obtained by rotating the reconstructions from both the adult group and the child group such that the bony portions of the ET and the tympanic orifices are aligned. This rotation suggests that the location of the pharyngeal orifice shifts on the average approximately 3 mm inferiorly and 3 mm laterally (with respect to this skull base coordinate frame) during maturation of both the face and the petrous apex. As an example of the lateral and inferior shifts of the pharyngeal orifice, Fig 5 shows the path of the midpoints of the ET of the 4-year-old case and the 28-year-old case viewed from 2 directions. Note that the bony portion is oriented along the pharyngeal orifice–tympanic orifice line in the child. The growth and change in the orientation of the cartilaginous ET, however, results in a significant deviation between the pharyngeal orifice–tympanic orifice line and the bony ET in adults. It is suggested that the combination of this inferior shift of the cartilaginous ET trajectory and the expansion of the lumen during adolescence are factors that promote clearance of the middle ear. Further, the elongation and increased curvature of the ET would promote protection of the middle ear. These morphological changes, then, may contribute to the reduced incidence of otitis media with effusion after 7 years of age.[1]

The path lengths of the ET lumen from our adult specimens are consistent with those from previous reports in the literature, which produced estimates ranging from 31 to 39.7 mm.[3-10] Minor discrepancies between our estimates and those of the previous studies may result from different definitions of the ET orifices, different methods of measurement, and the unavoidable 10% shrinkage of the specimens that is produced by histologic processing.[19] A systematic shrinkage artifact could produce a consistent underestimate of the length of the ET (and, hence, underestimates of the initial length and growth magnitude parameters for the exponential association relationships for growth curves, too). However, it should not affect either the rate constants, the ratio between the initial length and growth magnitude parameters (see below), or the statistical significance of the differences in deviation of the path length from the pharyngeal orifice–tympanic orifice axis. [In regard to said magnitude parameters, assume a 10% uniform shrinkage of the tissue. Let L designate the path length. Before processing, the growth of the path length is characterized by the relationship $L = A + B(1 - e^{-t/C})$, such that A is the initial length, B is the growth magnitude, and C is the rate constant. After the processing shrinkage of 10% occurs, this relationship for the data becomes $0.9L = 0.9A + 0.9B(1 - e^{-t/C})$. Note that the rate constant C is unaffected, and that the ratio of the initial length parameter (0.9A) to the growth magnitude parameter (0.9B) remains as A/B.]

ACKNOWLEDGMENTS — The authors express deep gratitude to Eugene N. Myers, MD, Professor and Chairman of the Department of Otolaryngology, University of Pittsburgh School of Medicine, and Charles D. Bluestone, MD, Professor of Otolaryngology, University of Pittsburgh School of Medicine, and Director, Department of Pediatric Otolaryngology, Children's Hospital of Pittsburgh, for their encouragement to study this subject. Appreciation is also expressed to Gloria Limetti for her assistance in this study.

REFERENCES

1. Bluestone CD, Klein JO. Otitis media, atelectasis, and eustachian tube dysfunction. In: Bluestone CD, Stool SE, Kenna MA, eds. Pediatric otolaryngology. 3rd ed. Philadelphia, Pa: WB Saunders, 1996:388-582.
2. Suzuki C, Balaban C, Sando I, Ganbo T, Kitagawa M. Postnatal development of eustachian tube: a computer aided three-dimensional reconstruction and measurement study. Acta Otolaryngol (Stockh) 1998;118:837-43.
3. Konstantinov VV, Senyukov MV. On asymmetry of the human eustachian tubes [in Russian]. Vestn Otorinolaringol

1965;27:29-33.

4. Doyle WJ. A functiono-anatomic description of eustachian tube vector relations in four ethnic populations: an osteologic study [Dissertation]. Pittsburgh, Pa: University of Pittsburgh, 1977.

5. Todd NW, Martin WS. Relationship of eustachian tube bony landmarks and temporal bone pneumatization. Ann Otol Rhinol Laryngol 1988;97:277-80.

6. Anson B, ed. Morris' human anatomy. New York, NY: McGraw-Hill, 1967:1145-6.

7. Anson B, Donaldson J. The surgical anatomy of the temporal bone and ear. Philadelphia, Pa: WB Saunders, 1967:29-30.

8. Clemente CD, ed. Gray's anatomy of the human body. 30th ed. Philadelphia, Pa: Lea & Febiger, 1984:1324.

9. Macbeth B. Some thoughts on the eustachian tube. Proc R Soc Med 1960;53:151-4.

10. Proctor B. Embryology and anatomy of the eustachian tube. Arch Otolaryngol 1967;86:503-14.

11. Sudo M, Sando I, Suzuki C. Three-dimensional reconstruction and measurement study of human eustachian tube structures: a hypothesis of eustachian tube function. Ann Otol Rhinol Laryngol 1998;107:547-54.

12. Graves GO, Edwards LF. The eustachian tube: review of its descriptive, microscopic, topographic, and clinical anatomy. Arch Otolaryngol 1944;39:359-97.

13. Sando I, Doyle WJ, Okuno H, Takahara T, Kitajiri M, Coury WJ III. A method for the histopathological analysis of the temporal bone and the eustachian tube and its accessory structures. Ann Otol Rhinol Laryngol 1986;95:267-74.

14. Takagi A, Sando I. Computer-aided three-dimensional reconstruction: a method of measuring temporal bone structures including the length of the cochlea. Ann Otol Rhinol Laryngol 1989;98:515-22.

15. Fujita S, Sando I. Postnatal development of the vestibular aqueduct in relation to the internal auditory canal: computer-aided three-dimensional reconstruction and measurement study. Ann Otol Rhinol Laryngol 1994;103:719-22.

16. Sudo M, Sando I, Ikui A, Suzuki C. Narrowest (isthmus) portion of eustachian tube: a computer-aided three-dimensional reconstruction and measurement study. Ann Otol Rhinol Laryngol 1997;106:583-8.

17. Vaughan VC III, Litt IF. Developmental pediatrics. In: Behrman RE, Vaughan VC III, eds. Nelson textbook of pediatrics. 13th ed. Philadelphia, Pa: WB Saunders, 1987:27-35.

18. Sadler-Kimes D, Siegel MI, Todhunter JS. Age-related morphologic differences in the components of the eustachian tube/middle ear system. Ann Otol Rhinol Laryngol 1989;98:854-8.

19. Schuknecht HF. Pathology of the ear. 2nd ed. Philadelphia, Pa: Lea & Febiger, 1993:1-29.

Ann Otol Rhinol Laryngol 109:2000

EFFECT OF WEB 2170 BS, PLATELET ACTIVATING FACTOR RECEPTOR INHIBITOR, IN THE GUINEA PIG MODEL OF MIDDLE EAR INFLAMMATION

R. MURAT KARASEN, MD
YAVUZ SUTBEYAZ, MD
BULENT AKTAN, MD
HASAN OZDEMIR, PHD
CEMAL GUNDOGDU, MD
ERZURUM, TURKEY

Platelet activating factor (PAF), a potent inflammatory mediator, is a biologically active phospholipid. Recent studies have shown that PAF may play an important role in the pathogenesis of otitis media (OM). WEB 2170 BS has been shown to be a PAF antagonist both in vitro and in vivo. In this study, the anti-inflammatory effects of WEB 2170 BS were investigated in a guinea pig model of OM induced by middle ear (ME) inoculation of killed *Staphylococcus aureus*. The outcome of treatment was determined by measurement of myeloperoxidase activity in the samples of ME mucosa, evaluation of temporal bone histopathology, and the presence of ME fluid. The myeloperoxidase activity in the WEB 2170 BS–treated group was found to be significantly lower than that in the control group. Histopathology of the temporal bones indicated decreased inflammation in the treated group as compared to the controls. In addition, ME fluid was absent in 16 of the 20 ears of the 10 treated animals. These results demonstrate that WEB 2170 BS can produce significant anti-inflammatory effects in this model of OM.

KEY WORDS — animal model of otitis media, platelet activating factor, platelet activating factor antagonist, WEB 2170 BS.

INTRODUCTION

Otitis media (OM) is the inflammatory response of the middle ear (ME) caused by multiple factors such as viral or bacterial infection, eustachian tube dysfunction, and allergy. This inflammatory response begins with cellular infiltration in the ME mucosa, followed by release of inflammatory mediators and enzymes such as platelet activating factor (PAF), metabolites of arachidonic acid (AA), histamine, kinin, hydrolytic enzyme, protease, and lysosomal enzymes, including myeloperoxidase (MPO), collagenase, elastase, and cathepsin G that have the capacity to destroy connective tissue matrix.[1,2] These increase vascular permeability and secretory activity. Metabolites of AA and PAF have been identified in human ME effusions, as well as in experimentally induced ME effusions of animals.[1,3-6]

Platelet activating factor (1-o-alkyl-2-acetyl-sn-glyceryl-3-phosphoryl-choline), a biologically active phospholipid, acts as a potent inflammatory mediator via a specific membrane receptor. It is known to have wide-ranging effects on a number of tissues and inflammatory cells.[1,7] It is released from human neutrophils, basophils, platelets, eosinophils, macrophages, mast cells, and vascular endothelial cells.[1,7,8] Its activities include induction of microvascular leakage, chemotaxis, bronchoconstriction, increased bronchial hyperresponsiveness, increased airway mucus secretion, hypotension, shock, and death.[1,7,8] It has been demonstrated in recent years that PAF plays an important role in the pathogenesis of ME inflammation.[1,3,8]

WEB 2170 BS is a potent and specific antagonist of PAF in vitro and in vivo. It is a synthesized hetrazepine PAF antagonist. It has been shown to produce significant anti-inflammatory effects in several models, including the guinea pig.[9-11] WEB 2170 BS has been reported to inhibit the PAF chemotaxis of inflammatory cells in a concentration-dependent manner (50% inhibitory concentration, 0.83 μmol/L in vitro).[11] In this study, we examined the anti-inflammatory activity of WEB 2170 BS in a guinea pig model of OM induced by ME inoculation of killed *Staphylococcus aureus*.

MATERIALS AND METHODS

Animals. We used 20 albino guinea pigs (400 to 500 g) obtained from the Research Institute of Animal Diseases, Erzurum, Turkey, with normal MEs as ascertained by otoscopy and tympanometry.

Chemicals. WEB 2170 BS [5-(2-chlorophenyl)-3, 4-dihydro-10-methyl-3-[(4-morpholinyl) carbonyl]-2H, 7H-cyclo penta [4,5] thieno [3,2-f] [1,2,4] triazolo [4,3-a] [1,4] diazepine (Bepafant)], was obtained from Boehringer Ingelheim KG, Ingelheim/Rein, Germany. Hexadecyltrimethyl ammonium bro-

---

From the Departments of Otolaryngology (Karasen, Sutbeyaz, Aktan) and Pathology (Gundogdu), School of Medicine, and the Division of Biochemistry, Faculty of Science (Ozdemir), Ataturk University, Erzurum, Turkey.
CORRESPONDENCE — R. Murat Karasen, MD, Ataturk Universitesi, PK 59, 25171, Erzurum, Turkey.

mide and glycine were purchased from Fluka Chemika, Germany. Hydrogen peroxide solution 30% was purchased from Merck, Germany. o-Dianisidine (3-3'-dimethoxy benzidine) was purchased from Eastman Organic Chemicals, Rochester, NY.

Preparation of WEB 2170 BS Solution. Each 100 mg of WEB 2170 BS was dissolved in 3 mL of 0.1 N hydrochloric acid; then, 2.3 mL of 0.1 N sodium hydroxide was immediately added, and the solution was diluted with distilled water to 10 mL. The pH of the final solution was 6 to 6.4.

Preparation of Staphylococcus *Suspension.* Suspended *S aureus* was killed by a sonicator and adjusted to a concentration of 1,100 × 10^6 of *S aureus* per milliliter by use of McFarland Nephelometer Standards 3, and the sterility of the killed *S aureus* was tested before inoculation of the animals by culture in the Department of Microbiology, School of Medicine, Ataturk University, Erzurum, Turkey.

Immunization of Animals. Three weeks before ME inoculation, all animals were sensitized with a single subcutaneous injection of a suspension of 0.2 mL of *S aureus* and 0.2 mL of *Bordetella pertussis* (with diphtheria and tetanus toxoids) to stimulate the immune response.[12]

Middle Ear Inoculation of Killed Bacteria. Under anesthesia induced by intraperitoneal ketamine hydrochloride (30 mg/kg), a volume of 0.2 mL of *S aureus* suspension was inoculated into the bilateral ME cavity of all animals through the inferior bulla.

Experimental Groups. The experimental groups were as follows. Group 1 was the WEB 2170 BS treatment group for MPO assay, observation of the presence of ME fluid, and histopathology of the temporal bone. Ten animals were injected intraperitoneally with 10 mg/kg of WEB 2170 BS 2 hours before ME inoculation. Administration was repeated every 12 hours for 48 hours.

Group 2 was the control group. Ten animals were injected intraperitoneally with only sterile saline solution 2 hours before ME inoculation.

Assays and Histopathology. At 48 hours, tympanometric examination was done before sacrifice. The animals in groups 1 and 2 were then killed painlessly by intracardiac 3% glutaraldehyde injection. The animals were then decapitated and the temporal bones were removed. The tympanic bulla of each ear was gently opened, the presence of ME fluids was observed, and a piece of ME mucosa was removed and stored frozen (–70°C). The temporal bones were fixed in phosphate-buffered 3% glutaraldehyde (pH 7.3) for 24 hours. The MPO activity was assayed as we reported previously.[2] The frozen samples were weighed, minced, and homogenized in phosphate-buffered saline solution (pH 6.0) containing 0.5% hexadecylammonium bromide by a Sonic Dismembrator (Fisher Scientific, USA). After homogenization and 2 freeze-thaw cycles with liquid nitrogen, the homogenates were centrifuged at –4°C, 2,500*g* for 30 minutes by a Heraus Sepatech Santrifuge (Germany). After centrifugation, we assayed the MPO activity in the supernatant by incubating 50 µL of diluted sample with 150 µL of potassium phosphate buffer (pH 6.0) containing o-dianisidine (0.2 mg/mL) and hydrogen peroxide (0.001%) at 37°C for 15 minutes. The reaction was then terminated by the addition of 100 µL of 0.4-mol/L glycine (pH 10). A blank was prepared by the addition of 50 µL of distilled water instead of supernatant. A spectrophotometer (LKB-Biochrom, Ultraspec-11 model 4050, Cambridge, England) was adjusted with the blank. The MPO activity was assayed spectrophotometrically by an absorbance reading at 450 nm. The fixed temporal bones were decalcified in 5% ethylenediaminetetraacetic acid for 5 days at 4°C, rinsed 3 times with the same buffer, dehydrated in graded ethanol, and embedded in paraffin. Each paraffin block was sectioned at 20 µm. Every 10th section was stained with hematoxylin and eosin for microscopic examination. Any inflammatory cell infiltration, edema, hemorrhage, and vascularization in the ME mucosa were noted.

Statistical evaluation of the data was performed by Student's *t*-test with significance assigned at $p < .05$.

RESULTS

Presence of ME Fluids. At 48 hours, ME fluids were present in only 4 of the 20 ears of the treated animals, but they were present in all saline controls except 1. Before sacrifice, a type B tympanogram (an indicator of the presence of ME fluids) was also found in the animals with ME fluids.

MPO Activity. The MPO activities of the WEB 2170 BS–treated and saline control groups are shown in the Table as absorbance values detected spectrophotometrically. The mean ± SD absorbance levels in the saline control group (0.439 ± 0.029) were approximately 2 times higher than those in the WEB-2170 BS–treated group (0.230 ± 0.028). Statistical analysis demonstrated a significant difference between the 2 groups' absorbance levels ($p < .001$). Consequently, absorbance levels as an indicator of MPO activity clearly showed that WEB 2170 BS (10 mg/kg intraperitoneally) significantly reduced polymorphonuclear leukocyte (PMN) infiltration at 48 hours, as assessed by the reduction in MPO activity.

Histopathology of Temporal Bone. In the saline

ABSORBANCE LEVELS AS INDICATOR OF MYELOPEROXIDASE ACTIVITY IN EARS OF WEB 2170 BS–TREATED ANIMALS AND SALINE CONTROLS

	Absorbance Levels at 450 nm (OD/min)	
	WEB 2170 BS–Treated Group (n = 20 ears)	*Saline Control Group (n = 20 ears)*
Range	0.188-0.288	0.397-0.486
Mean ± SD	0.230 ± 0.028*	0.439 ± 0.029
Median	0.236	0.440

OD — optical density.

*p < .001 relative to saline control group.

controls, the ME mucosa was dramatically thickened, with subepithelial edema and dilated capillaries in addition to focal hemorrhage and severe subepithelial infiltration of PMNs (see Figure, A,B). In the WEB 2170 BS–treated group, a significant reduction of inflammation, with only a mild amount of PMN infiltration and a minimally thickened subepithelial space, was observed (see Figure, C).

Inflammation was much less pronounced in the ME mucosa of the WEB 2170 BS–treated animals as compared to the controls. In addition, ME fluids were absent in 16 of the 20 ears of the treated animals, but were present in all control ears except 1, and the MPO activity was significantly lower in the treated group as compared to the control group. These findings made with this PAF antagonist emphasize the important role played by PAF as a mediator of inflammation in OM.

DISCUSSION

Platelet activating factor plays an important role in acute inflammatory reactions. It has been shown that PAF is released from inflammatory cells and vascular endothelial cells stimulated by various agents.[1,7] At the same time, the chemotactic action of PAF may induce infiltration of inflammatory cells such as PMNs, monocytes, eosinophils, and basophils.[1]

Several studies in recent years have suggested the possibility of PAF involvement in the pathogenesis of ME inflammation, and it has been shown to induce OM in vivo. Work done by Rhee et al[1] has clearly indicated that PAF alone is able to induce the production of ME fluid in the chinchilla ME cavity. Lin et al[8,13] have demonstrated that PAF has a stimulatory effect on mucous glycoprotein secretion in cultured chinchilla ME epithelial cells. Mucous glycoprotein is one of the troublesome components of ME inflammation.

Jung et al[3] determined high levels of PAF and leukotrienes (LTs) in ME fluid in an experimental model of OM induced by the ME inoculation of killed *Haemophilus influenzae*. Rhee et al[1] demonstrated that PAF stimulated the release of AA metabolites and additional PAF in an experimental model of OM induced by PAF. These findings indicate the importance of both PAF and LTs in the pathogenesis of OM.

Platelet activating factor is produced by or activates neutrophils, eosinophils and monocytes, macrophages, mast cells, and basophils to release lysosomal enzymes, including MPO, oxygen-free radicals, and AA metabolites, and increases vascular permeability in several animal species, including the guinea pig.[14-16] It is chemotactic for PMNs.[15] Accumulation of PMNs can be quantified by MPO activity.[2,17]

WEB 2170 BS is a potent, selective PAF receptor antagonist. Its effectiveness has been studied in ME inflammation by a few investigators. It inhibits most exogenous PAF-induced alteration in vitro and in vivo very effectively and irrespective of the route of administration. The in vivo PAF antagonists WEB 2086 and WEB 2170 BS have been studied extensively and were well proven for their inhibitory effects against various PAF actions.[9,11] Rhee et al[1] demonstrated that WEB 2170 BS effectively prevents PAF-induced OM. Lin et al[8] demonstrated in their study that WEB 2170 BS significantly inhibited PAF-stimulated mucous glycoprotein secretion from ME epithelium in ears with OM.

Jung et al[3] clearly demonstrated that inhibition of PAF and LTs by their antagonists WEB 2170 BS and SCH-37224 prevented the development of OM in an experimental model of OM induced by the ME inoculation of killed *H influenzae*, and it was found that treatment with a combination of both inhibitors prevented the development of OM better than treatment with either drug alone. In our previous study,[2] the effect of SC-41930, a potent selective LTB4 receptor antagonist, was investigated in a guinea pig model of OM induced by ME inoculation of killed *S aureus*. The outcome of treatment was determined by measurement of MPO activity in samples of ME mucosa, and the MPO activity in the treated group was found to be significantly lower than that in the control group.[2] In our present study, ME fluids were present only in 4 of the 20 ears of the treated animals, but were present in almost all controls. The absence of ME fluids in the majority of the treated animals may be explained by the inhibitory effect of WEB 2170 BS on PMN infiltration, on vascular permeability, and on activation of blood cells to release other inflammatory mediators, such as AA metabolites, that are known to be released from inflammatory cells stimulated by PAF.[1,18,19]

Several studies have demonstrated that in histopa-

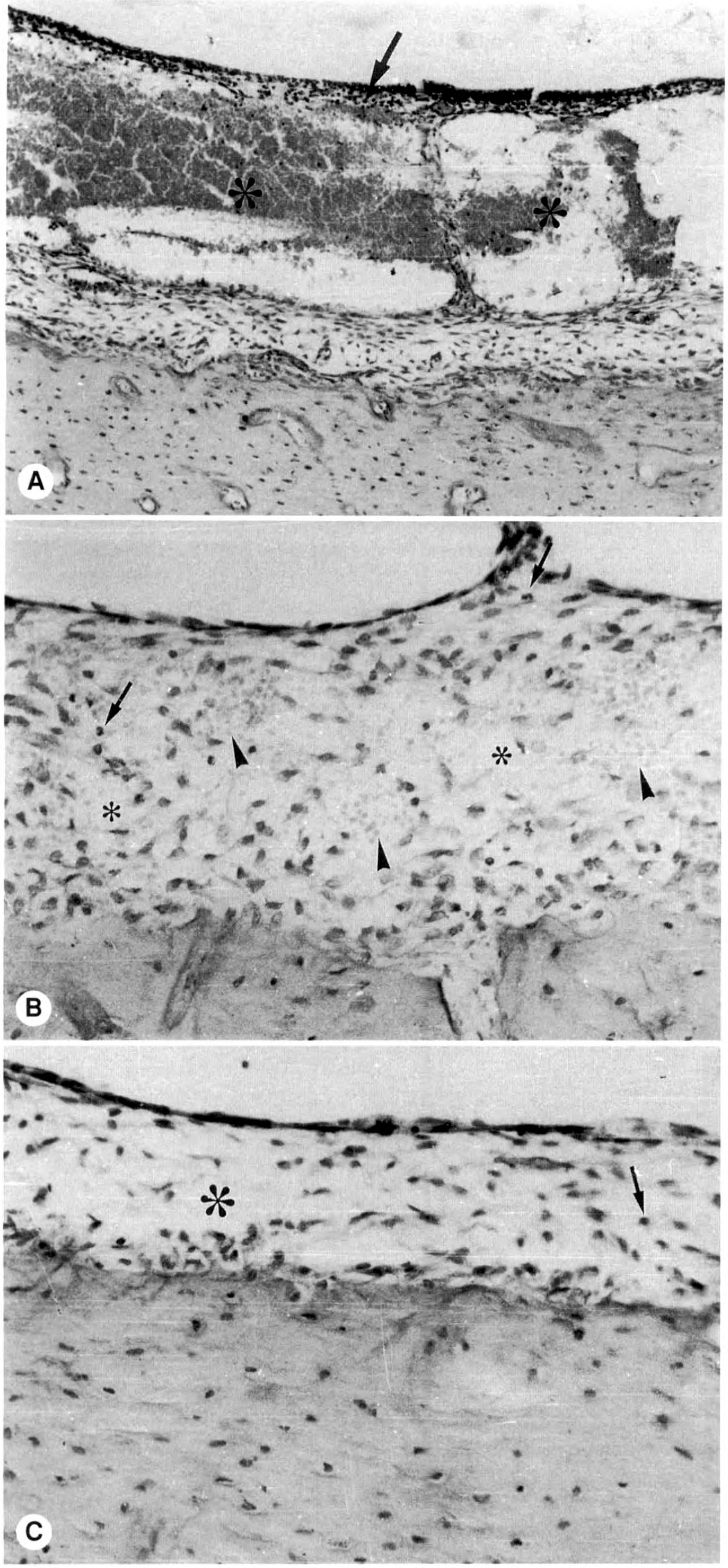

Photomicrographs of guinea pig middle ear mucosa. A,B) Saline control, showing dramatically thickened mucosa, subepithelial edema, and dilated capillaries (asterisks), severe subepithelial infiltration of polymorphonuclear leukocytes (arrows), and focal hemorrhage (arrowheads). A) H & E, original ×200. B) H & E, original ×400. C) After treatment with WEB 2170 BS, showing minimal edema (asterisk) and mild polymorphonuclear leukocyte infiltration (arrow), without focal hemorrhage (H & E, original ×200).

thology of temporal bones, edema and focal hemorrhage resulted from vascular permeability and vasodilation due to PAF and that leukocyte infiltration was pronounced in its chemotactic effect.[1,3] The findings in the PAF or other mediator antagonist–treated groups indicated a significant reduction of inflammation.[1-3] The inflammatory changes were found to be most severe in the ears of the saline control group. In the WEB 2170 BS–treated group, there was only a mild amount of PMN infiltration and a minimally thickened subepithelial space, confirming the histopathologic findings of previous studies.

CONCLUSION

Our findings confirm those of others indicating that PAF is an important mediator of inflammation in OM. This study demonstrated that PAF antagonists such as WEB 2170 BS effectively prevent the development of OM induced by killed *S aureus*, and that PAF antagonists and inhibitors of other inflammatory mediators may have an adjunctive role in the future treatment of ME inflammation.

REFERENCES

1. Rhee C-K, Jung TTK, Miller S, Weeks D. Experimental otitis media with effusion induced by platelet activating factor. Ann Otol Rhinol Laryngol 1993;102:600-5.
2. Sutbeyaz Y, Yakan B, Ozdemir H, Karasen M, Doner F, Kufrevioglu I. Effect of SC-41930, a potent selective leukotriene B4 receptor antagonist, in the guinea pig model of middle ear inflammation. Ann Otol Rhinol Laryngol 1996;105:476-80.
3. Jung TTK, Rhee CK, Park YS, Choi DJ, Miller S, Weeks D. Effect of the inhibitors of leukotriene and platelet activating factor on killed *H influenzae*–induced experimental otitis media. In: Mogi G, Honjo I, Ishii T, Takasaka T, eds. Recent advances in otitis media. Amsterdam, the Netherlands: Kugler, 1994:661-5.
4. Jung TTK, Shea D, Giebink GS, Juhn SK. Comparative histopathology of animal models of otitis media in chinchillas: a temporal bone study. In: Lim DJ, Bluestone CD, Klein JO, Nelson JD, eds. Recent advances in otitis media with effusion. Philadelphia, Pa: BC Decker, 1984:91-6.
5. Jung TTK, Rhee CK. Otolaryngologic approach to the diagnosis and management of otitis media. Otolaryngol Clin North Am 1991;24:931-45.
6. Cauwenberge P, Bernstein J. Inflammatory mediators in middle ear disease. In: Bernstein J, Ogra P, eds. Immunology of the ear. New York, NY: Raven Press, 1987:338-9.
7. Barnes P, Chung K, Page C. Platelet activating factor as a mediator of allergic disease. J Allergy Clin Immunol 1988;81: 919-34.
8. Lin J, Kim Y, Lees C, Juhn SK. Effects of platelet activating factor (PAF) receptor blockage on mucous glycoprotein secretion in cultured chinchilla middle ear epithelium. Acta Otolaryngol (Stockh) 1996;116:69-73.
9. Casals-Stenzel J, Muacevic G, Weber KH. Pharmacological actions of Web 2086, a new specific antagonist of platelet activating factor. J Pharmacol Exp Ther 1987;241:974-81.
10. Casals-Stenzel J, Weber KH. Triazolodiazepines: dissociation of their Paf (platelet activating factor) antagonistic and CNS activity. Br J Pharmacol 1987;90:139-46.
11. Heuer HO. Pharmacology of hetrazepines as Paf-antagonists. In: Braquet P, ed. Handbook of Paf and Paf antagonists. Boca Raton, Fla: CRC Press, 1991:171-202.
12. Baron EJ, Finegold SM. Diagnostic microbiology. Philadelphia, Pa: CV Mosby, 1990:171-94.
13. Lin J, Kim Y, Lees C, Juhn SK. Effects of platelet activating factor on secretion of mucous glycoprotein from cultured middle ear epithelial cells. Eur Arch Otorhinolaryngol 1995;252:92-6.
14. Calumbo M, Casolaro V, Warner J, MacGlashan D, Kagey-Sobotka A, Lichtenstein L. The mechanism of mediator release from human basophils induced by platelet activating factor. J Immunol 1990;145:3855-61.
15. Martins MA, Silva PM, Faria Neto HC, et al. Pharmacological modulation of PAF-induced rat pleurisy and its role in inflammation by zymosan. Br J Pharmacol 1989;96:363-71.
16. Giembycz M, Kroegel C, Barnes P. Platelet activating factor stimulates cyclo-oxygenase activity in guinea pig eosinophils. J Immunol 1990;144:3489-97.
17. Boughton-Smith NK, Wallace JL, Whittle JR. Relationships between arachidonic acid metabolism, myeloperoxidase activity and leukocyte infiltration in rat model of inflammatory bowel disease. Agents Actions 1988;25:115-23.
18. Nakashima S, Suganuma A, Sato M, Tohmatsu T, Nozawa Y. Mechanism of arachidonic acid liberation in platelet-activating factor–stimulated human polymorphonuclear neutrophils. J Immunol 1989;143:1295-302.
19. Voelkel N, Worthen S, Reeves J, Henson P, Murphy R. Nonimmunological production of leukotrienes induced by platelet-activating factor. Science 1982;218:286-8.

Ann Otol Rhinol Laryngol 109:2000

LARYNGEAL RADIONECROSIS AND HYPERBARIC OXYGEN THERAPY: REPORT OF 18 CASES AND REVIEW OF THE LITERATURE

GEORGE A. FILNTISIS, MD, PHD
ATHENS, GREECE
RICHARD E. MOON, MD
DURHAM, NORTH CAROLINA
KEVIN L. KRAFT, RN
DURHAM, NORTH CAROLINA
JOSEPH C. FARMER, MD
DURHAM, NORTH CAROLINA
RICHARD L. SCHER, MD
DURHAM, NORTH CAROLINA
CLAUDE A. PIANTADOSI, MD
DURHAM, NORTH CAROLINA

Laryngeal radionecrosis is a difficult late complication of radiotherapy. It is associated with hoarseness, edema, pain, weight loss, and upper airway obstruction. The medical treatment options are limited, and in severe cases, the patient may require tracheostomy or laryngectomy. We report clinical results in 18 patients treated with adjunctive hyperbaric oxygen (HBO) therapy for severe radionecrosis of the larynx. Of these 18 patients, 2 had grade 3 and 16 had grade 4 radionecrosis. The patients received a mean number of 41 HBO treatments (range, 6 to 80) at 2 atmospheres absolute for 2 hours, twice a day, 6 days a week. Thirteen patients (72.2%) had a major improvement after HBO therapy, and none of them required total laryngectomy. All patients preserved their voice and deglutition in good or normal condition. Five patients (27.8%) failed to have a good response to HBO and underwent total laryngectomy. One of these patients had local recurrence of his cancer 4 months later, and the other 3 had significant concurrent medical problems. The remaining patient received only 6 HBO treatments because of emergency heart surgery. These encouraging results are comparable to those of smaller previous studies suggesting that HBO has a beneficial effect in the management of advanced laryngeal radionecrosis.

KEY WORDS — hyperbaric oxygen, laryngeal necrosis, radiation injury.

INTRODUCTION

Radiotherapy (RT) is a primary or adjuvant therapy in the control and treatment of head and neck malignancies. Because the beneficial effects of RT are produced by tissue destruction, and the radiation dose cannot be restricted to the tumor cells alone, normal tissue is injured during the RT.[1,2] Radiotherapy is particularly effective for early stages of primary laryngeal squamous cell carcinoma (SCC), in which it can eradicate the disease and preserve the normal structure and function of the larynx. The local control rates reported for invasive SCC are in the range of 90% for T1, 70% for T2, and 50% to 60% for T3 and T4 disease. The larynx sometimes is included incidentally in the irradiation portal when irradiation is administered for head and neck tumors involving other anatomic sites.[3]

Radiation necrosis of the larynx presents with hoarseness, dyspnea, pain, dysphagia, weight loss, edema, and upper airway obstruction often requiring a tracheostomy. After cervical RT, almost all patients experience some discomfort due to acute mucositis and laryngeal edema. The acute reactions are relatively mild and in most cases resolve within a few weeks after the completion of RT. The voice begins to improve approximately 3 weeks later, usually reaching a plateau within 2 to 3 months.[3,4]

The most serious complications of head and neck RT generally occur after a latent period of 6 months or more and typically result from vascular compromise and tissue hypoxia secondary to reactive fibrosis and endarteritis. Persistent laryngeal edema is the most common complication that occurs after RT for glottic and supraglottic lesions, with a reported incidence of 13.7% at doses less than 7,000 cGy, rising to 46.2% at doses of 7,000 cGy and above. Soft tissue necrosis leading to chondritis (chondroradionecrosis) occurs in fewer than 1% of patients, usually in those who continue to smoke, at conventional daily fractions of 200 cGy to total doses of 7,000 cGy.[3,5,6] Adult cartilage generally resists RT unless it is infected or traumatized. Local tumor invasion also predisposes to chondronecrosis, which occurs in 2% of patients in T1 and T2 stages and 27% in the advanced stages T3 and T4.[7] Risk factors related to the tissue volume or the patient's use of alcohol or tobacco also affect the normal tissue tolerance to radiation. Moreover, combining RT with surgery or cytotoxic agents frequently decreases the tolerance of normal tissues to radiation.[3,7]

Injury to normal or radioresistant tissues may be caused by the radiation effect on the microvascula-

---

From the Duke Hyperbaric Center (Filntisis, Moon, Kraft, Piantadosi) and the Department of Surgery, Division of Otolaryngology (Farmer, Scher), Duke University Medical Center, Durham, North Carolina. Dr Filntisis is currently in the Department of Critical Care and Pulmonary Diseases, Athens University, Athens, Greece.

CORRESPONDENCE — Claude A. Piantadosi, MD, Duke Hyperbaric Center, DUMC 3315, Duke University Medical Center, Durham, NC 27710.

TABLE 1. GRADING SYSTEMS FOR RADIATION DAMAGE TO LARYNX

Radiation morbidity scoring criteria for larynx irradiation[1]		
Grade 1	Acute	Mild or intermittent hoarseness, cough not requiring antitussive, erythema of mucosa
	Late	Hoarseness, slight arytenoid edema
Grade 2	Acute	Persistent hoarseness but able to vocalize; referred ear pain, sore throat, patchy fibrinous exudate or mild arytenoid edema not requiring narcotic; cough requiring antitussive
	Late	Moderate arytenoid edema, chondritis
Grade 3	Acute	Whispered speech, throat pain or referred ear pain requiring narcotic, confluent fibrinous exudate, marked arytenoid edema
	Late	Severe edema, severe chondritis
Grade 4	Acute	Marked dyspnea, stridor, or hemoptysis with tracheostomy or intubation necessary
	Late	Necrosis
Chandler's grading system for laryngeal radionecrosis[4]		
Grade 1	Symptoms	Slight hoarseness, slight mucosal dryness
	Signs	Slight edema, telangiectasia
Grade 2	Symptoms	Moderate hoarseness, moderate mucosal dryness
	Signs	Slight impairment of vocal cord mobility, moderate cord edema and erythema
Grade 3	Symptoms	Severe hoarseness with dyspnea, moderate odynophagia and dysphagia
	Signs	Severe impairment of vocal cord mobility or fixation of 1 cord, marked edema, skin changes
Grade 4	Symptoms	Respiratory distress, severe pain, severe odynophagia, weight loss, dehydration
	Signs	Fistula, fetor oris, fixation of skin to larynx, laryngeal obstruction and edema occluding airway, fever

ture of the support tissues (stromal or parenchymal cells). Nontumor cells in the field of irradiation are heterogeneous in type and in sensitivity to radiation.[1,8] Radiation produces swelling, degeneration, and necrosis of the vascular endothelium. This results in edema, fibrosis, and thickening of the vessel wall, with degeneration of the elastic and muscular coating. Tissue vascularity and cellularity decline over time as cells degenerate and are not replaced. There are characteristic changes of obliterative endarteritis that progress slowly after radiation exposure to produce hypocellular, hypovascular, and hypoxic tissue beds.[9] Although the cellular mechanisms of radiation injury are not completely understood, DNA damage is one common denominator of injury. Radiation either can affect DNA directly or react with water to form oxygen free radicals, which disrupt chemical bonds in DNA and may lead to an inability of the cell to divide and to repair tissue injury.[10]

To assess the morbidity of RT, toxicity grading systems for various organs have been developed by the Radiology Tumor Oncology Group (RTOG) and the European Organization for Research and Tumor Control (EORTC).[1] Acute morbidity criteria are used in the first 90 days, and thereafter, the late criteria are used. Chandler[4] also has published a grading system for qualifying the severity of laryngeal radiation damage. These grading systems are useful for establishing guidelines for therapy and are summarized in Table 1.[1,4] Grade 1 and 2 radiation injuries are expected reactions and usually respond favorably to conservative treatment such as humidification, voice restraint, discontinuation of smoking, and antibiotics (in the presence of infection). In contrast, grade 3 and 4 reactions are more severe and are considered complications of therapy. These complications consist mostly of edema and fibrosis in less-severe reactions, and frank necrosis involving the cartilage in the most severe.[4]

Hyperbaric oxygen (HBO) therapy has been reported to reverse the progressive changes induced by RT. A daily increase in the oxygen tension in hypoxic tissue stimulates the growth of functional capillaries, fibroblast proliferation, and collagen synthesis. Hyperbaric oxygen has been proposed to repair vascular beds within the irradiated tissue, enabling the surgeon to debride the wound successfully and later reconstruct it. This process has been studied most extensively in osteoradionecrosis of the mandible, although responses to HBO therapy for radionecrosis in other locations, including the larynx, have been reported.[8,11] To date, a total of 25 patients who received HBO therapy for laryngeal radionecrosis have been reported in the literature.[12-17] In this paper, we report our clinical experience in 18 additional patients and summarize the literature on the treatment of laryngeal radionecrosis with HBO.

MATERIALS AND METHODS

Patient Population and Diagnosis. This report is an analysis of all patients referred for HBO therapy to the F. G. Hall Hyperbaric Center at Duke University Medical Center with the diagnosis of radiation-induced laryngeal damage between 1990 and 1996. The 18 patients (11 men and 7 women) were examined with panendoscopy and had tissue biopsies performed to confirm the presence of severe inflammation or necrosis and exclude recurrent tumor. At laryngoscopy, all patients were found to have marked edema. Three patients had biopsy changes consistent with fibrosis, inflammation, and edema; necrosis was not demonstrated in these biopsies. Fifteen patients had necrosis plus edema, and in 5, there was additional cartilage exposure and fragmentation, whereas in 1 patient there was additional marked mucosal ulceration. No evidence of persistent or recurrent tumor, local or distant, was found at the time of referral. All patients received symptomatic therapy as needed with parenteral antibiotics, steroids, racemic epinephrine, bronchodilators, and humidity before and during HBO therapy. All 18 patients had had clinical signs of severe radiation injury for at least 3 months with no improvement despite aggressive therapy. Patients who had already undergone total laryngectomy were not included in the study.

Grading System for Radionecrosis. Chandler's[4] system for grading the severity of radionecrosis was used in this analysis (Table 1). Two of the 18 patients presented with Chandler grade 3 necrosis, and 16 had grade 4 necrosis. The time between RT and development of radiation injury ranged from 3 months to 30 years. Three patients developed early (≤3 months) severe symptoms, and 4 patients developed late symptoms (>2 years). The majority of the patients developed clinical manifestations of radionecrosis within 9 months of therapy. Thirteen patients presented for HBO therapy with a tracheostomy in place for severe airway obstruction. (Four patients had required emergency tracheostomy, and 1 patient underwent tracheostomy early during the HBO treatment.) Two patients also had infection of the tracheostomy site with neck cellulitis, and 2 others had significant infections of the bronchi. Two patients were being fed by a nasogastric tube (patient 10) and a gastrostomy tube (patient 15) because of severe odynophagia and inability to eat. The time to referral for HBO therapy after a definitive diagnosis of radiation injury was made (usually by a biopsy) ranged from 3 to 150 days (average, 26 days).

The 2 patients with Chandler grade 3 necrosis had undergone RT combined with chemotherapy (5-fluorouracil, mitomycin), and 1 of them had been submitted to a laser excision of the primary cancer. Neither required a tracheostomy. Of the 16 patients who had Chandler grade 4 necrosis, 1 patient (No. 3) had undergone RT combined with chemotherapy (5-fluorouracil, cisplatin). One patient (No. 4) had undergone supraglottic laryngectomy and radical neck dissection before RT, and laser excision of redundant arytenoid tissue after RT. Another patient (No. 9) had undergone modified radical neck dissection before RT, and another (No. 11) was treated initially with laser debulking, followed by modified radical neck dissection after RT. A laser excision was performed in 1 patient (No. 5) for a local recurrence in the hypopharynx after RT, and in another patient (No. 17) for a polyp of the vocal cords after RT.

Hyperbaric Oxygen Therapy. Hyperbaric oxygen therapy was given 6 days a week, twice a day, for the desired number of treatments, usually 40, in a multiplace chamber. The chamber was compressed with air to a pressure of 2 atmospheres absolute for 2 hours while the patients breathed 100% oxygen through a head tent system that sealed around the neck. Air breaks were not used. Head tent oxygen and carbon dioxide concentrations were monitored continuously to ensure an oxygen concentration of >98% and a carbon dioxide concentration of <1%. For safety purposes, exhaust gases from the hood were evacuated into an overhead dump system in order to prevent the ambient oxygen concentration within the chamber from exceeding 23%. In 4 patients, bilateral myringotomy tubes were placed before they started HBO therapy. After the completion of HBO therapy, the patients were returned to the care of their referring otolaryngologist.

RESULTS

The patient population (11 men and 7 women; average age, 61 years) was heterogeneous. The characteristics of the patient group are given in Tables 2[4] and 3. As shown in Table 2, 15 of the 18 patients had biopsy-proven tissue necrosis. Biopsy results on the other 3 patients showed advanced radiation injury without definite necrosis (Table 2, patients 1, 7, and 9). Seventeen patients completed at least 20 HBO treatments, with a mean number of 43 treatments (range, 20 to 80). One patient underwent only 6 treatments because of a need for an emergency coronary artery bypass graft. Two patients underwent 2 courses of HBO. One patient had undergone only 19 treatments initially, and the other had his treatment interrupted for surgical repair of his tracheostomy with lysis of synechiae. None of the 18 patients had significant complications of the HBO therapy. The outcomes of HBO treatment are provided in Table 4.

Thirteen patients (72.2%) who underwent an average of 44 HBO treatments (range, 20 to 80) had ma-

TABLE 2. PATIENTS' CHARACTERISTICS

Pt No.	Age	Sex	Cancer Diagnosis, Site, and Stage	Radiation Dose (cGy)	Time RT to RN (mo)	Presentation of Radiation Injury	Chandler[4] Grade
1	41	F	1992: SCC left glottis T3N0	6,480	8	Severe hoarseness, difficult swallowing, progressive pain. Biopsy: fibrosis and inflammation.	3
2	66	F	1994: Larynx	7,000	9	Hoarseness, edematous epiglottis, difficult voice after biopsy. Biopsy: edema of vocal cords, exposed ligaments, areas of irritation and necrosis.	3
3	64	F	1992: SCC pyriform sinus T4N2bM0	7,000	3	Upper airway obstruction, weight loss, loss of consciousness. Biopsy: soft tissue and cartilage necrosis.	4, em trach
4	54	M	1993: SCC supraglottic T2N0M0	6,000	3	Upper airway obstruction after biopsy and laser excision. Copious fibrinous debris and focal necrosis.	4, trach
5	64	F	1994: SCC epiglottis T2N1	6,600	3	Hoarseness, odynophagia, swelling, upper airway obstruction. Biopsy: necrosis and inflammation.	4, trach
6	75	M	1995: SCC supraglottic T4N2cM0	7,545	4	Sore throat, pain, hoarseness, ulceration. Biopsy: inflamed necrotic tissue. 1994: Lung adenocarcinoma, T1N0, lobectomy.	4
7	60	F	1993: Ca larynx T1N0	6,600	4	Swelling and massive edema of larynx, infection. Biopsy: marked laryngeal edema.	4, em trach
8	55	M	1996: SCC supraglottic T4N1M0	7,450	6	Choking sensation, dyspnea, odynophagia, weight loss, skin changes, voice loss, supraglottic edema, exposed cartilage. Biopsy: necrotic debris.	4, trach
9	57	M	1996: SCC head and neck	5,760	6	Dehydration, severe dysphagia, airway occlusion, significant edema of larynx and hypopharynx. Oropharyngeal infection.	4
10	47	M	1993: SCC vocal cord T2N0M0	6,400	8	Upper airway obstruction, very edematous larynx, feeding tube. Biopsy: changes consistent with radionecrosis.	4, trach
11	54	F	1995: SCC supraglottic T3N0	7,450	9	Stridor, dyspnea, pain, dry mucus, dysphagia, neck cellulitis. Biopsy: extensive anterior necrosis, exposure of thyroid cartilage.	4, em trach
12	77	M	1993: SCC true vocal cord T2N0	5,000	9	Hoarseness, stridor, weight loss. Biopsy: inflammation and necrosis.	4, trach
13	49	M	1994: SCC true vocal cord T2N0	7,000	12	Hoarseness, dyspnea, odynophagia, weight loss, acute airway obstruction after biopsy. Biopsy: evidence of radionecrosis.	4, em trach
14	65	M	1990: SCC larynx T2N2	7,000	40	Odynophagia, swelling, difficult swallowing. Biopsy: necrosis, chronic laryngeal edema.	4, trach
15	65	F	1988: SCC epiglottis T1N0	6,600	72	Dysphagia, throat pain, difficult swallowing, weight loss, gastrostomy tube. Biopsy: necrosis and cartilage destruction.	4, trach
16	63	M	1980: Pharynx	7,000	204	Upper airway noise, dysphagia, dyspnea, fetor oris, weight loss, paralysis of left hemilarynx. 1981: Hyperbaric oxygen therapy for osteoradionecrosis of mandible (healed). Biopsy: radionecrosis.	4, trach
17	71	M	1965: Larynx	6,600	360	Severe hoarseness, dysphonia, weight loss, cellulitis. Biopsy: fracture of thyroid cartilage, sequestration, denudation, necrosis.	4
18	46	M	1990: SCC L pyriform sinus T2N0	6,000	7	Severe shortness of breath, hoarseness, difficult swallowing, weight loss. Biopsy: marked edema, fat necrosis, fibrosis, granulomatous inflammation.	4, trach

RT — radiotherapy, RN — radionecrosis, SCC — squamous cell carcinoma, em trach — emergency tracheostomy, trach — tracheostomy, Ca — carcinoma.

TABLE 3. PREDISPOSING FACTORS FOR LARYNGEAL RADIONECROSIS

Pt No.	*Chemotherapy*	*Surgery*	*Laser*	*Smoking**	*Other Diseases*	*Response to HBO*
1	+	–	+	+	–	+
2	+	–	–	+	–	+
3	+	–	–	+	Hyponatremia	+
4	–	+	+	+	–	+
5	–	–	+	–	Chronic renal failure, hypertension	–
6	–	–	–	–	COPD, lung carcinoma	+
7	–	–	–	++	Hypertension	+
8	–	–	–	++	Hypertension	+
9	–	+	–	+	Basal cell carcinoma of skin	+
10	–	–	–	+	–	–
11	–	+	+	–		+
12	–	–	–	–	Diabetes	+
13	–	–	–	+	COPD, angina	–
14	–	–	–	+	–	–
15	–	–	–	–	Rheumatoid arthritis, diabetes, steroid therapy	+
16	–	–	–	+	COPD	+
17	–	–	+	–	Diabetes	+
18	–	–	–	++	Alcohol abuse	–

HBO — hyperbaric oxygen, COPD — chronic obstructive pulmonary disease.

*+ — Ex-smoker; ++ — continued smoking.

jor improvement in their symptoms. These 13 patients were followed from 1 to 4 years after the completion of HBO therapy. None of them required a total laryngectomy, and all preserved their voice in good or normal condition. Four of the 8 patients of this group who underwent tracheostomy were able to be decannulated. Deglutition also improved so they were able to eat without difficulty. One patient had been treated previously in 1981 with HBO for a mandibular osteoradionecrosis, which healed completely. Three of the 13 patients developed metastatic or second primary tumors after the HBO therapy. One patient presented with lung cancer 1 year later (and died 2 years later). Another patient presented with a lymph node metastasis of his primary cancer and required radical neck dissection 13 months later, and the remaining patient presented with cervical cancer 4 years later and was treated with RT. These 2 patients, as well the other 10 patients in this group, were alive and well at the time of this report.

Five patients (27.8%) underwent a mean number of 34 HBO treatments (range, 6 to 60) and failed to have a good initial response to HBO treatment. Four patients underwent total laryngectomy 3, 4, 10, and 12 months after the HBO treatment. The fifth patient (No. 10) was found to have a local recurrence of his cancer 4 months later and underwent total laryngectomy. He died of myocardial infarction 3 years after HBO treatment. Two of the other 5 patients had significant concurrent medical problems. One (No. 5) had end-stage renal disease, and the other (No. 14) had ischemic heart disease and required a gastric feeding tube because of aspiration pneumonia after a stroke that occurred 2 years after HBO therapy. This patient underwent only 23 HBO treatments. Both of them were still alive, 28 months and 3 years after HBO treatment. The fourth patient (No. 18) continued to smoke and abuse alcohol heavily. His wound dehisced after laryngectomy and required a major pectoralis flap. He then underwent 43 HBO treatments, which resulted in complete healing of the wound. The patient who underwent only 6 HBO treatments (No. 13) underwent a total laryngectomy 10 months later, and was still alive 26 months later with a permanent tracheostomy and fistula.

DISCUSSION

Radiation necrosis is a complication of RT due primarily to a vascular inflammatory reaction secondary to the effect of radiation on blood vessels. The small vessels show extensive arteritis and thrombosis, which, in the larynx, reduce the blood supply to the hyaline cartilage, resulting in necrosis. Several clinical studies have shown that patients who do not develop overt clinical disease still have significant tissue damage. Uncompromised irradiated tissue, after doses of 6,000 to 8,000 cGy given for malignant tumors, shows a capillary density of only 20% to 40% of that of nonirradiated tissue. Irradiated tissue appears to be largely incapable of revascularization or recovery without intervention, because of a decrease in the number of viable fibroblasts and in sufficient

TABLE 4. RESULTS OF HBO TREATMENT

Pt No.	*No. of HBO*	*Complications*	*Time to Referral (d)**	*Clinical Outcome*	*Follow-up After HBO*
1	80	None†	30	Major improvement. Weight gain, less discomfort. At 6 mo, resolved radionecrosis. At 4 y, cervical carcinoma (radiotherapy).	Alive at 4 y
2	28	None	30	Hoarseness, persistent supraglottic edema, vocal difficulty. At 2 y, no swelling, dysphagia, or tracheostomy; normal voice.	Alive and well at 2 y
3	40	Mild OB	15	Voice improvement, decreased mucous drainage. At 1 y, lung carcinoma. At 2 y, spinal cord metastasis. Since initial laryngeal carcinoma treatment, had done reasonably well (tracheostomy in place, good voice, no dysphagia).	Died 2 y later (metastasis)
4	19 + 40	None†	5	First course, reduction of edema. Second course, major improvement in airway obstruction. At 21 mo, tracheostomy closed at rest, good voice, no dysphagia.	Alive and well at 21 mo
5	42	None	30	Initial improvement in voice and throat discomfort. Tracheostomy wound clean (no odor or exudate). At 3 mo later, total laryngectomy. At 7 mo later, skin flap, no dysphagia.	Alive and well at 28 mo
6	40	Mild OB	5	Ulceration healed, good voice. Computed tomogram of larynx showed no filling defects or mucosal abnormalities. At 13 mo, radical neck dissection (lymph node metastasis). Percutaneous esophagogastric tube placement. No tracheostomy or dysphagia.	Alive and well at 18 mo
7	20	None	15	At 2 mo, tracheostomy removed. At 40 mo, very well. Normal voice and breathing. No dysphagia, eats by mouth.	Alive and well at 40 mo
8	40	None	7	Minor resolution of supraglottic edema, major resolution of wound edema. At 6 mo, no voice, small area of necrotic tissue. At 9 mo, tracheostomy in place, eats well by mouth, good voice.	Alive and well at 9 mo
9	39	Mild OB†	30	Major resolution of edema, complete resolution of dysphagia.	Alive and well at 6 mo
10	40	None	3	Minor improvement of edema and voice. At 4 mo, local recurrence (total laryngectomy). At 6 mo, well, ability to eat, weight gain.	Died 3 y later (heart attack)
11	36	Anxiety†	3	Significant improvement. At 4 mo, decannulation. At 13 mo, no tracheostomy or dysphagia, good voice.	Alive and well at 13 mo
12	40 + 34	None	15	First course, minor improvement. Surgical repair. Second course, significant improvement. At 6 mo, well, stronger voice.	Alive and well at 6 mo
13	6	None	5	Therapy incomplete because of heart surgery. At 10 mo, total laryngectomy. At 26 mo, tracheostomy in place, fistula. No dyspnea or dysphagia.	Alive at 26 mo
14	23	None	150	Major resolution of pain and edema. HBO discontinued by surgeon. At 1 y, total laryngectomy. Feeding tube after stroke.	Alive at 3 y
15	40	None	60	Major improvement, decannulation, good voice, eats well by mouth.	Alive and well at 34 mo
16	23	None	7	At 15 mo, well, eats well by mouth, weight gain, decannulation.	Alive and well at 25 mo
17	48	Myopia, anxiety	30	At 1 mo, major improvement. Small opening in neck, no discharge, weight gain, no hoarseness. At 10 mo, eats well by mouth, voice preservation, very small hole in neck.	Alive and well at 10 mo
18	60	Myopia	30	Minor improvement. Return of edema. At 4 mo, total laryngectomy. Wound dehiscence. After muscle flap and 43 HBO (2nd course), healing.	Alive and well at 5 mo

OB — otic barotrauma.
*From radionecrosis to HBO referral.
†Had myringotomy tubes.

oxygen to synthesize collagen to support the capillary budding.[8] Fibroblast and leukocyte functions are severely impaired when tissue oxygen levels fall below normal levels. Because of the unique physics and pattern of tumoricidal radiation delivery, a shallow oxygen gradient is established from the nonirra-

TABLE 5. SUMMARY OF PUBLISHED LITERATURE ON TREATMENT OF LARYNGEAL RADIONECROSIS WITH HBO

Authors	*No. of Pts*	*Chandler[4] Grade*	*HBO Pressure (ATA × min)*	*Mean No. of HBO (range)*	*Outcome*
Hart and Mainous[12]	5	4	2 ×120	60	4 Improved, 1 died (aspiration)
Farmer et al[13]	1	4	2 ×120	40	Improved
Davis et al[14]	1	4	2.4 ×90	60	Improved
Strauss[15]	1	4	Not reported	20	Failed
Ferguson et al[16]	8	4 pts 3 4 pts 4	2 ×120	49 (39-76)	7 Improved, 1 failed
Feldmeier et al[17]	9	1 pts 3 8 pts 4	2.4 ×90	28 (8-41)	All improved
Present report	18	2 pts 3 16 pts 4	2 ×120	43 (6-80)	13 Improved, 4 failed, 1 inadequate number of treatments

ATA — atmospheres absolute.

diated tissue to the central zone of the irradiated field. Tissue oxygen measurements from the center to the edge of an irradiated field show a gradual increase in tissue oxygen tensions, from 5 to 10 mm Hg in the center of the injury to 50 to 60 mm Hg at the edge.[8,10,18]

The most common early manifestation of radiation injury is edema, which is present for 4 to 6 weeks after RT. All of our patients presented with severe progressive symptoms 3 or more months after the completion of RT; hence, it is unlikely that we were treating a self-limited process. This conclusion is in agreement with those of other authors.[17] Four of our patients manifested radionecrosis after 2 years, and 1 of them presented after 30 years, the longest delay for laryngeal radionecrosis in the literature.[19] When edema persists for months after RT, it may indicate the onset of laryngeal perichondritis and incipient chondronecrosis or recurrent malignancy. The changes secondary to radionecrosis are very similar to those of cancer, and this represents a major diagnostic dilemma for the otolaryngologist and pathologist.[20,21] Some authors recommend multiple biopsies at different sites and different times, if necessary[22]; however, surgical trauma to the irradiated tissue may further the necrotic process. Positron emission tomography may be useful in distinguishing benign from malignant changes in the irradiated larynx.[23] Laryngectomy has been recommended as a last resort when recurrent malignancy cannot be excluded and the biopsy specimens show severe necrosis.[4,22,24] The use of HBO in such patients is not dangerous[25]; it may improve tissue vascularity and make the patient a better surgical candidate. The "risk" of administering HBO to the patient with an undiagnosed local recurrence instead of radionecrosis would be to delay a potentially curative resection.

The most severe consequences of RT relate to the development of ischemia of tissues. Secondary infection often occurs in the compromised tissue, leading to major clinical problems such as progressive necrosis and sloughing of soft tissue and cartilage. Necessary surgery and deep tissue biopsy can worsen necrosis or promote fistula formation, and have even been associated with fatalities.[26] Impaired leukocyte function has been implicated as a key factor in poor wound healing and infection in hypoxic tissues, and recent evidence suggests that leukocyte function also may be impaired directly in irradiated tissue.[10] Gabka et al,[27] using an experimental rabbit wound cylinder model to determine the effect of irradiated tissue on neutrophil function, found functional leukocyte deficits such as diminished phagocytosis, superoxide production, and surface adhesion molecule expression.[27] These factors play an important role in the early inflammatory process, in bactericidal effects, and in the ability of neutrophils to migrate to inflammatory sites.

Other predisposing risks for the development of complications related to RT include alcohol, smoking, diabetes, hypertension, steroids, and infiltration of cartilage with tumor before treatment. Five of our patients with severe cartilage destruction continued to smoke or had advanced cancer, steroid therapy, or concurrent diseases such as diabetes and hypertension. These factors are known to affect vascularization and the wound healing process.[7,20,28] Three of these 5 patients did not improve with HBO (Table 3).

Radionecrosis is very difficult to treat, both medically and surgically,[29] particularly with higher grades of injury.[4] Conservative measures, including humidification, steroids, and antibiotics administered for up to 6 weeks, are usually sufficient for initial treatment of less-severe symptoms. Patients with more-severe symptoms may require a tracheostomy, a partial laryngectomy, or, in very severe cases, total laryngectomy. Hyperbaric oxygen therapy is recommended only for severe manifestations.[24,29,30]

Our report represents the largest experience with

TABLE 6. OUTCOME VERSUS NUMBER OF TREATMENTS

	Improved			*Not Improved*		
No. of HBO	*Grade 3*	*Grade 4*	*Totals*	*Grade 3*	*Grade 4*	*Totals*
<20		2	2		1	1
20-40	4	16	20		3	3
>40	3	10	13		4	4
Totals	7	28	35	0	8	8

Data are numbers of patients. Grades are in Chandler[4] system.

laryngeal radionecrosis treated with HBO as an adjunctive therapy to date and supports the trends of earlier reports. To date, a total of 25 patients who underwent HBO therapy for laryngeal radionecrosis have been reported in the literature.[12-17] Two of them had known, persistent tumor. Of the 25 patients, 22 had a significant improvement, whereas 2 failed to respond and required a total laryngectomy (1 patient underwent only 20 treatments, only half the usual number), and 1 died of aspiration (Table 5[4,12-17]). The data from this study and 2 previous reports from this institution[13,16] indicate a failure rate for HBO therapy of 22.2% (6/27). Table 6[4] shows the outcome of the 43 patients treated with HBO for laryngeal radionecrosis versus the number of HBO treatments.

The use of HBO therapy for radiation-damaged tissue was first introduced by Greenwood and Gilchrist[31] and Hart and Mainous.[12] Since that time, several treatment protocols have been developed. Marx[8] developed HBO protocols based on randomized, prospective clinical trials that have proven successful in oral and maxillofacial surgery after irradiation. Hyperbaric oxygen appears to reverse the ongoing reduction of vascularity by creating the steep oxygen gradient that is present naturally in noncompromised normal wounds. A steep oxygen gradient is one of the driving forces for normal wound healing. By acting as an important stimulus for release of growth factors from the macrophages that populate the wound space, HBO can increase the oxygen tensions in ischemic tissue and stimulate leukocyte bactericidal activity, enhance fibroblast and collagen formation, and facilitate angiogenesis. Leukocyte killing can increase by 40% when the Po_2 is increased from 45 to 150 mm Hg. Neovascularization has been shown to raise the oxygen tension in irradiated tissue to 75% to 80% of normal.[25,32-35]

It should be emphasized that HBO is adjunctive to surgery and other indicated medical measures, although we observed significant improvement or complete healing of the radiation injury in most of our patients. Healing was accompanied by decreased hoarseness and pain, so that the patients were able to preserve voice or to improve it. There was also reduction of edema and upper airway obstruction, so that breathing became more comfortable and tracheostomy was unnecessary. There was also reduction of dysphagia and mucous membrane dryness, so that the patients were able to eat by mouth and to gain weight. Finally, the avoidance of a total laryngectomy, even in patients with severe chondroradionecrosis, suggests an important positive effect of HBO therapy.

Persistent tumor continues to be of concern to physicians who manage patients who have radionecrosis. At this time, there is no convincing evidence that HBO stimulates tumor growth. A review of the literature showed that the majority of reports indicate no cancer growth enhancement by HBO exposure.[25] Two of our patients presented local recurrence (11.1%), and 2 more a second primary cancer (11.1%). This rate is below that reported for local and/or regional recurrence and second primary tumors in patients treated with radiation therapy (31% and 21%, respectively).[36,37]

In conclusion, Chandler[4] proposed 20 years ago that there might be a place for HBO in the treatment of laryngeal radionecrosis. At the time, the general unavailability of the therapy limited its usefulness. Today, on the basis of the increased availability of hyperbaric facilities and of our experience and the results of previous studies, we offer HBO as a relatively safe and useful adjunctive treatment for radionecrosis in patients with laryngeal damage refractory to more conservative measures.

REFERENCES

1. Perez CA, Brady LW. Overview. In: Perez CA, Brady LW, eds. Principles and practice of radiation oncology. Philadelphia, Pa: JB Lippincott, 1992:1-55.

2. Mettler FAJ, Upton AC. Medical effects of ionizing radiation. 2nd ed. Philadelphia, Pa: WB Saunders, 1995:214-301.

3. Mendenhall WM, Parsons JT, Mancuso AA, Cassisi NJ, Stringer SP, Million RR. Larynx. In: Perez CA, Brady LW, eds. Principles and practice of radiation oncology. Philadelphia, Pa: JB Lippincott, 1992:740-61.

4. Chandler JR. Radiation fibrosis and necrosis of the larynx. Ann Otol Rhinol Laryngol 1979;88:509-14.

5. Berger G, Freeman JL, Briant DR, Berry M, Noyek AM. Late post radiation necrosis and fibrosis of the larynx. J Otolaryngol 1984;13:160-4.

6. Emami B, Lyman J, Brown A, et al. Tolerance of normal tissues to therapeutic irradiation. Int J Radiat Oncol Biol Phys 1991;21:109-22.

7. Keene M, Harwood AR, Bruce DP, Van Nostrand AWP. Histopathologic study of radionecrosis in laryngeal carcinoma. Laryngoscope 1982;92:173-80.

8. Marx RE. Radiation injury to tissue. In: Kindwall EP, ed. Hyperbaric medicine practice. Flagstaff, Ariz: Best Publish-

ing Co, 1994:447-503.

9. Marx RE, Johnson RP. States in the radiobiology of osteoradionecrosis and their clinical significance. Oral Surg Oral Med Oral Pathol 1987;64:379-90.

10. Mathes SJ, Alexander J. Radiation injury. Surg Oncol Clin North Am 1996;5:809-24.

11. Camporesi EM. Radiation tissue damage. In: Hyperbaric oxygen therapy: a committee report. Kensington, Md: Undersea and Hyperbaric Medical Society, 1996:41-3.

12. Hart GB, Mainous EG. The treatment of radiation necrosis with hyperbaric oxygen. Cancer 1976;37:2580-5.

13. Farmer JC Jr, Shelton DL, Angelillo JD, Bennett PD, Hudson WR. Treatment of radiation-induced tissue injury by hyperbaric oxygen. Ann Otol Rhinol Laryngol 1978;87:707-15.

14. Davis JC, Dunn JM, Gates GA, Heimbach RD. Hyperbaric oxygen. A new adjuvant in the management of radiation necrosis. Arch Otolaryngol 1979;105:58-61.

15. Strauss M. Long term complications of radiotherapy confronting the head and neck surgeon. Laryngoscope 1983;93:310-3.

16. Ferguson BJ, Hudson WR, Farmer JC Jr. Hyperbaric oxygen therapy for laryngeal radionecrosis. Ann Otol Rhinol Laryngol 1987;96:1-6.

17. Feldmeier JJ, Heimbach RD, Davolt DA, Brakora MJ. Hyperbaric oxygen as an adjuvant treatment for severe laryngeal necrosis: a report of nine consecutive cases. Undersea Hyperb Med 1993;20:329-35.

18. Marx RE, Ehler WJ, Tayapongsak P, Pierce LW. Relationship of oxygen dose to angiogenesis induction in irradiated tissue. Am J Surg 1990;160:519-24.

19. Robson SC, Daws JDK. A case of perichondritis and necrosis of laryngeal cartilage 25 years after treatment with radium. J Laryngol Otol 1961;75:997-8.

20. Rowley H, Walsh M, McShane D, Fraser I, O'Dwyer TP. Chondroradionecrosis of the larynx: still a diagnostic dilemma. J Laryngol Otol 1995;109:218-20.

21. Bahadur S, Amatya RC, Kacker SK. The enigma of post-radiation oedema and residual or recurrent carcinoma of the larynx and pyriform fossa. J Laryngol Otol 1985;99:763-5.

22. Calcaterra TC, Stern F, Ward PH. Dilemma of delayed radiation injury of the larynx. Ann Otol Rhinol Laryngol 1972; 81:501-7.

23. Greven KM, Williams DW 3rd, Keyes JW Jr, et al. Distinguishing tumor from irradiation sequelae with positron emission tomography in patients treated for larynx cancer. Int J Radiat Oncol Biol Phys 1994;29:841-5.

24. Flood LM, Brightwell AP. Clinical assessment of the irradiated larynx. Salvage laryngectomy in the absence of histological confirmation of residual or recurrent carcinoma. J Laryngol Otol 1984;98:493-8.

25. Feldmeier JJ, Heimbach RD, Davolt DA, Brakora MJ, Sheffield PJ, Porter AT. Does hyperbaric oxygen have a cancer-causing or -promoting effect? A review of the pertinent literature. Undersea Hyperb Med 1994;21:467-75.

26. Robson MC. Disturbances of wound healing. Ann Emerg Med 1988;17:1274-8.

27. Gabka CJ, Benhaim P, Mathes SJ, et al. An experimental model to determine the effect of irradiated tissue on neutrophil function. Plast Reconstr Surg 1995;96:1676-88.

28. Matos LA, Nunez AA. Enhancement of healing in selected problem wounds. In: Kindwall EP, ed. Hyperbaric medicine practice. Flagstaff, Ariz: Best Publishing Co, 1994:589-612.

29. Oppenheimer RW, Krespi YP, Einhorn RK. Management of laryngeal radionecrosis: animal and clinical experience. Head Neck 1989;11:252-6.

30. Balm AJM, Hilgers FJM, Baris G, Keus RB. Pectoralis major muscle transposition: an adjunct to laryngeal preservation in severe chondroradionecrosis. J Laryngol Otol 1993;107: 748-51.

31. Greenwood TW, Gilchrist AJ. Hyperbaric oxygen and wound healing in post-irradiation head and neck surgery. Br J Surg 1973;60:394-7.

32. Kindwall EP. Hyperbaric oxygen's effects on radiation necrosis. Clin Plast Surg 1993;20:473-83.

33. Hunt TK. The physiology of wound healing. Ann Emerg Med 1988;17:1256-73.

34. Miller SH, Rudolph R. Healing in the irradiated wound. Clin Plast Surg 1990;17:503-8.

35. LaVan FB, Hunt TK. Oxygen and wound healing. Clin Plast Surg 1990;17:463-72.

36. Morris MR, Canonico D, Blank C. A critical review of radiotherapy in the management of T1 glottic carcinoma. Am J Otolaryngol 1994;15:276-80.

37. Shimm DS, Coulthard SW. Radiation therapy for squamous cell carcinoma of the supraglottic larynx. Am J Clin Oncol 1989;12:17-23.

Ann Otol Rhinol Laryngol 109:2000

AIRWAY FLOW DYNAMICS AND VOICE ACOUSTICS AFTER AUTOLOGOUS FASCIA AUGMENTATION OF PARALYZED VOCAL FOLD

ANTTI SAARINEN, MD
HEIKKI RIHKANEN, MD, PHD
SARI LEHIKOINEN-SÖDERLUND, MSC
ANSSI R. A. SOVIJÄRVI, MD, PHD
HELSINKI, FINLAND

The aim of this study was to assess the effect of vocal fold medialization, accomplished by injection of autologous fascia, on airflow dynamics and voice acoustics. Ten patients with unilateral vocal fold paralysis were included. Flow-volume spirometry, body plethysmography, and acoustic analysis of voice were performed within 1 week before injection of autologous fascia and 4 to 14 months after operation. Medialization of the paralyzed vocal fold decreased the mean peak inspiratory flow (PIF) from 4.63 L to 4.10 L ($p = .012$). The acoustic characteristics of the voice improved: the values of jitter, shimmer, and mean noise-to-harmonics ratio decreased significantly ($p = .006$, $p = .017$, and $p = .047$, respectively), and the mean maximal phonation time almost doubled ($p = .002$). Changes in PIF and shimmer showed a negative correlation ($r = -.857$, $p = .007$). In conclusion, injection of autologous fascia improves voice acoustics, but induces a slight abnormal limitation on PIF. The results also suggest that improvement in voice acoustics is most prominent in subjects with the least deterioration in inspiratory airflow.

KEY WORDS — autologous fascia injection, body plethysmography, flow-volume spirometry, medialization of vocal fold, vocal fold paralysis, voice acoustics.

INTRODUCTION

Unilateral vocal fold paralysis is a not-uncommon disorder that causes dysphonia and aspiration.[1] Some patients also complain of noisy inspiration in deep breathing or dyspnea. When voice therapy does not sufficiently improve glottic closure, surgery is indicated to restore the volume and increase the tension of the vocal fold. Teflon injections have been performed for decades, but because of their unfavorable side effects,[2] thyroplasty type I[3] has gained popularity in medialization of the paralyzed vocal fold. More recently, autologous fat,[4,5] collagen,[6] and fascia[7] have been used as injectable materials.

Controlled studies concerning the impact of medialization of the paralyzed vocal fold on the ventilatory function have been carried out after Teflon injections. The results of those studies have been somewhat discrepant. Cormier et al[8] found improved maximal expiratory flow at the level of 50% of forced expiratory volume (MEF50) after intracordal Teflon injections. In another study, a transient decrease of forced inspiratory flow in the first second (FIV1) and an increase of upper airway resistance were found.[9] Moreover, Woo et al[10] showed a statistically significant decrease in both inspiratory and expiratory flow-volume parameters after medialization of the paralyzed vocal fold by Teflon injection. Patient materials in these studies included subjects with progressive pulmonary diseases.

Vocal performance has been studied carefully after thyroplasty type I, but few reports exist of acoustic voice analysis after Teflon or autologous tissue injections. The great variety in normal and pathological voices makes the assessment a difficult task. However, acoustic analysis yields objective data and gives numeric values enabling statistical evaluation. Sustained vowels are preferred over running speech, because cutting out the prosodic features facilitates the interpretation of voice samples. Perturbations of the signal present period-to-period variations and have been shown to correlate with vocal fold disorders.[11] Jitter stands for a variability of the pitch period and is shown to correlate with roughness of the perceived voice.[12] Shimmer is another component of hoarseness and denotes period-to-period amplitude variation, which is known to correlate with breathiness.[13] The noise-to-harmonics ratio gives an estimation of the proportion of aperiodic noise to the periodic signal produced by the vocal folds and is considered an important tool for assessing hoarseness.[13] Previously, no attempts have been made to relate the changes of voice acoustics induced by vocal fold medialization to simultaneous changes in airflow dynamics in the large airways, including the larynx.

From the Laboratory of Clinical Physiology (Saarinen, Sovijärvi) and the Department of Otolaryngology (Rihkanen, Lehikoinen-Söderlund), Helsinki University Hospital, Helsinki, Finland. This study has been supported by Helsinki University Hospital research project TYH0033.

CORRESPONDENCE — Anssi R. A. Sovijärvi, MD, PhD, Helsinki University Hospital, Laboratory of Clinical Physiology, PL 360, 00029 HYKS, Helsinki, Finland.

TABLE 1. SUBJECT CHARACTERISTICS

Subject	*Age (y)*	*Height (cm)*	*Body Mass Index (kg/m^2)*	*Sex*	*History of Regular Smoking*	*Cause of Paralysis*
1	64	171	30	M	No	Thyroid cancer
2	58	158	26	F	No	Thyroid operation
3	46	169	25	M	Yes	Idiopathic
4	59	157	27	F	Yes	Thyroid operation
5	48	188	27	M	No	Idiopathic
6	50	162	21	F	No	Thyroid operation
7	65	177	27	M	No	Thyroid operation
8	65	160	26	F	No	Thyroid operation
9	57	172	26	F	No	Thyroid operation
10	58	166	25	F	No	Thyroid operation
Mean	57	169	26			

The aim of the present study was to assess the effect of vocal fold medialization by injection of autologous fascia on voice acoustics and airflow dynamics during both forced and quiet breathing in patients with unilateral vocal fold paralysis. Special attention was paid to the possible relationship between ventilatory function and voice acoustics.

MATERIALS AND METHODS

Ten adults with unilateral recurrent laryngeal nerve paralysis whose symptoms had not greatly improved with voice therapy alone were given the opportunity to participate in the present prospective study. Subject characteristics are shown in Table 1. The mean duration of vocal fold paralysis had been 13 months (range, 6 to 30 months) before entry into the study. The cause of unilateral vocal fold paralysis was a thyroid operation in 7 patients, idiopathic in 2 patients, and thyroid cancer in 1 patient. Subjects with a history of chronic pulmonary diseases were not included in the material. Medialization of the paralyzed vocal fold was achieved by a recently published technique of injecting autologous fascia into the vocal fold.[7] The transplant was harvested from fascia lata under local anesthesia and cut into small pieces with a scalpel, and the mass thus formed was placed in a 1-mL pressure syringe. The injection was performed on the lateral aspect of the vocal fold under general anesthesia using jet ventilation via a laryngoscope. An average volume of 0.4 to 0.6 mL was injected. In addition, for 1 subject, an arytenoid adduction procedure was performed in order to optimize the tonus of the vocal fold.

The preoperative voice samples were recorded within 1 week before the medialization, and postoperative samples from 2 to 12 months (mean, 6 months) after the injection. The subjects did not receive any voice therapy after the operation. Recording of the voice samples took place in a soundproof booth. The mouth-to-microphone distance (30 cm) and the setup of the digital audiotape recorder (Casio DA-7, Casio Computer Co Ltd, Japan) were kept constant. The maximum sustained phonation time was measured with the vowel /a/. Acoustic analysis was also performed on a vowel /a/ voiced at a comfortable loudness and pitch level. The first second of the sample was cut off, and the 2 successive seconds were used for the analysis. In the few cases in which the length of the sample was shorter than 4 seconds, 25% of the first and of the last parts of the vowel samples was discarded. This ensured that the beginning and the end of voicing did not affect the final result. Kay Elemetrics Corp (USA) CSL model 4300B (version 5.X) and Multispeech Voice Program model 4305 were used for processing and for the analysis of the fundamental frequency, jitter, shimmer, and noise-to-harmonics ratio. The sampling rate was 50,000 Hz.

Ventilatory function tests were performed within 1 week before the operation and 4 to 14 months (mean, 8 months) after the operation. Maximal flow-volume curves were recorded with a rolling-seal flow-volume spirometer (CPI 220, Cardiopulmonary Instruments, Houston, Tex) connected to a microcomputer system (Medikro 202, Medikro OY, Kuopio, Finland). The highest flow values of at least 3 successive determinations were recorded by use of the envelope technique. Forced inspiratory volume in 1 second (FIV1), forced vital capacity (FVC), peak inspiratory and expiratory flows (PIF, PEF), forced expiratory volume in 1 second (FEV1), and maximal flow at the level of 50% of the FVC (MEF50) were measured. A constant-volume body plethysmograph (Body Screen 2, Erich Jaeger GmbH, Würtzburg, Germany) was used for the measurement of airway resistance (Raw) and airway specific conductance (SGaw) during tidal breathing (breathing frequency of 30 breaths per minute). The mean value of 3 to 5

TABLE 2. MEAN VALUES, RANGE, AND STATISTICAL COMPARISON OF ACOUSTIC VARIABLES OF VOICE BEFORE AND AFTER VOCAL FOLD MEDIALIZATION (N = 10)

	Preoperative	*Postoperative*	*p*
Maximal phonation time (s)	5.7 (2.3-12.0)	10.3 (4.0-24.0)	.002
Jitter (μs; normal <83.2)	564 (20-1,211)	136 (25-427)	.006
Shimmer (%; normal <3.81)	20.19 (4.72-46.40)	10.08 (2.20-21.69)	.017
Noise-to-harmonics ratio (dB/dB; normal <0.19)	0.52 (0.12-0.98)	0.25 (0.10-0.68)	.047

Normal values are according to Kay Elemetrics instruction manual.

successive determinations was recorded. The measured values of the respiratory function tests were compared to Finnish reference values determined by gender, age, and height.[14]

Mann-Whitney and Wilcoxon signed-ranks tests were applied for statistical analysis. Statistical significance was defined as $p < .05$. Relationships between changes in acoustic variables (shimmer, jitter, noise-to-harmonics ratio) and respiratory function test variables were analyzed by Spearman's correlation analysis.

TABLE 3. MEAN VALUES AND RANGE OF VARIABLES OF FLOW VOLUME SPIROMETRY AND BODY PLETHYSMOGRAPHY BEFORE AND AFTER VOCAL FOLD MEDIALIZATION

	Preoperative		*Postoperative*	
	Measured	*%Predicted**	*Measured*	*%Predicted**
FVC	3.99 L (2.84-7.24) (n = 10)	103% (81-126)	3.90 L (2.87-7.49) (n = 10)	100% (79-130)
FEV1	3.05 L (2.29-5.48) (n = 10)	99% (75-121)	2.97 L (2.31-5.20) (n = 10)	96% (69-130)
PEF	7.05 Ls^{-1} (5.28-10.99) (n = 10)	89% (64-107)	6.93 Ls^{-1} (5.28-10.59) (n = 10)	87% (61-108)
MEF50	2.92 Ls^{-1} (1.66-4.45) (n = 10)	70% (66-92)	2.84 Ls^{-1} (1.24-4.17) (n = 10)	67% (67-94)
FIV1	3.17 L (2.06-4.11) (n = 8)		3.16 L (2.13-4.17) (n = 8)	
PIF	4.63 Ls^{-1} (2.84-7.51) (n = 8)	78% (58-105)	4.03 Ls^{-1}† (2.27-6.68) (n = 8)	70%† (44-90)
Raw	0.31 kPa $s^{-1}L$ (0.15-0.57) (n = 9)	182% (81-264)	0.28 kPa $s^{-1}L$ (0.17-0.50) (n = 9)	168% (104-234)
SGaw	1.34 $kPa^{-1}s^{-1}$ (0.84-2.76) (n = 9)	73% (41-163)	1.26 $kPa^{-1}s^{-1}$ (0.84-2.0) (n = 9)	71% (54-118)

FVC — forced vital capacity; FEV1 — forced expiratory volume in 1 second; PEF — peak expiratory flow; MEF50 — maximal expiratory flow at 50% of FVC; FIV1 — forced inspiratory volume in 1 second; PIF — peak inpiratory flow; Raw — airway resistance; SGaw — specific airway conductance.

*Predicted values are according to Viljanen et al.[14]

†p = .012, Wilcoxon matched-pairs signed-ranks test.

RESULTS

After the operation, the mean maximal phonation time measured with the vowel /a/ almost doubled, increasing from 5.7 seconds to 10.3 seconds; the difference was statistically significant (Table 2). The phonation time did not decrease in any patient after the injection. The mean value of jitter decreased by 76%, that of shimmer by 50%, and that of the noise-to-harmonics ratio by 52% after the operation; the changes were statistically significant (Table 2). The mean fundamental frequency did not change significantly, although after the operation, the mean fundamental frequency for male patients was slightly lower, and for females, higher, than before the procedure.

The results of the preoperative and postoperative flow-volume spirometry and body plethysmography are shown in Table 3.[14] The only significant change in the variables of airway flow dynamics was the fact that the PIF decreased by 13% (p = .012) as a consequence of the medialization. However, the PIF was below the normal range (predicted value ± 2 SD) in only 3 subjects after the operation. The FEV1, FIV1, PEF, FVC, MEF50, Raw, and SGaw did not change significantly after the operation.

There was a significant negative correlation between the changes in PIF and shimmer (r = –.857, p = .007) caused by the medialization (see Figure). No other significant correlations between changes in the variables of the respiratory function tests and the vari-

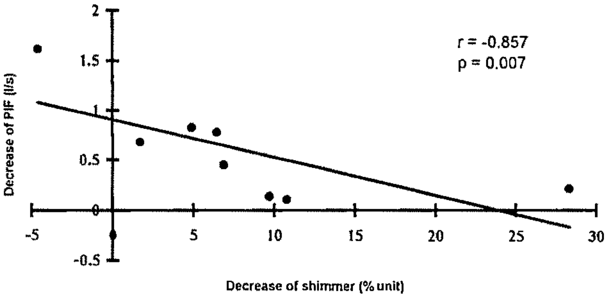

Correlation of changes in peak inspiratory flow (PIF) and shimmer induced by vocal fold medialization in 8 patients with unilateral vocal fold paralysis.

ables of the voice acoustics were found.

DISCUSSION

In the present study, medialization of a paralyzed vocal fold by injection of autologous fascia improved significantly the variables of voice acoustics. The procedure probably decreases the cross-sectional area of the glottis, and this change could explain the slight decrease in PIF found in this study. We did not find any significant deterioration in other respiratory function variables measured during forced or quiet breathing. This differed from the findings made by Woo et al[10] after Teflon injections. The present result is in accordance with the findings of Cormier et al,[8] who did not find statistically significant changes in forced inspiratory flow values after Teflon injections, and with those of Ejnell et al,[9] who found only a transient impairment in forced inspiration 1 week after the operation.

In the present series, unlike in the studies by Cormier et al,[8] Ejnell et al,[9] and Woo et al,[10] subjects with a history of chronic pulmonary diseases were excluded to avoid the confounding effect on ventilatory function variables. The discrepant results in the earlier studies cited may have been caused by the small number of subjects and by the volume and location of the injected material. Teflon creates a foreign body reaction and thereby stiffens the vocal fold.[2] If the paralyzed vocal fold is fixed in the midline and inflammation does not allow a functioning mucosal wave, voice and airflow dynamics will be affected. When Teflon is placed far away from the medial edge, the foreign body inflammation does not necessarily interfere with the vocal performance. It may, however, have an effect on airflow dynamics. In the studies cited above, the description of laryngeal function was very brief, and no attempt was made to correlate the postoperative vocal fold position or function to airflow dynamics during maximal respiratory efforts.

Decreased airflow during forced inspiration with normal expiratory flow-volume variables is a characteristic finding in variable extrathoracic airway obstruction.[15] If the vocal fold is rigid and is fixed in the midline by the medialization procedure, one would expect to find a constant rather than a variable airflow obstruction. The former is indicated by a simultaneous decrease in PEF and PIF. It is, however, likely that medialization does not decrease the cross-sectional area of the glottis enough to cause a fixed central airway stenosis. When the vocal fold is pliant, the medialization may be considered dynamic, rather than fixed. This means that negative pressure in the subglottic airways during a forced inspiration (the Bernoulli effect) probably causes a slight collapse of the pliable airways, resulting in a decreased PIF. Forced expiration, however, is less likely to be affected, because of the conical shape of the larynx, the elasticity of the vocal muscle, and positive intraluminal pressure. It is assumed that autologous fascia, used in the present work, creates minimal inflammation and remains soft in the paralyzed muscle. This would explain the slight but consistent decrease in PIF without a significant change in PEF, ie, the variable extrathoracic obstruction, found in our series.

Resistance of the airways (Raw) and specific conductance of the airways (SGaw), which are sensitive variables in central airway obstruction, did not change after vocal fold medialization in our study. This finding indicates that the procedure had no significant limiting effect on airflow in quiet breathing.

As a consequence of medialization, the values of PIF and shimmer decreased in most of the subjects. We found a clear and significant negative correlation between the changes in these 2 variables. The improvement in shimmer was greatest in the subjects with the least deterioration in PIF. This might indicate the dynamic nature of the present procedure. According to our hypothesis, the mucosal wave that occurs during phonation may be most regular in patients with a well-preserved subepithelial space and elasticity of the vocal fold. It is possible that the more resilient the paralyzed vocal fold is, the less its position influences the airflow dynamics in the larynx. To confirm this hypothesis, videostroboscopic investigations combined with flow-volume recordings should be performed.

In conclusion, injection of autologous fascia into a paralyzed vocal fold successfully improves the acoustic properties of the voice while slightly impairing the airflow at the level of the larynx during forced inspiration. Quiet breathing and forced expiration are not disturbed by the procedure. The results also suggest that a better improvement of voice acoustics is associated with a less-pronounced impairment of the PIF and a less-pronounced variable obstruction at the level of the vocal folds.

ACKNOWLEDGMENT — We thank the personnel of the Laboratory of Clinical Physiology of Helsinki University Hospital for performing the respiratory function tests.

REFERENCES

1. Clerf LH, Suehs OW. Paralysis of the larynx. Ann Otol Rhinol Laryngol 1941;50:762-8.

2. Lewy RB. Teflon injection of the vocal cord: complications, errors, and precautions. Ann Otol Rhinol Laryngol 1983;

92:473-4.

3. Isshiki N, Morita H, Okamura H, Hiramoto M. Thyroplasty as a new phonosurgical technique. Acta Otolaryngol (Stockh) 1974;78:451-3.

4. Shindo ML, Zaretsky LS, Rice DH. Autologous fat injection for unilateral vocal fold paralysis. Ann Otol Rhinol Laryngol 1996;105:602-6.

5. Zaretsky LS, Shindo ML, deTar M, Rice DH. Autologous fat injection for vocal fold paralysis: long-term histologic evaluation. Ann Otol Rhinol Laryngol 1995;104:1-4.

6. Staskowski PA, Ford CN, Inagi K. The histologic fate of autologous collagen injected into the canine vocal fold. Otolaryngol Head Neck Surg 1998;118:187-90.

7. Rihkanen H. Injection of autologous fascia in augmentation of vocal fold paralysis. Laryngoscope 1998;108:51-4.

8. Cormier Y, Kashima H, Summer W, Menkes H. Airflow in unilateral vocal cord paralysis before and after Teflon injection. Thorax 1978;33:57-61.

9. Ejnell H, Månsson I, Bake B, Stenborg R. Laryngeal obstruction after Teflon injection. Acta Otolaryngol (Stockh) 1984; 98:374-9.

10. Woo JKS, van Hasselt CA, Chan HS. Teflon injection for unilateral vocal cord paralysis and its effect on lung function. Clin Otolaryngol 1992;17:497-500.

11. Rontal E, Rontal M, Jacob HJ, Rolnick MI. Quantitative and objective evaluation of vocal cord function. Ann Otol Rhinol Laryngol 1983;92:421-3.

12. Dejonckere PH, Lebacq J. Acoustic, perceptual, aerodynamic and anatomical correlations in voice pathology. ORL J Otorhinolaryngol Relat Spec 1996;58:326-32.

13. Yumoto E. The quantitative evaluation of hoarseness. Arch Otolaryngol 1983;109:43-52.

14. Viljanen AA, Halttunen PK, Kreus K-E, Viljanen BC. Spirometric studies in non-smoking healthy adults. Scand J Clin Lab Invest Suppl 1982;42(suppl 159):5-20.

15. Miller A. Pulmonary function tests in clinical and occupational lung disease. Orlando, Fla: Harcourt Brace Jovanovich Publishers, 1986:58.

≈

CARE OF THE PROFESSIONAL VOICE

The Voice Foundation's 29th Annual Symposium: Care of the Professional Voice will be held June 28 to July 2, 2000, in Philadelphia, Pennsylvania. For information, contact The Voice Foundation, 1721 Pine St, Philadelphia, PA 19103; telephone (215) 735-7999; fax (215) 735-9293.

Ann Otol Rhinol Laryngol 109:2000

EFFECTS OF DEHYDRATION ON PHONATION IN EXCISED CANINE LARYNGES

JACK JIANG, MD, PHD
CHICAGO, ILLINOIS

KATHERINE VERDOLINI, PHD
BOSTON, MASSACHUSETTS

BEN AQUINO, MS
CHICAGO, ILLINOIS

JENNIE NG
CHICAGO, ILLINOIS

DAVID HANSON, MD
CHICAGO, ILLINOIS

The effects of exposure to dry air on phonation were measured in an ex vivo model of vocal fold vibration. Excised canine larynges were mounted on an apparatus and made to phonate at a constant subglottal pressure by means of unhumidified airflow. The phonation threshold pressure (PTP), glottal airflow, sound intensity of the acoustic output, and effects on vocal efficiency were also assessed. Student's *t*-test was performed on the results. In 17 larynges, the average PTP increased from 10.0 cm H_2O to 15.0 cm H_2O after exposure to dry airflow ($p < .001$). In addition, the average flow increased from 585 mL/s to 801 mL/s at a constant suprathreshold subglottal pressure ($p < .001$), and from 323 mL/s to 610 mL/s at the PTP ($p < .001$). The average acoustic output levels, measured during stable phonation segments, markedly decreased with exposure to the dry airflow, from 91.5 dB to 88.5 dB ($p < .001$). The average vocal efficiency decreased from 3.63×10^{-4} to 7.00×10^{-5} ($p < .001$). No such changes were seen in control larynges phonated with 100% humidified air used for driving the airflow. The results support previously reported modeling and experimental findings that dehydration of the vocal fold generally degrades laryngeal performance.

KEY WORDS — canine, dehydration, excised larynx, phonation, phonation threshold pressure, subglottal pressure, vocal efficiency.

BACKGROUND

For years, hydration has been a topic of interest in voice management. Clinically, dehydration has been considered to contribute to dysphonia, and hydration has been considered to assist in its prevention. Various types of humidification therapies include ambient humidification,[1-3] direct steam or fog inhalations,[2,4] mucolytic drug administration,[4] nose breathing,[1,3,5] lozenges,[2] propylene glycol solutions,[4] lemon juice, and herbal teas.[5] Voice patients are routinely advised to avoid drying influences[5,6] such as dry environments, primary and secondary smoke, alcohol, caffeine and other diuretics,[1,3,5,6] antihistamines,[1,5] nasal sprays and decongestants,[3,7] and mouth breathing.[1]

Theoretical analysis and animal experiments support the hypothesis that dehydration of the vocal folds will degrade voice performance by making phonation more "difficult"[8,9] — increasing the subglottic pressure required to drive the folds — and that hydration will improve performance and make it easier. Some experimental evidence consistent with these proposals has been provided. In 2 studies assessing normal adults, phonation threshold pressures (PTPs) were reduced after hydration as compared with placebo[10,11] and control[12] treatments, particularly at high pitches. Similarly, excised canine larynx studies have shown that PTPs are smallest after baths involving the greatest water transport across the mucosal barrier and greatest after baths involving the least water transport.[8]

An important question addresses the mechanisms by which hydration and dehydration treatments may affect vocal performance. Wexler et al[13] described the role of the gelatinous and relatively compliant nature of the lamina propria, which is influenced by hydration, in the responsiveness of laryngeal tissue to vibration. However, no physical model has been developed that demonstrates the quantitative relationship between laryngeal hydration status and phona-

---

From the Department of Otolaryngology–Head and Neck Surgery, Northwestern University Medical School, Chicago, Illinois (Jiang, Aquino, Ng, Hanson), and the Voice and Speech Laboratory, Massachusetts Eye and Ear Infirmary, the Department of Communication Sciences and Disorders, Harvard Medical School, and Massachusetts General Hospital Institute of Health Professions, Boston, Massachusetts (Verdolini). Supported by National Institutes of Health grants P60 DC 94-002-02, R01 DC 00254-11, and T32 DC 0015-15. This study was performed in accordance with the PHS Policy on Humane Care and Use of Laboratory Animals, the NIH *Guide for the Care and Use of Laboratory Animals*, and the Animal Welfare Act (7 U.S.C. et seq.); the animal use protocol was approved by the Institutional Animal Care and Use Committee (IACUC) of Northwestern University.

CORRESPONDENCE — Jack Jiang, MD, PhD, Dept of Otolaryngology–Head and Neck Surgery, Northwestern University Medical School, Searle Building 12-561, 303 E Chicago Ave, Chicago, IL 60611.

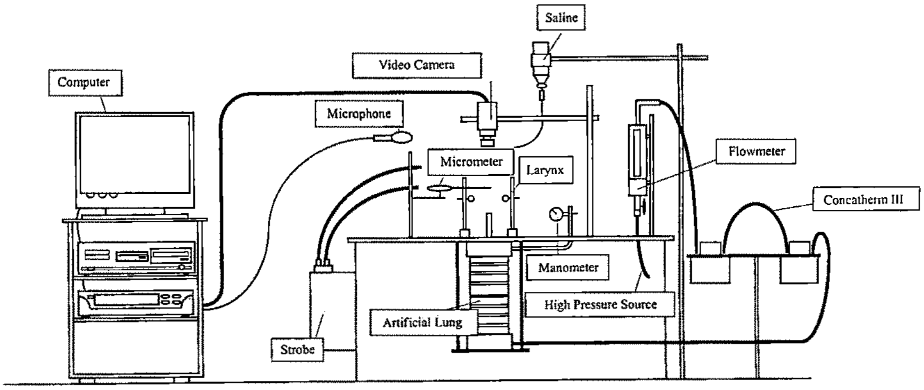

Fig 1. Experimental setup used to create and monitor laryngeal performance.

tion. Furthermore, previous studies have not empirically distinguished the effects of superficial versus systemic dehydration on phonation.[10-12]

The present study addresses these issues with an in vitro model in which the effects of surface dehydration are explored. An attempt was made to induce surface, or superficial, dehydration in excised canine larynges by driving the folds with a desiccated airflow source (room humidity). Such flow is likely to produce water loss and mucosal dryness. If extraction of fluid from the vocal fold surface is one mechanism of PTP change, then PTPs should increase with increasing exposure to the dry air. A further question regarded the time course of vocal degradation with exposure to dry air. Ancillary questions regarded the effects of the exposure on glottal airflow, sound intensity, and glottal efficiency.

MATERIALS AND METHODS

Larynges. Seventeen larynges were harvested 15 to 30 minutes postmortem from large, healthy laboratory dogs after demise from other causes. The larynges were kept refrigerated and used in an experimental trial 24 to 48 hours after excision. Information about the age and gender of the animals was not recorded. Gender does not appear to affect the range and quality of phonation for dogs.[14] Fifteen larynges were used for dehydration trials. Two larynges were used as controls, for hydration trials (below).

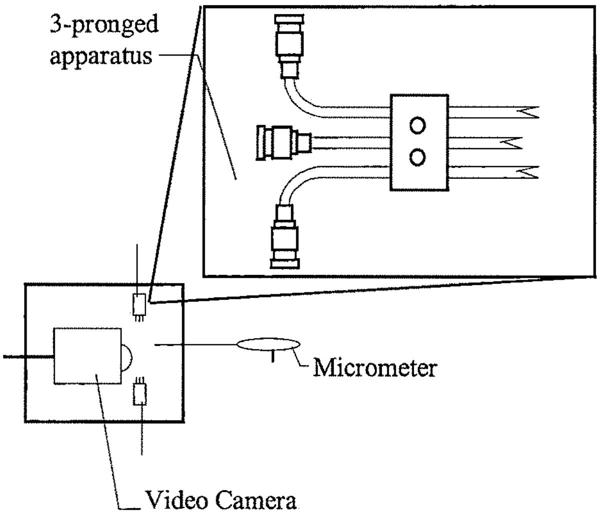

Fig 2. Three-pronged apparatus and micrometer system used for precise control of elongation and adduction of vocal folds.

Excision and Preparation of Larynx. Excision of the larynx was performed by a procedure described by Jiang and Titze.[15] After excision, the larynx was placed in a 9% saline solution and refrigerated. Immediately before use, the larynges were trimmed in preparation for mounting by the method described by Jiang and Titze.

Apparatus and Mounting of Larynx. Figure 1 shows the general experimental setup used to create and monitor laryngeal phonation. Before mounting, the resting length of the vocal folds and the position of the arytenoid cartilages during fixed adduction were established. The larynx was then mounted with a section of trachea on top of a pipe, and the trachea was tightly clamped to the pipe with a 1-mm hose clamp. A 3-pronged device was used to stabilize the arytenoid cartilages bilaterally, allowing for micrometer control of adduction and abduction (Fig 2). A second micrometer system was attached by stitching a rod to the anterior tip of the thyroid lamina with a blue monofilament polypropylene type B suture. Turning of this micrometer system controlled the elongation of the vocal folds. The larynx was stabilized at its resting length and adduction as established before mounting. Vocal fold elongation and adduction were held constant within each larynx for all experimental trials.

As shown in Fig 1, an air compressor was used to generate the airflow. The flow was stabilized in a chamber before being passed through the larynx. The flow quantity was controlled throughout the experiment with a valve, and measured with a flowmeter. For the dehydration trials, which were the focus of the experiment, room air was used to induce phonation (20% to 30% relative humidity). The humidity levels and temperature were measured with an Omega RH-10 hygrometer and a thermometer. Humidified trials were also conducted on a limited number of larynges as a control condition. For those trials, humidified airflow was conditioned to 100% humidity at 36°C to 38°C by passing the air through 2 ConchaTherm III heater-humidifiers placed in series. Constant dripping of saline onto the vocal folds also prevented desiccation of the vocal folds.

Instrumentation, Calibration, and Data Processing. A video camera was used to record the glottal image from above, and the image was viewed online on a color monitor. The camera was mounted 35 to 40 cm from the larynx, with the view perpendicular to the midline axis of the glottis. A pressure sensor mounted on the pipe directly beneath the vocal folds monitored the subglottal pressure throughout the trials. The acoustic signal was recorded with an ECM-T150 Sony microphone mounted 45° perpendicular to the long axis of the larynx and facing the glottis at a distance of 8 to 10 cm. The signal picked up by the microphone was preamplified, then recorded. A TDS 420A oscilloscope was used to monitor sound signal intensities. Voltage signals were monitored on 4 channels: flow/volts, sound intensity/volts, frequency/volts, and pressure/volts. A sound level meter (Radio Shack 32-2050) was used for measuring acoustic output.

Calibrations of pressure, flow, sound intensity, and fundamental frequency were performed before each experimental run by means of a known flow resistor. Calibrations were obtained for known levels of both flow and pressure. The sound intensity was also calibrated at 2 different decibel levels: 74 and 84 dB. A calibration curve was then determined relating the voltages to their respective decibel units. Voltage signals for pressure, airflow, sound level, and fundamental frequency were acquired and calibrated to their respective units of measurement: centimeters of water, milliliters per second, decibels, and hertz.

The computer data acquisition used a National Instruments MIO16-E2 AD board. The data were acquired, stored, and analyzed with custom-made software based on the Labview 4.0 platform. SigmaStat 2.0 was used to analyze the data.

Measurement Environment. All measurements were carried out in a sound-treated room that minimized background noise and allowed stability of temperature and humidity levels. All dehydration measurements were performed at a room temperature of 20°C with a room humidity level of 20% to 30%. The hydration trials used 100% humidified airflow at temperatures of 36°C to 38°C.

The dehydration conditions consisted of sequential 10-second periods of blowing dry air through the larynx, followed by 3 seconds of rest. During each 10-second drying period, the airflow was manually adjusted to produce a constant subglottal pressure to reach PTP. The flow was then increased to achieve a suprathreshold pressure that produced a strong, stable voice, below the pressure that would produce irregular, rough, suprathreshold voicing. The total drying periods averaged 5 minutes. Throughout the process, saline was withheld from the larynges to ensure maximal surface dehydration.

Control Larynges. Two control larynges underwent sequential 10-second treatments of phonation using hydrated air, followed by 3 seconds of rest. The subglottal pressure was regulated as for the dehydration trials. The total amount of phonation time averaged 5 minutes.

Data Analysis. After the laryngeal manipulations were completed, the PTP, flow, and sound intensity levels were manually evaluated. Calculations of vocal efficiency were based upon the ratio of radiated acoustic power to aerodynamic (subglottic) power.[14] Acoustic power (pascals [Pa]) was determined by the equation $Pa = 4\pi r^2 I$ where I equals sound pressure level (SPL) in watts per square meter (W/m^2) and r equals the distance to the microphone in meters. The SPL was converted with the following equation: $SPL = 10^{\text{No. of dB}/10} \times 10^{12}\ W/m^2$.

The subglottic power was determined by multiplying the flow in milliliters per second by the subglottic pressure in kilopascals (1 cm H_2O = 98 Pa). The values for pressure, flow, and sound intensity were standardized with a z-transformation. A linear regression was drawn through all the data points in the plot, and p values were determined for each parameter.

RESULTS

It was important to establish to what extent any variations in results during dehydration periods were attributable to fatigue or other possible tissue changes related to vibration and time. For the hydrated control periods, there was no significant change in PTP, flow, sound intensity, or efficiency across the 5-minute experimental period ($p < .340$, $p < .627$, $p < .377$, and $p < .383$, respectively). Thus, the effects of the dehydration periods on the measures were thought to be due to the exposure to dry air.

The global results for the dehydration periods are indicated in the Table and discussed in detail below. As shown in the Table, exposure to dry air significantly influenced PTP, flow, sound intensity, and vocal efficiency, at the <.001 level of confidence.

AVERAGES OF RESULTS OBTAINED IN PHONATION OF DEHYDRATED LARYNGES

	PTP (cm H2O)	*Flow at PTP (mL/s)*	*Flow at Constant SGP (mL/s)*	*Maximum SGP Intensity (dB)*	*Maximum Intensity (dB)*	*Vocal Efficiency*
Initial	10.04 (1.08)	323 (3.69)	585 (5.06)	91.5 (0.89)	91.77 (0.85)	3.63×10^{-4} (2.35×10^{-4})
Final	15.00 (1.34)	610 (6.29)	801 (6.77)	88.5 (1.00)	89.73 (0.88)	7.00×10^{-5} (1.51×10^{-5})
p	<.001	<.001	<.001	<.001	<.001	<.001

Numbers in parentheses represent error values.

PTP — phonation threshold pressure; SGP — subglottal pressure.

Phonation Threshold Pressure for Dehydration Periods. The PTP increased significantly ($p < .001$) as the exposure to dry air continued. The initial PTP values ranged from 4.12 to 18.6 cm H2O; the final PTP values ranged from 6.02 to 25.4 cm H2O. During phonation induced by room air, the PTP values increased on average from 10.0 to 15.0 cm H2O. A typical curve is shown in Fig 3A. Average data are shown in Fig 3B.

Glottal Airflow at PTP for Dehydration Trials. The airflow at PTP increased significantly ($p < .001$) as the phonation with room air continued. The initial flow values ranged from 26.4 to 846 mL/s; the final flow values ranged from 60.2 mL/s to 1.60×10^3 mL/s. The average flow across specimens increased from 323 to 610 mL/s. Figure 4A,B shows typical changes in airflow and average changes at PTP.

Glottal Airflow at Suprathreshold Subglottic Pressure for Dehydration Trials. The airflow at a constant subglottal pressure increased significantly ($p < .001$) as the phonation with room air continued. The initial flow values ranged from 73.0 mL/s to 1.35×10^3 mL/s; the final flow values ranged from 267 mL/s to 1.70×10^3 mL/s. The average flow across specimens increased from 585 to 801 mL/s. Figure 4C shows the average changes in suprathreshold airflow levels.

Sound Intensity at Suprathreshold Subglottal Pressure for Dehydration Trials. The phonatory intensity was measured in decibels for suprathreshold trials. The initial sound intensity levels ranged from 84.7 to 99.5 dB; the final sound intensity levels ranged from 80.5 to 93.9 dB. The average sound intensity across larynges decreased from 91.5 to 88.5 dB. Figure 5A shows typical significant decreases in sound intensity levels; Fig 5B shows the average decreases with progressive dehydration ($p < .001$).

Maximum Sound Intensity for Dehydration Trials. The maximum phonation intensity was measured in decibels SPL. The initial maximum intensity levels ranged from 86.1 to 99.6 dB; the final maximum intensity levels ranged from 81.6 to 94.0 dB. The average maxima across larynges decreased from 91.8 to 89.7 dB ($p < .001$).

Glottal Efficiency for Suprathreshold Dehydration Trials. Glottal efficiency relates the emitted acoustic power to the pneumatic driving subglottic power. The initial vocal efficiency values for the suprathreshold trials ranged from 4.26×10^{-6} to 4.10×10^{-3}. The final efficiency values ranged from 3.74×10^{-6} to 2.04×10^{-4}. The mean efficiency was reduced significantly ($p < .001$), from 3.63×10^{-4} to 7.00×10^{-5} after de-

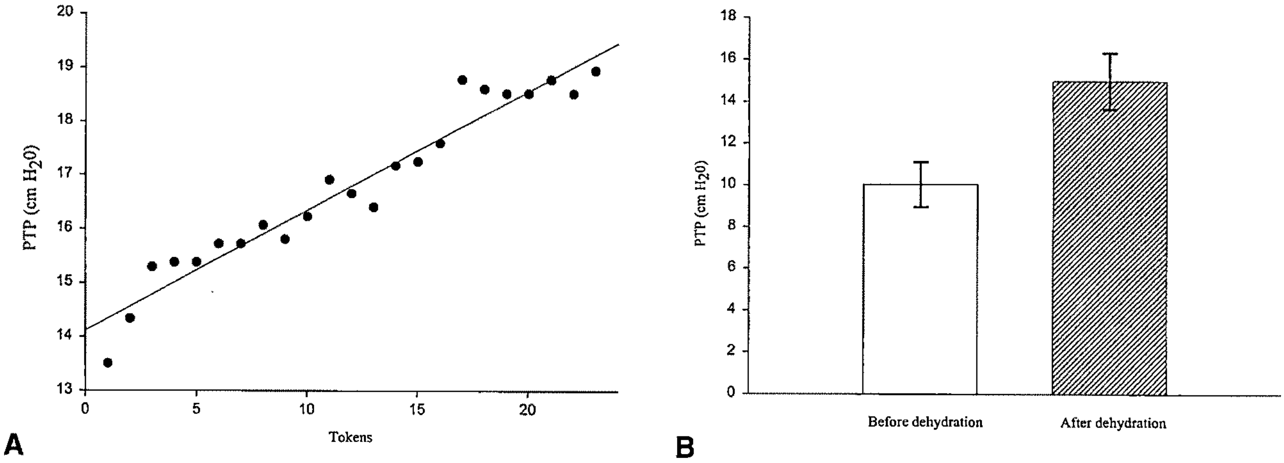

Fig 3. Phonation threshold pressure (PTP). A) Typical example of PTP levels as dehydration occurred. B) Mean PTP levels before and after dehydration.

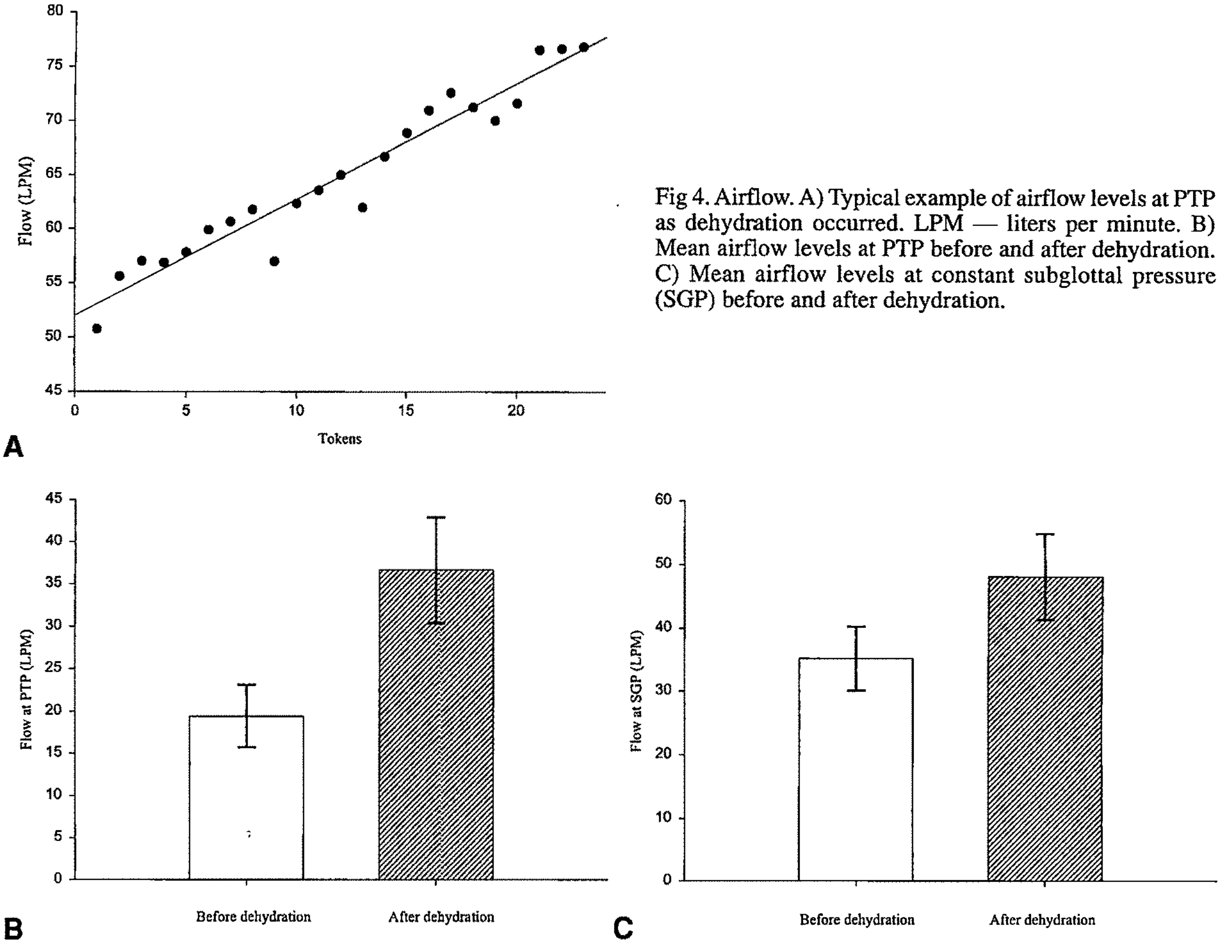

Fig 4. Airflow. A) Typical example of airflow levels at PTP as dehydration occurred. LPM — liters per minute. B) Mean airflow levels at PTP before and after dehydration. C) Mean airflow levels at constant subglottal pressure (SGP) before and after dehydration.

hydration. The typical and average effects of dehydration on efficiency are shown in Fig 6.

DISCUSSION

After 5 minutes of oscillation induced by the delivery of dry air to the larynx, the PTP values increased significantly ($p < .001$) on average, from 10.0 to 15.0 cm H2O. The airflow levels at each PTP showed a significant increase ($p < .001$), from 323 to 610 mL/s, and the airflow levels at a constant subglottal pressure also showed a significant increase ($p < .001$), from 585 to 801 mL/s. The average sound intensity at a constant subglottal pressure significantly decreased, from 91.5 to 88.5 dB ($p < .001$), and the average maximum sound intensity significantly decreased, from 91.8 to 89.7 dB ($p < .001$). The mean efficiency was reduced from 3.63×10^{-4} to 7.00×10^{-5} ($p < .001$) after dehydration. It is clear

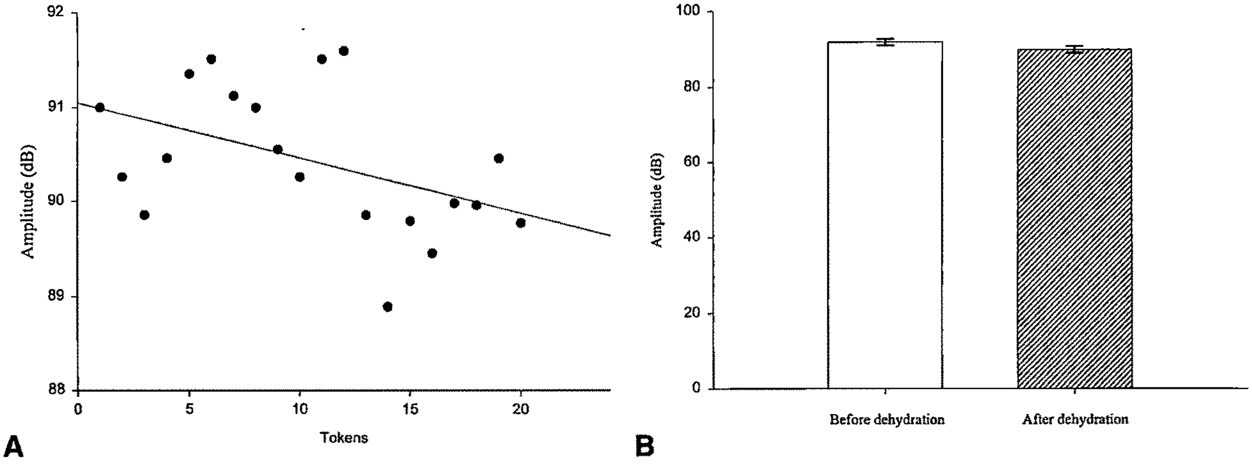

Fig 5. Sound intensity levels. A) Typical example of sound intensity levels as dehydration occurred. B) Mean sound intensity levels before and after dehydration.

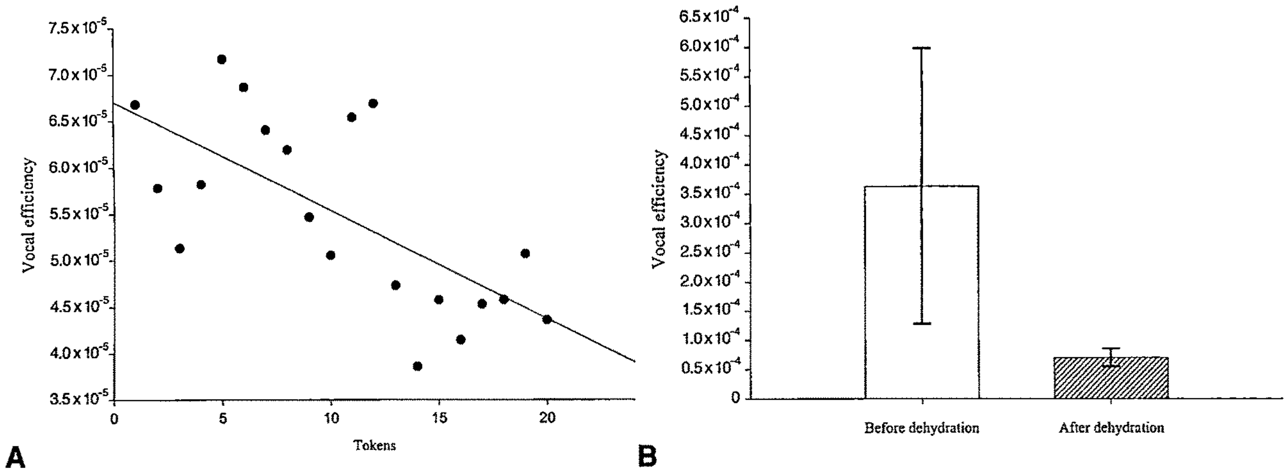

Fig 6. Vocal efficiency levels. A) Typical example of vocal efficiency levels as dehydration occurred. B) Mean vocal efficiency levels before and after dehydration.

that the delivery of dry air to the vocal fold surface desiccates the surface epithelium and possibly also the lamina propria. Thus, this experiment provided clear evidence that surface dehydration is one mechanism that can quickly increase the PTP. This evidence supplements other information, indicating that dehydration induced in humans by systemic means (diuretics) can also increase PTPs (Verdolini et al, unpublished observations). In addition, the threshold and suprathreshold glottal airflow, radiated sound intensity, and vocal efficiency deteriorated significantly with surface dehydration of the vocal folds.

The changes obtained from the dehydration trials were not likely to be due to fatigue or a change in the tissues that occurred over time during the experiment. Two control larynges underwent similar phonation trials using hydrated air. The changes in PTP, flow, sound intensity, and efficiency occurring over time with phonation were not statistically significant for these preparations ($p < .340$, $p < .627$, $p < .377$, and $p < .383$, respectively).

From these results, it appears that one possible mechanism by which dehydration affects phonation ex vivo is through drying effects on the superficial mucus and the surface layer of the vocal fold tissue. The structure of the vocal fold is made up of tissue layers; the outer layer is made up of epithelium and the superficial layer of the lamina propria that is normally covered by a layer of mucus. The intermediate and deep layers of the lamina propria are made up of elastic and collagenous fibers, respectively, and constitute a transition layer to underlying muscle. Dry air certainly influences the epithelium, and possibly the lamina propria as well.

Clearly, there are differences with respect to the in vivo human situation. In live subjects, the tissue of the vestibular fold contains many mucous glands that empty into the saccule and distribute lubricating mucus to the surface of the vocal folds, where microridges hold and spread a thin layer of mucus covering the fold. This thin layer of mucus appears to be critical to normal phonation. It seems possible that dry air involved in vocal fold oscillation would desiccate the adherent mucus and also extract water through the epithelium, producing effects similar to those seen in this experiment.

Another difference with respect to in vivo human situations is that normally, the airflow through the glottis from the lungs is totally saturated with moisture. (The vapor pressure is approximately 47 mm Hg.) When dry atmospheric air (vapor pressure << 47 mm Hg) is passed through the vocal folds instead, such as may occur with rapid inhalation through the mouth, there is an osmotic gradient between the outer and inner areas of the vocal fold epithelium. With time, we would expect moisture evaporation from the tissues due to the dry passing air. However, in living tissue, the process of dehydration is slowed, as osmosis of water into the intercellular spaces creates an elevated concentration of ions in the cells and a negative osmotic gradient. The circulating blood of the microvilli flows through the basement membrane of the epithelium cells and restores fluid. Further, as already noted, mucous glands also normally secrete and distribute mucus to the vocal folds, preventing excessive dehydration by inhaled air. However, even with these mechanisms to maintain hydration of the vocal folds, the ambient air humidity clearly can, in our clinical experience, be an important factor in causing phonatory problems. Vocalists who move from a high-humidity environment to a low-humidity environment often experience transient difficulty with voice quality, which can be remedied by providing adequate humidification and hydration.

Thus, although similar effects *may* be found in vivo with the passage of dry air through the larynx, the effects noted in this experiment are likely exaggerated with respect to the human situation because of the absence of fluid replacement from blood vessels and mucus-secreting glands. Therefore, loss of water from the surface into the dry airstream is not counterbalanced.

Despite these cautions about the limitations of generalization to humans, in fact, similar dehydration effects have been shown in humans[11,12] (also Verdolini et al, unpublished observations). In one study (Verdolini et al), systemic dehydration with furosemide was associated with an increase in PTP, with a lag of several hours. Clinically, the importance of the vocal fold hydration state on phonation has been documented in studies showing an increased ease of phonation (decreased PTP) after hydration, at least in vocally normal subjects.[11,12] In those studies, hydration treatments involved a combination of systemic and superficial interventions, including water intake, mucolytic drugs, and humidified air. Acoustic perturbation and lesion status may also be improved with therapeutic hydration in patients with vocal nodules.[10] The present findings are consistent with these human reports and represent an attempt to specifically assess surface dehydration, which has not yet been reported in the literature.

In addition to the physiological perspective, biomechanical considerations have been proposed to explain the findings from both excised canine larynx and human studies. Titze[9] has proposed that the PTP depends on a series of parameters: $PTP = (2k/T)(Bc)(w/2)$ where k is a dimensionless transglottal pressure coefficient, T is vocal fold thickness, B is a damping coefficient that is proportional to vocal fold tissue viscosity, c is the velocity of mucosal wave propagation (which depends on vocal fold stiffness), and $w/2$ is the prephonatory glottal half-width at the vocal processes of the arytenoids. Superficial dehydration, induced in the present experiment by dehumidified air, would be expected to increase vocal fold tissue stiffness and viscosity, and to some degree may decrease vocal fold thickness by drying of the superficial mucus layer and thus increase PTP. Vocal efficiency also decreases, in part because it depends on phonatory subglottic pressure.

The present study is the first to demonstrate similar effects with superficial as with internal or systemic dehydration. The effects demonstrated in these experiments probably overestimate the in vivo effects, because of the lack of normal physiological hydration mechanisms in excised preparations. However, these experiments demonstrate that superficial dehydration from dry air can be associated with rapid deterioration in key physical parameters of the biomechanics of phonation, and suggest that the superficial mucus layer over the vocal folds is a very important factor in voice quality.

CONCLUSION

Data from these experiments demonstrated that progressive dehydration of the surface of the vocal folds incrementally and rapidly increased the minimum required phonatory subglottal driving pressures and phonatory airflow, and progressively decreased phonatory efficiency. The results are consistent with those previously reported regarding the relationship between PTP and hydration levels.[16] They support the modeling with experimental findings indicating that dehydration of the vocal folds will degrade laryngeal performance. Whereas previous work has demonstrated the effects of systemic dehydration on phonatory subglottic pressure, the present study demonstrates the effects of superficial dehydration on excised preparations. These biomechanical observations cannot be directly generalized to living human larynges; however, further studies examining how ambient air humidity affects in vivo human larynges would be of clinical importance.

REFERENCES

1. Bradley M. Prevention and correction of vocal disorders in singers. NATS Bull 1980;36:38-41.

2. Lawrence VL. Handy household hints: to sing or not to sing. NATS Bull 1981;37:23-5.

3. Verdolini K. Practice good vocal health and prevent those voice disorders. Choristers Guild Lett 1988;2:40-4.

4. Sataloff RT. The professional voice: part III. Common diagnoses and treatments. J Voice 1987;1:283-92.

5. Sataloff RT. The professional voice: part I. Anatomy, function, and general health. J Voice 1987;1:92-104.

6. Bastian RW, Lawrence VL. Hoarseness in singers. NATS Bull 1984;40:26-7.

7. Sataloff RT, Baron BC, Brodnitz FS, et al. Discussion: acute medical problems of the voice. J Voice 1988;2:345-53.

8. Finkelhor BK, Titze IR, Durham PL. The effect of viscosity changes in the vocal folds on the range of oscillation. J Voice 1988;1:320-5.

9. Titze IR. Regulation of vocal power and efficiency by subglottic pressure and glottal width. In: Fujimura O, ed. Vocal physiology: voice production, mechanisms and function. New York, NY: Raven Press, 1988:227-38.

10. Verdolini K, Sandage M, Titze IR. Effect of hydration treatments on laryngeal nodules and polyps and related voice measures. J Voice 1994;8:30-47.

11. Verdolini K, Titze IR, Fennell A. Dependence of phonatory effort on hydration level. J Speech Hearing Disord 1994;37:1001-7.

12. Verdolini K, Titze IR, Druker DG. Changes in phonation threshold pressure with induced conditions of hydration. J Voice

1990;4:142-51.

13. Wexler DB, Jiang J, Gray SD, Titze IR. Phonosurgical studies: fat-graft reconstruction of injured canine vocal cords. Ann Otol Rhinol Laryngol 1989;98:668-73.

14. Durham P, Titze IR, Scherer R. Development of excised larynx procedures for studying mechanisms of phonation. Technical report VABL-1. Iowa City, Iowa: Voice Acoustics and Biomechanics Laboratory, Department of Speech Pathology and Audiology, The University of Iowa, 1987.

15. Jiang JJ, Titze IR. A methodological study of hemilaryngeal phonation. Laryngoscope 1993;103:872-82.

16. Jiang JJ, Ng J, Verdolini K, Hanson DG. The effects of rehydration on phonation in excised canine larynges. J Voice 1999;13:51-9.

≈

INTERNATIONAL CONFERENCE ON NEWBORN HEARING SCREENING DIAGNOSIS AND INTERVENTION

The International Conference on Newborn Hearing Screening Diagnosis and Intervention will be held in Milan, Italy, October 12-14, 2000. In Europe, contact Dr Ferdinando Grandori, Center of Biomedical Engineering, Polytechnic of Milan, piazza Leonardo da Vinci 32, I-20133 Milan, Italy; fax +39.02.2399.3360; e-mail NHS2000@biomed.polimi.it. In the United States, contact Dr Deborah Hayes, The Children's Hospital, 1056 E 19th Ave, B030, Denver, CO 80218; telephone (303) 861-6424; fax (303) 764-8220; e-mail: Hayes.deborah@tchden.org.

Ann Otol Rhinol Laryngol 109:2000

LARYNGEAL REFLEXOMYOGRAPHIC RESPONSES IN RABBITS: A NEUROLARYNGOLOGICAL STUDY OF GLOTTAL MOVEMENT

SHENGGUANG YIN, MD
WILLIAM W. QIU, MD, MA
FRED J. STUCKER, MD
SHREVEPORT, LOUISIANA

The role of the laryngeal reflex in glottal movement has been reported, but its mechanism remains unclear. To further investigate the neurophysiological characteristics of glottal movement, we recorded the laryngeal reflexomyographic responses (LRMRs) to electrical stimulation of the superior laryngeal nerve (SLN) in rabbits. The procedure involved simultaneous recording of the LRMRs from the thyroarytenoid muscles by means of bipolar hooked wire electrodes after electrical stimulation to the SLN. The results demonstrated characteristic patterns of the responses, consisting of R1 and R2, similar to those found in humans. The R1 response was obtained with a latency of 10.7 ± 0.78 ms. The ipsilateral R2 response was obtained with a latency of 43.76 ± 4.67 ms in all rabbits, and the contralateral R2 response with a latency from 42.6 to 50.2 ms in 4 rabbits. It was concluded that LRMRs may serve as a potential central laryngeal function test in the investigation of glottal movement control.

KEY WORDS — glottal movement, laryngeal reflexomyographic responses, larynx, R1, R2, rabbit.

INTRODUCTION

The laryngeal muscles, nerves, and joints are the anatomic structures involved in glottal movement. Proper positioning, articulation, and coordination of these structures are essential for glottal activity. Investigations have demonstrated that glottal movement is under the fine control of the central laryngeal system, particularly the brain stem.[1-5] This control is necessary for maintaining laryngeal muscular activity and the associated articulation, glottal configuration, and physiological positioning of the laryngeal structures. The larynx thus functions as a powerful coordinator for phonation, respiration, and swallowing. The study of glottal motor control, therefore, is a key to understanding complex laryngeal functions and their regulation.

Recording laryngeal muscle responses to stimulation of the laryngeal nerves has been used as an efficient method for studies of glottal motor control in animals and humans.[1,2,6,7] The nerves that are stimulated to elicit responses in the laryngeal muscles include the superior laryngeal nerve (SLN), recurrent laryngeal nerve (RLN), vagal nerve, and other cranial nerves.[1,8,9] Laryngeal motor control depends on central and peripheral inputs. The afferent system of the laryngeal pathways carries sensory impulses from the laryngeal receptors such as mechanoreceptors and chemoreceptors[10] to the nucleus tractus solitarii. These receptors and the ends of nerve fibers and their interactions in the vocal tract are responsible for triggering varied responses to peripheral stimulation. A technique for electrostimulation of the SLN has been used in evoked electromyography (EMG) studies of laryngeal functions in humans[6,11] and animals.[12,13] This technique is widely used because the SLN contains the afferent fibers and because the stimulation to the SLN, whether magnetic, electrical, or vibratory, is accessible and controllable.

Recently, laryngeal reflexomyographic responses (LRMRs) R1 and R2 have been elicited from the thyroarytenoid muscle (TA) with electrostimulation of the laryngeal nerves in humans,[6-8] electrostimulation of the SLN in cats,[14] electrostimulation of the RLN in cats and dogs,[2] and electrostimulation of the RLN with a conditioning stimulus of vibration.[14] In general, the characteristic patterns of LRMRs are similar to those recorded with the blink reflex, which elicits responses R1 and R2.[15] Considering the graphs of the response spectrum, length of window, and latency marks, the responses first reported by Sasaki and Suzuki[1] may be classified as R1. The similarity in patterns of R1 and R2 in animals to patterns of responses to stimulation of the SLN in humans[7] indicates that R1 and R2 are the product of integration of central laryngeal activities, and the responses to stimulation of the SLN may share a part of the laryngeal pathways. Although the ipsilateral R2 response is often noted, the R2 pathway is little known. Particularly,

---

From the Department of Otolaryngology–Head and Neck Surgery, Louisiana State University Medical Center, Shreveport, Louisiana. This study was performed in accordance with the PHS Policy on Humane Care and Use of Laboratory Animals, the NIH *Guide for the Care and Use of Laboratory Animals*, and the Animal Welfare Act (7 U.S.C. et seq.); the animal use protocol was approved by the Institutional Animal Care and Use Committee (IACUC) of Louisiana State University in Shreveport (proposal 96016).

CORRESPONDENCE — Shengguang Yin, MD, Dept of Otolaryngology–Head and Neck Surgery, Louisiana State University Medical Center in Shreveport, 1501 Kings Highway, Shreveport, LA 71130-3359.

the contralateral R2 response in anesthetized animals has rarely been reported in the literature. It is assumed that the LRMRs to varied stimulation reflect the balance of excitatory and inhibitory activities within the laryngeal nuclei in the brain stem. Therefore, it is expected that LRMRs serve as a test for evaluation of both laryngeal peripheral and central functions. Rabbits have been used as animal models for neurophysiological studies of the larynx.[16-19] If LRMRs can be recorded in rabbits, this species could serve as a useful model to further characterize R1 and R2 and investigate their central origins.

This study was designed to record LRMRs in rabbits. The possible role of LRMRs in control of the glottal movement was also discussed. We hypothesized that both R1 and R2 participate in the symmetric adductor reflex of the glottis.

METHODS

Data were collected from 5 adult New Zealand White rabbits, weighing from 3.5 to 5.0 kg. Anesthesia was induced in the animals with an initial intramuscular dose of ketamine hydrochloride (40 mg/kg) and xylazine hydrochloride (5 mg/kg). The rabbits were then placed in a supine position, and an adequate level of anesthesia was maintained by supplemental intravenous doses of ketamine hydrochloride (10 mg/kg) and xylazine hydrochloride (1.25 mg/kg) throughout the experiment, and body temperature was maintained by the use of a heating pad. All surgical procedures were carried out under aseptic conditions. The rabbit was fixed with a stereotaxic holder in a prone position with the head inclined downward at an angle of 45°. An endotracheal tube was inserted via the oral cavity, below the second ring of the trachea, for appropriate respiration. The larynx and trachea were exposed with a vertical midline incision in the neck. The connective tissue and prelaryngeal muscle layers were then sectioned. The SLNs were explored around the middle portion of the posterior edge of the thyroid cartilage, and the RLNs were isolated in the esophagotracheal groove.

Bioelectric activities from the laryngeal muscles were recorded with Spirit System (Nicolet Biomedical Inc, Madison, Wis), which has recording and stimulating capabilities. The passband on the EMG filters was set between 100 and 5,000 Hz, and the sensitivity at 100 to 500 μV. The hooked-wire electrodes used for EMG recordings from both TAs consisted of 2 stainless steel wires (0.0508 mm diameter) stripped of insulation for 1 mm at the end, and were contained in a 27-gauge needle. The electrodes were directly inserted through the cricothyroid space into the TA at an angle of 35°. Electrode location in the TAs was confirmed by the following criteria: muscle activity with respiration, contraction of the TA after stimulation of the RLN, and anatomic identification after the study.

For stimulation of the internal branch of the SLN, a bipolar platinum wire electrode (60 μm diameter) was hooked to the proximal stump of the SLN and embedded in paraffin with a low melting point (43°C). A rectangular pulse of 0.1 ms in duration and 0.5 to 0.8 mA in intensity was delivered to the proximal part of the SLN with a frequency of 0.7 to 2 Hz. Each stimulus mode was repeated twice to demonstrate response repeatability. Validity of stimulation was confirmed by observing the contraction of the ipsilateral cricothyroid muscle (CTr) with stimulation of the external branch of the SLN before cutting off the SLN. Vocal fold adduction was examined by means of a flexible fiberoptic laryngoscope (ENF-P2, Olympus America Inc, New York, NY) during stimulation of the SLN. The intensity of stimulation of the SLN was set at zero and incremented until a consistent threshold response was observed in at least 1 muscle on the screen. There were 2 distinct EMG responses recorded in LRMR waveforms: R1 and R2. The results from the TA were stored on computer disks for later analysis. In each test, waveforms were measured to calculate onset latency, duration, and amplitude.

In this study, *optimal stimulation* was defined as the stimulation intensity at which the optimal laryngeal muscle response was elicited; *latency* was defined as the interval between the onset of stimulation and the onset of the evoked responses; *amplitude* was defined as the maximum peak voltage of the LRMR; and *duration* was defined as the interval between the onset and offset of the LRMR.

RESULTS

The bilateral baseline EMG activities observed in the TA were synchronous with abdominal respiratory movement. To identify the nerve selected for stimulation, the response in the CTr was recorded first. There were 3 components in the waveform of the responses to stimulation of the SLN in the CTr — muscular responses, R1, and R2 — as the threshold of stimulation of the SLN was reached before cutting off the SLN.

When the optimal stimulation level was obtained, the LRMRs measured were of different intensities. The threshold level ranged from 0.32 to 3.0 mA. The function of frequency of the response to stimulation intensity was observed in rabbit 4. As the stimulation intensity was increased to a level of 0.28 mA, the incidences of ipsilateral and contralateral R1 re-

TABLE 1. EFFECTS OF STIMULATION INTENSITY ON INCIDENCE OF LRMR IN ONE RABBIT

		Intensity (mA)		
		0.20	*0.28*	*0.32 or 0.40*
Ipsilateral	R1	0.0	75.0	100.0
	R2	75.0	100.0	100.0
Contralateral	R1	0.0	37.5	100.0
	R2	0.0	100.0	100.0

Data are incidence of laryngeal reflexomyographic response (LRMR) expressed as percentage.

TABLE 2. LRMR IN THYROARYTENOID MUSCLES TO STIMULATION OF RIGHT SUPERIOR LARYNGEAL NERVE IN RABBITS

LRMR	*Latency (ms)*	*Duration (ms)*	*Amplitude (μV)*
Ipsilateral R1	10.62 ± 1.31 (8.40-11.80)	5.62 ± 1.88 (3.40-8.00)	67.20 ± 52.20 (31.00-158.00)
Contralateral R1	10.67 ± 0.57 (10.00-11.00)	3.48 ± 1.93 (2.00-5.60)	60.70 ± 14.60 (47.00-59.00)
Ipsilateral R2	37.70 ± 10.30 (25.00-50.00)	17.26 ± 4.25 (12.50-22.40)	108.40 ± 74.10 (44.80-223.00)
Contralateral R2	38.47 ± 8.07 (26.50-43.70)	20.33 ± 2.52 (17.00-22.60)	104.00 ± 51.40 (51.00-157.00)

Data are mean ± SD. Range is in parentheses. There was significant difference in latency and amplitude between R1 and R2 ($p < .05$).

sponses were 75% and 37.5%, respectively, whereas the incidence of the R2 response was 100%; this difference suggests that the neurons involving the pathway of R2 have a lower threshold than that of R1 in that animal (Table 1).

Electrostimulation of the SLN elicited reflexomyographic responses in the ipsilateral and contralateral TAs in the rabbits tested. The LRMRs, consisting of R1 and R2 components, were clearly identified during an optimum stimulation of the SLN in this study (Fig 1). All rabbits had ipsilateral R1 and R2 responses in the TA. Three of them had contralateral R1 responses in the TA, and 4 had contralateral R2 responses. Ipsilateral R1 responses had a 100% repeatable configuration, latency, duration, and amplitude. Although the contralateral R1 showed a latency similar to that of the ipsilateral R1, the configuration is significantly different. Whether the contralateral R1 is an artifact or a genuine response requires further study.

Two-sample *t*-tests were computed to compare the latency, duration, and amplitude of R1 and R2 in the ipsilateral and contralateral sides. Ipsilateral and contralateral means and standard deviations of the R1 and R2 response latencies, amplitudes, and durations among the 5 rabbits are summarized in Table 2. The range, as well as the mean and standard deviation, is listed because of the small number of animals studied. The early response, R1, had a shorter latency than the later response, R2 ($p < .01$), but there were no significant differences between ipsilateral and contralateral sides in latency, duration, or amplitude ($p > .05$). Moreover, no significant difference in R2 was found between the 2 sides in latency, duration, or amplitude ($p > .05$).

When observed with a flexible fiberoptic endoscope, glottal movement during stimulation of the SLN showed adduction of the vocal folds. The characteristic adduction elicited by electrostimulation of the SLN is a movement from the natural respiratory position to the midline position. In gross anatomic terms, we found no crossing fibers or other anatomic connections between the SLN and RLN (both were exposed) or between the left and right sides peripherally.

DISCUSSION

Reflexomyography or evoked laryngeal EMG has been used recently to study the physiology of the larynx and the pathogenesis of spasmodic dysphonia[9] and laryngeal paralysis in humans[20] and in animals.[18] There are other terms to describe these responses in the literature, including "early and late response," "neuromusculographic response," "reflex response," "thyroarytenoid evoked response," "adduction re-

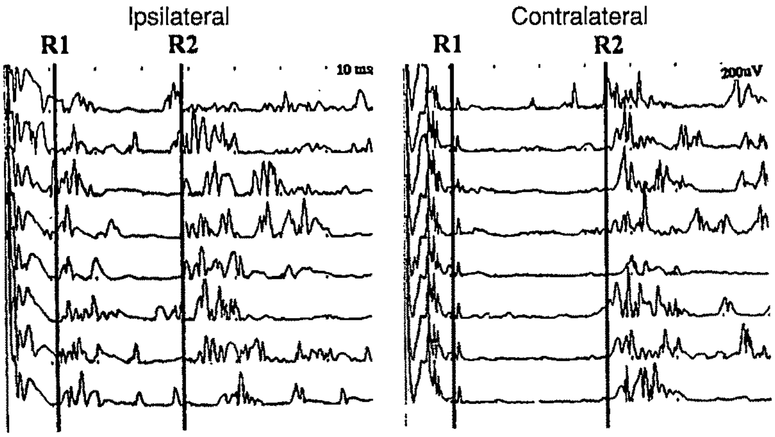

Fig 1. Integrated and averaged electromyographic signals from thyroarytenoid muscles in response to electrical stimulation of superior laryngeal nerve in rabbits. Two vertical lines indicate latency of R1 and R2 responses for 8 recorded tracings.

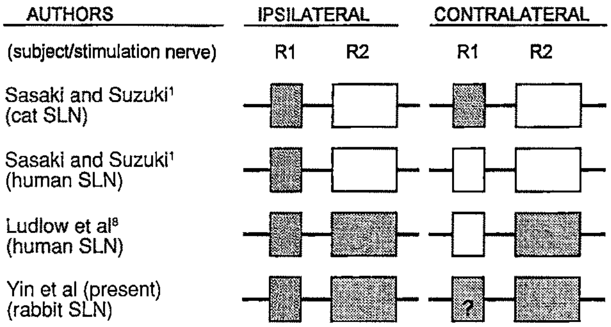
AUTHORS
(subject/stimulation nerve)
IPSILATERAL
CONTRALATERAL
R1
R2
R1
R2
Sasaki and Suzuki1 (cat SLN)
Sasaki and Suzuki1 (human SLN)
Ludlow et al8 (human SLN)
Yin et al (present) (rabbit SLN)
?

Fig 2. Schematic representation of findings in thyroarytenoid muscle in response to laryngeal nerve stimulation in different studies in literature.[1,8] Solid blocks indicate recordable response, and empty blocks indicate no measurable response.

sponse," "laryngeal late response," and "evoked compound action potential."[1,8,9,21] However, these terms do not specify whether the responses come from the brain stem or from the target muscles. The term "LRMR" was chosen for this study to emphasize that the responses are recorded in the laryngeal muscles via the reflex arc.

In comparison with R1, R2 showed a longer latency with a larger variance and a greater range of duration. This may suggest that the reflex is mediated via a pathway that separates from that of R1. The variability and longer latency of R2 also indicate that R2 involves more complex pathways than R1. It is interesting to note that R2 revealed a lower threshold than that of R1 in 1 rabbit (Table 1). The significance of this phenomenon is still unclear. We believe that the excitability of the reflex arc for R1 is probably different from that of R2, because the threshold of R1 exceeded that of R2 in the rabbit studied. Such a discrepancy in the excitability of the reflex arcs responsible for R1 and R2 evoked by electrostimulation of the SLN may suggest that the responses are generated from different origins, excited fibers, and pathways. The phenomena of discrepancy in threshold of R1 and R2 were similar to those observed in awake humans.[7] Our working hypothesis is that different reflex thresholds maintain basic tonic tension of the laryngeal muscles for vigilance before eliciting the glottal adduction reflex. When the intensity of stimulation reaches the threshold of either R1 or R2, both R1 and R2 are present and enforced. Physiologically, the presence of R1 may shorten the onset time of the laryngeal responses, further increase muscular tone, and reinforce the responses for the required laryngeal functions.

Whether the crossed adductor reflex exists in both humans and animals is still controversial. The data from Sasaki and Suzuki[1] show that the crossed adductor reflex is present in cats but not in humans. Ludlow et al[8] reported that R2 was more likely to be responsible for vocal fold adduction than R1 in humans. Considering the similarities in the latencies, lateralization distributions, and configurations of waveforms, it is most likely that the TA evoked responses reported by Sasaki and Suzuki[1] are analogous to the ipsilateral R1 demonstrated in our studies (Fig 2[1,8]). The results of the bilateral R2 responses, with a latency of 43.76 ± 4.67 ms in 4 rabbits, seem to demand a reconsideration of the presence of the crossed laryngeal reflex. It is still unclear whether there are crossed fibers in the pathway of R2 in the animal brain stem. From the results of this preliminary study, we hypothesize that both R1 and R2 participate in the adductor reflex of the glottis by different mechanisms. The differential contributions of these components still await further study.

In summary, this preliminary study demonstrated R1 and R2 responses in rabbits. Although the existence of LRMRs in rabbits may reflect some important aspects of laryngeal motor control, it is too early to conclude that either R1 or R2 corresponds to a specific physiological function. The interactions between R1 and R2 and the central nervous pathways remain to be elucidated.

ACKNOWLEDGMENTS — We are grateful to Henry H. Nguyen, MD, and Barbara M. Batchelor, EdD, MCD, for their editorial and technical assistance during the study and the preparation of our manuscript.

REFERENCES

1. Sasaki CT, Suzuki M. Laryngeal reflexes in cat, dog, and human. Arch Otolaryngol 1976;102:400-2.

2. Suzuki M. Laryngeal reflexes. In: Hirano M, ed. Neurolaryngology: recent advances. Boston, Mass: College Hill Press, 1983:142-55.

3. Berke GS, Moore DM, Hantke DR, Hanson DG, Gerratt BR. Laryngeal modeling: theoretical, in vitro, in vivo. Laryngoscope 1987;97:871-81.

4. Yajima Y, Hayashi Y. GABAA receptor–mediated inhibition in the nucleus ambiguus motoneuron. Neuroscience 1997; 79:1079-88.

5. Yin SG, Qiu WW, Stucker FJ, Wang ZM. The quest for neurolaryngology I. Ophthalmol Otolaryngol Chin 1998;3:155-60.

6. Suzuki M, Sasaki CT. Initiation of reflex glottic closure. Ann Otol Rhinol Laryngol 1976;85:382-6.

7. Yamashita T, Nash EA, Tanaka Y, Ludlow CL. Effects of stimulus intensity on laryngeal long latency responses in awake humans. Otolaryngol Head Neck Surg 1997;117:521-9.

8. Ludlow CL, Van Pelt F, Koda J. Characteristics of late responses to superior laryngeal nerve stimulation in humans. Ann Otol Rhinol Laryngol 1992;101:127-34.

9. Ludlow CL, Schulz GM, Yamashita T, Deleyiannis FWB. Abnormalities in long latency responses to superior laryngeal

nerve stimulation in adductor spasmodic dysphonia. Ann Otol Rhinol Laryngol 1995;104:928-35.

10. Sant'Ambrogio G, Mathew OP. Laryngeal receptors and their reflex responses. Clin Chest Med 1986;7:221-2.

11. Satoh I. Evoked electromyographic test applied for recurrent laryngeal nerve paralysis. Laryngoscope 1978;88:2022-31.

12. Misuhashi T. A physiological study of the effect of vibration on reflexive control of cats' larynx: the change in respiratory phase and the role of the internal branch of the superior laryngeal nerve. Nippon Jibiinkoka Gakkai Kaiho 1990;93:1020-33.

13. Bellingham MC, Lipski J. Morphology and electrophysiology of superior laryngeal nerve afferents and postsynaptic neurons in the medulla oblongata of the cat. Neuroscience 1992;48:205-16.

14. Mochida A. Reflex control on laryngeal functions — vibration effect of the laryngeal mucosa on recurrent laryngeal nerve reflexes. Nippon Jibiinkoka Gakkai Kaiho 1990;93:938-48.

15. Kimura J, Wilkinson JT, Damasio H, Adams HR, Shivapour E, Yamada T. Blink reflex in patients with hemispheric cerebrovascular accident (CVA). J Neurol Sci 1985;67:15-28.

16. Yin SG, Wang PW, Xiao J. Experimental research of the deviated glottis in rabbits. J Chin Otorhinolaryngol 1986;21:292-4.

17. Davis PJ, Nail BS. Quantitative analysis of laryngeal mechanosensitivity in the cat and rabbit. J Physiol (Lond) 1987;388:467-85.

18. Lewis WS, Crumley RL, Blanks RHI, Pitcock JK. Does intralaryngeal motor nerve sprouting occur following unilateral recurrent laryngeal nerve paralysis? Laryngoscope 1991;101:1259-63.

19. Kitamura S, Nagase Y, Chen K, Shigenaga Y. Nucleus ambiguus of the rabbit: cytoarchitectural subdivision and myotopical and neurotopic representations. Anat Rec 1993;237:109-23.

20. Thumfart WF. Electrodiagnosis of laryngeal nerve disorders. Ear Nose Throat J 1988;67:380-93.

21. Sherrey JH, Megirian D. Spontaneous and reflexly evoked laryngeal abductor and adductor muscle activity of cat. Exp Neurol 1974;43:487-98.

≈

FIFTH INTERNATIONAL CONFERENCE ON HEAD AND NECK CANCER

The Fifth International Conference on Head and Neck Cancer will be held July 29–August 2, 2000, in San Francisco, California. For information, contact Concepts in Meetings & Events, Robin L. Wagner, President, 7819 Lloyd Ave, Pittsburgh, PA 15218-1941; telephone (412) 243-5156; fax (412) 243-5160; e-mail: rlwa@med.pitt.edu.

Ann Otol Rhinol Laryngol 109:2000

SITE OF AIRWAY COLLAPSE IN OBSTRUCTIVE SLEEP APNEA AFTER UVULOPALATOPHARYNGOPLASTY

LTC WAYNE C. FARMER, MC, USA
FORT MONMOUTH, NEW JERSEY

LT STANLEY C. GIUDICI, MC, USN
NEW BERN, NORTH CAROLINA

The objective of this prospective study was to determine the site and pattern of upper airway collapse by a multiple-catheter technique in subjects demonstrated to have obstructive sleep apnea (OSA) after uvulopalatopharyngoplasty (UPPP). Standard diagnostic nocturnal polysomnography (PSG) was done on all subjects. The PSG recordings included electroencephalogram, electrooculogram, electrocardiogram, chin and leg electromyograms, nasal and oral airflow, and abdominal effort. Polysomnography with a multiport flexible airway Gaeltec catheter was performed in 22 subjects. The Gaeltec flexible airway catheter has 4 high-fidelity pressure sensors to aid in determining the primary site of airway collapse. The primary site of airway collapse was determined by differential pressure gradients between pressure ports and by visual inspection of the pressure tracings. Forty-two subjects with prior UPPP from a total of 60 (39 men and 3 women, ages 33 to 61) agreed to be to studied by the standard PSG technique. Thirty-five subjects complained of excessive daytime sleepiness. Ten had mild OSA, 10 had moderate OSA, 12 had severe OSA, and 10 were "normal." Of the 22 subjects who had airway catheter monitoring, 3 of the normals were reclassified as having upper airway resistance (mean peak negative esophageal pressure of −28 cm H_2O); 2 patients demonstrated airway obstruction in the nasopharynx, 2 at the oropharynx, and 11 at the level of the hypopharynx. Postoperative nocturnal PSG data were compared to data gathered prior to UPPP. The mean respiratory disturbance index (RDI) for the catheter group was 54 events per hour prior to UPPP, and the mean RDI after surgery was 44. There was no correlation between the severity of OSA and the stage of sleep. We conclude that the majority of patients who complain of excessive daytime sleepiness following UPPP have OSA with the primary site of obstruction at the level of the hypopharynx. The severity of airway collapse is variable during each stage of sleep. Esophageal pressure monitoring during sleep should be considered when evaluating symptoms of persistent OSA in patients who have had UPPP.

KEY WORDS — airway collapse, obstructive sleep apnea, uvulopalatopharyngoplasty.

The objective of this prospective study was to determine the site and pattern of upper airway collapse by a multiple-catheter technique in subjects demonstrated to have obstructive sleep apnea (OSA) after uvulopalatopharyngoplasty (UPPP).

BACKGROUND

Persistent OSA has been found in up to 50% of patients following UPPP.[1-4] An increase in mortality due to OSA has been reported.[5] Furthermore, anatomic and functional airway changes may greatly complicate the surgical treatment and perioperative course.[6] Guilleminault et al[7] reported that there is a high probability of upper airway resistance (UAR) in subjects who have excessive daytime sleepiness (EDS) and habitual snoring.

The precise site of airway collapse in patients with OSA can be localized.[8,9] Launois et al[10] have demonstrated that the site of airway collapse can predict the outcome of surgery. Persistent, habitual post-UPPP snoring has not been well documented. It is often difficult to differentiate obstructive hypopneas from mixed apneas and central hypopneas by means of conventional thoracic and abdominal strain gauges. The protocol in this study included the use of a multiport pressure esophageal catheter to more accurately define respiratory events and to identify the type and location of respiratory obstruction. The polysomnography (PSG) profile of OSA has traditionally been defined as cessation of respiration for 10 seconds or longer, in the presence of continued respiratory effort. Central apnea is defined as cessation of respiration for 10 seconds or longer, in the absence of respiratory effort. Mixed apnea is defined as cessation of respiration for 10 seconds or longer, in the presence of respiratory effort following an initial period of absent effort.[11,12] Obstructive sleep apnea is believed to represent a continuum of disease beginning with snoring and UAR and progressing to apnea.[13] Numerous studies have documented that OSA is associated with an increased prevalence of cardiovascular complications such as systemic hypertension, pulmonary hypertension, congestive heart failure, cardiac arrhythmias, and stroke.[14-17] Polysomnography is done to 1) confirm the diagnosis, 2) ascertain the severity of the respiratory event, 3) evaluate the response to nasal continuous positive airway pressure (CPAP), and 4) recommend the type of surgical procedure. There have been significant advances in

---

From the Department of Pulmonary and Sleep Medicine, Walter Reed Army Medical Center, Washington, DC. This study was approved by the Department of Clinical Investigation, Walter Reed Army Medical Center.

Presented at the Annual Meeting of The American College of Chest Physicians, New Orleans, Louisiana, October 26-30, 1997.

CORRESPONDENCE — Wayne C. Farmer, DO, 14 Schank Rd, Holmdel, NJ 07733.

TABLE 1. POLYSOMNOGRAPHY RESULTS FROM FIRST STUDY NIGHT

No. of Subjects	*Diagnosis*	*RDI*	*LSAT*
10	Mild OSA	10.8 ± 3.5	89.2 ± 4.5
10	Moderate OSA	22.1 ± 4.5	84.6 ± 5.1
12	Severe OSA	60.0 ± 18.3	81.4 ± 6.8
10	Normal		

Data are mean ± SD.

RDI — respiratory distress index (apnea events per hour); LSAT — lowest oxygen saturation (percent); OSA — obstructive sleep apnea.

TABLE 2. MEAN PEAK NEGATIVE INTRATHORACIC PRESSURES DURING SLEEP ON SECOND STUDY NIGHT

No. of Subjects	*Diagnosis*	*Sleep Stages*				*RDI*
		1	*2*	*3 & 4*	*REM*	
4	Mild OSA	−22.7	−22.5	−25.0	−21.3	13.9-18.6
5	Moderate OSA	−20.7	−27.0	−25.5	−22.3	21.3-28.0
6	Severe OSA	−29.7	−34.5	−20.0	−26.0	40.5-73.0
4	Normal					
3	UAR					

Note: patients with moderate or severe OSA had decreased slow-wave sleep.

Data are in centimeters of water for sleep stages, and apnea events per hour for RDI.

REM — rapid eye movement; UAR — upper airway resistance.

surgery for OSA.[18] If the site of airway collapse is at the oropharynx or hypopharynx, it is unlikely that UPPP will be of benefit. In addition, airway pressure monitoring allows recognition of the UAR syndrome in patients who have EDS and nocturnal habitual snoring.

METHODS

This is a prospective study of 42 patients from a total of 60 who were previously documented to have OSA prior to UPPP. The UPPP was performed more than 6 months prior to this study. Of the 42 subjects studied after UPPP, 22 had airway catheter monitoring. Postoperative nocturnal PSG data were compared to data gathered prior to UPPP. Patients were identified from records in the Sleep Disorders Center and otolaryngology clinic at The Walter Reed Army Medical Center. Initial anthropometric measures included age, weight, height, and body mass index. All subjects were interviewed by one of the investigators prior to the study. A detailed sleep history was obtained to include the Stanford Sleepiness Scale, the Epworth Sleepiness Scale, and the Visual Analog Scale. Standard PSG was recorded on a multichannel Sensor Medics analysis system. Recordings included electroencephalography, electrocardiography, submental and limb electromyography, nasal air and oral airflow, thoracic and abdominal effort, oxygen saturation, arterial blood pressure, and a snore microphone. The Gaeltec flexible airway catheter has 4 high-fidelity pressure sensors to aid in determining the primary site of airway collapse. The catheter port at the level of C1-2 reflects the site of obstruction in the nasopharynx, the catheter port at C3-4 reflects obstruction in the oropharynx, and the catheter port at C5 reflects obstruction in the hypopharynx. The site of collapse was defined by a differential pressure gradient of greater than 10 cm H_2O between airway sites and by visual inspection of the pressure tracings showing either partial or complete airway collapse according to Shepard and Thawley.[19] In our experience, a progressive increase in peak negative pressure across the various sites of obstruction preceded visual recognition of the site of collapse. The magnitude of the pressure gradient is more apparent during obstructive hypopneas and after termination of the obstructive event. The esophageal pressure port recorded the total intrathoracic pressure that developed during respiratory efforts. The mean values for airway pressures were calculated over 30-minute segments of non–rapid eye movement (NREM) and rapid eye movement (REM) sleep and were compared to the respiratory disturbance index (RDI) during each stage of sleep. Concomitant measures of the number of obstructive apneas (complete airway obstruction), hypopneas (partial airway obstruction), the actual amount of sleep spent in apnea (total apnea time), and the oxygen saturation levels reached during each apnea were evaluated. On the first night of the study, standard diagnostic PSG was done. During the second night, diagnostic PSG was performed with a multiport flexible airway Gaeltec catheter to access the site of upper airway collapse. A lateral neck radiograph confirmed placement of the pressure ports. A third nocturnal CPAP titration study was performed with the catheter on subjects with OSA and UAR.

RESULTS

Forty-two subjects participated in the study. Thirty-five subjects had persistent symptoms of EDS. There were 39 men and 3 women, ages 33 to 61. The mean body mass index for the entire group was 28.9 (range, 18.9 to 43; SD, 4.5). On the first study night, 10 subjects were classified as "normal," 10 had mild OSA, 10 had moderate OSA, and 12 had severe OSA (Table 1). Seven of the "normal" subjects participated in the catheter study; 3 were reclassified as having UAR (mean peak negative intrathoracic pressure of −28 cm H_2O). The mean RDI for the catheter group was 54 events per hour prior to UPPP and 44 after surgery. Table 2 shows the mean peak negative intrathoracic pressures as measured by the esophageal catheter during sleep. Mild persistent snoring was seen

TABLE 3. SITE OF AIRWAY OBSTRUCTION AND SEVERITY OF OSA

Site	*Mild OSA*	*Moderate OSA*	*Severe OSA*
Nasopharynx		2	
Oropharynx	1		1
Hypopharynx	3	3	5

Data are numbers of subjects.

in half of the UPPP subjects. There were 2 patients with airway obstruction in the nasopharynx, 2 at the oropharynx, and 11 at the level of the hypopharynx (Table 3). Nocturnal snoring was reported in only 1 patient. The presence of snoring on the PSG did not differentiate normals or UAR or OSA subjects from each other. One of the UAR subjects demonstrated partial airway collapse at the level of the hypopharynx. A control population was not studied. Among our post-UPPP subjects, there were no significant differences among the scores on the Epworth Sleepiness Scale, the body mass index, and the lowest oxygen saturation. The RDI did not predict the site of airway obstruction. As previously reported, there was a correlation among the RDI, the lowest oxygen saturation, and the total arousal index.[20] The severity of OSA did not predict the site of airway collapse (Table 3).

DISCUSSION AND CONCLUSIONS

While the outcome of UPPP in our patients is comparable to that in the study by Launois et al,[10] the primary site of airway collapse in the majority of our patients was at the level of the hypopharynx. Our definition of the site of collapse differs from that of other studies. The site of obstruction was determined when there was an increase in the peak negative pressure of greater than 10 cm H_2O between pressure ports confirmed by visual inspection of pressure tracings that showed either partial or complete airway collapse. Upper airway resistance was best determined during hypopneas prior to partial or complete obstruction. It is unclear why the majority of patients who are post-UPPP with complaints of EDS have OSA with the primary site of collapse at the level of the hypopharynx. Perhaps our population of "physically fit" military patients differs from other study groups. The severity of airway collapse indicated by esophageal pressure was not significantly different among the different sleep stages. Recent evidence indicates that post-UPPP, secondary sites of narrowing or airway collapse may be more collapsible at a lower level after the original site is corrected.[21] It is possible that unmasking a lower level of airway obstruction accounts for UPPP failures and the often quoted "50% reduction" in the RDI after UPPP.

The weakness of our study is apparent, as there were no catheter data taken prior to UPPP and no endoscopic technique. The selection for UPPP in our patients may have been motivated in part by the inability to use CPAP during military deployment.

CLINICAL IMPLICATIONS

Esophageal pressure monitoring should be considered in evaluating symptoms of persistent OSA in patients who have had UPPP surgery.

REFERENCES

1. Gislason T, Lindholm C-E, Almquist M, et al. Uvulopalatopharyngoplasty in the sleep apnea syndrome. Predictors of results. Arch Otolaryngol Head Neck Surg 1988;114:45-51.
2. Wetmore SJ, Scrima L, Snyderman NL, Hiller FC. Postoperative evaluation of sleep apnea after uvulopalatopharyngoplasty. Laryngoscope 1986;96:738-41.
3. Rodenstein D. Assessment of uvulopalatopharyngoplasty for the treatment of sleep apnea syndrome. Sleep 1992;15(suppl 1):S56-S62.
4. Sher AE, Thorpy MJ, Shprintzen RJ, Spielman AJ, Burack B, McGregor PA. Predictive value of Müller maneuver in selection of patients for uvulopalatopharyngoplasty. Laryngoscope 1985;95:1483-7.
5. He J, Kryger MH, Zorich FJ, Conway W, Roth T. Mortality and apnea index in obstructive sleep apnea. Chest 1988;94:9-14.
6. Piper JG, Dirks BA, Traynelis VC, Van Gilder JC. Perioperative management and surgical outcome of acromegalic patients with sleep apnea. Neurosurgery 1995;36:70-5.
7. Guilleminault C, Stoohs R, Clerk A, Meistros PA. A cause of excessive daytime sleepiness: the upper airway resistance syndrome. Chest 1993;104:781-7.
8. Crumley RL, Stein M, Gamsu G, Golden J, Dermon S. Determination of obstructive site in obstructive sleep apnea. Laryngoscope 1987;97:301-8.
9. Shepard JW, Thawley SE. Evaluation of the upper airway by computerized tomography in patients undergoing uvulopalatopharyngoplasty for obstructive sleep apnea. Am Rev Respir Dis 1989;140:711-6.
10. Launois SH, Feroah TR, Campbell WM. Site of pharyngeal narrowing predicts outcome of surgery for obstructive sleep apnea. Am Rev Respir Dis 1993;147:182-9.
11. Guilleminault C, Tilkian A, Dement WC. The sleep apnea syndrome. Annu Rev Med 1976;27:465-84.
12. Guilleminault C, Van Den Hoed J, Miller MM. Clinical review of the sleep apnea syndromes. In: Guilleminault C, Dement WC, eds. Sleep apnea syndromes. New York, NY: Academic Press, 1978:1-12.
13. Lugaresi E, Cirignotta F, Coccagna G, Piana C. Some epidemiological data on snoring and cardiocirculatory disturbances. Sleep 1980;3:221-4.
14. Koskenvuo M, Kaprio J, Partinen M, Telakivi T. Snoring as a risk factor for hypertension and angina pectoris. Lancet 1985;1: 893-6.

15. Lavie P, Yoffe N, Berger J, Peled R. The relationship between the severity of sleep apnea syndrome and 24 hour blood pressure values in patients with obstructive sleep apnea. Chest 1993;103:717-21.

16. Carlson JT, Hedner JA, Ejnell H, Peterson LE. High prevalence of hypertension in sleep apnea patients independent of obesity. Am J Respir Crit Care Med 1994;150:72-7.

17. Silverberg D, Oksenberg A. Essential hypertension and abnormal upper airway resistance during sleep. Sleep 1997;20: 794-806.

18. Riley R, Powell N, Guilleminault C. Current surgical concepts for treating obstructive sleep apnea syndrome. J Oral Maxillofac Surg 1987;45:149-57.

19. Shepard TW, Thawley SE. Localization of upper airway collapse in obstructive sleep apnea. Am Rev Respir Dis 1990; 141:1350-5.

20. Giudici S, Farmer W. Lack of predictive value of the Epworth Sleepiness Scale in patients following uvulopalatopharyngoplasty [Abstract]. Annual Meeting, American College of Chest Physicians, San Francisco, California, 1996:356.

21. Dundar A, Gerek M. Patient selection and surgical results in obstructive sleep apnea. Eur Arch Otolaryngol Suppl 1997(suppl 25A):S1157-S1161.

≈

SAN FRANCISCO OTOLOGY & NEUROTOLOGY UPDATE 2000

The San Francisco Otology & Neurotology Update 2000 will be held October 26-28, 2000, in San Francisco, California. For information, contact University of California, San Francisco, Office of Continuing Medical Education, Room LH-450, San Francisco, CA 94143-0742; telephone (415) 476-4251; fax (415) 476-0318; e-mail: palmerk@ocme.ucsf.edu.

Ann Otol Rhinol Laryngol 109:2000

PHARYNGEAL PRESSURE ANALYSIS BY THE FINITE ELEMENT METHOD DURING LIQUID BOLUS SWALLOW

SUNG MIN KIM, PHD
SEOUL, KOREA

TIMOTHY M. MCCULLOCH, MD
IOWA CITY, IOWA

KWAN RIM, PHD
SEOUL, KOREA

The human pharynx is unique, acting as a complex interchange between the oral cavity and the esophagus, and between the nasal cavity and the lungs. It is actively involved in the transport of food and liquid, producing the forces that guide the bolus into the upper esophagus and away from the adjacent larynx and lungs. This study developed a biomechanical computer model of the human pharynx, utilizing a finite element method (FEM). Control 2-dimensional cine computed tomography images were obtained during 10-mL barium paste swallows at 8 levels extending from the tongue base to the cricopharyngeal level in order to encompass the entire pharynx. Three-dimensional finite element models of the pharynx were reconstructed from the geometric information obtained from the images at each level. Using an inverse dynamic approach with the addition of known tissue properties, we analyzed the 8 models under estimated pressure histories during swallow. Within each model, changes in the cross-sectional intraluminal area were calculated and compared with the area from the computer-generated FEM model. Area matching allowed estimation of intraluminal pressure gradients during swallow. The estimated pressure gradients were distributed through a range from 10 to 55 mm Hg, varying from one region to another and showing different patterns for the upper 4 levels and the lower 4 levels. The contraction velocity for the upper 4 levels was much higher than that for the lower 4 levels. The higher contraction velocities and pressure gradients in the upper levels are consistent with the bolus velocities required for efficient swallow.

KEY WORDS — biomechanical modeling, finite element analysis, inverse dynamic, pharynx, swallowing.

INTRODUCTION

The pharyngeal phase of swallow requires rapid, complex, and coordinated neuromuscular action of the structures of the mouth, pharynx, and larynx. The ability to track the gross movements and trajectories of key structures in the pharyngeal phase of swallowing (kinematics of swallowing) has clinical relevance and is crucial to researchers for biomechanical modeling. An improved understanding of the physiology of swallow will come from investigations of muscle activation and the relationship between muscle activation and bolus propulsion.[1,2] Information about muscle group activity is important, because contracting muscles provide the driving force at the initiation of the swallow and generate the pressure gradients necessary for bolus movement into the esophagus. Additionally, muscle contractions change the structure of the pharynx, producing anatomic and pressure barriers that prevent the bolus from entering the airway.

McConnel et al[3,4] used manofluorometry to describe bolus motion. Pharyngeal bolus transit occurs in 2 phases: an initial thrust phase and a mucosal clearance phase. Bolus thrust, which propels most of the bolus into the esophagus, is provided by lingual propulsion, laryngeal elevation, and gravity. The tongue has been likened to a piston, pumping the bolus through the pharynx. The tongue has a much greater muscle mass than the adjacent constrictors, and drives the bolus head through the pharynx before pharyngeal peristalsis has begun. Patients with tongue impairment cannot generate large bolus driving forces despite an intact pharyngeal constrictor mechanism. Hyoid and laryngeal elevation along with cricopharyngeal relaxation decreases upper esophageal sphincter pressure, aiding in bolus motion toward the esophagus. The elevated larynx holds the pharyngeal lumen open to minimize pharyngeal resistance.[3] Intrabolus pressures may not build up in the esophageal region of normal subjects, because the bolus passes into the esophagus along a path of low resistance. However, when the anatomy and tissues are changed, as in laryngectomy, pharyngeal resistance increases, causing prolonged transit times and increased lingual pressures.[4]

The mucosal clearance phase occurs in a sequential fashion through the pharynx due to close contact between the anterior and posterior mucosal surfaces. In the oropharynx, it is related to squeezing between the tongue base and the posterior pharynx followed

---

From the Department of Biomedical Engineering, College of Engineering (Kim, Rim), and the Department of Otolaryngology–Head and Neck Surgery, College of Medicine (McCulloch), University of Iowa, Iowa City, Iowa.

CORRESPONDENCE — Timothy M. McCulloch, MD, Dept of Otolaryngology, University of Iowa Hospitals and Clinics, 200 Hawkins Dr (E230GH), Iowa City, IA 52242.

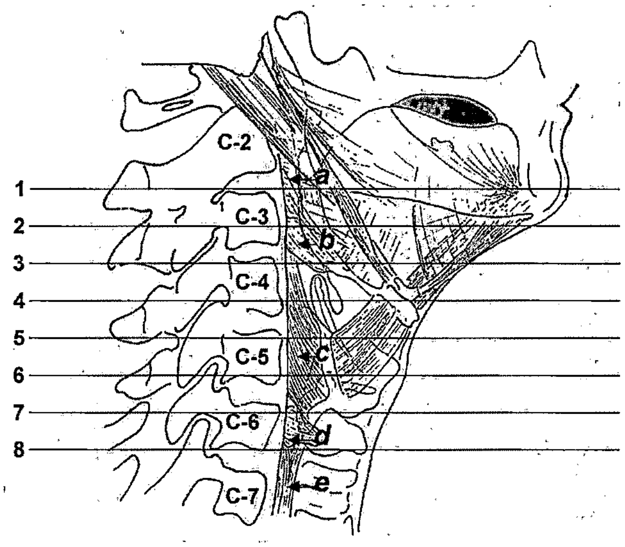

Fig 1. Levels of cine computed tomography scan from tongue base to esophageal inlet. a — superior constrictor muscle; b — middle constrictor muscle; c — inferior constrictor muscle; d — cricopharyngeus muscle; e — esophagus.

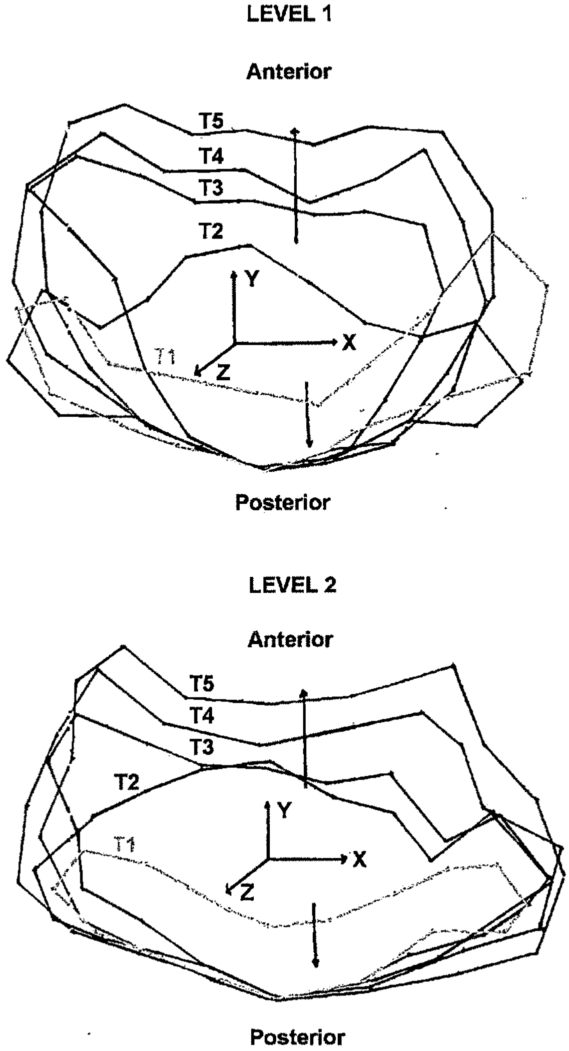

Fig 2. Intraluminal areas extracted from cine computed tomography, levels 1 and 2, times T1 (near closure) to T5 (maximum expansion). Each step is separated by 0.1 second.

by the "pharyngeal peristaltic wave."[5,6] Bolus passage is continued through the hypopharynx as the larynx descends and contacts the hypopharyngeal peristaltic wave and is completed with cricopharyngeal closure.

In this study, a computer-based finite element model is generated from kinematic data obtained from 10-mL barium swallows recorded with a cine computed tomography (CT) scanner. These kinematic data, when coupled with known physical properties of pharyngeal tissue, allow the development of a simple biomechanical model capable of simulating the pharyngeal phase of swallow. One objective of the model was to estimate regional swallowing intrabolus pressure gradients for the purpose of examining swallowing performance of the pharynx in the normal state. However, once established, a reasonably accurate model would allow noninvasive investigation of swallowing dysfunction.

MATERIALS AND METHODS

Kinematic Observation of Pharyngeal Swallowing. Control 2-dimensional (2-D) cine CT images with simultaneous temporal information were obtained from the base of the tongue through the cricopharyngeal level. Three-dimensional (3-D) reconstruction of pharyngeal geometry from the 2-D cine CT images was performed based on a finite element method (FEM). A brief description of the procedure follows. In a single healthy 36-year-old male subject swallowing approximately 10 mL of radiopaque contrast, 2-D cine CT images were obtained, 2 levels at a time, along the pharyngeal region with a 0.7-cm image thickness (Fig 1). The pharyngeal lumen borders of the swallowing event, together with the orientation data, were used as input for the FEM. By means of hard copy images from each pharyngeal-level lumen, borders were manually digitized and then reconstructed with a finite element computer program. Reference times and dimensions were also recorded from the images to correlate with the pharyngeal bolus swallowing sequence. At each level, 5 consecutive images were transferred to the FEM model, with each image separated in time by 0.1 second, with the first postbolus point of maximum pharyngeal segment dilatation designated as time 5 (T5). Time 1 or T1 represented the image 0.5 second into the pharyngeal contraction, in most cases representing near-complete closure (Fig 2).

This method of CT image analysis has been used in other studies, and has been found to be a reason-

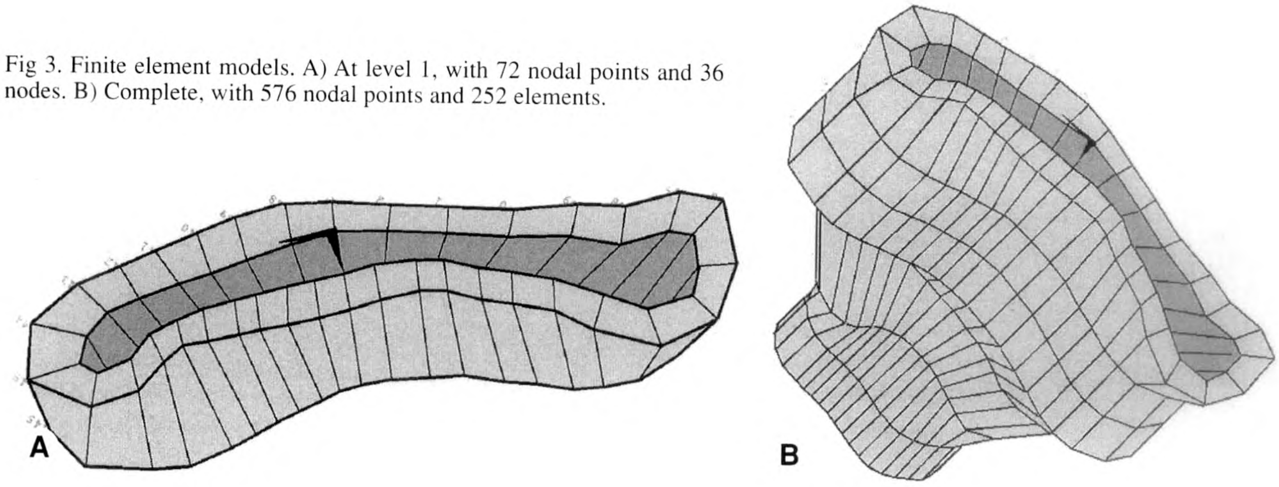

Fig 3. Finite element models. A) At level 1, with 72 nodal points and 36 nodes. B) Complete, with 576 nodal points and 252 elements.

ably accurate method of defining regional geometry. From the transferred lumen border data, a finite element mesh was formed. In order to generate finite elements of nearly equal volumes and to avoid skewed shapes, we defined 72 nodal points for each level, creating 36 nodes in each level (Fig 3A).

A standard coordinate system was defined and fixed with the origin located at the center of the upper pharyngeal contour. The z-axis is defined as the line connecting the origin (upper pharyngeal level) to the center of the upper esophageal sphincter (UES) contour. The x-axis and y-axis are defined as the lines perpendicular to the z-axis (x-axis medial-to-lateral, y-axis anterior-to-posterior). The digitized data for the pharyngeal regions are transformed to the standard coordinate system with an interactive conversion program.

This simple model assumes uniform wall thickness in the pharynx. By stacking the reconstructed 2-D cross sections of the pharynx proximal-to-distal, it is possible to obtain a 3-D shape simulating the entire pharyngeal geometry. The total reconstructed finite element mesh is composed of 576 nodal points and 252 elements (Fig 3B).

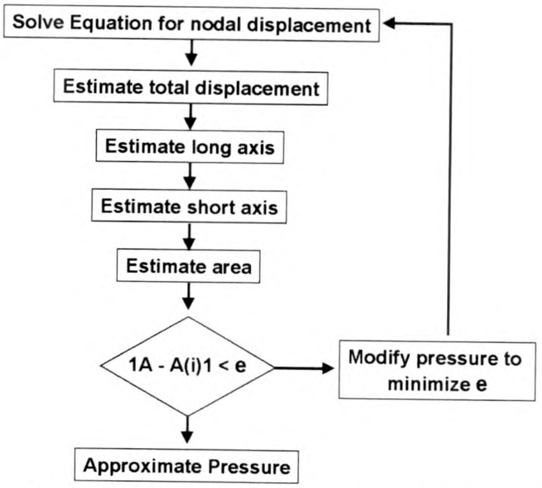
Solve Equation for nodal displacement
Estimate total displacement
Estimate long axis
Estimate short axis
Estimate area
1A - A(i)1 < e
Modify pressure to minimize e
Approximate Pressure

Fig 4. Diagram of optimization procedure. 1A — known area; A(i)1 — estimated area; e — error.

In this simple model, all elements were assigned the same material properties. Poisson's ratios of reasonably assumed values are taken to approximate the incompressible material. The modulus of elasticity was estimated from nonlinear stress-strain relationship data obtained from studies of the mechanical properties of the pharyngeal tissues.^{7}

Finite Element Analysis of Pharynx Subjected to Assumed Forces. In this study, the output parameters of the model are the physiological cross-sectional area and the geometric parameters describing the position coordinates of the pharyngeal lumen along the x-axis and y-axis. All input and output variables are presented with respect to the coordinate system fixed in the most superior level. The output variables of the model are the resultant displacements of the internal lumen of the pharynx, and the pressure necessary to counterbalance the external load on the pharyngeal wall. Each solution is obtained from an optimization procedure (Fig 4). The resultant counterbalance pressure magnitude is then equivalent to the intraluminal "swallowing" pressure.

In the usual finite element analysis, the geometry of, the material properties of, and the loading conditions on a structure are known, and the nodal displacements (the deformation) are directly solved. However, in the present study, the pharyngeal geometry of the "deformed" structure, which comes from a cine CT image, is known, and the loading condition (in this case, pressure) remains the unknown variable (inverse dynamic approach). The finite element computer program is used to determine the geometry of the pharynx during swallowing, corresponding to an assumed force history. The nodes

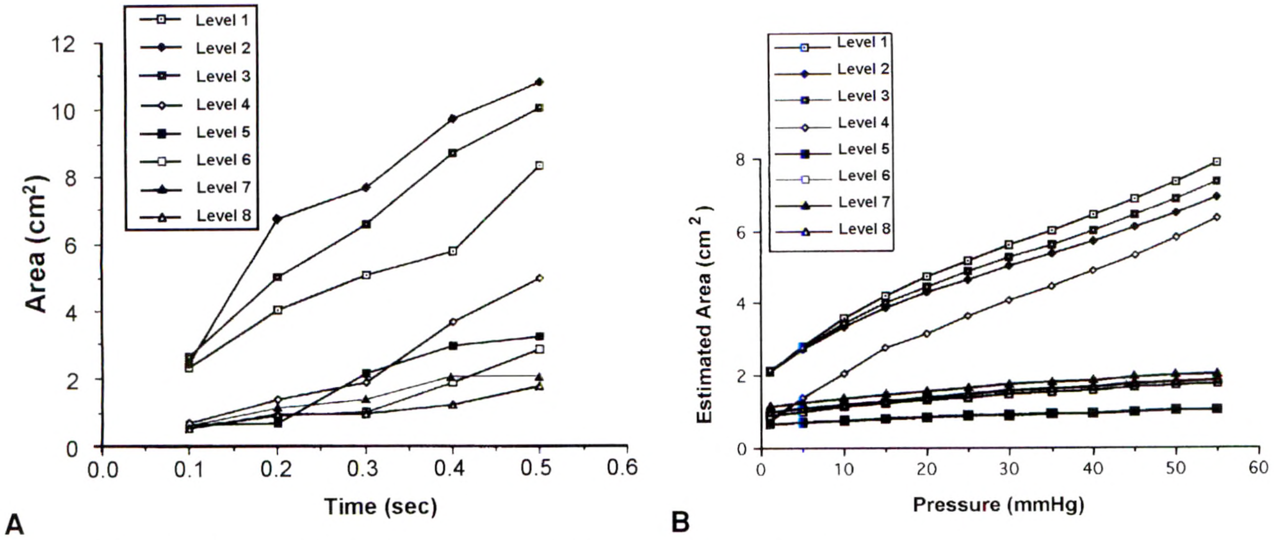

Fig 5. Results. A) Recorded areas at each level of cine computed tomography. Liquid swallow is 10 mL; 0.1 second is time 1 (see text), and 0.5 second is time 5. B) Finite element model of estimated area according to intraluminal pressure.

on the uppermost level (base of tongue) are fixed and served as fixed boundary conditions. The central portion of the posterior pharyngeal geometry is constrained by the cervical spine, and this was also considered a fixed boundary condition. The analysis is completed with a series of different assumed pressure patterns acting on the inner surface of the pharynx with spatial, as well as temporal, variation. The computer-predicted geometry of the pharynx is compared with the geometry of the pharynx as depicted by the cine CT scan images at corresponding instances. The difference between the observed geometry and the computer-predicted geometry is defined as a percent error and is to be minimized via multiple modeling iterations. When the percent error approximates zero, a good kinematic match occurs, and hence, the corresponding pressures are expected to be reliable estimates of the intraluminal pressure gradients of pharyngeal swallowing.

RESULTS

The recorded areas at each level of the cine CT scans, from T1 to T5, are graphically represented in Fig 5A. The final result of the optimization procedure for each level is represented in Fig 5B. These data are then interpolated to represent the estimated pressure gradients for each level related to the changing intraluminal area. From the FEM analysis, the estimated pressure gradients are distributed through a pressure range from 10 to 55 mm Hg. The estimated pressure gradients differ significantly between the superior 4 levels and the inferior 4 levels. The relative slopes of these curves imply more rapid contraction in the upper pharyngeal levels relative to the lower levels. The completed FEM model graphically depicts the simplified pharyngeal anatomy, which allows representation of bolus transfer, pressure changes, and geometric changes during swallow.

DISCUSSION

The anatomy and thus the geometry differ between the levels of the human pharynx. The contraction velocities for the upper 4 levels are higher than those for the lower 4 levels. The reason may be rooted in the physiological flexibility in the upper levels (tongue base) and the anatomic constraints in the lower levels (pyriform sinus and cricopharyngeus muscle). Rigid structures — the cricoid and thyroid cartilages anterior and the cervical spine posterior — are components of these inferior levels. Therefore, displacements in the x and y directions at these levels are relatively small, resulting in a small change in cross-sectional area.

McConnel et al[4,8] investigated the pressure distribution and the bolus transport during pharyngeal swallow in normal subjects and laryngectomized patients. Their results show that the change in pharyngeal pressure that was generated during a 10-mL bolus swallow ranged from 20 to 80 mm Hg. Another important study, by Sokol et al,[9] based on simultaneous cineradiographic data with manometry of 3 pharyngeal regions, also demonstrated that pharyngeal pressure varied from 20 to 70 mm Hg. Cerenko et al[5] made a quantitative assessment of pharyngeal bolus driving forces, and reported the mean pressure values of the pharyngeal clearing force and the oropharyngeal propulsion pump. Those pressure results in normal pharyngeal swallowing are compatible with the pressures estimated from our model.

The estimated swallowing pressure gradients in the region below level 4 (levels 5 and 6), which is located near the UES, tend to decrease, implying that below this level the pressure gradient has different values. As the level changes from proximal to distal, the pressure gradient generated tends to decrease. Below the arytenoid and in the postcricoid area (below level 4), there are expected to be no significant geometric changes induced by pharyngeal pressures, since this region incorporates both the thyroid cartilage and the cricoid cartilage.

In a series of reports by Kahrilas et al,[10-12] pharyngeal lumen changes occurring during swallowing were estimated from dynamic CT scanning. These studies addressed the change in luminal area created by various swallowing volumes; however, they did not correlate the area change with the swallowing pressure generated by pharyngeal tissue. The range of measured and estimated areas from our study was similar to the results in their reports.

It is observed that during swallowing the magnitude of the maximum pharyngeal structural deformation is greater in the anterior walls, where the curvatures of the cross section are largest. Further, some compressive local stresses may develop at the innermost posterior pharyngeal walls in the pharynx, where the cervical spine is located.

CONCLUSION

On the basis of the 3-D reconstruction techniques and the results discussed above, it is possible to accurately estimate the changes in cross-sectional shape and dimension at any site along the proximal-to-distal axis of the pharyngeal structure throughout a complete swallowing cycle. In this study, we describe how the FEM model can be applied to these reconstructed cross sections for investigating the regional characteristics of the pharyngeal structure deformation. The estimated pressure gradients were distributed through a range from 10 to 55 mm Hg. The estimated pharyngeal pressure gradient varies from one region to another, and showed different patterns for the upper 4 levels and the lower 4 levels. The contraction velocity for the upper 4 levels is much higher than that for the lower 4 levels. The higher contraction velocities and pressure gradients in the upper levels are consistent with the bolus velocities required for efficient swallow.

In this analysis, the pharynx was approximated with a cylindrical shape of uniform wall thickness. All cross-sectional deformations occur relative to assumed boundary conditions and forces. The initial modeling conditions assume the pharynx is in a passive state and then applies force under uniform internal pressure. For contraction analysis, the procedure must incorporate time-dependent changes in pharyngeal tissue stiffness, as well as displacement induced by the active muscle contraction. This type of information is not currently available; however, the necessary contraction information may be derived from future studies incorporating intramuscular electromyography. Factors commonly incorporated in fluid dynamic models — viscosity, frictional forces, and bolus composition — are not included in this current FEM modeling. Validation of such a complex model could be difficult, but would facilitate the investigation of all aspects of pharyngeal dysfunction.

ACKNOWLEDGMENTS — The authors thank Drs Brad Thompson and William Stanford of the Department of Radiology at The University of Iowa for providing the computed tomography images.

REFERENCES

1. Kahrilas PJ, Dodds WJ, Dent JA, Logemann JA, Shaker R. Upper esophageal sphincter function during deglutition. Gastroenterology 1988;95:52-62.
2. Kahrilas PJ, Logemann JA, Gibbons P. Food intake by maneuver: an extreme compensation for impaired swallowing. Dysphagia 1992;5:155-60.
3. McConnel FMS. Analysis of pressure generation and bolus transit during pharyngeal swallowing. Laryngoscope 1988;98:71-8.
4. McConnel FMS, Mendelsohn MS, Logemann JA. Examination after total laryngectomy using manofluorography. Head Neck Surg 1986;9:3-12.
5. Cerenko D, McConnel FMS, Jackson RT. Quantitative assessment of pharyngeal bolus driving forces. Otolaryngol Head Neck Surg 1989;100:57-63.
6. Curtis DJ, Cruess DF, Dachman AH. Normal erect swallowing. Normal function and incidence of variations. Invest Radiol 1985;20:717-26.
7. Kim SM, McCulloch TM, Rim K. Evaluation of the viscoelastic properties of pharyngeal tissue. Tissue Eng 1998;4:389-401.
8. McConnel FMS, Cerenko D, Mendelsohn MS. Dysphagia after laryngectomy. Otolaryngol Clin North Am 1988;21:721-6.
9. Sokol EM, Heitmann P, Wolf BS, Cohen BR. Simultaneous cineradiographic and manometric study of the pharynx, hypopharynx and cervical esophagus. Gastroenterology 1966;51:960-74.
10. Kahrilas PJ, Lin S, Chen J, Logemann JA. Oropharyngeal accommodation to swallow volume. Gastroenterology 1996;111:297-306.
11. Kahrilas PJ, Lin S, Chen J, Logemann JA. Three-dimensional modeling of the oropharynx during swallowing. Radiology 1995;194:575-9.
12. Pouderoux P, Kahrilas PJ. Deglutitive tongue force modulation by volition, volume, and viscosity in humans. Gastroenterology 1995;108:1418-26.

Ann Otol Rhinol Laryngol 109:2000

CARCINOMA OF THE HYPOPHARYNX AND CERVICAL ESOPHAGUS IN YOUNG ADULTS

PATRICK R. AXON, FRCS (ORL)
MANCHESTER, ENGLAND

RICARD SIMO, FRCS (ORL)
LONDON, ENGLAND

NEIL FERGIE, FRCS
MANCHESTER, ENGLAND

ROBERT H. TEMPLE, FRCS
MANCHESTER, ENGLAND

W. TREVOR FARRINGTON, FRCS
MANCHESTER, ENGLAND

Squamous cell carcinoma of the hypopharynx and cervical esophagus usually presents in the late-middle-aged and elderly. When diagnosed in young adults, the disease process is often thought to be more aggressive and have a worse long-term outcome. Four hundred ninety patients presented to the Christie Hospital and Manchester Royal Infirmary between 1981 and 1990 with squamous cell carcinoma of the hypopharynx and cervical esophagus. Of this group, 24 patients (5%) received their diagnosis before the age of 45. A comparison is made with a control group of 156 (32%) patients who presented between the ages of 60 and 69 years. Analysis of tumor and nodal staging at presentation demonstrates no statistically significant difference between the 2 age groups. There is a higher incidence of a combination of smoking and alcohol abuse in the older age group, but it is of no statistical significance. There is no difference in 5-year survival results between the 2 groups. We conclude that patients with squamous cell carcinoma of the hypopharynx and cervical esophagus who receive their diagnosis under the age of 45 show no difference in tumor stage or long-term outcome when compared with a control group encompassing the mean age of presentation.

KEY WORDS — cervical esophagus, hypopharynx, squamous cell carcinoma, young adult.

INTRODUCTION

Squamous cell carcinoma arising in the head and neck is an unexpected finding in a patient under the age of 45 years. Its rarity, coupled with the often-high emotions associated with diagnosis, makes these cases easy to recall, especially when associated with a poor outcome. This can leave the impression that hypopharyngeal carcinoma in the young follows a more aggressive course.

Most studies examining squamous cell carcinoma in the young adult include data that encompass the entire head and neck region so that the numbers presented give meaningful results.[1-4] This practice, however, leads to the analysis of a series of tumors with different characteristics, including different ages at presentation, causations, tumor and nodal stages at presentation, treatment options, and long-term outcomes. This study analyzes a group of patients with squamous cell carcinoma of the hypopharynx and cervical esophagus who received their diagnoses under the age of 45. It compares this group with a larger series of patients, with diagnoses made over the same time period, whose age range encompassed the mean age of presentation.

PATIENTS AND METHODS

A retrospective case note review was performed on 490 patients presenting to the Christie Hospital and Manchester Royal Infirmary between 1981 and 1990 with a diagnosis of squamous cell carcinoma of the hypopharynx and cervical esophagus. Exclusion criteria included having undergone previous treatment for the same lesion at other hospitals. Tumor and nodal staging according to the UICC (1992) was confirmed by clinical examination, diagnostic imaging, and direct examination under general anesthesia, which enabled biopsy of the lesion for pathological diagnosis.

Twenty-four patients (5%) were under the age of 45 (33 to 44 years) at the time of diagnosis and are classified as young adults. The overall age range for patients presenting with squamous cell carcinoma of the hypopharynx and cervical esophagus was 33 to 95 years, with a mean age of 67.4 years. This study compares the young adult group with a control group of 166 patients who presented between the ages of 60 and 69 years. The control group was chosen because it encompasses the average age of presentation and excludes elderly patients who would affect crude 5-year survival figures because of alternative treatment protocols and a presumed higher rate of intercurrent illness.

The treatment protocols for both patient groups

From the Department of Otolaryngology–Head and Neck Surgery, Manchester Royal Infirmary, Manchester, England.

CORRESPONDENCE — Patrick R. Axon, FRCS (ORL), Dept of Otolaryngology–Head and Neck Surgery, Manchester Royal Infirmary, Oxford Road, Manchester, M13 9WL, England.

COMPARISON OF TREATMENT METHODS IN BOTH AGE GROUPS

Patient Age (y)	*Palliative or No Treatment*	*Surgery*	*Radiotherapy*	*Surgery and Radiotherapy*	*Chemotherapy and Radiotherapy*	*Chemotherapy*
Under 45	8 (33%)	1 (4%)	8 (33%)	5 (21%)	2 (8%)	
60 to 69	64 (39%)	13 (8%)	76 (46%)	7 (4%)	4 (2%)	2 (1%)

are listed in the Table. Eight (33%) young adults and 64 (39%) control patients had palliative or no treatment. This was either because of patient refusal of more radical treatment options or because of advanced disease.

Single-method treatment was administered to 9 (38%) and 91 (55%) of the young adults and control patients, respectively. Surgical resection included pharyngolaryngoesophagectomy with mobilization of the stomach through the posterior mediastinum to enable pharyngogastric anastomosis. If there was palpable metastatic spread to the lymph nodes, a radical neck dissection was performed. The patients undergoing radiotherapy received a dose of 50 to 55 Gy administered over 21 days in 15 fractions. The treatment field encompassed the primary tumor, extending 3 cm below its inferior extent to include possible submucosal spread. Lower cervical nodes were included as standard, and the treatment field extended to include other regions of the neck if there was palpable metastatic lymph node spread.

Combination therapy was performed in 13 (54%) and 11 (7%) of the young adults and control patients, respectively. This included either radical neck dissection of palpable metastatic lymph node spread followed by radiotherapy to the primary site or radiotherapy followed by salvage surgery if tumor recurrence was deemed resectable. Chemotherapy was administered to a small group of patients as an adjunct to radiotherapy.

Data were analyzed for tumor and nodal staging at diagnosis, subsite, etiologic factors, including smoking and alcohol abuse, and 5-year survival status. The results are analyzed by the χ^2 test, with Yates' correction for continuity where appropriate (p value of <.05 is regarded as significant). Kaplan-Meier estimates of the different age group survival functions for both curative and palliative therapy are given and analyzed with a stratified log rank test.

RESULTS

Fifteen (63%) of the young adults were male, compared with 88 (53%) control patients ($\chi^2 = 0.456$, p = not significant). Subsite analyses showed only a minor difference between the patient groups (Fig 1A). Tumor was localized to the pyriform fossa in 8 (33%) young adults and 76 (46%) control patients, the postcricoid area in 11 (46%) young adults and 37 (22%)

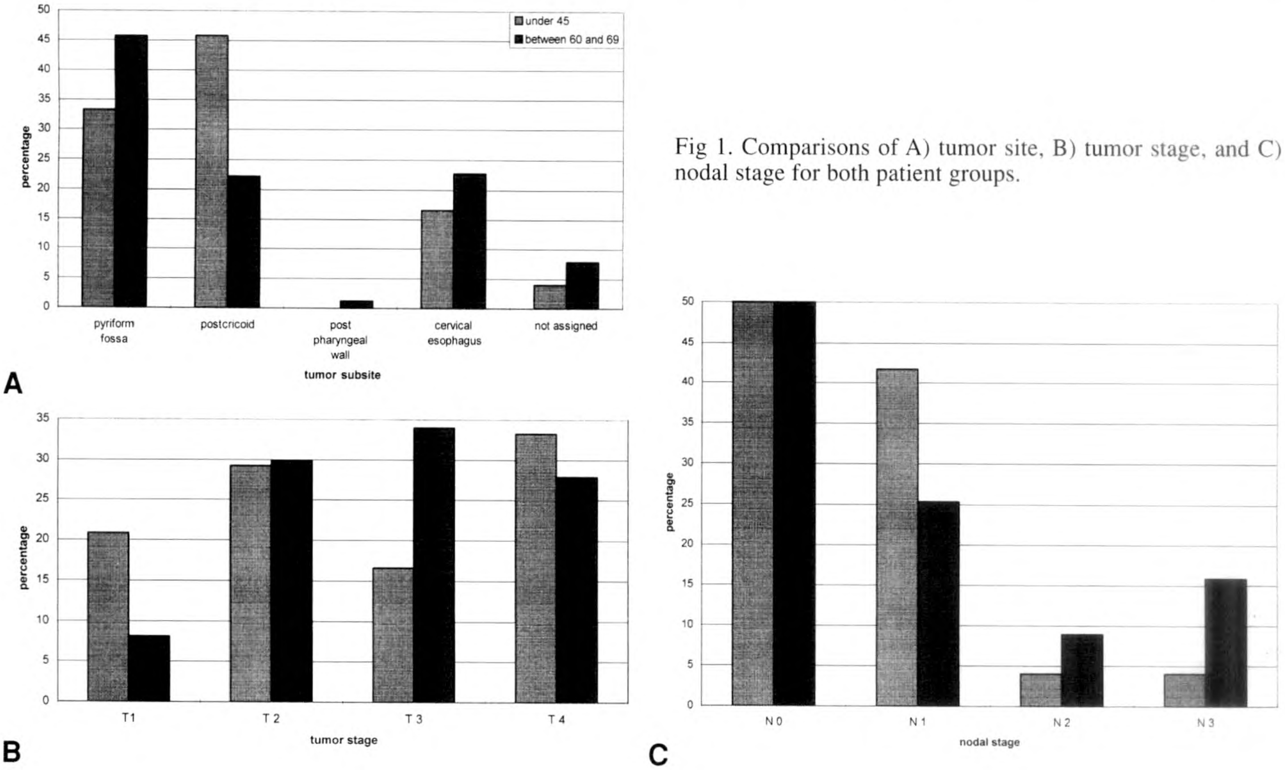

Fig 1. Comparisons of A) tumor site, B) tumor stage, and C) nodal stage for both patient groups.

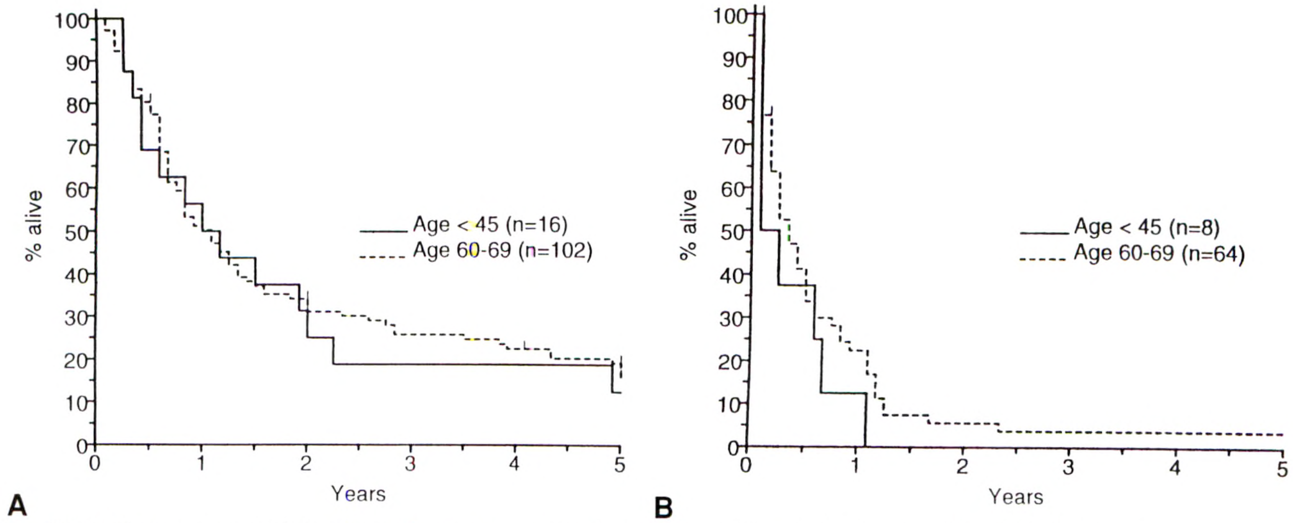

Fig 2. Five-year survival data for both age groups after A) treatment with curative intent and B) palliative or no treatment.

control patients, and the cervical esophagus in 4 (17%) young adults and 38 (23%) control patients ($\chi^2 = 5.79$, p = not significant). Tumor localized to the posterior pharyngeal wall was extremely rare, with only 2 (1%) patients presenting in the control group. A tumor subsite was unable to be assigned in 1 (4%) young adult and 13 (8%) control patients because of advanced disease at presentation (Fig 1A).

The UICC (1992) TNM tumor stage was calculated separately for the 2 groups of patients (Fig 1B). The number of young adults with tumor stage 1 was 5 (21%), tumor stage 2 was 7 (29%), tumor stage 3 was 4 (17%), and tumor stage 4 was 8 (33%). The number of patients in the control group presenting with tumor stage 1 was 12 (8%), tumor stage 2 was 44 (30%), tumor stage 3 was 50 (34%), and tumor stage 4 was 41 (28%; $\chi^2 = 5.5$, p = not significant). Tumor stage data were not available for 19 patients in the control group, who are therefore excluded.

Twelve (50%) of the young adults had nodal stage 0, 10 (42%) had nodal stage 1, 1 (4%) had nodal stage 2, and 1 (4%) had nodal stage 3 (Fig 1C). The number of patients in the control group with no nodal metastatic spread was 79 (50%), nodal stage 1 was 40 (25%), nodal stage 2 was 14 (9%), and nodal stage 3 was 25 (16%; $\chi^2 = 4.67$, p = not significant). There were incomplete nodal data for 8 patients in the control group, who are therefore excluded.

Etiologic factors, including smoking and heavy alcohol intake, were recorded in 18 (75%) and 131 (79%) of the young adults and control patients, respectively. Five (28%) young adults and 68 (52%) control patients had a combination of these 2 factors ($\chi^2 = 2.78$, p = not significant).

Sixteen (67%) young adults were treated with curative intent, and 8 (33%) were offered palliative therapy because of the advanced nature of the disease. This compared with 99 (60%) patients who had curative treatment in the control group. Of those treated with curative intent, a higher percentage of young adults received combination therapy as compared with the control group (see Table).

Kaplan-Meier estimates of the group survival functions are illustrated in Fig 2. The young adults who had curative therapy had a 5-year survival rate of 13%, and the patients in the control group had a 5-year survival rate of 16% (Fig 2A). The results of an analysis of survival for the patients undergoing palliative therapy were 0% and 3% for the young adults and the control group, respectively (Fig 2B). There was no statistically significant difference between these figures (stratified log rank test, p = .55).

DISCUSSION

The length of time between exposure to a carcinogen and the development of carcinoma is estimated to be in the region of 25 years.[1] As expected, squamous cell carcinoma of the hypopharynx and cervical esophagus arising in the young adult is uncommon, presumably because of the reduced period of exposure to recognized etiologic factors such as smoking and alcohol abuse. Nevertheless, patients do present within the third and fourth decades; therefore, other predisposing factors may play a role.

Basic science research has suggested that there is increased chromosome fragility after mutagen exposure in young adults with head and neck cancer when compared with the normal population.[5] The immunologic profiles, including lymphocyte function and humoral immune status, were found to be normal,[6] although 2 studies documented the development of head and neck carcinoma after immunosuppressive therapy.[2,7] It is recognized that the 2 main carcinogens, smoking and alcohol, are known to act synergistically.[8-10] A higher percentage of young adults would therefore be expected to have a combination of these 2 etiologic factors. Our study demonstrated a higher percentage of the control group as having a history of smoking and alcohol abuse, but the difference was of no statistical significance, a point that has been noted by Schantz et al.[11] If increased chromosome fragility after mutagen exposure is an important factor, carcinogens other than those associated with smoking and alcohol may be involved.

The young adults presented with less-advanced disease as assessed by the TNM classification, but the difference was of no statistical significance. This finding may indicate the younger patient's greater awareness of the gravity of his or her symptoms, unlike a possibly more stoical older age group. Delayed referral of young patients because of a lack of importance placed on often vague and nonspecific symptoms is unfounded.

Between 60% and 70% of patients were treated with curative intent — a low percentage when compared with other studies[1,4] analyzing the treatment outcome of upper aerodigestive tract carcinoma in young adults — perhaps because squamous cell carcinoma of the hypopharynx and cervical esophagus often presents late, has significant posttreatment morbidity, and is associated with a poor outcome.

A higher proportion of young adults received combination therapy, as either postoperative radiotherapy or salvage surgery. This difference most probably reflects the clinician's lower threshold for a second treatment method when confronted with tumor recurrence in the younger patient. There is, however, little difference in 5-year survival curves, indicating that age is not a significant factor for patient outcome. The more-aggressive treatment protocols that were used in some patients may have affected outcomes, but because only a small proportion underwent combination therapy, we do not believe this factor played a significant role. These data support the findings of other studies that the age of the individual does not determine prognosis.[1,4,12] The often-held perception that patients who present young have a worse outcome is most probably an indication of the greater impact that the case has on the clinician.

CONCLUSION

Young adults presenting with squamous cell carcinoma of the hypopharynx and cervical esophagus have a tumor and nodal staging at presentation similar to that of patients presenting between the ages of 60 and 69. Kaplan-Meier estimates of group survival rates indicate no statistical difference after treatment with curative intent. This study supports the increasing evidence that patient age is not a significant factor for determining prognosis in head and neck cancer.

REFERENCES

1. Clarke RW, Stell PM. Squamous carcinoma of the head and neck in the young adult. Clin Otolaryngol 1992;17:18-23.
2. Clark RM, Rosen IB, Laperriere NJ. Malignant tumors of the head and neck in a young population. Am J Surg 1982; 144:459-62.
3. Benninger MS, Roberts JK, Levine HL, Wood BG, Tucker HM. Squamous cell carcinoma of the head and neck in patients 40 years of age and younger. Laryngoscope 1988;98:531-4.
4. Lund VJ, Howard DJ. Head and neck cancer in the young: a prognostic conundrum? J Laryngol Otol 1990;104:544-8.
5. Schantz SP, Hsu TC, Ainslie N, Moser RP. Young adults with head and neck cancer express increased susceptibility to mutagen-induced chromosome damage. JAMA 1989;262:3313-5.
6. Schantz SP, Liu FJ. An immunologic profile of young adults with head and neck cancer. Cancer 1989;64:1232-7.
7. Newman AN, Rice DH, Ossoff RH, Sisson GA. Carcinoma of the tongue in persons younger than 30 years of age. Arch Otolaryngol 1983;109:302-4.
8. Decker J, Goldstein JC. Risk factors in head and neck cancer. N Engl J Med 1982;306:1151-5.
9. Wynder EL, Mushinski MH, Spivak JC. Tobacco and alcohol consumption in relation to the development of multiple primary cancers. Cancer 1977;40:1872-8.
10. Langman MJ. Epidemiology of cancer of the oesophagus and stomach. Br J Surg 1971;58:792-3.
11. Schantz SP, Byers RM, Goepfert H, Shallenberger RC, Beddingfield N. The implication of tobacco use in the young adult with head and neck cancer. Cancer 1988;62:1374-80.
12. von Doersten PG, Cruz RM, Rasgon BM, Quesenbury CP Jr, Hilsinger RL Jr. Relation between age and head and neck cancer recurrence after surgery: a multivariate analysis. Otolaryngol Head Neck Surg 1995;113:197-203.

Ann Otol Rhinol Laryngol 109:2000

SECRETORY DIFFERENTIATION OF SERIALLY PASSAGED NORMAL HUMAN NASAL EPITHELIAL CELLS BY RETINOIC ACID: EXPRESSION OF MUCIN AND LYSOZYME

JOO-HEON YOON, MD
KYUNG-SU KIM, MD
JEUNG-GWEON LEE, MD
SUNG-SHIK KIM, MD
IN YONG PARK, MD
SEOUL, KOREA

The purpose of this study was to subculture normal human nasal epithelial (NHNE) cells without compromising their ability to differentiate into secretory and ciliated cells and to study the effect of retinoic acid on mucous and serous secretions in passaged cells and to compare the expression of mucin and lysozyme in cultured cells with those in in vivo nasal epithelium. The subcultured cells were tested after every passage for secretory differentiation in air-liquid interface cultures. The cultured NHNE cells secreted mucin and lysozyme. The cells became squamous and mucin secretion decreased when retinoic acid was deleted from the culture media. Cells from passage 1 through passage 2 remained able to differentiate into mucous or squamous cells. Mucin gene 4 (MUC4), MUC5AC, MUC7, MUC8, and lysozyme messenger RNAs were expressed in passage 2 NHNE cells. In conclusion, passage 2 NHNE cell cultures retain features of normal epithelium and are suitable for many studies of upper airway cell biology.

KEY WORDS — lysozyme, mucin, normal human nasal epithelial cells, retinoic acid, subculture.

INTRODUCTION

Culturing airway epithelial cells is a very useful method for studying the effects of environmental pollution, viral and bacterial infections, and chemical carcinogens on the function of differentiated airway epithelial cells. At present, many kinds of epithelial cell culture methods have been introduced, including submerged,[1] suspension,[2] floating,[3] and air-liquid interface (ALI)[4,5] techniques. Until now, most studies were conducted on animal airway epithelial cells from guinea pigs,[6] rats,[7] and hamsters.[8] As well, some studies used primary culture cells from human airway epithelium. However, using primary cultures from human airway epithelial cells causes several problems, such as a limited amount of material available from 1 donor, contamination with pathogens, and significant donor-to-donor variability. Therefore, tumor cells, which are relatively easy to grow, and cell lines such as BEAS-2B or 9HTEo$^-$ have been used for studies of cellular response or physiological characteristics instead of human specimens. However, there have been continuing demands for a normal human airway epithelial cell culture, because of the fact that tumor cells cannot appropriately represent the physiological characteristics and cellular response of normal airway epithelial cells. In 1996, Gray et al[9] succeeded in subculturing passage 1 (P1) normal human tracheobronchial epithelial cells and completed their characterization.

Although the incidence of airway disease is much higher in the upper airway compared to the lower airway, only minor progress has been made in the field of research on upper airway epithelial cells. We wanted to obtain enough normal human nasal epithelial cells to conduct many studies on upper airway cell biology. The purpose of this study was 1) to subculture normal human nasal epithelial (NHNE) cells without compromising their ability to differentiate into secretory and ciliated cells, 2) to study the effect of retinoic acid (RA) on mucous and serous secretions in passaged cells, and 3) to compare the expression of mucin and lysozyme in cultured cells with those in in vivo nasal epithelium.

MATERIALS AND METHODS

Expansion, Subculturing, and Cryopreservation of NHNE Cells. Human nasal tissues were obtained during surgery from inferior turbinate mucosa of 5 patients suffering from septal deviation or maxillary cancer. Specimens used in these studies were from the macroscopically normal areas adjacent to the tumor. This procedure was approved by the Ethics Committee of Yonsei University College of Medicine. Tissues were treated with 1.0% Pronase (type XIV protease, Sigma, St Louis, Mo) in a 1:1 mixture of Dulbecco's modified Eagle's medium and Ham's nutrient F12 (DMEM/F12) supplemented with penicillin G sodium (50 IU/mL) and streptomycin sulfate (50 μg/mL) for 16 to 20 hours at 4°C. Dissociated epithelial cells were washed 3 times in DMEM/F12 con-

---

From the Department of Otorhinolaryngology, Yonsei University College of Medicine, Seoul, Korea.

CORRESPONDENCE — Joo-Heon Yoon, MD, Dept of Otorhinolaryngology, Yonsei University College of Medicine, CPO Box 8044, Seoul, Korea 120-752.

taining antibiotics and suspended in DMEM/F12 supplemented with antibiotics and 10% fetal bovine serum. Cells were preplated on a plastic dish at 37°C for 1 hour in order to eliminate fibroblasts by differential attachment to plastic. Suspended epithelial cells were seeded at 3×10^4 cells per dish (500 cells per square centimeter) into 10-cm plastic tissue culture dishes. The culture medium used was bronchial epithelial growth medium (BEGM; Clonetics Corp) containing hydrocortisone 21-hemisuccinate (0.5 µg/mL), insulin (5 µg/mL), transferrin (10 µg/mL), epinephrine hydrochloride (0.5 µg/mL), 3,3',5-triido-L-thyronine (6.5 ng/mL), gentamicin sulfate (50 µg/mL), and amphotericin B (50 µg/mL), all supplied by Clonetics and further supplemented with epidermal growth factor (EGF; 25 ng/mL; Collaborative Research, Bedford, Mass), all-trans RA (10^{-7} mol/L; Sigma), bovine serum albumin (1.5 µg/mL; Sigma), and bovine pituitary extract (1% vol/vol; Pel-Freez Biologicals, Rogers, Ark). Cultures were maintained at 37°C in an atmosphere of 5% carbon dioxide in air. The culture medium was changed on day 1 after seeding and every other day thereafter until the cultures reached 50% to 60% confluency, at which time they were dissociated with trypsin–ethylenediaminetetraacetic acid (EDTA) treatment by means of the methods and reagents supplied by Clonetics Corp. The cell number was determined by hemocytometer, and cultures were seeded as described above for subsequent passages. Cells not used for reestablishing cultures were either suspended in supplemented BEGM containing 10% dimethyl sulfoxide at 1 to 2 $\times 10^6$ cells per milliliter and stored frozen in liquid nitrogen for future use, or else were tested for their differentiation competence.

Air-Liquid Interface Culture. Serially passaged NHNE cells (10^5 cells per culture, 2×10^4 cells per square centimeter) were seeded in 0.5 mL of culture medium onto the surface of rat tail, collagen type 1 gel–coated (3.0 g/mL; Collaborative Research), 24.5-mm, 0.45-µm pore size, Transwell-clear (Costar Co, Cambridge, Mass) culture inserts. Cells were cultured in a 1:1 mixture of BEGM:DMEM containing the same concentrations of all supplements described above, except that 0.5 ng/mL of EGF was used. The cultures were grown submerged for the first 7 days, during which time the culture medium was changed on day 1 and every other day thereafter. The ALI was created on day 9 by removing the apical medium and feeding the cultures only from the basal compartment. The culture medium was changed daily after creation of an ALI. To dissociate cells grown on collagen gels in ALI cultures, the culture medium was removed and both the apical and basal compartments were washed with 1.5 mL of phosphate buffered saline (PBS). The apical wash was saved for detecting secretions produced by the cultures. One milliliter of 3× trypsin-EDTA (10× stock; GIBCO-BRL, Grand Island, NY) was added to the apical compartment. Cultures were incubated at 37°C until cell detachment occurred. The cells were resuspended in PBS and visually counted by hemocytometer or used for cytospin slides for immunocytochemical staining.

Histology and Immunocytochemistry. Cultures were fixed with 10% neutral buffered formalin and embedded in paraffin. Five micron–thick sections were cut and stained with hematoxylin and eosin. Cytospin slides were made with 2×10^4 cells per each slide and fixed in a 1:1 mixture of acetone and methanol and stored at 4°C until stained. Secretory cells were detected with a monoclonal antimucin antibody (H6C5; a generous gift from Dr C. W. Davis, University of North Carolina, Chapel Hill, NC), and an antibody against β-tubulin (Sigma) was used to stain ciliated cells. The mean number of positive cells with β-tubulin and H6C5 antibody was determined by scoring 3,000 cells on each slide, and statistical comparisons were made by Student's *t*-test.

Immunodetection and Quantitation of Mucin and Lysozyme. Apical secretions accumulating over a 24-hour period were collected. Intracellular levels of mucin and lysozyme were measured from cell lysates obtained from enzymatically isolated in vivo surface epithelial cells and cultures of passage 2 (P2) NHNE cells. Dissociated cells were pelleted, washed, and lysed with 50-mmol/L Tris buffered saline containing 1% Tween-20 (Bio-Rad, Hercules, Calif), 1-mmol/L EDTA, and protease inhibitors (Complete, Boehringer Mannheim, Indianapolis, Ind) and briefly sonicated. Mucin and lysozyme were detected by immunoblot assay. Purified mucin (a generous gift from Dr C. W. Davis) and lysozyme (Sigma) were used as standards. Mucin was detected with the monoclonal antimucin antibody H6C5, and lysozyme was detected with a polyclonal anti-human lysozyme antibody (DAKO, Carpinteria, Calif). Dilutions of apical secretions and standards were applied to nitrocellulose membranes, incubated with the appropriate primary antibody, and reacted with horseradish peroxidase–conjugated goat anti-mouse or anti-rabbit IgG. The signal was detected by chemiluminescence (ECL kit; Amersham, Little Chalfont, England), and a standard curve was generated by a linear regression analysis from which the concentration of individual samples could be determined. The specificity of the human anti-human lysozyme antibody was confirmed by Western blot analysis. The number of cells per culture was determined by visual cell counts on dissociated cell suspensions with a hemocytometer. The data were represented as the mean ± SD of triplicate cultures from the same experiment. Statistical comparisons were made with Student's *t*-test.

RT-PCR for Mucin and Lysozyme mRNA. Because the lysozyme messenger RNA (mRNA) levels were not reliably detected by Northern blot analysis and the analysis of mucin gene expression by Northern analysis is complicated by the polydispersity of most mucin messages, which makes specific detection and reliable measurement tenuous, we used a reverse transcription (RT)–polymerase chain reaction (PCR) (RT-PCR) for the detection of mucin and lysozyme mRNA. Oligonucleotide primers were designed according to the published sequences for human mucin gene 2 (MUC2; Genbank accession No. L21998, 440 base pair [bp], 5' primer: TGCCTGGCCCTGTCTTTG; 3' primer: CAGCTCCAGCATGAGTGC); human MUC4 (Genbank accession No. M64594, 303 bp, 5' primer: TTAAATACTGCCCTGCAC; 3' primer: TTTCTTCCTGATGAGCAC); human MUC5AC (Genbank accession No. U06711, 680 bp, 5' primer: TCCGGCTCATCTTCTTCC, 3' primer: ACTTGGGCACTGGTGCTG); human MUC5B (Genbank accession No. Z72496, 338 bp, 5' primer: ACTCCAGAGACTGTCCACAC, 3' primer: TACCACTGGTCTGTGTGCTA); human MUC7 (Genbank accession No. L13283, 209 bp, 5' primer: CCACACCTAATTCTTCCC, 3' primer: CTATTGCTCCACCATGTC); human MUC8 (Genbank accession No. U14383, 239 bp, 5' primer: ACAGGGTTTCTCCTCATTG, 3' primer: CGTTTATTCCAGCACTGTTC); and human lysozyme (Genbank accession No. J03801, 5' primer: CTCTCATTGTTCTGGGGC; 3' primer: ACGGACAACCCTCTTTGC). Oligonucleotide amplimers for β2 microglobulin (β2M, which was used as a control gene for RT-PCR) were purchased from Clontech Laboratories; they generated a 335 bp PCR fragment. The RT-PCRs were performed with a Perkin Elmer Cetus DNA Thermal Cycler according to the manufacturer's recommendations. Total RNA (1 μg per 20 μL reaction volume) was reverse-transcribed into complementary DNA (cDNA) with random hexanucleotide primers and Moloney murine leukemia virus reverse transcriptase. Forty percent for mucin and lysozyme or 4% for β2M of the resulting cDNA was amplified with 0.2 mmol/L of each primer. The optimized concentration of magnesium chloride in the PCR was 1.5 mmol/L for MUC4, MUC5AC, MUC5B, MUC7, MUC8, lysozyme, and β2M and was 2.5 mmol/L for MUC2. Denaturation was carried out at 95°C for 1 minute. The annealing temperature was 55°C for MUC4, MUC7, MUC8, and lysozyme, and 60°C for MUC2, MUC5AC, and β2M for 1 minute; extension was performed at 72°C for 1 minute.

We used comparative kinetic analysis to compare mRNA levels for each gene for each set of culture conditions. The PCR products were separated by electrophoresis on a 2% Seakem agarose gel (FMC, Rockland, Me) containing 50-ng/mL ethidium bromide and photographed with Polaroid type 55 film. The negatives were scanned on a Molecular Dynamics densitometer (Sunnyvale, Calif), and the signal was analyzed with ImageQuant software. The linear range for the PCR was established by plotting the intensity of the signal versus the PCR cycle number. The linear range for lysozyme was found to be between 25 and 30 cycles, and that for β2M, between 26 and 31 cycles. In order to verify that the amplified products were from mRNA and not genomic DNA contamination, negative controls were performed by omitting reverse transcriptase from the RT reaction. In the absence of reverse transcriptase, no PCR products were observed. Specific amplification of lysozyme mRNAs was confirmed by the sequencing (dsDNA Cycle Sequencing System, Gibco-BRL) or PCR fragments.

RESULTS

Expansion of NHNE Cells. Suspended epithelial cells were seeded at 3 × 10^4 cells per dish (500 cells per square centimeter) into 10-cm plastic tissue culture dishes. When the cultures reached 50% to 60% confluency, they were subcultured. At each passage, aliquots of cells not used for subculturing were frozen in liquid nitrogen. The cultures grew rapidly for the first 3 passages, resulting in a 20- to 40-fold expansion with each subculture. However, P4 cells attached well to plastic dishes, but grew very poorly. The original cell inoculum had undergone more than 500-fold expansion, including P3 cells.

Growth Curve and Mucus Secretion of Passage 2 NHNE Cells in ALI Cultures as Function of Time. Passage 2 cells were seeded on collagen type 1 gel–coated permeable membranes at a seeding density of 10^5 cells per membrane, ie, 2 × 10^4 cells per square centimeter, in a 1:1 mixture of BEGM and DMEM to test the differentiating potential. Cells grew rapidly and reached 90% confluency on day 9. An ALI was created on day 9 for all subsequent experiments. The number of cells increased in a time-dependent manner between days 9 and 16 and thereafter decreased slightly (Fig 1A). Peak cell densities of >2 × 10^6 cells per culture between days 16 and 22 were noted. In these cultures, mucin secretion increased in a time-dependent manner between days 9 and 18 after plating (Fig 1B). The mucin secretions at each time point were 130.7 ± 19.8 μg/10^6 cells on day 16, 213.0 ± 11.5 μg/10^6 cells on day 18, and 165.6 ± 12.6 μg/10^6 cells on day 22. Because cell growth and mucin secretion reached a plateau phase on day 16, mucin

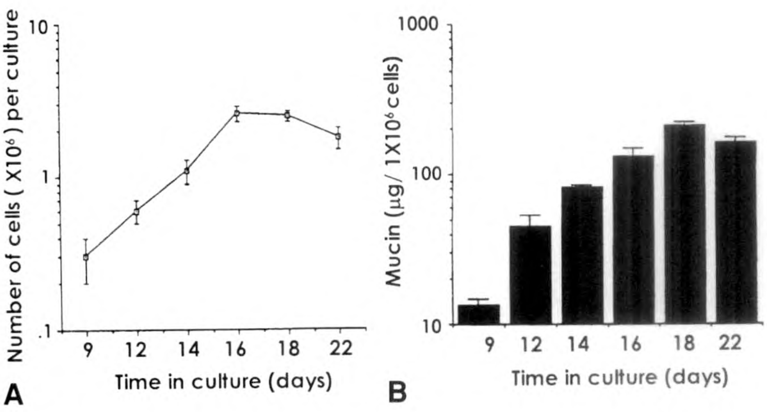

Fig 1. Growth and mucus secretion of passage 2 normal human nasal epithelial (NHNE) cells in air-liquid interface culture. A) 10^5 Cells were plated in bronchial epithelial growth medium and Dulbecco's modified Eagle's medium (1:1); duplicate cultures per time points. B) Dot blot analysis of apical secretions using H6C5 antibody. Values represent mean ± SD of triplicate cultures.

and secretion were routinely quantitated on day 16. Ciliogenesis confirmed by immunocytochemistry using the β-tubulin antibody usually started on day 12 in some areas in which focal high cell density existed and there were less than 10% ciliated cells in RA-sufficient cultures (Fig 2).

Secretory Cell Differentiation of Serially Passaged NHNE Cells on Day 16 Culture. Cytospin slides for immunostaining were made on day 16. The mean number of positive cells with an antimucin antibody (H6C5) was determined by scoring 3,000 cells on each slide with passaged cells. The numbers of cells on day 16, with P1, P2, and P3 cells, were 4.3 ± 0.6 ($\times 10^6$), 2.5 ± 0.3 ($\times 10^6$), and 1.8 ± 0.6 ($\times 10^6$), respectively. The number of cells decreased slightly with succeeding passages (Table 1). We defined β-tubulin–positive cells as secretory cells in this study. The percentages of secretory cells in P1, P2, and P3 cells were 38% ± 2.6%, 39.1% ± 2.0%, and 35.1% ± 3.6%, respectively. There was no difference in the percentage among serially passaged cells. Passage 4 cells attached to plastic dishes, but failed to grow (Table 1).

Effect of RA on Mucin and Lysozyme Secretion and Histology. The apical secretions from day 16 cultures grown in the absence or presence of RA were collected and assayed. Table 2 summarizes the data from 1 representative experiment. In all, 3 experiments were conducted showing the same RA effects. The levels of mucin secretion in passaged cells were 26.8 ± 0.4 µg/10^6 cells in P1, 50.8 ± 5.9 µg/10^6 cells in P2, and 62.4 ± 13.8 µg/10^6 cells in P3 in the presence of RA. When we removed RA from the culture medium, the levels of mucin secretion were undetectable in P1, 1.5 ± 0.3 µg/10^6 cells in P2, and 12.8 ± 3.0 µg/10^6 cells in P3. Removal of RA from the culture medium resulted in a marked reduction of mucin irrespective of the passage. However, when we removed RA from the culture medium with the P3 cells, the level of mucin secretion increased about 8.5-fold compared to that of P2 cells in the absence of RA, while P3 cells secreted 47.8% of the level of mucin secretion of P1 cells in the presence of RA. This suggested that P3 cells may be losing a characteristic of RA responsiveness (Table 2).

In the presence of RA, the levels of lysozyme secretion in passaged cells were 0.5 ± 0.03 µg/10^6 cells in P1, 1.4 ± 0.02 µg/10^6 cells in P2, and 2.7 ± 1.1 µg/

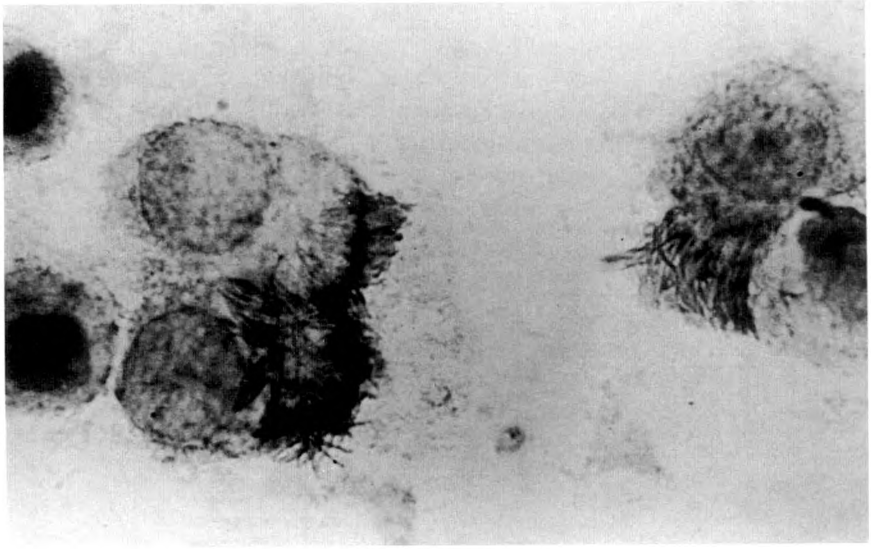

Fig 2. Immunocytochemistry of passage 2 NHNE cells on day 16 using β-tubulin antibody. Heavily stained cilia are evident.

TABLE 1. GROWTH AND SECRETORY CELL DIFFERENTIATION OF SERIALLY PASSAGED NORMAL HUMAN NASAL EPITHELIAL CELLS ON DAY 16 OF CULTURE

Passage	*No. of Cells per Culture*	*Secretory Cells (%)*
1	4.3 ± 0.6	38.0 ± 2.6
2	2.5 ± 0.3	39.1 ± 2.0
3	1.8 ± 0.2	35.1 ± 3.6
4	Cells did not grow	

Data are mean ± SD.

Secretory cells — anti-mucin antibody (H6C5)–positive cells.

10^6 cells in P3. When we removed RA from the culture medium, the levels of lysozyme secretion were 6.8 ± 0.7 μg/10^6 cells in P1, 5.9 ± 0.3 μg/10^6 cells in P2, and 1.5 ± 0.1 μg/10^6 cells in P3. In the absence of RA, 5- to 15-fold higher levels of lysozyme were detected in all 3 experiments when we used P1 and P2 cells. However, when we removed RA from the culture medium with the P3 cells, the level of lysozyme secretion decreased about 4-fold compared to that of P2 cells in the absence of RA, while P3 cells secreted 40% of the level of lysozyme secretion for P1 cells in the presence of RA. This also suggested that P3 cells may be losing a characteristic of RA responsiveness (Table 2).

Histologic examination of day 16 cultures in P1 and P2 cells revealed a uniform, stratified squamous epithelium in the absence of RA (Fig 3B). In contrast, RA-sufficient cultures showed mostly mucociliary epithelium (Fig 3A), although the morphology of the RA-sufficient cultures varied. However, P3 cells in the absence of RA did not show a typical morphology for squamous epithelium (data not shown). All these results also suggested that P3 cells might lose some characteristics of RA responsiveness.

Comparison of Protein and mRNA Levels of Mucin and Lysozyme in NHNE Cells From In Vivo Tissue and Fully Differentiated Passage 2 NHNE Cells. We next wanted to compare the intracellular protein levels and mRNA levels of mucin and lysozyme between the surface epithelial cells from in vivo tissue and fully differentiated P2 NHNE cells. The level of intracellular mucin was 814.9 μg/10^6 cells and the level of intracellular lysozyme was 20.0 μg/10^6 cells in the surface epithelial cells from in vivo tissue. The level of intracellular mucin was 131.4 ± 9.1 μg/10^6 cells and the level of intracellular lysozyme was 7.6 ± 2.3 μg/10^6 cells in fully differentiated P2 NHNE cells. The levels of mucin and lysozyme in cultured cells were 16% and 38%, respectively, of those in in vivo cells (Table 3).

TABLE 2. MUCIN AND LYSOZYME SECRETION OF CULTURED NORMAL HUMAN NASAL EPITHELIAL CELLS ON DAY 16 OF CULTURE IN PRESENCE OR ABSENCE OF RETINOIC ACID

	Mucin		*Lysozyme*	
Passage	*–RA*	*+RA*	*–RA*	*+RA*
1	ND	26.8 ± 0.4*	6.8 ± 0.7	0.5 ± 0.03*
2	1.5 ± 0.3	50.8 ± 5.9*	5.9 ± 0.3	1.4 ± 0.02*
3	12.8 ± 3.0	62.4 ± 13.8*	1.5 ± 0.3	2.7 ± 1.1

Data are mean ± SD in micrograms per 1 × 10^6 cells.

RA — retinoic acid, ND — not detected.

*$p < .05$ compared to RA-deficient cultures.

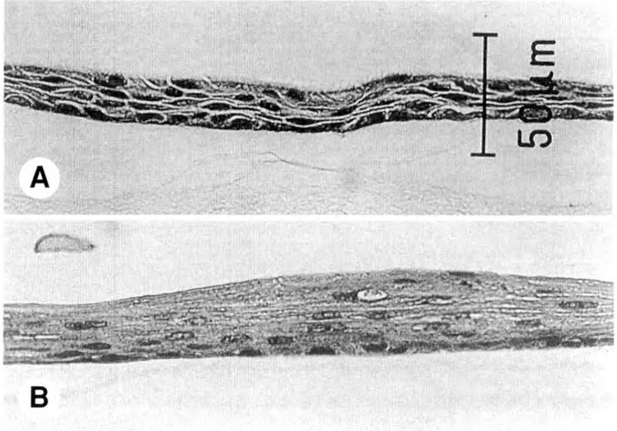

Fig 3. Histologic appearance of passage 2 NHNE cells on day 16 cultures in A) presence and B) absence of retinoic acid. A) Polarized, cuboidal cells with cilia. B) Number of stratified cells with horizontal nucleus.

We determined the levels of MUC2, MUC4, MUC5AC, MUC5B, MUC7, and MUC8 mRNAs and lysozyme mRNA in NHNE cells from in vivo tissue, fully differentiated P2 NHNE cells, and human tracheal RNA (Fig 4). All genes tested in this study were expressed in NHNE cells from in vivo tissue and human tracheal RNA, although their signal intensity varied. The MUC2 and MUC5B mRNA levels were similarly expressed in NHNE cells from in vivo tissue and human tracheal RNA, but not in fully differentiated P2 NHNE cells. The MUC4 mRNA levels were weakly expressed in NHNE cells from in vivo tissue and human tracheal RNA, but were strongly expressed in fully differentiated P2 NHNE cells. The MUC5AC mRNA levels were similar among the 3 groups. The MUC7 mRNA levels were weakly expressed in NHNE cells from in vivo tissue

TABLE 3. COMPARISON OF MUCIN AND LYSOZYME PROTEIN LEVELS BETWEEN NORMAL IN VIVO NASAL EPITHELIUM AND FULLY DIFFERENTIATED CULTURED NASAL EPITHELIUM

	Mucin	*Lysozyme*
Normal in vivo nasal epithelium (mean)	814.9	20.0
Fully differentiated cultured nasal epithelium (mean ± SD)	131.4 ± 9.1	7.6 ± 2.3

Data are micrograms per 10^6 cells.

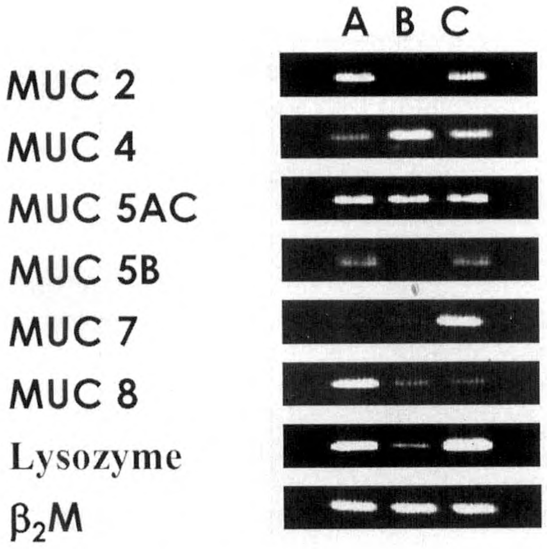

Fig 4. Comparison of mucin messenger RNA (mRNA) levels and lysozyme mRNA levels in NHNE cells from in vivo tissue (A), fully differentiated passage 2 NHNE cells (B), and human tracheal RNA (C) by reverse transcription–polymerase chain reaction. Levels of MUC2, MUC5B, MUC8, and lysozyme mRNA decreased in fully differentiated passage 2 NHNE cells compared to NHNE cells from in vivo tissue. However, MUC5AC mRNA levels were not altered. MUC7 mRNA levels were strongly expressed in human tracheal RNA compared to NHNE cells whether they were cultured or not. MUC8 mRNA levels were strongly expressed in NHNE cells from in vivo tissue compared to fully differentiated passage 2 NHNE cells and human tracheal RNA. Control gene, β2M, was not altered.

and fully differentiated P2 NHNE cells, but were strongly expressed in human tracheal RNA. The MUC8 mRNA was expressed in all groups, but strongly expressed in NHNE cells from in vivo tissue. The lysozyme mRNA levels were weakly expressed in fully differentiated P2 NHNE cells, but were strongly expressed in NHNE cells from in vivo tissue and human tracheal RNA. The β2M mRNA levels were not altered.

DISCUSSION

Owing to the development of cell culture techniques, it is presently possible to induce differentiation of airway epithelial cells having morphological, physiological, and biochemical characteristics similar to those in in vivo airway epithelial cells. The current drawback in research on human airway epithelial cells is the difficulty in obtaining a sufficient number of cells. This limitation can be overcome by accomplishing subculture of airway epithelial cells while maintaining their ability to differentiate into secretory and ciliated epithelial cells.

The authors succeeded in subculturing NHNE cells down to P4 on plastic dishes containing serum-free culture media using cells from 5 different donors. On day 16 of culture, the amount of mucin secretion by P2 cells from each donor was sufficient, ranging from 50 to 150 μg, and the differentiation had reached its plateau phase. Thus, day 16 of culture can be considered as the appropriate time for collecting cells to analyze the results.

Although the number of nasal epithelial cells on day 16 of culture decreased as the passage progressed from P1 to P4, the percentage of secretory cells was not significantly changed, as confirmed by immunocytochemistry using antimucin antibody H6C5 (Table 1). The amount of mucin secretion showed a tendency to slightly increase as the passage progressed, even though the percentage of secretory cells did not show any significant changes between different passages. This result suggests that the amount of mucin secretion from a uniform number of cells increases as the passage progresses.

Regarding the characteristics of cells in each passage, we noticed that P1 and P2 cells maintained their secretory ability, as well as their potential to differentiate into secretory or ciliated epithelial cells. We also observed that P3 cells can differentiate into mucin-secreting ciliated epithelial cells in the presence of RA. However, in the absence of RA, typical squamous epithelial cells were not seen, and the amount of mucin secretion by P3 cells increased 8.5 times and the amount of lysozyme showed a 25% decrease compared to those of P2 cells. These results imply that the cellular response to RA becomes a little insensitive. Therefore, we can predict that P3 cultured NHNE cells partially lose the characteristics of airway epithelial cells. In addition, as the passage progressed, the number of cells on day 16 of culture decreased (Table 1), possibly due to the aging of cells. Differentiated P1 and P2 cells showed no significant morphological or physiological differences from in vivo cells. By contrast, P4 cells could not be differentiated, even though the cells initially attached to the plastic culture dishes. Therefore, P2 cells are thought to be the most appropriate subcultured cells for multipurpose research, including nasal secretion and differentiation of upper airway epithelial cells.

Two major cells producing airway secretion are mucous cells secreting mucin and serous cells producing lysozyme lactoferrin, secretory IgA, and secretory leukocyte protease inhibitor. There are 2 types of airway secretion by 2 different types of epithelial cells: serous and mucous. Mucin is the major airway secretion produced by mucous cells, and nonmucin secretions such as lysozyme, lactoferrin, secretory IgA, and secretory leukocyte protease inhibitor are secreted by serous cells.[10] The authors selected mucin as a major mucous secretion and lysozyme as a serous secretion to study airway secretion. Quantitation of lysozyme secretion was obtained by calculating the amount of intracellular lysozyme per 10^6 epithelial cells. Since sufficient amounts of mucin and lysozyme were detected in serially subcultured nasal epithelial cells by immunoblot, cultured nasal epithelial cells were shown to be capable of secreting airway secretions similar to those in vivo.

As previously reported, retinoids are a well-known important factor for growth and differentiation of airway epithelial cells. In many animals, such as mice, hamsters, and rabbits, airway epithelial cells cultured with serum-free media without RA undergo squamous metaplasia.[11-13] However, by contrast, other studies have reported that cells from RA-deficient cultures can still differentiate into mucociliary epithelia.[14,15] It is not exactly clear why such a discrepancy resulted, but in some instances, it may be due to a saturated amount of RA already present in the serum that prevented epithelium from undergoing squamous metaplasia. Moreover, if bovine pituitary extract or hypothalamus extract is used instead of serum, the amount of retinoids can vary depending on the collection methods. Therefore, reinvestigation of the effect of RA in our culture media containing bovine pituitary extract is needed. In our culture system, the minimal concentration of RA required for cultured cells to differentiate into mucociliary epithelium was 10^{-9} mol/L, and squamous metaplasia occurred uniformly below that concentration (data not shown). In addition, the authors found that RA increased the amount of mucin secretion 50 times, although that is somewhat opposed to results of another study showing that retinol lowered the level of MUC2, 1 of the 9 mucin genes.[16]

Another interesting fact is that lysozyme secretion decreased while mucin secretion increased, which correlated well with the results of Gray et al,[9] even though these 2 kinds of secretions originate from the same epithelial cells. The difference in the amount of secretions may indicate that these 2 secretions have different regulation mechanisms, or it may be the result of a secondary phenomenon, that of morphological changes in the cultured cells mainly caused by RA.

The authors also investigated the amount of intracellular mucin and lysozyme along with their mRNA levels in fully differentiated P2 NHNE cells, and compared them to those of in vivo human nasal epithelial cells. The levels of intracellular mucin and lysozyme in cultured cells were 6 times and 2.5 times lower than those of in vivo cells. This may be due to morphologically immature mucous cells in cultured nasal epithelium, which is incapable of producing a sufficient amount of secretion.

For the message level of mucin, MUC3 and MUC6, which had been previously reported not to be expressed in human nasal mucosa, and membrane-bound mucin (MUC1) were excluded from this study. In our study, MUC2, MUC4, MUC5AC, MUC5B, MUC7, MUC8, and lysozyme were all expressed in human nasal epithelial cells, as well as human tracheal RNA, which was used as a positive control. However, MUC2 and MUC5B were barely expressed in fully differentiated P2 NHNE cells. The MUC4 mRNA expression was stronger in cultured nasal epithelial cells than in cells from in vivo tissue, but MUC8 and lysozyme mRNA expression was stronger in cells from in vivo tissue than cultured NHNE cells. Meanwhile, mRNA levels of MUC5AC and MUC7 were similarly expressed in both NHNE cells from in vivo tissue and fully differentiated P2 NHNE cells. These results indicate that there is organ specificity in mucin genes. When the results of message and protein levels were compared, cultured NHNE cells showed an 84% decrease in the amount of mucin secretion compared to that of cells from in vivo tissue. This result was considered to be related to the decreased levels of MUC2, MUC5B, and MUC8 in cultured NHNE cells. In the evaluation of lysozyme, there was a decrease in the level of protein in cultured NHNE cells compared to cells from in vivo tissue. The level of lysozyme mRNA was significantly lower in cultured NHNE cells. This suggests that secretory cells of cultured epithelial cells are not in a fully matured status.

In conclusion, the authors succeeded in subculturing human nasal epithelial cells without the cells' losing their potential capability of differentiation. As well, a differentiation method for P2 human nasal epithelial cells using an ALI culture technique was considered to be very effective in providing an excellent experimental model for research regarding the differentiation of human upper airway epithelial cells and their secretions.

ACKNOWLEDGMENTS — We thank Paul Nettesheim for his advice, William C. Davis for his gifts of purified mucin and antimucin antibody (H6C5), and Ja Seok Koo for his technical assistance.

REFERENCES

1. Ostrowski LE, Nettesheim P. Inhibition of ciliated cell differentiation by fluid submersion. Exp Lung Res 1995;21:957-70.
2. Bridges MA, Walker DC, Harris RA, Wilson BR, Davison AGF. Cultured human nasal epithelial multicellular spheroids: polar cyst-like model tissues. Biochem Cell Biol 1991;69:102-8.

3. Emerman JT, Pietelka DR. Maintenance and induction of morphological differentiation in dissociated mammary epithelium on floating collagen membrane. In Vitro 1977;13:316-28.

4. Adler KB, Schwarz JE, Whitcutt MJ, Wu R. A new chamber system for maintaining differentiated guinea pig respiratory epithelial cells between air and liquid phases. Biotechniques 1987;5:462-7.

5. Yoon JH, Gray T, Guzman K, Koo JS, Nettesheim P. Regulation of the secretory phenotype of human airway epithelium by retinoic acid, triiodothyronine, and extracellular matrix. Am J Respir Cell Mol Biol 1997;16:724-31.

6. Adler KB, Cheng PW, Kim KC. Characterization of guinea pig tracheal epithelial cells maintained in biphasic organotypic culture: cellular composition and biochemical analysis of released glycoconjugates. Am J Respir Cell Mol Biol 1990;2:145-54.

7. Kaartinen L, Nettesheim P, Adler KB, Randel SH. Rat tracheal epithelial cell differentiation in vitro. In Vitro Cell Dev Biol Anim 1993;29A:481-92.

8. Niles R, Kim KC, Hyman B, Christensen T, Wasano K, Brody J. Characterization of extended primary and secondary cultures of hamster tracheal epithelial cells. In Vitro Cell Dev Biol Anim 1988;24:457-63.

9. Gray T, Guzman K, Davis CW, Abdullah L, Nettesheim P. Mucociliary differentiation of serially-passaged normal human tracheobronchial epithelial cells. Am J Respir Cell Mol Biol 1996;14:104-12.

10. Basbaum CB, Jany B, Finkbeiner WE. The serous cell. Annu Rev Physiol 1990;52:97-113.

11. Marchok AC, Cone MV, Nettesheim P. Induction of squamous metaplasia (vitamin A deficiency) and hypersecretory activity in tracheal organ culture. Lab Invest 1975;33:451-6.

12. Chopra DP. Squamous metaplasia in organ culture of vitamin A–deficient hamster trachea: cytokinetic and ultrastructural alterations. J Natl Cancer Inst 1982;69:895-905.

13. Jetten AM, Brody AR, Deas MA, Hook ER, Rearick JI, Thacher SM. Retinoic acid and substratum regulate the differentiation of rabbit tracheal epithelial cells into squamous and secretory phenotype. Lab Invest 1987;56:654-64.

14. DeJong PM, van Sterkenberg MAJA, Kempenaar JA, Dijkman JH, Ponec M. Serial culturing of human bronchial epithelial cells derived from biopsies. In Vitro Cell Dev Biol Anim 1994;29A:379-87.

15. Christensen T, Breuer GR, Haddad CE, Niles RM. Quantitative ultrastructural analysis of the relationship between cell growth, shape change, and mucosecretory differentiation in cultured hamster tracheal epithelial cells exposed to retinoic acid. Am J Respir Cell Mol Biol 1993;9:287-94.

16. An G, Luo G, Wu R. Expression of MUC2 gene is down-regulated by vitamin A at the transcriptional level in vitro in tracheobronchial epithelial cells. Am J Respir Cell Mol Biol 1994;10:546-51.

≈

FUNCTIONAL ENDOSCOPIC SINUS SURGERY

Functional Endoscopic Sinus Surgery — Basic and Advanced Techniques will be held in Graz, Austria, September 7-9, 2000. For more information, contact Claire Zwerina, Secretary to Prof Stammberger, ENT-Department, University Hospital, Auenbruggerplatz 20, A-8036 Graz, Austria; fax ++43/316/385/3425.

Ann Otol Rhinol Laryngol 109:2000

CLINICAL NOTE

LARYNGEAL DIVERSION AND TRACHEOTRACHEAL SPEECH FISTULA FOR CHRONIC ASPIRATION

DESHENG WANG, MD
FUZHOU, CHINA

PAVEL DULGUEROV, MD
GENEVA, SWITZERLAND

Intractable aspiration is a life-threatening problem and often requires a procedure for blocking or separating the larynx from the bronchial tree. The disadvantage of these techniques is a compromise of phonation. We report the use of a speech fistula after laryngotracheal diversion to restore voice. It allows for the definitive treatment of aspiration, while maintaining the use of the vocal folds for phonation.

KEY WORDS — aspiration, laryngotracheal diversion, tracheotracheal speech fistula.

The normal human larynx has 3 major functions: as an air conduit, in airway protection, and in phonation. Phonatory ability is not essential for survival, and under certain circumstances, the voice has to be compromised in an effort to preserve the airway and prevent aspiration.

The treatment of aspiration comprises conservative management and surgical procedures. Patients who can handle their secretions, can talk, and do not present episodes of recurrent pneumonia may be managed with a variety of conservative techniques such as nasogastric or gastrostomy tubes, swallowing rehabilitation, food texture changes, head position adjustments, breath-holding, and postswallow volitional cough. For severe aspiration, a surgical intervention is necessary.

The surgical management of aspiration can be divided into adjuvant and definitive procedures.[1] The adjuvant procedures include tracheostomy, cricopharyngeal myotomy,[2,3] laryngeal suspension,[4] cricoid resection,[5] and various vocal fold medialization techniques.[6,7] If the patient presents intractable life-threatening aspiration, more definitive surgical procedures should be applied. The definitive procedures consist of various techniques for blocking or separating the larynx and the trachea and include laryngeal stenting,[8] glottic and supraglottic laryngeal closure,[9,10] laryngeal diversion,[11,12] and total laryngectomy. An obvious disadvantage of these definitive procedures is the compromise of phonation.

CASE REPORT

An 80-year-old man had had a left tonsillar squamous cell carcinoma that was treated with radical neck dissection and irradiation 21 years earlier. He developed progressive dysphagia, and a gastrostomy had been performed at another facility 7 months earlier. He presented with moderate dyspnea, and a stenosis of the oropharynx was diagnosed.

The stenosis was circumferential at the lower level of the tonsils. A tracheostomy and a transoral carbon dioxide laser resection of the stenosis were performed. A surprising finding was the presence of a separate exophytic lesion of the aryepiglottic fold, the biopsy of which revealed verrucous carcinoma. The performed treatment was a horizontal supraglottic laryngectomy, complicated by a large wound dehiscence. The pharyngocutaneous fistula required a pectoralis major myocutaneous flap for closure. However, the tongue–to–thyroid cartilage sutures were lost, with the result that the larynx was unsuspended and unprotected.

Severe aspiration ensued. Videofluoroscopy revealed a lack of pharyngeal contraction, cricopharyngeal dysfunction, a lack of laryngeal elevation, and severe aspiration. Despite intensive swallowing therapy, the situation did not improve, and a tracheostomy tube with an inflated cuff remained necessary. Even though the voice remained excellent, a total laryngectomy was considered.

Lindeman's technique[11] of laryngeal diversion and separation was used to manage the problem. The upper part of the trachea was dissected and separated from the esophagus, and severed between the second and third tracheal rings. The proximal stump was then sutured to the esophagus in an end-to-side anastomosis. The distal portion was sutured to the neck skin. The remaining larynx was kept intact.

From the Division of Head and Neck Surgery, Geneva University Hospital, Geneva, Switzerland. Dr Wang is currently in the ENT Department, Affiliated Union Hospital, Medical University of Fujian, Fuzhou, China.

CORRESPONDENCE — Pavel Dulguerov, MD, Division of Head and Neck Surgery, Geneva University Hospital, 24, rue Micheli-du-Crest, 1211 Geneva 14, Switzerland.

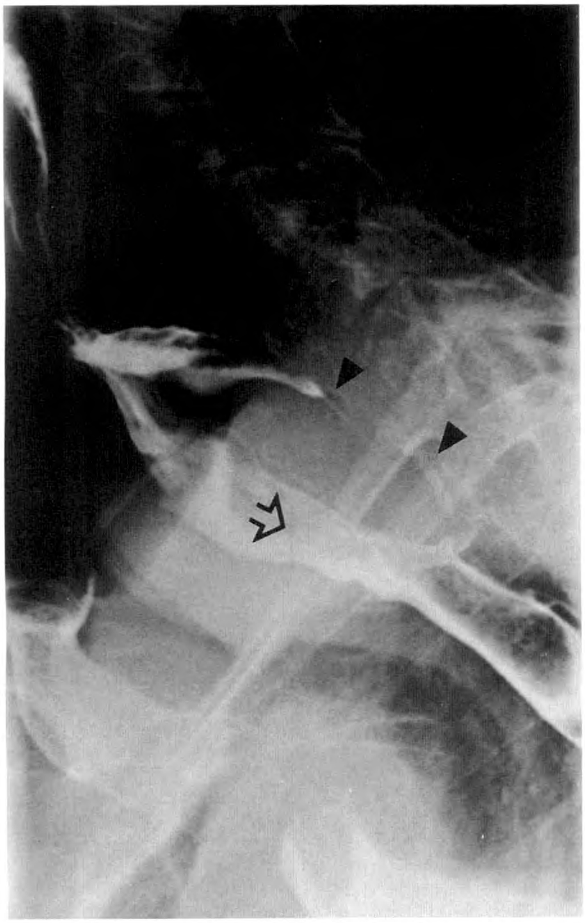

Fig 1. Postoperative videofluoroscopy still image print. Majority of contrast material passes through larynx and tracheoesophageal anastomosis (open arrow). Small portion of contrast material takes normal route through upper esophagus (arrowheads).

After this intervention, aspiration was totally controlled. The patient could swallow normally, and the tracheostomy tube was removed. Videofluoroscopy revealed that half of the contrast material was passing through the laryngeal-tracheal-esophageal route (Fig 1).

Two weeks later, to rehabilitate the phonation function, a fistula was created between the upper wall of the tracheostoma and the subglottic area, and an indwelling Blom-Singer prosthesis was placed under endoscopic guidance (Fig 2). The voice quality was satisfactory, and there was no aspiration. Finally, the gastrostomy was closed.

DISCUSSION

Aspiration can occur in patients with various pathological processes. It is important to determine the underlying cause, because this conditions the overall prognosis and hence will guide therapeutic decisions. For patients with intractable aspiration, the described procedures often result in alteration or loss of phonation. Laryngotracheal diversion appears to be the most frequently selected management,[11-15] because it allows a satisfactory treatment of aspiration while the larynx remains intact. Because the procedure is reversible, rehabilitation of dysphagia could result in an anatomically normal upper aerodigestive tract. In patients whose underlying disease process precludes any hope of resumption of safe swallowing, total narrow-field laryngectomy is advocated, although phonation is compromised permanently.

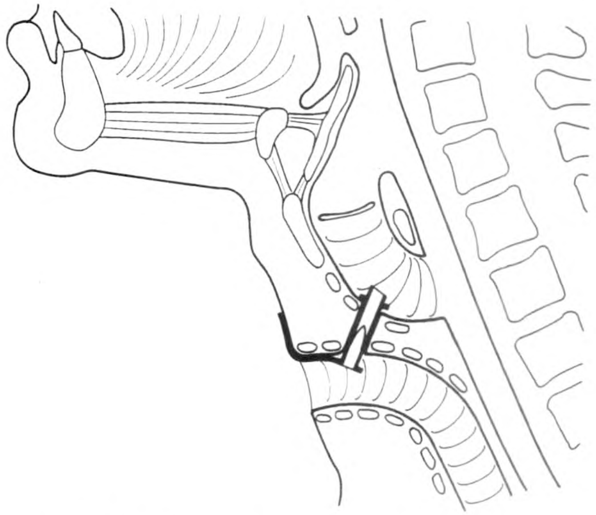

Fig 2. Schematic drawing of postoperative status. Tracheoesophageal anastomosis is depicted as performed for laryngeal diversion procedure. Tracheotracheal speech fistula is shown between 2 portions of transected trachea. Normal supraglottic structures are shown, contrary to situation in our patient.

In the case reported, the patient had no hope for recovery of safe swallowing. The severity of aspiration was due to several independent factors: the patient's advanced age, delayed effects of irradiation (poor pharyngeal function, cricopharyngeal dysfunction, decreased laryngeal ascension with swallowing[16]), the circumferential resection of the pharyngeal constrictors, the supraglottic laryngectomy, and the presence of an adynamic segment between the tongue and the glottis. Because of all these factors, success from swallowing reeducation and other surgical procedures appeared dim, and total laryngectomy was considered. In order to conserve the vocal folds, a laryngotracheal separation and diversion procedure was selected, in association with a Blom-Singer prosthesis for voice rehabilitation. Because the prosthesis is placed between the upper wall of the tracheostoma and the subglottic area, the vocal folds retain their normal vocal function when the patient phonates. The voice quality achieved is excellent.

Various tracheoesophageal prostheses have been widely used for voice rehabilitation after total laryngectomy. To our knowledge, there is no report about their use after laryngotracheal separation intervention, probably because few patients who undergo this procedure have the intact neuromuscular laryngeal control necessary for phonation.

We think that there is a potential for the use of speech prostheses in association with laryngotracheal diversion. The procedure allows for the definitive treatment of aspiration, while maintaining the use of the vocal folds for phonation. Further, the placement of a speech fistula does not preclude the reversibility of laryngotracheal diversion. Although we staged the procedures, both could be performed during the same general anesthesia.

REFERENCES

1. Miller FR, Eliachar I. Managing the aspirating patient. Am J Otolaryngol 1994;15:1-17.

2. Sasaki CT, Suzuki M, Horiuchi M, Kirchner JA. The effect of tracheostomy on the laryngeal closure reflex. Laryngoscope 1977;87:1428-33.

3. Berg HM, Jacobs JB, Persky MS, Cohen NL. Cricopharyngeal myotomy: a review of surgical results in patients with cricopharyngeal achalasia of neurogenic origin. Laryngoscope 1985;95:1337-40.

4. Goode RL. Laryngeal suspension in head and neck surgery. Laryngoscope 1976;86:349-52.

5. Krespi YP, Pelzer HJ, Sisson GA. Management of chronic aspiration by subtotal and submucosal cricoid resection. Ann Otol Rhinol Laryngol 1985;94:580-3.

6. Koufman JA, Isaacson G. Laryngoplastic phonosurgery. Otolaryngol Clin North Am 1991;24:1151-77.

7. Isshiki N, Tanabe M, Sawada M. Arytenoid adduction for unilateral vocal fold paralysis. Arch Otolaryngol 1978;104:555-8.

8. Weisberger EC, Huebsch SA. Endoscopic treatment of aspiration using a laryngeal stent. Otolaryngol Head Neck Surg 1982;90:215-22.

9. Montgomery WW. Surgical laryngeal closure to eliminate chronic aspiration. N Engl J Med 1975;292:1390-1.

10. Habel MB, Murray JE. Surgical treatment of life-endangering chronic aspiration pneumonia. Plast Reconstr Surg 1972;49:305-11.

11. Lindeman RC. Diverting the paralyzed larynx: a reversible procedure for intractable aspiration. Laryngoscope 1975;85:157-80.

12. Baron BC, Dedo HH. Separation of the larynx and trachea for intractable aspiration. Laryngoscope 1980;90:1927-32.

13. Lindeman RC, Yarington CT Jr, Sutton D. Clinical experience with the tracheoesophageal anastomosis for intractable aspiration. Ann Otol Rhinol Laryngol 1976;85:609-12.

14. Eisele DW, Yarington CT Jr, Lindeman RC, Larrabee WF Jr. The tracheoesophageal diversion and laryngotracheal separation procedures for treatment of intractable aspiration. Am J Surg 1989;157:230-6.

15. Eibling DE, Snyderman CH, Eibling C. Laryngotracheal separation for intractable aspiration: a retrospective review of 34 patients. Laryngoscope 1995;105:83-5.

16. Lazarus CL, Logemann JA, Pauloski BR, et al. Swallowing disorders in head and neck cancer patients treated with radiotherapy and adjuvant chemotherapy. Laryngoscope 1996;106:1157-66.

Ann Otol Rhinol Laryngol 109:2000

CLINICAL NOTE

ACTINOMYCOSIS IMITATING NASOPHARYNGEAL CARCINOMA

CHING-WEN CHIANG, MD
YIH-LEONG CHANG, MD
PEI-JEN LOU, MD
TAIPEI, TAIWAN

The incidence of nasopharyngeal actinomycosis is exceedingly rare. To our knowledge, only 1 case has been reported previously. This article presents 4 cases of actinomycosis involving the nasopharynx that imitated nasopharyngeal carcinoma. Acidic gas exposure and farming of aquatic products are possibly involved in the pathogenesis of nasopharyngeal actinomycosis. Patients in the case studies completely recovered after 4 weeks of oral antibiotic treatment. We recommend including actinomycosis in the differential diagnosis of nasopharyngeal neoplasms.

KEY WORDS — actinomycosis, nasopharyngeal carcinoma.

INTRODUCTION

Actinomyces, a gram-positive, anaerobic filamentous organism, is an intermediate between bacteria and fungus. This organism is also considered a commensal saprophyte of the normal mouth flora. It becomes a pathogen when some form of trauma allows access to an anaerobic environment. The most commonly involved sites are cervicofacial (55% of all cases), with the majority of cases occurring in the oral cavity.[1] Nasopharyngeal actinomycosis is exceedingly rare. Only 1 case has been reported.[2] In this article, we present 4 cases of nasopharyngeal actinomycosis that imitated nasopharyngeal carcinoma (NPC), an endemic malignancy in our country. The clinical manifestations, possible pathogenetic factors, and treatment results are discussed.

CASE REPORTS

Actinomycosis of the nasopharynx was diagnosed in 4 patients at our outpatient clinic from February 1998 to April 1998. The Table summarizes the clinical data. The patients visited our clinic with symptoms of blood-tinged sputum (1 case), aural fullness (1 case), and a neck mass (3 cases). Physical examination by indirect rhinoscopy and nasopharyngeal fiberscopy (Fig 1) revealed granular tumors involving the roof of the nasopharynx. Three of the patients underwent a computed tomography scan, which clearly demonstrated a prominent tumor of the nasopharynx (Fig 2). Both clinical and imaging findings suggested the diagnosis of NPC. Punch biopsies of the tumors were performed. Pathological examinations indicated suppurative inflammation with the formation of abscesses that contained 1 or more actinomycotic granules (organized aggregates of filaments), and were surrounded by fibrosing granulation tissue (Fig 3). Bacterial cultures by nasopharyngeal swabs were obtained from 3 patients, but no *Actinomyces* growth was revealed. A thorough review of the pa-

SUMMARY OF CLINICAL DATA OF PATIENTS WITH NASOPHARYNGEAL ACTINOMYCOSIS

Case No.	*Age (y)*	*Sex*	*Occupation*	*Trauma History*	*Symptoms*	*Physical Findings*	*Treatment*
1	43	M	Aquatic products farming	No	Blood-tinged sputum for 1 mo	Nasopharyngeal tumor	Penicillin V potassium 500 mg orally every 6 h for 4 wk
2	44	M	Aquatic products farming	Submucosal diathermy of inferior turbinates	Aural fullness sensation for 1 mo	Nasopharyngeal tumor, neck mass	Penicillin V potassium 500 mg orally every 6 h for 4 wk
3	46	M	Automobile electrician	No	Neck mass for 1 y	Nasopharyngeal tumor, neck mass	Minocycline hydrochloride 100 mg orally every 12 h for 4 wk
4	37	M	Aquatic products farming	No	Neck mass for 10 d	Nasopharyngeal tumor, neck mass	Minocycline hydrochloride 100 mg orally every 12 h for 4 wk

---

From the Departments of Otolaryngology (Chiang, Lou) and Pathology (Chang), National Taiwan University Hospital, Taipei, Taiwan.
CORRESPONDENCE — Pei-Jen Lou, MD, Dept of Otolaryngology, National Taiwan University Hospital, #7 Chung Shan South Rd, Taipei, Taiwan.

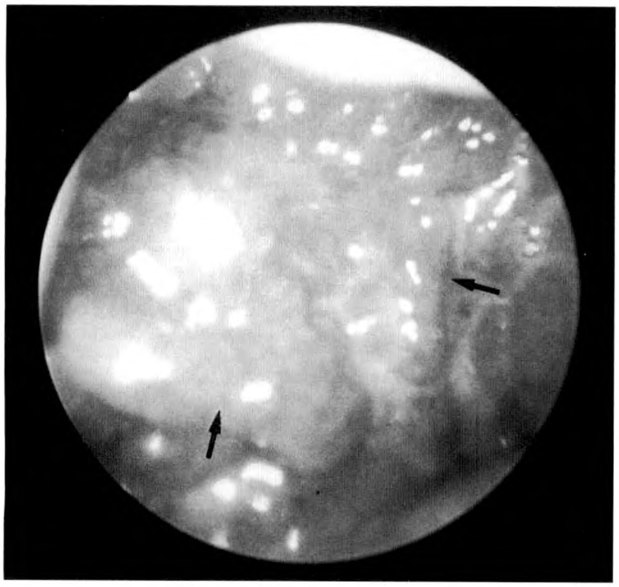

Fig 1. Endoscopic view of nasopharyngeal actinomycosis shows granular mass at nasopharynx (arrows).

tients' medical histories confirmed that none of them had underlying systemic disease. Only 1 patient had undergone electrical submucosal cautery 3 months earlier. Three of the patients are farmers of aquatic products (fish and turtles). One patient is an automobile electrician. Two of them are brothers (cases 1 and 2) and live near a glass factory. They were treated with oral antibiotics for 4 weeks, and the lumpy lesions subsided. The patients are being followed up in the outpatient department and show no signs of recurrence.

DISCUSSION

The incidence of NPC is significantly higher in Taiwan than in Western countries, where cases are rarely observed.[2] The presenting symptoms and signs of NPC include a neck mass, blood-tinged sputum or nasal secretions, unilateral aural fullness, and tinnitus.[2] Our otolaryngologists routinely check the nasopharynx of every patient on his or her first visit to our outpatient clinics. We consider a diagnosis of NPC if the patients have the aforementioned symptoms and signs and a nasopharyngeal mass is detected. Then biopsy is performed to confirm the diagnosis. We think this biopsy largely accounts for why 4 cases of nasopharyngeal actinomycosis were observed in such a short period. Diagnosing actinomycosis may

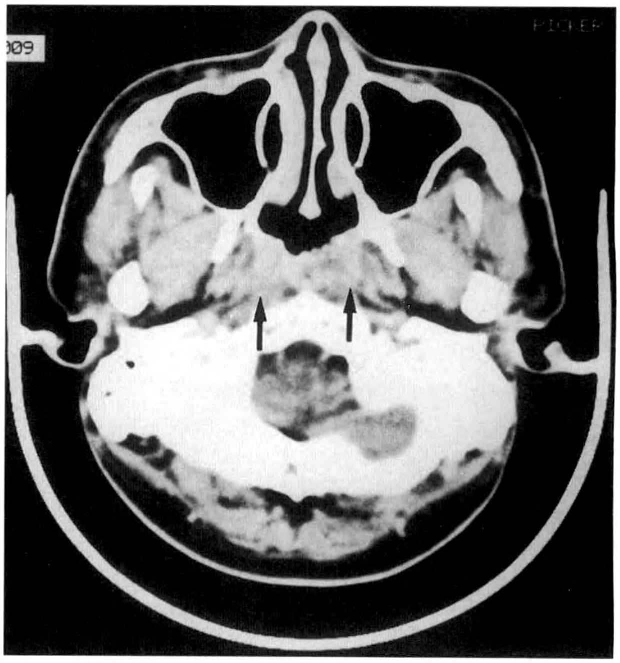

Fig 2. Computed tomography scan of nasopharyngeal actinomycosis shows marked thickening of posterior wall of nasopharynx (arrows).

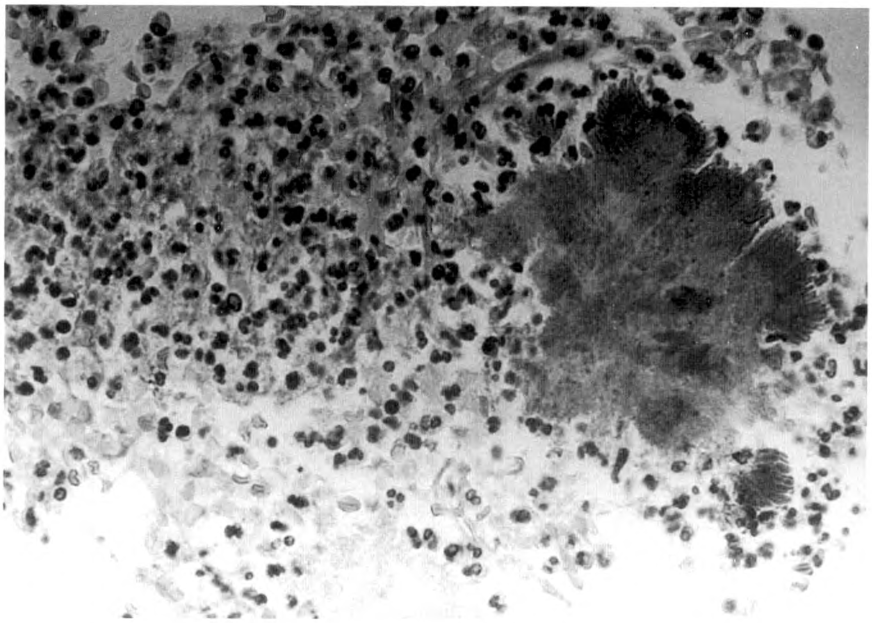

Fig 3. Single granule with filaments and peripheral clubs, which is intimately surrounded by neutrophils (H & E, original ×132).

be difficult. *Actinomyces* is difficult to grow, with fewer than 50% of clinically suspected cases identified by culture.[3] Characteristic colonies of *Actinomyces*, the sulfur granules, are easily missed in one biopsy and are present in only about one third of the material sent for examination.[4] Pus or tissue samples from neck lesions are not routinely sent for anaerobic culture, and patients are often already taking antibiotics by the time of collection. Therefore, the actual number of cases of nasopharyngeal actinomycosis is undoubtedly higher than reported.

Previous reports have proposed the hypothesis of a 2-step pathogenesis of actinomycosis.[5,6] First, the mucosal lining of the affected area is traumatized. One investigation found trauma to the nasopharynx by nasal suction during nasal surgery to be the precipitating factor of nasopharyngeal actinomycosis.[5] Second, another organism acts in a synergistic fashion to create an anaerobic environment for the actinomyces to multiply. However, 3 of our 4 patients had no history of trauma. The remaining patient underwent submucosal diathermy for nasal obstruction relief 3 months before the diagnosis of nasopharyngeal actinomycosis. Using the suction trauma hypothesis to account for how nasopharyngeal actinomycosis developed in our patients is extremely difficult. Environmental factors may play an important role; 2 of our patients (cases 1 and 2) live together with a glass factory in close proximity to their residence. The glass factory could release acidic gas into the air, and it could damage the mucosa of the nasopharynx. The storage battery of an automobile (case 3) may also be a source of acidic gas. *Actinomyces* species are common in saliva and dental plaque; their existence in tonsil crypts is also identified.[7] We postulate that *Actinomyces* may also exist in the nasopharynx, possibly in the adenoids, and become pathogenic once the mucosa is traumatized. The farming of aquatic products (cases 1, 2, and 4) may predispose people to *Actinomyces* infection, possibly by providing an anaerobic environment or promoting synergistic effects between microorganisms.

In conclusion, the results of this study demonstrate that the actual incidence of nasopharyngeal actinomycosis may be higher than expected. In addition, acidic gas exposure and farming of aquatic products are possibly involved in its pathogenesis. Moreover, the differential diagnosis of nasopharyngeal neoplasms should include nasopharyngeal actinomycosis.

REFERENCES

1. Weese WC, Smith IM. A study of 57 cases of actinomycosis over a 36-year period. Arch Intern Med 1975;135:1562-8.
2. Hsu MM, Tu SM. Nasopharyngeal carcinoma in Taiwan: clinical manifestations and results of therapy. Cancer 1983;52:362-8.
3. Burden P. Actinomycosis. J Infect 1989;19:95-9.
4. Burns BV, Al-Ayoubi A, Ray J, Schofield JB, Shoton JC. Actinomycosis of the posterior triangle: a case report and review of the literature. J Laryngol Otol 1997;111:1082-5.
5. Osborne JE, Blair RL, Christmas HE, McKenzie H. Actinomycosis of the nasopharynx: a complication of nasal surgery. J Laryngol Otol 1988;102:639-40.
6. Bennhoff DF. Actinomycosis: diagnostic and therapeutic considerations and a review of 32 cases. Laryngoscope 1984;94:1198-217.
7. Slack JM. The source of infection in actinomycosis. J Bacteriol 1942;43:193-209.

Ann Otol Rhinol Laryngol 109:2000

IMAGING CASE STUDY OF THE MONTH

SPHENOETHMOIDAL MUCOCELE PRESENTING WITH BILATERAL VISUAL COMPROMISE

TODD A. LOEHRL, MD
MILWAUKEE, WISCONSIN

DONALD A. LEOPOLD, MD
LINCOLN, NEBRASKA

INTRODUCTION

Mucoceles are mucus-containing cysts that are frequently diagnosed from the symptoms produced when they expand into surrounding structures. We present the case of a patient with bilateral visual compromise as a result of optic nerve compression from a large sphenoethmoidal mucocele.

CASE REPORT

A 58-year-old woman presented with a 3-year history of right eye blindness and a progressive loss of visual acuity in the left eye over the previous 6 weeks. The patient had undergone evaluation at another institution when she lost vision in her right eye 3 years earlier. She reportedly had radiographic evidence of a sphenoid sinus lesion. Biopsy at that time "did not reveal any pathology," and the patient was subsequently lost to follow-up. She presented to our institution with a 6-week history of progressive vision loss in the left eye. She denied epistaxis, nasal airway obstruction, facial pain, headaches, or changes in olfaction. Ophthalmologic evaluation revealed blindness of the right eye and light perception only in the left eye. She also was unable to abduct her right eye. Nasal endoscopy revealed a right sphenoethmoidal recess fullness that lateralized the right superior turbinate. The overlying mucosa was pink and slightly edematous. The rest of the physical examination findings were unremarkable.

Imaging studies revealed a cystic lesion of the right ethmoid sinus and entire sphenoid sinus with erosion of the optic canals bilaterally (Fig 1). There was also intracranial extension through the ethmoid roof and cribriform plate on the right side. Results of magnetic resonance imaging with gadolinium were consistent with a nonvascular lesion with no definite solid component.

Initially, the patient was managed endoscopically in the clinic under local anesthesia. The lesion was identified in the right sphenoethmoidal recess, and a 25-gauge spinal needle was inserted into the lesion. This resulted in no significant hemorrhage and a slow ooze of thick, brown fluid. At that point, an opening approximately 2 cm in diameter was made into the wall of the lesion, and approximately 20 mL of thick, brown fluid was removed. The histologic examination revealed benign squamous epithelium with cholesterol granules, but no multinucleated giant cells. The histologic, operative, and radiographic findings were consistent with a mucocele. The postoperative imaging studies were as noted below (Fig 2). Unfortunately, the patient's vision did not improve after decompression of the lesion.

A follow-up examination 2 weeks later revealed that the opening had closed. Imaging studies revealed reaccumulation of the cystic contents, and the patient was therefore scheduled for endoscopic sinus surgery with wider marsupialization of the mucocele. The entire floor of the mucocele was removed while leaving the roof intact. This resulted in excellent ventilation of the mucocele cavity. There were no complications, and the mucocele had not recurred at 1 year. The histologic findings from the second procedure were similar to those of the first. A postoperative ophthalmologic examination showed no improvement in the patient's vision.

DISCUSSION

Mucoceles are mucus-containing cysts that often start within the paranasal sinuses and result in surrounding bony changes characterized by progressive thinning and distention of the sinus bony walls. Symptoms depend on the anatomic area involved. Presenting symptoms can include facial pain, headaches, diplopia, decreased visual acuity, orbital globe displacement, facial swelling, nasal obstruction, and meningitis.

Several different entities can present with a similar radiographic appearance. The differential diagno-

---

From the Department of Otolaryngology–Head and Neck Surgery, Johns Hopkins Medical Institutions, Baltimore, Maryland.
CORRESPONDENCE — Todd A. Loehrl, MD, Medical College of Wisconsin, 9200 W Wisconsin Ave, Milwaukee, WI 53226.

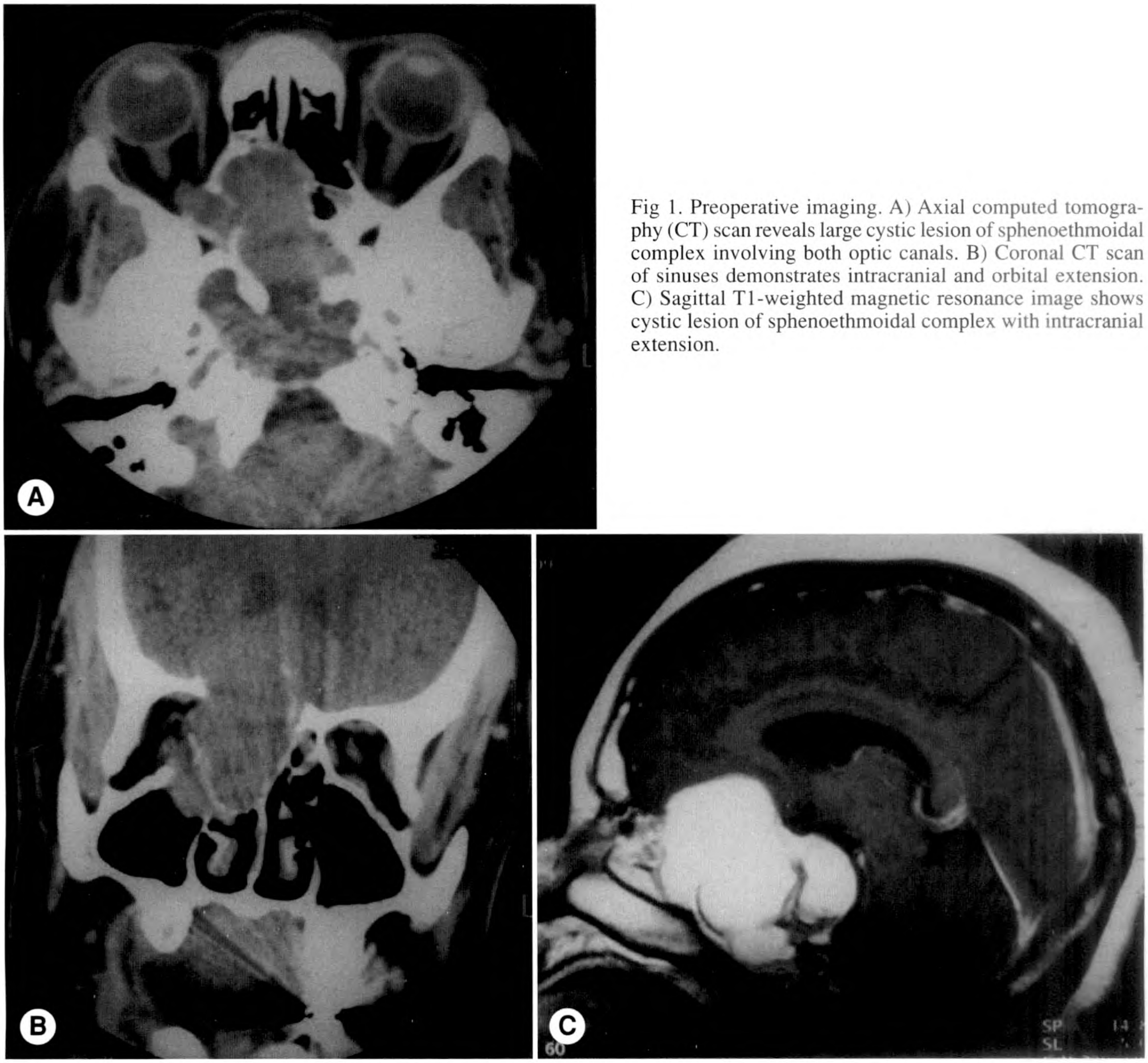

Fig 1. Preoperative imaging. A) Axial computed tomography (CT) scan reveals large cystic lesion of sphenoethmoidal complex involving both optic canals. B) Coronal CT scan of sinuses demonstrates intracranial and orbital extension. C) Sagittal T1-weighted magnetic resonance image shows cystic lesion of sphenoethmoidal complex with intracranial extension.

sis includes congenital lesions such as encephaloceles and other non-neoplastic lesions such as cholesterol granulomas or epidermoid cysts. A wide variety of neoplastic processes need to be considered. Benign lesions include, but are not limited to, meningiomas, chordomas, fibro-osseous conditions, neurofibromas, and salivary adenomas. Benign vascular lesions include hemangiopericytomas, paragangliomas, and juvenile nasopharyngeal angiofibroma. Malignant neoplasms should be considered, as well. In addition, mucoceles may be associated with a neoplastic process because of sinus ostial obstruction.[1] Imaging studies are often helpful in differentiating between these entities, as noted below.

The etiologic mechanism of mucoceles is not fully understood, but they are often associated with sinus ostial obstruction. They occur most frequently in the frontal and ethmoid sinuses, and with about equal frequency in men and women.[2] They can be a sequela of sinus obstruction from chronic rhinosinusitis, nasal polyps, or tumors.[1] Facial trauma, in particular that involving the ethmoid and frontal sinuses, has been associated with extensive mucoceles that extend into the orbit, soft tissue of the forehead, and cranium. Previous sinus surgery can also result in ostial obstruction and subsequent mucocele development.[3,4]

Mucoceles tend to continually expand and remodel the surrounding bone. The pathophysiological mechanism of mucocele expansion has been debated. Pressure-induced osteolysis, bone devascularization, and osteolytic enzymes may all play a role.[5] An acute infection of the mucocele (mucopyocele) may induce an acute orbital or intracranial complication.

The diagnosis of mucoceles is primarily radio-

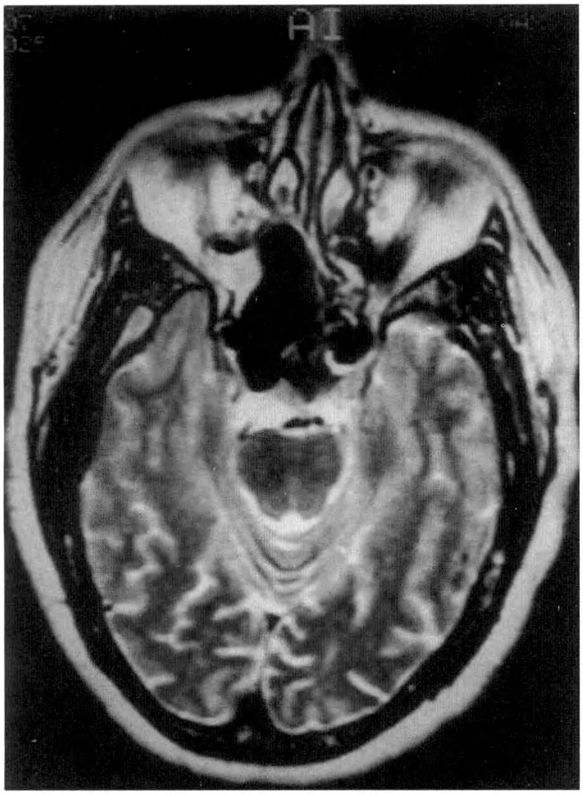

Fig 2. Axial T2-weighted magnetic resonance image shows postoperative decompression of sphenoethmoidal mucocele.

graphic. Computed tomography scans are helpful in making the diagnosis, demonstrating bony involvement, assessing intracranial or orbital extension, and helping with preoperative planning. Magnetic resonance imaging may be helpful in ruling out a neoplastic process, but is not very helpful in demonstrating the bony anatomy.[2]

Several approaches have been used to surgically treat mucoceles. Historically, frontal mucoceles have been treated with more radical exenterative procedures. These include the Riedel, Lynch-Howarth, and Sewall-Boyden procedures and the osteoplastic flap with obliteration. Each has its own advantages and disadvantages, which are discussed in detail elsewhere.[2] However, more recently, transnasal endoscopic management has been reported to yield excellent results.[2,6,7] The goal of endoscopic management of frontal sinus mucoceles is marsupialization and preservation of nasofrontal recess patency. The advantages of endoscopic management include good visualization, less morbidity, and minimal trauma to surrounding mucosa with preservation of the nasofrontal recess bony anatomy. In many cases, the operation can be completed as an outpatient procedure with the patient under local anesthesia. In addition, endoscopic visualization is useful for following the patient after surgery.[2]

Sphenoid and ethmoid mucoceles are commonly treated with wide marsupialization allowing for ventilation and drainage. Several authors have reported excellent results with the endoscopic approach here, as well.[2,4,6,8,9] With intracranial or orbital extension, the wall of the mucocele may be left intact with good results, as long as the lesion is well ventilated.[3,8] Attempted removal in this situation may increase morbidity by injuring the periorbita or dura.[8]

After surgery, mucoceles should be cleaned frequently in the office. Nasal saline irrigations help with removal of any residual debris. Regular follow-up in the office with nasal endoscopy is important, as was demonstrated in our patient. Imaging, either computed tomography or magnetic resonance imaging, may be helpful in following these patients after operation, especially if recurrent disease is suspected. Patients should be informed that long-term follow-up is necessary because mucocele development may take long periods of time.

REFERENCES

1. Holt GR, Standefer JA, Brown WE, Gates GA. Infectious diseases of the sphenoid sinus. Laryngoscope 1984;94:330-5.

2. Kennedy DW, Josephson JS, Zinreich SJ, Mattox DE, Goldsmith MM. Endoscopic sinus surgery for mucoceles: a viable alternative. Laryngoscope 1989;99:885-95.

3. Daniilidis J, Nikolaou A, Knodopoulos V. An unusual case of sphenoid sinus mucocele with severe intracranial extension. Rhinology 1992;31:131-7.

4. Moriyama H, Hesaka T, Honda Y. Mucoceles of ethmoid and sphenoid sinus with visual disturbance. Arch Otolaryngol Head Neck Surg 1992;118:142-6.

5. Lund VJ, Henderson B, Song Y. Involvement of cytokines and vascular adhesion receptors in the pathology of fronto-ethmoidal mucoceles. Acta Otolaryngol (Stockh) 1993;113:540-6.

6. Hoffer ME, Kennedy DW. The endoscopic management of sinus mucoceles following orbital decompression. Am J Rhinol 1994;8:61-5.

7. Wigand ME, Hosemann WG. Endoscopic surgery for frontal sinusitis and its complications. Am J Rhinol 1991;5:85-9.

8. Benninger MS, Marks S. The endoscopic management of sphenoid and ethmoid mucoceles with orbital and intranasal extension. Rhinology 1995;33:157-61.

9. Har-El G, Balwally AN, Lucente FE. Sinus mucoceles: is marsupialization enough? Otolaryngol Head Neck Surg 1997;117:633-40.

Ann Otol Rhinol Laryngol 109:2000

CLINICOPATHOLOGICAL CONSULTATION

HERPES SIMPLEX VIRAL LARYNGITIS

JEFFREY T. VRABEC, MD
GALVESTON, TEXAS

CLAUDIA P. MOLINA, MD
GALVESTON, TEXAS

BRIAN WEST, MD
NEW YORK, NEW YORK

The true incidence of herpetic infections of the larynx is unknown. This entity may be underreported because of the difficulty in establishing the diagnosis. This report describes an immune-competent patient in whom extubation failed because of mass lesions of the posterior glottis. A biopsy specimen of the lesions revealed herpes simplex virus. We review the clinical presentation and histopathologic findings in this patient.

INTRODUCTION

Herpetic infections of the larynx are either uncommon or rarely recognized. Accurate diagnosis requires clinical suspicion and a highly specific method of confirming the presence of the virus. Unfortunately, physical findings in herpetic infections are often nonspecific and sometimes transient, easily allowing these infections to escape diagnosis. Confirmation of herpesvirus infection is achieved by culturing the virus from laryngeal tissue in appropriate cell lines. The sensitivity of this method is limited, because the virus may not be recovered from older ulcerative lesions. In addition, it is somewhat impractical to obtain an appropriate specimen in an outpatient setting. Herpesvirus infection may also be detected by the presence of characteristic intranuclear inclusions in histologic sections and may be confirmed by immunocytochemical staining for herpesvirus antigens.

The laryngeal manifestations of herpetic infection are quite variable. Vesicles, ulcers, bulky fibrinous lesions of the endolarynx, and vocal cord paralysis have been described.[1-6] Several of these findings are usually present, although each may occur in isolation. Ulcerative lesions may involve the supraglottis or glottis, whereas edema is most commonly described in the subglottic region. Stridor is a prominent initial symptom in infants, but may also occur in older patients. The vocal cord paralysis has been described as transient or permanent. Unilateral superior or recurrent laryngeal nerve palsy and bilateral vocal cord paralysis have been reported.[5-8] Chronic symptoms, resulting from multiple recurrences, have sometimes been incorrectly attributed to malignancy.[9-11]

Laryngeal infection may occur in isolation, in conjunction with other cranial nerve dysfunction, or as part of a widespread infection of the respiratory tract. Herpes simplex viruses 1 and 2 (HSV-1, HSV-2) and varicella zoster virus (VZV) infections have all been reported to cause laryngeal inflammation, ulcerative lesions, and vocal cord paralysis. In this report, a case of HSV laryngitis arising after endotracheal intubation is described. The correct diagnosis was not suspected at the initial laryngeal examination, but was suggested by histopathologic examination and confirmed by immunocytochemical analysis.

CASE REPORT

A 59-year-old man was hospitalized after a stroke involving the right basal ganglia and cerebellum. Stridor developed, necessitating endotracheal intubation. Assisted ventilation was required for 1 day; then, the patient was extubated without incident. The patient had moderate dysphagia from the stroke and was examined in the otolaryngology clinic. The pharyngeal and laryngeal musculature demonstrated normal mobility, and there were no mucosal lesions. A second episode of dyspnea occurred 3 weeks later, requiring a second endotracheal intubation. Mechanical ventilation was required for 4 days. The patient became immediately stridulous on extubation and was intubated for a third time.

At direct laryngoscopy, large plaquelike lesions were found emanating from the posterior glottis bilaterally. The posterior commissure was uninvolved. Presumably, these plaques would occlude the glottis during inspiration. The lesions were excised and sent for histopathologic examination.

The specimens were fixed in 10% neutral buffered

From the Departments of Otolaryngology (Vrabec) and Pathology (Molina, West), University of Texas Medical Branch, Galveston, Texas.
CORRESPONDENCE — Jeffrey T. Vrabec, MD, Dept of Otolaryngology, 301 University Blvd, JSA 7.104, Galveston, TX 77555-0521.

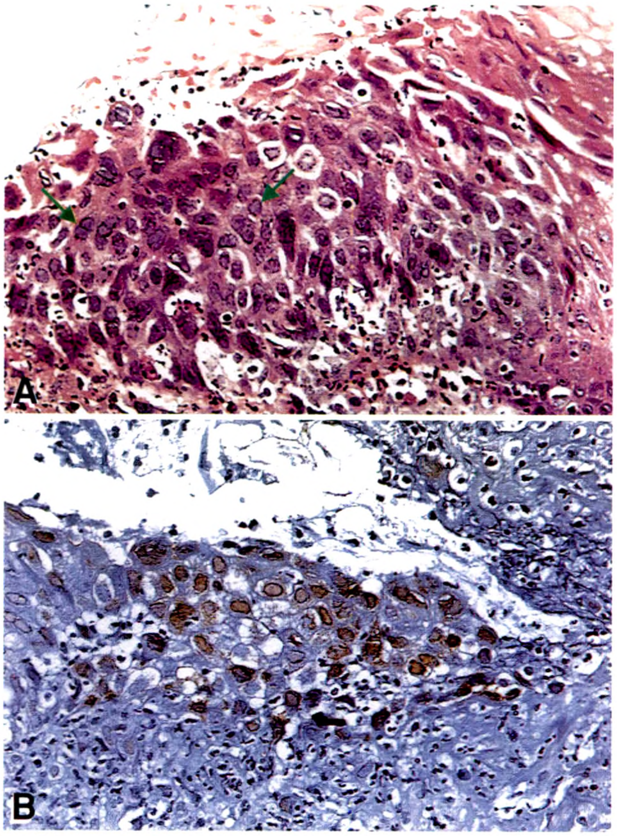

Vocal cord biopsy shows squamous epithelium at edge of ulcer. A) Acutely inflamed mucosa with enlarged squamous cells (arrows) containing single or multiple ground-glass nuclei with amphophilic inclusions and peripheral chromatin (H & E, original ×230). B) Immunocytochemical stain for herpes simplex shows positive immunoreactivity (brown) in ground-glass nuclei (hematoxylin counterstain, original ×250).

formalin, embedded in paraffin, and sectioned. Biopsies of both vocal cords showed necroinflammatory exudate with subjacent mucosal ulceration. Squamous epithelial cells at the edge of the ulcers were swollen and contained single or multiple enlarged nuclei with pale, amphophilic ground-glass inclusions and peripheral chromatin, typical of HSV and VZV infections[12] (see Figure). Immunocytochemical staining with a cocktail of rabbit polyclonal antibodies to HSV-1 and HSV-2 (Dako, Carpinteria, Calif) at 1:4,000 dilution with avidin-biotin peroxidase amplification with diaminobenzidine as chromogen and a light hematoxylin counterstain showed positive immunoreactivity of intranuclear inclusions, confirming their identity as HSV.

A tracheotomy was performed to allow extubation. The patient was started on intravenous acyclovir. Rapid resolution of the glottic lesions allowed prompt decannulation.

DISCUSSION

In the case outlined above, the possibility of a herpesvirus infection was not suspected at the time of laryngoscopy. The finding of intranuclear inclusions in the epithelial layer on histologic examination suggested the diagnosis. An immunocytochemical analysis confirmed the presence of HSV. The histologic differential diagnosis of laryngeal ulceration includes benign and malignant lesions. Among the latter, squamous cell carcinoma is by far the most common and must be distinguished from pseudoepitheliomatous hyperplasia at the ulcer edge. Rarer tumors such as adenoid cystic, basaloid, mucoepidermoid, neuroendocrine, and small cell carcinoma occur infrequently, as do a variety of mesenchymal tumors and lymphomas. Benign ulcers arise on occasion in mucosa overlying mass lesions such as laryngeal nodules, lobular capillary hemangiomas (pyogenic granulomas), and amyloid deposits; after instrumentation or other trauma (contact ulcers); and in immunodeficient patients because of infection with fungi (notably, *Candida*), cytomegalovirus (CMV), or herpes. The cytomegalic changes of CMV infection are characteristic, and fungi are readily demonstrated by the use of periodic acid–Schiff or appropriate silver stains. The histologic appearances of ulcers due to HSV and VZV are identical. At the stage of ulceration in which the typical intranuclear inclusions are present, herpesvirus infections are readily distinguished from other forms of benign laryngeal ulcers in routine sections stained with hematoxylin and eosin. The diagnosis can then be confirmed by immunohistochemical analysis. Later in their development, however, the inclusions disappear, and the histologic appearance is nonspecific.

There are few articles on herpesvirus infections of the larynx that present a large number of cases. Laryngeal involvement due to VZV infection is more commonly reported.[4,13] In these cases, the presence of mucosal lesions in the larynx and associated cranial nerve findings establishes VZV as a potential cause. Laryngeal infection due to HSV is less commonly recognized, possibly because the mucosal lesions are more transient and the associated cranial nerve dysfunction is less common.

Certain patient populations are known to have a high incidence of herpesvirus infections involving the airway. Patients who suffer burns are likely to have laryngeal involvement in conjunction with lower respiratory tract infection.[14] Transplant recipients, immunocompromised patients, and those who undergo cardiothoracic surgery have been noted to have a high incidence of lower respiratory tract herpesvirus infections.[15] These reports do not discuss laryngeal findings, but immunocompromised individuals may develop laryngeal involvement in conjunction with widespread pulmonary herpesvirus infections. A high index of suspicion is necessary when evaluating these patients for failure of extubation. Isolated laryngeal lesions occur in both immune-competent and immune-compromised individuals.

Laryngeal herpetic infections occur both as primary infections and as reactivation of latent virus. There are several case reports of neonates who developed severe laryngeal inflammation secondary to perinatally acquired HSV-2.[3,16] Reactivation of latent virus is the likely mechanism in cases of laryngeal zoster. In our case, airway trauma associated with endotracheal intubation is presumed to have caused reactivation of latent HSV. This mechanism has been observed in VZV infection of the larynx.[17]

The treatment of laryngeal herpesvirus infections depends on the degree of airway compromise. Isolated laryngeal inflammation is usually self-limited, but can recur. Most patients are not in acute respiratory distress when they first seek medical care. Dysphonia, dysphagia, and otalgia are the usual presenting symptoms. Antiviral medications and steroids have been effective in this setting. Prompt resolution of the inflammation is expected.

Recurrent laryngeal nerve paresis or paralysis is described in most cases of VZV infection, but in only one third of patients with HSV infection. In most instances, the dysfunction is transient. Review of selected case reports of HSV-induced dysfunction reveals recovery of normal function or improvement in 4 of 5 cases.[5,6,8,18,19] The fifth case had a reported follow-up of only 8 months. In 13 cases of VZV-induced dysfunction, improvement or return of normal motion was reported in 11.[4,12,16,19-21] It is difficult to determine from the available reports whether the recovery profiles are different for HSV and VZV infections.

Neonates with stridor due to herpesvirus infection have not required endotracheal intubation.[3,16] Patients with acute respiratory distress from edema or bilateral vocal cord paralysis have required urgent tracheotomy.[4,6,18] If endotracheal intubation is necessary to secure the airway, elective tracheotomy may minimize damage to the larynx from the combined effects of viral inflammation and mechanical trauma.[1,2] Bulky endolaryngeal lesions precluded extubation in our patient; therefore, tracheotomy was performed in conjunction with lesion excision. In the only other reported case of viral reactivation due to endotracheal intubation, excision of the lesion alone was sufficient to facilitate extubation.[17] Recurrence of inflammatory mass lesions was not observed in our case, although others have reported this.[10] Follow-up laryngoscopy to document healing of the posterior glottis is essential before decannulation.

Long-term sequelae of herpesvirus infections are unusual among the referenced studies. Persistent vocal cord paralysis is the most prevalent, occasionally requiring a medialization procedure. Incomplete return of function would be expected in some cases if recovery from virally mediated vocal cord paralysis is similar to that from facial paralysis. The use of a standardized system for grading recovery from facial paralysis allows better documentation of outcomes. A partial recovery of vocal cord mobility is poorly defined, and some cases of mild dysfunction or synkinesis may be overlooked.

Recurrent ulcerations and mass lesions have been described. An early anterior commissure web was noted by Pahor.[4] It is conceivable that herpesvirus infections could contribute to the development of webbing, granuloma formation, or laryngeal stenosis, but the evidence is circumstantial.

A high index of suspicion is necessary for diagnosis of herpetic infection involving the larynx. The increasing clinical use of polymerase chain reaction techniques in the diagnosis of viral infections may allow earlier and more accurate diagnosis of herpesvirus infections.

REFERENCES

1. D'Angelo AJ Jr, Zwillenberg S, Olekszyk JP, Marlowe FI, Mobini J. Adult supraglottitis due to herpes simplex virus. J Otolaryngol 1990;19:179-81.

2. Harris JB, Lusk R, Wagener JS, Andersen RD. Acute viral laryngotracheitis complicated by herpes simplex virus infection. Otolaryngol Head Neck Surg 1987;96:190-3.

3. Nadel S, Offit PA, Hodinka RL, Gesser RM, Bell LM. Upper airway obstruction in association with perinatally acquired herpes simplex virus infection. J Pediatr 1992;120:127-9.

4. Pahor AL. Herpes zoster of the larynx — how common? J Laryngol Otol 1979;93:93-8.

5. Flowers RH III, Kernodle DS. Vagal mononeuritis caused by herpes simplex virus: association with unilateral vocal cord paralysis. Am J Med 1990;88:686-8.

6. Magnussen CR, Patanella HP. Herpes simplex virus and recurrent laryngeal nerve paralysis: report of a case and review of the literature. Arch Intern Med 1979;139:1423-4.

7. Adour KK, Schneider GD, Hilsinger RL Jr. Acute superior laryngeal nerve palsy: analysis of 78 cases. Otolaryngol Head Neck Surg 1980;88:418-24.

8. Bachor E, Bonkowsky V, Hacki T. Herpes simplex virus type I reactivation as a cause of a unilateral temporary paralysis of the vagus nerve. Eur Arch Otorhinolaryngol 1996;253:297-300.

9. Yeh V, Hopp ML, Goldstein NS, Meyer RD. Herpes simplex chronic laryngitis and vocal cord lesions in a patient with acquired immunodeficiency syndrome. Ann Otol Rhinol Laryn-

gol 1994;103:726-8.

10. Karnauchow PN, Kaul WH. Chronic herpetic laryngitis with oropharyngitis. Ann Otol Rhinol Laryngol 1988;97:286-8.

11. Schwenzfeier CW, Fechner RE. Herpes simplex of the epiglottis. Arch Otolaryngol 1976;102:374-6.

12. Khalifa MA, Lack EE. Herpes simplex virus infection. In: Connor DH, Chandler FW, Schwartz DA, Manz HJ, Lack EE, eds. Pathology of infectious diseases. Stamford, Conn: Appleton & Lange, 1997:147-52.

13. Sandberg N. Herpes zoster and paralysis of cranial nerves. In: Portmann M, ed. Proceedings of the Fifth International Symposium on the Facial Nerve. New York, NY: Masson Publishing, 1985:408-12.

14. Nash G, Foley FD. Herpetic infection of the middle and lower respiratory tract. Am J Clin Pathol 1970;54:857-63.

15. Klainer AS, Oud L, Randazzo J, Freiheiter J, Bisaccia E, Gerhard H. Herpes simplex virus involvement of the lower respiratory tract following surgery. Chest 1994;106(suppl 1):8S-14S.

16. Nyquist AC, Rotbart HA, Cotton M, et al. Acyclovir-resistant neonatal herpes simplex virus infection of the larynx. J Pediatr 1994;124:967-71.

17. Wackym PA, Gray GF Jr, Avant GR. Herpes zoster of the larynx after intubational trauma. J Laryngol Otol 1986;100:839-41.

18. Pou A, Carrau RL. Bilateral abductor vocal cord paralysis in association with herpes simplex infection: a case report. Am J Otolaryngol 1995;16:216-9.

19. Mesolella M, Testa B, Mesolella C, Giuliano A, Testa G. Herpes of the larynx: apropos of 3 cases [in French]. Ann Otolaryngol Chir Cervicofac 1993;110:337-40.

20. Nishizaki K, Onoda K, Akagi H, Yuen K, Ogawa T, Masuda Y. Laryngeal zoster with unilateral laryngeal paralysis. ORL J Otorhinolaryngol Relat Spec 1997;59:235-7.

21. Hiraide F, Kakoi H, Miyoshi S, Morita M. Acute profound deafness in Ramsay Hunt syndrome: two case reports. Acta Otolaryngol Suppl (Stockh) 1988(suppl 456):49-54.

* * *

EUROPEAN ACADEMY OF FACIAL PLASTIC SURGERY

The annual meeting of the European Academy of Facial Plastic Surgery will be held September 15-17, 2000, in Thessaloniki, Greece. For information, contact Prof Dr J. Daniilidis, ENT Dept, Aristotelian University of Thessaloniki–AHEPA Hospital, 540 06 Thessaloniki, Greece; telephone 0030/31/994.761-2; fax 0030/31/994.916.

Ann Otol Rhinol Laryngol 109:2000

BASILAR ARTERY AND VERTIGO

LOUIS W. WELSH, MD

JOHN J. WELSH, MD BERNARD LEWIN, MD

JENKINTOWN, PENNSYLVANIA

Our goal was to identify by magnetic resonance angiography the specific vascular abnormalities of the basilar artery that can be related to hypoperfusion disorders and produce symptoms of vertebrobasilar insufficiency. A classification of regional vascular perfusion disorders based on developmental malformations and intrinsic and extrinsic angiopathies was formulated from an analysis of individuals with these disorders. Specific angiographic abnormalities such as tortuosity, stenosis, thrombosis, and dolichoectasia were identified in subjects with vestibulocerebellar dysfunction. Charts and radiographic images were examined with respect to the history, physical evidence, and vascular configuration, and the data were integrated for comprehensive analysis. We found that abnormalities identified by magnetic resonance angiography could be correlated with symptoms due to vascular insufficiency. Cases are presented that document the developmental and acquired arterial disorders that may be considered the etiologic factors for regional perfusion deficits.

KEY WORDS — magnetic resonance angiography, vertebrobasilar arterial system, vertigo.

We investigated the vascular basis of vestibulocerebellar dysfunction by magnetic resonance angiography (MRA). Confirmation of segmental arterial insufficiency in the vertebrobasilar artery (VBA) system may explain the dysfunctional symptoms of vertigo, gait disturbance, incoordination, and imbalance. The specific goals of this study included 1) examination by MRA of abnormalities of the basilar artery (BA) that may be considered potential factors in vestibulocerebellar dysfunction; 2) identification of specific abnormal vascular structures and morphologies and the resulting impact on volumetric flow and regional perfusion; 3) establishment of criteria for the use of regional angiography during the evaluation of vertigo; and 4) presentation of illustrative cases correlating clinical disorders with regional arterial disease.

ANATOMY AND PATHOPHYSIOLOGY

There are fundamental data that are required for an appropriate analysis of the function of the BA. This material is briefly summarized in the following abstracts.

Configuration and Specifics of Anatomy. The dimensions of the BA[1] involve length (25 to 39 mm; mean, 33.3 mm), diameter (2.7 to 4.3 mm; mean, 4.1 mm), and morphology (straight in 25%, S-pattern in 16%, and curved, variably, in about 60%). The volumetric flow of the VBA system is 18% of the total cerebral perfusion.[2] The volume[3] is 164 ± 12 mL/mm, and the velocity[3] is 40 ± 3 cm/s.

Developmental Variants. Developmental variants[4] of the VBA system include persistent trigeminal artery and persistent hypoglossal artery. In the scenario of incompetence of the anterior circulation, for example, due to occlusive carotid disease, vertebrobasilar insufficiency (VBI) secondary to anomalous shunting mechanisms may become clinically apparent. Alternatively, hypoplasia of the VBA system may impair regional hindbrain flow with resulting symptoms of VBI.[5,6]

Collateralization. Because the cerebellar arteries develop peripheral arborization serving the hindbrain,[7,8] occlusive disease of specific branches can reflect different syndromal components according to the developmental anatomy of the regional distribution.[7,8] The importance of shunting through the circle of Willis compensating for VBA insufficiency has been described by numerous authors.[9-13] In addition, collateralization between the posterior cerebral artery and the superior cerebellar artery is recognized, and the relationships between the lower cerebellar arteries have been identified.

Several pathological situations relating to collateralization, shunting, and compensatory flows involving the BA are possible and are considered in our case presentations and discussion. These include the following: 1) hypoperfusion in the watershed area may not be compensated by shunting through an incomplete circle of Willis (a developmental anomaly); 2) diminished antegrade perfusion through the VBA system may be compensated by posteriorly directed flow from the anterior circle of Willis; 3) absence or hypoplasias of the posterior communicating arteries may interrupt the potential for anteroposterior shunting in the presence of VBI; and 4) unilateral carotid

CORRESPONDENCE — Louis W. Welsh, MD, 179 Washington Lane, Jenkintown, PA 19046.

artery system occlusion, in conjunction with the absence of an anterior and/or posterior communicating artery, may provide the terminal dynamic for regional infarction.

VASCULAR SOURCES OF VERTIGO AND LONGITUDINAL ANALYSIS

The BA supplies the neural components of the vestibulocerebellar complex through the cerebellar branches. The peripheral cochlear labyrinthine apparatus is perfused by the internal auditory artery (IAA); the eighth cranial nerve and the vestibular nuclei are served by the anterior inferior cerebellar artery (AICA) and the posterior inferior cerebellar artery (PICA); the central vestibular connections within the brain stem are served by the AICA and the superior cerebellar arteries; and, finally, the cerebellum is served by each of the above.

The vestibular function may be compromised by circulatory embarrassment at any level within the extensive neuronal cascade and result in vertigo. Although the cortical sensory level for vertigo is located in the temporal lobe and lesions within this area may produce a dysfunction of spatial relationships, this area is not associated with the VBA system and is not further discussed in this report.

Valvassori[14] commented that permanently or transiently reduced perfusion to the hindbrain is the major cause of vestibular disorders and is responsible for 80% of the central type of dysfunction.

Variations in the clinical presentation of vertiginous individuals were described by Welsh et al,[8] who presented several combinations of neurologic deficits contingent on the site and local perfusion of specific arterial branches. Developmental inconsistencies in the arterial anatomy within the hindbrain may contribute to pseudolabyrinthine symptoms similar to a peripheral vestibular dysfunction. The diagnostic confusion of central versus peripheral lesions is contingent on the division and collateralization of the PICA.[15]

Extrinsic compression by spondylosis or arthritis of the cervical vertebrae on the vertebral arteries with consequent diminished BA flow is well recognized.[16] Additional obstruction due to cervical rotation further narrows the arterial lumen, possibly provoking the symptom of transient instability. A similar event has been reported during the stretch position in adolescence.[17]

Rancurel et al[18] considered the etiologic factors of VBI and described the separate dynamic mechanisms as follows: 1) thromboembolic transient ischemic attack (TIA; 21%); 2) positional hemodynamic TIA (46%); 3) combination of factors 1 and 2 (21%); and 4) an unclassified segment (12%). The importance of primary vascular disease such as atherosclerotic stenosis or occlusion, extrinsic compression, and intravascular obstruction was emphasized.

The longitudinal concern for vertiginous patients was emphasized by Grad and Baloh.[19] They noted that 29% of 84 patients ultimately sustained a confirmed infarction within the VBA region before the final occlusive event.[19]

A study by Kim and Heo[20] presented the longitudinal prognosis of vertiginous subjects (154 individuals). Progression from isolated vertigo to an overt neurologic deficit was observed and confirmed by radiographic analysis in 20% of this cohort. The lesion was isolated by computed tomography (CT) or magnetic resonance imaging (MRI) within the cerebellum (19 patients), pons (8 patients), and medulla oblongata (3 patients). Finally, the evolution from the early phase of isolated vertigo to final infarction occurred between 4 hours and 7 days after the initial onset in 27% of this group, suggesting a progressive vascular obstructive phenomenon.

METHODS AND MATERIALS

Magnetic resonance angiography is an established radiographic investigation with a high correlation to contrast angiography. In addition, and of paramount importance, the complications and morbidity of an invasive study are spared, and consequently, this examination may be used routinely for medical evaluations.[4]

We suggest that the interested reader refer to the article by Patrux et al[21] that describes the technique of MRA. The images were examined with maximum-intensity projection and source views when available. The images of the circle of Willis were assessed primarily by the composite skull base (axial) view and the lateral projection exaggerating the relationship to the BA. The following areas were considered: 1) the presence, dimensions in millimeters, configuration (tortuous, straight, S-curvature), and areas of stenosis; 2) the direction of flow, either antegrade or retrograde; and 3) the data derived from examination of the vertebral arteries (VAs), the source of antegrade BA flow, as integrated into the composite structural and functional status of the VBA system.

The investigation was limited to vertiginous subjects, and the subgroup previously reported as having "syndromal vertigo" was deleted from this review. The remaining individuals complained of transient, isolated vertigo and dysfunctional vestibulocerebellar symptoms of nausea, vomiting, and gait and visual disturbance. Insofar as possible, other fac-

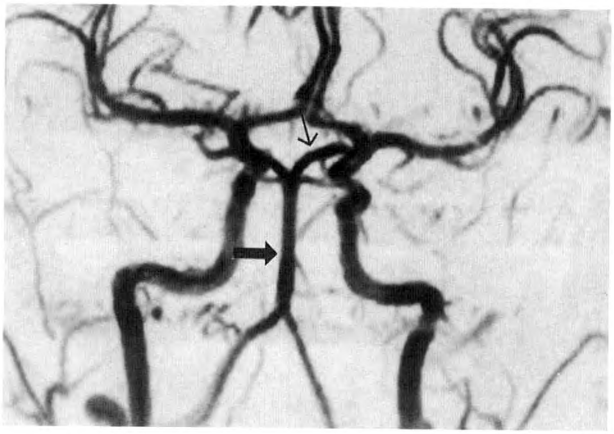

Fig 1. (Case 1) Eighteen-year-old man evaluated for basilar migraine. Magnetic resonance angiography (MRA) in anteroposterior (AP) projection for circle of Willis shows normal findings. Note wide lumen of basilar artery (large arrow). Posterior cerebral arteries are symmetric and widely patent (small arrow).

tors beyond regional vascular insufficiency were evaluated, including cardiogenic disease (specifically, arrhythmias and the hemodynamic disorders of anemia), orthostatic hypotension, and psychogenic problems. The authors also eliminated from the review the subjects whose complaints were based on these factors. The typical subject was in the 6th to 9th decade. As anticipated, a broad medical survey revealed that many of the subjects suffered the metabolic and vascular diseases of advancing age, but, in comparison with matched asymptomatic subjects, these disorders were not of higher incidence in the investigated segment.

In addition, the recognized primary neuronal or cochlear disturbances producing vertigo, such as Meniere's disease, vestibular neuronitis, acoustic neuromas, and positionally induced peripheral syndromes, were eliminated from this investigation.

DATA

We examined the MRA findings for each subject and classified the configurations on the basis of developmental variants and acquired intrinsic vascular disorders that have an impact on regional blood flow.

We have extracted from this database a variety of vascular disorders for illustrative purposes. The specific analysis of the complete cohort was presented in previous publications with the final conclusion that approximately 50% of the subjects revealed some morphological or perfusion disorder.[7,8]

The following illustrations and brief clinical summaries integrate the radiologic evidence with the vestibulocerebellar dysfunction. The common denominator of each case in this study is vertigo. We emphasize that these neuro-otologic cases are not homogeneous; they depict the wide panorama of dysfunctions of the brain stem and cerebellum. The motor disorders of visual tracking and of the vestibulo-ocular reflexes and incoordination of the trunk or extremities are observed variably and in accordance with the primary regions of disease.

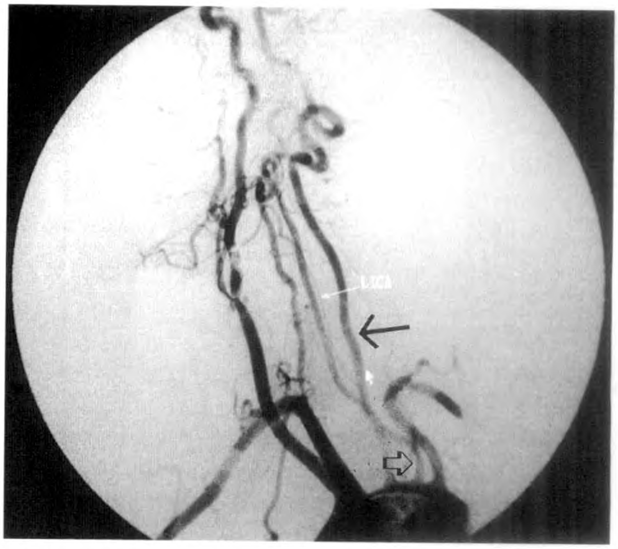

Fig 2. (Case 2) Contrast angiogram, arch study. Left vertebral artery (VA; solid arrow and small white arrow) is identified below atlas loop, and origin (open arrow) is from arch of aorta. LICA — left internal carotid artery.

Case 1 (Normal Images). This 18-year-old man was investigated for symptoms compatible with basilar migraine. The presenting complaints were headaches, nausea and vomiting, fluctuating hearing loss in the left ear, and gait ataxia. The medical evaluation and neurologic examination performed between episodes revealed normal findings. An MRI study of the brain and MRA of the circle of Willis and cervical vessels were performed; these were considered to show normal findings (Fig 1).

Case 2 (Developmental Abnormalities). This 65-year-old man was examined for intermittent brief symptoms of lightheadedness and occasional vertigo with episodic weakness of the right extremities over several months. The neurologic survey performed between occurrences yielded normal findings. A contrast angiogram revealed a rare anatomic variant of the VA with the point of origin arising directly from the arch of the aorta (Fig 2). The volumetric flow through the VBA system appeared to be competent. Further examination of the angiogram revealed a significant stenosis of the carotid artery, which was alleviated by surgical correction and total recovery.

Case 3. A relatively rare persisting right trigeminal artery was observed in this 72-year-old man who was investigated for "dizziness" and vertigo (Fig 3).

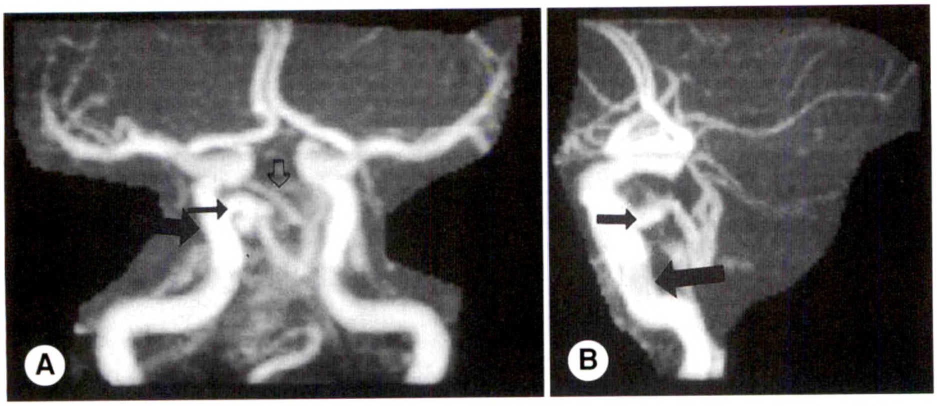

Fig 3. (Case 3) A) MRA of circle of Willis. AP projection reveals origin of persistent trigeminal artery (small arrow) from internal carotid artery (ICA; large arrow). Note hypoplastic posterior cerebral artery (open arrow). B) MRA in lateral projection. Internal carotid artery is identified by large arrow, and origin of persistent trigeminal artery by small arrow.

The neuro-otologic examination results were normal, though advanced presbycusis was measured bilaterally. The MRI revealed brain shrinkage compatible with aging and evidence of microvascular focal ischemia. After a thorough study, we concluded that this embryological anomaly, which provides posterior brain perfusion by way of shunting, in conjunction with carotid insufficiency, was a likely factor in inducing the presenting complaints.

Case 4. A persistent hypoglossal artery was identified in a 73-year-old woman who complained of intermittent vertigo, instability, and lightheadedness (Fig 4). The findings of auditory and visual assessments were normal; the positive findings included a wide-based gait and failure of the tandem test.

Case 5 (Collateral Cervical Circulation). A 72-year-old man was surveyed for lightheadedness, transient vertigo, episodic nausea and vomiting, and dysequilibrium occurring within the previous 6 months. Additional complaints included fluctuating hearing with progressive loss in the left ear of a sensorineural type, and gait ataxia. The neuro-otologic examination revealed normal cranial function (excluding the auditory disability), incoordination of upper extremities, failure of tandem gait, and unsteady, broad-based walking. The MRI revealed a left parietal infarction with numerous areas of small vessel ischemia. The cervical MRA identified an occlusion of the left internal carotid artery, an absent left VA, and a cervical collateral merging with the adjacent VA into the BA (Fig 5).

Case 6 (Basilar Artery Stenosis). A 74-year-old woman complained of intermittent transient vertigo, blurring of vision, nausea, and brief episodes of staggering and unstable gait (Fig 6). Six months before these episodes, the patient had suffered a right temporoparietal lobe infarction that was associated with a persistent swallowing disorder that included mild

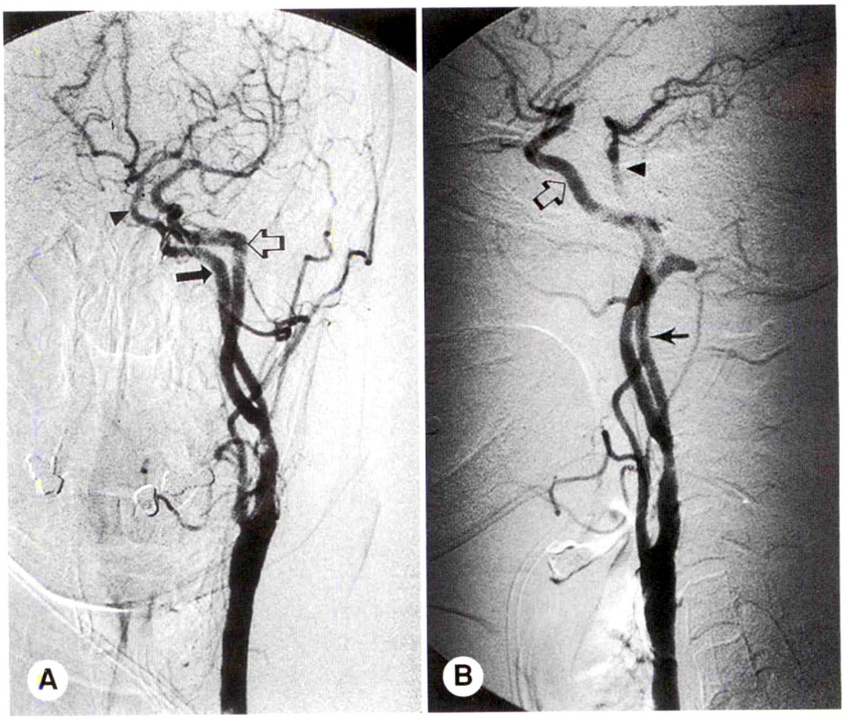

Fig 4. (Case 4) A) Digital subtraction angiogram in AP projection. Apparent duplication of ICA actually represents persistent hypoglossal artery (PHA; solid arrow), with point of origin above carotid bifurcation. Note intracranial ICA (open arrow) and basilar artery (arrowhead). B) Digital subtraction angiogram in lateral projection. Separation of ICA (open arrow) from PHA (solid arrow) is evident. Anterior artery proceeds intracranially, displaying normal configuration (open arrow). Arterial variant (PHA) courses posteriorly and continues into basilar artery (arrowhead).

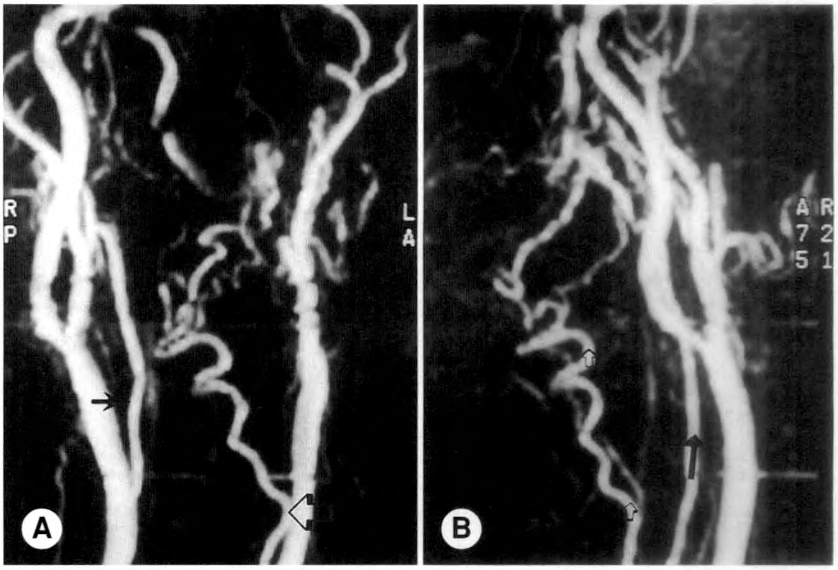

Fig 5. (Case 5) A) AP projection of cervical arteries identifies right VA (solid arrow) and extremely tortuous vessel (open arrow) that ultimately merges into basilar artery (not seen in this image). B) Lateral projection depicts normal VA (solid arrow) and deep collateral tortuous cervical artery (open arrows).

symptoms of obstruction and delay of passage. Examination revealed normal neuro-otologic findings except for poor pharyngeal function, wide-based walk, failure of tandem gait, and age-related presbycusis.

Case 7 (Basilar Artery Dolichoectasia). A 72-year-old man was examined for otalgia, right-sided hearing impairment (sensorineural type), intermittent facial paresthesias, and occasional lightheadedness with minor complaints of vertigo (Fig 7). The neurologic examination, with special attention to the vestibular function and electro-oculography, showed normal findings.

DISCUSSION

We examined this group of vertiginous patients by the standard neuro-otologic techniques, including audiometry, quantitative measurement of spontaneous and latent nystagmus, ocular tracking, positional and caloric vestibular stimulation, the electrophysiological measurement of the early far-field acoustic response, and MRI and MRA. The cranial nerve functions were grossly intact in this complement of subjects; nonlocalizing vestibulocerebellar dysfunctions were observed in each individual. Integration of the above tests (excluding MRI and MRA) failed to localize the site of the lesion producing vertigo. Sufficient data were examined to conclude that although the auditory brain stem response might be abnormal, there were such inconsistencies of morphology, amplitude, and interaural or intra-aural peak latencies that a correlation among symptoms, data, and localization could not be established.

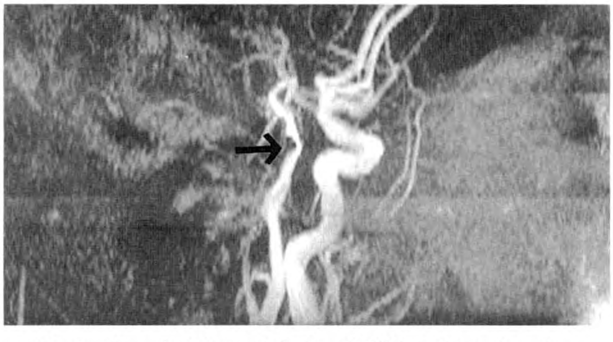

Fig 6. (Case 6) MRA of circle of Willis in lateral projection. Lumen of proximal basilar artery is of normal caliber until point of severe stricture (arrow) in distal segment, imaged below bifurcation into posterior cerebral arteries.

A similar conclusion was drawn from the various components of electro-oculography and the associated studies from positional and caloric stimulation. The dichotomy between peripheral and central vestibular derangements could not be confirmed in this series. This conclusion was supported by a longitudinal assessment of subjects with heretofore-considered peripheral disease, some of whom eventually had cerebellar infarctions.

Consequently, and with little diagnostic or localizing value from the previously described tests, we have considered the vascular component of hindbrain dysfunction as a potential etiologic source of vertigo.[22] This report, while illustrating some of the possible abnormalities of the hindbrain circulation, supports the concept that intrinsic vascular disease can produce a hypoperfusion state without MRI evidence of infarction and may initiate the vestibulocerebellar disorders characterized in these patients' abstracts.

Whereas the relationships among carotid artery stenosis, flow rates through the narrowed area, and volumetric flow are established,[23] the authors postulate a similar construction for the VBA system. The

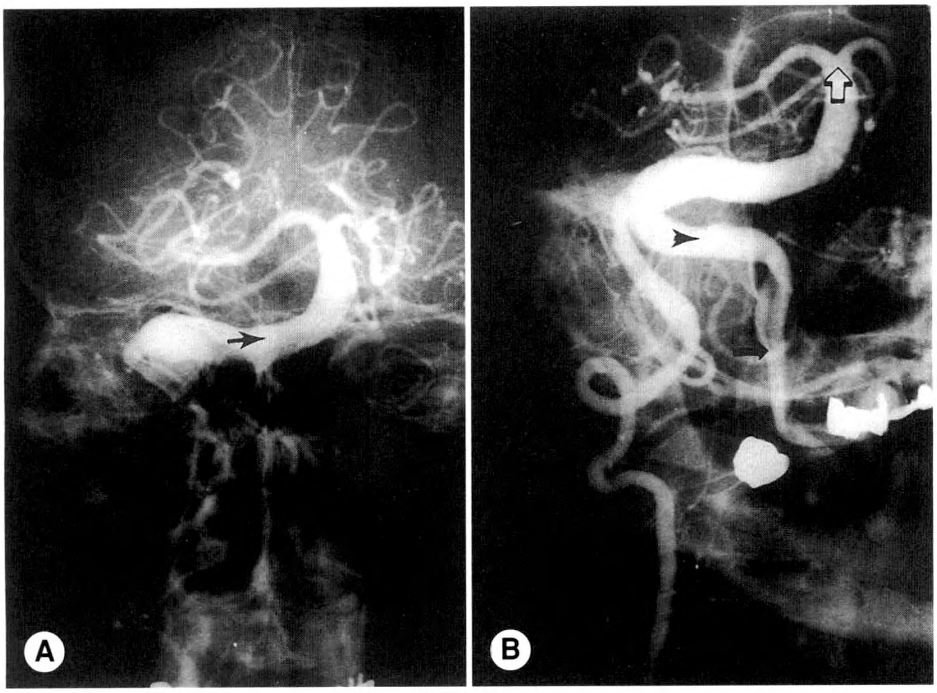

Fig 7. (Case 7) A) Contrast angiography of cerebral circulation in coronal view demonstrates massive dilatation of basilar artery (arrow) with obvious displacement from midline. B) Oblique view with contrast-filled VA reveals retrograde flow into opposite VA (solid arrow), and distorted and dilated basilar artery (arrowhead). Note bifurcation into posterior cerebral arteries (open arrow).

magnitude of the volumetric flow through the VBA, ie, 20% of the cerebral perfusion, suggests the impact of partial stenosis on the BA.[24] A previous report by the authors considered the varieties of vascular configurations, including tortuosity, intrinsic narrowing, stenosis, and collateral circulation, and their effects on the posterior brain vascular flow.[22] The evidence suggests that these hemodynamic factors, in conjunction with the abnormalities noted in this material, are sufficient to compromise vascular flow and cause a symptom-producing hypoxemic state — in effect, a transient ischemic event. After relief from extrinsic compression or resumption of adequate flow (eg, correction of arrhythmias, postural hypotension, or cervical rotation or extension), relatively normal function may resume.[16-18,20,25]

As a preliminary to MRA, the cerebral status must be examined by MRI. Failing a specific diagnosis such as tumor or infarction, the authors investigated the vascular patterns of the neck and brain in an attempt to identify radiographic evidence of arterial insufficiency. These studies were limited to those subjects whose diagnosis could not be established by the standard chronological survey, symptom complex, and objective evidence of recognized entities. These disorders included Meniere's disease, viral or vestibular neuronitis, cochleovestibular trauma, and benign postural vertigo.

After review of our data, we suggest that MRA should be considered in the following circumstances: 1) unknown diagnosis, barring the above recognized syndromes or entities; 2) a potential vascular component suggested by initiation or aggravation of vestibular systems due to positional change or rotation and extension of the neck; 3) an acute vertiginous episode with significant dysfunction in gait, nystagmus, nausea and vomiting, and associated cranial nerve dysfunction, ie, the vertiginous syndrome; 4) recurrent vertiginous episodes, without hearing impairment or cranial nerve dysfunction; and 5) crescendo-type vertigo with increasing disability.

An analysis of the cases suggests a variety of conclusions based on the developmental anatomy and the incremental damages of local atherosclerosis, regional osteoarthritis, and fibromuscular compression. The developmental abnormalities illustrated in cases 2, 3, and 4 provide sufficient perfusion through anomalous vessels until the secondary impact of regional arterial stenosis intervenes. In these cases, diminished flow through the associated carotid artery impacts downstream on the embryonic remnant connecting to the VBA system. In this instance, although the primary disorder, ie, carotid artery stenosis, generally impacts on the anterior circle of Willis and the associated peripheral branches, the perfusion deficit is clinically represented through the decreased hindbrain circulation.

Collateral circulation via cervical anastomoses can be impaired at the origin or termination of these vessels, as in case 5. In addition, multivessel disease with cerebral infarction was noted in the parietal area in this individual subsequent to internal carotid artery occlusion.

Basilar artery stenosis (case 6) can be of such significantly narrowed dimensions that the critical volumetric flow is diminished below the level necessary to maintain competent vestibulocerebellar function.[6,26] Progression to complete stenosis can be life-threatening or compensated by posterior shunting via the circle of Willis.

The uncommon entity of severe dolichoectasia (case 7) is associated with the recognized hemodynamic disorders of turbulence, slow marginal intravascular flow, stasis, and the potential for thrombosis and secondary embolization.

The authors examined the issue of unifocal versus multifocal and extracranial or intracranial arterial disease as it might impact on the posterior circulation. The carotid circulation is impaired by stenoses or occlusion in approximately 10% of this series. The status of the VBA system on MRA analysis reveals abnormalities that include mild to extreme tortuosity, stenosis, or occlusion in approximately 50% of the subjects. We conclude that although the majority of vertiginous patients in this investigation revealed some degree of circulatory embarrassment in the hindbrain, a subset had coexistent carotid flow disturbances to the forebrain that contributed to the vestibular disturbance.

We propose that there is a prominent role for analysis of the vascular system of the hindbrain during the investigation of vertigo. We submit that analysis of the VBA system relating to the vestibulocerebellar apparatus may have a diagnostic value when the scenario of perfusion disorders is probable on the basis of historical and physical evidence. We have eliminated the MRA when other factors of neuronal damage such as viral, neoplastic, traumatic, or degenerative sources are sufficiently evident to be diagnostic. The concept of vascular diseases characterized by the symptoms of recurrent hypoperfusion with a progressive evolution into complete occlusion and the consequent classic neurologic syndromal deficits can finally be confirmed in a segment of vertiginous subjects by a longitudinal study of our patients and the reports of others.[19,20]

The event of isolated vertigo without additional neurologic findings continues to be of concern. We concluded from this study that the diagnostic evaluation by the current otoneurologic survey for isolated vertigo provides some degree of objective measure of abnormalities, but little specificity, and inadequate evidence for localization within the vestibulocerebellar system at this time. On the basis of this report, we encourage further investigation into potential vascular disorders during the analysis of isolated or syndromal vertigo.

We conclude that despite the application of advanced neuroradiologic techniques, infrequent or isolated events of vertigo continue to be a medical problem. We submit that longitudinal studies may ultimately provide the underlying pathological answers for this complaint.

And finally, the less common, but certainly more dramatic, vertiginous syndromes occurring subsequent to regional occlusive disease can be identified and therapeutically programmed on the basis of the existing composite of clinical and radiographic evidence.

ACKNOWLEDGMENT — We acknowledge and appreciate the contribution by Orlando Alvarez, MD, in providing radiologic consultation.

REFERENCES

1. Takahashi M. Basilar artery. In: Newton TH, Potts DG, eds. Radiology of skull and brain. St Louis, Mo: Mosby, 1974: 1775-95.

2. Marks MP, Pelc NJ, Ross MR, et al. Determination of cerebral blood flow with a phase-contrast one MR imaging technique. Evaluation of normal subjects and patients with arteriovenous malformation. Radiology 1992;182:467-76.

3. VonBudingen HJ, Staudachen T. Evaluation of vertebrobasilar disease. In: Newell DW, Aaslid R, eds. Transcranial Doppler. New York, NY: Raven Press, 1993:167-96.

4. Osborn AG. Introduction to cerebral angiography. Philadelphia, Pa: Harper and Row, 1980.

5. Luxon LM. Signs and symptoms of vertebrobasilar insufficiency. In: Hofferberth B, Brune GG, Sitzer G, Weger HD, eds. Vascular brain stem diseases. Basel, Switzerland: Karger, 1990:93-111.

6. Bradshaw P, McQuaid P. The syndrome of vertebro-basilar insufficiency. Q J Med 1963;32:279-96.

7. Welsh LW, Welsh JJ, Jaffe SC, Healy MP. Evaluation of the vestibular system by magnetic resonance angiography. Laryngoscope 1996;106:1138-43.

8. Welsh LW, Welsh JJ, Jaffe SC, Healy MP. Syndromal vertigo identified by magnetic resonance imaging and angiography. Laryngoscope 1996;106:1144-51.

9. Riggs HE, Rupp C. Variation in form of circle of Willis. Arch Neurol 1963;8:24-30.

10. Alpers BJ, Berry RG, Paddison RM. Anatomical studies of the circle of Willis in normal brain. Arch Neurol Psychiatry 1959;81:409-18.

11. Alpers BJ, Berry RG. Circle of Willis in cerebral vascular disorders. Arch Neurol 1963;8:398-402.

12. Battacharji SK, Hutchinson EC, McCall AJ. The circle of Willis — the incidence of developmental abnormalities in normal and infarcted brains. Brain 1967;90:747-58.

13. Krabbe-Hartkamp M, DeLeeuw PE, DeRoot JC, et al. Circle of Willis: morphologic variation in small three-dimensional time-of-flight MR angiograms. Radiology 1998;207:103-11.

14. Valvassori GE. Vertigo in vertebral-basilar insufficiency.

Rev Laryngol 1985;106:215-8.

15. Amarenco P, Roullet E, Hommel M, Chaine P, Marteau R. Infarction in the territory of the medial branches of the posterior inferior cerebellar artery. J Neurol Neurosurg Psychiatry 1990;53:731-5.

16. Sakai F, Ishii K, Igarashi H, et al. Regional cerebral blood flow during an attack of vertebrobasilar insufficiency. Stroke 1988;19:1426-30.

17. Sturzeneggar M, Newell DW, Douville CM, Byrd S, Schoonover KD, Nicholls SC. Transcranial Doppler and angiographic findings in adolescent stretch syncope. J Neurol Neurosurg Psychiatry 1995;58:367-70.

18. Rancurel G, Kieffer E, Arzimanoglou A, Vitte E, Freyss G. Hemodynamic vertebrobasilar ischemia: differentiation of hemodynamic and thromboembolic mechanisms. In: Berguer R, Caplan L, eds. Vertebrobasilar arterial disease. St Louis, Mo: Quality Medical Publishing, 1992:40-51.

19. Grad A, Baloh RW. Vertigo of vascular origin. Arch Neurol 1989;46:281-4.

20. Kim GW, Heo JH. Vertigo of cerebrovascular origin proven by CT scan or MRI: pitfalls in clinical differentiation from vertigo and aural origin. Yonsei Med J 1996;37:47-61.

21. Patrux S, Laissy JP, Jouini S, et al. Magnetic resonance angiography (MRA) of the circle of Willis: a prospective comparison with conventional angiography in 54 subjects. Neuroradiology 1994;36:193-7.

22. Welsh LW, Welsh JJ, Lewin B. Vertigo: analysis by magnetic resonance imaging and angiography. Ann Otol Rhinol Laryngol 2000;109:239-48.

23. Kerber CW, Liepsch D. Flow dynamics for radiologists: practical considerations in the live human. AJNR Am J Neuroradiol 1984;15:1076-86.

24. Litt AW. MR angiography of the central nervous system. Basic flow phenomena. Magn Reson Imaging Clin N Am 1995;3:375-90.

25. Kline RA, Berguer R. Vertebral artery reconstruction. In: Taylor LM Jr, ed. Basic data underlying clinical decision making. Ann Vasc Surg 1993;7:497-501.

26. Biemond A. Thrombosis of the basilar artery and vascularization of the brain stem. Brain 1951;74:300-17.

≈

SAN FRANCISCO OTOLOGY & NEUROTOLOGY UPDATE 2000

The San Francisco Otology & Neurotology Update 2000 will be held October 26-28, 2000, in San Francisco, California. For information, contact University of California, San Francisco, Office of Continuing Medical Education, Room LH-450, San Francisco, CA 94143-0742; telephone (415) 476-4251; fax (415) 476-0318; e-mail: palmerk@ocme.ucsf.edu.

Ann Otol Rhinol Laryngol 109:2000

SURGICAL MANAGEMENT OF UNCOMPLICATED OTITIS MEDIA IN A PEDIATRIC MEDICAID POPULATION

STEPHEN BERMAN, MD
PATRICIA J. BYRNS, MD
JESSICA BONDY, MHA
DENNIS LEZOTTE, PHD

DENVER, COLORADO

The objective of this study was to document the frequency and timing of otitis media–related visits, audiological consultations, and surgical interventions following a new episode of otitis media. A retrospective descriptive study was performed on a Medicaid administrative database that follows individual patients over time. The study included 14,453 children enrolled in Medicaid during 1991 and 1992 who were 30 months of age or younger and had a "new" episode of otitis media. Among 14,321 patients with an uncomplicated episode of otitis media, there were 10,443 with additional otitis media visits. Audiological testing was performed in 1,134 (10.9%). The testing occurred within 2 months of the onset of otitis media in 52.2% of the children and within 3 months in 66.6%. Physicians referred 400 children (3.8%) to an otolaryngologist; 299 (75%) underwent 1 or more surgical procedures. These surgical interventions included placement of ventilating tubes in 296 children, adenoidectomy in 34 children (all of whom also had placement of ventilating tubes), mastoidectomy in 2 children, and tympanoplasty in 1 child. The proportion of children who underwent surgical placement of ventilating tubes who had prior audiological testing was 174 of 296 (58.8%). The overall surgical rate for ventilating tubes was 2.9%. Among children who underwent surgery, the procedure occurred within 2 months of the onset of otitis media in 21.4% of children. Attempts to rationalize the management of otitis media in early childhood must deal with the difficulties in distinguishing among the otitis media conditions. The findings of this study suggest a need to know whether insertions of ventilating tubes within 3 months after a new episode of otitis media are related to unresponsive or recurrent infections.

KEY WORDS — Medicaid, otitis media, surgical management.

INTRODUCTION

Otitis media, an inflammation of the middle ear, is associated with middle ear effusion or otorrhea. Otitis media can be further classified by its associated clinical symptoms, otoscopic findings, duration, frequency, and complications into acute otitis media, otitis media with effusion, unresponsive otitis media, recurrent otitis media, otitis media with complications, and chronic suppurative otitis media. Acute otitis media is commonly defined as inflammation of the middle ear with a rapid onset of symptoms such as earache, fever, irritability, anorexia, or vomiting. Cough, congestion, irritability, and fever may result from the associated viral upper respiratory tract infection.[1-3] The otoscopic findings of middle ear inflammation include decreased tympanic membrane mobility, a bulging contour with impaired visibility of the ossicular landmarks, a yellow or red color, exudate on the membrane, and bullae. When our patients with a history of recurrent otitis media were screened monthly, approximately one third of children with bulging red or yellow eardrums with decreased or absent mobility were otherwise asymptomatic.[4] Otitis media with effusion is defined as an asymptomatic middle ear effusion. Findings that suggest otitis media with effusion include visualization of air fluid levels, middle ear fluid, and decreased membrane mobility. When a membrane is translucent, the character of the middle ear fluid may be appreciated; however, when the tympanic membrane is more opaque, it is difficult to visualize the middle ear effusion. Etiologic studies document the frequent isolation of middle ear pathogens in middle ear effusions by tympanocentesis regardless of the type of effusion or associated symptoms.[4,5] Unresponsive acute otitis media is said to occur when the initial antibiotic therapy is not associated with resolution of the clinical symptoms or improvement of the otoscopic signs of middle ear inflammation. As a result, the clinician administers another antibiotic.

Recurrent otitis media is said to occur when a child has 3 or more episodes of acute otitis media within 6 months. How physicians manage children with acute otitis media, unresponsive otitis media, recurrent otitis media, and otitis media with effusion varies widely.[5-10] Our prior publications reported findings on the use of all otitis media–related services (not limited to new episodes of otitis media) and antibiotic prescribing patterns.[7,8] The current study documents the frequency and timing of otitis visits, prescriptions, audiological testing, and surgical interventions after a new episode of uncomplicated otitis media.

From the Department of Pediatrics (Berman), and the Department of Preventive Medicine and Biometrics (Bondy, Byrns, Lezotte), University of Colorado Health Sciences Center, Denver, Colorado. This study was supported by a grant from the Agency for Health Care Policy and Research (RO1 HS07816-03).

CORRESPONDENCE — Stephen Berman, MD, The Children's Hospital, 1056 E 19th Ave, B032, Denver, CO 80218.

METHODS

The study cohort consisted of 14,453 children enrolled in Medicaid in Colorado during 1991 and 1992 who were 30 months of age or younger at the time of a "new" episode of otitis media. The index visit for this "new" episode was defined as an ambulatory visit with a diagnosis of otitis media and prescription of an antibiotic. When otitis media was not diagnosed in the previous 3 months, all antibiotics prescribed during this period had to have an appropriate diagnostic explanation other than otitis. Thus, a child would have been included in the cohort if given an antibiotic in the previous 3 months for another diagnosis, such as impetigo, but would have been excluded by our criteria if this antibiotic prescription had been filled without an associated diagnosis. For example, children with recurrent otitis media who were being treated with antibiotic prophylaxis but who did not visit a physician would have been excluded from the cohort. Likewise, children with persistent middle ear effusions who were being treated with antibiotics would have been excluded.

Children with an appropriate index visit had to meet the following additional criteria for inclusion: their age at the time of the index visit was 30 months or younger; they were enrolled in Medicaid for 6 months after the index visit; they had no hospitalizations within 24 days of the index visit for possible sepsis, bronchiolitis, croup, meningitis, sinusitis, pneumonia, or mastoiditis; and their index visit did not have a secondary diagnosis of mastoiditis, cholesteatoma, or perforation.

The data obtained from an extract of the Medicaid Medical Events Database (MMED) included patient demographics, provider information (including physician specialty and primary care provider status), and claims paid by Medicaid for prescriptions, outpatient office and clinic visits, emergency department visits, and inpatient hospitalizations. The MMED and the artificial intelligence software developed by the research team have been described in prior publications.[7,8,11] Colorado Medicaid eligibility during this time period conformed to mandatory federal requirements. During the period of the study, more than 95% of the state's Medicaid recipients obtained services in a fee-for-service environment. The analyses followed individual patients over time by means of the unique Medicaid recipient identification numbers that are maintained across interrupted periods of enrollment, name changes, and moves to different counties.

The International Classification of Diseases (ICD-9) diagnostic codes were used to identify visits for otitis media on the basis of studies that have documented physicians' coding practices related to otitis media.[6,9] Visits and procedures associated with acute otitis media, otitis media with effusion, and chronic otitis media were included. Therefore, the more generic term otitis media is used in this study. Otitis media–related visits that occurred within 90 days of the index visit were documented. An antibiotic was considered to have been prescribed to treat otitis media if dispensed up to 24 hours before or within 48 hours after an encounter that included a diagnosis of otitis media as described in a prior publication.[7] We considered unresponsive otitis to have occurred when another antibiotic was prescribed within 24 days after initiation of antibiotic therapy for a new episode of otitis media. Antibiotics administered during a visit after 24 days could have been prescribed for otitis media with effusion, unresponsive otitis media, or a new infection. Children who had no additional documented visits with a diagnosis of otitis media, antibiotic fills, or surgical procedures within 90 days of the index visit were considered to have resolved episodes. This is an assumption, because we have no data to determine what happened with these children. We assumed that if the children continued to be symptomatic or developed a recurrence of symptoms, they would either seek care and have another diagnosis of otitis or call their physician and have an antibiotic ordered over the phone. If either of these interventions happened, they would have been noted in the claims data. Therefore, these patients without follow-up documented in the claims data either were seen at well child care visits and were noted to have normal ears and did not have a diagnosis of otitis media coded, or were not brought back to the physician because they became asymptomatic. However, we cannot exclude the possibility that some of these children had ongoing disease that was not recognized during the following 3 months.

The patient demographic variables included age, sex, urban versus rural residence, ethnicity, and enrollment category (Aid to Families with Dependent Children [AFDC], etc). Residence referred to the first county of residence during the study year, with "urban" defined by the Census Bureau's metropolitan statistical areas. The classification for ethnicity included Caucasian, Hispanic, African-American, Native American, and other.

RESULTS

For 1991 and 1992, we identified a total of 14,453 children between 3 and 30 months of age with a new episode of otitis media who had a subsequent 6 months of continuous Medicaid enrollment. The 74 children who were hospitalized at the index visit and 58 addi-

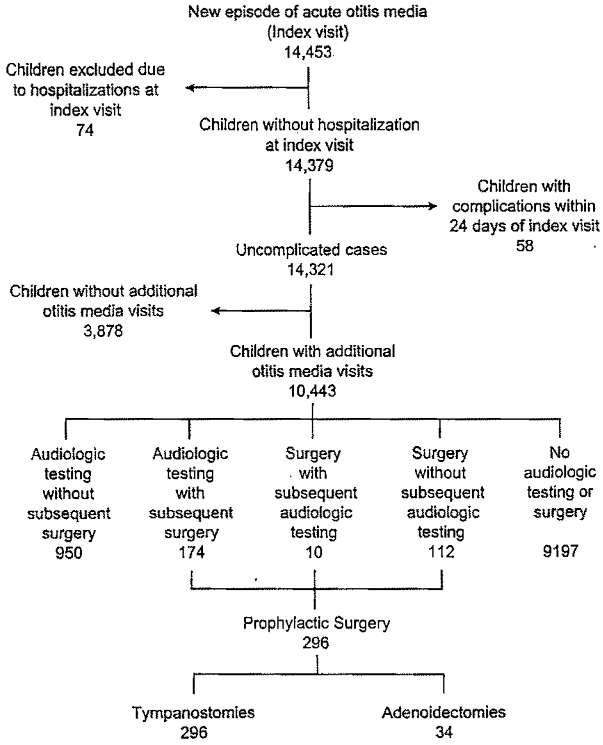
New episode of acute otitis media (Index visit) 14,453
Children excluded due to hospitalizations at index visit 74
Children without hospitalization at index visit 14,379
Children with complications within 24 days of index visit 58
Uncomplicated cases 14,321
Children without additional otitis media visits 3,878
Children with additional otitis media visits 10,443
Audiologic testing without subsequent surgery 950
Audiologic testing with subsequent surgery 174
Surgery with subsequent audiologic testing 10
Surgery without subsequent audiologic testing 112
No audiologic testing or surgery 9197
Prophylactic Surgery 296
Tympanostomies 296
Adenoidectomies 34

Management of acute otitis media in children 3 to 36 months of age enrolled in Colorado Medicaid program in 1991 and 1992.

tional children who had complications or later hospitalizations were excluded from the analysis. Among these 132 children, there were 3 with mastoiditis, 1 with meningitis, 2 with sinusitis, 16 with pneumonia, 58 with bronchiolitis, and 21 with possible sepsis. Some children had multiple diagnoses. The algorithm in the Figure reviews the management of children with uncomplicated cases who were included in the initial cohort. Among the 14,321 children with uncomplicated cases who were initially included in the cohort, 3,893 (27.2%) had no documented additional visits with a diagnosis of otitis media, antibiotic fills, or surgical procedures within 90 days of the index visit. We assume that the episodes of acute otitis media resolved in these children, many of whom probably received ear checks during well child care visits.

Frequency and Timing of Additional Otitis Media Visits. The first subsequent otitis media–related visit occurred within 11 days for 11.0%, from 11 to 24 days for 33.3%, from 24 to 45 days for 29.8%, and from 46 to 90 days for 25.9% of the children. During the following 6 months of follow-up, 39.3% had 2 otitis media–related visits, 21.9% had 3 visits, 37.0% had 4 to 9 visits, and 1.8% had 10 or more visits.

Frequency and Timing of Audiological Testing. Among the 10,443 children with uncomplicated cases who had documented otitis media–related follow-up visits, 1,134 (10.9%) had audiological testing documented. The age-specific referral rates for audiological testing, shown in Table 1, vary from 9.3% to 11.7%. The age of the patient (at the index visit) does not greatly influence the referral rate for audiological testing. As shown in Table 2, a higher proportion of Caucasian (11.6%) and Hispanic (11.8%) children were referred for audiological testing than African-American children (4.2%). Children who always (12.5%) or sometimes (11.3%) had a primary care provider were also more likely to have their hearing tested than were children who never had a primary care provider (8.8%). The timing of the referrals for audiological testing in relation to the initial index visit for children with uncomplicated cases is shown in Table 3. The testing occurred within 2 months of the onset of otitis media in 66.6% of children and within 3 months in 77.6%. Audiological testing was performed before the first follow-up visit in 44.8% of children, after the first follow-up visit in 16.0%, after the second follow-up visit in 14.8%, and after 3

TABLE 1. AGE-SPECIFIC REFERRAL RATES FOR AUDIOLOGICAL TESTING AND SURGICAL INSERTION OF VENTILATING TUBES

Age (mo)	*No. of Patients*	*Audiological Testing (%)*	*Ventilating Tubes (%)*
3 to 6	3,047	10.9	3.4
7 to 12	4,008	11.2	2.5
13 to 18	2,760	9.3	3.0
19 to 24	2,507	11.7	2.7
25 to 30	1,999	11.1	1.9
Total	14,321	10.9	2.8

TABLE 2. DEMOGRAPHIC CHARACTERISTICS

	*No. of Patients**	*Audiological Testing (%)*	*Ventilating Tubes (%)*
Gender†			
Male	3,191	11.1	2.8
Female	2,756	10.7	2.5
Ethnicity			
Native American	53	11.3	0
Hispanic	3,394	11.8	1.5
Caucasian	5,847	11.6	3.6
African-American	990	4.2	2.5
Other	159	4.4	1.9
Locale			
Urban	8,497	10.9	2.8
Rural	1,946	10.5	2.5
Primary care provider access			
Always	2,894	12.5	2.7
Sometimes	4,271	11.3	2.9
Never	3,278	8.8	2.7

*Number of children with uncomplicated cases who had follow-up visits.

†Gender information is available only for 1992.

TABLE 3. TIMING OF REFERRALS FOR AUDIOLOGICAL TESTING AND VENTILATING TUBES

Months From Index Visit	Audiological Testing		Ventilating Tubes	
	No.	%	No.	%
<1	373	32.9	3	1.0
1	219	19.3	12	4.0
2	163	14.4	49	16.4
3	125	11.0	53	17.7
4	110	9.7	58	19.4
5	99	8.7	78	26.1
6	45	4.0	46	15.4

or more follow-up visits in 24.4%. Among the 1,134 children with hearing tests, 174 (15.3%) underwent subsequent surgical intervention. The proportion of children who underwent surgical placement of ventilating tubes who had prior audiological testing was 174 of 296 (58.8%).

Frequency and Timing of Referrals to Otolaryngologists for Surgery. Physicians referred 400 children (3.8%) to an otolaryngologist for a consultation, and 299 (75%) underwent 1 or more surgical procedures. These surgical interventions included placement of ventilating tubes in 296 children, adenoidectomy in 34, mastoidectomy in 2, and tympanoplasty in 1 child. Adenoidectomy was performed in 34 children at the time of ventilating tube insertion. The overall surgical rate for placement of ventilating tubes was 296 of 10,443 (2.8%). The age-specific rates for placement of ventilating tubes, shown in Table 1, vary from 1.9% for the oldest group to 3.4% for the youngest group. The surgical rates were similar for boys (2.8%) and girls (2.5%).

Surgery was performed before the fourth follow-up visit in 32.2% of children, between the fourth and ninth follow-up visits in 61.0%, and after the ninth follow-up visit in 6.7%. The timing for the surgical procedure in relation to the new episode index visit is shown in Table 3. The surgery occurred within 2 months of the onset of otitis media in 21.4% of children and within 3 months in 39.1%. The mean duration from the index visit to surgery was 3.87 months when the referring physician was a pediatrician and 3.64 months when he or she was a family physician. The mean duration from the index visit to surgery was 3.84 months for Hispanic children, 3.93 months for Caucasian children, and 3.68 months for African-American children.

The average number of antibiotic courses administered before surgery was 4.1. The age-specific numbers of antibiotic courses were 5 for children 3 to 6 months of age, 3.9 for children 7 to 12 months of age, 4.0 for children 13 to 18 months of age, 3.4 for children 19 to 24 months of age, and 3.1 for children 25 to 30 months of age.

The influence of demographic characteristics on rates of ventilating tube surgery is shown in Table 2. A higher proportion of Caucasian children (3.6%) was referred for surgery than Hispanic (1.5%) and African-American children (2.5%). The proportions of children in whom ventilating tubes were implanted who lived in urban (2.8%) and rural areas (2.5%) were similar. Although the rates were not greatly influenced by access to a primary care provider, a prior publication reported that the timing of the referral was affected by access to a primary care provider.[8]

DISCUSSION

In this analysis, we selected a cohort who did not have a history of otitis media in the 3 months before the diagnosis of a new episode and did not receive antibiotic prophylaxis for recurrent acute otitis media or antibiotics to treat persistent middle ear effusion. This method of selection was chosen to focus on surgical management of the otitis media continuum during a 6-month period of continuous Medicaid enrollment after a new episode of otitis media. We arbitrarily considered unresponsive otitis to have occurred when another antibiotic was prescribed within 24 days after initiation of antibiotic therapy for an episode of otitis media, despite the possibility that some clinicians may use antibiotics to treat otitis media with effusion within 24 days. After 24 days, no attempt was made to distinguish episodes of otitis media with effusion from unresponsive acute otitis media or another otitis episode, because of difficulties in diagnosis and coding. Middle ear effusions often remain for 6 weeks after diagnosis of otitis regardless of antibiotic therapy.[12] It is also possible that some children, especially those 3 to 6 months of age, experienced recurrent otitis media episodes after their index visit.

The rationale for surgical intervention in the cohort children could include the prevention of recurrent episodes of acute otitis media, as well as the management of otitis media with effusion or unresponsive acute otitis media. Among children in whom ventilating tubes were implanted, 21.4% underwent the procedure by the end of the second month after their index visit. The indication for ventilating tube insertion in children who had tubes placed within 2 months of their index visit with a new episode of acute otitis media was more likely to be unresponsive acute otitis media than recurrent acute otitis or persistent middle ear effusion.

This study highlights ethnic differences in patterns of care related to the management of otitis media. Financial considerations should not have affected these patterns, because all children in the cohort had continuous fee-for-service insurance coverage with Medicaid for the 6 months of data collection. Physicians referred African-American children for audiological testing less frequently than Native American, Hispanic, and Caucasian children. Physicians referred African-American and Hispanic children for ventilating tube placement less frequently than Caucasian children. These differences could be explained by ethnic differences in the severity of disease and the frequency of unresponsive acute otitis media, persisting middle ear effusions, and recurrent acute otitis media. Alternatively, there may be cultural differences in willingness to undergo surgical procedures or physician bias in referral patterns. Minority populations may be served disproportionately by physicians who work in clinics and community health centers and have different practice styles compared with physicians in private practice.

Although national guidelines recommend audiological testing before insertion of ventilating tubes for otitis media with effusion, the guidelines do not address the use of this testing when surgery is being considered for recurrent or unresponsive otitis media.[5] It is unclear whether the 41.8% who underwent surgery without prior audiological testing reflect the other indications for surgery or a failure to perform audiological testing in children with otitis media with effusion. Further studies should focus on the indications for surgery being performed within 3 months of a new episode of otitis media. It is also important to better understand the relative impact of recurrent otitis media compared with otitis media with effusion in children who undergo surgery 5 and 6 months after the index visit.

In summary, it is important to determine how clinicians are managing unresponsive acute otitis media, otitis media with effusion, and recurrent acute otitis media in order to design education efforts to reduce the variability in practice patterns. Attempts to rationalize the management of otitis media in early childhood must deal with the difficulties in distinguishing among the conditions included in the otitis media continuum. The findings of this study suggest a need to know whether current insertions of ventilating tubes within 3 months after a new episode of otitis media are related to unresponsive or recurrent infections. It would also be valuable to explore further the reasons for ethnic differences in referral rates for both audiological testing and ventilating tube surgery.

REFERENCES

1. Koivunen P, Kontiokari T, Niemela M, Pokka T, Uhari M. Time to development of acute otitis media during an upper respiratory tract infection in children. Pediatr Infect Dis J 1999; 18:303-5.

2. Heikkinen T, Ruuskanen O. Signs and symptoms predicting acute otitis media. Arch Pediatr Adolesc Med 1995;149:26-9.

3. Niemela M, Uhari M, Jounio-Ervasti K, Luotonen J, Alho OP, Vierimaa E. Lack of specific symptomatology in children with acute otitis media. Pediatr Infect Dis J 1994;13:765-8.

4. Berman S. Current concepts: otitis media in children. N Engl J Med 1995;332:1560-5.

5. The Otitis Media Guideline Panel and Consortium: Stool SE, Berg AO, Berman S, et al. Otitis media with effusion in children. Guideline Technical Report Number 12. AHCPR Publication No. 94-0621. Rockville, Md: Agency for Health Care Policy and Research, Public Health Service, US Department of Health and Human Services, July 1994.

6. Roark R, Petrofski J, Berson E, Berman S. Practice variations among pediatricians and family practice physicians in the management of otitis media. Arch Pediatr Adolesc Med 1995; 149:839-44.

7. Berman S, Byrns PJ, Bondy J, Smith PJ, Lezotte D. Otitis media–related antibiotic prescribing patterns, outcomes, and expenditures in a pediatric Medicaid population. Pediatrics 1997;100:585-92.

8. Byrns PJ, Bondy J, Glazner JE, Berman S. Utilization of services for otitis media by children enrolled in Medicaid. Arch Pediatr Adolesc Med 1997;151:407-13.

9. Thompson D, Oster G, McGarry LJ, Klein JO. Management of otitis media among children in a large health insurance plan. Pediatr Infect Dis J 1999;18:239-44.

10. Gonzalez-Vallejo C, Sorum PC, Stewart TR, Chessare JB, Mumpower JL. Physicians' diagnostic judgements and treatment decisions for acute otitis media in children. Med Decis Making 1998;18:149-62.

11. Wade TD, Byrns PJ, Steiner JF, Bondy J. Finding temporal patterns: a set-based approach. Artif Intell Med 1994;6: 263-71.

12. Claessen JQPJ, Appelman CLM, Touw-Otten FWMM, De Melker RA, Hordijk GJ. Persistence of middle ear dysfunction after recurrent acute otitis media. Clin Otolaryngol 1994; 19:33-40.

Ann Otol Rhinol Laryngol 109:2000

EFFECT OF A BETA-STIMULANT ON THE INNER EAR STRIA VASCULARIS

KOSUKE ISHII, MD

WEI GANG ZHAI, MD

MASUMI AKITA, MD

SAITAMA, JAPAN

In vivo and in vitro experiments were conducted to investigate the effect of α-isoproterenol on the inner ear stria vascularis with intracellular cytochrome oxidase activity used as an index. Intraperitoneal injection of α-isoproterenol (5 mg/kg) was performed in 10 rats, and that of physiological saline in 4 rats, for 21 consecutive days. After the 3-week treatment, bilateral cochleas were excised for frozen sections and stained for cytochrome oxidase. The staining density of the stria vascularis for the enzyme was analyzed with a computer. Electron microscopic observation was also performed for some specimens. As for the in vitro experiments, bilateral cochleas from 6 normal rats were excised for cell culture. Cochlear cells from the right ear were cultured with medium containing α-isoproterenol (10-μmol/L concentration), and those from the left ear with medium alone. After 3-day culture, the enzyme activity of cytochrome oxidase in the stria vascularis was quantified by the same method used for the in vivo experiments. Cytochrome oxidase activity was markedly elevated in the α-isoproterenol group. The activity tended to be higher in the lower turns of the cochlea. Electron microscopy revealed that numerous mitochondria were present in marginal cells that protruded into the endolymphatic space. The enzyme activity was also elevated in the stria vascularis from cochlear specimens in the α-isoproterenol group of the in vitro experiment. The above results suggest that α-isoproterenol accelerated the metabolic activity of the cells that constitute the stria vascularis. The increase in activity was probably attributable to direct pharmaceutical effects of the β-stimulant, rather than an increase in blood flow. It is possible that the cells that constitute the stria vascularis may have β-receptors.

KEY WORDS — beta-stimulant, cytochrome oxidase, electron microscopy, organ culture, stria vascularis.

INTRODUCTION

Blood pressure and heart rate increase during vertigo attacks in patients with Meniere's disease, probably because of the vestibulospinal reflex. The autonomic nervous system may be closely involved in inner ear disorders, because the presence of an underlying autonomic imbalance has been suggested in such patients. The autonomic nervous system regulates blood flow to the brain and inner ear. The tension of the cervical sympathetic nerves often shows laterality. The hemodynamics of the vertebral artery may be different between the right side and the left side in patients with vertigo.[1] Disturbed blood flow causes inner ear disorders. However, the inner ear disorder is not always found on the same side as lower blood flow in the vertebral artery.[2] In most cases, the origin of vertigo cannot be explained by disturbed blood flow caused by a difference in the tension of the cervical sympathetic nerves. On the other hand, it is still unknown whether autonomic agents have direct actions on the inner ear cells. To investigate the effect of autonomic agents on the inner ear, we conducted in vivo and in vitro experiments. The effect of α-isoproterenol (sympathetic β-stimulant) on the inner ear function was analyzed by using the enzyme activity of cytochrome oxidase, a mitochondrial respiratory enzyme, as an index.

METHODS

In Vivo Experiment. Fourteen adult rats with a normal Preyer's reflex were used in the in vivo experiment. Intraperitoneal injection of α-isoproterenol (5 mg/kg), a sympathetic β-stimulant, was performed for consecutive 21 days in 10 animals, while that of physiological saline was performed for the same period in 4 animals as a control group.

After the 3-week treatment, 6 of the 10 rats in the α-isoproterenol group and 3 of the 4 rats in the control group were painlessly killed by an overdose injection of anesthetics. Cochleas bilaterally excised from these animals were fixed with 3% paraformaldehyde for about 1 hour, decalcified with ethylenediaminetetraacetic acid (EDTA), frozen, and embedded in Tissue-Tek OCT compound (Miles Inc, Elkhart, Ind). Cochlear frozen sections with a 6-μm thickness were reacted with diaminobenzidine, hydrogen peroxide, and 1% manganese chloride at 37°C for 1 hour, and then with 1% cupric sulfate (hydrate) for 5 minutes.[3,4] After the completion of the reactions, the sections were mounted on a glass slide. The above serial procedures were performed under the same conditions for each specimen. Color pic-

---

From the Department of Otorhinolaryngology, Jichi Medical School, Tochigi (Ishii), and the Departments of Otorhinolaryngology (Zhai), and Anatomy (Akita), Saitama Medical School, Saitama, Japan.

CORRESPONDENCE — Kosuke Ishii, MD, Dept of Otorhinolaryngology, Omiya Medical Center, Jichi Medical School, Amanuma-cho, Omiya-shi, Saitama-ken, 330-8503, Japan.

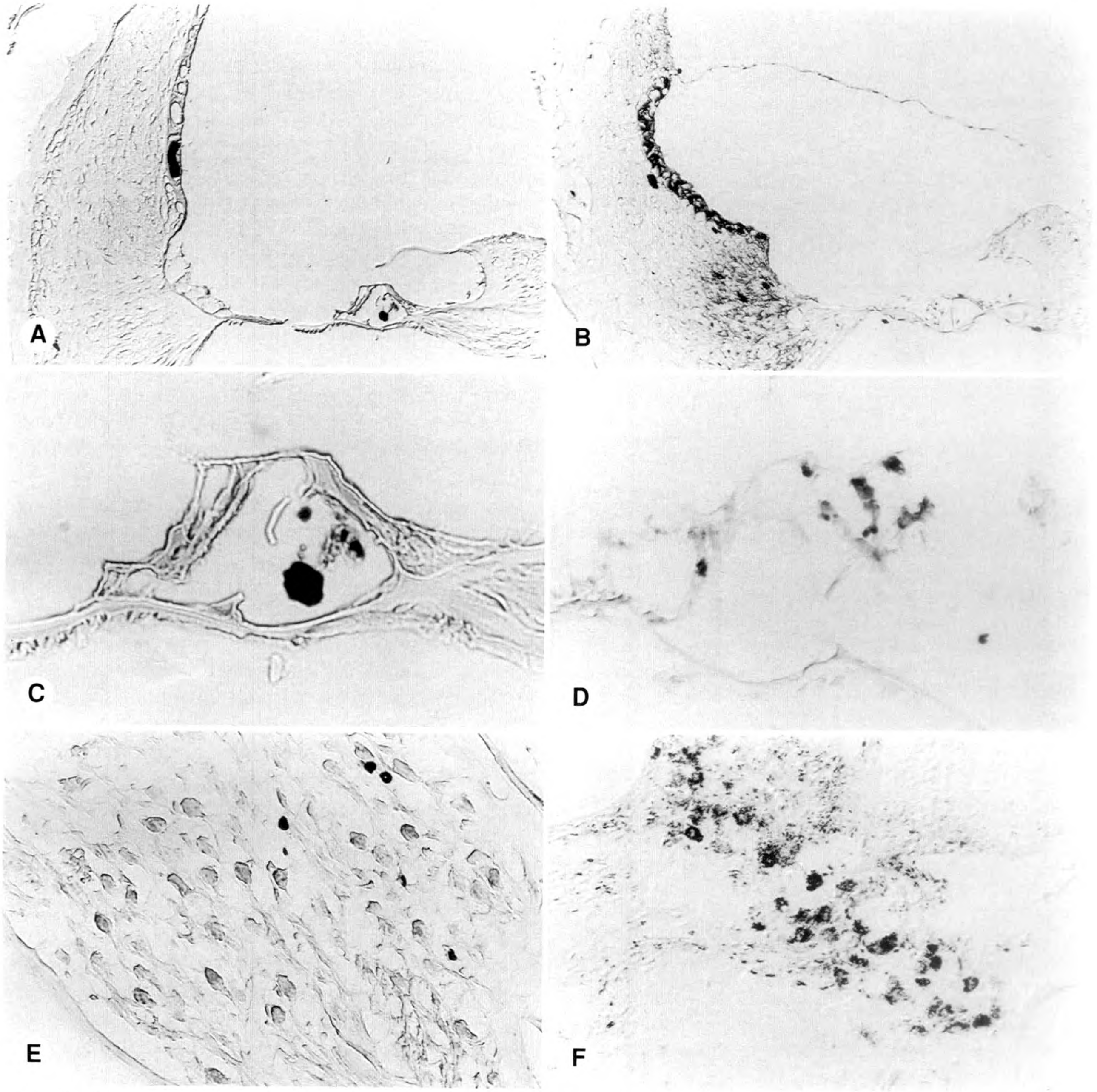

Fig 1. Light microscopic views of A,B) cochlea (original ×50); C,D) outer and inner hair cells (original ×200); and E,F) spiral ganglia (original ×200). A,C,E) Control. B,D,F) After 3-week administration of α-isoproterenol.

tures were taken for computer-assisted image processing. Images sampled by a Canon scanner at 256 gradations were used for the measurement of staining density for cytochrome oxidase with NIH Image. Cochleas excised from the remaining 4 animals in the α-isoproterenol group and 1 animal in the control group were fixed with 2% glutaraldehyde, postfixed with 1% osmic acid, decalcified with EDTA, dehydrated, and embedded in epoxy resin. After electron staining, ultrathin sections of the specimens were observed under a transmission electron microscope.

In Vitro Experiment. Six adult rats with a normal Preyer's reflex were used in the in vitro experiment. Bilateral cochleas were excised from animals painlessly killed by an overdose injection of anesthetics. The lateral wall of the cochlea was removed as much as possible and cultured in a medium (Ham F-12 + 20% fetal bovine serum, 50 U/mL of penicillin, 50 μg/mL of ascorbic acid, 10 μg/mL of nonessential amino acids) for 3 days. α-Isoproterenol (10 mol/L) was added to the culture solution for cochlear cells from the right ear. Cochlear cells from the left ear were cultured in the medium alone. After the 3-day culture, all the cochlear specimens were fixed with 3% paraformaldehyde for 30 minutes, decalcified

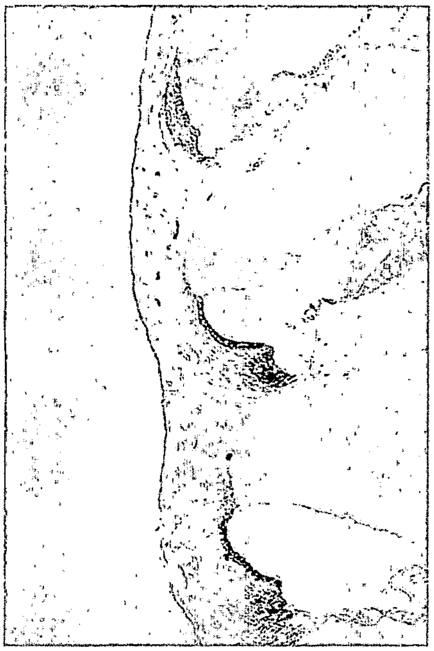

Fig 2. Light microscopic view of cochlea after 3-week administration of α-isoproterenol (original ×20). Staining density of stria vascularis tended to be greater in lower turns. There was no endolymphatic hydrops.

with EDTA, frozen, and embedded in Tissue-Tek OCT compound. Frozen sections of the specimens were made to quantify cytochrome oxidase activities of the cochlear cells by the computer-aided image processing technique described for the in vivo experiment.

All light microscopic photographs were taken by Nomarski interference microscopy.

This study was performed according to the guidelines of the Declaration of Helsinki.

RESULTS

In Vivo Experiment. To preserve the cytochrome oxidase activity in the tissues, the specimens were fixed relatively weakly with paraformaldehyde. Therefore, there were some structural changes in the rat cochlea.

The cytochrome oxidase activity in the stria vascularis, outer and inner hair cells, and spiral ganglia was markedly increased in the α-isoproterenol group, whereas it was only slightly recognizable in the control group (Fig 1). The cytochrome oxidase activity in the spiral ligament facing the endolymphatic space was also markedly increased in the α-isoproterenol group. The staining density tended to be greater in the lower turns (greater in the second turn than in the third turn, and greater in the first turn than in the second turn) of the cochleas in the α-isoproterenol group. There were no deviations of Reissner's membrane or findings suggesting endolymphatic hydrops in any specimen (Fig 2). Results of the computerized analysis of the staining density in the cochlear stria vascularis were as follows. As shown in Fig 3A, the overall staining density of the cochlea was significantly greater in the α-isoproterenol group than in the control group. The staining density tended to be greater in the lower turns of the cochlea (greatest in the first turn) in both groups, but this tendency was more evident in the α-isoproterenol group (Fig 3B). Transmission electron microscopic examination of the cochlea revealed the stria vascularis to be normal in morphology in the control group (not shown). In the α-isoproterenol group, marginal cells protruded into the endolymphatic space. Numerous mitochondria were observed in the cells in the stria vascularis (Fig 4). These changes were most evident in the basal turn of the cochlea.

In Vitro Experiment. After the 3-day culture, some cells that constituted the stria vascularis were detached from the spiral ligament and showed degeneration. However, the cytochrome oxidase activity in the cells remained detectable in both groups. It appeared that the enzyme activity was greater in the α-isoproterenol group than in the control group (Fig 5). Computer analysis of staining density confirmed greater enzyme activity in the α-isoproterenol group (Fig 6).

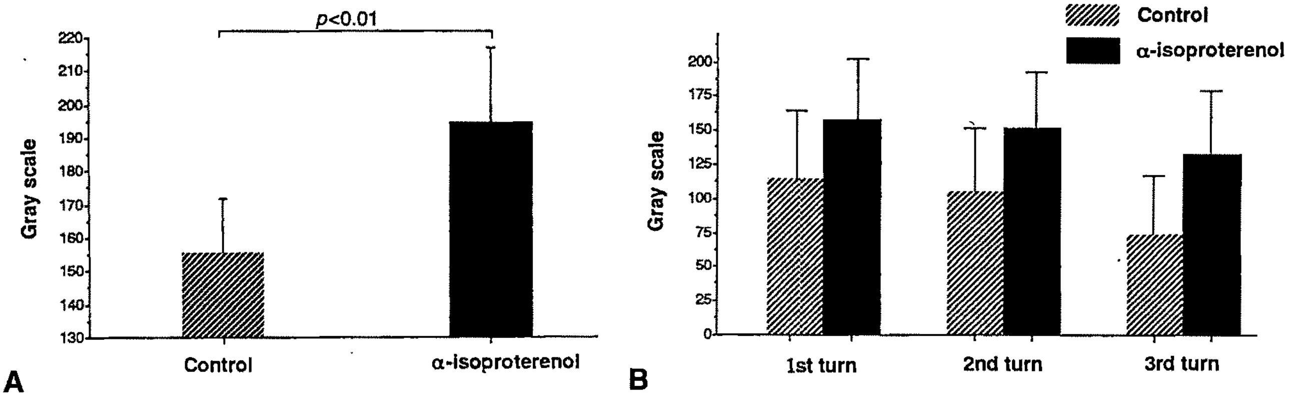

Fig 3. Cytochrome oxidase activity in cochlea. A) All turns. B) By turn.

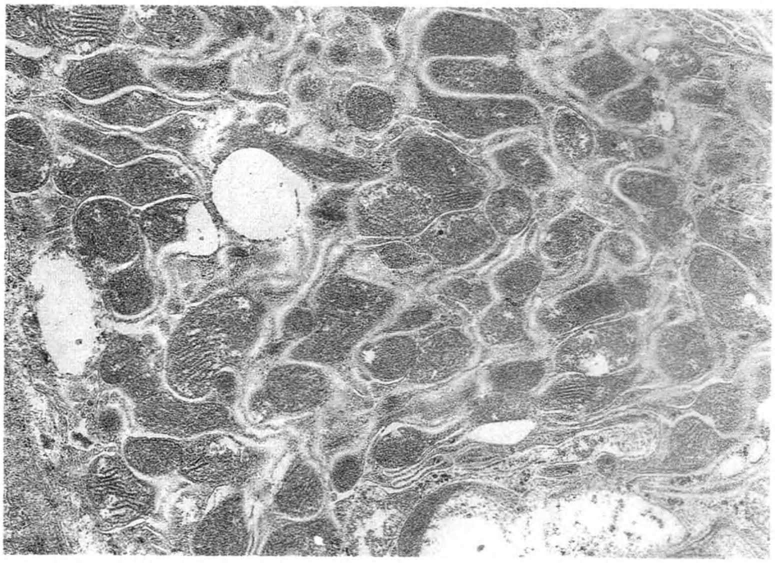

Fig 4. Electron microscopic view of marginal cells in cochlear stria vascularis after 3-week administration of α-isoproterenol (original ×10,000). Numerous mitochondria were seen in cell.

DISCUSSION

In this study, the tissue was reacted for cytochrome oxidase activity according to the procedure of Wong-Riley.[5] This technique has high specificity for cytochrome oxidase activity. White and Vaughan[3] studied age-related denervation muscle atrophy in rats with this technique. We have also used this technique to analyze the hypermetabolic effects of isoproterenol on the orbicularis oculi and stapedius muscles.[4] An increased cytochrome oxidase activity corresponds to an elevated metabolic level of the cell. Cytochrome oxidase has been detected in the inner and outer hair cells and stria vascularis from normal cochlear specimens.[6] The cochlear distribution of cytochrome oxidase in the control group in the present study was the same as that reported in previous studies. Hsu[7] reported that cytochrome oxidase activity was reduced in the hair cells and stria vascularis of the cochlea in animals with experimental hydrops. He suggested decreased cellular activities in the cochlear regions in such animals.

The marked effects of the autonomic nervous system on inner ear function are clinically well known. A number of electrophysiological studies have also been conducted on experimental animals. These have mainly focused on the effect of stimulation or blockage of the cervical sympathetic nerves on cochlear function. Some investigators have reported that electrical stimuli applied to the upper cervical sympathetic nerves caused an increase in compound action potential amplitude.[8] In subsequent studies, however, the above finding was not observed.[9] In most studies, sectioning of the upper sympathetic ganglion induced no detectable changes in compound action potential threshold.[8] Acute stimulation or blockage of the cervical or general sympathetic nerves may not cause changes in cochlear sensitivity for sound near the threshold level. However, the present study suggests that long-term administration of sympathetic agents influences the cochlear function. Wada et al[10] reported that the compound action potential threshold shifts at 8,000 Hz after an auditory trauma were

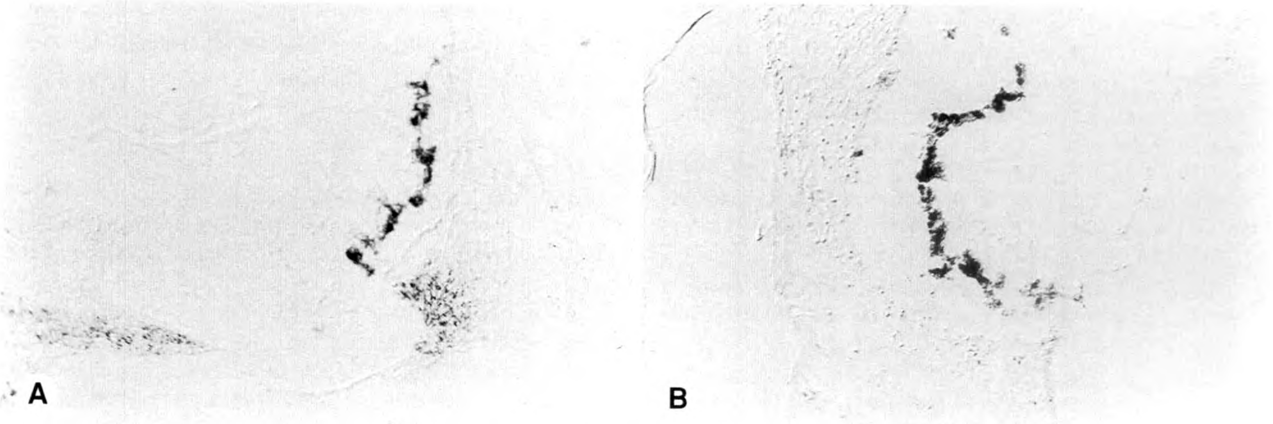

Fig 5. Light microscopic views of rat cochlear stria vascularis after 3-day culture showing cytochrome oxidase activity (original ×360). A) Control. B) After 3-day administration of α-isoproterenol.

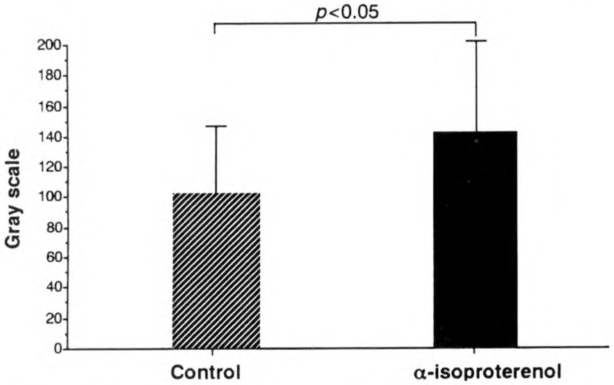

Fig 6. Cytochrome oxidase activity in rat cochlear stria vascularis after 3-day culture.

significantly smaller on the electrical stimulation side. They concluded that the cervical sympathetic nerves act to protect against traumatic sound stimuli. Although we used generalized stimuli with a sympathetic agent rather than localized stimuli on the cervical sympathetic nerves, increased activity of cytochrome oxidase, a mitochondrial respiratory enzyme, was found in cells constituting the stria vascularis. This finding suggested that aerobic metabolism was increased in these cells. α-Isoproterenol possibly protects against cochlear injury. The increase in cytochrome oxidase activity was greater in the basal turn than in the apical turn. This result may support the finding by Wada et al that threshold shifts were smaller at higher frequencies.

Most electrophysiological studies on animals and clinical investigations have suggested that the effect of the sympathetic nerves on the cochlea is produced via changes in the cochlear blood flow. A reason for this is that the stria vascularis and inner or outer hair cells may not be innervated by the autonomic nervous system.[11] However, in the in vitro experiment, α-isoproterenol had a direct effect on cells constituting the stria vascularis, with no influence on blood flow. We considered that this might be attributable to the presence of β-receptors on the surface of the cells constituting the stria vascularis. In smooth muscle cells, the following mechanism has been posited by Stryer[12] as a cause for the increase in cytochrome oxidase activity that occurs after the administration of isoproterenol. The administration of isoproterenol causes an increase in mitochondrial cyclic adenosine 3',5'-monophosphate via β-receptors on the cell membrane. Cyclic adenosine 3',5'-monophosphate–dependent protein kinase is activated thereafter. This enzyme phosphorylates phosphorylase kinase and accelerates glycogenolysis. Accelerated glycogenolysis produces abundant acetyl coenzyme A, a raw material for the tricarboxylic acid cycle, which results in an increase in cytochrome oxidase activity.[12] Therefore, it is speculated that α-isoproterenol has an effect on the stria vascularis by the same mechanism. Even if sympathetic fibers do not reach the cochlear cells, autonomic agents in the blood flow may have a direct effect on these cells in vivo.

Transmission electron microscopic examination of the cochlea revealed numerous mitochondria in the marginal cells of the stria vascularis. Cells with more mitochondria may be more influenced by α-isoproterenol. Therefore, it is probable that the increase in cytochrome oxidase activity in the stria vascularis was most strongly influenced by changes in the enzyme activity in marginal cells. Transmission electron microscopy demonstrated marginal cells protruding in the endolymphatic space and expanded intercellular spaces. Although we could not identify the cause of these findings, similar morphological changes have been reported after the administration of diuretics.[13] Hyperkalemia was considered to be responsible for the changes. α-Isoproterenol may cause hyperkalemia, and this is a possible explanation for the above findings. Increased intracellular vesicles and expanded intercellular spaces may indicate an increased production of endolymphatic fluid. However, there were no findings suggesting the presence of hydrops in any cochlear specimens. We considered that the absorption of the endolymphatic fluid was enhanced in the endolymphatic sac. A functional balance was thus maintained between the stria vascularis and the endolymphatic sac. If the balance were to be upset by some disorder, hydrops might easily develop.

REFERENCES

1. Matsunaga T. Ultrasonic blood rhenography in vertebral artery of vertigo patients (Doppler method). With the glass model experiments. Med J Osaka Univ 1974;25:43-56.

2. Uemura T, Itoh M, Kikuchi N. Autonomic dysfunction on the affected side in Meniere's syndrome. Acta Otolaryngol (Stockh) 1980;89:109-17.

3. White KK, Vaughan DW. The effects of age on atrophy and recovery in denervated fiber types of the rat nasolabialis muscle. Anat Rec 1991;229:149-58.

4. Ishii K, Zhai W, Akita M. The effects of isoproterenol on the orbicularis oculi and stapedius muscles. ORL 1998;60:98-102.

5. Wong-Riley M. Changes in the visual system of monocularly sutured or enucleated cats demonstrable with cytochrome oxidase histochemistry. Brain Res 1979;171:11-28.

6. Vosteen KH. Oxygen metabolism in inner ear. Laryngoscope 1960;70:351-62.

7. Hsu CJ. Changes in activity of cytochrome oxidase in the cochleae of guinea pigs with experimental endolymphatic hydrops. J Formos Med Assoc 1992;91:258-62.

8. Pickles JO. An investigation of sympathetic effects on hearing. Acta Otolaryngol (Stockh) 1979;87:69-71.

9. Lee AH, Moller AR. Effects of sympathetic stimulation of the round window compound action potential in the rat. Hear Res 1985;19:127-34.

10. Wada T, Takahashi K, Kimura S, Ase Y, Hara A, Kusakari J. The effect of the sympathetic nervous system upon susceptibility to acoustic trauma. Auris Nasus Larynx 1995;22:86-92.

11. Hozawa K, Kimura RS. Cholinergic and noradrenergic nervous systems in the cynomolgus monkey cochlea. Acta Otolaryngol (Stockh) 1990;110:46-55.

12. Stryer L. Biochemistry. New York, NY: WH Freeman, 1991.

13. Quick CA, Duvall AJ. Early changes in the cochlear duct from ethacrynic acid: an electronmicroscopic evaluation. Laryngoscope 1970;80:954-65.

≈

CALL FOR PAPERS

Pediatric Diabetes (Mark A. Sperling, MD, Editor-in-Chief; masp+@pitt.edu) is pleased to solicit manuscripts for publication in forthcoming issues and will consider full-length papers, preliminary communications with important new information, clinical reports, and reviews of major topics. Invited editorials and perspectives will be a regular feature. Full-length papers and reviews of major topics should generally not exceed a total of 5,000 words (approximately 20 double-spaced typewritten pages) for the text, references, tables, figures, and figure legends, excluding running title page, title page, and abstract. Preliminary communications with important new information, clinical reports, invited editorials, and perspectives should generally not exceed 2,000 words. For more information, please contact our web site at: www.munksgaard.dk, go to Scientific Journals, and click on the mock-up of the journal cover. Also, you can contact the Editorial Office at: Editorial Assistant, Sandra K. Arjona, MLS, arjonas@chplink.chp.edu, Children's Hospital of Pittsburgh, 3705 Fifth Ave, Pittsburgh, PA 15213; telephone (412) 692-7765; fax (412) 692-7813. Manuscripts can be submitted electronically as an e-mail attachment, or as hard print copy sent in quadruplicate to the above address.

Ann Otol Rhinol Laryngol 109:2000

COMPARISON OF FUNCTIONAL ENDONASAL SINUS SURGERY WITH AND WITHOUT PARTIAL MIDDLE TURBINATE RESECTION

THOMAS E. HAVAS, FRACS DAVID S. G. LOWINGER, MB BS

SYDNEY, AUSTRALIA

The aim of endonasal sinus surgery is to ameliorate sinonasal symptoms and to achieve a functional nose. Although the importance of opening the ostiomeatal complex is accepted, the role of middle turbinate surgery remains controversial. Although some surgeons emphasize the importance of maintaining the middle turbinate as a physiological humidifier and anatomic landmark, others resect it without adverse sequelae. To date, there have only been limited reviews published to support either approach. This paper examines 1,106 matched patients who underwent similar functional endonasal sinus surgery with (509 patients) or without (597 patients) middle turbinate surgery. We demonstrate a paucity of complications and the potential outcome benefits of judicious partial middle turbinate resection in some patients with more severe rhinosinusitis.

KEY WORDS — complications, middle turbinate, recurrent sinusitis, sinus surgery.

INTRODUCTION

Chronic rhinosinusitis is thought to be a disease secondary to obstruction caused by anatomic anomalies and reactive mucosal engorgement. Subsequent to obstruction, inflammation occurs, and with this, the morphology of the lining mucosa of the nasal sinuses changes. The goal of treating sinus disease with surgery has evolved from removing all diseased sinus mucosa to specific exenteration of the tissue causing obstruction. Once ventilation is restored, it is postulated that the mucosa may regain near-normal appearance and function.

Thanks largely to the teachings of Stammberger[1-4] and Kennedy et al,[5-7] based on the work of Messerklinger,[8-10] the ostiomeatal complex has become the center of attention in sinus surgery. As part of the ostiomeatal complex, the anterior ethmoid is in a key location. Homeostasis of the large maxillary and frontal sinuses, with their ostia located within the anterior ethmoidal complex, is dependent on the proper physiological condition of this region.

The anterior part of the middle turbinate, lying just medial to this area, may exhibit anatomic deformity and mucosal hyperreactivity, exacerbating restrictions to sinus ventilation. After surgery to the ostiomeatal complex, adhesion or synechiae formation between the middle turbinate and the lateral nasal wall is a common complication[11-13] and may lead to restenosis of the region and recurrent disease.[6,14] Various techniques of managing the middle turbinate have been suggested, but it is still most controversial whether the middle turbinate should be resected as a part of functional endonasal sinus surgery (FESS).

Today, there remain 2 schools of opinion, largely based on surgeons' training. There are those who favor anterior middle turbinate preservation (MTP),[4,5,14,15] and others who practice total or partial middle turbinate resection (MTR).[16-18] Therefore, most published series present the outcome of 1 of these approaches, rather than a comparison.

This review intends to analyze the postoperative course of a large series of well-matched patients who had comparable disease and technically similar endonasal sinus surgery with the exception of the performance or nonperformance of partial MTR. By comparing the 2 groups, we aim to assess the safety and efficacy of MTR and determine when this approach is clinically indicated.

METHOD

Patients. The initial study population consisted of 1,233 patients who underwent bilateral FESS between January 1987 and June 1996. For the purpose of results analysis for this paper, only patients who attended at least 12 months of follow-up are included in the report. Of the total cohort, 127 did not complete this obligatory follow-up; 54 patients were from the MTR group, and 73 from the MTP group. These were excluded from this study, leaving 1,106 patients.

Before surgery, the patients were randomly divided into 2 groups according to an odds-and-evens system with regard to their position on the operating list; 509 patients had partial MTR as part of their procedure, and in 597 cases, the middle turbinates were

---

From the Department of Otolaryngology, Head and Neck Surgery, The Prince of Wales Hospital, Sydney, Australia.

Presented at the XVIIth European Rhinologic Society and International Symposium on Infection and Allergy of the Nose combined conference, Vienna, Austria, July 28–August 1, 1998.

CORRESPONDENCE — Thomas E. Havas, FRACS, Suite 506, 253 Oxford St, Bondi Junction, NSW 2022, Australia.

TABLE 1. PATIENT DETAILS

	MTP	*MTR*
Total patients	597	509
Female	318	236
Male	279	273
Age range (y)	15-87	15-87

MTP — middle turbinate preservation, MTR — middle turbinate resection.

preserved (MTP). The age range for the patients was 15 to 87 years, with 554 female patients and 552 male patients. The demographics of the patients in both treatment groups were well matched (Table 1).

On initial presentation, all patients had a complete history recorded and a careful ear, nose, and throat examination including nasal endoscopy. If sinusitis symptoms continued while they were on maximum medical therapy, axial and coronal computed tomography scans of the paranasal sinuses were obtained. Patients with persisting symptomatic and radiologic evidence of disease were offered surgery. The stage of disease was assessed according to the number of sinus groups involved, conforming to the Kennedy classification system[19] (stages 1 to 4; Fig 1). Only in stage 3 was there a slight significant difference in group numbers ($p = .00118$), with more having had MTP surgery. If we combine stages 1 and 2 as "mild" disease and stages 3 and 4 as "severe" disease, there is no significant difference in group populations.

Olfactory Assessment. A subset of 149 patients, whose major symptoms included an altered sense of smell, underwent preoperative and postoperative olfactory assessment. Olfactory acuity was assessed with the Olfactolab Clinical Smell Test Kit from 1987 to 1993. In 1993, this was replaced by the Sensonic University of Pennsylvania Smell Identification Test (UPSIT). For the purposes of this study, hyposmia (as defined by the Olfactolab reporting system) and microsmia (as determined by the Sensonic test) are equated and referred to as hyposmia.

Procedure. The MTP patient group had a standard FESS performed.[4,6] Dissecting and cutting forceps rather than powered instruments were used. At all times, great care was taken to spare mucosa and not to traumatize the lateral edge of the middle turbinate. If a concha bullosa was present, the lateral side was resected with scissors and the medial portion left intact. If necessary, an ointment-coated absorbent roll was placed in the middle meatus for a few days.

For the MTR patient group, partial MTR was performed at the beginning of the procedure. After we allowed time for vasoconstriction, the middle turbinate was gently medialized with a Freer dissector. A straight crushing forceps was applied for a few moments to assist hemostasis. Then, using curved endoscopic scissors, we resected only the anterior-inferior third of the turbinate. Any residual bleeding point was carefully cauterized by diathermy via a modified insulated sucker. Then the FESS was undertaken as described above. Patients were routinely discharged within 24 hours. All were prescribed saline nasal douche and appropriate analgesia. Operative times, blood loss, complications, and discharge delays were recorded.

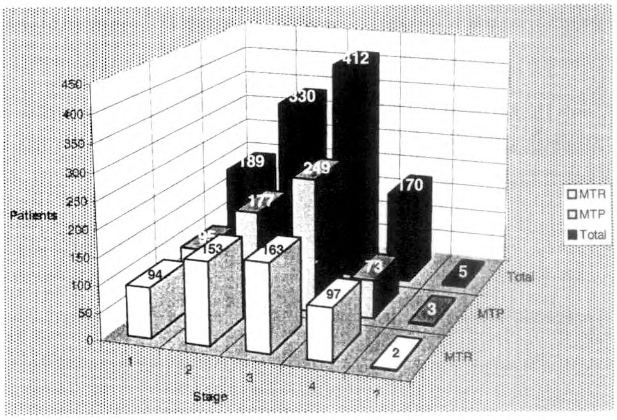

Fig 1. Computed tomographic staging[19] of initial rhinosinusitis. MTR — middle turbinate resection, MTP — middle turbinate preservation.

Progress. The patients were initially reviewed weekly 3 times and then at increasing intervals. At postoperative review, office nasal endoscopy was performed, the sinus and nasal mucosal healing assessed, the middle meatus cleaned, and topical antibiotic ointment applied as needed. At 3 months, olfaction was objectively reassessed. The progress of the patients' symptoms was continually reviewed and recorded. If a patient complained of recurrent symptoms, they were investigated and managed appropriately. Although the need for ongoing investigations and management were also determined by the endoscopic appearance, the presence of synechiae alone in asymptomatic patients did not lead to any additional investigation or imaging.

The patients included in this study were required to attend follow-up for a minimum of 12 months. The overall mean follow-up period was 50 months (4.2 years).

A χ^2 analysis was applied to determine an association between the operative technique and the various operative complications and outcomes. Analysis incorporating the initial disease stage was also undertaken. A p value of less than .05 was considered to be statistically significant.

TABLE 2. MAIN PRESENTING COMPLAINT

	MTP	*MTR*
Sinus disease	531	444
Facial pain and headache	47	49
Other	19	16
Total	597	509

RESULTS

Chronic sinusitis with acute exacerbations usually manifesting in nasal obstruction, purulent rhinorrhea, postnasal discharge, and facial pain was the presenting problem in 975 of the 1,016 patients. Sinonasal headache with associated nasal symptoms was the main feature in 96 patients, and 35 patients had other primary concerns, including halitosis and chronic cough (Table 2).

Olfaction. Of the 149 patients tested for olfactory acuity, 88 had objective evidence of preoperative hyposmia. Thirty-six of these patients underwent FESS with MTR, and 52 with MTP. In the MTR group, 22 of 36 patients remained hyposmic, compared with 32 of 52 in the MTP group. Comparing the groups showed that there was no adverse effect on smell caused by MTR, and there was a slight smell outcome benefit (p = .000603; Fig 2). Patients with more severe initial disease were more likely to have hyposmia and a poor response to surgery. There was no iatrogenic hyposmia.

Operative Complications. There were no intraoperative complications, such as diathermy burns, iatrogenic trauma, excessive bleeding, problems with endoscopic vision, or a prolonged average anesthetic time, related to MTR.

Immediate Complications. No patients experienced any significant immediate postoperative complication that required blood transfusion, surgical intervention, or prolonged hospitalization. Minor primary epistaxis occurred in 7 patients overall, and all responded to conservative management before leaving the recovery ward. A major epistaxis was considered to be one that delayed discharge or required readmission. This occurred in 3 patients, all of whom were controlled with packing. Of the 2 cases of bleeding following MTR, 1 was a primary hemorrhage in a patient with occult hepatic dysfunction, and the other a secondary bleed at 10 days. The 1 epistaxis in the MTP group was also a secondary hemorrhage. Another patient in the MTR group experienced an orbital hematoma that settled with conservative measures without sequelae. There were no cases of epistaxis requiring transfusion, no visual, cerebrospinal fluid, or neurologic complications (Table 3), and no unexpected postoperative discomfort.

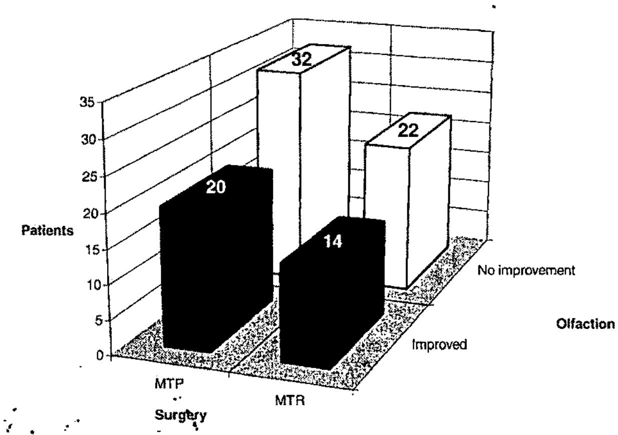

Fig 2. Olfactory outcome for hyposmic patients.

TABLE 3. OPERATIVE COMPLICATIONS AND OUTCOME

	MTP	*MTR*	*Significant Difference*
Total patients	597	509	
Epistaxis	1	2	No
Orbital hematoma	0	1	No
CSF leaks	0	0	
Meningitis	0	0	
Synechiae	51	0	Yes, p < .05
Revision required	93	36	Yes, p < .05

CSF — cerebrospinal fluid.

Long-term Complications. The mean postoperative follow-up period was 4.2 years, with some follow-ups up to 10 years. In the patients who had MTR, there have been no cases of chronic crusting, drying, or atrophic rhinitis to date. However, as such changes may take over 7 years to develop, we continue to monitor our patients.

Synechiae and Revision Surgery. Of the 509 MTR patients, 36 (7.1%) had recurrent symptoms requiring revision surgery. Predominantly, the endoscopic findings in these patients were of widespread mucosal disease associated with recurrent polyposis. Persistent synechiae were not seen.

In the MTP cohort of 597 patients, 93 (15.6%) had symptomatic recurrences sufficient to warrant revision surgery (Table 4). Of these 93 patients, 51 had developed obvious synechiae between the middle turbinate and the lateral wall of the nose that were thought to have contributed to the recurrence of symptoms and the failure of surgery. When the initial stage of rhinosinusitis is taken into account, paired χ^2 analysis shows that the type of surgery made little statistical difference in revision rates for those with mild disease (stages 1 and 2; p = .129). With severe disease (stages 3 and 4), there was an outcome benefit with MTR (p = .0000198). Overall, revision was more likely for patients with a worse initial disease

TABLE 4. TABLE OF REVISION INCIDENCE BY STAGE FOR EACH SURGICAL GROUP AND SIGNIFICANT DIFFERENCE OF MTR VERSUS MTP

Stage[19]	*No. of Patients Requiring Revision*	*MTP (%)**	*MTR (%)**	*Significant Difference*
1	5	3.2	2.1	No
2	18	6.2	4.6	No
3	43	11.2	9.2	Yes, $p < .05$
4	63	69	12.4	Yes, $p < .05$
Overall	129	15.6	7.1	Yes, $p < .05$

*Percentage of patients requiring revision surgery as classified by surgical option and initial disease stage.

stage (Table 4[19]).

DISCUSSION

The physiological foundation for FESS is that the major sinuses are capable of reversal of mucosal disease if ventilation is reestablished. The key area for this surgery is the ostiomeatal complex. This includes the uncinate process, ethmoidal bulla, and anterior third of the middle turbinate.[20] When structural or mucosal changes cause obstruction in this region, drainage of the nearby sinuses is compromised, with resultant infection. Optimum ventilation of the ostiomeatal complex may be achieved with removal of an obstructing uncinate process, bulla ethmoidalis, polyps, and, in some cases, an adjacent hyperplastic, deformed, flaccid, or malpositioned anterior portion of the middle turbinate.

The controversy surrounding MTR has been present since the modern era of transnasal surgery. In 1925, Pratt[21] suggested that the middle turbinate should be retained because removal may predispose patients to meningitis. Williams and Mousel[22] agreed that the nose should be left in its normal physiological state and felt it important not to disturb the middle turbinate. Upon reviewing FESS techniques of the 1970s and early 1980s, Eichel[23] proposed that a portion of the middle turbinate ought to be resected, although he strongly recommended preservation of its medial wall. In 1974, Kidder et al[24] concluded that the effectiveness of intranasal ethmoidectomy seemed directly related to the completeness of the operation. They found that the removal of the middle turbinate yielded a lower rate of polyp recurrence without any increase in postoperative morbidity.[24] Morganstein and Krieger,[18] too, resected the middle turbinate if it was obstructive, if there was a contact point with the septum, or if there was a concha bullosa. Davis et al[25] found that the most important correlate for post-FESS patency of the middle meatal antrostomy was MTR, and Beidlingmaier[17] proffered that FESS with MTR gave excellent symptomatic results. However, with the evolution of the current concept of increasingly conservative endoscopic sinus surgery, most tend to practice preservation of the middle turbinate, apart from the grand lamella, which has to be removed in order to enter the posterior ethmoidal cells or a pneumatized turbinate.

Although anatomic variations of the middle turbinate, such as paradoxical curvature, bony distortion, and concha bullosa, may be seen in asymptomatic patients, in the crowded or reactive nose they may contribute to ostiomeatal obstruction, rhinosinusitis, and septal-turbinate contact point headaches.[26] A paradoxical middle turbinate, with a convex curve on the lateral aspect, occurs in around 11% to 29% of patients and may be associated with ipsilateral sinusitis.[27] Hypertrophic pneumatization of the middle turbinate was described by Zuckerlandl[28] in 1885 and was called concha bullosa. This may occur as part of normal fetal development of the ethmoidal labyrinth[29] and involves pneumatization of the lamella or bulbous parts of the turbinate, or both.[30] Concha bullosa has been found in 9% to 20% of cadaveric dissections[27] and in 17% to 80% of patients suffering from recurrent chronic sinusitis.[31] Pneumatized middle turbinates may harbor mucosal disease, including polyps, cysts, aspergilloma,[26] pyoceles,[32] and mucoceles. Chronic osteitis has also been found on histologic analysis of middle turbinates resected from chronic sinusitis patients, particularly those with grade 3 to 4 sinusitis on computed tomography.[33] Preservation of the middle turbinate in these cases may leave diseased tissue within the key area of the ostiomeatal complex.[33,34]

The anterior part of the middle turbinate has also been found to be an important area in the secretion of vasoactive sensory neuropeptides, which results in hypersecretion, mucosal edema, polyp formation, and the development of chronic rhinosinusitis. The neuropeptides calcitonin gene–related peptide, substance P, and neurokinin A, found in a subpopulation of unmyelinated sensory nerve fibers in the nasal mucosa, have been implicated in the pathophysiological mechanism of chronic allergic and nonallergic rhinosinusitis.[35-37] Chemical irritation or mechanical (contact) stimulation of the anterior middle turbinate mucosa causes a local axon reflex provoking the local secretion of these neuropeptides.[38] Pochon and Lacroix[31] found that in patients with chronic nonallergic rhinosinusitis, there was a twofold increase in the concentration of calcitonin gene–related peptide in the middle turbinate mucosa, and Lacroix et al[39] found that these levels correlated with symptom intensity. On the basis of these findings, that group suggested that the resection of the anterior part of a pneumatized middle turbinate should be considered on physiological grounds.

Other important nasal neuroepithelia include the olfactory cells, which are thought to be located mainly on the superior turbinate and extending to the uppermost septum,[40] although there may be marked variability.[41] Previous reports indicate a risk of anosmia after FESS, with either MTR or MTP, of around 1%,[33,42] with no increased risk associated with MTR.[43,44] Using the UPSIT, a prospective study of 64 patients showed little objective change after FESS and no significant difference in olfactory acuity with MTR compared with MTP.[44] We found that patients with more extensive initial disease had a higher incidence of preoperative hyposmia and the least improvement after surgery. There was a slight outcome benefit with MTR in this patient group. We did not experience any iatrogenic anosmia or hyposmia in either group.

The most frequent complication of FESS is lateralization of the middle turbinate, which may promote the formation of scars and synechiae in the operated middle meatus, between the turbinate and the lateral wall of the nose.[45,46] The reported incidences vary from 1.2%[14] to 43%.[47] Ramadan and Allen,[48] in a review of 337 patients, found that synechiae developed in 5.3% of MTR patients and 9.3% of MTP patients. This compares with 0% (MTR) and 8.5% (MTP) in our revision patients. Vleming et al[14] also found no synechiae after MTR. In order to preserve the middle turbinate while avoiding synechiae and scarring, some have tried turbinoplasty procedures. Har-El and Slavit[49] performed 63 operations in which the concha bullosa was incised, curetted, and crushed. Although few patients developed adhesions, there were no details of symptomatic improvement or an influence on the presence of rhinosinusitis. Another method described is suture medialization of the turbinates, which is technically challenging.[50] Bolgerization of the turbinate is also popular.

Complications other than synechiae and hyposmia may occur with FESS. Atrophic rhinitis and squamous metaplasia, which may be the sequelae of changes in airflow and humidification in the hypoplate nose and may take years to develop, have not yet occurred in our patients and have not been reported in other series in which MTR was practiced.[17,18,51] The serious problems of cerebrospinal fluid leaks, bleeding, and iatrogenic orbital damage have been reported, with an incidence of usually less than 1%. Vleming et al, in a review of 593 patients, found that absence of the middle turbinate was a risk factor for serious complications on revision FESS,[14] as the middle turbinate is an important landmark for the FESS surgeon, particularly for identification of the anterior skull base and frontal recess. We would, therefore, not advocate extensive turbinectomy. However, with judicious amputation of the anteroinferior portion of the turbinate, the important superior insertion remains. In our MTR operations, we were able to complete FESS with no neurologic or orbital complications other than a single case of periorbital hematoma. We also found no difficulty with using the middle turbinate remnant as the landmark in revision cases.

In our series, revision surgery was required in 7% of MTR and 14% of MTP patients. A similar rate of polyp recurrence, 17%, was seen by Eichel[23] in his (MTP) series. Recurrent polypoid rhinosinusitis most commonly led to the need for revision in the MTR patients, whereas synechiae were a major factor in our MTP group. This outcome correlates with Beidlingmaier's results of FESS with MTR, in which patients who failed were those with proliferative polypoid disease,[17] and with other studies that found that with the MTP technique, recurrent sinus disease requiring revision was mainly secondary to synechiae and adhesions involving the middle turbinate.[46,52] Our results also concur with Kennedy's findings that the most important predictive factor of the success of FESS is the extent of rhinosinusitis before surgery.[19] In both of our patient groups, those with a higher stage of disease initially were more likely to require revision surgery. When including disease stage as a confounding factor, we found a statistically significant outcome benefit of MTR only in stage 3 and 4 patients.

CONCLUSION

The middle turbinate is a dynamic structure, in a crucial position, that may play a significant role in the pathogenesis of rhinosinusitis and headaches. Its vasoactive response to exogenous factors, release of sensory neuropeptides, and proximity to the ostiomeatal complex underlie its importance in sinonasal disease. Anatomic variations, pneumatization, infection, and contact points may also be contributing factors to disease causation and recurrence.

Judicious partial MTR is an option in the treatment of chronic sinusitis and middle turbinate headache in certain circumstances. It may be an adjuvant technique in the improvement and maintenance of ventilation of the infundibular meatal complex, especially when an anatomic anomaly or concha bullosa is present. In our series, MTR has minimized iatrogenic obstruction due to synechiae and led to less recurrent disease requiring revision surgery in patients with more severe initial disease. Enhanced access for office endoscopic examination and cleaning of the maxillary sinus, ethmoidal infundibulum, and frontonasal recess was also achieved. By leaving the superior and posterior parts of the turbinate, we preserved the anatomic landmarks. No significant short- or long-term complications have resulted from our partial resection of the middle turbinate. On the basis of these results, we suggest that surgeons consider the inclusion of partial MTR, by the described technique, when performing FESS for patients in whom there is extensive mucosal disease or the potential for middle turbinate lateralization or scarring.

ACKNOWLEDGMENTS — The authors recognize Annette Kowalcyzk, RN, for her dedication, skill, and assistance with this paper. We also acknowledge the commitment to patient care and research of the operating room personnel of the Prince of Wales Hospital, Randwick, and St Luke's Hospital, Darlinghurst. We also thank Lindsay Oakes, BAppSc, for his assistance.

REFERENCES

1. Stammberger H. Endoscopic surgery for mycotic and chronic recurring sinusitis. Ann Otol Rhinol Laryngol Suppl 1985;94(suppl 119).

2. Stammberger H. Endoscopic endonasal surgery: concepts in treatment of recurring rhinosinusitis I. Anatomic and pathophysiologic considerations. Otolaryngol Head Neck Surg 1986; 94:143-7.

3. Stammberger H. Endoscopic endonasal surgery: concepts in treatment of recurring rhinosinusitis II. Surgical technique. Otolaryngol Head Neck Surg 1986;94:147-56.

4. Stammberger H. Functional endoscopic sinus surgery. Philadelphia, Pa: BC Decker, 1991.

5. Kennedy DW, Zinreich SJ, Rosenbaum A, Johns ME. Functional endoscopic sinus surgery: theory and diagnostic evaluation. Arch Otolaryngol 1985;111:567-82.

6. Kennedy DW. Functional endoscopic sinus surgery: technique. Arch Otolaryngol 1985;111:643-9.

7. Kennedy DW, Zinreich SJ. The functional endoscopic approach to inflammatory sinus disease: current perspectives and technique modifications. Am J Rhinol 1988;2:89-96.

8. Messerklinger W. Zur Endoskopietechnik des mittleren Nasenganges. Eur Arch Otorhinolaryngol Suppl 1978(suppl 221):297-305.

9. Messerklinger W. Endoscopy of the nose. Baltimore, Md: Urban and Schwarzenberg, 1978.

10. Messerklinger W. Die Rolle der lateralen Nasenwand in der Pathogenese: Diagnose und Therapie der Rezidivierenden und chronischen Rhinosinusitis. Laryngol Rhinol Otol (Stuttg) 1987;66:293-9.

11. Kinsella JB, Calhoun KH, Bradfield JJ, Hokanson JA, Bailey BJ. Complications of endoscopic sinus surgery in a residency training program. Laryngoscope 1995;105:1029-32.

12. Ramadan HH, Allen GC. Complications of endoscopic sinus surgery in a residency training program. Laryngoscope 1995;105:376-9.

13. Schaefer SD, Manning S, Close LG. Endoscopic paranasal sinus surgery: indications and considerations. Laryngoscope 1989;99:1-5.

14. Vleming M, Middelweerd RJ, de Vries N. Complications of endoscopic sinus surgery. Arch Otolaryngol Head Neck Surg 1992;118:617-23.

15. Thornton RS. Middle turbinate stabilization technique in endoscopic sinus surgery. Arch Otolaryngol Head Neck Surg 1996;122:869-72.

16. Friedman WH. Surgery for chronic hyperplastic rhinosinusitis. Laryngoscope 1975;85:1999-2011.

17. Beidlingmaier JF. Endoscopic sinus surgery with middle turbinate resection: results and complications. Ear Nose Throat J 1993;72:351-5.

18. Morganstein KM, Krieger MK. Experiences in middle turbinectomy. Laryngoscope 1980;90:1596-603.

19. Kennedy D. Prognostic factors, outcomes and staging in ethmoid sinus surgery. Laryngoscope 1992;102:1-18.

20. Zinreich SJ, Kennedy DW, Rosenbaum AE, Gayler BW, Kumar AJ, Stammberger H. Paranasal sinuses: CT imaging requirements for endoscopic surgery. Radiology 1987;163:769-75.

21. Pratt JA. The present status of the intranasal ethmoid operation. Arch Otolaryngol 1925;1:42-50.

22. Williams HL, Mousel LH. Diagnosis and treatment of chronic disease of the paranasal sinuses. Ann Otol Rhinol Laryngol 1940;49:466-89.

23. Eichel BS. Revision sphenoidethmoidectomy. Laryngoscope 1985;95:300-4.

24. Kidder TM, Toohill RJ, Unger JD, Lehman RH. Ethmoid sinus surgery. Laryngoscope 1974;84:1525-34.

25. Davis WE, Templer JW, LaMear WR, Davis WE Jr, Craig SB. Middle meatus antrostomy: patency rates and risk factors. Otolaryngol Head Neck Surg 1991;104:467-72.

26. Massegur H, Adema JM, Lluansi J. The middle turbinate as the cause of sinonasal pathology. Acta Otorrinolaringol Esp 1995;46:27-9.

27. Tonia A, Baba S. Anatomic variations of the bone in sinonasal CT. Acta Otolaryngol Suppl (Stockh) 1996(suppl 525):9-13.

28. Zuckerlandl E. Anatomie normale et pathologique des fosses nasales et de leurs annexes pneumatiques. Paris: Masson, 1885.

29. Wang RG, Jaing SC. The embryonic development of the human ethmoid labyrinth from 8-40 weeks. Acta Otolaryngol (Stockh) 1997;117:118-22.

30. Bolger WE, Butzin CA, Parsons DS. Paranasal sinus bony anatomic variations and mucosal abnormalities: CT analysis for endoscopic sinus surgery. Laryngoscope 1991;101:56-64.

31. Pochon N, Lacroix JS. Incidence and surgery of concha bullosa in chronic rhinosinusitis. Rhinology 1994;32:11-4.

32. Badia L, Parika A, Brookes GB. Pyocele of the middle turbinate. J Laryngol Otol 1994;108:783-4.

33. Biedlingmaier JF, Whelan P, Zoarski G, Rothman M. Histopathology and CT analysis of partially resected middle turbinates. Laryngoscope 1996;106:102-4.

34. Milbrath MM, Madredo G, Toohill RJ. Histopathological analysis of the middle turbinate after ethmoidectomy. Am J Rhinol 1994;8:37-42.

35. Lundberg JM, Alving K, Lacroix JS, Matran R. Local and central reflex mechanisms in the neural control of airway microcirculation. Eur Respir J Suppl 1990;12(suppl):624s-628s.

36. Stjarne P, Lundblad L, Anggard A, Hokfelt T, Lundberg JM. Tachykinins and calcitonin gene related peptide: coexistence in sensory nerves of the nasal mucosa and effects on blood flow. Cell Tissue Res 1989;256:439-46.

37. Lacroix JS, Buvelot JM, Polla BS, Lundberg JM. Improvement of symptoms of nonallergic chronic rhinitis by local treatment with capsaicin. Clin Exp Allergy 1991;21:595-600.

38. Stammberger H, Wolf G. Headaches and sinus disease: the endoscopic approach. Ann Otol Rhinol Laryngol Suppl 1988; 97(suppl 134).

39. Lacroix JS, Kurt AM, Pochon N, Bretton C, Lundberg JM, Deshusses J. Neutral endopeptidase activity and concentration of sensory neuropeptides in the human nasal mucosa. Eur Arch Otorhinolaryngol 1995;252:465-8.

40. McMinn RMH, ed. Last's anatomy. Regional and applied. 8th ed. Edinburgh, Scotland: Churchill Livingstone, 1990:468-75.

41. Smith CG. Incidence of atrophy of the olfactory nerves in man. Arch Otolaryngol 1941;34:553.

42. Kimmelman CP. The risk to olfaction from nasal surgery. Laryngoscope 1994;104:981-8.

43. Lawson W. The intranasal ethmoidectomy: an experience with 1,077 procedures. Laryngoscope 1991;101:367-71.

44. Friedman M, Caldarelli DD, Venkatesan TK, Pandit R, Lee Y. Endoscopic sinus surgery with partial middle turbinate resection: effects on olfaction. Laryngoscope 1996;106:977-8.

45. Uchida Y, Sugita T. Endonasal findings using a fiberoptic telescope in postoperative cases of chronic sinusitis. Rhinology 1981;19:161-5.

46. Schaefer SD, Manning S, Close LG. Endoscopic paranasal sinus surgery: indications and considerations. Laryngoscope 1989;99:1-5.

47. Lazar RH, Younis RT, Long TE, Gross CW. Revision functional endonasal sinus surgery. Ear Nose Throat J 1992;71: 131-3.

48. Ramadan HH, Allen GC. Complications of endoscopic sinus surgery in a residency training program. Laryngoscope 1995;105:336-97.

49. Har-El G, Slavit DH. Turbinoplasty for concha bullosa: a non–synechiae-forming alternative to middle turbinectomy. Rhinology 1996;34:54-6.

50. Thornton RS. Middle turbinate stabilization technique in endoscopic sinus surgery. Arch Otolaryngol Head Neck Surg 1996;112:869-72.

51. LaMear WR, Davis WE, Templer JW, McKinsey JP, Del-Porto H. Partial endoscopic middle turbinectomy augmenting functional endoscopic sinus surgery. Otolaryngol Head Neck Surg 1992;107:382-9.

52. Hinohira Y, Yumoto E, Hyodo M, Joko H. Revision endoscopic sinus surgery. Long term follow up and operative findings. Nippon Jibiinkoka Gakkai Kaiho 1995;98:1285-90.

Ann Otol Rhinol Laryngol 109:2000

COMBINATION OF ANGIOGENESIS INHIBITOR TNP-470 WITH CYTOTOXIC DRUGS IN EXPERIMENTAL THERAPY OF NASOPHARYNGEAL CARCINOMA

CHAO-NAN QIAN, MD, PHD
HUA-QING MIN, MD
HAN-LIANG LIN, MD
MING-HUANG HONG, MD
GUANGZHOU, PEOPLE'S REPUBLIC OF CHINA

This study was conducted to evaluate the effectiveness of angiogenesis inhibitor 6-*O*-(*N*-chloroacetyl-carbamoyl)-fumagillol (TNP-470, AGM-1470) in the treatment of nasopharyngeal carcinoma (NPC) alone and in combination with cytotoxic agents. Forty-two male BALB/c nude mice bearing human NPC cell line CNE-2 were randomized into 6 groups: those treated with saline solution, TNP-470, cisplatin (DDP), fluorouracil (5-FU), TNP-470 + DDP, and TNP-470 + 5-FU, respectively. In every treatment group, tumor growth was suppressed significantly. The combination of 5-FU with TNP-470 showed significant enhancement in antitumor efficacy. TNP-470 also enhanced the inhibitory effect of DDP, although not to statistical significance. All animals gained in body weight, although treatment with 5-FU caused slight, reversible diarrhea of 2 to 3 days' duration. The results showed that TNP-470 suppressed the growth of the human NPC cell line and enhanced the antitumor effect of 5-FU without increasing its toxicity. The combination of angiogenesis inhibitors with conventional cytotoxic agents is promising in the treatment of NPC.

KEY WORDS — AGM-1470, angiogenesis inhibitor, antiangiogenic therapy, nasopharyngeal carcinoma, TNP-470.

INTRODUCTION

Nasopharyngeal carcinoma (NPC) is considerably radiosensitive. But the high incidence of locoregional and/or systemic failure has undermined the survival rate, especially in patients with stage IV NPC, for whom the best reported 5-year survival rate was only 30%.[1] Cytotoxic chemotherapy has been recommended in metastatic and/or recurrent NPC for decades. In recent years, induction chemotherapy has shown statistically significant improvement in freedom from distant metastasis, in disease-free survival rate, and in overall survival rate for patients with locoregional stage IV NPC, without increasing treatment-related morbidity.[2] Cisplatin (DDP) and fluorouracil (5-FU) are regarded as first-line cytotoxic drugs for chemotherapy of NPC by many investigators.[2,3] However, drug resistance has occurred in some cases after certain cycles of chemotherapy, and in one study only 10% of the patients with metastatic NPC could be cured by chemotherapy alone.[1]

The rationale of antiangiogenic therapy is based on the fact that aggressive growth and metastatic dissemination of solid tumors are angiogenesis-dependent. Angiogenesis is an essential process characterized by the recruitment of new blood vessels.[4,5] So, suppression of capillary growth could suppress tumor growth.[6] A potent angiogenesis inhibitor, the fumagillin analog 6-*O*-(*N*-chloroacetyl-carbamoyl)-fumagillol (TNP-470, AGM-1470), has been reported to reduce growth of different tumors with little toxicity and few side effects in animal models.[7-9] Our previous observation also found that TNP-470 was effective in the inhibition of tumor growth of a human NPC cell line in an animal model without obvious toxicity.[10] Moreover, antiangiogenic therapy with TNP-470 does not induce drug resistance in Lewis lung carcinoma.[11] Exploration of the possibility of integrating TNP-470 with conventional therapeutic approaches is therefore essential in the development of a multidisciplinary therapeutic strategy of improving survival rates and overcoming drug resistance of NPC. However, it is still not clear whether TNP-470 can play a positive role in combination with conventional cytotoxic agents in the treatment of NPC.

In the present study, we investigated the effect of TNP-470 in combination with DDP or 5-FU in the experimental treatment of NPC. Animals bearing the human NPC cell line CNE-2[12] were treated with TNP-470, DDP, and 5-FU alone and in combination for a specific period of time.

MATERIALS AND METHODS

Cell Line. CNE-2 was provided by the Pathology Department, Cancer Center, Sun Yat-sen University of Medical Sciences (SUMS). It was maintained in

---

From the Department of Nasopharyngeal Carcinoma, Cancer Center (Qian, Min, Hong), and the Department of Pathology (Lin), Sun Yat-sen University of Medical Sciences, Guangzhou, People's Republic of China.

CORRESPONDENCE — Chao-Nan Qian, MD, Dept of Nasopharyngeal Carcinoma, Cancer Center, Sun Yat-sen University of Medical Sciences, 651 Dongfeng East Road, Guangzhou 510060, People's Republic of China.

TABLE 1. SUPPRESSION OF SUBCUTANEOUSLY IMPLANTED CNE-2 NASOPHARYNGEAL CARCINOMA AS EXPRESSED BY TUMOR VOLUME

		Tumor Volume		*p*			
Drug	*No. of Mice*	*mm³ (Mean ± SD)*	*% (T/C)*	*Versus Control*	*Versus TNP-470*	*Versus DDP*	*Versus 5-FU*
Control	7	901.3 ± 273.9	100.00				
TNP-470	7	484.6 ± 114.3	53.77	.003			
DDP	7	612.1 ± 205.6	67.92	.045			
5-FU	7	435.3 ± 165.7	48.30	.002			
TNP-470 + DDP	7	414.1 ± 171.4	45.94	.002	.383	.074	
TNP-470 + 5-FU	7	233.2 ± 65.7	25.87	<.001	<.001		.011

Listed are data from day 13. TNP-470 (20 mg/kg, subcutaneously) was given on days 4, 6, 8, 10, and 12 after tumor implantation, either alone or in combination. DDP (4 mg/kg, intraperitoneally) was given on day 4. 5-FU (60 mg/kg, subcutaneously) was given on days 4 and 6.

T/C — ratio of tumor volume in treated animals versus control animals. See text for other abbreviations.

culture medium RPMI-1640 supplemented with 10% fetal bovine serum at 37°C. A single cell suspension of approximately 2 × 10^6 cells in 0.5 mL of culture medium was inoculated subcutaneously in 2 male BALB/c nude mice to make source tumors. These source tumors were excised when they grew to approximately 1 cm^3, and then 2 to 3 mm^3 of minced tumor tissue was implanted subcutaneously into the left axial region of the flank of each BALB/c nude mouse on day 0.

Animals. BALB/c nude mice (nu/nu) 4 weeks old were purchased by the Animal Laboratory of the Cancer Center, SUMS, and reared under specific pathogen–free conditions. On day 4 after tumor implantation, 42 tumor-bearing male nude mice were randomized into 6 groups with 7 mice each: a control group treated with saline solution, a TNP-470–treated group, a 5-FU–treated group, a DDP-treated group, a TNP-470 + 5-FU group, and a TNP-470 + DDP group. Treatment also began on day 4. The average tumor volumes and animal weights in the treatment groups and control group were almost equal at the beginning of treatment.

Drugs. The TNP-470 was a kind gift from Takeda Chemical Industries, Ltd (Osaka, Japan). It was stored dry at −20°C. A stock solution of 10% (wt/vol) TNP-470 in 100% ethanol could be stored in 4°C for about 3 months. Immediately before injections, a treatment solution was made by diluting the stock solution of TNP-470 in 0.9% normal saline solution (20-µL stock solution per 1 mL saline solution).

The DDP and 5-FU were purchased from David Bull Laboratories (Melbourne, Australia) and diluted in saline solution immediately before injections.

Antitumor Therapy. TNP-470 20 mg/kg was given by subcutaneous injection on days 4, 6, 8, 10, and 12 after tumor implantation to the TNP-470 group and both of the combination groups. DDP 4 mg/kg was given by intraperitoneal injection on day 4 to the DDP group and the DDP + TNP-470 group. 5-FU 60 mg/kg was given subcutaneously on days 4 and 6 to the 5-FU group and the 5-FU + TNP-470 group. The control group received saline solution 10 mL/kg subcutaneously on days 4, 6, 8, 10, and 12.

Tumor Growth and Animal Weights. The tumor dimensions were measured every 2 to 3 days with a dial caliper. The tumor volumes were calculated with the formula[7] $\text{width}^2 \times \text{length} \times 0.52$. The tumor volume is also expressed by the ratio of the mean tumor volume in the treated animals to the mean tumor volume in the control animals (T/C ratio). The mice were weighed every 2 to 3 days so as to adjust the doses of the drugs.

The experiment was terminated on day 13 after tumor implantation. The animals were painlessly killed by continuous inhalation of ether. All animals were weighed before autopsy, at which time the tumor weights were also obtained. The net animal weights at the time of autopsy were calculated by subtracting the tumor weight from the animal weight before autopsy. The mean body weight of the animals is also expressed by the ratio of the mean body weight in the treated animals to the mean body weight in the control animals (T/C ratio).

Statistics. Student's t-test for independent samples was used for comparing the means of the tumor volumes, tumor weights, and body weights.

RESULTS

Antitumor Effects. Before treatment, the mean tumor volumes among the groups were approximately the same. The mean tumor volumes of all groups at the end of the experiment are shown in Table 1. Tumor growth curves are illustrated in the Figure. The mean tumor weights are shown in Table 2. Significant inhibitory efficacy was obtained in every treatment group. When combined with 5-FU, TNP-470 showed significant enhancement in antitumor effect

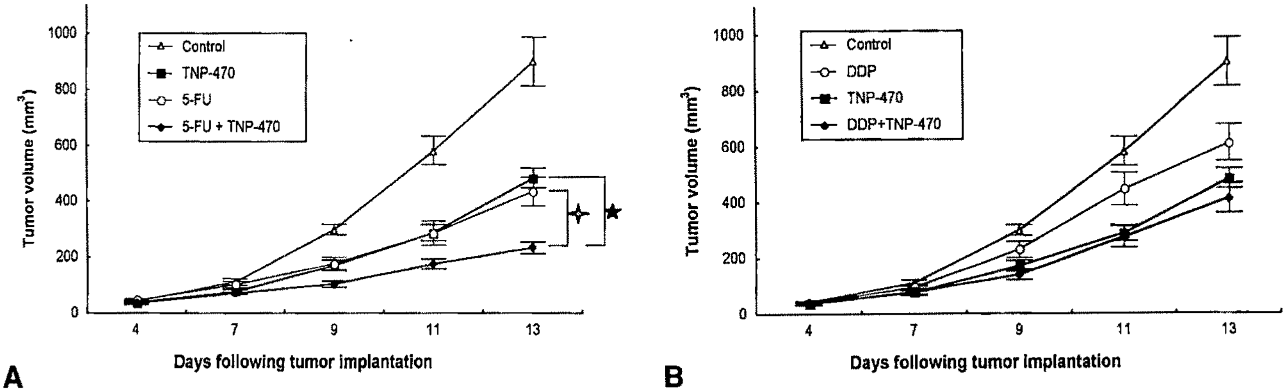

Growth suppression of CNE-2. Points — mean; bars — ±SE. A) By 5-FU (60 mg/kg, subcutaneously, on days 4 and 6 after tumor implantation) and TNP-470 (20 mg/kg, subcutaneously, on days 4, 6, 8, 10, and 12), either alone or in combination. Cross — $p = .011$; star — $p < .001$. B) By DDP (4 mg/kg, intraperitoneally, on day 4 after tumor implantation) and TNP-470 (20 mg/kg, subcutaneously, on days 4, 6, 8, 10, and 12), either alone or in combination. Significant enhancement did not result from combination treatment compared to corresponding single-drug treatments ($p > .05$).

compared to the corresponding single-drug treatment. TNP-470 also enhanced the inhibitory effect of DDP, although the enhancement did not reach statistical significance.

Toxicity. In the groups with 5-FU treatment and 5-FU + TNP-470 treatment, most of the mice had reversible, slight diarrhea of 2 to 3 days' duration starting from day 7 after tumor implantation. But the diarrhea was not prolonged in the combination-treatment group of 5-FU with TNP-470, and all animals had gained in body weight by 2 to 3 g at the terminal day. The net body weights of the mice at the terminal day are listed in Table 2. No significant difference in body weight was found among the control and treatment groups ($p > .05$). There was no other evident drug-related toxicity (ie, diminished activity, anorexia, or seizure activity) in any group.

DISCUSSION

As a common malignancy in south China, NPC is often diagnosed when it is locally advanced or has already spread to lymph nodes because of its deep location, rapid growth, and high potential for metastasis.[1] The chemosensitivity of NPC has been proven for many years.[1,2,13] It is anticipated that induction chemotherapy will reduce the rate of distant metastases, whereas concomitant chemotherapy will increase the probability of locoregional control in patients with locally advanced NPC.[2]

In this study, we investigated another novel therapeutic strategy for NPC, namely, antiangiogenic therapy with TNP-470 alone or in combination with conventional cytotoxic agents. TNP-470 has a cytostatic effect on rapidly proliferating endothelial cells, including tumor endothelial cells.[14] But the endothelial cells regrow after cessation of TNP-470.[15] Additive effects of TNP-470 in combination with other cytotoxic drugs have been demonstrated in other tumors, but not in NPC.[16,17]

We found in the present study that TNP-470 inhibited the growth of human NPC cell line CNE-2 in vivo with an inhibitory rate (1 – T/C) of 46.23% ($p = .003$). Compared to the results of our previous study,[10] earlier treatment with a smaller dose of TNP-470 and a shorter schedule was more effective in the inhibition of the growth of CNE-2. In the previous experiment, treatment was started after 6 days of tumor implantation, while the tumor-bearing animals received TNP-470 at a dose of 30 mg/kg every other day by subcutaneous injection, and an inhibitory rate

TABLE 2. TUMOR WEIGHTS AND BODY WEIGHTS AT TERMINAL DAY

		p				*Body Weight*	
Drug	*Tumor Weight (g; mean ± SD)*	*Versus Control*	*Versus TNP-470*	*Versus DDP*	*Versus 5-FU*	*g (mean ± SD)*	*% (T/C)*
Control	0.764 ± 0.246					22.3 ± 2.2	100.0
TNP-470	0.357 ± 0.127	.002				24.0 ± 1.9	107.6
DDP	0.486 ± 0.177	.032				23.7 ± 3.3	106.3
5-FU	0.353 ± 0.160	.003				23.1 ± 1.4	103.6
TNP-470 + DDP	0.321 ± 0.125	.001	.606	.068		22.5 ± 1.6	100.9
TNP-470 + 5-FU	0.163 ± 0.052	.001	.003		.019	24.1 ± 4.1	108.1

Animal body weights have been adjusted by tumor weights. Number of animals in each group is 7.

of only 27% was obtained after 15 days of treatment. Our finding was consistent with those of others,[8] in which delayed administration of TNP-470 on day 6 after inoculation of Renca murine tumor cell subcutaneously in BALB/c mice did not result in inhibition of tumor growth, whereas it inhibited the tumor growth significantly when the treatment began on day 1. So, it is suggested that administration of TNP-470 would be more effective if the treatment begins at an earlier stage, because of its timing-dependent characteristics.

Another important discovery in the present study was that TNP-470 could enhance the efficacy of conventional cytotoxic agents in the treatment of NPC. The inhibitory rate of 5-FU was increased, from 51.7% to 74.13% (ie, significantly), by concomitant administration of TNP-470. Although the elevation did not reach statistical significance, TNP-470 also elevated the inhibitory rate of DDP, from 32.08% to 54.08% ($p = .074$). Development of an optimum therapy combination of TNP-470 with DDP may finally clarify this interaction issue. These results were also consistent with the results of experimental treatments of other cancers,[16,17] and the mechanism of enhancement of the antitumor effect in combined therapy was reported as being an increase in the tissue levels of cytotoxic drugs by administration of TNP-470.[17] Reversible, slight diarrhea of 2 to 3 days' duration occurred in both the group with 5-FU treatment and the group with 5-FU + TNP-470 treatment. This is a typical kind of toxicity of 5-FU, and it was not aggravated by the combination of 5-FU with TNP-470. In fact, all animals had gained in body weight by the terminal day.

The therapeutic interaction of TNP-470 with fractionated radiotherapy has also been investigated in mammary carcinoma in vivo.[18] An additive effect of TNP-470 was found when it was given after the end of fractionated radiotherapy. But, when TNP-470 was given during fractionated radiotherapy, it decreased the radiocurability by inhibiting reoxygenation of the tumor cells, which is an essential process in maintaining the radiosensitivity of tumor cells. So, the effect of combining TNP-470 with radiotherapy is strongly dependent on the timing of the drug administration.

CONCLUSIONS

TNP-470 inhibits the growth of the human NPC cell line alone, and an additive effect was demonstrated when TNP-470 was combined with 5-FU. Side effects did not result from the administration of TNP-470 at the dose of 20 mg/kg, and the toxicity of conventional drugs was not aggravated by TNP-470.

ACKNOWLEDGMENTS — We thank Yan-Li Ye and Lian-Gui Wang, Animal Laboratory, Cancer Center, Sun Yat-sen University of Medical Sciences, for providing us the facilities for the animal experiments. We also appreciate Takeda Chemical Industries, Ltd, Osaka, Japan, for providing us the TNP-470.

REFERENCES

1. Fandi A, Altun M, Azli N, Armand JP, Cvitkovic E. Nasopharyngeal cancer: epidemiology, staging and treatment. Semin Oncol 1994;21:382-97.

2. Geara FB, Glisson BS, Sanguineti G, et al. Induction chemotherapy followed by radiotherapy versus radiotherapy alone in patients with advanced nasopharyngeal carcinoma. Cancer 1997;79:1279-86.

3. Al-Sarraf M, McLaughlin PW. Nasopharyngeal carcinoma: choice of treatment. Int J Radiat Oncol Biol Phys 1995;33:761-3.

4. Folkman J. What is the evidence that tumors are angiogenesis dependent? J Natl Cancer Inst 1990;82:4-6.

5. Qian CN, Min HQ, Liang XM, Zheng SS, Lin HL. Primary study of neovasculature correlating with metastatic nasopharyngeal carcinoma using computer image analysis. J Cancer Res Clin Oncol 1997;123:645-51.

6. Folkman J. Clinical applications of research on angiogenesis. N Engl J Med 1995;333:1757-63.

7. Brem H, Folkman J. Analysis of experimental antiangiogenic therapy. J Pediatr Surg 1993;28:445-51.

8. Fujioka T, Hasegawa M, Ogiu K, Matsushita Y, Sato M, Kubo T. Antitumor effects of angiogenesis inhibitor *O*-(chloroacetyl-carbamoyl)-fumagillol (TNP-470) against murine renal cell carcinoma. J Urol 1996;155:1775-8.

9. Yanase T, Tamura M, Fujita K, Kodama S, Tanaka K. Inhibitory effect of angiogenesis inhibitor TNP-470 on tumor growth and metastasis of human cell lines in vitro and in vivo. Cancer Res 1993;53:2566-70.

10. Qian CN, Min HQ, Lin HL, Hong MH, Ye YL. Primary study in experimental antiangiogenic therapy of nasopharyngeal carcinoma with AGM-1470 (TNP-470). J Laryngol Otol 1998;112:849-53.

11. Brem H, Goto F, Budson A, Saunders L, Folkman J. Minimal drug resistance after prolonged anti-angiogenic therapy with AGM-1470. Surg Forum 1994;45:674-7.

12. Zhang SZH, Gao XK, Zeng Y. Cytogenetic study on an epithelial cell line derived from poorly differentiated nasopharyngeal carcinoma. Int J Cancer 1983;31:587-90.

13. Al-Sarraf M, Pajak TF, Cooper JS, Mohiuddin M, Herskovic A, Ager PJ. Chemo-radiotherapy in patients with locally advanced nasopharyngeal carcinoma: a radiation therapy oncology group study. J Clin Oncol 1990;8:1342-51.

14. Folkman J. Tumor angiogenesis. Adv Cancer Res 1985;43:175-203.

15. Kusaka M, Sudo K, Matsutani E, et al. Cytostatic inhibition of endothelial cell growth by the angiogenesis inhibitor TNP-470 (AGM-1470). Br J Cancer 1994;69:212-6.

16. Kato T, Sato K, Kakinuma H, Matsuda Y. Enhanced suppression of tumor growth by combination of angiogenesis inhibitor *O*-(chloroacetyl-carbamoyl)-fumagillol (TNP-470) and cytotoxic agents in mice. Cancer Res 1994;54:5143-7.

17. Teicher BA, Dupuis NP, Robinson MF, Emi Y, Goff DA. Antiangiogenic treatment (TNP-470/minocyclin) increases tissue levels of anticancer drugs in mice bearing Lewis lung carcinoma. Oncol Res 1995;7:237-43.

18. Murata R, Nishimura Y, Hiraoka M. An antiangiogenic agent (TNP-470) inhibited reoxygenation during fractionated radiotherapy of murine mammary carcinoma. Int J Radiat Oncol Biol Phys 1997;37:1107-13.

≈

FUNCTIONAL ENDOSCOPIC SINUS SURGERY

Functional Endoscopic Sinus Surgery — Basic and Advanced Techniques will be held in Graz, Austria, September 7-9, 2000. For more information, contact Claire Zwerina, Secretary to Prof Stammberger, ENT-Department, University Hospital, Auenbruggerplatz 20, A-8036 Graz, Austria; fax ++43/316/385/3425.

Ann Otol Rhinol Laryngol 109:2000

LACK OF PREDICTIVE VALUE OF THE EPWORTH SLEEPINESS SCALE IN PATIENTS AFTER UVULOPALATOPHARYNGOPLASTY

STANLEY GIUDICI, MD
IOWA CITY, IOWA
WAYNE FARMER, DO
HOLMDEL, NEW JERSEY
ANTHONY DOLLINGER, MS
WALKERSVILLE, MARYLAND
TIMOTHY ANDRADA, MS
CHEVERLY, MARYLAND
KENNETH TORRINGTON, MD
WASHINGTON, DC
KRISHNAN RAJAGOPAL, MD
SILVER SPRING, MARYLAND

The Epworth Sleepiness Scale (ESS) has been recognized as a valid measure of sleep propensity. Statistically significant correlations between ESS scores, the respiratory disturbance index (RDI), and the lowest arterial oxygen saturation (LSAT) have been described in patients with surgically untreated obstructive sleep apnea (OSA). We investigated whether the same relationships hold true after uvulopalatopharyngoplasty (UPPP). Forty-two adults with documented OSA treated by UPPP were reevaluated with the ESS questionnaire and 8-hour diagnostic nocturnal polysomnography (nPSG). We found no significant correlation between the ESS scores and the RDI or LSAT in patients after UPPP. Because postoperative ESS scores do not correlate with the RDI or LSAT, we conclude that the ESS is not a reliable surrogate for nPSG testing.

KEY WORDS — diagnosis, polysomnography, questionnaires, sleep apnea, therapy, uvulopalatopharyngoplasty.

Obstructive sleep apnea (OSA) is a relatively common condition that affects 2% to 4% of the adult population.[1] The initial treatment for most patients involves the use of nasal continuous positive airway pressure (nCPAP). However, some patients cannot tolerate nCPAP on a long-term basis.[2] In selected patients, uvulopalatopharyngoplasty (UPPP) provides effective treatment.[3,4] After surgery, many patients undergo follow-up nocturnal polysomnography (nPSG) to evaluate their response to surgery and to determine whether the need for further treatment exists. This determination remains largely based on the respiratory disturbance index (RDI).

Patients are often reluctant to undergo postoperative testing, and insurance companies are commonly unwilling to pay for expensive overnight sleep studies. Without the benefit of nPSG, can physicians be confident of the success of UPPP? It would be ideal if a simple, effective screening method existed that would assist physicians in further patient management and not subject the patient to time-consuming and costly testing.

The Epworth Sleepiness Scale (ESS) was developed as a simple and easy-to-administer questionnaire that provides quantitative measurements of sleep propensity in adults. It distinguishes normals and primary snorers from those with sleep disorders.[5] The study was conducted in Melbourne, Australia; adult subjects (n = 55) had documented OSA, but had no surgery for their condition. It found a significant correlation between ESS scores and the RDI ($r = +.550$, $p < .001$) and between ESS scores and the lowest arterial oxygen saturation (LSAT; $r = -.457$, $p < .001$).

The primary objective of this study was to evaluate the relationship between ESS scores and the RDI and LSAT after surgery and to address whether the ESS could be used as an indicator for further studies in OSA patients after UPPP. Two secondary objectives were to determine whether ESS scores correlate with the degree of fragmented sleep as measured by the total arousal index (TAI) and to determine whether ESS scores correlate with sleep latency (SL) as a measure of sleep propensity in OSA patients after UPPP.

METHODS

This is a prospective analysis of patients with OSA previously documented with nPSG (RDI, >5) and surgically treated with UPPP at Walter Reed Army Medical Center. All patients were more than 18 years of age and were recruited from a population of active-duty and retired military personnel and their families. Initially identified from records in the Walter Reed Sleep Disorders Center and otolaryngology clinics, the patients had undergone UPPP a minimum of 4 months before enrollment. An investigator (S.G.) contacted the patients during the 6-month period between February and September 1996 and invited them to participate in a follow-up evaluation to assess their response to surgery. Of the patients contacted, 70% voluntarily agreed to participate and gave informed consent to the study, which had been approved by the Walter Reed Army Medical Center Department

---

From the Pulmonary and Critical Care Medicine Service, Walter Reed Army Medical Center, Washington, DC.

CORRESPONDENCE — Stanley Giudici, MD, University of Iowa College of Medicine, Depts of Internal Medicine and Psychiatry, 2-202/MEB, Iowa City, IA 52242-1000.

TABLE 1. SLEEP SCORING AND DEMOGRAPHIC CHARACTERISTICS OF 42 STUDY PATIENTS

	Minimum	*Maximum*	*Mean*	*SD*
ESS	2.0	23.0	11.9	4.9
RDI	0.0	101.0	24.9	25.5
LSAT (%)	73.0	95.0	86.6	6.5
TAI	1.7	112.4	36.5	24.9
SL (min)	0.0	32.0	6.7	7.9
Age (y)	19	71	48	11.6
BMI	18.9	43.0	28.9	4.5

ESS — Epworth Sleepiness Scale, RDI — respiratory disturbance index, LSAT — lowest arterial oxygen saturation, TAI — total arousal index, SL — sleep latency, BMI — body mass index (weight in kilograms divided by height in meters, squared).

of Scientific Review and Human Use Committees. Patients were disqualified if they had other types of airway surgery besides UPPP for treatment of OSA, if they were taking medications with sedative side effects, if they had an additional sleep disorder, or if they had used nCPAP before enrollment. The studies were conducted at the Walter Reed Sleep Disorders Center.

On the study night, each subject completed the ESS questionnaire and then underwent 8-hour diagnostic nPSG that was recorded with a Grass Instruments model 78 (Astro-Med, Inc, West Warwick, RI) interfaced with a Somnostar 4100 recording and analysis system (SensorMedics Corporation, Yorba Linda, Calif). The subjects were monitored with standard continuous polysomnography, including electroencephalographic activity from central and occipital leads, eye movements, submental electromyography, electrocardiography, snore microphone, oxyhemoglobin saturation, and continuous blood pressure. Respiration was monitored with 2-channel reusable trace thermocouples (Pro-Tech Services, Inc, Woodinville, Wash) with sensor tips to record nasal and oral airflow and by crystal trace respiration belts (Pro-Tech Services, Inc) to detect respiratory effort. A 4-sensor Gaeltec catheter, model CT/S4 (Medical Measurements, Inc, Hackensack, NJ), with pressure ports located in the posterior nasopharynx, oropharynx, hypopharynx, and distal esophagus, recorded pressures in the upper airway and esophagus. After each sensor was individually balanced and calibrated (+100 to −100 cm H2O), the nasal passage was numbed with 2% viscous Xylocaine and the catheter was inserted. Catheter placement was verified with a lateral-view radiograph of the head and neck. The subjects were continuously monitored by way of infrared closed-circuit cameras and were videotaped for analysis of body position and movement. Resting levels of esophageal pressure, oxyhemoglobin saturation, and heart rate were obtained with continuous recordings while the subjects lay in bed quietly awake for 10 minutes before lights-out, and for 10 minutes after lights-on in the morning.

TABLE 2. PEARSON CORRELATION BETWEEN ESS SCORES AND SLEEP STUDY VARIABLES

	ESS	*RDI*	*LSAT*	*TAI*	*SL*
ESS	1.000	.296	−.299	.284	−.376
RDI	.296	1.000	−.710*	.889*	−.167
LSAT	−.299	−.710*	1.000	−.688*	.112
TAI	.284	.889*	−.688*	1.000	.035

*Correlation is significant at .01 level (2-tailed).

Sleep was scored manually in 30-second epochs by standard criteria.[6] Swallows and movement artifacts were deleted from the analysis. The SL was scored from time of lights-out to first occurrence of stage II sleep or 3 consecutive epochs of stage I sleep. Apneas and hypopneas were scored and categorized for obstructive, central, and mixed events. Hypopneas and obstructive apneas were events that were associated with increasing negative fluctuations in esophageal pressure or increased thoracoabdominal effort with little or no airflow until termination of the event. Central apnea scores were based on absence of airflow, respiratory effort, and esophageal pressure fluctuation. Increasing negative intrathoracic pressure with transient arousals but no obstructive apneas or hypopneas and no change in oxygen saturation identified an upper airway resistance syndrome (UAR). The RDI was calculated as the number of apneas and hypopneas that caused a drop of >4% in the arterial oxygen saturation per hour of sleep. The TAI was calculated as the total number of arousals, awakenings, and alpha intrusions per hour of sleep.

The primary response variables were the ESS scores, RDI, LSAT, TAI, and SL. The relationships between the ESS scores and sleep study variables were determined from a simple correlation analysis with alpha set to 0.01.

RESULTS

Forty-two male patients from a total recruitment of 60 participated in this study. Of the total patients recruited, 8 were not compliant or dropped out, 7 refused to participate, and 3 left the area and were lost to follow-up. Of those who participated, their ESS scores, sleep study variables, age, and body mass index (BMI) are given in Table 1. Using a Pearson correlation coefficient, we found no statistical association between the ESS scores and the sleep study variables RDI, LSAT, TAI, and SL (Table 2). Significant correlations between the RDI, LSAT, and TAI were noted.

We determined whether the severity of disease had

TABLE 3. ESS SCORES AND SLEEP STUDY VARIABLES IN MILD, MODERATE, AND SEVERE OSA

OSA	*N*	*ESS*	*RDI*	*LSAT (%)*	*TAI*
Mild	10	10.6 ± 4.5	10.8 ± 3.5	89.2 ± 4.5	19.4 ± 12.5
Moderate	10	12.5 ± 3.6	22.1 ± 4.5	84.6 ± 5.1	42.2 ± 18.6
Severe	12	13.2 ± 5.9	60.0 ± 18.3	81.4 ± 6.8	63.4 ± 20.1

Data are mean ± SD.

OSA — obstructive sleep apnea.

an impact on the relationship of the ESS to sleep study variables, and divided the groups into mild (RDI, >5 to <15), moderate (RDI, ≥15 to <30), and severe OSA (RDI, ≥30). The descriptive values are given in Table 3. We found no significant correlation between the ESS and the sleep study variables, including the SL. Neither did we find a significant correlation among the ESS scores, age, and BMI.

DISCUSSION

The means, standard deviations, and ranges of age and ESS scores differed little from Johns' data.[5] However, we found no significant correlation between the ESS scores and the RDI and LSAT, and conclude that the ESS is not a valid predictor of these variables in patients after UPPP. Moreover, we conclude that the ESS is not a reliable measure of sleep propensity in OSA patients after UPPP, as evidenced by no significant correlation between the ESS and the SL.

A lack of a significant relationship between the ESS and both the RDI and LSAT may reflect changes in upper airway dynamics after surgery whereby obstructive events are less frequent and airway resistance is more evident.[7,8] This syndrome, known as the UAR, has been studied with respect to excessive daytime sleepiness (EDS). Investigators believe the link between the UAR and EDS is frequent arousals and fragmented sleep associated with the UAR.[9] Regarding our patients, however, fewer than 7% developed a UAR after surgery. Moreover, if frequent arousals and fragmented sleep were a factor in our findings, we would expect to see a significant correlation between the ESS scores and the TAI, which we did not find.

Further insight into the development of the ESS questionnaire sheds light on the discrepancies that we find in our study between the ESS scores and the sleep study variables. The ESS' development was conceptually based on the nature and occurrence of daytime sleepiness. Sleepy people often describe how they doze off while engaged in activities that involve low levels of stimulation and immobility. Early questionnaire surveys identified situations commonly encountered in daily life that are soporific.[10] A survey (n = 116) among adults in New Mexico asked the frequency of falling asleep in 5 situations, and the 3 "most sleepy" questions showed a statistically significant correlation between the SL and answers to the questions ($r = -.32$, $p < .001$).[11] However, the extent to which these answers influenced the variations in SL was determined from the coefficient of determination, which was only 10%. Therefore, 90% of the SL variability in this survey remained influenced by or accounted for by other factors. Though not a strong predictor of the SL, this survey contributed to the development of the ESS in both methodology and content. The ESS, likewise, is based on questions referring to 8 such situations, some known to be very soporific, others less so. If a subject could not remember facing a particular situation, he or she was asked to estimate how it might affect him or her. This method and approach obviously left room for error, either from memory failure or from biased estimates due to misperceptions of one's level of daytime sleepiness.

The response to the ESS is based partly on perceived sleepiness. If a patient subjectively feels the level of daytime sleepiness has improved after surgery, he or she would be less likely to report a tendency to doze off in certain situations. Discrepancies and a lack of significant correlation between subjective responses and objective findings after UPPP have been well documented.[12-18] A study that examined the effects of UPPP on daytime sleepiness among nonresponders (those with no reduction in their RDI after surgery) showed no significant improvement in their Mean Sleep Latency Test scores after surgery, even though 70% reported subjective improvement in excessive sleepiness.[19] Our study might have shown a tighter relationship between ESS scores and sleep study variables in patients before surgery, as previously reported in the literature.

Biased estimates or reliance on memory can produce varied responses from patients who complete a survey questionnaire such as the ESS. Johns' study[5] (n = 55) did not show a particularly strong influence ($r = +.55$) of RDI values on ESS scores; this outcome may simply reflect sample variation or result from other variables such as memory failure. In practice, non-sampling errors such as memory failure or biased estimates can be extremely difficult to control. These factors ultimately result in diminishing a survey's power to accurately predict and assess measurable clinical parameters.

In summary, the assessment of sleep characteristics in patients who have undergone UPPP requires nPSG testing. The ESS is not a reliable indicator of sleep quality in such patients.

ACKNOWLEDGMENT — We acknowledge Jose Munoz (Naval Hospital, Rota, Spain) in appreciation for his statistical analysis of the data.

REFERENCES

1. Young T, Palta M, Dempsey J, Skatrud J, Weber S, Badr S. Occurrence of sleep disorder breathing among middle-aged adults. N Engl J Med 1993;328:1230-5.

2. Lojander J, Maasilta P, Partinen M, Brander P, Salmi T, Lehtonen H. Nasal-CPAP, surgery, and conservative management for treatment of obstructive sleep apnea syndrome. A randomized study. Chest 1996;110:114-9.

3. Shepard J, Olsen K. Uvulopalatopharyngoplasty for treatment of obstructive sleep apnea. Mayo Clin Proc 1990;65:1260-7.

4. Gislason T, Lindholm C, Almquist M, Birring E. Uvulopalatopharyngoplasty in the sleep apnea syndrome. Predictors of results. Arch Otolaryngol Head Neck Surg 1988;114:45-51.

5. Johns M. A new method for measuring daytime sleepiness: the Epworth Sleepiness Scale. Sleep 1991;14:540-5.

6. Rechtschaffen A, Kales A. A manual of standardized terminology: techniques and scoring system for sleep stages of human subjects. Los Angeles, Calif: UCLA Brain Information Service/Brain Research Institute, 1968.

7. Polo O, Brissaud L, Fraga J, Dejean Y, Billiard M. Partial upper airway obstruction in sleep after uvulopalatopharyngoplasty. Arch Otolaryngol Head Neck Surg 1989;115:1350-4.

8. Woodson B. Upper airway resistance syndrome after uvulopalatopharyngoplasty for obstructive sleep apnea syndrome. Otolaryngol Head Neck Surg 1996;114:457-61.

9. Guilleminault C, Stoohs R, Clerk A, Cetel M, Maistros P. A cause of excessive daytime sleepiness: the upper airway resistance syndrome. Chest 1993;104:781-7.

10. Roth T, Roehrs T, Carskadon M, Dement W. Daytime sleepiness and alertness. In: Kryger M, Roth T, Dement W, eds. Principles and practice of sleep medicine. 2nd ed. Philadelphia, Pa: WB Saunders, 1994:40-9.

11. Schmidt-Nowara W, Wiggins C, Walsh J, Bauer C. Prevalence of sleepiness in an adult population. Sleep Res 1989;18:302.

12. Wetmore S, Scrima L, Snyderman N, Hiller F. Postoperative evaluation of sleep apnea after uvulopalatopharyngoplasty. Laryngoscope 1986;96:738-41.

13. Schoen L, Anand V, Weisenberger S. Upper-airway surgery for treating obstructive sleep apnea. Measuring and predicting success. Arch Otolaryngol Head Neck Surg 1987;113:850-3.

14. Zohar Y, Finkelstein Y, Talmi Y, Bar-Ilan Y. Uvulopalatopharyngoplasty: evaluation of postoperative complications, sequelae, and results. Laryngoscope 1991;101:775-9.

15. Larsson H, Carlsson-Nordlander B, Svanborg E. Longtime follow-up after UPPP for obstructive sleep apnea syndrome. Results of sleep apnea recordings and subjective evaluation 6 months and 2 years after surgery. Acta Otolaryngol (Stockh) 1991;111:582-90.

16. Rodenstein D. Assessment of uvulopalatopharyngoplasty for the treatment of sleep apnea syndrome. Sleep 1992;15(suppl):S56-S62.

17. Davis J, Fine E, Maniglia A. Uvulopalatopharyngoplasty for obstructive sleep apnea in adults: clinical correlation with polysomnographic results. Ear Nose Throat J 1993;72:63-6.

18. Lu S, Chang S, Shiao G. Comparison between short-term and long-term postoperative evaluation of sleep apnea after uvulopalatopharyngoplasty. J Laryngol Otol 1995;109:308-12.

19. Zorick F, Roehrs T, Conway W, Fujita S, Witting R, Roth T. Effects of uvulopalatopharyngoplasty on the daytime sleepiness associated with sleep apnea syndrome. Bull Eur Physiopathol Respir 1983;19:600-3.

Ann Otol Rhinol Laryngol 109:2000

ULTRASTRUCTURE OF THE VOCAL PROCESS OF THE ARYTENOID CARTILAGE

KIMINORI SATO, MD, PHD

MINORU HIRANO, MD TADASHI NAKASHIMA, MD

KURUME, JAPAN

An investigation of the ultrastructure of the vocal process of the arytenoid cartilage was performed on excised human adult larynges. The results are summarized as follows. 1) The size of the chondrocytes is small and their density is high at the tip of the vocal process. 2) The size of the chondrocytes increases and their density decreases toward the posterior portion of the vocal process. 3) At the tip of the vocal process, the collagenous fibers are thin and run in various directions. 4) The thickness of the collagenous fibers increases and they form thick bundles toward the posterior portion of the vocal process. 5) The elastic fibers are dense at the tip of the vocal process, and their number decreases toward the posterior portion of the vocal process. 6) The elastic fibers, which are slender, branched, and anastomosed to form a loose network, run among the collagenous fibers at the tip of the vocal process. 7) Elaunin fibers are the predominant elastic fibers at the tip of the vocal process. 8) Even in the hyaline cartilage portion of the vocal process, elastic fibers are found. 9) The vocal processes are firm in forming the framework of the glottis and are more pliable toward the tip. 10) The 3-dimensional structure of the gradual changes in stiffness between the vocal fold and the vocal process makes a functional contribution to the roles of the vocal folds and the vocal processes.

KEY WORDS — arytenoid cartilage, elaunin fibers, larynx, ultrastructure, vocal process.

INTRODUCTION

The basic functions of the larynx are to act as a protective sphincter and as a passageway for air and to act in sound production. During swallowing, respiration, and phonation, the vocal processes always move and form the shape of the glottis.[1]

Among the laryngeal cartilages, only the arytenoid cartilage is composed of 2 types of cartilage, ie, elastic and hyaline cartilages. The 2 types of cartilages are very different in structure. Our previous investigations of the vocal process by light microscopy revealed that the elastic cartilage portion of the vocal process plays an important role in the physiological function of the arytenoid.[2]

In this paper, the ultrastructure of the vocal process of the arytenoid cartilage is investigated, and its functional implications are discussed.

MATERIALS AND METHODS

We used 5 normal human adult larynges obtained from autopsy cases with ages ranging from 32 to 52 years (3 men and 2 women).

For transmission electron microscopy, the specimens were fixed in 2.5% glutaraldehyde at 4°C for 2 hours, rinsed with cacodylate buffer solution, and postfixed in 2% osmium tetroxide at 4°C for 2 hours. They were then dehydrated in a graded series of concentrations of ethanol and embedded in epoxy resin. Semithin sections were prepared with an ultramicrotome, stained with 1% toluidine blue, and examined with a light microscope. Thin sections were made with an ultramicrotome, stained with uranyl acetate and lead citrate, and stained with tannic acid to make elastin apparent. These sections were then observed under a JEM-2000EX transmission electron microscope.

For scanning electron microscopy, each specimen was fixed in 2.5% glutaraldehyde at 4°C for 2 hours. After rinsing with cacodylate buffer solution, chemical digestion methods were used. To observe the 3-dimensional (3-D) structure of the collagenous fibers, the elastic fibers and the ground substance of the vocal process were chemically digested. All specimens were immersed in 2N sodium hydroxide for 7 days at room temperature. To observe the 3-D structure of the elastic fibers and the relationship between the elastic and collagenous fibers, the ground substance of the vocal process was chemically digested. All specimens were immersed in 2N sodium hydroxide for 6 hours at 37°C. These specimens were washed in physiological saline solution and then postfixed in 2% osmium tetroxide at 4°C for 2 hours. Postfixation was followed by dehydration in a graded series of concentrations of ethanol, immersion in tert-butyl alcohol, and drying by the tert-butyl alcohol freezing method. The specimens were then sputter-coated with gold and examined under a Hitachi S-

---

From the Department of Otolaryngology–Head and Neck Surgery, Kurume University, School of Medicine, Kurume, Japan.

CORRESPONDENCE — Kiminori Sato, MD, PhD, Dept of Otolaryngology–Head and Neck Surgery, Kurume University, School of Medicine, 67 Asahi-machi, Kurume 830-0011, Japan.

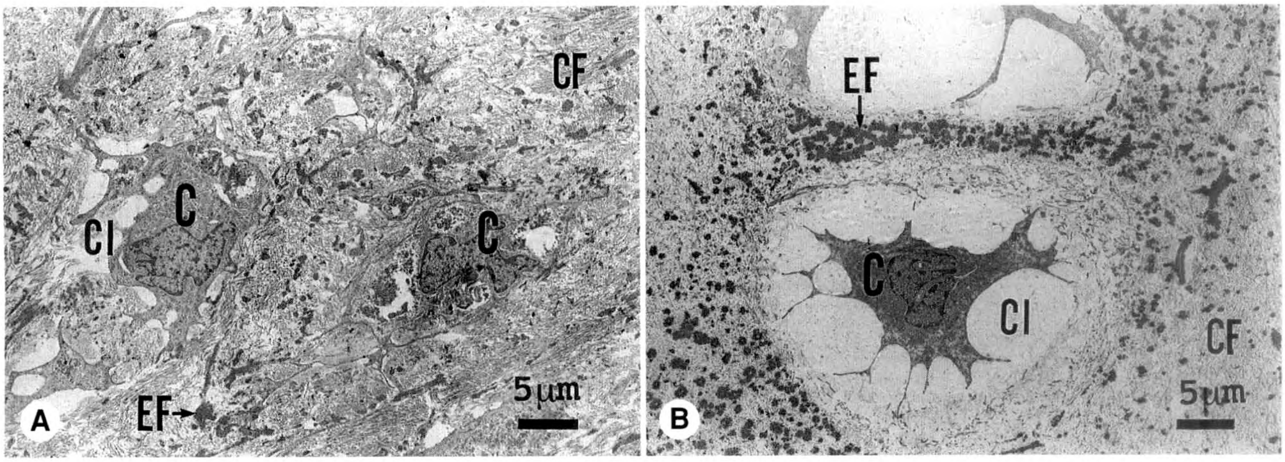

Fig 1. Transmission electron microscopic findings in vocal process (tannic acid stain). C — chondrocyte, Cl — cartilage lacuna, CF — collagenous fibers, EF — elastic fibers. A) Elastic cartilage portion. B) Hyaline cartilage portion.

800 scanning electron microscope.

RESULTS

The cartilage of the vocal process was composed of chondrocytes, collagenous fibers, elastic fibers, and ground substance (Fig 1). This cartilage was also composed of elastic and collagenous cartilages (Fig 1). The elastic cartilage is found not only at the tip of the vocal process, but also at its superior portion. The tip of the vocal process was attached to the posterior macula flava anteriorly. The transition between the vocal process and the posterior macula flava was gradual, and the border between them was not clearly delineated.

Chondrocytes. The chondrocytes that had small cartilage lacunae were relatively small at the tip of the vocal process, ie, the elastic cartilage portion of the vocal process (Fig 1A). The density of chondrocytes was high in these portions (Fig 1A), and they synthesized fibers and ground substance. The size of the chondrocytes increased and their density decreased toward the posterior portion of the vocal process. The chondrocytes that had large cartilage lacunae were relatively large in the posterior portion of the vocal process, ie, the hyaline cartilage portion of the vocal process (Fig 1B). The density of chondrocytes was low in these portions (Fig 1B). The transition between the elastic and hyaline cartilage portions was gradual, and the border between them was not clearly delineated.

Collagenous Fibers. Figure 2 shows scanning electron microscopy findings for collagenous fibers in the vocal process. Collagenous fibers alone remained after treatment by the sodium hydroxide maceration method.

At the tip of the vocal process (Fig 2A), ie, the elastic cartilage portion, the collagenous fibers were thin and ran in various directions. The thickness of the collagenous fibers increased and they formed thick bundles toward the posterior portion of the vocal process (Fig 2B).

Elastic Fibers. Figure 3A shows scanning elec-

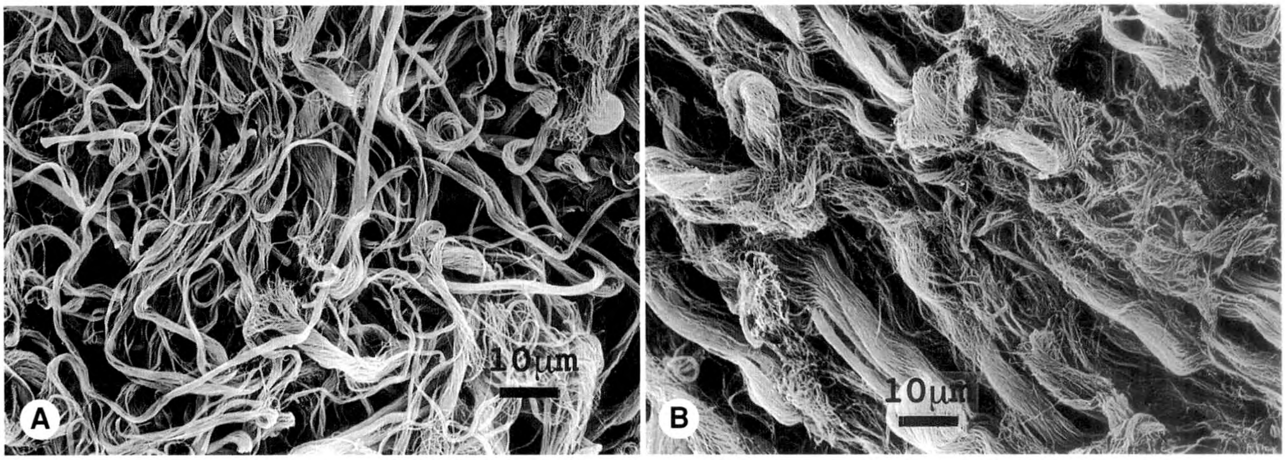

Fig 2. Scanning electron microscopic findings of collagenous fibers at A) tip of vocal process and B) posterior portion of vocal process.

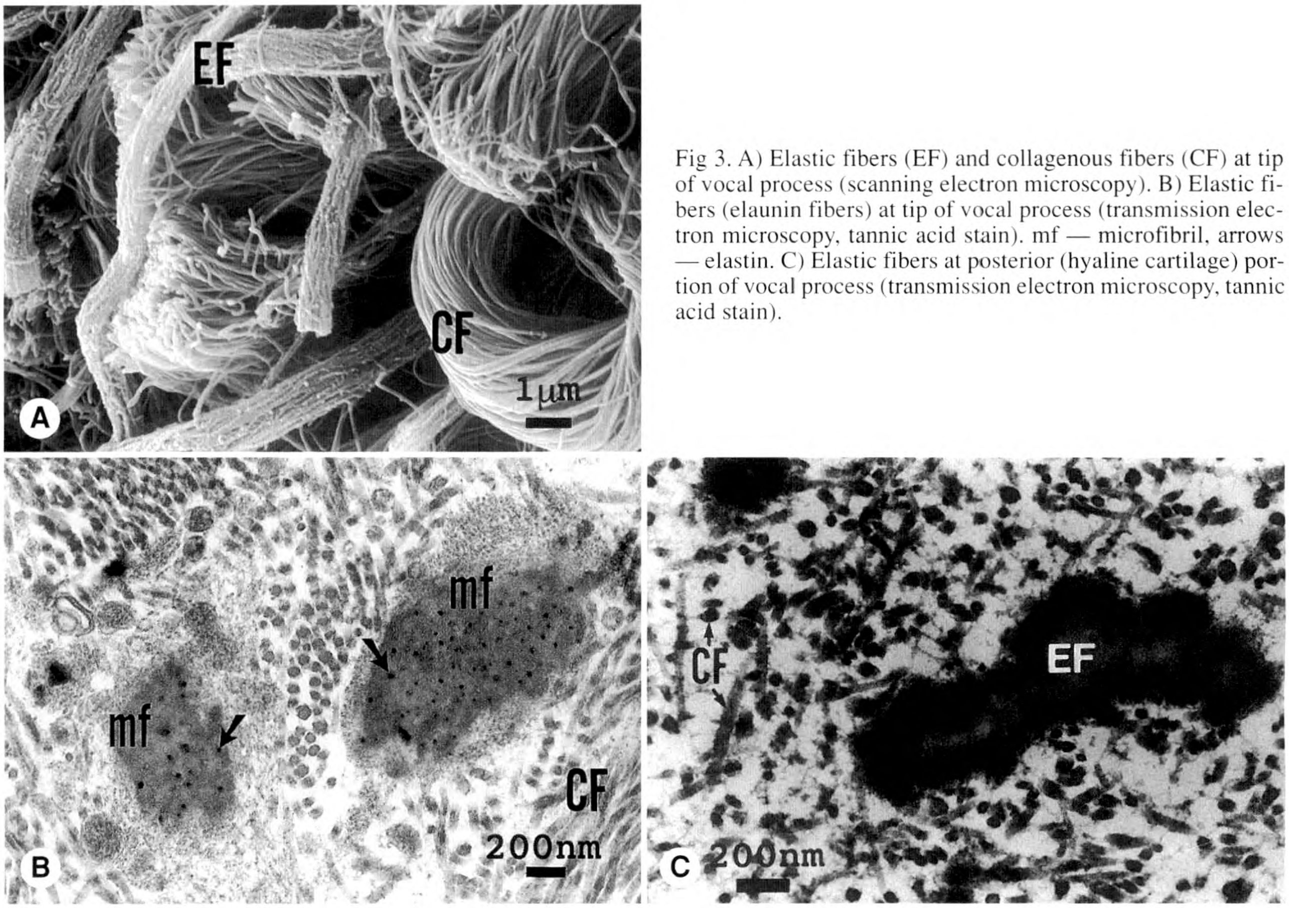

Fig 3. A) Elastic fibers (EF) and collagenous fibers (CF) at tip of vocal process (scanning electron microscopy). B) Elastic fibers (elaunin fibers) at tip of vocal process (transmission electron microscopy, tannic acid stain). mf — microfibril, arrows — elastin. C) Elastic fibers at posterior (hyaline cartilage) portion of vocal process (transmission electron microscopy, tannic acid stain).

tron microscopy findings for elastic fibers at the tip of the vocal process. To observe the elastic fibers and the relationship between the elastic and collagenous fibers, we used the sodium hydroxide maceration method to leave the elastic and collagenous fibers.

The elastic fibers were slender and ran among the collagenous fibers. The elastic fibers were cylindrical or elliptical in shape. The spaces among the fibers were relatively large.

The elastic fibers were dense at the tip of the vocal process, ie, the elastic cartilage portion (Figs 1A and 3A). Elaunin fibers were the predominant elastic fibers there. The elaunin fibers were elastic-related fibers in which the fibrillary component (microfibril) was quite prominent but the elastic component (elastin, stained black with tannic acid stain) was not as abundant as in the elastic fibers (Fig 3B). The number of elastic fibers decreased toward the posterior portion of the vocal process. Even in the hyaline cartilage portion of the vocal process, elastic fibers were found (Figs 1B and 3C).

DISCUSSION

Arytenoid cartilage is composed of elastic and hyaline cartilages. These 2 types of cartilages have very different properties. Elastic cartilage is soft and pliable. Hyaline cartilage is firm and plays a role as a framework for the larynx.

Our previous investigation of the vocal process by light microscopy revealed that the elastic cartilage was found not only at the tip of the vocal process, but also at the superior portion of the arytenoid cartilage, from the vocal process to the apex.[2] The transition between the elastic and hyaline cartilage portions is gradual, and the border between them is not clearly delineated.[2,3] The tip of the vocal process bends at the elastic cartilage portion during adduction and abduction, and the arytenoids come into contact mainly at the superior portion, ie, the elastic cartilage portion.[2,4] The elastic cartilage portion of the arytenoid cartilage does not become ossified, hence the elastic cartilage in the arytenoid is able to perform its role throughout the individual's lifetime.[2,5] The tip of the vocal process is attached to the posterior macula flava anteriorly.[6] In this study, the ultrastructure of the vocal process was investigated.

Cellular Component. The chondrocytes that had small cartilage lacunae were relatively small and their density was high at the tip of the vocal process, ie, the elastic cartilage portion of the vocal process. In this portion, many chondrocytes synthesized fibers and ground substance, and the size of each chondrocyte was relatively small. The vocal process bends at the elastic cartilage portion during adduction and abduction.[2,4] From the functional point of view, the chondrocytes synthesize fibers and ground substance at the tip of the vocal process to maintain a pliable and strong structure. Numerous but small chondrocytes cannot prevent the pliable movement there.

Fibrous Component. At the tip of the vocal process, ie, the elastic cartilage portion, the fibrous components were dense. The collagenous fibers were thin and ran in various directions. The elastic fibers were slender and ran among the collagenous fibers. A 3-D study of these structures demonstrates that the tip of the vocal process not only is pliable but also has a relatively strong structure.

The thickness of the collagenous fibers increased and they formed thick bundles toward the posterior portion of the vocal process. The 3-D study showed that the collagenous fibers play a role as a strong framework for the posterior glottis at the posterior portion of the vocal process.

Elastic fibers were dense at the tip of the vocal process, ie, the elastic cartilage portion. At the tip of the vocal process, elaunin fibers were predominantly elastic fibers. Elaunin fibers, which are elastic-related fibers having small amounts of elastin, are probably related to mechanical resistance and provide a support mechanism.[7,8] In fact, these fibers have been described in areas in which they may have that function.[7,8] During abduction and adduction, the tip of the vocal process bends at the elastic cartilage portion,[2,4] and there is much mechanical stress at the tip of the vocal process. The elaunin fibers at the tip of the vocal process are suggested to have mechanical resistance and serve as a support mechanism.

The number of elastic fibers decreased toward the posterior portion of the vocal process. Even in the hyaline cartilage portion of the vocal process, elastic fibers were found. Usually, hyaline cartilage does not contain elastic fibers.[9] The hyaline cartilage of the vocal process has a more pliable structure than other hyaline cartilages found in other parts of the body.

The vocal ligament ran between the anterior and posterior macula flavae.[6] The posterior macula flava is attached to the tip of the vocal process posteriorly.[6] The transition between the macula flava and the elastic cartilage portion of the vocal process is gradual, and the transition between its elastic and hyaline cartilage portions is also gradual. The borders between them are not clearly delineated. This electron microscopic investigation revealed that there are gradual changes in stiffness between the vocal fold and the vocal process. The vocal process of the arytenoid cartilage is firm in forming a framework for the glottis and is more pliable toward the tip. Gradual changes in stiffness between the vocal fold and the vocal process may absorb shock during phonation and prevent mechanical damage to the tip of the vocal process, and the tip of the vocal process bends easily during adduction and abduction. The 3-D structure of gradual changes in stiffness between the vocal fold and the vocal process makes a functional contribution to the roles of the vocal folds and vocal processes.

ACKNOWLEDGMENTS — We are grateful to Dr Yuuji Ito and Dr Yasuhiro Nakamura, St Mary's Hospital, Kurume, for their thoughtful consideration of the cadaver larynges.

REFERENCES

1. Hirano M, Kurita S, Kiyokawa K, Sato K. Posterior glottis. Morphological study in excised human larynges. Ann Otol Rhinol Laryngol 1986;95:576-81.

2. Sato K, Kurita S, Hirano M, Kiyokawa K. Distribution of elastic cartilage in the arytenoids and its physiologic significance. Ann Otol Rhinol Laryngol 1990;99:363-8.

3. Hirano M, Sato K. Histological color atlas of the human larynx. San Diego, Calif: Singular Publishing Group, 1993.

4. Hirano M, Yoshida T, Kurita S, Kiyokawa K, Sato K, Tateishi O. Anatomy and behavior of the vocal process. In: Baer T, Sasaki C, Harris K, eds. Laryngeal function in phonation and respiration. San Diego, Calif: Singular Publishing Group, 1991:3-13.

5. Sato K, Sakaguchi S, Kurita S, Hirano M. A morphological study of aged larynges. Larynx Jpn 1992;4:84-94.

6. Sato K, Hirano M. Histologic investigation of the macula flava of the human vocal fold. Ann Otol Rhinol Laryngol 1995; 104:138-43.

7. Cotta-Pereira G, Kattenbach WM, Rodrigo G. Elastic-related fibers in basement membranes. Front Matrix Biol 1979;7: 90-100.

8. Cotta-Pereira G, Rodrigo G, Bittencourt-Sampaio S. Oxytalan, elaunin, and elastic fibers in the human skin. J Invest Dermatol 1976;66:143-8.

9. Fawcett DW. A textbook of histology. Philadelphia, Pa: WB Saunders, 1986:188-98.

Ann Otol Rhinol Laryngol 109:2000

RECURRENT LARYNGEAL NERVE MONITORING DURING CRICOTRACHEAL RESECTION

KEVIN CAVANAUGH, MD ALBERT H. PARK, MD

MAYWOOD, ILLINOIS

Cricotracheal resection has been advocated in the management of severe subglottic stenosis. One of the possible complications of this procedure is injury to the recurrent laryngeal nerve (RLN). We describe a new technique in which electrodes are placed directly through the thyroid cartilage to monitor the RLN intraoperatively. Nine cats' left vocal cords were monitored, and 3 cats had unilateral vocal cord injury postoperatively: 1 right cord and 2 left cords. Even though this technique was efficacious, our ability to monitor the RLNs was difficult secondary to difficulty interpreting the nerve monitor's wave morphologies. The future use of RLN nerve monitoring during cricotracheal resection will depend upon the ability to distinguish true stimulation from artifact. Monitoring of the RLN could be beneficial in patients with previous operations for subglottic stenosis.

KEY WORDS — cat, cricotracheal resection, nerve monitoring, recurrent laryngeal nerve, subglottic stenosis.

INTRODUCTION

Because of the close proximity of the recurrent laryngeal nerve (RLN) to the cricothyroid joint, RLN injury during cricotracheal resection is a potential complication. Several methods of RLN monitoring have been described, including palpation,[1] pressure transduction,[2] electromyography (EMG) electrode placement via direct laryngoscopy[3-5] or indirectly via the cricothyroid membrane,[6] an EMG endotracheal tube,[7] and a postcricoid laryngeal surface monitor.[8] Intraoperative RLN monitoring has been used for thyroid surgery[6] and cranial base surgery.[9]

Partial cricoid resection with tracheal reanastomosis is a recently described procedure for the treatment of severe pediatric subglottic stenosis.[10] One of the concerns about this procedure is the potential for injury to the RLN. This injury can lead to hoarseness, difficulty with speech and swallowing, and failure to decannulate the patient. This study reviews our experience with RLN monitoring in a cat model.

METHODS AND MATERIALS

Nine tabby cats weighing 2.6 to 4.7 kg were used in this study (Institutional Animal Care and Use Committee No. 97-048). After intramuscular sedation with a mixture of ketamine hydrochloride, butorphanol tartrate, and acepromazine maleate, the vocal cords were evaluated for function. The cats were intubated and monitored with an esophageal heart monitor (Bickford, USA). The cats were anesthetized with halothane.

A NIM-2 Nerve Integrity Monitoring Unit (Xomed-Treace, Jacksonville, Fla) was used to monitor the left RLNs in all the surgeries. Standard surface EMG electrodes were placed in the forehead to use as a ground and the left shoulder as an anode for stimulation with a Prass monopolar flush-tip stimulator probe (Xomed-Treace). Two EMG electrodes were also placed in the left vocal cord.

Cricotracheal resection was performed following a tracheotomy. The cricoid was separated with a vertical midline incision, and the vocal cords were identified after moving the previously placed oral endotracheal tube (ET) proximally. Variable portions of the cricoid were removed, with the inferior cornu of the thyroid cartilage used as a landmark for the RLN. In some of the operations, the inferior cornu was separated from its attachment to the cricoid, and the RLNs were able to be identified. When the cricothyroid joint was not separated, the RLNs were not seen. Reanastomosis involved mobilizing the trachea and suturing it to the posterior cricoid, the remaining lateral portions of the cricoid, and the anterior thyroid cartilage with 4.0 Vicryl suture. Vocal cord function was evaluated endoscopically following surgery.

The larynges and the RLNs were stained with hematoxylin and eosin postmortem at various periods after surgery, and then they were evaluated by 2 pathologists who were blinded to the results.

RESULTS

Nine tabby cats, including 7 females and 2 males,

From the Department of Otolaryngology–Head and Neck Surgery, Loyola University Medical Center, Maywood, Illinois. This study was performed in accordance with the PHS Policy on Humane Care and Use of Laboratory Animals, the NIH *Guide for the Care and Use of Laboratory Animals*, and the Animal Welfare Act (7 U.S.C. et seq.); the animal use protocol was approved by the Institutional Animal Care and Use Committee (IACUC) of Loyola University Medical Center.

CORRESPONDENCE — Albert H. Park, MD, Dept of Otolaryngology, Loyola University Medical Center, 2160 S First Ave, Bldg 105, Maywood, IL 60153.

COMPARISON OF POSTOPERATIVE VOCAL CORD FUNCTION BY TYPE OF RECURRENT LARYNGEAL NERVE MONITORING

Cat No.	*Vocal Cord Function Preop*	*Recurrent Laryngeal Nerves Seen Intraop*	*Vocal Cord Function Postop*	*Type of Monitoring**
1	+	+	L paralysis	1
2	+	+	R paralysis	1
3	+	+	Mobile	1
4	+	+	Mobile	2
5	+	−	Mobile	2
6	+	−	L paralysis	3
7	+	−	Mobile	3
8	+	−	Mobile	3
9	+	+	Mobile	3

*1 — electrodes placed endoscopically; 2 — electrodes placed via operative field into vocal cords; 3 — electrodes placed via thyroid cartilage.

underwent cricotracheal resections and RLN monitoring of their left vocal cords. Vocal cord function was normal in all of the cats preoperatively. Postoperatively, 3 cats (33%) were noted to have unilateral vocal cord paralysis. One cat (No. 2) had a hypomobile right cord, of which the function greatly improved until it was only very slightly hypomobile on postoperative day 28. Another cat (No. 1) had a hypomobile left cord that was not reevaluated, because the cat died prematurely. Finally, 1 cat (No. 6) had a hypomobile-to-immobile left cord that was immobile on postoperative day 28. Thus, 11% of the control cords and 22% of the monitored cords were affected by the surgery (see Table).

The pathology of cat 6 revealed both severe degeneration of a section of the left RLN and severe neuropathic atrophy of 1 cord. The pathology of cat 2 showed very little injury to the RLNs, but 1 cord illustrated muscular injury with both degenerating and regenerating skeletal muscle fibers. Finally, cat 1 had no injury to its left RLN or its cords, but this cat died before muscular changes could be studied to see if there was injury. No vocal cord hematomas or obvious electrode injuries were seen pathologically.

The RLNs of the cats were only identified if the inferior cornu of the thyroid cartilage was separated from its attachment to the cricoid. The RLNs were seen in 2 of the cats with vocal cord impairment (Nos. 1 and 2), but not in the third cat with vocal cord impairment (No. 6).

Five of the cats had hoarse meows postoperatively, which did not improve, and meows were not appreciated in the 4 remaining cats.

DISCUSSION

The method of monitoring the RLN changed during the course of this study (Fig 1). In the first 3 monitored surgeries, 2 standard EMG electrodes were placed endoscopically into the left vocal cords. However, this method was abandoned secondary to technical difficulty, inability to see the electrodes intraoperatively, false mucosal readings after dislodgment,

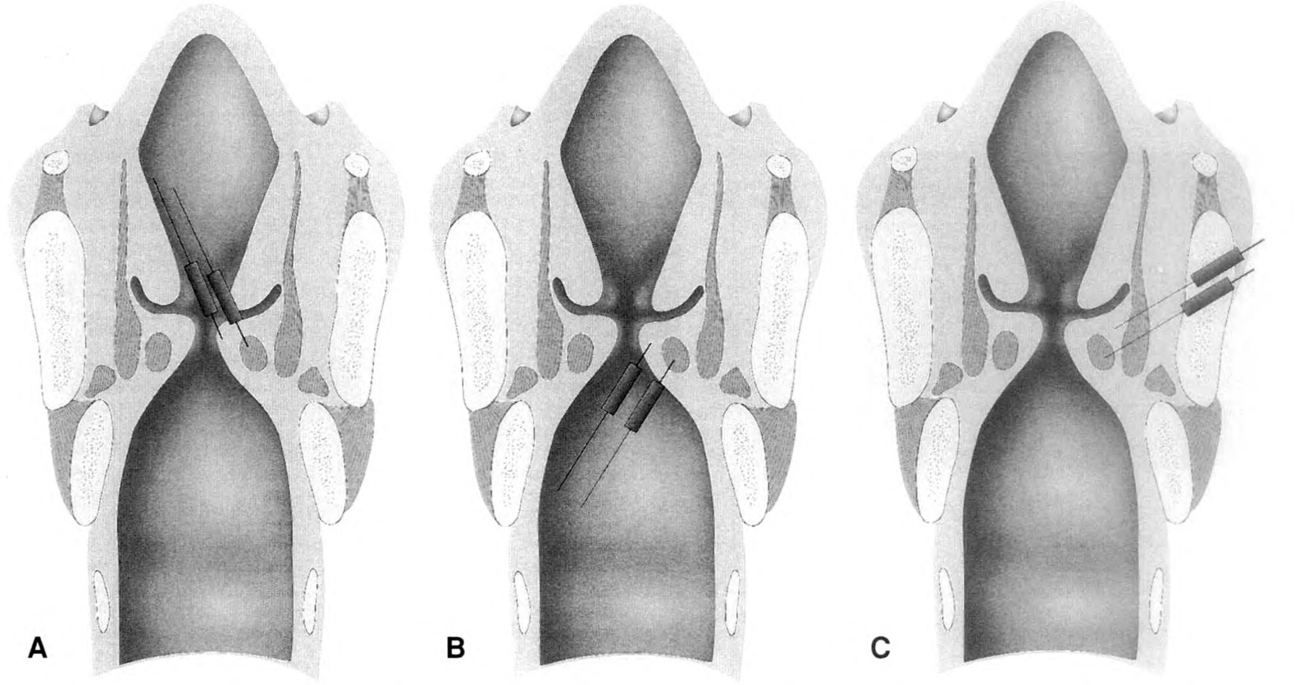

Fig 1. Methods of monitoring. A) Electrodes placed endoscopically. B) Electrodes placed via operative field into vocal cords. C) Electrodes placed via thyroid cartilage.

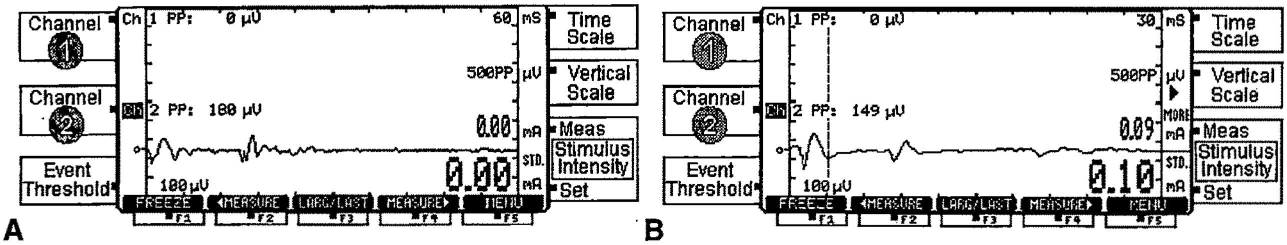

Fig 2. Comparison of A) artifact versus B) true stimulation.

and the need to "unscrub" (remove the sterile gown and gloves) to replace dislodged electrodes. In the next 2 monitored operations, the electrodes were placed directly into the left vocal cords via the operative field. This method was abandoned secondary to the electrodes' interfering with the operative field. In the last 4 monitored surgeries, the electrodes were placed through the strap muscles and thyroid cartilage and into the left vocal cord. This method worked well, since it stabilized the electrodes and kept them visible but out of the operative field.

Two of the 9 monitored RLNs were hypomobile or immobile postoperatively, whereas only 1 of the 9 control RLNs was hypomobile, and it improved postoperatively. Thus, the nonmonitored side had less morbidity to the vocal cords than the monitored side did. The electrodes in the injured monitored cats were placed endoscopically via direct laryngoscopy in 1 cat (No. 1), and through the thyroid cartilage in the other cat (No. 6). The RLNs of 2 of the 3 injured vocal cords were identified intraoperatively, whereas the RLN of cat 6 was not seen intraoperatively.

Possible reasons for the RLN injuries could include transection or ligation of the nerve. However, neither of these causes was seen when we dissected the RLNs during autopsies. Other reasons for nerve impairment could include electrical or thermal injury from electrical cautery or injury from stretching. Injury secondary to nerve stimulation is doubtful, since stimulation was only at 0.25 mA — a value that is well within the range of previously used levels.[11] Injury secondary to the placement of the electrodes is a consideration, especially for cat 2. No evidence of vocal cord injury secondary to electrode placement could be found in the literature, except for transient vocal cord edema and hemorrhage.[9] There were no vocal cord hematomas seen grossly or histologically in this study.

The only complete vocal cord paralysis involved cat 6, in which the electrode was placed via the thyroid cartilage. Pathology revealed that this injury was neuropathic. This method was used in 4 cats. Whether or not this method caused direct injury to the RLN or the vocal cord or whether the surgery itself caused the injury is unknown. The likelihood of injury to the RLN is not suspected to be high, especially since the electrode is placed superior to the RLN's entrance into the larynx. Furthermore, dissections of the RLN on other cats revealed that the RLN divides into several small branches after crossing the cricoid. Thus, it is difficult to tell if individual branches were injured by the electrode, although injury is a possibility.

In addition to the EMG electrode monitoring used in this study, there are 2 other types of RLN monitoring devices available. One involves an EMG ET, which most likely could not be placed secondary to the subglottic stenosis. If this ET could be placed, it would be in the middle of the operative field. Further, this ET was also not available for pediatric use at the time of this study. However, one could fabricate a pediatric EMG ET by a previously described method.[12]

A postcricoid laryngeal monitor (RLN Systems, Jefferson City, Mo) is also available. It would be difficult to use in this operation, since manipulation of the cricoid during resection would probably lead to artifact and thus frustration with the use of nerve monitoring. Further, the postcricoid laryngeal monitor can become dislodged during the operation, and it is only available in 1 (adult) size. Even though it can be trimmed, it would still be too large in pediatric patients.

One of the main drawbacks of intraoperative nerve monitoring is the false readings that are obtained secondary to artifact or mechanical stimulation. The operative team must be familiar with the different wave morphologies that can be produced (Fig 2). It is often difficult to distinguish the difference between the morphologies. If the various waveforms cannot be identified or there is artifact or mechanical stimulation, then the nerve monitor becomes more of a nuisance than a help — a situation that occurred frequently in this study. There was certainly a learning curve that occurred in this study concerning the nerve monitor and its readings. It was difficult to determine whether or not many of the readings were true, despite several consultations with our staff and the monitor manufacturer (Xomed-Treace).

Further, during cricotracheal resection, every maneuver is closely related to the location of the RLN. This fact led to artifact's being picked up by the monitor and thus to distraction and/or frustration for the operating team. Thus, the ability to decrease artifact would help make RLN monitoring more useful.

By placing the electrode through both the thyroid cartilage and the strap muscles, we also monitored the electrical and mechanical activity in the strap muscles. Thus, the false activity secondary to strap muscle stimulation could be eliminated by placing the electrode only through the thyroid cartilage.

Finally, the question of whether intraoperative nerve monitoring is necessary during cricotracheal resection needs to be addressed. Apart from the added cost and the possibility of false readings, one could argue that monitoring is unnecessary. In the first study by Monnier et al[10] on partial cricoid resections on previously unoperated children in which the RLNs were identified, there were no RLN injuries. In that group's second study, with 16 patients, no RLN injuries were reported.[13] Further, Stern et al[14] performed partial cricotracheal resections without identifying the RLNs on 16 pediatric patients, including 11 patients who had undergone previous surgeries. In that study, 9 of the patients had impaired vocal cord mobility preoperatively, and only 1 patient was noted to have a new vocal cord injury postoperatively. In our study, there were fewer RLN injuries on the unmonitored side compared to the monitored side. One of the advantages of the nerve monitor is that it can be used for nerve identification; however, in this study the RLNs were easily identified by using the cricothyroid joint as an anatomic landmark. Further, since the vocal cords are directly visible after splitting the cricoid open, a nerve stimulator could be used to identify the RLN.

Nevertheless, intraoperative nerve monitoring could play an important role in patients who have undergone previous operations for subglottic stenosis. If the patient has undergone a previous anterior cricoid split or a laryngotracheal reconstruction, the ability to use anatomic landmarks to identify the RLN is difficult secondary to scarring. Thus, monitoring the RLN during these reoperations could possibly be beneficial.

CONCLUSION

By placing EMG electrodes via the thyroid cartilage into the vocal cords, a surgeon can monitor the RLNs during cricotracheal resection. However, RLN monitoring was difficult in this study secondary to artifact and trouble in differentiating the nerve monitor's morphologies. Whether or not RLN monitoring is necessary during these operations will be determined as more of these operations are performed. Monitoring of the RLN might be more useful if it is only used during the lateral cricoid resection and anastomosis and if the morphologies become easier to differentiate. Further, the necessity of using nerve monitoring will most likely be higher in patients undergoing reoperation.

ACKNOWLEDGMENTS — We acknowledge John M. Lee, MD, PhD, and Aliya Husain, MD, for their preparation and readings of the pathology slides. We also acknowledge Xomed-Treace for loaning the NIM-2 monitor.

REFERENCES

1. James AG, Crocker S, Woltering E, Ferrara J, Farrar W. A simple method of identifying and testing the recurrent laryngeal nerve. Surg Gynecol Obstet 1985;161:185-6.
2. Zini C, Grandolfi A. Facial nerve and vocal-cord monitoring during otoneurosurgical operations. Arch Otolaryngol Head Neck Surg 1987;113:1291-3.
3. Beck DL, Maves MD. Recurrent laryngeal nerve monitoring during thyroid surgery. In: Kartush J, Bouchard K, eds. Neuromonitoring in otology and head and neck surgery. New York, NY: Raven Press, 1992:151-62.
4. Lipton RJ, McCaffrey TV, Litchy WJ. Intraoperative electrophysiologic monitoring of laryngeal muscle during thyroid surgery. Laryngoscope 1988;98:1292-6.
5. Rice DH, Cone-Wesson B. Intraoperative recurrent laryngeal nerve monitoring. Otolaryngol Head Neck Surg 1991; 105:372-5.
6. Flisberg K, Lindholm T. Electrical stimulation of the human recurrent laryngeal nerve during thyroid operation. Acta Otolaryngol [Suppl] (Stockh) 1970(suppl 263):63-7.
7. Goldstone AC, Schettino RL. The electrode endotracheal tube: a state of the art method for monitoring recurrent laryngeal nerve–vocal cord integrity in the intubated patient [Abstract]. Otolaryngol Head Neck Surg 1990;103:249.
8. Rea JL, Khan AL. Recurrent laryngeal nerve location in thyroidectomy and parathyroidectomy: use of an indwelling laryngeal surface electrode with evoked electromyography. Oper Tech Otolaryngol Head Neck Surg 1994;5:91-6.
9. Lanser MJ, Jackler RK, Yingling CD. Regional monitoring of the lower (IXth through XIIth) cranial nerves. In: Kartush J, Bouchard K, eds. Neuromonitoring in otology and head and neck surgery. New York, NY: Raven Press, 1992:131-50.
10. Monnier P, Savary M, Chapuis G. Partial cricoid resection with primary tracheal anastomosis for subglottic stenosis in infants and children. Laryngoscope 1993;103:1273-83.
11. Eisele DW. Intraoperative electrophysiologic monitoring of the recurrent laryngeal nerve. Laryngoscope 1996;106:443-9.
12. Sercarz JA, Berke GS, Rothschiller J, Ming Y. Fabrication of a custom endotracheal tube. Laryngoscope 1991;101: 1024-5.
13. Monnier P, Lang F, Savary M. Partial cricotracheal resection for severe pediatric subglottic stenosis: update of the Lausanne experience. Ann Otol Rhinol Laryngol 1998;107:961-8.
14. Stern Y, Gerber ME, Walner DL, Cotton RT. Partial cricotracheal resection with primary anastomosis in the pediatric age group. Ann Otol Rhinol Laryngol 1997;106:891-6.

Ann Otol Rhinol Laryngol 109:2000

INFLUENCE OF PHONATION ON BASEMENT MEMBRANE ZONE RECOVERY AFTER PHONOMICROSURGERY: A CANINE MODEL

SEUNG-HO CHO, MD
SEOUL, KOREA
HYUNG-TAE KIM, MD
SEOUL, KOREA
IN-JA LEE, MD
TAEJON CITY, KOREA
MIN-SIK KIM, MD
SEOUL, KOREA
HAN-JONG PARK, MD
SEOUL, KOREA

The process of wound healing at the basement membrane zone of the vocal folds after phonomicrosurgery was investigated. The influence of phonation and the implied optimal period of voice rest were considered. Phonomicrosurgery was performed on both vocal folds of 20 adult dogs. In 10 dogs, the left recurrent laryngeal nerve was simultaneously resected to simulate iatrogenic voice rest; the remaining 10 dogs were allowed to phonate normally. The healing process of the vocal folds of each group was observed at 1, 2, 4, 8, and 12 weeks after surgery with immunohistochemical staining and transmission electron microscopy. In the voice rest group, the basement membrane was completely re-formed in 2 weeks, and the "cover" appeared completely rearranged by 8 weeks. The results of the phonation group were characterized by a delayed healing process and basement membrane changes. These results suggest that voice rest of at least 2 weeks after surgery may be beneficial and that vocal hygiene should be maintained for as long as 8 weeks.

KEY WORDS — anchoring fiber, basement membrane zone, collagen, laminin, phonomicrosurgery, vocal folds, voice rest, wound healing.

INTRODUCTION

The vocal fold has a well-organized architecture for withstanding great vibratory and shearing stress, and its pathophysiological characteristics are unlike those of any other body portion. Ever since Hirano and Kakita[1] defined the "cover and body" structure of the human vocal fold in great detail, remarkable insights have been uncovered in the areas of the basement membrane zone (BMZ) and the morphological ultrastructure of the vocal fold. These have improved our understanding of normal phonatory physiology and the response of the vocal folds to benign lesions.[2-4]

Phonomicrosurgery can be performed for benign laryngeal diseases, such as vocal polyps and nodules, that do not respond to voice therapy. However, studies assessing the role of voice rest after phonomicrosurgery have generally been anecdotal and have not been substantiated with objective data. The specific histologic healing processes of the ultrastructure of the vocal fold after surgery have not been documented. This may be the first report to describe the sequential healing processes of the BMZ of the "cover," which plays a significant role in tissue vibration and in the mucosal wave of the vocal fold.

The purpose of this study was to investigate wound healing at the ultrastructural level in the vocal folds after phonomicrosurgery and to study the influence of phonation on BMZ recovery. This was accomplished by demonstrating differences between the healing of the BMZ in dogs with sectioned recurrent laryngeal nerves (voice rest group) and in those in a control group that were allowed to phonate (phonation group with intact recurrent laryngeal nerves). This study was designed to provide some objective data to substantiate the desirability of voice rest after phonomicrosurgery.

MATERIALS AND METHODS

Twenty-two adult dogs with normal microscopic findings of the vocal folds and body weights between 7 and 10 kg were the subjects for this experiment. Two of the 22 dogs were used as control subjects. The other 20 dogs were anesthetized with ketamine hydrochloride (Ketalar 50 mg/kg, intramuscular injection) and thiopental sodium (Thionyl 25 mg/kg, intravenous injection) before phonomicrosurgery was performed with a microscope under a suspension laryngoscope. Segments of vocal fold mucosa measuring about 2 × 4 mm were bilaterally excised with mi-

---

From the Department of Otolaryngology–Head and Neck Surgery, St Mary's Hospital, College of Medicine, The Catholic University of Korea (Cho, H.-T. Kim), and the Department of Otolaryngology–Head and Neck Surgery, Kangnam St Mary's Hospital, College of Medicine, The Catholic University of Korea (M.-S. Kim, Park), Seoul, and the Department of Otolaryngology–Head and Neck Surgery, DaeJeon St Mary's Hospital, College of Medicine, The Catholic University of Korea, Taejon City (Lee), Korea.

CORRESPONDENCE — Hyung-Tae Kim, MD, Dept of Otolaryngology–Head and Neck Surgery, St Mary's Hospital, The Catholic University of Korea, College of Medicine, 62 Yoido-dong, Youngdungpo-ku, Seoul, Korea 150-010.

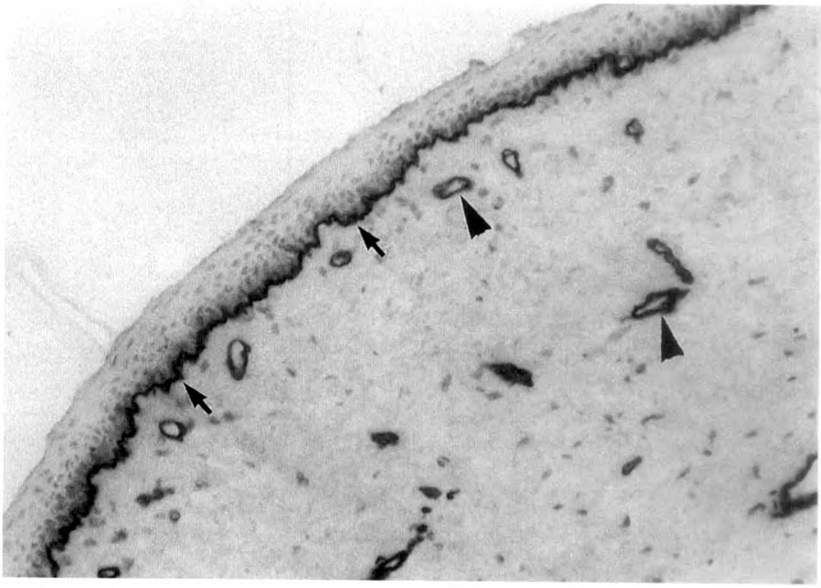

Fig 1. Photomicrograph of normal canine vocal fold stained for laminin (original ×100). Continuous linear pattern of positive staining for laminin is shown beneath normal vocal fold epithelium, indicating basement membrane (BM; arrows). Note staining of BM around arterioles and capillary structures, which served as control to verify accuracy of staining technique (arrowheads).

croforceps and microscissors at the junction of the anterior and middle thirds of the membranous portion. In 10 of the 20 dogs, the left recurrent laryngeal nerve was simultaneously resected to simulate, or create an artificial, voice rest (voice rest group). The remaining 10 dogs were induced to phonate for 10 minutes every 6 hours (phonation group with intact recurrent laryngeal nerve). Two dogs were randomly selected from each test group at 1, 2, 4, 8, and 12 weeks after phonomicrosurgery, and their vocal folds were obtained after total laryngectomy.

The 42 vocal folds from the 22 canine larynges were examined with immunohistochemical staining and transmission electron microscopy (TEM). One of the 22 dogs was taken out of the study because of postoperative infection to the vocal fold. The right vocal folds obtained after total laryngectomy were fixed with 10% formaldehyde solution for immunohistochemical study. The left vocal folds were immediately fixed in 2% paraformaldehyde and 2.5% glutaraldehyde in 0.1-mol/L phosphate buffer (4°C, pH 7.0) for TEM.

For the immunohistochemical studies of laminin, the avidin-biotin complex immunoperoxidase technique (ABC method) of Hsu et al[5] was used. Five-micrometer-thick adjacent sections just in the middle of the excised wound region of the paraffin-embedded specimen were mounted on chrome gelatin–coated glass microscope slides and dried overnight at room temperature. Deparaffinized sections were treated with 3% hydrogen peroxide and washed in phosphate-buffered saline solution for 5 minutes. The tissue was then predigested with 1% pepsin reagent (M77, Biomeda Corp, Foster City, Calif). A 5% normal goat serum was used as a suppressor serum for laminin immunostaining. The tissue was incubated at 45°C with polyclonal antilaminin (No. 68-125, ICN Biomedicals, Inc, Costa Mesa, Calif) for 20 minutes and then with biotinylated goat antimouse immunoglobulin and with avidin-biotin complex for 10 minutes each. The slides were washed with chilled phosphate-buffered saline solution after each incubation. The slides were then developed with chromogen 3-amino-9-ethyl-carbazole for 10 minutes and lightly counterstained with Mayer's hematoxylin before being coverslipped in crystal mount. For negative control specimens, we omitted the primary antibody and substituted nonimmune serum of the same species as the primary antibodies in parallel tissue sections.

For TEM, the fixed tissue blocks were rinsed in 6.8% saccharose in 0.1-mol/L phosphate buffer (pH 7.4). Subsequently, the samples were dehydrated in graded ethanols and then embedded in Epon 812. One-micrometer sections were cut and stained with toluidine blue. The vocal fold wound site was localized in the 1-μm sections, and the block was trimmed off for thin-section localization. Ultrathin sections (80 nm) were cut just in the middle of the excised wound region and placed on 300-mesh copper grids, stained with uranyl acetate for 20 minutes and lead citrate for 1 minute, rinsed in filtered distilled water, and viewed under a JEOL 1200EX electron microscope (Tokyo, Japan).

RESULTS

In the normal control group, linearly continuous red stain beneath the normal vocal fold epithelium indicated deposition in the basement membrane (BM; Fig 1).

In the voice rest group, immunostaining 1 week

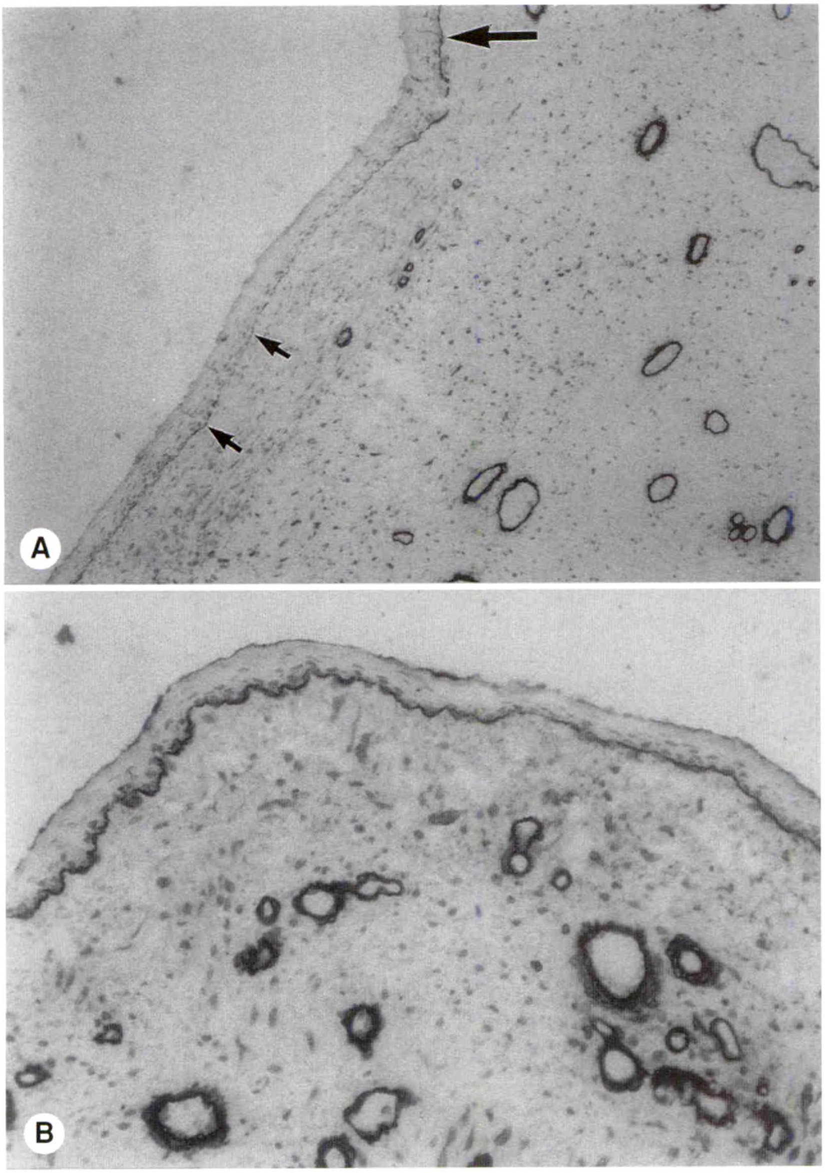

Fig 2. Immunolocalization of laminin in vocal fold BM of voice rest group (original ×100). A) At 1 week after phonomicrosurgery, wounded epithelium of vocal fold has been completely resurfaced, laminin is localized in discontinuous patches, and fragments of BM appear in resurfacing epithelium of vocal fold (small arrows). Normal linear staining of laminin in unwounded vocal fold mucosa is noticed, which was strictly compared with resurfaced epithelium (large arrow). B) Continuous linear laminin immunoreactivity in BM 2 weeks after operation indicates complete formation and organization of BM.

after surgery revealed that the wound bed was epithelialized completely, but scant and discontinuous laminin stains were observed beneath the reepithelialized region (Fig 2A). This reaction indicates that the early stages of BM organization have been initiated. Laminin staining 2 weeks after operation showed a continuous linear red stain, which indicates complete polymerization and organization of the BM (Fig 2B). The 4-week, 8-week, and 12-week findings also showed similar laminin staining features.

In the phonation group, there was negative immunostaining of laminin in the completely reepithelialized vocal fold wound within 1 week after operation, and fragmented and interrupted laminin immunoreactivity in the BM was observed under the reepithelialized region in the second week after operation (Fig 3A). This fragmented immunoreactivity of laminin indicates incomplete restitution and initiation of rearrangement of the BM. The restitution of the BM was delayed longer in the phonation group than in the voice rest group. The findings 4 weeks after surgery showed a broad but weak band (Fig 3B). A weak band may indicate incomplete assembly and incomplete polymerization of glycoproteins in the BM.[3] A broad band, however, indicates extensive disorganization and injury of the BM.[3] Continuous linear laminin staining was observed at 8 and 12 weeks, reflecting complete polymerization and organization of the BM.

Electron microscopy revealed that the canine larynges showed epidermal and lamina propria structures similar to those described in humans. In the control group, the BM is composed of 2 layers of different electron densities: the lamina rara (or lamina lucida), the colorless, continuous line beneath the basal cell membrane, and the lamina densa, the continu-

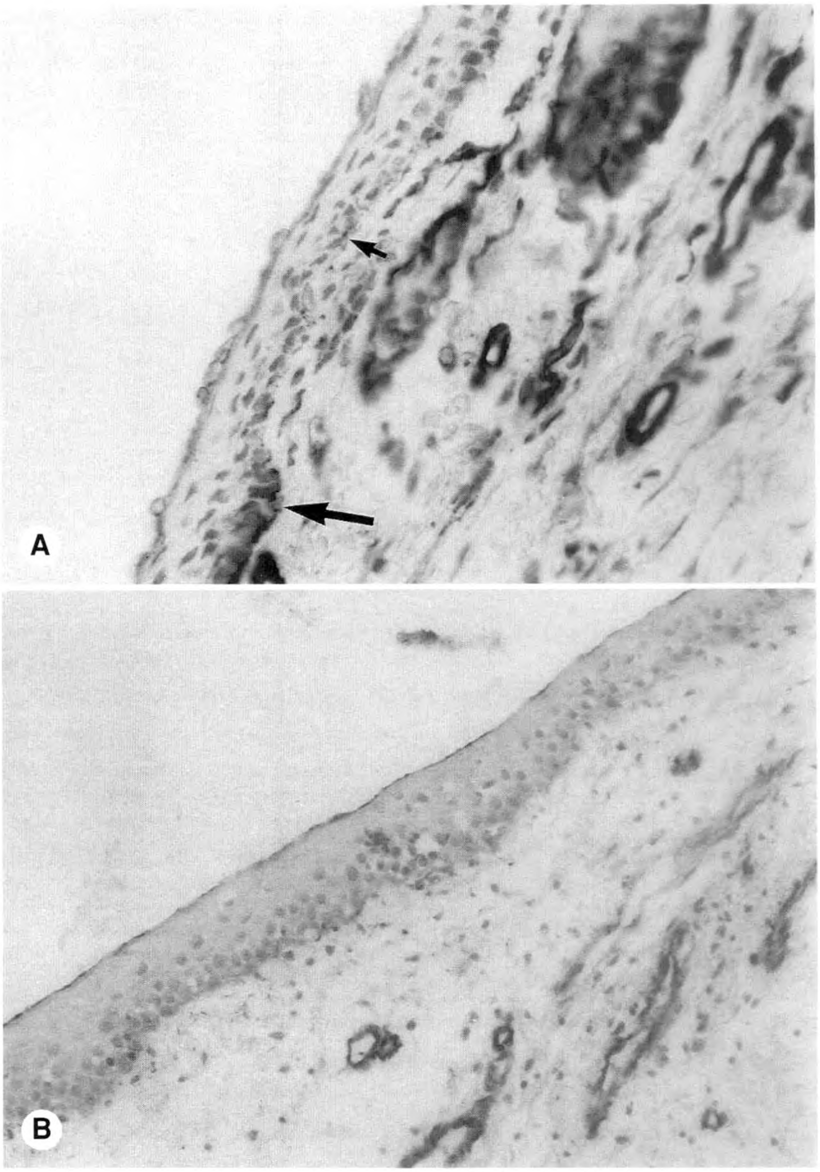

Fig 3. Immunolocalization of laminin in vocal fold BM of phonation group (original ×200). A) At 2 weeks after operation, interrupted and fragmented laminin immunoreactivity indicates incomplete polymerization of BM (small arrow). Normal linear staining of laminin in unwounded normal vocal fold epithelium is noticed, which was strictly compared with resurfaced epithelium (large arrow). B) At 4 weeks after surgery, weak and broad-band laminin staining is noticed, indicating incomplete assembly and disorganization of proteins in BM.

ous black line under the lamina rara. The areas of dense basal cell membrane represent hemidesmosomes. Collagen type III fibers of the superficial layer of the lamina propria and small anchoring fibers making small loops into the lamina propria were seen. All of the above-mentioned components are ultrastructures of the "cover" (Fig 4).[2,6]

In Fig 5A, TEM confirmed that the initial development of hemidesmosomes was under way in the basal cell membrane of the epithelium 1 week after operation in both the voice rest and phonation groups. The BM was not detected, but electron-dense macromolecules, which may have contributed to the formation of the BM, were detected under the basal cell layer.

In the voice rest group, the BM was completely rearranged and hemidesmosomes were partly present at 2 weeks. The anchoring fibers and collagen type III fibers of the superficial layer of the lamina propria were not observed under the BM (Fig 5B). In the phonation group, however, various alterations of the BM — attenuation, interruption, or loss — were observed in underlying hemidesmosomes (Fig 6A). It appears from this experiment that hemidesmosomes are areas of special attachment between the basal cells and the BM.

Four weeks after surgery, in the voice rest group, anchoring fibers and collagen type III fibers were present in the superficial layer of the lamina propria; a well-organized BMZ was also found (Fig 5C). At 8 and 12 weeks, TEM showed that the BM, anchoring fibers, and collagen type III fibers of the superficial layer of the lamina propria were completely organized. In the phonation group, the BM was thoroughly organized under the basal cell layer, but was

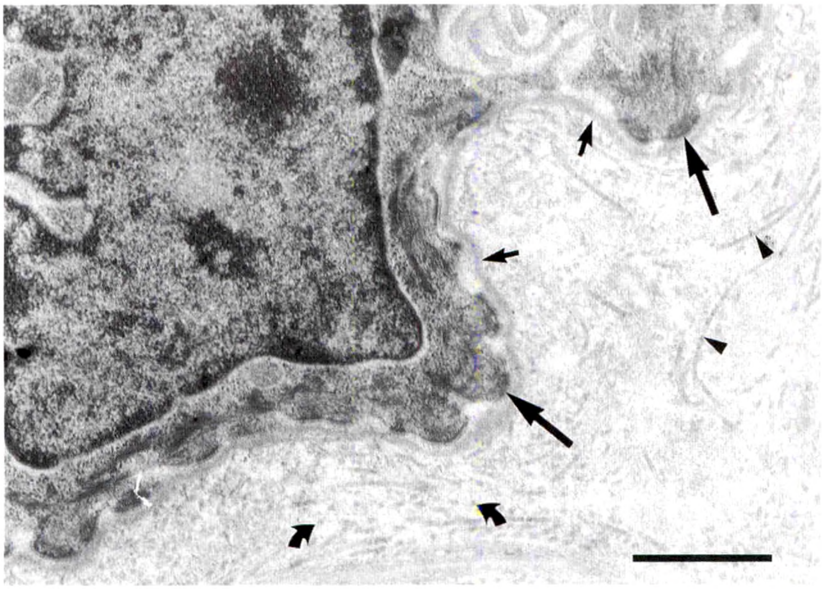

Fig 4. Transmission electron micrograph of epithelial–lamina propria junction of normal canine vocal fold. Note hemidesmosome in basal lamina of basal cell layer (large arrows), lamina lucida, lamina densa (small arrows), and collagen type III fibers (arrowheads) in superficial layer of lamina propria, and some anchoring fibers making loops into lamina propria (curved arrows). Scale bar — 1 μm.

separated from the basal cell layer and formed multiple layers (Fig 6B). This finding may suggest that the BM was separated from the hemidesmosomes of the basal cell layer by phonatory trauma during the organization and ongoing formation of the BM.[4] In conclusion, the BM was disorganized, and it formed multiple layers. Anchoring fibers were detected. The multiple-layered BM was somewhat condensed 8 weeks after operation, but the double layer and the partially developed multiple layers remained at 12 weeks (Fig 6C). This result may imply that this stage of BM development is permanent, because no change in the disorganized BM was observed for several weeks.

DISCUSSION

The vocal fold has an epidermal–lamina propria junction, with no dermis. This junction is termed the BMZ. The epithelium, the BMZ, and the superficial layer of the lamina propria possess similar mechanical properties and behave collectively as 1 tissue, which is commonly referred to as the "cover."[1] The vocalis muscle is referred to as the "body," and an intervening layer — consisting of the intermediate and deep layers of the lamina propria — as the "transition" layer.[1,2] The BMs are ubiquitous extracellular matrices found at the boundary between the epithelial cells and the superficial layer of the lamina propria. The BM has 5 principal components: laminin, heparan sulfate proteoglycan, entactin (nidogen), collagen type IV, and fibronectin. The BM is segmented into 2 layers of different electron microscope–detectable densities: the lamina rara or lamina lucida and the lamina densa.[7] The lamina lucida is adjacent to the basal cell membrane, and the lamina densa is adjacent to the underlying lamina propria. The BM is attached to the basal cell layer by hemidesmosomes. Several kinds of structures attach the BM to the lamina propria, namely, lamina densa extensions and anchoring fibers or microfibrils, which form the other layer of the BMZ, the pars fibroreticularis.[7] Anchoring fibrils are specialized structures that mediate close contact between the lamina densa and the underlying connective tissue.[6,7] The BMZ consists of the BM and the pars fibroreticularis. The superficial layer of the lamina propria is a loosely arranged fibrous network of collagen type III and elastin fibers in a ground substance matrix of hyaluronic acid and mucopolysaccharides.[6] The BMZ and the superficial layer of the lamina propria provide the "cover" with sufficient flexibility for phonation. These structures also appear to furnish the "cover" with the ability to resist injury from phonation.[4]

In normal human vocal folds, the BMZ is similar to human skin in construction and thickness. During the healing process of epithelium in human skin 1 day after injury, keratinocytes in the basal cell layer of the epithelium have migrated into the wound surface after the release of a metalloproteinase series, causing degradation of the BM and causing separation between the basal cell layer and the BM.[8] At 2 or 3 days, reepithelialization is completed by keratinocytes, the differentiation of keratinocytes occurs, and the synthesis and release of components of the BM from myofibroblasts has been initiated.[8,9] In the time-dependent rearrangement of the epithelial BM in a human skin wound, laminin and heparan sulfate proteoglycan are first detectable approximately 1.5 days after injury, and collagen type IV is observed along the epithelial-stromal interface at 4 to 10 days.[10,11] In our study, we used laminin for detecting the time of initiation of the rearrangement of the

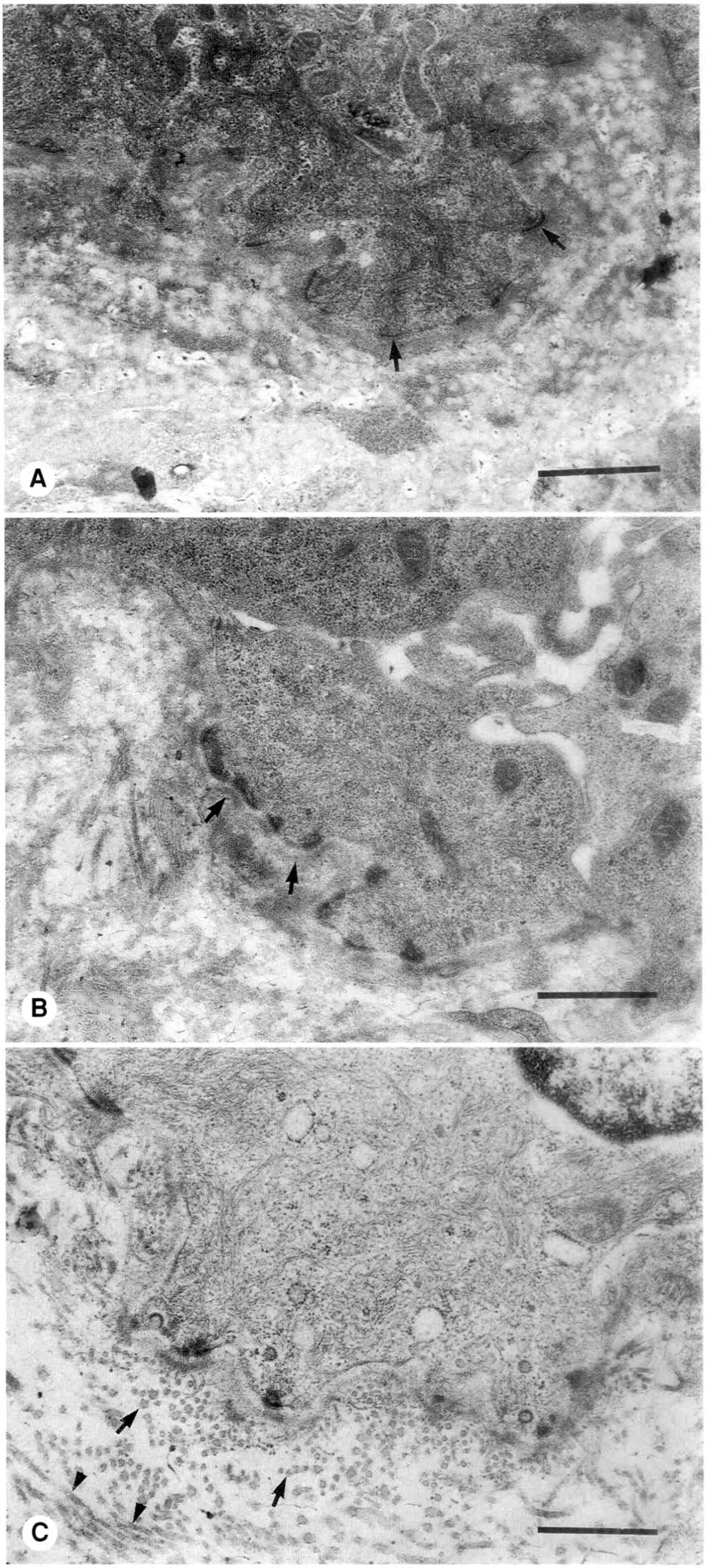

Fig 5. Transmission electron micrographs of voice rest group. Scale bars — 1 μm. A) One week. Hemidesmosomal plaque structures are present with their sub-basal dense plate (arrows), but no obvious lamina densa of basal lamina is evident. B) Two weeks. Lamina densa of basal lamina is continuous and subjacent to each hemidesmosome (arrows), but no anchoring fibers or collagen type III fibers are seen. C) Four weeks. Numerous anchoring fibers (arrows) and some collagen type III fibers (arrowheads) are seen.

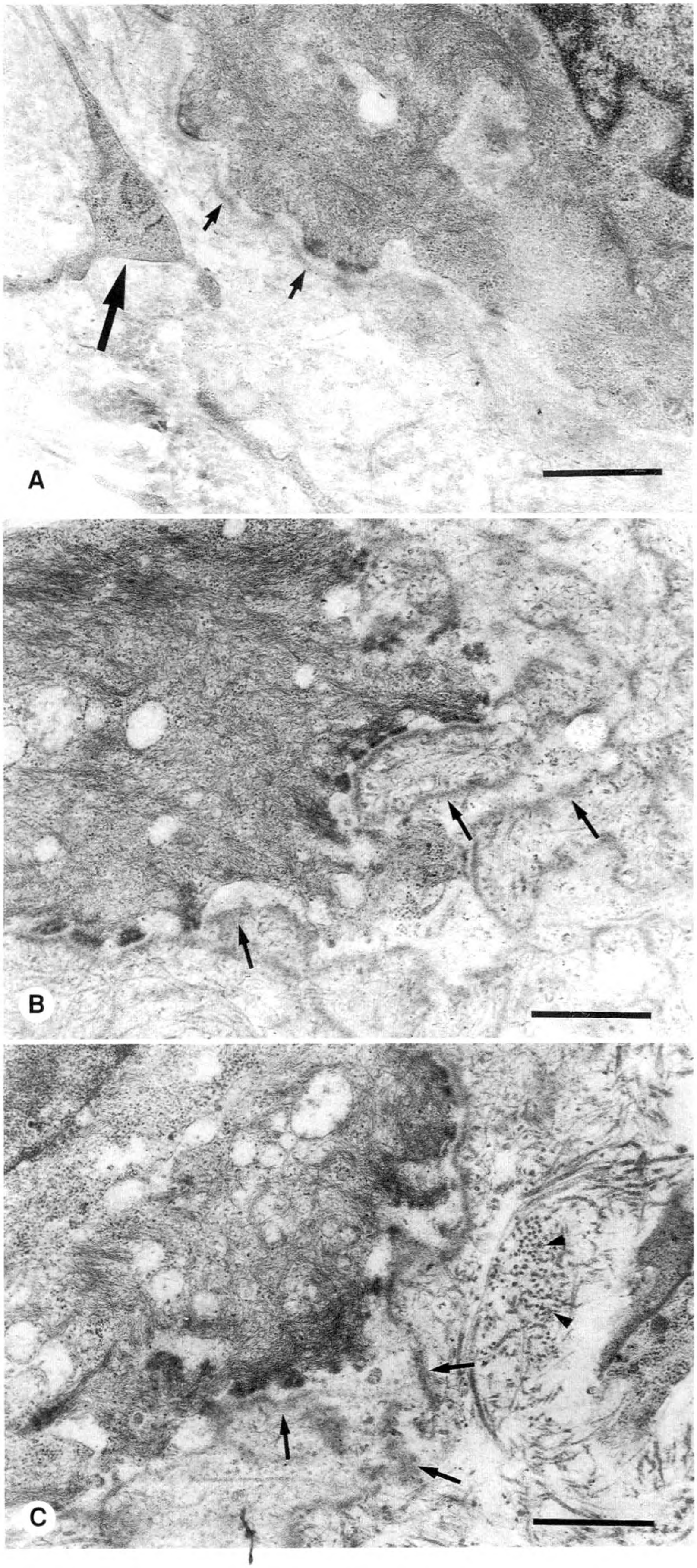

Fig 6. Transmission electron micrographs of phonation group. Scale bars — 1 μm. A) Two weeks. Some hemidesmosomes are noted, as well as many areas in which lamina densa of basal lamina is discontinuous and only occurs immediately underlying hemidesmosomes (small arrows). Fibroblast is noticed (large arrow). B) Four weeks. Lamina densa is loosely attached to hemidesmosomes in basal cell membrane, and BM is separated from basal cell layer and forms multiple layers (arrows). C) Eight weeks. Continuous multiple layers of BM are present, although BM has been condensed (arrows), and well-developed anchoring fibers (arrowheads) and collagen type III fibers are seen.

BM, because it is the first restitution component of the BM. Collagen type VII was detected along the wound bed from 11 days to 5 weeks.[9,11,12] Complete restoration of the BMZ with a normal configuration of the pars fibroreticularis occurred between 13 days and 5 weeks after the wound was produced.[10,12-14] It is likely that there are other differences, not addressed here, in time-dependent pericellular expression between the wound healing of the epidermal-dermal interface in the skin and the wound healing of the epithelial–lamina propria interface in the vocal fold.

In this study, measurable differences were observed between the voice rest group and the phonation group in the sequential histopathologic healing process of the ultrastructures of the BMZ after phonomicrosurgery. In the voice rest group, postoperative reepithelialization of the wound site in the vocal folds was completed within 1 week, with the release of molecular components and the polymerization of the BM initiated. Within 2 weeks after surgery, the BM was completely synthesized. The anchoring fibers and collagen type III fibers, constituting the pars fibroreticularis, were detectable at 4 weeks; complete restitution of the "cover" was evident from BMZ formation at 8 weeks. In the phonation group, the organization of the ultrastructures was delayed compared with that of the voice rest group. The re-formation of the BM in the wound site was incomplete at 2 weeks and complete at 4 weeks, but the multiple-layered formation of the BM indicated BM injury. The multiple layers and the double layers of the BM remained continuously present through 12 weeks. It is suggested that the disorganized BM changes in the phonation group may be permanent.

The BMZ is an extracellular scaffold and has biological characteristics such as molecular binding and strength. The histopathologic changes of the BMZ and the extracellular matrix of the lamina propria occurring after microsurgical injury may induce permanent voice change.[3,6] Supporting the above contention, these changes, observed in vocal nodules and occasionally in vocal polyps, restrict the mucosal wave and the vibration of the vocal folds. It is suggested that careful voice rest after phonosurgery is necessary for restoring a more normal voice and for promoting a normal rearrangement of the BMZ and lamina propria and a complete re-formation of the vocal "cover" during the wound healing process; furthermore, voice rest might prevent permanent voice change. Considerable experience has shown that in some patients with postoperative dysphonia who failed to practice careful voice rest, a restricted mucosal wave of the vocal folds is observed during stroboscopic examination.

It may be concluded from this study that the thickened and injured BM induced by phonation after surgery may be one of the primary causes of postoperative dysphonia. According to the histopathologic characteristics of wound healing of the vocal folds observed in this study, the BMZ portion of the injured tissues plays a significant role in the inducement of voice change. Because this study dealt with a canine model, however, there may be some behavior in the wound healing process of the vocal folds of humans that is not fully predicted by this study. The human vocal fold consists of a thick epithelial layer and a soft lamina propria, but canine vocal folds contain only a rudimentary vocal ligament and have a thicker lamina propria layer than their human counterpart.[4] Although these differences are likely to provide the canine vocal folds with a different capacity for resistance to phonotrauma than human vocal folds, there may be no appreciable differences in the wound healing process of the respective BMZs in the vocal folds; furthermore, the "cover" in both canine and human vocal folds is composed of a BMZ and a superficial layer of lamina propria, and they are structurally similar.

The appropriate period of voice rest after phonomicrosurgery is controversial, but observations within this study provide some clues: complete rearrangement of the BM occurs by about 2 weeks, and complete regeneration of the "cover" without changes of the histopathologic ultrastructure of the vocal fold wound occurs at about 8 weeks. It may be suggested that voice rest for at least 2 weeks after phonomicrosurgery might be beneficial, and that vocal hygiene should be maintained for as long as 8 weeks. It should be noted, however, that because the degree of voice rest in this study was absolute, it cannot be discerned conclusively whether mere voice restrictions would produce the same histopathologic results.

CONCLUSION

The sequential ultrastructural rearrangement of the BMZ during the wound healing of the vocal folds after phonomicrosurgery was investigated, and the influence of phonation and the optimal period of voice rest were studied. This was a qualitative study, and the investigation period was somewhat long; if the follow-up period had been shortened, with shorter observation intervals, the milestones of rearrangement and organization of the BMZ might have been more informative. The authors hope that further studies will be conducted on the sequential formation and changes of BMZ structural proteins and the extracellular matrix of the lamina propria in the wound healing process.

REFERENCES

1. Hirano M, Kakita Y. Cover-body theory of vocal fold vibration. In: Daniloff RG, ed. Speech science. San Diego, Calif: College-Hill Press, 1985:1-46.

2. Dikkers FG, Hulstaert CE, Oosterbaan JA, Cervera-Paz FJ. Ultrastructural change of the basement membrane zone in benign lesions of the vocal folds. Acta Otolaryngol (Stockh) 1993;113:98-101.

3. Gray SD, Hammond E, Hanson DF. Benign pathologic responses of the larynx. Ann Otol Rhinol Laryngol 1995;104:13-8.

4. Gray SD, Titze I. Histologic investigation of hyperphonated canine vocal cords. Ann Otol Rhinol Laryngol 1988;97:381-8.

5. Hsu SM, Raine L, Fanger H. Use of avidin-biotin-peroxidase complex (ABC) in immunoperoxidase technique: a comparison between A-B-C and unlabeled antibody (PAP) procedure. J Histochem Cytochem 1981;29:577-83.

6. Gray SD, Pignatari SSN, Harding P. Morphologic ultrastructure of anchoring fibers in normal vocal fold basement membrane zone. J Voice 1994;8:48-52.

7. Leblond CP, Inoue S. Structure, composition, and assembly of basement membrane. Am J Anat 1989;185:367-90.

8. Matsubara M, Zieske JD, Fini ME. Mechanism of basement membrane dissolution preceding corneal ulceration. Invest Ophthalmol Vis Sci 1991;32:3221-37.

9. Stock EL, Kurpakus MA, Sambol B, Jones JC. Adhesion complex formation after small keratectomy wounds in the cornea. Invest Ophthalmol Vis Sci 1992;33:304-13.

10. Betz P, Nerlich A, Wilske J, et al. Time-dependent pericellular expression of collagen type IV, laminin, and heparan sulfate proteoglycan in myofibroblasts. Int J Legal Med 1992;105:169-72.

11. McGrath JA, Leigh IM, Eady RA. Intracellular expression of type VII collagen during wound healing in severe recessive dystrophic epidermolysis bullosa and normal human skin. Br J Dermatol 1992;127:312-7.

12. Mommaas AM, Teepe RG, Leigh IM, Mulder AA, Koebrugge EJ, Vermeer BJ. Ontogenesis of the basement membrane zone after grafting cultured human epithelium: a morphologic and immunoelectron microscopic study. J Invest Dermatol 1992;99:71-7.

13. Oksala O, Salo T, Tammi R, et al. Expression of proteoglycans and hyaluronan during wound healing. J Histochem Cytochem 1995;43:125-35.

14. Boyce ST, Foreman TJ, English KB, et al. Skin wound closure in athymic mice with cultured human cells, biopolymers, and growth factors. Surgery 1991;110:866-76.

Ann Otol Rhinol Laryngol 109:2000

VASCULAR AND EPIDERMAL EFFECTS OF FIBROBLAST GROWTH FACTOR ON IRRADIATED AND NONIRRADIATED SKIN FLAPS

DAVID B. HOM, MD
TIM C. SIMPLOT, MD
J. CARLOS MANIVEL, MD
KERRI J. PERNELL, MS
CHANG W. SONG, PHD
MINNEAPOLIS, MINNESOTA

Head and neck cancer surgeons are often faced with the challenge of managing previously irradiated soft tissue that has poor vascularity and slower epithelialization. This study investigates the effect of supplemental basic fibroblast growth factor (bFGF) on flap vascularity, tissue oxygenation, and epidermal regeneration in nonirradiated ($n = 40$) and irradiated porcine skin flaps ($n = 40$). Supplemental bFGF increased vascularity in nonirradiated flaps by 80% ($p = .005$), with a trend to a higher tissue oxygen level by day 14. The irradiated bFGF-treated flaps did not show increased vascularity or higher tissue oxygen levels 2 weeks after surgery. However, in both irradiated and nonirradiated groups, epidermal regeneration increased by greater than 70% with supplemental bFGF ($p < .002$). The results of this study suggest that supplemental bFGF can increase tissue vascularity in nonirradiated tissues and epidermal regeneration in both nonirradiated and irradiated conditions.

KEY WORDS — epithelium, fibroblast growth factor, neovascularization, radiation effects, surgical flaps.

INTRODUCTION

Head and neck cancer surgeons are frequently faced with the challenge of ensuring adequate wound healing in the setting of previous irradiation. Impaired wound healing from irradiation is a significant source of patient morbidity, resulting in fistula formation, fibrosis, carotid artery rupture, or even death. Postoperative complications after radiation exposure have been reported to occur in as many as 67% of patients.[1] Impaired wound healing in irradiated tissue can be a frustrating and challenging problem for head and neck surgeons and oncologists.

The effects of irradiation on local tissue healing have been attributed to several factors, including endarteritis obliterans, excessive fibrosis, and decreased cellular replication. Disruption of wound healing by irradiation is largely a result of tissue ischemia caused by vascular damage and impaired angiogenesis.[2]

Local tissue oxygen concentration plays several key roles in the reparative process after wounding.[3] Without adequate tissue oxygen levels, wounds are more susceptible to infection, collagen production and fibroblast function is reduced, angiogenesis is hindered, and reepithelialization of the wound surface is impaired.[3-6] To stimulate healing in chronic wounds, hyperbaric oxygen has been used clinically to increase tissue oxygen levels to increase angiogenesis and blood flow.[7]

Fibroblast growth factors (FGFs) have shown promise in increasing vascularity in wounds and incisional wound strength in ischemic and nonischemic animal models.[8-13] The objectives of this study were 1) to quantify tissue oxygen levels in nonirradiated and irradiated skin flaps treated with supplemental basic FGF (bFGF), 2) to compare skin flap vascularity in nonirradiated and irradiated skin flaps treated with supplemental bFGF, and 3) to characterize the epidermal regenerative effects of bFGF in skin flaps in nonirradiated and irradiated conditions.

METHODS

Twenty white male Yorkshire-Hampshire–cross pigs weighing 10 to 12 kg were used in the study (10 irradiated and 10 nonirradiated animals). All animal care followed strict regulation guidelines according to laboratory animal medicine protocol. Animal use was approved by the Minneapolis Medical Research Foundation Animal Care Committee. For all surgi-

---

From the Division of Facial Plastic and Reconstructive Surgery, Department of Otolaryngology–Head and Neck Surgery (Hom, Simplot, Pernell), the Department of Laboratory Medicine and Pathology (Manivel), and the Department of Therapeutic Radiology (Song), University of Minnesota School of Medicine and Hennepin County Medical Center, Minneapolis, Minnesota. This work was supported by a research grant from the National Institutes of Health/National Institute of Dental and Craniofacial Research (No. R29 DE12005 to D.B.H.). This study was performed in accordance with the PHS Policy on Humane Care and Use of Laboratory Animals, the NIH *Guide for the Care and Use of Laboratory Animals*, and the Animal Welfare Act (7 U.S.C. et seq.); the animal use protocol was approved by the Institutional Animal Care and Use Committee (IACUC) of the Minneapolis Medical Research Foundation.

Presented at the meeting of the American Academy of Facial Plastic and Reconstructive Surgery, San Antonio, Texas, September 10, 1998.

CORRESPONDENCE — David B. Hom, MD, Division of Facial Plastic and Reconstructive Surgery, Dept of Otolaryngology–Head and Neck Surgery, University of Minnesota School of Medicine, Box 396, 420 Delaware St SE, Minneapolis, MN 55455.

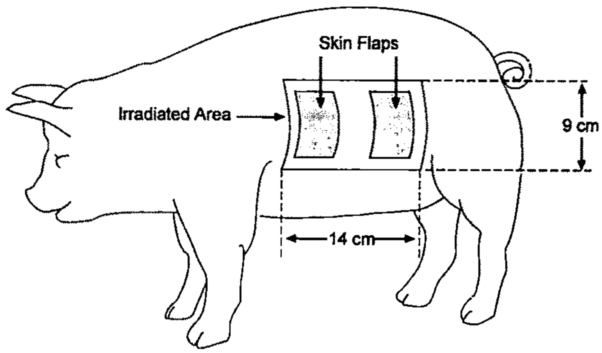

Fig 1. Pig skin flap model with orientation of irradiation ports.

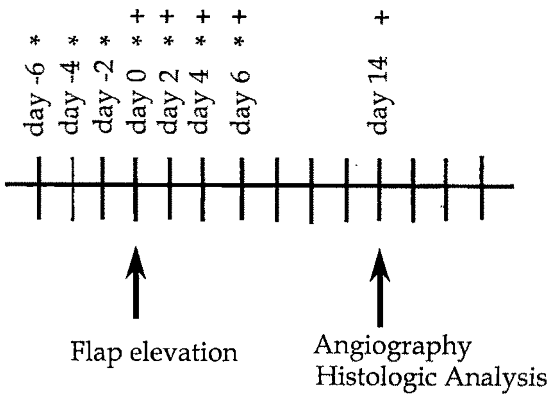

Fig 2. Time frame of flap model. * — Time of tissue injection of basic fibroblast growth factor (bFGF) or phosphate-buffered saline solution. + — Time of subcutaneous tissue oxygen measurement in skin flaps.

cal procedures, the animals were sedated with intramuscular ketamine hydrochloride (30 mg/kg) and xylazine hydrochloride (15 mg/kg) and anesthetized with 2% halothane by oral intubation.

Each animal had four 7 × 4-cm arterial skin flaps elevated (2 flaps on each side). All flaps were elevated along the vascular distribution of the ventral intercostal arteries of the superficial epigastric artery (Fig 1). The surgical plane of elevation was directly under the panniculus carnosus muscle. After the flaps were raised, they were stapled back to their original anatomic position and monitored for 14 days. On each side, one flap served as the treated flap and the other served as the control. This model enabled each animal to serve as its own control.

Recombinant bFGF (donated by Amgen, Boulder, Colo) was reconstituted with phosphate-buffered saline solution (PBS) and was injected in an intracuticular fashion (10 µg/cm^2; 0.1 mL/cm^2) within a marked 7 × 4-cm grid (1 cm^2; 280 µg per flap) in a serial fashion. The concentration of bFGF chosen exceeded the levels that were necessary to induce an angiogenic response in previous skin flap models.[8,9] The repeat procedure was performed on control flaps with an equal volume of PBS (0.1 mL/cm^2). All injections were done on days 6, 4, and 2 before surgery, the day of flap elevation just before surgery, and days 2, 4, and 6 after surgery (Fig 2).

Before flap elevation on the day of surgery, the degree of inflammatory edema elicited by the intracuticular injections was clinically evaluated and scored on a scale from 0 to 5. A rating of 0 was designated as no clinical evidence of inflammation, 1 as scant, 2 as mild, 3 as moderate, 4 as significant, and 5 as complete rubor and raised edema of the injected skin surface. On day 14 after surgery, the level of inflammatory edema was again recorded.

In irradiated subjects, the skin was subjected to orthovoltage radiation by an x-ray machine (Philips Medical Co, Shelton, Conn). The irradiation parameters were 250 kV peak, 15 mA, and filtration of 1.0 mm aluminum plus 0.35 mm copper. The dose rate was 95.4 cGy per minute, and the skin-to-source distance was 60 cm. Six weeks before skin flap elevation, the area of the planned skin incisions was marked with India ink and then irradiated with 650 cGy in 2 sessions 1 week apart (total, 1,300 cGy). The 1,300-cGy dose was confirmed with standard thermoluminescent dosimetry. The surrounding body of the pig was protected with a 4-mm lead shield.

A radiation dose of 1,000 cGy or more given within 3 weeks of wounding significantly reduces soft tissue wound healing.[14] A dose of 1,000 cGy significantly reduces the number of capillaries in several animal models.[15,16] Previous unpublished pilot studies in this laboratory demonstrated that 1,000 cGy irradiation induced enteritis in this pig model. For this reason, 2 separate fractions of 650 cGy were better tolerated, which is the biological equivalent of about 900 cGy in a single fraction. All animals tolerated this dosing regimen without problems.

Tissue Oximetry. On days 0, 2, 4, 6, and 14, all pigs were sedated with intramuscular ketamine hydrochloride (30 mg/kg) and xylazine hydrochloride (15 mg/kg) and sterilely prepared for subcutaneous tissue oxygen partial pressure ($P_{sc}O_2$) measurements underneath the previously elevated skin flaps. No inhalational anesthetic agents or supplemental oxygen were used during the $P_{sc}O_2$ measurements, because these can produce artifacts in the tissue oxygen readings.[17] Tissue oxygen measurements were then performed with the Tissutrak tissue perfusion monitoring system (Diametrics Medical Ltd, Bucks, England). The monitor was calibrated before all measurements at ambient temperature by placing the probe in a normal saline solution–filled sheath at a barometric pressure of 760 mm Hg. After calibration, the probe was inserted subcutaneously underneath the skin flap through one side of the incisional line (3 cm from distal flap edge) with an 18-gauge spinal needle. Care was taken to ensure that the sensor portion of the probe was a minimum of 3 cm from its cutaneous insertion site. All measurements were done on both control and treated flaps on the right side of the pig. After 15 minutes of equilibration, 3 recordings were taken 5 minutes apart. The values for each flap were then averaged for statistical comparison within each of the 4 groups (nonirradiated, irradiated, with bFGF, without bFGF) at each time interval. All tissue oximetry measurements were taken in an operating suite with the environment controlled for temperature in room air. Blood oxygen saturation, core body temperature (rectal), and tissue temperature levels were recorded for all oxygen saturation measurements.

The Tissutrak consists of a Clark-type polarographic bipolar oxygen electrode with a thermocouple temperature sensor. An alternating current–powered monitor applies the polarization voltage to the electrode and measures the electrical current generated by the presence of oxygen. Using the Stern-Volmer equation that incorporates temperature, the monitor software calculated the $P_{sc}O_2$ level relative to the calibrated PO_2.[18] Similar systems have been shown to reliably record tissue oxygenation levels in prior animal studies.[18-21]

During the tissue oxygen measurements, the pig was kept properly hydrated in a controlled temperature environment with any pain or discomfort controlled. To avoid excessive temperature fluctuations, the pig was monitored to ensure a stable body temperature. The $P_{sc}O_2$ levels were then statistically evaluated and compared within groups by Student's paired *t*-test.

Angiography. On postoperative day 14, after completion of tissue oximetry measurements, each animal was sedated by means of the regimen described previously, and porcine heparin (1 mg/kg) was administered by intravenous injection. A thoracotomy was performed, and the aorta was cannulated through the left ventricle. An incision was then done in the right atrium to exsanguinate the animal. With the previously placed cannula, a continuous infusion of 30% micropaque (fine-ground barium sulfate) was initiated with a manometric pump system at 160 mm Hg as described previously.[22]

Treated and control flaps were then harvested from the side of the pig by means of the previous incision lines. Angiograms of the harvested flaps were then taken by mammography techniques (stationary mammography system × 1 mm focal spot molybdenum target with Kodak OM film and a Kodak min-r screen; 10 mA, 28 kV peak for 0.20 seconds) and magnified (2×) to augment resolution of flap vascularity.[23] The radiopaque infusate in the flap vessels represents the flap vascularity.

The vascularity of each flap was computer digitized by the Lumisys model 200 film digitizer (Lumisys, Sunnyvale, Calif). Image analysis was performed with software custom-written for this project in IDL 3.1.1 language (Research Systems Inc, Boulder, Colo). Flap vascularity was compared by selecting equal-sized rectangular regions of interest on the distal third of each flap in each group. In a blinded fashion, each control and treated region of interest was combined into a single rectangular working image, which was then treated as a whole for the procedure of calculating the background mask image and segmenting the vasculature.[24,25] The working image was then divided back into the same control and treated regions for calculation of the percentage of vascularity in each sample. These values were then compared with Student's paired *t*-test.

Histologic Analysis. Sections of all harvested flaps were taken at the proximal 4.5 cm of the flap 2 cm from the flap edge. Wound margins and areas of ischemic damage were avoided. One treated flap and 1 control flap in each pig were analyzed with 4 stains (hematoxylin and eosin [H & E], Masson trichrome, Alcian blue, and Sirius red F3BA). All specimens were fixed in neutral buffered 10% formaldehyde, dehydrated in graded ethyl alcohol through xylene, and embedded in paraffin. Histomorphometric measurements were performed on the flap epidermis of each specimen with Masson trichrome stains. In a blinded fashion, the area of epidermal thickness was measured. Specifically, photographs at a magnification of 40× were taken of representative segments of treated and control flap epidermis in a blinded fashion. By means of the Zeiss Interactive Digital Analysis System (ZIDAS, Carl Zeiss, Inc), the area of the epidermis was calculated and recorded in absolute units for comparison of treated and control specimens. In a blinded fashion, 3 measurements were taken and then averaged for statistical comparison by Student's paired *t*-test. Qualitative analysis and comparisons between treated and control specimens and between radiated and nonirradiated specimens were also done for all stains (H & E, Masson trichrome, Alcian blue, and Sirius red F3BA).

Statistical Analysis. Student's paired *t*-test was used to compare the means within each group ($\alpha = 0.05$). Repeated-measures analysis of variance, focusing on the significance of irradiation and the differences in $P_{sc}O_2$ levels measured in the bFGF and control flaps over 14 days, was also performed. All analyses were performed with the aid of Microsoft Excel, Systat,

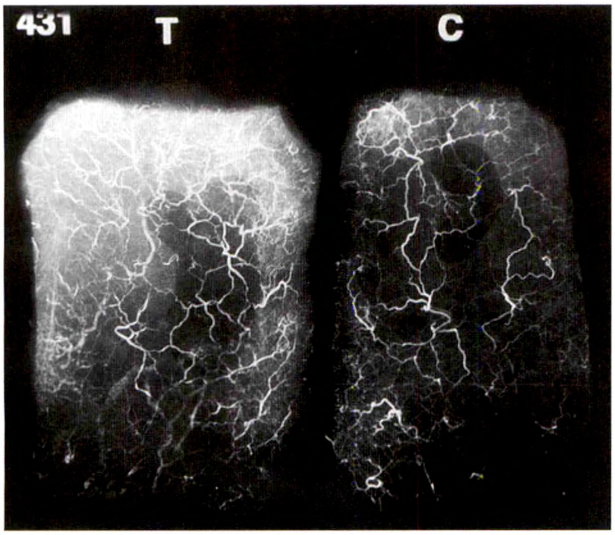

Fig 3. Angiograms depicting vascularity of bFGF-treated flap (T) and control flap (C) within same animal in nonirradiated group.

and the Statistical Package for the Social Sciences (SPSS).

RESULTS

All 20 animals survived to the completion of the study. Evaluation of tissue oxygenation and histomorphometric results was done with 10 animals in each group, irradiated and nonirradiated. Evaluation of the angiographic results was done with 7 animals in each group; 2 pigs in each group were not included because of technical errors in performing angiography, and 1 pig in each group was not included because of infection of the flap undergoing angiography. The design of the study allowed each animal to serve as its own control.

Tissue Oxygenation. Two days after surgery, the PscO2 levels (±SD) had decreased significantly in all skin flaps compared with the day of flap surgery (32.8 ± 12.0 mm Hg versus 45.8 ± 12.2 mm Hg; p < .005). By day 14, the PscO2 remained significantly decreased in comparison with the day of flap surgery (39.1 ± 12.4 mm Hg versus 45.8 ± 12.2 mm Hg; p < .01).

In the nonirradiated group, bFGF-treated flaps did have a trend toward a higher PscO2 level than that of the flap controls; however, this difference was not statistically significant on day 14. The mean (±SD) PscO2 level for the bFGF-treated flaps was 41.9 ± 13.8 mm Hg, versus 36.8 ± 10.7 mm Hg for their flap controls (p = .10). In the irradiated group, no statistically significant PscO2 difference was found between the bFGF-treated flaps and control flaps on day 14 (38.4 ± 11.3 mm Hg versus 39.5 ± 14.6 mm Hg; p = .42). Thus, by day 14 in this study, a significant change of PscO2 levels was not apparent after bFGF application.

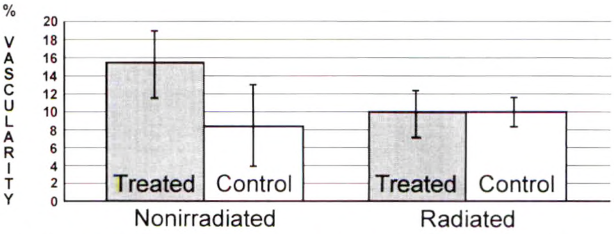

Fig 4. Skin flap vascularity differences between bFGF-treated and control flaps in nonirradiated group (p = .005) and in irradiated group (p = .928).

In regard to systemic body oxygen saturation levels, no significant difference was found between irradiated and nonirradiated animals. On postoperative day 14, the mean systemic oxygen saturation level (±SD) for the nonirradiated animal group (n = 10) was 94% ± 2.4%, and for the irradiated group (n = 10), the mean value was 93.3% ± 1.9% (p = .14).

Subcutaneous flap tissue temperature recordings were also taken for all tissue oximetry readings. No statistically significant differences were found in flap tissue temperature readings between treated and control flaps in the irradiated and nonirradiated animals. However, there was a significant difference in body core temperature between irradiated and nonirradiated groups. The nonirradiated animals had a mean (±SD) body core temperature of 37.5°C ± 0.93°C. The irradiated animals had a mean body core temperature of 38.0°C ± 0.85°C (p = .009).

Angiography. Digital imaging analysis in the nonirradiated group demonstrated a large difference in vascularity between the bFGF-treated flaps and the control flaps 14 days after flap elevation (Fig 3). The control flaps had a mean (±SD) area of vascularization of 8.57% ± 4.51% (p = .005), whereas the treated flaps had a mean area of vascularization of 15.44% ± 3.6%, which was an 80% increase. Such an increase in vascularization by bFGF was not observed in the irradiated flaps. The mean area of vascularization in the treated flaps was 9.91% ± 2.62%; the mean value in the control flaps was 10.06% ± 1.6% (p = .928; Fig 4).

Clinical Analysis. Clinically, the bFGF-treated flaps appeared to have more capillary bleeding and were more edematous on the day of flap construction. This change became less apparent over the following 2 weeks.

In regard to the degree of inflammatory edema elicited by the intracuticular bFGF injections over the 20-day time course (inflammation scale score 0 to 5), a wheal reaction became evident on the bFGF flaps within 3 days after the initial injection. This wheal

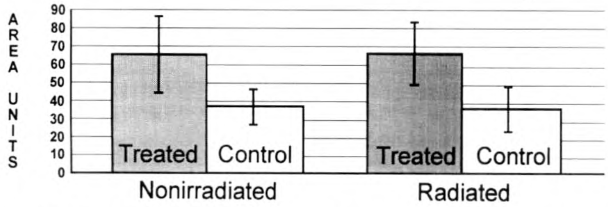

Fig 5. Skin flap epidermal area thickness differences between bFGF-treated and control flaps in nonirradiated group (p = .002) and in irradiated group (p = .001).

reaction peaked 6 days after the initial injection and was limited to the area of injection. This reaction was significantly more pronounced in the nonirradiated animals than in the irradiated animals (mean [±SD] scaled score, 2.6 ± 0.7 versus 1.6 ± 0.8; p = .01). After the last day of bFGF injections, this wheal reaction appeared to diminish spontaneously; by day 14, the reaction had fully resolved. In the PBS-injected control flaps of both irradiated and nonirradiated groups, no inflammatory edema was at all evident; thus, all were given a score of 0. The bFGF-injected flaps therefore had a significantly greater amount of clinical inflammatory edematous change compared with the control flaps.

Histologic Analysis. Histomorphometric measurements of nonirradiated and irradiated flaps showed a significantly increased epidermal cross-sectional area in bFGF-treated tissue over control specimens. In the nonirradiated group, the bFGF-treated flaps had a mean (±SD) epidermal area of 65.5 ± 21.1 units, whereas the untreated control flaps had a mean epidermal area of 36.6 ± 9.4 units (p = .002). In irradiated animals, a similar difference was also found between treated and control flaps. The treated flaps in this group had a mean epidermal area of 66.6 ± 18.2 units, whereas the untreated control flaps had a mean epidermal area of 37.0 ± 12.1 units (p = .001; Fig 5).

Histologically, the epidermis of the nonirradiated bFGF-treated flaps showed more prominent papillomatosis and acanthosis. The epidermal cells were hyperplastic, with prominent rete ridges. An increased

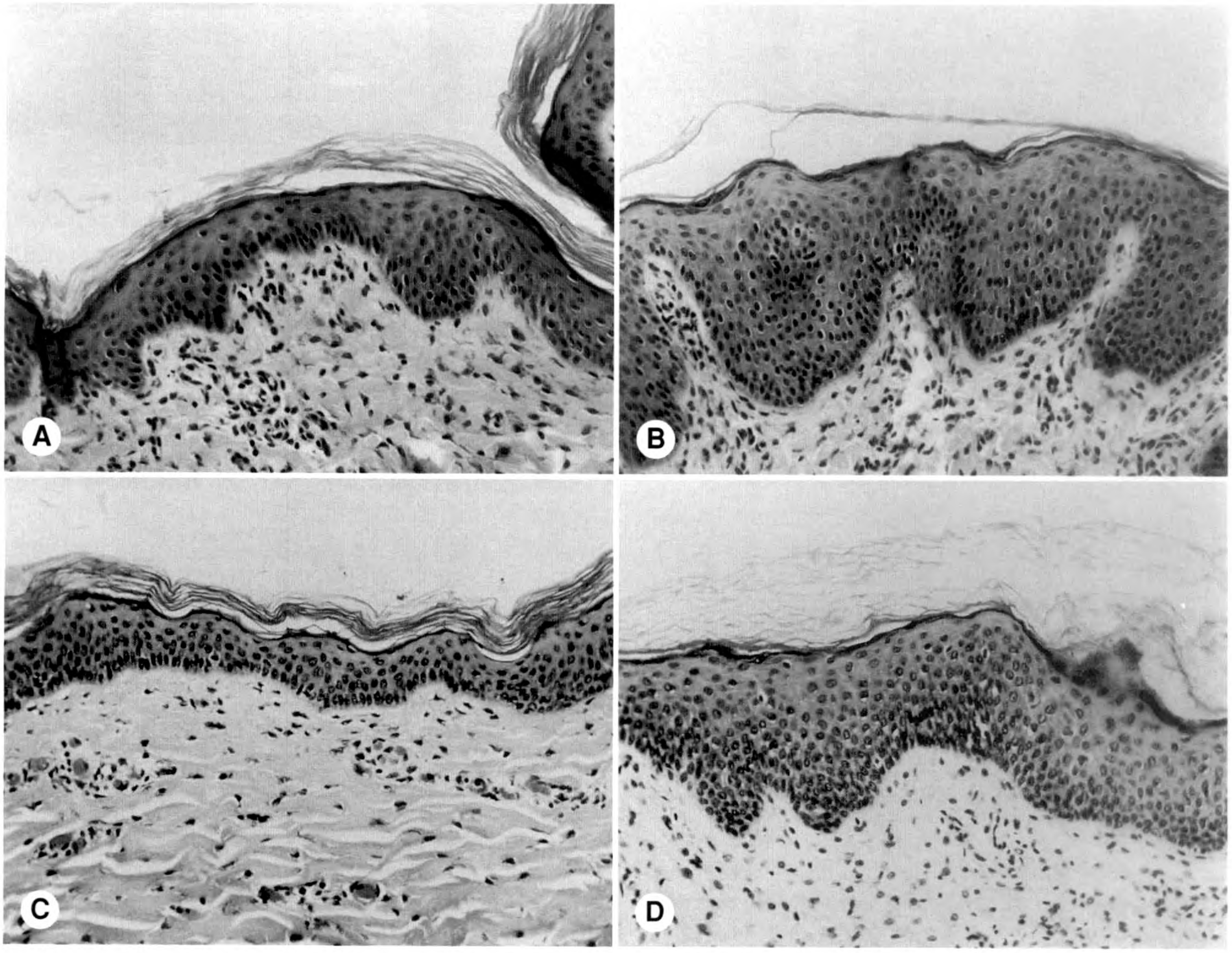

Fig 6. Epidermal comparison of skin flaps (Masson trichrome, original ×40) shows more epithelial cell hyperplasia and more prominent rete ridges in bFGF-treated versus control specimens in nonirradiated and irradiated flaps. A) Nonirradiated control flap. B) Nonirradiated bFGF-treated flap. C) Irradiated control flap. D) Irradiated bFGF-treated flap.

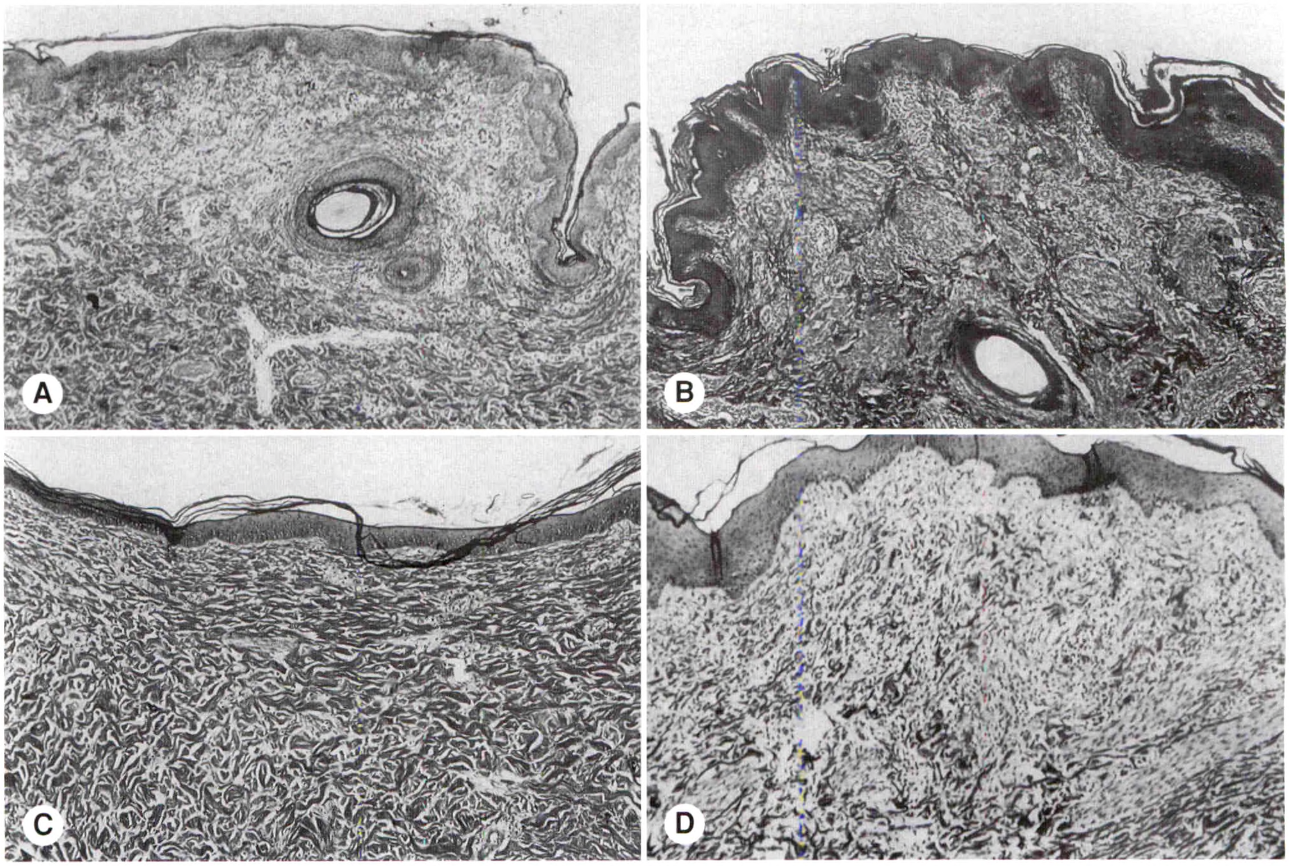

Fig 7. Cutaneous comparison of skin flaps (Masson trichrome, original ×10) demonstrates increased epidermal thickness, more arrectores pilorum muscles, and increased space between collagen fibers in bFGF-treated versus control specimens in nonirradiated and irradiated flaps. A) Nonirradiated control flap. B) Nonirradiated bFGF-treated flap. C) Irradiated control flap. D) Irradiated bFGF-treated flap.

number of epithelial cell nuclei per surface area were evident (Fig 6). In the dermis, the cellularity in the treated group was 2 to 3 times greater than that in the control group. This increase in cellularity was caused in part by an inflammatory infiltrate composed of lymphocytes and eosinophils located predominantly in perivascular regions. In addition, increased numbers of fibroblasts and scattered lymphocytes and eosinophils were present. The arrectores pilorum muscles in the treated group were more prominent, having an increased number of smooth muscle nuclei. The number of smooth muscle cells was approximately twice that of the control group; their nuclei were more plump and displayed occasional mitotic figures. Further, a marked increase in the number of perivascular spindle-shaped cells with morphological features of fibroblasts or fibroblast precursors was present.

The changes observed in the irradiated group were qualitatively similar to those seen in the nonirradiated group, although they were quantitatively less prominent. Again, in the bFGF-treated irradiated tissue the epidermal cells were hyperplastic, with more prominent rete ridges than those in the nontreated irradiated tissue. The dermal cellularity in the nontreated irradiated tissue was approximately one half that in nontreated nonirradiated tissues. Inflammatory cells were less abundant in the treated irradiated group compared with the treated nonirradiated group.

Trichrome stains showed a slight increase in the space between collagen fibers in the bFGF-treated group because of the accumulation of extracellular fluid. This histologic finding is consistent with the clinical observation that the bFGF-treated flaps appeared to be more edematous (Fig 7). No increased number of mature collagen fibers was evident with this stain. As estimated by Alcian blue stains, no apparent difference in the content of acid mucopolysaccharides was evident. No appreciable differences were observed in the ratio of mature versus immature collagen fibers between the treated and nontreated controls, as evaluated with the Sirius red stain. Similarly, no differences in this ratio were noted between the irradiated and the nonirradiated groups.

DISCUSSION

This study demonstrates the vascular effects, tissue oxygen changes, and epidermal effects of exogenous bFGF in nonirradiated and irradiated skin flaps. In this study, supplemental bFGF significantly increased the vascularity of nonirradiated flaps. In the bFGF-treated flaps, flap angiograms showed an 80% increase in vascularity compared with the PBS controls. Thus, supplemental bFGF in this study was most effective in increasing vascularity in the nonirradiated condition. In the nonirradiated group, the bFGF-treated flaps showed a trend toward a higher $P_{sc}O_2$ level than that in the flap controls; however, this difference was not statistically significant by day 14. The reason for the lack of recordable early improvement of $P_{sc}O_2$ with exogenous bFGF in the skin flaps may be that it could take longer than 14 days for sufficient neovascularization and tissue perfusion to occur before an increased $P_{sc}O_2$ level is seen. Another possible explanation may be that the flap angiograms document the existence of blood vessels greater than several hundred micrometers in diameter, whereas the $P_{sc}O_2$ level correlates more with the tissue's physiological oxygen state, which is dependent on arteriolar-capillary blood flow, arterial-venous shunting, and temperature.

Adequate tissue oxygenation is critical for effective wound healing to occur. A minimal oxygen tension of 20 mm Hg in the presence of ascorbate and ferrous ions is required for the hydroxylation of proline and lysine to form procollagen.[26] When the tissue PO_2 level is lower than 20 mm Hg, collagen synthesis stops; however, collagen lysis continues. In this hypoxic environment, the wound is more susceptible to dehiscence.[27] A tissue PO_2 level higher than 30 to 40 mm Hg is necessary for the development of a collagen matrix for capillary budding in avascular areas and for collagen synthesis.[28] Within the wound, the PO_2 level is lowest in the areas furthest from the intact vasculature (9 to 10 mm Hg) in which macrophages, capillaries, and immature fibroblasts proliferate. In close proximity to maturing vessels, PO_2 levels are 40 to 80 mm Hg.[29]

Wound healing will only progress when a sharp tissue oxygen gradient exists between the viable wound margin and the hypoxic tissue of the wound center.[30] It is interesting to note that endogenous cytokines are released in a hypoxic wound environment; however, the actual cellular repair process of wound healing depends on oxygen.[31]

We originally hypothesized that the $P_{sc}O_2$ levels in irradiated flaps would be lower than those in nonirradiated flaps because of decreased vasculature; however, this finding was not evident in this study. One possible reason is that the baseline $P_{sc}O_2$ levels may have been falsely elevated because the body core temperature of the irradiated group was increased by 0.5°C over that of the nonirradiated group. This elevated body temperature would have increased vasodilation and resulted in increased blood perfusion. However, the flap temperature was not different between the groups.

We realize that measuring the $P_{sc}O_2$ level at the flap site does not evaluate its distribution within the whole flap. Prior studies have shown that tissue PO_2 levels can be 60 mm Hg at the flap base while they are 10 mm Hg at the flap tip.[32] To standardize the $P_{sc}O_2$ flap measurements in our study, one area of the flap (3 cm from the distal edge) was consistently measured throughout the study.

In the irradiated group, significantly increased vascularity was not found in the bFGF-treated flaps. Previous studies that used irradiated animal models in conjunction with FGFs have shown mixed results in irradiated conditions. In vitro studies of bFGF on irradiated endothelial cells suggest that bFGF can be a potent inducer of repair of potentially lethal radiation cellular damage.[33] Chang et al,[22] using a porcine model, found a 62% increase in vascularity in irradiated flaps treated with bFGF. The difference between our results and those of Chang et al may be related to different methods of flap angiogram comparison. A different computer program for flap digitization and comparison was used. A second contributing factor could be that in the study by Chang et al, the angiogram comparison was of randomly chosen 2 × 4-cm segments, whereas our study evaluated the distal third of each flap. In another study, Hom et al[34] found enhanced flap viability and vascularity with endothelial cell growth factor, a crude form of FGF with heparin, in irradiated tissue. Mustoe et al[35] found bFGF to be angiogenic under ischemic conditions in a rabbit ear dermal ulcer model. In addition, Uhl et al[36] showed increased angiogenesis with supplemental bFGF in an ischemic dermal ulcer mouse model. However, Wu et al[37] found that bFGF gave more optimal neogranulation tissue in an ischemic rabbit ear dermal ulcer model when hyperbaric oxygen was given. Hence, the effects of bFGF may be dependent on tissue oxygen tension in the wound area.

In this study, the vascular effects of supplemental bFGF were hindered by previous irradiation. It is possible that previous irradiation may have caused a decreased endothelial cell receptor activity to bFGF, either by diminishing bFGF binding or by making a lower number of bFGF receptors available. Another possible explanation could be that irradiation modifies the environmental matrix, reducing endothelial cell replication and mobility, or causing endothelial cell damage.[38]

In both irradiated and nonirradiated conditions, bFGF significantly increased the epidermal cross-sectional area, by 80%, as compared with control flaps. Previous studies have shown bFGF to be a potent mitogenic stimulant for keratinocytes.[39,40] Several studies in a porcine model have shown increased epithelialization with supplemental bFGF in partial-thickness excisional wounds and partial-thickness burns.[41,42] Hebda et al,[41] who used a partial-thickness excisional wound in a porcine model, showed that topical application of bFGF gave a 20% acceleration of epidermal healing. Our study used an intracuticular route for bFGF delivery by serial injections, which may have further contributed to the increased bFGF epidermal effects.

In our model, skin flaps were subjected to previous irradiation to simulate a delayed healing condition due to irradiation. Mustoe et al[35] showed that supplemental bFGF did not significantly increase reepithelialization in full-thickness excisional dermal ulcers subjected to ischemia. However, with the addition of hyperbaric oxygen to this model, increased reepithelialization was seen.[37] Thus, a previously irradiated wound may have different bFGF epithelial response properties than an ischemic wound.

This study demonstrates that bFGF stimulates epidermal regeneration in previously irradiated skin. Thus, the cellular mechanism by which bFGF stimulates epidermal proliferation is not diminished by irradiation in this model. This finding supports the contention that supplemental bFGF affects the epidermis and vascularity independently in the setting of previous irradiation.

ACKNOWLEDGMENT — We thank biostatistician Bob Sherman, PhD, for his assistance in this study.

REFERENCES

1. Habel DW. Surgical complications in irradiated patients. Arch Otolaryngol 1967;82:382-6.

2. Tibbs M. Wound healing following radiation therapy: a review. Radiother Oncol 1997;42:99-106.

3. Van Meter K. Baromedicine as an aid in resolution of chronic wounds. J Geriatr Dermatol 1996;4:210-25.

4. Jonsson K, Hunt TK, Mathes SJ. Oxygen as an isolated variable influences resistance to infection. Ann Surg 1988;208:783-7.

5. Knighton DR, Halliday B, Hunt TK. Oxygen as an antibiotic: the effect of inspired oxygen on infection. Arch Surg 1984;119:199-204.

6. Boykin JV. Hyperbaric oxygen therapy: a physiologic approach to selected wound healing. Wounds 1996;8:183-98.

7. Knighton DR, Silver IA, Hunt TK. Regulation of wound healing angiogenesis — effect of oxygen gradients and inspired oxygen concentration. Surgery 1981;90:262-70.

8. Im MJ, Kim YS, Edwards RJ, Hoopes JE, Fenselau A. The effect of bovine basic fibroblast growth factor on skin flap survival in rats. Ann Plast Surg 1992;28:242-5.

9. Ishiguro N, Yabe Y, Shimizu T, Iwata H, Miura T. Basic fibroblast growth factor has a beneficial effect on the viability of random skin flaps in rats. Ann Plast Surg 1994;32:356-60.

10. McGee GS, Davidson JM, Buckley A, et al. Recombinant basic fibroblast growth factor accelerates wound healing. J Surg Res 1988;45:145-53.

11. Khouri RK, Brown DM, Leal-Khouri SM, Tark KC, Shaw WW. The effect of basic fibroblast growth factor on the neovascularization process: skin flap survival and staged flap transfers. Br J Plast Surg 1991;44:585-8.

12. Hom DB, Assefa G. Effects of endothelial cell growth factor on vascular compromised skin flaps. Arch Otolaryngol 1992;118:624-8.

13. Slavin J, Hunt JA, Nash JR, Williams DF, Kingsnorth AN. Recombinant basic fibroblast growth factor in red blood cell ghosts accelerates incisional wound strength. Br J Surg 1992;19:918-21.

14. Drake DB, Oishi S. Wound healing considerations in chemotherapy and radiation therapy. Clin Plast Surg 1995;22:31-7.

15. Dimitrievich GS, Fischer-Dzoga K, Griem M. Radiosensitivity of vascular tissue. I. Differential radiosensitivity of capillaries: a quantitative in vivo study. Radiat Res 1984;99:511-34.

16. Doyle JW, Li Y, Salloum A, Fitzgerald TJ, Walton RL. The effects of radiation on neovascularization in a rat model. Plast Reconstr Surg 1996;98:129-35.

17. Lancaster JF, Leaper DJ. Effects of inhalational anaesthetic agents on oxygen electrodes. Eur Surg Res 1987;19:1-12.

18. Hjortdal VE, Timmenga EJ, Knolseth D, et al. Continuous direct tissue oxygen tension measurement. Ann Chir Gynaecol 1991;80:8-13.

19. Hopf HW, Hunt TK. Comparison of Clark electrode and optode for measurement of tissue oxygen tension. Adv Exp Med Biol 1994;345:841-7.

20. Hofer SOP, Timmenga EJF, Christiano R, Bos KE. An intravascular oxygen tension monitoring device used in myocutaneous transplants: a preliminary report. Microsurgery 1993;14:304-9.

21. Hjortdal VE, Henriksen TB, Djurhuus JC, Gottrup F. Tissue oxygen tension in myocutaneous flaps. Eur J Surg 1991;157:307-11.

22. Chang HS, Hom DB, Agarwal RP, Pernell K, Manivel JC, Chang S. Effects of basic fibroblast growth factor on irradiated porcine skin flaps. Arch Otolaryngol Head Neck Surg 1998;124:307-12.

23. Erol O, Spira M, Levy B. Microangiography: a detailed technique of perfusion. J Surg Res 1980;29:406-13.

24. Panda DP, Rosenfeld A. Image segmentation by pixel classification in gray level, edge value space. IEEE Trans Comput 1978;C-27:875-80.

25. Thackray BD, Nelson AC. Semi-automatic segmentation of vascular network images using a rotating structure element

(ROSE) with mathematical morphology and dual feature thresholding. IEEE Trans Med Imaging 1993;12:385-92.

26. Hunt TK, Pai MP. Effect of varying ambient oxygen tensions on wound metabolism and collagen synthesis. Surg Gynecol Obstet 1972;135:561-7.

27. Goodson W, Hunt T. Wound healing. In: Kinney J, ed. Nutrition and metabolism in patient care. Philadelphia, Pa: WB Saunders, 1988:635-42.

28. Nemiroff PM. Hyperbaric oxygen in skin grafts and flaps. In: Kindwall EP, ed. Hyperbaric medicine practice. Flagstaff, Ariz: Best Publishing Co, 1995:566-79.

29. Remensnyder J. Oxygen gradients in healing wounds. Am J Pathol 1968;52:302-8.

30. Hunt TK, Twomey P, Zederfeldt B, Dunphy JE. Respiratory gas tension and pH in healing wounds. Am J Surg 1967;114: 302-7.

31. Davis JC, Buckley CJ, Barr PO. Compromised soft tissue wounds: correction of wound hypoxia. In: Davis JC, Hunt TK, eds. Problem wounds: the role of oxygen. New York, NY: Elsevier, 1988:143-4.

32. Calderon W. Chang KN, Mathes SJ. Comparison of the effect of bacterial inoculation in musculocutaneous and fasciocutaneous flaps. Plast Reconstr Surg 1986;77:785-92.

33. Haimovitz-Friedman A, Vlodavsky I, Chanhuri A, Witte L, Fuks Z. Autocrine effects of fibroblast growth factor in repair of damage in endothelial cells. Cancer Res 1991;51:2552-8.

34. Hom DB, Assefa G, Song CW. Endothelial cell growth factor (ECGF) application to irradiated soft tissue. Laryngoscope 1993;103:165-70.

35. Mustoe TA, Ahn ST, Tarpley JE, Pierce GF. Role of hypoxia in growth factor responses: differential effects of basic fibroblast growth factor and platelet derived growth factor in an ischemic wound model. Wound Repair Regeneration 1994;2: 277-83.

36. Uhl E, Barker JH, Bondar I, et al. Basic fibroblast growth factor accelerates wound healing in chronically ischemic tissue. Br J Surg 1993;80:977-80.

37. Wu L, Pierce GF, Ladin DA, Zhao LL, Rogers D, Mustoe TA. Effects of oxygen on wound responses to growth factors: Kaposi's FGF, but not basic FGF, stimulates repair in ischemic wounds. Growth Factors 1995;12:29-35.

38. Reinhold HS, Buoisman GH. Radiosensitivity of capillary endothelium. Br J Radiol 1973;46:54-7.

39. O'Keefe EJ, Chin ML, Payne RE. Stimulation of keratinocytes by basic fibroblast growth factor. J Invest Dermatol 1988;90:767-9.

40. Shipley GD, Keeble WW, Hendrickson JE, Coffey RJ, Pittelkow MR. Growth of normal human keratinocytes and fibroblasts is stimulated by acidic and basic fibroblast growth factor. J Cell Physiol 1989;138:511-8.

41. Hebda PA, Klingbeil CK, Abraham JA, Fiddes JC. Basic fibroblast growth factor stimulation of epidermal wound healing in pigs. J Invest Dermatol 1990;95:626-31.

42. Eriksson E, Breuing K, Johansen LB, Miller DR. Growth factor solutions for wound treatment in pigs. Surg Forum 1989; 40:618-20.

Ann Otol Rhinol Laryngol 109:2000

CERVICAL VERSUS THORACIC EPIDURAL MORPHINE FOR THE TREATMENT OF HEAD AND NECK CANCER PAIN

LOUCAS GEORGIOU, MD, PHD
CHRISTINA SKLAVOU, MD
IOANNIS YIOTAKIS, MD, PHD
ANTONIOS LOUIZOS, MD
LEONIDAS MANOLOPOULOS, MD, PHD
GEORGIOS ADAMOPOULOS, MD, PHD
ATHENS, GREECE

We studied 29 patients in the final stage of head or neck cancer who were suffering pain that was not relieved by oral morphine. Cervical or thoracic epidural morphine was administered to relieve the pain. The quality of analgesia was equally good for both techniques. However, cervical epidural administration appeared to be superior, because much smaller doses of morphine were required in order to induce more rapid and longer analgesia.

KEY WORDS — analgesia, cancer pain, cervical epidural administration, morphine, pain, thoracic epidural administration.

INTRODUCTION

Pain in cancer victims can be well treated with oral opioids. Sometimes, in the final stage of the disease, cancer pain becomes refractory to this treatment. In such cases the epidural administration of opioids is an alternative solution.

Opioids administered in small doses in the epidural region provide excellent analgesia, usually with few side effects. Morphine is the opioid most commonly used for this purpose. Given that morphine is a hydrophilic drug and has the capability to reach the cerebrospinal fluid (CSF) after being introduced in the epidural region,[1-4] it may be administered therapeutically at some distance from the painful area.

The aim of this study was to investigate the effectiveness of epidural morphine administration in intervertebral spaces near to or far from the site of pain in patients with head or neck cancer.

MATERIALS AND METHODS

During the last 3 years, we studied 29 patients suffering from head or neck cancer. All patients were in the final stage of the disease and suffered pain that could not be controlled by oral morphine. For this reason, it was decided to administer the drug through the epidural route. The patients were randomized into 2 groups, according to which intervertebral space was used. Group A contained 16 patients in whom the catheter was placed in the thoracic region, at the level of the T7-8 intervertebral space. Group B contained 13 patients in whom the epidural catheter was placed in the cervical region, at the level of the C7-T1 space. Initially, a temporary epidural catheter was inserted, for 3 to 4 days, through which bolus doses of morphine were given in order to rate the therapeutic analgesic dose. The temporary catheter was then replaced with a permanent one. After the patient had given consent, the permanent epidural catheter was placed by means of subcutaneous tunneling under local anesthesia, with the Portex subcutaneous epidural catheter set. Most patients then returned home, where the morphine administration was undertaken by trained persons from their locality. The morphine was given in intermittent doses when the patient was in pain. A special team of physicians and nurses monitored the patients until they died.

To estimate the score of pain, we used a visual analog scale (VAS) from 0 (no pain) to 100 (worst pain).[5,6] The patients were trained how to use the scale.

The following parameters were recorded to evaluate the effectiveness of the 2 methods in combating cancer pain: the effective bolus dose; the total dose over 24 hours; the latency of onset of analgesia; the duration of analgesia after bolus dose; the pain score, using a VAS, evaluated over a 24-hour period on the 1st, 2nd, 5th, and 10th days of treatment; and the total duration of treatment. Any complications were also noted.

Results were expressed as mean and SD. The statistical analysis of the results concerning the patients' characteristics, the latency of onset of analgesia, the duration of analgesia, and the quantity of morphine given was carried out by Student's *t*-test. The pain

---

From the Departments of Anesthesiology (Georgiou, Louizos, Sklavou) and Otolaryngology (Manolopoulos, Yiotakis, Adamopoulos), "Hippokration" General Hospital, Athens, Greece.

CORRESPONDENCE — Ioannis Yiotakis, MD, PhD, 98 Vas. Sofias Avenue, GR 11528, Athens, Greece.

PATIENT DATA FOR TWO GROUPS

	Thoracic	*Cervical*
Age (y)*	68 ± 7	69 ± 4
Weight (kg)*	65 ± 5	63 ± 7
Sex (M/F)	15/1	13/0
Therapy (d)*	53 ± 11	45 ± 8

*Mean ± SD.

score was analyzed by 1- and 2-way ANOVAs for repeated measurements. The statistical package used was MS Excel 97 for Windows 95. A p level of <.05 was considered statistically significant.

RESULTS

The patients' characteristics and the duration of treatment did not differ significantly between the 2 groups (see Table). Both the bolus dose administered and the total daily dose of morphine were significantly lower ($p < .05$) in group B (Fig 1). The latency of onset of analgesia was also significantly lower ($p < .05$) in group B (Fig 2), whereas the duration of analgesia after each bolus dose of morphine was at least 4 hours longer in group B ($p < .05$, Fig 2).

There was no significant difference in the pain score, either between the 2 groups on the specific measurement days (1st, 2nd, 5th, and 10th days) or between the measurement days in individual patients of both groups (Fig 3).

Nausea and vomiting were observed in 8 patients of group A (50%) and in 4 of group B (31%). Urinary retention occurred in 2 patients of group A. Ten patients in group A (62%) and 5 in group B (38%) suffered constipation. Pruritus occurred in 5 patients of group A (31%) and in 2 of group B (15%). Respiratory inhibition and local infection were not seen in any patient of either group.

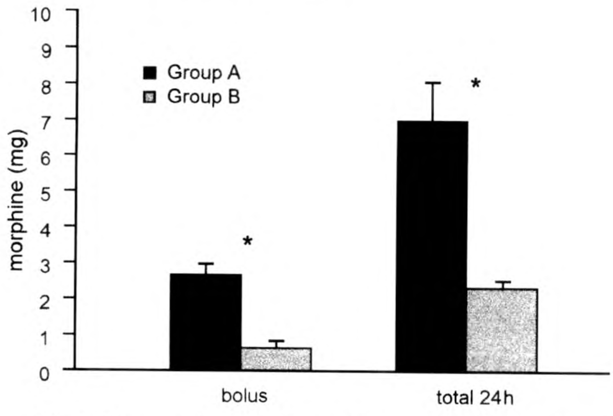

Fig 1. Dosage of epidural morphine administered to patients in 2 groups at each bolus dose and total administered over 24 hours (mean and SD). Asterisks — $p < .05$; group A — thoracic administration; group B — cervical administration.

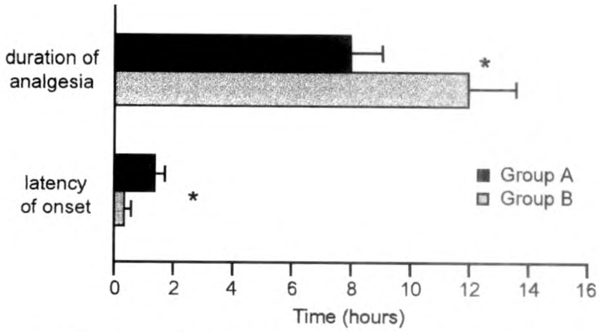

Fig 2. Time until onset of analgesia after administration of epidural morphine and duration of analgesia after bolus dose (mean and SD). Asterisks — $p < .05$.

DISCUSSION

Analgesia may be achieved by epidural or subarachnoid administration of an opioid. Cancer pain, which is transmitted through the A delta and C afferent fibers, can be greatly reduced by the spinal administration of opioids, which selectively relieve the pain without causing mobility, sensory, or sympathetic disturbances.[1,2] Thus, the epidural administration of opioids is becoming a widely accepted method for treating cancer pain in a home care environment[3,4] as an alternative when oral opioid treatment is discontinued. This method is founded on the action of opioids on receptors located in the substantia gelatinosa of the spinal cord.[7]

This study shows that patients who are given cervical epidural morphine for the relief of cancer pain need much smaller bolus doses and gain significantly longer analgesia than do those who receive epidural morphine via the thoracic route. The former method thus reduces the "pain" problem for the patient and family and also requires much smaller daily amounts of the opioid. The latency of onset of analgesia in patients who received thoracic epidural morphine was more than double that in the patients treated via the cervical route. This difference can be attributed to the time required for the drug to penetrate the CSF when it is administered in the thoracic region.

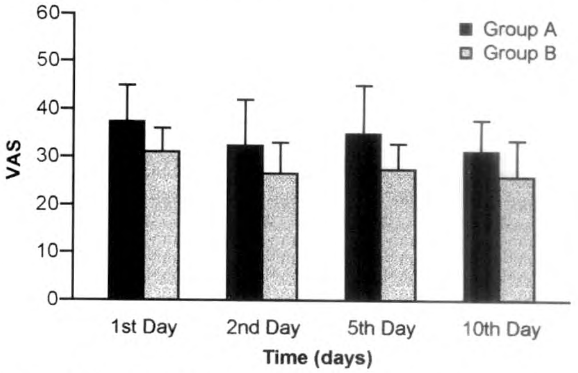

Fig 3. Visual analog scale (VAS) scores of pain on 1st, 2nd, 5th, and 10th days of treatment (mean and SD).

This is in agreement with the findings of other studies that support the rostral spread of morphine into the CSF after epidural administration.[8-11]

Even though long-term intraspinal opioids are mainly recommended for the treatment of difficult cancer pain in the lower part of the body,[10-12] from the present study it appears that the epidural administration of morphine in the thoracic or cervical regions of the spine offers equally effective analgesia in the treatment of cancer pain in the head or neck.

Nausea and vomiting, when they occurred, were usually of moderate degree and were treated well with metoclopramide hydrochloride and dehydrobenzperidol. The pruritus was mild and was tolerated by the majority of patients in whom it occurred. Constipation was the most frequent problem. These side effects all occurred much more frequently in the patients who were given thoracic epidural morphine, probably because of the larger dosages that were required in these patients. The urinary retention that was observed in 2 patients who received thoracic epidural morphine disappeared after the administration of naloxone hydrochloride.

In conclusion, it appears that cervical epidural administration of morphine for the relief of pain caused by head or neck cancer is indicated when oral administration is ineffective, as may be the case in the final stage of the disease. The technique has the advantages of high-quality and long-lasting analgesia with very small doses of morphine, thus reducing the side effects associated with opioid treatment.

REFERENCES

1. Cousins MJ, Mather LE. Intrathecal and epidural administration of opioids. Anesthesiology 1984;61:276-310.

2. Yaksh TL. Spinal opiates: a review of their effect on spinal function with an emphasis on pain processing. Acta Anaesthesiol Scand Suppl 1987;85:25-37.

3. Smith DE. Spinal opioids in the home and hospice setting. J Pain Symptom Manage 1990;5:175-82.

4. Crawford ME, Andersen HB, Augustenborg G, et al. Pain treatment on outpatient basis using extradural opiates: a Danish multicenter study comprising 105 patients. Pain 1983;16:41-7.

5. Huskisson EL. Visual analogue scales. In: Melzack R, ed. Pain measurement and assessment. New York, NY: Raven Press, 1983:33-7.

6. Jensen MP, Karoly P, Braver S. The measurement of clinical pain intensity: a comparison of six methods. Pain 1986;27:117-26.

7. Atweh S, Kurah M. Autoradiographic localization of opiate receptors in rat brain. 1. Spinal cord and lower medulla. Brain Res 1977;124:53-67.

8. Bromage PR, Camporesi EM, Durant PAC, Nielsen CH. Rostral spread of epidural morphine. Anesthesiology 1982;56:431-6.

9. Gourlay GK, Cherry DA, Cousins MJ. Cephalad migration of morphine in CSF following lumbar epidural administration in patients with cancer pain. Pain 1985;23:317-26.

10. Larsen VH, Iversen AP, Christiensen P, Andersen PK. Postoperative pain treatment after upper abdominal surgery with epidural morphine at thoracic or lumbar level. Acta Anaesthesiol Scand 1985;29:566-71.

11. Sullivan SR, Cherry DA. Pain from an invasive facial tumor relieved by lumbar epidural morphine. Anesth Analg 1987;66:777-9.

12. Du Pen SL, Williams AR. Management of patients receiving combined epidural morphine and bupivacaine for the treatment of cancer pain. J Pain Symptom Manage 1992;7:125-7.

Ann Otol Rhinol Laryngol 109:2000

CLINICAL NOTE

CAT-SCRATCH DISEASE OF THE PAROTID GLAND: AN OFTEN-MISDIAGNOSED ENTITY

SHELTON MALATSKEY, MD
JACOB BEN-DAVID, MD
MILO FRADIS, MD
LUDWIG PODOSHIN, MD
HAIFA, ISRAEL

A case of cat-scratch disease involving the parotid area in a young adult is presented. Thanks to meticulous history-taking, the correct diagnosis was suggested and later established, thus preventing unnecessary surgery. The pertinent literature is discussed.

KEY WORDS — cat-scratch disease, parotid gland.

INTRODUCTION

Several inflammatory processes can cause cervical nodules or swelling in the neck and face, and a complete physical examination and extensive laboratory testing are required to establish the diagnosis.[1] Cat-scratch disease, also known as benign nonbacterial regional lymphadenitis, may well be one of the more common causes of lymphadenopathy in children and young adults.[2] Cat-scratch disease can cause a very diverse and fascinating array of clinical syndromes and is capable of affecting organs other than skin and lymph nodes.[3] These atypical manifestations, together with serious complications, usually occur more often in the pediatric population and also in immunocompromised hosts.[4]

The first report of cat-scratch disease was made by Greer and Keefer[5] in 1951, although the entity was first identified by Dubre in 1931.[2] Although large series of patients with cat-scratch disease have been detailed in the literature,[6,7] involvement of the parotid parenchyma is rare.[6,8] We thought it would be of interest to report a case of cat-scratch disease involving the parotid parenchyma in a patient who was spared surgical exploration thanks to a correct diagnosis of the disease.

CASE REPORT

A 23-year-old manual worker was admitted to our otolaryngology department in February 1995 for a swelling in the right parotid area that had appeared 2 weeks before his admission. He had been treated with amoxicillin, but the swelling had continued to grow, and he was referred for surgical excision of what appeared to be a tumor. In taking the patient's history, a history of contact with cats 4 to 6 weeks previously was elicited. No other significant diseases were reported by this otherwise healthy patient.

On examination, a soft, elastic, 5 × 4-cm mass in the right parotid area was found (Fig 1A). The skin covering the mass had a reddish color, but the mass was not painful. The Stensen duct opening was examined and found to be normal, with normal salivary secretion. No enlarged lymph nodes in the neck were found. The remaining findings on the otolaryngological examination were normal. No obvious site of inoculation was observed. A minor scratch of unknown origin was found on the patient's right arm, but he could not relate the scratch to any animal contact, and it could have been due to his field of work. The physical examination findings were otherwise normal. Chest radiographs and laboratory tests, including those for syphilis (VDRL test) and human immunodeficiency virus, were negative. A fine-needle aspiration was performed, and pus rich in neutrophils was aspirated. The pus that had been collected in the syringe was transported immediately to the bacteriologic laboratory. The bacteriologic examination included cultures for aerobic and anaerobic bacteria, which were sterile. A Gram stain and a Ziehl-Neelsen stain were performed and found to be negative. The pus was also cultured in a Loewenstein-Jensen medium for *Mycobacterium*, and this culture was also negative.

An ultrasound examination of the parotid area showed a cystic lesion in the right parotid gland. A computed tomography scan of the area showed enlargement of the right parotid region with nonhomogeneous hyperdense areas (Fig 2). A tentative diag-

---

From the Department of Otolaryngology–Head and Neck Surgery, Bnai Zion Medical Center (all authors), and The Bruce Rappaport Faculty of Medicine, Technion-Israel Institute of Technology (Fradis, Podoshin), Haifa, Israel.

CORRESPONDENCE — Milo Fradis, MD, Dept of Otolaryngology–Head and Neck Surgery, Bnai Zion Medical Center, POB 4940, 31048 Haifa, Israel.

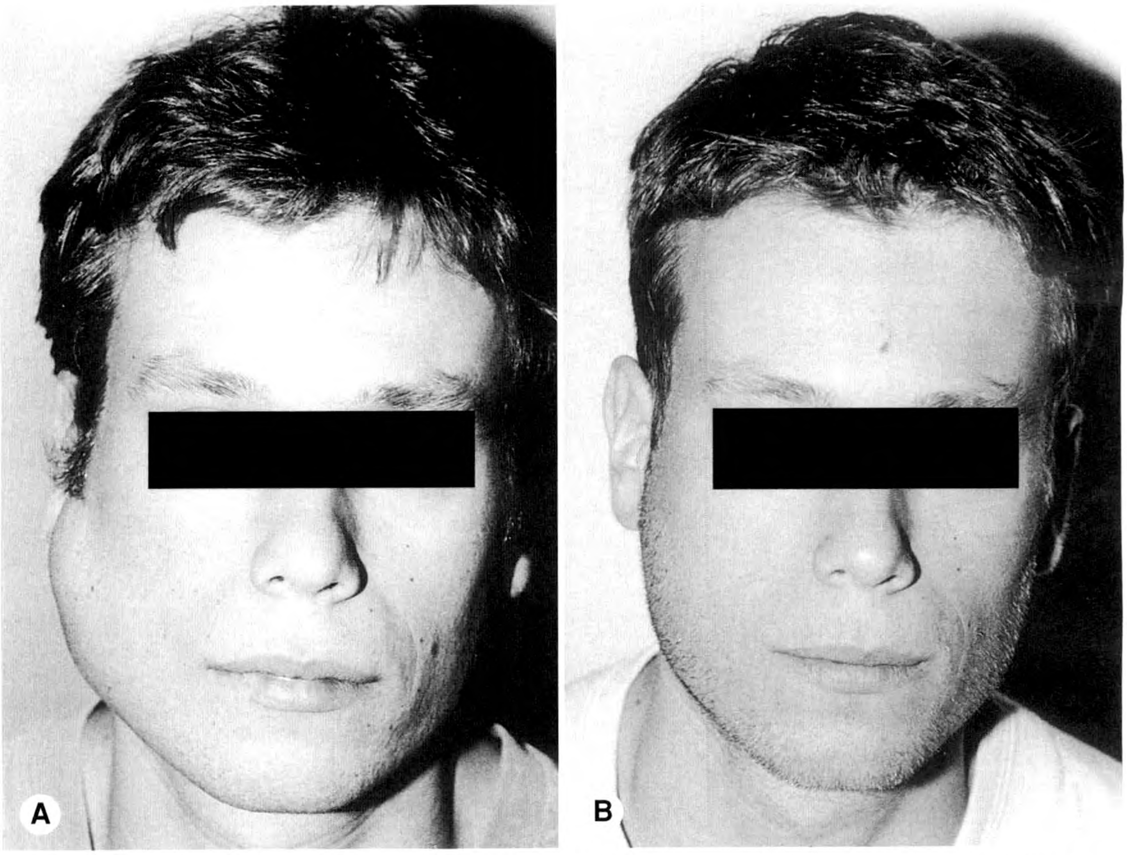

Fig 1. Patient A) at admission, with extent of swelling clearly evident, and B) 2 months later, after swelling of parotid area had subsided.

nosis of cat-scratch disease was proposed, and an intradermal test for cat-scratch disease was performed. Pus obtained from a previous patient sensitive for cat-scratch disease was used. The pus was subcultured for *Mycobacterium* and tested for hepatitis B and C. It then underwent a process of activation at 60°C for 2 hours on 2 consecutive days and was introduced into ampules. Further inactivation at 56°C for 1 hour on 2 consecutive days was performed. Once the subcultures had returned negative, 0.1 mL of pus was then injected intracutaneously and examined for induration over 48 to 72 hours. The test was strongly positive after 48 hours, and the diagnosis of cat-scratch disease was confirmed. Therefore, the patient was not operated on; and, as no specific treatment for cat-scratch disease is known, he was reassured that the disease is benign and self-limited and that the mass would subside in 1 or 2 months. After 2 months without any treatment, the parotid mass disappeared (Fig 1B).

DISCUSSION

In 38% to 73% of patients with cat-scratch disease, head and neck adenopathy can be found.[2,6,7,9] The disease is primarily one of children and young adults,[10] most probably as a consequence of the route of inoculation. A history of animal contact, usually with cats or even newborn kittens (scratches, bites, or even licking by a cat) was elicited in 67% to 90% of the reported cases.[11] Monkey, dog, and rabbit scratches have also been implicated as vectors.[2,11]

In the past, a viral source was suggested as a specific agent, and studies of lymphocyte responsiveness tended to support this hypothesis.[12] Kalter et al[13] described herpes-like virus particles in affected cells that were not found in control lymph nodes.[14] Others[15] implicated a small bacillus as the etiologic agent. Only very recently has the true origin been identified as *Bartonella henselae*,[16] a gram-negative bacterium. A polymerase chain reaction assay to detect *Bartonella* DNA has been developed to identify the agent.[17] Lately, furthermore, serologic testing of cat-scratch disease patients has shown titers of 1:64 or higher for antibodies to *B henselae*.[18]

In most cases, an inoculation site is evident, and an erythematous papule or pustule develops within 2 weeks at the site, the head and neck being very common sites. Most such lesions clear within 1 to 3 weeks. Proximal lymphadenitis appears 1 to 2 weeks after inoculation, and usually only 1 site is involved,[6] as in our patient. Exocrine tissues are usually not

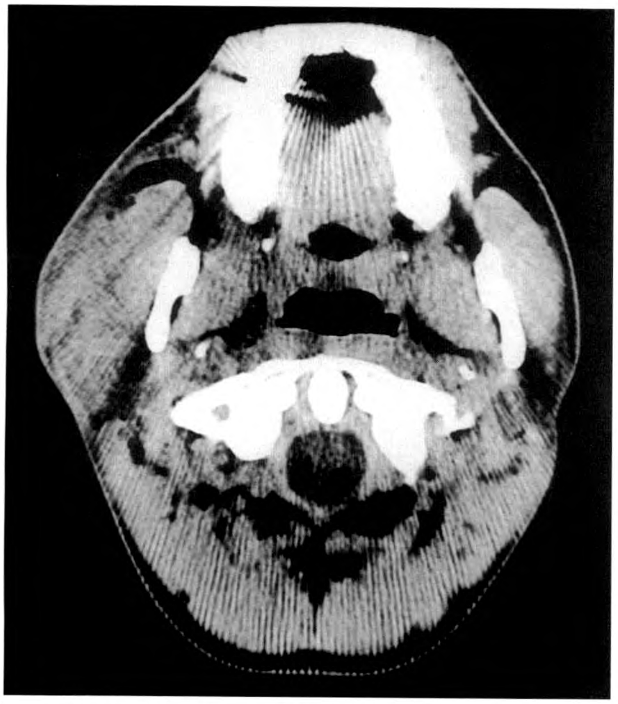

Fig 2. Enlargement of right parotid area on computed axial tomography.

involved in cat-scratch disease, but meticulous examination of the entire computed tomography scan that was performed could not identify enlarged lymph nodes, and we assume that in our patient the parotid gland itself was involved. The emphasis of our case is placed on the importance of recognizing the correct microbiological origin and, by doing so, preventing unnecessary surgery.

Cat-scratch disease can be diagnosed clinically, especially if the skin lesion is present. Pus obtained by needle aspiration may be negative, but a Warthin-Starry silver impregnation stain will demonstrate typical organisms.[19,20] The intradermal skin test is positive in 90% of cases 3 to 4 weeks after the scratch. False-positive skin tests have been found in 1.8% to 4.1% of the general population.[19] On the other hand, a positive reaction may persist for years after a previous infection. An excisional biopsy reveals no specific granulomatous changes of cat-scratch disease[7] and, if possible, should be avoided. Incisional biopsy can lead to a continuously draining sinus tract. Indirect immunofluorescent antibody assays[21] are now available commercially and should always be included among the diagnostic criteria, once cat-scratch disease has been proposed. This is especially true in the case of an uncommon clinical presentation or one with an obscure history of animal contact.

Treatment consists mainly of supportive therapy and reassurance, as antibiotics have not been shown to be effective in shortening the course of the disease, despite recent trials with pefloxacin.[22] Up to now, there is still no standard therapy for cat-scratch disease. Rifampin, ciprofloxacin hydrochloride, or trimethoprim-sulfamethoxazole can be considered for cat-scratch disease with severe symptoms, with efficacies of 88%, 84%, and 58%, respectively, in clinical trials.[23] Steroids have not been shown to be effective.[19]

By being alert to a history of animal contact in the presence of unilateral head and neck lymphadenopathy, a discerning clinician can establish a correct diagnosis without reverting to surgery that is probably unnecessary, in the light of an otherwise excellent prognosis, as in our case. The lymphadenopathy usually disappears within 2 to 3 months without complications or sequelae.

REFERENCES

1. Damion J, Hybels RL. The neck mass. 2. Inflammatory and neoplastic causes. Postgrad Med 1987;81:97-100, 103, 106-7.

2. Heroman WM, McCurley WS. Cat scratch disease. Otolaryngol Clin North Am 1982;15:649-58.

3. Thurnheer U, Wiprachtiger U. Katzenkratzkrankheit. Schweiz Rundsch Med Prax 1995;84:122-6.

4. Shinall EA. Cat-scratch disease: a review of the literature. Pediatr Dermatol 1990;7:11-8.

5. Greer WER, Keefer CS. Cat-scratch fever. A disease entity. N Engl J Med 1951;244:545-8.

6. Margileth AM. Cat scratch disease: nonbacterial regional lymphadenitis. The study of 145 patients and a review of the literature. Pediatrics 1968;42:803-18.

7. Margileth AM. Cat scratch disease in 65 patients: evaluation of cat scratch skin test antigens in 109 subjects. Clin Proc Child Hosp Dist Columbia 1971;27:213-23.

8. Travis LW, Hecht DW. Acute and chronic inflammatory diseases of the salivary glands: diagnosis and management. Otolaryngol Clin North Am 1977;10:329-38.

9. Warwick WJ. The cat-scratch syndrome: many diseases or one disease? Prog Med Virol 1967;9:256-301.

10. Bruyn HB. Cat scratch disease in the young adult. J Am Coll Health Assoc 1969;18:169-72.

11. Miura T, Torinurki W, Tanahashi Y. Cat scratch disease. Tohoku J Exp Med 1975;117:373-80.

12. Schulkind ML, Ayoub EM. Cell-mediated immunity in cat-scratch disease. J Pediatr 1974;85:199-203.

13. Kalter SS, Kim CS, Heberling RL. Herpes-like virus particles associated with cat scratch disease [Letter]. Nature 1969; 224:190.

14. Gross BD, Case D. Cat scratch disease. Report of a case. Oral Surg Oral Med Oral Pathol 1977;43:698-701.

15. Margileth AW, Wear DJ, Hadfield TL, Schlagel CJ, Spigel GT, Muhlbauer JE. Cat-scratch disease. Bacteria in skin at the primary inoculation site. JAMA 1984;252:928-31.

16. Jerris RC, Regnery RL. Will the real agent of cat-scratch

disease please stand up? Annu Rev Microbiol 1996;50:707-25.

17. Bergmans AMC, Groothedde J-W, Schellekens JFP, van Embden JDA, Ossewaarde JM, Schouls LM. Etiology of cat scratch disease: comparison of polymerase chain reaction detection of *Bartonella* (formerly *Rochalimaea*) and *Afipia felix* DNA with serology and skin tests. J Infect Dis 1995;171:916-23.

18. Dreher A, Grevers G. Katzenkratzkrankheit. Eine Ubersicht fur den HNO-Arzt. Laryngorhinootologie 1996;75:403-7.

19. Carithers HA, Carithers CM, Edwards RO Jr. Cat-scratch disease. Its natural history. JAMA 1969;207:312-6.

20. Johnson WT, Helwig EB. Cat-scratch disease. Histopathologic changes in the skin. Arch Dermatol 1969;100:148-54.

21. Diaz F, de la Viuda JM, Urkijo JC, Mendoza F. Enfermedad por aranazo de gato. Descripcion de cuatro casos y revision de la literatura. Rev Clin Esp 1997;197:28-30.

22. Patey O, Breuil J, Bouhali R, Roucayrol AM, Chaplain C, Lafaix C. Pefloxacine et maladie des griffes du chat. Pathol Biol (Paris) 1989;37:582-4.

23. Margileth AM. Antibiotic therapy for cat-scratch disease: clinical study of therapeutic outcome in 268 patients and a review of the literature. Pediatr Infect Dis J 1992;11:474-8.

≈

INTERNATIONAL CONFERENCE ON NEWBORN HEARING SCREENING DIAGNOSIS AND INTERVENTION

The International Conference on Newborn Hearing Screening Diagnosis and Intervention will be held in Milan, Italy, October 12-14, 2000. In Europe, contact Dr Ferdinando Grandori, Center of Biomedical Engineering, Polytechnic of Milan, piazza Leonardo da Vinci 32, I-20133 Milan, Italy; fax +39.02.2399.3360; e-mail NHS2000@biomed.polimi.it. In the United States, contact Dr Deborah Hayes, The Children's Hospital, 1056 E 19th Ave, B030, Denver, CO 80218; telephone (303) 861-6424; fax (303) 764-8220; e-mail: Hayes.deborah@tchden.org.

Ann Otol Rhinol Laryngol 109:2000

CLINICAL NOTE

LIPOSARCOMA OF THE TONGUE: CASE REPORT AND LITERATURE UPDATE

YORIHISA ORITA, MD
KAZUNORI NISHIZAKI, MD
TOSHIAKI OGAWARA, MD
ICHIRO YAMADORI, MD
SATOSHI YORIZANE, MD
HIROFUMI AKAGI, MD
YU MASUDA, MD
OKAYAMA, JAPAN

Liposarcoma is an exceedingly rare tumor in the oral cavity. We report a case of a 70-year-old man with liposarcoma that presented as a lump on the tongue. The excised tumor was diagnosed as a well-differentiated lipoma-like liposarcoma. The majority of cases of well-differentiated liposarcoma follow a relatively benign course, but the disease has a high recurrence rate. It appears that accurate clinical and histopathologic diagnosis of this lesion is difficult. The prognosis seems to depend on the histologic type, size, and location of the lesion. Wide surgical excision is important for successful management of these liposarcomas.

KEY WORDS — diagnosis, liposarcoma, prognosis, tongue.

INTRODUCTION

Liposarcomas may arise wherever there is adipose tissue normally present, but the majority occur in the retroperitoneum and deep soft tissue of the proximal aspects of the extremities.[1] Liposarcomas of the oral cavity are exceedingly rare, and fewer than 40 cases have been reported in the literature. Liposarcoma of the tongue was first described by Larson et al[2] in 1976, and to our knowledge, only 6 cases of its occurrence in the tongue have been reported in English at the time of this writing. We now present a case of well-differentiated lipoma-like liposarcoma of the tongue and discuss the disease's clinical and histologic features, histopathologic diagnosis, and patient prognosis in light of the literature.

CASE REPORT

A 70-year-old Japanese man presented at Okayama National Hospital with the chief complaint of saliva-dribbling from the mouth for about 1 month. He did not have any other symptoms, eg, dysgeusia, dysphagia, pain, or a feeling of an enlarging mass. The patient had undergone surgery for total removal of an intracranial meningioma 10 years before. Oral examination showed a 1 × 3.5-cm, slightly yellowish, soft mass on the right lateral border of the tongue (see Figure, A). A biopsy of the tongue surface was done. The surface epithelium and the connective tissue under the epithelium were not remarkable, but a small area of fatty tissue attached under the connective tissue contained some myxomatous matrix and, intermingled among mature adipocytes, many plurivacuolated lipoblasts with enlarged nuclei (see Figure, B). Liposarcoma was considered possible, and a second biopsy of the deep tissue of the tongue was done. The histologic findings were the same, and liposarcoma was highly suspected. The patient subsequently underwent a hemiglossectomy. The cut surface of the resected tongue was almost entirely replaced by a lobulated growth of fatty tissue (see Figure, C). Histologic examination showed that bundles of striated muscle fibers were separated by a lobular proliferation of fatty tissue (see Figure, D). Its infiltration reached the bottom margin of the operated material. The fatty tissue was mainly composed of mature adipocytes simulating a lipoma, but areas with myxomatous matrix or connective tissue contained many plurivacuolated lipoblasts that were of the same morphological type as those in the biopsy specimen. Mitotic figures were not found, but the nuclei of these lipoblasts were atypical. Accordingly, this tumorous lesion was diagnosed as a well-differentiated lipoma-like liposarcoma.

DISCUSSION

Liposarcoma of the oral cavity is very rare and shows a predilection for the cheek, where it presents most commonly as a painless, enlarging mass.[3] The difficulty in clinical and histologic differentiation of lipomatous oral masses has been recognized by several authors.[4-7] Liposarcomas of the head and neck

---

From the Department of Otorhinolaryngology, Okayama University Medical School (Orita, Nishizaki, Akagi, Masuda), and the Departments of Otorhinolaryngology (Ogawara, Yorizane) and Pathology (Yamadori), Okayama National Hospital, Okayama, Japan.

CORRESPONDENCE — Yorihisa Orita, MD, Dept of Otorhinolaryngology, Okayama University Medical School, Shikata-cho 2-5-1, 700-8558, Okayama, Japan.

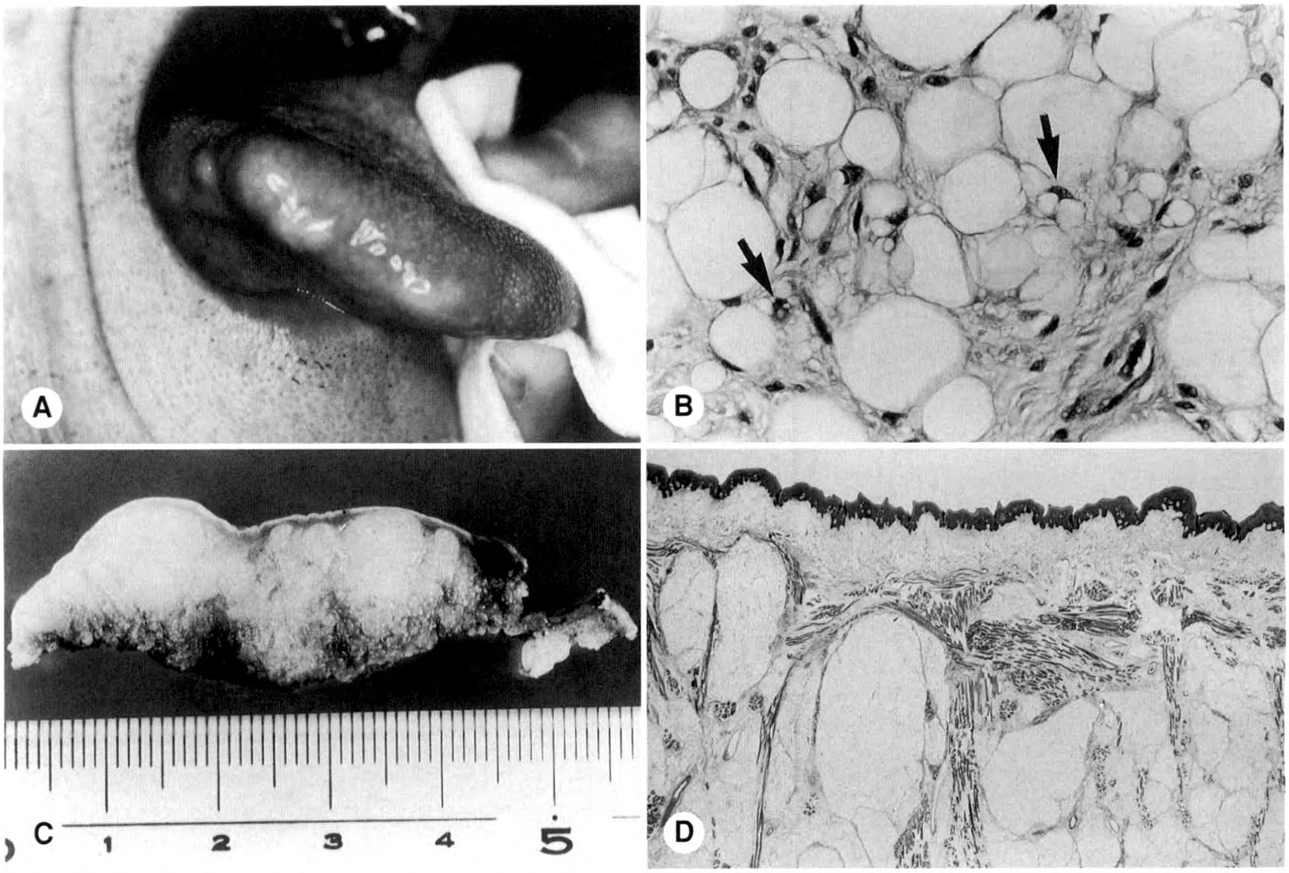

Liposarcoma of tongue. A) Lesion at right lateral border of tongue. B) Histology of biopsy specimen (H & E, original ×132). Fatty tissue contains plurivacuolated lipoblasts with atypical nuclei (arrows). C) Cut surface of resected tongue specimen. Tongue is totally infiltrated by lobular growth of fatty tissue. D) Low-power view of resected tongue (H & E, original ×3.1). Lobular proliferation of adipocytes separates bundles of striated muscle fibers.

seem to have high recurrence rates,[8,9] and the long latent period between the original diagnosis and the first recurrence seems to make it more difficult to give an accurate clinical and histopathologic diagnosis of this lesion.[6,7] Two previous case reports on liposarcoma of the tongue indicated that the first recurrence in 1 case occurred 18 years, and that in the other, 12 years, after the first presentation.[6,7] This tumor must be discriminated from lipoma, neurofibroma, mesenchymoma, angiofibroma, granular cell tumor, myxoma, and irritation fibroma.[6,7,10] Most authors recognize 4 histologic types of liposarcoma

SEVEN LIPOSARCOMAS OF TONGUE

Authors	*Date*	*Age*	*Sex*	*Race*	*Histopathologic Classification*	*Treatment, Size*	*Progress or Prognosis*
Larson et al[2]	1976	42	F	Black	Well differentiated	Hemiglossectomy, 1.5 × 1.5 cm	No follow-up available
Wescott and Correll[6]	1984	61	M	Not specified	Myxoid, well differentiated	Tumor excision, 3.5 × 3.0 × 2.0 cm	First presentation at age 24, recurrences at 42 and 54
Guest[18]	1992	71	M	Not specified	Myxoid, well differentiated	Tumor excision, 1 cm in diameter	No recurrence 2 years after surgery
Minic[3]	1995	68	F	White	Myxoid, well differentiated	Tumor excision, 2.5 × 1.5 × 1 cm	No recurrence 3 years after surgery
Saddik et al[7]	1996	76	M	Not specified	Well differentiated	Tumor excision, 2.5 cm in greatest diameter	First presentation at age 53, recurrences at 65, 67, 71, and 74
Nelson et al[10]	1998	37	M	White	Well differentiated	Tumor excision, 3.0 × 3.0 × 3.0 cm	No recurrence 18 months after surgery
This study	1999	70	M	Japanese	Well differentiated, lipoma-like	Hemiglossectomy, 1 × 3.5 cm	No recurrence 8 months after surgery

following the classification of Stout and Lattes[11]: 1) well-differentiated myxoid liposarcoma; 2) poorly differentiated myxoid liposarcoma; 3) round cell liposarcoma; and 4) mixed-type liposarcoma. Enzinger and Weiss[1] classified liposarcomas into 4 groups: 1) myxoid; 2) round cell; 3) pleomorphic, which was called mixed-type in the Stout and Lattes classification; and 4) well differentiated, which is subclassified into lipoma-like, sclerosing, inflammatory, and dedifferentiated. The well-differentiated myxoid liposarcoma of Stout and Lattes is called lipoma-like or sclerosing liposarcoma in this classification. Most oral liposarcomas are myxoid or well differentiated. Particularly well-differentiated lipoma-like liposarcomas are not infrequently misdiagnosed as lipomas, because of their inconspicuous microscopic atypical changes.[12] On the contrary, lipomas of the tongue may be mistaken for liposarcomas.[13] The only certain method of determining the exact nature of the tumor is histopathologic examination.[14] Because liposarcomas extend by infiltration, immediate good fixation and good biopsy sampling that includes all margins of the lesion are essential for the accurate evaluation of liposarcomas.[15] The characteristics that serve to distinguish an intramuscular lipoma from a liposarcoma are the absence of lipoblastic proliferation, cellular pleomorphism, increased vascularity, and mitotic activity.[13] The most important aspect of the diagnosis of liposarcoma is the positive identification of lipoblasts.[3] Saddik et al[7] proposed that deep adipose tissue neoplasms of the head and neck should be considered malignant even in the absence of unequivocal features of malignancy such as increased mitosis, anaplasia, and dedifferentiation, because they are most likely to behave in a malignant fashion.

Liposarcomas generally behave in accordance with their histologic type.[1] The prognosis of myxoid and well-differentiated forms seems to be better than that of pleomorphic or round cell variants,[1,15] and they do not appear to metastasize,[5] whereas poorly differentiated tumors in adults metastasize in 40% of cases, primarily to the lungs, pleura, liver, and brain.[11] For well-differentiated liposarcomas, wide local excision with a tumor-free margin is recommended,[16] and incomplete excision often leads to local recurrence.[8,9,17] The prognosis of liposarcomas of the oral tissue is generally favorable, most probably because of the dominance of myxoid and well-differentiated varieties, as well as their small size. Wide excision is greatly limited in the oral and maxillofacial regions, because of their cosmetic and physiological importance.[8] Thus, the prognosis of liposarcomas in this region seems to depend on their location and size. In our case, the tumor was relatively large, and the surgical margins seem to have been inadequate. But the patient is being followed without additional excision, because of his age and physiological status, and the slow growth rate typical of the tumor.

Including the current case, only 7 liposarcomas of the tongue have appeared in the literature. Only 2 liposarcomas were followed up long-term (see Table[2,3,6,7,10,18]). All were well differentiated and underwent surgical excision. No metastasis was reported. The average age was 55 years at first presentation of the tumor, with a range from 24 to 71 years. A predilection for males was found. The maximum size of the tumors was 3.5 cm in diameter.

In conclusion, an adipose tissue neoplasm in the oral cavity should undergo complete surgical excision with as wide a margin as possible considering its histologic type, the anatomic region's cosmetic and physiological functions, the patient's age, and the long latent period between the first presentation and the first recurrence.

ACKNOWLEDGMENT — We acknowledge the advice of Dr Kohji Taguchi, Okayama University Medical School, in consultation on the pathology of this case.

REFERENCES

1. Enzinger FM, Weiss SW. Liposarcoma. In: Enzinger FM, Weiss SW, eds. Soft tissue tumors. 3rd ed. St Louis, Mo: CV Mosby, 1995:431-66.
2. Larson DL, Cohn AM, Estrada RG. Liposarcoma of the tongue. J Otolaryngol 1976;5:410-4.
3. Minic AJ. Liposarcomas of the oral tissues: a clinicopathologic study of four tumors. J Oral Pathol Med 1995;24:180-4.
4. Guillou L, Dehon A, Charlin B, Madarnas P. Pleomorphic lipoma of the tongue: case report and literature review. J Otolaryngol 1986;15:313-6.
5. Azumi N, Curtis J, Kempson RL, Hendrickson MR. Atypical and malignant neoplasms showing lipomatous differentiation: a study of 111 cases. Am J Surg Pathol 1987;11:161-83.
6. Wescott WB, Correll RW. Multiple recurrences of a lesion at the base of the tongue. J Am Dent Assoc 1984;108:231-2.
7. Saddik M, Oldring DJ, Mourad WA. Liposarcoma of the base of tongue and tonsillar fossa. A possibly underdiagnosed neoplasm. Arch Pathol Lab Med 1996;120:292-5.
8. Zheng J, Wang Y. Liposarcoma in the oral maxillofacial region: an analysis of 10 consecutive patients. J Oral Maxillofac Surg 1994;52:595-8.
9. Wenig BM, Heffner DK. Liposarcomas of the larynx and hypopharynx: a clinicopathologic study of eight new cases and a review of the literature. Laryngoscope 1995;105:747-56.
10. Nelson W, Chuprevich T, Galbraith DA. Enlarging tongue mass. J Oral Maxillofac Surg 1998;56:224-7.
11. Stout AP, Lattes R. Tumors of the soft tissues. In: Atlas of tumor pathology. Second series, Fascicle 1. Washington, DC:

Armed Forces Institute of Pathology, 1967:116-26.

12. Kingdom LG, Angervall L, Jarlstedt J. Liposarcoma of the neck: a clinicopathologic study of 4 cases. Cancer 1978;42:774-80.

13. Garavaglia J, Gnepp DR. Intramuscular (infiltrating) lipoma of the tongue. Oral Surg Oral Med Oral Pathol 1987;63:348-50.

14. Correll RW, Wescott WB, Potter DM. Nonulcerated, sessile nodule of the lower lip. J Am Dent Assoc 1982;104:206-8.

15. Baden E, Newman R. Liposarcoma of the oropharyngeal region. Oral Surg Oral Med Oral Pathol 1977;44:889-902.

16. Evans HL, Soule EH, Winkelmann RK. Atypical lipoma, atypical intramuscular lipoma, and well differentiated retroperitoneal liposarcoma. Cancer 1979;43:574-84.

17. Das Gupta T. Management of soft tissue sarcomas. Surg Gynecol Obstet 1973;137:1012-3.

18. Guest PG. Liposarcoma of the tongue: a case report and review of the literature. Br J Oral Maxillofac Surg 1992;30:268-9.

≈

FIFTH INTERNATIONAL CONFERENCE ON HEAD AND NECK CANCER

The Fifth International Conference on Head and Neck Cancer will be held July 29–August 2, 2000, in San Francisco, California. For information, contact Concepts in Meetings & Events, Robin L. Wagner, President, 7819 Lloyd Ave, Pittsburgh, PA 15218-1941; telephone (412) 243-5156; fax (412) 243-5160; e-mail: rlwa@med.pitt.edu.

Ann Otol Rhinol Laryngol 109:2000

CLINICAL NOTE

AIRWAY BURNS AND ATELECTASIS IN AN ADOLESCENT FOLLOWING ASPIRATION OF MOLTEN WAX

SHARON EINAV, MD

ITZHAK BRAVERMAN, MD
AVRAHAM AVITAL, MD

IDO YATSIV, MD
MOSHE ROTHSCHILD, MD

JERUSALEM, ISRAEL

Scald injuries caused by hot liquids are not a frequently reported cause of pediatric respiratory and alimentary tract burns. Aspiration of molten wax with subsequent pharyngeal or laryngeal burns has not been described at all, to the best of our knowledge. A case of an adolescent who presented with airway burns and atelectasis subsequent to aspiration of molten wax is herein described and discussed.

KEY WORDS — airway, aspiration, atelectasis, burn, caustic ingestion, scald, thermal injury, wax.

CASE REPORT

An 11-year-old boy had been forming decorative candles by suction of molten wax via a straw when he inadvertently drew a large amount of wax into his mouth and throat. Pain and discomfort upon swallowing appeared immediately. Medical advice was, however, sought only 12 hours later.

Physical examination upon arrival at the emergency room revealed a blood pressure of 90/60 mm Hg, a pulse of 90/min, a rectal temperature of 37.2°C, and a respiratory rate of 32 breaths per minute. The patient was drooling, dysphagic, and aphonic. There were burns on the tongue and hypopharynx. Decreased breathing sounds were auscultated over the base of the left lung.

Laboratory examinations included arterial blood gases and a complete blood count that were normal except for 14,700 white blood cells per square millimeter. Chest radiography demonstrated complete atelectasis of the lingula and left lower lobe.

Indirect laryngoscopy revealed burns on the tongue, supraglottic regions, hypopharynx, and arytenoids. The vocal cords were normal.

Flexible laryngobronchoscopy, performed with a pediatric Olympus 3C20 bronchoscope (3.5-mm external diameter), revealed diffuse edema and irritation of the trachea, burns and edema of the arytenoids, erythema and edema of the epiglottis, and irritation and small burns on the left main bronchus and surrounding the lingular opening (see Figure). There was no evidence of a foreign body or wax throughout the entire upper and lower airways. Multiple lavages were performed via the lingular aperture in order to alleviate the atelectasis.

Nasal fiberoptic intubation was performed with a 5.5-mm–internal diameter tube, and the patient was sedated and mechanically ventilated. Treatment was initiated with intravenous dexamethasone sodium phosphate 0.5 mg/kg per day and cefuroxime sodium 100 mg/kg per day. Follow-up chest radiographs were normal.

Three days later, the boy underwent rigid laryngoscopy and esophagoscopy. Most of the burns were healed, with pale edema of the subglottic area. The child was extubated and discharged a day later. On follow-up a week later, he was completely healthy.

DISCUSSION

Damage to the airways and alimentary tract following ingestion of caustics and smoke inhalation is frequently reported. In a search of the literature we found, however, no more than 2 cases of scald injury as a result of ingestion or aspiration of hot fluids.[1,2] To the best of our knowledge, aspiration of molten wax has never been described.

Early endoscopic evaluation has been shown to aid greatly in determining further management of ingestion of caustic substances.[3,4] In our case, flexible bronchoscopy was performed with the intent of both assessing airway damage and achieving atraumatic prophylactic intubation during direct visualiza-

---

From the Departments of Anesthesia and Critical Care Medicine (Einav), Otolaryngology–Head and Neck Surgery (Braverman), and Pediatric Intensive Care (Yatsiv) and the Institute of Pulmonology (Avital, Rothschild), Hadassah Hebrew University Medical Center, Jerusalem, Israel.

CORRESPONDENCE — Sharon Einav, MD, Hadassah Hebrew University Medical Center, PO Box 12000, Jerusalem, Israel.

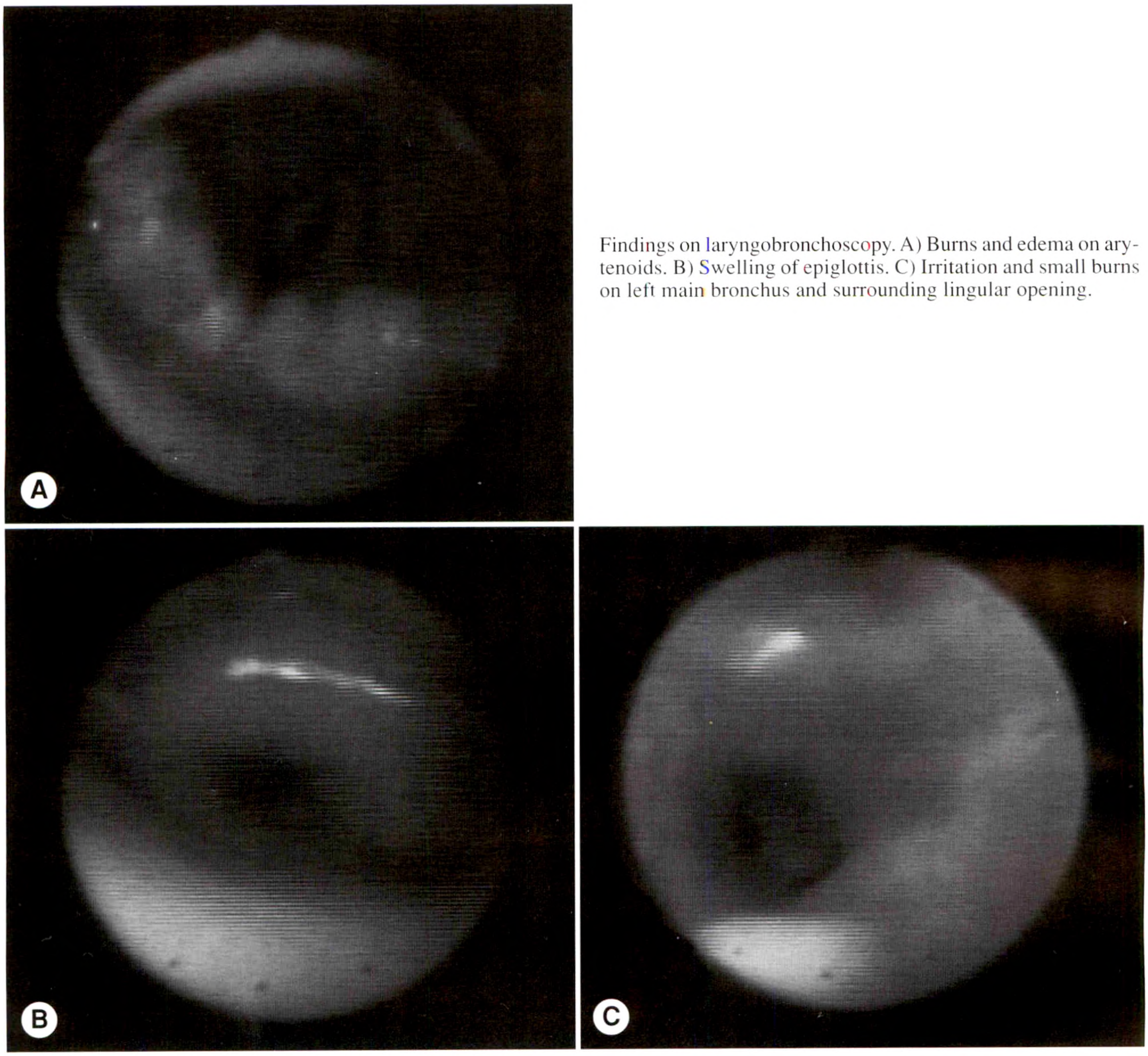

Findings on laryngobronchoscopy. A) Burns and edema on arytenoids. B) Swelling of epiglottis. C) Irritation and small burns on left main bronchus and surrounding lingular opening.

tion of the airway. Because concern was raised as to airway patency, spontaneous ventilation together with minimal irritation of the airway during direct visualization was considered the best option for airway management.

We found that the complications of molten wax aspiration included damage to both upper and lower airways. If left untreated for several hours, upper airway damage may be clinically similar to epiglottitis, with drooling, dysphagia, and stridor. These symptoms are caused by thermal injury of the glottic region, with superficial and deep burns, edema, and erythema of the arytenoids and epiglottis.

Upper airway obstruction has been described after caustic ingestion.[5] After smoke inhalation, upper airway burns warrant almost routine prophylactic intubation because of the risk of severe resultant edema and obstruction. In our case, the tube inserted was at least 1 mm (internal diameter) smaller than those usually inserted at this age — proof of already existing airway edema. We believe this edema was related to thermal injury caused by hot wax fumes. Steroid treatment was initiated in order to decrease the edema.

Additional damage along the lower airway may manifest either as burns and ulcerations or as foreign body obstruction. In the case of burns or ulcerations, resultant edema may also cause secondary obstruction of the lower airways. Foreign body obstruction may result from accumulation of debris or reactive secretions, as in smoke inhalation.

A unique theoretical complication of wax in the airway is the possibility of late coagulation of the molten wax with airway obstruction. Should wax coagulate in small airways that are inaccessible to a bronchoscope, this may become a more serious problem. As no wax was found within the bronchial tree during our bronchoscopy, we believe that the atelectasis in this case was due to thermic and chemical irritation from wax fumes that caused profuse secretions and edema of the bronchus. Insertion of the fiberoptic bronchoscope reopened the bronchus and enabled lung ventilation. Further maintenance of positive airway pressure with ongoing ventilation prevented recurrent obstruction and collapse. Fluid aspiration could not be excluded under the circumstances; however, no evidence of particulate matter was found. Antibiotic treatment was initiated because of the time interval between aspiration and referral for treatment.

Wax fumes have been implicated in a decreased carbon monoxide diffusion capacity persisting for at least 24 hours in cross-country skiers.[6] In the same study, dynamic and static lung volumes remained the same. Blood gases were not disturbed in our case. No attempt was made to evaluate pulmonary volumes, because the patient was intubated in order to preserve the airway and placed on a respirator.

To summarize, aspiration of molten wax should probably be considered a combination of smoke inhalation and hot fluid scald. We recommend rapid flexible laryngobronchoscopy in order to evaluate the extent of damage and clear the bronchial tree of debris and secretions. Should clinical examination or bronchoscopy findings give rise to doubt as to later airway patency, prophylactic intubation is recommended. The benefit of ventilation with positive end expiratory pressures should be weighed against the possibility of barotrauma. Treatment with steroids is recommended when significant airway edema is present.

REFERENCES

1. Garland JS, Rice TB, Kelly KJ. Airway burns in an infant following aspiration of microwave-heated tea. Chest 1986;90: 621-2.
2. Sente M, Rakic N. Hot water burns of the upper aerodigestive tract. Med Pregl 1991;44:233-5.
3. Zargar SA, Kochhar R, Nagi B, Mehta S, Mehta SK. Ingestion of corrosive acids. Spectrum of injury to upper gastrointestinal tract and natural history. Gastroenterology 1989;97: 702-7.
4. Sugawa C, Lucas CE. Caustic injury of the upper gastrointestinal tract in adults: clinical and endoscopic study. Surgery 1989;106:802-7.
5. Moulin D, Bertrand JM, Buts JP, Nyakabasa M, Otte JB. Upper airway lesions in children after accidental ingestion of caustic substances. J Pediatr 1985;106:408-10.
6. Knopfli B, Gutensperger U, Schibler A, Villiger B. Acute deterioration of the CO diffusion capacity following exposure to ski wax vapors. Schweiz Rundsch Med Prax 1992;81:884-7.

Ann Otol Rhinol Laryngol 109:2000

IMAGING CASE STUDY OF THE MONTH

INTERNAL CAROTID ARTERY ANEURYSM PRESENTING AS A LARGE PHARYNGEAL MASS

TOMOKAZU YOSHIZAKI, MD
OSAMU MATSUI, MD
SHIGEKAZU TERANISHI, MD
MITSURU FURUKAWA, MD

KANAZAWA, JAPAN

INTRODUCTION

Aneurysms of the extracranial internal carotid artery (ICA) are rare. We report a case of an ICA aneurysm that presented as a large mass extending from the nasopharynx to the hypopharynx. A 3-dimensional (3-D) computed tomography (CT) scan revealed the striking appearance of this giant aneurysm. The patient was successfully treated with coil embolization of the ICA. Although rare, aneurysms should be considered in the differential diagnosis of a carotid space mass. Three-dimensional CT scanning is noninvasive and useful for discerning the entire structure of ICA aneurysms.

CASE REPORT

A 46-year-old woman was referred to the otolaryngology unit from an outside institution for evaluation of a large pharyngeal mass with pulsation. There was no evidence of cranial nerve palsy. Review of the cervical CT scan showed a large parapharyngeal space mass with dramatic enhancement (Fig 1). At that time, the ICA could not be observed in its usual location.

Three-dimensional reconstruction of the CT scan demonstrated an ellipse-shaped parapharyngeal aneurysm that was sequential to the ICA (Fig 2). Although a conventional arteriogram also showed similar findings, the shape of the aneurysm was not as clearly defined as on the 3-D CT scan (Fig 3). The patient was neurologically intact and had no evidence of ischemic symptoms from embolization of the aneurysm. Large and irregular enhancement of the lumen of the aneurysm indicated the existence of a thrombus. Surgical resection of the aneurysm would

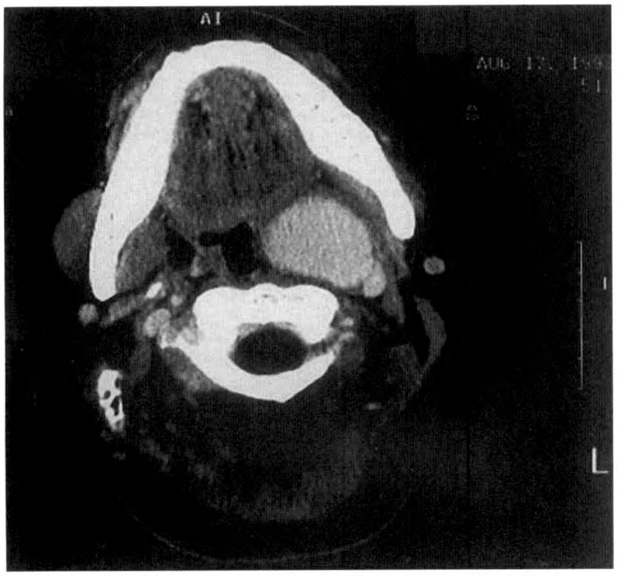

Fig 1. Axial contrast computed tomography (CT) scan at level of mandibular angle before coil embolization. High-signal mass is detected at carotid lesion.

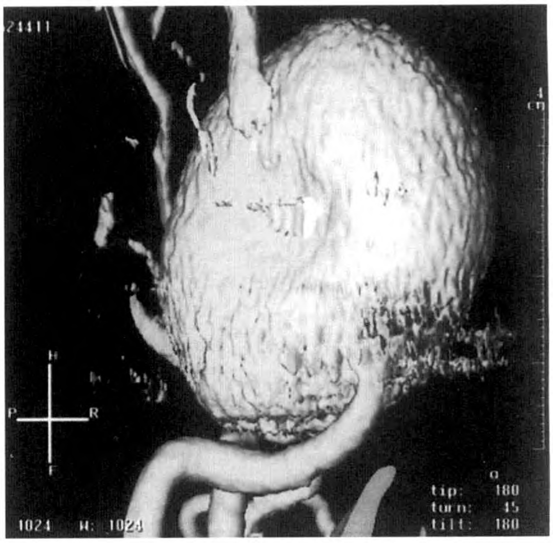

Fig 2. Lateral view of 3-dimensional reconstruction of mass depicted in Fig 1.

From the Departments of Otolaryngology (Yoshizaki, Teranishi, Furukawa) and Radiology (Matsui), School of Medicine, Kanazawa University, Kanazawa, Japan.

CORRESPONDENCE — Tomokazu Yoshizaki, MD, Dept of Otolaryngology, School of Medicine, Kanazawa University, 13-1 Takaramachi, Kanazawa, 920-0934, Japan.

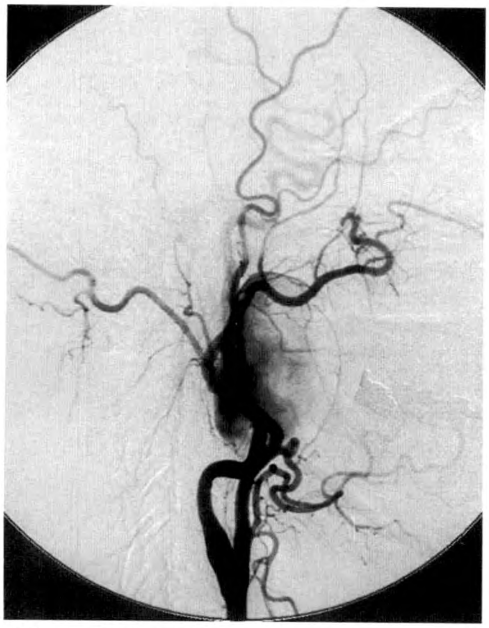

Fig 3. Lateral view of left common carotid angiogram. Lumen of aneurysm is irregularly depicted.

have required exposure of multiple cranial nerves and removal of the skull base. A balloon occlusion Matas' test showed no neurological change.

These clinical factors led us to plan a coil embolization of this aneurysm for the prevention of rupture and cerebral infarction. To avoid iatrogenic spread of thrombus while passing a catheter through the lumen of the aneurysm, we embolized only the proximal end of the aneurysm with titanium coils. Two weeks after coil embolization, a follow-up CT scan demonstrated satisfactory obliteration of the lumen of the aneurysm (Fig 4). There have been no symptoms of cerebral infarction in 18 months of observation.

DISCUSSION

Aneurysms of the extracranial ICA are rare. Houser and Baker[1] found only 8 extracranial aneurysms in their study of 5,000 carotid arteriograms. Today, most patients who had a large cervical mass would be examined with CT scans and magnetic resonance imaging. The differential diagnosis of a carotid space mass is relatively limited. The most common are schwannomas arising from cranial nerves IX, X, or XI or from a sympathetic nerve. Schwannomas are typically identified posterior to the carotid artery. A carotid body tumor or vagal paraganglioma may present as a carotid space mass. Carotid body tumors are usually in the vicinity of the carotid bifurcation and between the ICA and the external carotid artery. Vagal paragangliomas typically are located between the ICA and the jugular vein.[2] Although most head and neck surgeons would consider the equally uncommon carotid body tumor in their differential diagnosis of a hypervascular and pulsating neck mass, few would consider a carotid artery aneurysm. Therefore, most extracranial ICA aneurysms have been diagnosed from arteriograms. Although arteriography remains the gold standard for establishing the diagnosis of extracranial ICA aneurysm, it is less helpful in determining the entire extent of an aneurysm, especially in the case of an aneurysm with a thrombus. Three-dimensional reconstruction of a CT scan visualizes the external surface shape regardless of the endoluminal condition of the aneurysm, and is unequivocally less invasive than conventional catheter arteriography. Head and neck surgeons should be aware of the diagnostic value of 3-D CT scanning whenever a pulsating cervical mass is encountered.

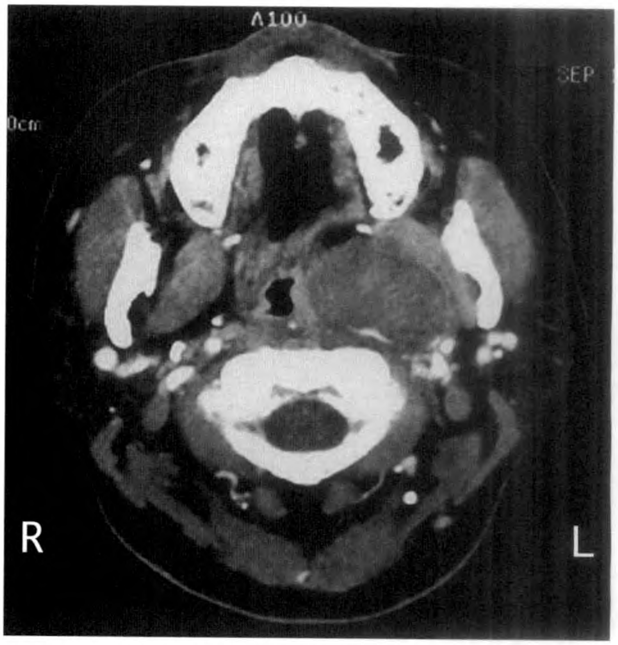

Fig 4. Axial contrast CT scan at level of mandibular angle after coil embolization. Lumen of aneurysm is well thrombosed.

The decision to use endoluminal coil embolization rather than perform open surgery was based mainly on the difficulty of exposing the ICA between the aneurysm and the skull base. According to recent ICA aneurysm reports, most cases have been treated with endoluminal embolization after an occlusion Matas' test.[3,4] Although endoluminal manipulation has the risk of spreading thrombus, the possibility was considered to be remote as long as the coils were placed in the portion of the ICA proximal to the aneurysm. A follow-up CT scan of this patient showed successful obliteration of the lumen of the aneurysm.

According to the literature, trauma seems to be the most common cause of cervical carotid artery aneurysm. Alternatively, infection, arteriosclerosis, fibromuscular dysplasia, Ehlers-Danlos syndrome, and radiotherapy are also reported causes.[5-7] The patient's history of tonsillectomy led us to suspect that an ICA might have been damaged by the operation.

In summary, aneurysm should always be considered in the differential diagnosis of a carotid space mass. Three-dimensional reconstruction of a CT scan offers beneficial information for the diagnosis of ICA aneurysms.

REFERENCES

1. Houser OW, Baker HL. Fibromuscular dysplasia and other uncommon diseases of the cervical carotid arteries. Am J Roentgenol 1968;104:201-12.

2. Kyriakos M. Pathology of selected soft tissue tumors of the head and neck. In: Thawley SE, Panje WR, eds. Comprehensive management of head and neck tumors. 1st ed. Vol 2. Philadelphia, Pa: WB Saunders, 1987:1241-97.

3. Sorimachi T, Takeuchi S, Koike T, Minakawa T, Tanaka R. Intra-aneurysmal pressure changes during angiography in coil embolization. Surg Neurol 1997;48:451-7.

4. Komiyama M, Yasui T, Nishikawa M. Endovascular treatment of an extracranial internal carotid artery aneurysm at the skull base with mechanically detachable coils. Neurol Med Chir 1995;35:745-8.

5. Lyons AJ, Barker CS, Flood TR. Carotid aneurysm: a rare cause of cervical swelling. J Oral Maxillofac Surg 1997;55:77-9.

6. Cunningham MJ, Rueger RG, Rothfus WE. Extracranial carotid artery aneurysm: an unusual neck mass in a young adult. Ann Otol Rhinol Laryngol 1989;98:396-9.

7. McCollum CH, Wheeler WG, Noon GP, DeBakey ME. Aneurysms of the extracranial carotid artery: twenty-one years' experience. Am J Surg 1979;137:196-200.

≈

EUROPEAN ACADEMY OF FACIAL PLASTIC SURGERY

The annual meeting of the European Academy of Facial Plastic Surgery will be held September 15-17, 2000, in Thessaloniki, Greece. For information, contact Prof Dr J. Daniilidis, ENT Dept, Aristotelian University of Thessaloniki–AHEPA Hospital, 540 06 Thessaloniki, Greece; telephone 0030/31/994.761-2; fax 0030/31/994.916.

Ann Otol Rhinol Laryngol 109:2000

CLINICOPATHOLOGICAL CONSULTATION

BURKITT'S LYMPHOMA: HISTORICAL BACKGROUND AND RECENT INSIGHTS INTO CLASSIFICATION AND PATHOGENESIS

ANTONINO CARBONE, MD
AVIANO, ITALY
VINCENZO CANZONIERI, MD
AVIANO, ITALY
ANNUNZIATA GLOGHINI, PHD
AVIANO, ITALY
ALESSANDRA RINALDO, MD
UDINE, ITALY
GIANLUCA GAIDANO, MD, PHD
NOVARA, ITALY
ALFIO FERLITO, MD
UDINE, ITALY

In this paper, the authors evaluate the historical evolution of the definition of Burkitt's lymphoma (BL) and of its clinicoepidemiological (endemic, sporadic, and acquired immunodeficiency syndrome–associated BL) and morphological variants. On the basis of the morphological, immunologic, genetic, and clinical characteristics of these tumors, the authors also emphasize the importance of precise disease definitions for biological and epidemiological studies. These principles were used in accordance with the Revised European-American classification of lymphoid neoplasms (REAL), which proposed that disease entities should be defined by a constellation of pathobiological and clinical features.

INTRODUCTION

It is now widely recognized that Burkitt's lymphoma (BL) occurs 1) in East Africa (endemic form; eBL); 2) outside Africa (sporadic [American] form; sBL); and 3) in the human immunodeficiency virus (HIV) setting (acquired immunodeficiency syndrome [AIDS]–associated form; AIDS-BL). However, it has been pointed out that not all cases derived from Africa should be considered eBL because of their geographic location.[1] Also, there is no reason to suppose that sBL does not occur in endemic areas. Moreover, the high prevalence of HIV infection in Africa may determine a high percentage of AIDS-BL, probably unrelated to the endemic form.[1]

Cases of sBL usually occur in North America and Europe, where sBL accounts for approximately one third of pediatric lymphomas. Cases of eBL occur primarily in equatorial Africa and Papua–New Guinea, where BL accounts for approximately 50% of childhood cancer. Although sBL and eBL display many morphological similarities, the 2 epidemiological BL variants differ in their natural history and clinical behavior, particularly with respect to the involvement of body sites.[2] Further clinical heterogeneity of BL is due to the fact that some cases present with massive involvement of the bone marrow and peripheral blood. Such cases had been traditionally termed acute lymphoblastic leukemia (ALL), L3 type, according to the FAB (French-American-British) classification of ALL. In the past few years, however, several investigators have stated that such leukemic cases should be classified as BL because of their biological features and their response to therapy. In 1994, the revised European-American classification of lymphoid neoplasms (REAL) formally acknowledged that L3-ALL and classic BL represent different manifestations of the same disease.[2]

The present review is aimed at providing a general excursus on classic BL and on morphologically related malignancies. The commentary has also been addressed to the head and neck localization of these lymphomas.

HISTORICAL BACKGROUND

The first reference to jaw tumors in children is found in the clinical records of the first missionary hospital in the Mengo district of Kampala (Uganda) and dated around 1904.[3] In a period of about 50 years, other meaningful reports from the "Gold Coast" and the "Belgian Congo" by Edington[4] and Thijs[5] were related to "maxillary lymphosarcomas in young children," "reticulum cell sarcomas," and "atypical round cell sarcomas of the jaw." However, the first exhaustive description of the clinical features of these tumors was published in 1956 by De Smet,[6] who described cases of maxillary, orbital, paraspinal, and intra-abdominal lymphosarcomas consistent with the morphology of BL.

From the Division of Pathology, Centro di Riferimento Oncologico, National Cancer Institute, Aviano (Carbone, Canzonieri, Gloghini), the Department of Otolaryngology–Head and Neck Surgery, University of Udine, Udine (Rinaldo, Ferlito), and the Division of Internal Medicine, Department of Medical Sciences, "Amedeo Avogadro" University of Eastern Piedmont, Novara (Gaidano), Italy. This work has been supported in part by the Ministero della Sanità, Istituto Superiore di Sanità, AIDS projects 1998, Rome, Italy, and by the Associazione Italiana per la Ricerca sul Cancro, Milan, Italy.

CORRESPONDENCE — Alfio Ferlito, MD, Dept of Otolaryngology–Head and Neck Surgery, University of Udine, Policlinico Città di Udine, Viale Venezia 410, 33100 Udine, Italy.

The entity now recognized as BL was reported as a sarcoma of the jaw of African children by Dennis Burkitt,[7] a British surgeon practicing in Uganda in 1958, and identified as a non-Hodgkin's lymphoma (NHL) by O'Conor and Davies[8] 2 years later. In 1965, O'Conor et al[9] and Dorfman[10] independently reported childhood lymphoma cases resembling "Burkitt tumor" in the United States, suggesting that this lymphoma may occur sporadically outside East Africa. One year later, Wright[11] in England and Vecchione and Landi[12] in Italy reported 2 European cases of this tumor.

After these observations were made, reports of this lymphoma from many countries were published, with confusing and conflicting results.[13] Therefore, in 1967, an expert committee commissioned by the World Health Organization (WHO) conducted an objective study of cases gathered from Africa and other continents to establish whether this tumor was a clinical syndrome, a clinicopathological syndrome, or a pathological entity.[13] The committee established that "Burkitt's tumor" is a pathological entity with cytologic features distinct from those of other poorly differentiated lymphomas; it was recommended that the tumor be termed "malignant lymphoma, undifferentiated, Burkitt's type."[14]

Fifteen years later, Doll and List[15] reported the first case of undifferentiated lymphoma resembling, or identical to, BL in a male homosexual with infections; Ziegler et al,[16] independently, reported that homosexual men with AIDS have an increased incidence of BL. After these observations were made, the association between aggressive lymphomas, predominantly BL, and HIV infection was recognized in the United States and in Europe.[17-21]

TERMINOLOGY AND MORPHOLOGICAL CLASSIFICATION

In the original Rappaport[22] classification of NHL, dated 1966, BLs were included in the group "undifferentiated cell type" because of the predominance of cells showing no appreciable lymphocytic or histiocytic differentiation. The term "undifferentiated" was used to denote a pathological, rather than a biological, concept. Lukes and Collins[23] suggested that BL was of follicular center cell origin and proposed the term small noncleaved cell (SNC) lymphoma to define this entity.

In the International Working Formulation classification for clinical usage (WF), BL was called SNC lymphoma,[24] according to the Lukes and Collins[23] terminology. The SNC lymphoma group of the WF[24] includes 2 main pathological variants: Burkitt's and non-Burkitt's lymphomas. The case is subclassified as Burkitt's-type when it satisfies the morphological criteria for BL as published by the WHO in 1969[14] (Fig 1A). This variant was called "without plasmablastic differentiation" by Lennert's group.[25] Although the boundaries between the 2 morphological variants of SNC lymphomas are not sharp, the other main subtype, ie, non-Burkitt's SNC, may be recognized by its cellular heterogeneity, variations in nuclear size, and presence of large nucleoli (Fig 1B). This variant was interpreted as BL "with plasmablastic differentiation" by Lennert's group.[25] Burkitt's lymphoma was removed from the B-lymphoblastic category of the original Kiel classification and included separately as a morphologically and immunophenotypically distinct entity in the updated classification.[26]

Subsequently, the REAL classification recognized the non-Burkitt's type of SNC lymphoma, also named BL with plasmablastic differentiation, as a provisional entity under the comprehensive term of Burkitt's-like lymphoma.[2] This category includes a group of lymphomas that usually occur in the setting of AIDS and feature cell sizes and morphological characteristics intermediate between BL variants and diffuse large cell lymphoma (DLCL).

The chronicle of BL classification has not come to an end. A new WHO classification for hematologic malignant neoplasms is being developed under the auspices of the Society for Hematopathology and the European Association of Hematopathology. A preliminary comprehensive scheme of this classification has recently appeared in a progress report by members of the Steering Committee.[27] The main principles of the proposed system are derived from the REAL classification, because the morphological, immunophenotypic, genetic, and clinical features define the individual pathological entities. As a result, some provisional entities of the REAL classification have been revised with the intent of eliminating diagnostic uncertainties. One of these provisional entities was the category of Burkitt's-like lymphomas; with this classification, a fraction of Burkitt's-like lymphomas would be included either in the BL category or in the large cell (centroblastic or immunoblastic) lymphoma group as atypical BL variants (Fig 1C). The case separation would mainly rely on the size, shape, and morphological features of the neoplastic cells. The immunophenotypic and genetic characteristics of the tumor clone may also be used as discriminating features.

MORPHOLOGICAL FEATURES AND DIAGNOSIS

The Table[2,14,24,27] summarizes the morphological definitions adopted by various classifications for clas-

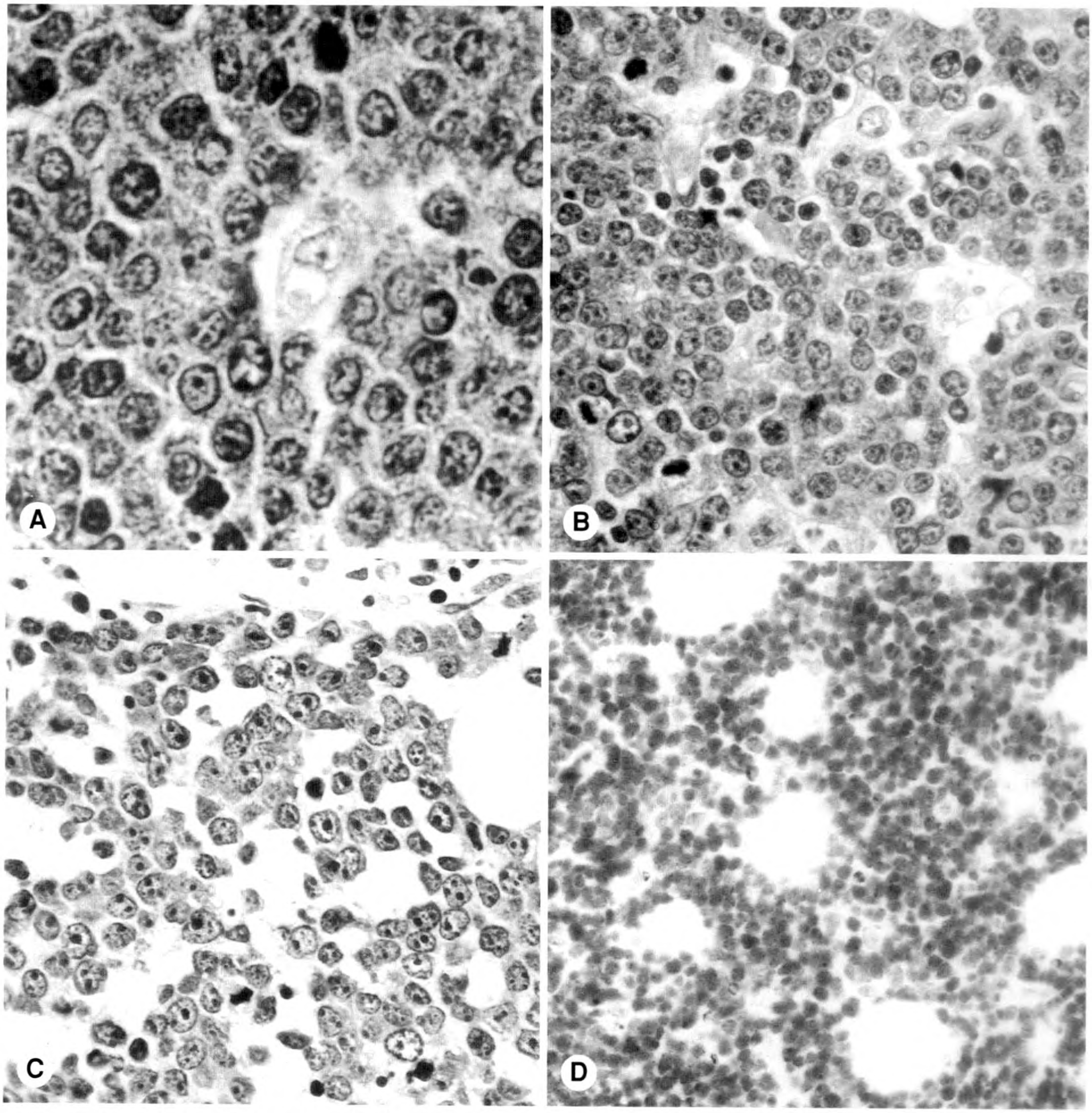

Fig 1. Histopathological specimens. A) Classic Burkitt's lymphoma (Giemsa staining, original ×1,000, oil immersion). Tumor consists of homogeneous proliferation of medium-sized cells displaying cohesive pattern. Tumor cells have round nuclei, multiple centrally located nucleoli, and limited basophilic cytoplasm. Macrophage is present at center of field. B) Small noncleaved cell lymphoma, non-Burkitt's type (H & E, original ×630). Tumor shows cohesive pattern and consists of medium-sized cells displaying morphological heterogeneity. Cells resembling centroblasts can be recognized. C) Burkitt's-lymphoma–like tumor (atypical variants; H & E, original ×630). Tumor cell population is mainly composed of medium-sized cells resembling centroblasts or immunoblasts. D) Classic Burkitt's lymphoma (alkaline phosphatase–anti–alkaline phosphatase method, original ×250). Most tumor cells express BCL-6 protein. Staining pattern is nuclear.

sic BL and BL variants. The histologic pattern of classic BL is characterized by diffuse cellular infiltration of small-to-medium neoplastic cells with obliteration of normal tissue structure, and a "starry-sky" background due to reactive histiocytes[23,24]; neoplastic follicles may be identified in some cases. The nuclei of neoplastic cells are of the same size as or smaller than those of reactive histiocytes. They are round and uniform, with distinct and prominent nuclear membranes, and usually exhibit fine granular chromatin, 2 to 5 small but distinct nucleoli, and a large number of mitotic figures. The cytoplasm is small or medium in size, with cohesive cell borders (Fig 1A).

The non-Burkitt's SNC (Burkitt-like) lymphomas include histologic variants that may be closely related to Burkitt's-type SNC and histologic variants resembling large cell lymphoma[28] (Fig 1B,C). Small

MORPHOLOGICAL DEFINITION ADOPTED FOR CLASSIC BL AND BL VARIANTS BY WF AND REAL CLASSIFICATIONS FOR NON-HODGKIN'S LYMPHOMAS AND BY WHO PROPOSAL

- Classic BL[14]
    - Homogeneous proliferation of medium-sized cells
    - Round nuclei
    - Multiple centrally located nucleoli
    - Limited basophilic cytoplasm
    - Cohesive pattern
    - Starry-sky appearance
- Burkitt's-like lymphoma (REAL)[2]
    - Cell size and nuclear morphology intermediate between those of typical Burkitt's lymphoma and typical large cell lymphoma
    - High proliferation rate
    - With or without starry-sky pattern
- SNCCL, non-Burkitt's type (WF)[24]
    - Cohesive pattern
    - Medium-sized cells
    - Morphological heterogeneity
    - Cells resembling centroblasts or immunoblasts with plasma cell differentiation
- Burkitt's-lymphoma–like (atypical) variants (WHO)[27]
    - Medium-sized cells resembling small centroblasts or immunoblasts
    - High growth fraction
    - Starry-sky pattern

BL — Burkitt's lymphoma; WF — Working Formulation Classification; REAL — Revised European-American Classification of Lymphoid Neoplasms; WHO — World Health Organization; SNCCL — small noncleaved cell lymphoma.

noncleaved cell non-Burkitt's lymphomas contain SNCs, but large noncleaved cells are present as well, in addition to a greater nuclear variability (pleomorphism and multinucleation), with nuclei containing 1 or 2 eosinophilic large nucleoli.[29] According to the REAL classification, the cell size and nuclear morphological characteristics of Burkitt's-like lymphoma are intermediate between those of typical BL and those of typical large cell lymphoma; further, Burkitt's-like lymphomas show a high proliferative rate and may or may not have a starry-sky pattern[2] (Fig 1B,C). In 1987, an "ultrastructural morphometric and immunophenotypic" study of BL and Burkitt's-like lymphoma focused on the morphophenotypic similarities and dissimilarities useful in making a clinically relevant distinction between the 2 entities.[30] Interestingly, the only effective discriminator was the number of nucleoli, ie, BLs usually have multiple nucleoli, and Burkitt's-like lymphomas have only 1 centrally located nucleolus.[30]

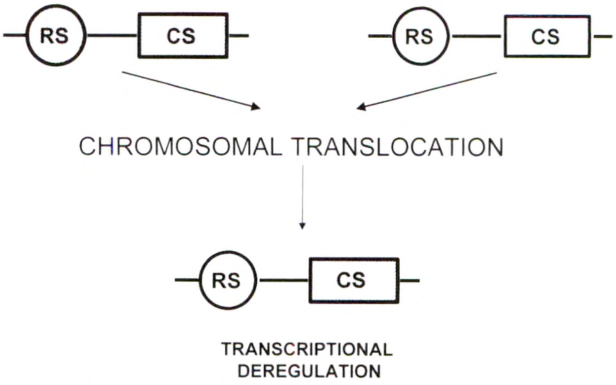

Fig 2. Model of chromosomal translocations in non-Hodgkin's lymphoma. Two genes involved in translocation are represented by relative coding sequences (CS), identified by rectangle, and by regulatory sequences (RS). Two genes are identified by different colors (white boxes versus hatched boxes). Germline configuration of 2 genes is shown in upper part of Figure. Coding sequence of each gene is proximal to its physiological regulatory elements, which coordinate normal expression of gene. As effect of chromosomal translocation, normal regulatory sequences of proto-oncogene (in this case, white gene) are removed and substituted with regulatory sequences derived from partner chromosome. In B-cell non-Hodgkin's lymphoma, novel regulatory sequences most commonly derive from immunoglobulin genes.

IMMUNOLOGIC FEATURES

Immunologic studies have shown that BLs are B-cell lymphomas with light chain restriction; moreover, the selective involvement of germinal centers (GCs) in a percentage of cases of these lymphomas has suggested a relation to GCs.[31,32] This linkage has been strengthened by the recently observed association between AIDS-BL and the expression of BCL-6 (Fig 1D), a protein selectively expressed by GC B-cells.[33,34]

Immunophenotypic findings in BL include constancy of B-cell antigen expression (CD19+, CD20+, CD22+, CD74+, CDw75+, CD79a+); frequent expression of Ia antigens and CD10; absence or low expression of LFA1/CD11a and LFA3/CD58; and absence of CD5, CD43, and CD23.[35-39] Compared to other high-grade B-cell tumors, BL manifests a much higher incidence of surface immunoglobulin expression of μ or heavy chains.[30,35]

The immunophenotypic profiles of all epidemiological BL variants are similar overall, with the exception of CD45RO, which is expressed at higher frequency in AIDS-BL than in other epidemiological BL variants.[40]

On the other hand, some differences between BL and Burkitt's-like lymphoma emerge. Burkitt's lymphomas demonstrated more consistent CD10 expression; moreover, they are largely of the μ isotype, without evidence of further heavy chain switching to γ or α,[30,35] whereas Burkitt's-like lymphomas frequently demonstrated α heavy chain switch, like large cell lymphomas.[35]

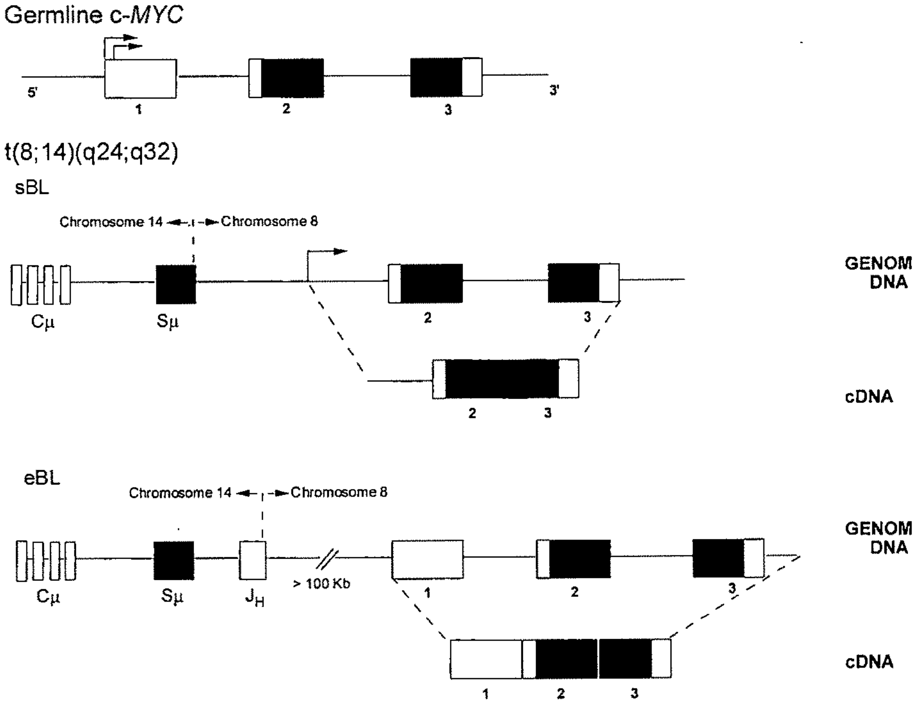

Fig 3. Schematic representation of chromosomal translocations involving c-*MYC* gene. In its germline configuration (upper panel), c-*MYC* is composed of 3 exons. Coding region of c-*MYC* is indicated by black boxes, and noncoding exons (or portions of exons) are indicated by white boxes. c-*MYC* promoters are indicated by arrows. Molecular consequences of most frequent c-*MYC* translocation, ie, t(8;14), are depicted in middle and lower panels. Two molecular subtypes of t(8;14) are recognized, which tend to associate with sporadic Burkitt's lymphoma (sBL; middle panel) and endemic Burkitt's lymphoma (eBL; lower panel), respectively. For each molecular subtype of t(8;14), both genomic configuration and resulting complementary DNA (cDNA) of representative translocated c-*MYC* allele are shown. In case of t(8;14) of sBL (middle panel), chromosome 8 breakpoint involves sequences within c-*MYC*, which is deprived of its exon 1. Because physiological promoters are removed by translocation, transcription is driven by otherwise silent promoter located within c-*MYC* intron 1 (indicated by arrow in Figure). On chromosome 14, breakpoint maps in proximity of switch μ (Sμ) region. Notably, translocation leaves intact gross configuration of coding sequence of c-*MYC*. However, at nucleotide level, c-*MYC* translocated alleles frequently harbor point mutations within exon 2 coding sequence, leading to amino acid substitutions in c-*MYC* protein. cDNA encoded by translocated c-*MYC* alleles includes exons 2 and 3 of gene, as well as abnormally transcribed sequence of intron 1 starting from novel transcriptional initiation site within c-*MYC* intron 1. Because c-*MYC* coding region is intact, normal-size c-*MYC* protein is translated by t(8;14) of sBL. In case of t(8;14) of eBL (lower panel), c-*MYC* breakpoint involves sequences on chromosome 8 at undefined distance (>100 kb) 5' to c-*MYC* and sequences on chromosome 14 within or in proximity to Ig JH region. Internal genomic configuration of translocated c-*MYC* allele is thus apparently preserved.

GENETIC FEATURES AND MOLECULAR PATHOGENESIS

Sporadic and Endemic Forms. All the clinicoepidemiological variants of BL, including sBL, eBL, and L3-ALL, consistently share a common genetic background represented by chromosomal translocations of c-*MYC* and 1 of the immunoglobulin loci. Other genetic lesions associate at variable frequencies with cases of BL and include infection of the tumor clone by Epstein-Barr virus (EBV) and mutations of *p53*.

Chromosomal breaks at 8q24 are found in 100% of cases of sBL, eBL, and L3-ALL.[2] Chromosomal breaks at 8q24 share the common denominator of NHL translocations, ie, the presence of a proto-oncogene mapping to the proximity of the chromosomal recombination site. The translocations alter the expression pattern of the target proto-oncogene by juxtaposing it to heterologous regulatory sequences derived from the partner chromosome, a mechanism called proto-oncogene deregulation (Figs 2 and 3). The heterologous regulatory regions responsible for proto-oncogene deregulation derive from antigen receptor loci and are consistently characterized by high levels of expression in the normal cellular population from which lymphoma is thought to arise. In BL, all 8q24 breaks lead to a common final consequence, ie, deregulation of the expression of the c-*MYC* proto-oncogene.[41] The product of the c-*MYC* proto-oncogene is a ubiquitously expressed nuclear phosphoprotein that functions as a transcriptional regulator controlling cell proliferation, differentiation, and apoptosis. Depending on the Ig locus involved, the c-*MYC* gene may be involved in 3 distinct translocations (Fig 3).[41-46] In 80% of cases, the translocation involves IgH, leading to t(8;14)(q24;q32). In the remaining 20% of cases, c-*MYC* juxtaposes either to Igκ, leading to t(2;8)(p11;q24) (15% of cases), or to

Igλ, leading to t(8;22)(q24;q11) (5% of cases). Throughout the spectrum of B-cell neoplasms recognized by the REAL classification, breaks at 8q24 selectively cluster with all BL variants, whereas they are virtually absent in all other NHL categories.[2]

The common functional effect of t(8;14), t(2;8), and t(8;22) is that c-*MYC* translocated alleles undergo constitutive expression in tumor cells, whereas in physiological conditions, c-*MYC* levels are tightly regulated during B-cell proliferation and differentiation.[47-49]

Several lines of experimental evidence document that the deregulated expression of c-*MYC* can influence the growth of B-cells in vitro and in vivo. In vitro, the expression of c-*MYC* oncogenes transfected into EBV-immortalized human B-cells, a potential natural target for c-*MYC* activation in EBV-positive BL, leads to their malignant transformation.[50] In addition, antisense oligonucleotides directed against translocated c-*MYC* alleles are able to reverse the tumorigenicity of BL.[51,52] In vivo, the targeted expression of c-*MYC* oncogenes in the B-cell lineage of transgenic mice leads to the development of B-cell malignancies at a very high rate.[53]

In addition to c-*MYC* translocations, the molecular pathogenesis of BL also involves infection of the tumor clone by EBV, inactivation of the *p53* tumor suppressor gene, and deletions of 6q. Infection by EBV occurs in virtually all cases of eBL and in approximately 30% of cases of sBL.[54,55] The precise pathogenetic significance of EBV infection in BL is not clearly understood. On the one hand, the consistent monoclonality of EBV infection in BL, as assessed by molecular analysis of EBV terminal repeats, suggests that infection precedes clonal expansion of the tumor, consistent with a pathogenetic role of the virus.[56] On the other hand, however, BL cells fail to express the EBV-encoded antigens LMP-1 (latent membrane protein–1) and EBNA-2 (EBV nuclear antigen–2), which are transforming for B-cells.[54,55] Inactivation of *p53* is detected in approximately 30% to 40% of BL cases, independent of their geographic origin or of the presence of EBV infection.[57] As in other human cancers,[58] *p53* inactivation in BL occurs most commonly through deletion of one allele and mutation of the other. These genetic alterations cause inactivation of the normal *p53* function and therefore relieve cells of a major checkpoint in cell cycle control and regulation. As are many other NHL types, BL is also associated with deletions of 6q.[59]

Acquired Immunodeficiency Syndrome–Related Form. As mentioned above, BL was the first type of NHL reported in HIV-infected individuals.[15,16] Also, AIDS-BL may develop in the presence of relatively sustained peripheral blood CD4 levels and may be the first manifestation of AIDS in a significant fraction of cases. The molecular pathogenesis of AIDS-BL is complex and involves antigen stimulation and selection, as well as accumulation of genetic lesions. The role of genetic lesions in AIDS-BL has been studied in particular depth, and it is now well established that the molecular pathway of AIDS-BL involves activation of c-*MYC*, inactivation of *p53*, and infection by EBV.

In common with all the epidemiological and clinical BL variants, 100% of cases of AIDS-BL harbor a reciprocal chromosomal translocation between band 8q24 and one of the Ig gene loci: alternatively, IgH at 14q32, Igκ at 2p11, or Igλ at 22q11.[60-64] On 8q24, the involved proto-oncogene is represented by c-*MYC*.

Infection by EBV occurs in 30% of cases of AIDS-BL. Generally, EBV infection in AIDS-NHL is monoclonal, consistent with the hypothesis that the virus has been present in the tumor progenitor cell since the early phases of its clonal expansion and thus putatively contributed to lymphoma development.[56,63,64] The precise role of EBV in AIDS-BL pathogenesis, however, has remained controversial. On the one hand, in fact, EBV infection is considered to be a predisposing factor for subsequent development of lymphoma in the context of HIV-related persistent generalized lymphadenopathy (PGL).[65] On the other hand, though, EBV-positive AIDS-BLs fail to express the EBV transforming antigens EBNA-2 and LMP-1, which are key inducers of the transformed phenotype in other B-cell models.[66] Overall, these observations suggest that EBV is not a major pathogenetic element in AIDS-BL, although, in association with other factors, it may contribute to lymphoma development in specific settings such as PGL.

Inactivating mutations and deletions of the *p53* tumor suppressor gene occur in 60% of cases, a rate that is substantially higher than that detected in sBL and eBL (30%).[57,63] Mutations of *RAS* genes, which are otherwise univocally negative in sBL and eBL, are found in a fraction of AIDS-BL cases.[63] The recurrency of 1q21-q25 chromosomal abnormalities in AIDS-BL, particularly in EBV-positive cases, suggests that this genomic site harbors a novel, presently unknown, cancer-related gene relevant to AIDS-related lymphomagenesis.[67]

Recently, AIDS-BL has been extensively investigated for alterations of the *BCL*-6 proto-oncogene. *BCL*-6 is a transcriptional repressor involved in GC formation and function. Structural alterations of *BCL*-6 include chromosomal translocations leading to gene rearrangement, as well as point mutations of the gene regulatory regions. Among AIDS-NHL, chromosomal translocation of *BCL*-6 typically associates with the AIDS-DLCL subtype. In AIDS-BL, the main value of *BCL*-6 studies has been to elucidate the histogenesis of the lymphoma. Whereas AIDS-BL is typically devoid of gross rearrangements of *BCL*-6, small mutations clustering in the 5' regions of the gene are detectable in 60% of cases.[68,69] *BCL*-6 mutations are regarded as a marker of GC derivation of B-cells, because mutations of *BCL*-6 among B-cell NHLs of the immunocompetent host cluster with lymphoma categories deriving from cells that reside in or have transited through the GC, whereas they are rare or absent in tumors originating from precursor or virgin B-cells.[70] On this basis, the frequent detection of *BCL*-6 5' mutations in AIDS-BL indicates that this lymphoma type is related to GC B-cells.

CLINICAL FEATURES

The most striking feature of eBL is its predilection for the jaw and other facial bones; this feature occurs in approximately 60% of affected individuals. Conversely, jaw involvement is much less common in sBL,[31] which most often presents in the abdomen, mainly involving the distal ileum and cecum, as well as the ovaries, breasts, and kidney, and may disseminate widely to the central nervous system and bone marrow.[71] Few cases manifest as acute leukemia with Burkitt's tumor cells (L3-ALL).

Only approximately one fourth of patients with sBL have head and neck disease. Cervical lymphadenopathy enlargement, which is very rare in eBL, is more common in sBL. Virtually all head and neck sites may be affected in association with, or independent of, nodal disease, but there is a predilection for the jaw[72,73] and tonsil.[74-76] Possible sites involved by disease include the maxilla,[77] oral cavity,[78] parapharyngeal space,[79-82] cheek,[75] orbit,[83] nasopharynx,[75] paranasal sinuses,[84] mastoid,[85] and larynx.[86] The signs and symptoms vary according to the site of occurrence. Patients with multiple sites of involvement present with overlapping signs and symptoms.

In HIV-positive patients, BL usually accounts for 20% to 30% of all AIDS-related NHLs and is clinically characterized by widespread tumors. The vast majority of these tumors pertain to extranodal sites, including meningeal or primary central nervous system involvement and bone marrow infiltration. It is not unusual for patients to have more than 1 extranodal site of disease. Conventional tomography or computed tomographic scanning is valuable in showing the extension of the lesion.

Burkitt's lymphoma is one of the fastest-growing neoplasms, with a cell doubling time of 24 hours, requiring immediate diagnosis and treatment. The clinical course of BL in untreated patients is progressive, with rapid wide dissemination followed by death. Modern treatment schedules are now able to cure a significant number of patients.[87] Burkitt's lymphoma is highly responsive to aggressive chemotherapeutic agents. Tumor debulking or resection improves the probability of survival, but surgery is not the treatment of choice. Radiotherapy is not indicated as a sole method of treatment. With current chemotherapeutic regimens, patients with disease confined to the head and neck carry a good prognosis, and tumor-free survival can be expected for at least 2 years in up to 90% of cases.[88]

A different clinical presentation pertains to SNC non-Burkitt's lymphomas (or Burkitt's-like lymphomas). They occur mostly in adult patients and affect lymph nodes more than extranodal sites. Burkitt's-like lymphomas appear to be highly aggressive tumors in adulthood, whereas they behave like BLs in children. On the whole, patients with BL experience a higher rate of complete remission after therapy, and a longer median survival rate, than Burkitt's-like lymphoma patients.

REFERENCES

1. Wright DH. What is Burkitt's lymphoma? [Editorial]. J Pathol 1997;182:125-7.
2. Harris NL, Jaffe ES, Stein H, et al. A revised European-American Classification of lymphoid neoplasms: a proposal from the International Lymphoma Study Group. Blood 1994; 84:1361-92.
3. Davies JNP, Elmes S, Hutt MSR, Mtimavalye LAR, Owor R, Lorna S. Cancer in African community, 1897-1956. An analysis of the records of Mengo Hospital, Kampala, Uganda. Part I. Br Med J 1964;1:259-64.
4. Edington GM. Malignant disease in the Gold Coast. Br J Cancer 1956;10:41-54.
5. Thijs A. Considerations sur le tumeurs malignes des indigenes du Congo belge et du Ruanda-Urundi. A propos de 2,536 cas. Ann Soc Belg Med Trop 1957;37:483-514.
6. De Smet MP. Observations cliniques de tumeurs malignes des tissus reticuloendotheliaux et des tissus hemolymphopoietiques au Congo. Ann Soc Belg Med Trop 1956;36:53-70.
7. Burkitt D. Sarcoma involving jaws in African children. Br J Surg 1958;46:218-25.
8. O'Conor GT, Davies JNP. Malignant tumors in African children. J Pediatr 1960;56:526-35.
9. O'Conor GT, Rappaport H, Smith EB. Childhood lymphoma resembling Burkitt's lymphoma in the United States. Cancer 1965;18:411-7.
10. Dorfman RF. Childhood lymphosarcoma in St Louis, Missouri, clinically and histologically resembling Burkitt's lymphoma. Cancer 1965;18:418-30.
11. Wright DH. Burkitt's tumour in England. A comparison

with childhood lymphosarcoma. Int J Cancer 1966;1:503-4.

12. Vecchione A, Landi E. Su un caso di linfosarcoma a localizzazione ovarica. Quad Clin Ostet Ginecol 1966;21:799-810.

13. Cossman J, Berard CW. Histopathology of childhood non-Hodgkin's lymphomas. In: Graham-Pole J, ed. Non-Hodgkin's lymphomas in children. New York, NY: Masson, 1980:13-36.

14. Berard CW, O'Conor GT, Thomas LB, Torloni H. Histopathological definition of Burkitt's tumor. Bull World Health Organ 1969;40:601-7.

15. Doll DC, List AF. Burkitt's lymphoma in a homosexual [Letter]. Lancet 1982;1:1026-7.

16. Ziegler JL, Drew WL, Miner RC, et al. Outbreak of Burkitt's-like lymphoma in homosexual men. Lancet 1982;2:631-3.

17. Ziegler JL, Beckstead JA, Volberding PA, et al. Non-Hodgkin's lymphoma in 90 homosexual men. Relation to generalized lymphadenopathy and the acquired immunodeficiency syndrome. N Engl J Med 1984;311:565-70.

18. Lowenthal DA, Straus DJ, Campbell SW, Gold JWM, Clarkson BD, Koziner B. AIDS-related lymphoid neoplasia. The Memorial Hospital experience. Cancer 1988;61:2325-37.

19. Knowles DM, Chamulak GA, Subar M, et al. Lymphoid neoplasia associated with the acquired immunodeficiency syndrome (AIDS). The New York University Medical Center experience with 105 patients (1981-1986). Ann Intern Med 1988;108:744-53.

20. Raphael M, Gentilhomme O, Tulliez M, Byron P-A, Diebold J, The French Study Group of Pathology for Human Immunodeficiency Virus–Associated Tumors. Histopathologic features of high-grade non-Hodgkin's lymphomas in acquired immunodeficiency syndrome. Arch Pathol Lab Med 1991;115:15-20.

21. Carbone A, Tirelli U, Vaccher E, et al. A clinicopathologic study of lymphoid neoplasias associated with human immunodeficiency virus infection in Italy. Cancer 1991;68:842-52.

22. Rappaport H. Tumors of the hematopoietic system. In: Atlas of tumor pathology. Section 3. Fascicle 8. Washington, DC: Armed Forces Institute of Pathology, 1966:97-161.

23. Lukes RJ, Collins RD. Immunologic characterization of human malignant lymphomas. Cancer 1974;34:1488-503.

24. The Non-Hodgkin's Lymphoma Pathologic Classification Project. National Cancer Institute sponsored study of classifications of non-Hodgkin's lymphomas. Summary and description of a working formulation for clinical usage. Cancer 1982;49:2112-35.

25. Hui PK, Feller AC, Lennert K. High-grade non-Hodgkin's lymphoma of B-cell type. I. Histopathology. Histopathology 1988;12:127-43.

26. Stansfeld AG, Diebold J, Noel H, et al. Updated Kiel classification for lymphomas. Lancet 1988;1:292-3.

27. Jaffe ES, Harris NL, Diebold J, Muller-Hermelink H-K. World Health Organization classification of neoplastic diseases of the hematopoietic and lymphoid tissues. A progress report. Am J Clin Pathol 1999;111(suppl 1):S8-S12.

28. Cossman J. Diffuse, aggressive non-Hodgkin's lymphomas. In: Jaffe ES, ed. Major problems in pathology: surgical pathology of the lymph nodes and related organs. Vol 16. Philadelphia, Pa: Saunders, 1985:203-17.

29. Grogan TM, Warnke RA, Kaplan HS. A comparative study of Burkitt's and non-Burkitt's "undifferentiated" malignant lymphoma. Immunologic, cytochemical, ultrastructural, cytologic, histopathologic, clinical and cell culture features. Cancer 1982;49:1817-28.

30. Payne CM, Grogan TM, Cromey DW, Bjore CG Jr, Kerrigan DP. An ultrastructural morphometric and immunophenotypic evaluation of Burkitt's and Burkitt's-like lymphomas. Lab Invest 1987;57:200-18.

31. Pavlova Z, Parker JW, Taylor CR, Levine AM, Feinstein DI, Lukes RJ. Small noncleaved follicular center cell lymphoma: Burkitt's and non-Burkitt's variants in the US. II. Pathologic and immunologic features. Cancer 1987;59:1892-902.

32. Mann RB, Jaffe ES, Braylan RC, et al. Non-endemic Burkitt's lymphoma. A B-cell tumor related to germinal centers. N Engl J Med 1976;295:685-91.

33. Carbone A, Gaidano G, Gloghini A, et al. BCL-6 protein expression in AIDS-related non-Hodgkin's lymphomas: inverse relationship with Epstein-Barr virus–encoded latent membrane protein–1 expression. Am J Pathol 1997;150:155-65.

34. Carbone A, Gaidano G, Gloghini A, et al. Differential expression of BCL-6, CD138/syndecan-1 and EBV-encoded latent membrane protein–1 identifies distinct histogenetic subsets of acquired immunodeficiency syndrome–related non-Hodgkin's lymphomas. Blood 1998;91:747-55.

35. Garcia CF, Weiss LM, Warnke RA. Small noncleaved cell lymphoma. An immunophenotypic study of 18 cases and comparison with large cell lymphoma. Hum Pathol 1986;17:454-61.

36. Brownell MD, Sheibani K, Battifora H, Winberg CD, Rappaport H. Distinction between undifferentiated (small noncleaved) and lymphoblastic lymphoma. An immunohistologic study on paraffin-embedded, fixed tissue sections. Am J Surg Pathol 1987;11:779-87.

37. Billaud M, Rousset F, Calender A, et al. Low expression of lymphocyte function–associated antigen (LFA)–1 and LFA-3 adhesion molecules is a common trait in Burkitt's lymphoma associated with and not associated with Epstein-Barr virus. Blood 1990;75:1827-33.

38. Raphael MM, Audouin J, Lamine M, et al. Immunophenotypic and genotypic analysis of acquired immunodeficiency syndrome–related non-Hodgkin's lymphomas: correlation with histologic features in 36 cases. Am J Clin Pathol 1994;101:773-82.

39. Carbone A, Gloghini A, Gaidano G, et al. AIDS-related Burkitt's lymphoma. Morphologic and immunophenotypic study of biopsy specimens. Am J Clin Pathol 1995;103:561-7.

40. Gloghini A, De Paoli P, Gaidano G, Franceschi S, Carbone A. High frequency of CD45RO expression in AIDS-related B-cell non-Hodgkin's lymphomas. Am J Clin Pathol 1995;104:680-8.

41. Dalla-Favera R. Chromosomal translocations involving the c-myc oncogene in lymphoid neoplasia. In: Kirsch IR, ed. The causes and consequences of chromosomal aberrations. Boca Raton, Fla: CRC Press, 1993:312.

42. Dalla-Favera R, Bregni M, Erikson J, Patterson D, Gallo RC, Croce CM. Human c-myc oncogene is located on the region of chromosome 8 that is translocated in Burkitt lymphoma cells. Proc Natl Acad Sci U S A 1982;79:7824-7.

43. Dalla-Favera R, Martinotti S, Gallo RC, Erikson J, Croce CM. Translocation and rearrangements of the c-myc oncogene

in human undifferentiated B-cell lymphomas. Science 1983;219: 963-7.

44. Davis M, Malcolm S, Rabbits TH. Chromosome translocation can occur on either side of the c-myc oncogene in Burkitt lymphoma cells. Nature 1984;308:286-8.

45. Hollis GF, Mitchell KF, Battey J, et al. A variant translocation places the lambda immunoglobulin genes 3' to the c-myc oncogene in Burkitt's lymphoma. Nature 1984;307:752-5.

46. Taub R, Kirsch I, Morton C, et al. Translocation of c-myc gene into the immunoglobulin heavy chain locus in human Burkitt lymphoma and murine plasmacytoma cells. Proc Natl Acad Sci U S A 1982;79:7837-41.

47. ar-Rushdi A, Nishikura K, Erikson J, Watt R, Rovera G, Croce CM. Differential expression of the translocated and untranslocated c-myc oncogene in Burkitt's lymphoma. Science 1983;222:390-3.

48. Hayday AC, Gillies SD, Saito H, et al. Activation of a translocated human c-myc gene by an enhancer in the immunoglobulin heavy chain locus. Nature 1984;307:334-40.

49. Rabbits TH, Forster A, Baer R, Hamlyn PH. Transcriptional enhancer identified where the human C immunoglobulin heavy chain gene is unavailable to the translocated c-myc gene in a Burkitt's lymphoma. Nature 1983;306:806-9.

50. Lombardi L, Newcomb EW, Dalla-Favera R. Pathogenesis of Burkitt lymphoma: expression of an activated c-myc oncogene causes the tumorigenic conversion of EBV-infected human B lymphoblasts. Cell 1987;49:161-70.

51. Magrath IT. Prospects for the therapeutic use of antisense oligonucleotides in malignant lymphomas. Ann Oncol 1994;5 (suppl 1):S67-S70.

52. McManaway ME, Neckers LM, Loke SL, et al. Tumor-specific inhibition of lymphoma growth by an antisense oligodeoxy-nucleotide. Lancet 1990;335:808-11.

53. Adams JM, Harris AW, Pinkert CA, et al. The c-myc oncogene driven by immunoglobulin enhancers induces lymphoid malignancy in transgenic mice. Nature 1985;318:533-8.

54. Hamilton-Dutoit SJ, Pallesen G. A survey of Epstein-Barr virus gene expression in sporadic non-Hodgkin's lymphomas. Detection of Epstein-Barr virus in a subset of peripheral T-cell lymphomas. Am J Pathol 1992;140:1315-25.

55. Kieff E, Leibowitz D. Oncogenesis by herpesvirus. In: Weinberg RA, ed. Oncogenes and the molecular origin of cancer. Cold Spring Harbor, NY: Cold Spring Harbor Laboratory Press, 1989:259.

56. Neri A, Barriga F, Inghirami G, et al. Epstein-Barr virus infection precedes clonal expansion in Burkitt's and acquired immunodeficiency syndrome–associated lymphoma. Blood 1991;77:1092-5.

57. Gaidano G, Ballerini P, Gong JZ, et al. p53 Mutations in human lymphoid malignancies: association with Burkitt lymphoma and chronic lymphocytic leukemia. Proc Natl Acad Sci U S A 1991;88:5413-7.

58. Hollstein M, Sidransky D, Vogelstein B, Harris CC. p53 Mutations in human cancers. Science 1991;253:49-53.

59. Gaidano G, Hauptschein RS, Parsa NZ, et al. Deletions involving two distinct regions of 6q in B-cell non Hodgkin lymphoma. Blood 1992;80:1781-7.

60. Chaganti RS, Jhanwar SC, Koziner B, Arlin Z, Mertelsmann R, Clarkson BD. Specific translocations characterize Burkitt's-like lymphoma of homosexual men with the acquired immunodeficiency syndrome. Blood 1983;61:1265-8.

61. Groopman JE, Sullivan JL, Mulder C, et al. Pathogenesis of B cell lymphoma in a patient with AIDS. Blood 1986;67: 612-5.

62. Subar M, Neri A, Inghirami G, Knowles DM, Dalla-Favera R. Frequent c-myc oncogene activation and infrequent presence of Epstein-Barr virus genome in AIDS-associated lymphoma. Blood 1988;72:667-71.

63. Ballerini P, Gaidano G, Gong JZ, et al. Multiple genetic lesions in acquired immunodeficiency syndrome–related non-Hodgkin's lymphoma. Blood 1993;81:166-76.

64. Gaidano G, Parsa NZ, Tassi V, et al. In vitro establishment of AIDS-related lymphoma cell lines: phenotypic characterization, oncogene and tumor suppressor gene lesions, and heterogeneity in Epstein-Barr virus infection. Leukemia 1993;7:1621-9.

65. Shibata D, Weiss LM, Nathwani BN, Brynes RK, Levine AM. Epstein-Barr virus in benign lymph node biopsies from individuals infected with the human immunodeficiency virus is associated with concurrent or subsequent development of non-Hodgkin's lymphoma. Blood 1991;77:1527-33.

66. Carbone A, Tirelli U, Gloghini A, Volpe R, Boiocchi M. Human immunodeficiency virus–associated systemic lymphomas may be subdivided into two main groups according to Epstein-Barr viral latent gene expression. J Clin Oncol 1993;11: 1674-81.

67. Polito P, Cilia AM, Gloghini A, et al. High frequency of EBV association with non-random abnormalities of the chromosome region 1q21-25 in AIDS-related Burkitt's lymphoma–derived cell lines. Int J Cancer 1995;61:370-4.

68. Gaidano G, Lo Coco F, Ye BH, et al. Rearrangements of the BCL-6 gene in acquired immunodeficiency syndrome–associated non-Hodgkin's lymphoma: association with diffuse large-cell subtype. Blood 1994;84:397-402.

69. Gaidano G, Carbone A, Pastore C, et al. Frequent mutation of the 5' noncoding region of the BCL-6 gene in acquired immunodeficiency syndrome–related non-Hodgkin's lymphomas. Blood 1997;89:3755-62.

70. Migliazza A, Martinotti S, Chen W, et al. Frequent somatic hypermutation of the 5' noncoding region of the BCL-6 gene in B-cell lymphoma. Proc Natl Acad Sci U S A 1995;92: 12520-4.

71. Levine PH, Kamaraju LS, Connelly RR, Berard CW, Dorfman RF, Magrath I, Easton JM. The American Burkitt's Lymphoma Registry: eight years' experience. Cancer 1982;49: 1016-22.

72. Robbins KT, Fuller LM, Manning MD, et al. Primary lymphoma of the mandible. Head Neck Surg 1986;8:192-9.

73. Sariban E, Donahue A, Magrath IT. Jaw involvement in American Burkitt's lymphoma. Cancer 1984;53:1777-82.

74. Kraus M, Fliss DM, Argov S, Leiberman A, Benharroch D. Burkitt's lymphoma of the tonsil. J Laryngol Otol 1990;104: 991-4.

75. Wang MB, Strasnick B, Zimmerman MC. Extranodal American Burkitt's lymphoma of the head and neck. Arch Otolaryngol Head Neck Surg 1992;118:193-9.

76. Tewfik TL, Bond M, Al-Ghamdi K, Bernard C. Burkitt's lymphoma of the tonsil in children. J Otolaryngol 1996;25:205-8.

77. Standefer JA, Mattox DE, Aufdemorte TB, Geiser CF,

Gates GA. Midfacial Burkitt's lymphoma. Otolaryngol Head Neck Surg 1985;93:262-7.

78. Takahashi H, Fujita S, Okabe H, Tsuda N, Tezuka F. Immunophenotypic analysis of extranodal non-Hodgkin's lymphomas in the oral cavity. Pathol Res Pract 1993;189:300-11.

79. Bauer GP, Volk MS, Siddiqui SY, et al. Burkitt's lymphoma of the parapharyngeal space. Arch Otolaryngol Head Neck Surg 1993;119:117-20.

80. Topping JW III, Kennedy JL, Sharon BI, Mafee MF, Tojo DP. Pathologic quiz case 1. Arch Otolaryngol Head Neck Surg 1997;123:230, 232-3.

81. Vinayak BC, Reddy KTV, Fulton J, Milford CA. Pediatric nonendemic Burkitt's lymphoma of the head and neck. Ann Otol Rhinol Laryngol 1994;103:238-40.

82. Lazar RH, Gurucharri MJ, Edwards O, Presbury G. Pathologic quiz case 2. Arch Otolaryngol Head Neck Surg 1989;115: 636-7, 639.

83. Edelstein C, Shields JA, Shields CL, et al. Non-African Burkitt lymphoma presenting with oral thrush and an orbital mass in a child. Am J Ophthalmol 1997;124:859-61.

84. Weisberger EC, Davidson DD. Unusual presentations of lymphoma of the head and neck in childhood. Laryngoscope 1990;100:337-42.

85. Welling DB, McCabe BF. American Burkitt's lymphoma of the mastoid. Laryngoscope 1987;97:1038-42.

86. Michaels L. Pathology of the larynx. Berlin, Germany: Springer-Verlag, 1984:334-5.

87. Philip T, Pikerton R, Biron P, et al. Effective multiagent chemotherapy in children with advanced B-cell lymphoma: who remains the high risk patient? Br J Haematol 1987;65:159-64.

88. Anavi Y, Kaplinsky C, Calderon S, Zaizov R. Head, neck, and maxillofacial childhood Burkitt's lymphoma: a retrospective analysis of 31 patients. J Oral Maxillofac Surg 1990;48:708-13.

Ann Otol Rhinol Laryngol 109:2000

MORPHOLOGICAL AND FUNCTIONAL STUDY OF REGENERATED CHORDA TYMPANI NERVES IN HUMANS

TAKEHISA SAITO, MD
YOSHIYUKI SHIBAMORI, MD
YASUHIRO MANABE, MD
TAKAHIRO YAMAGISHI, MD
TAKEHITO YAMAMOTO, MD
TOSHIO OHTSUBO, MD
HITOSHI SAITO, MD
FUKUI, JAPAN

It is still unclear whether the chorda tympani nerves in humans regenerate after being severed during middle ear surgery, although functional studies have demonstrated recovery of taste 1 to 2 years after surgery. To date, 12 cases of regenerated chorda tympani nerves have been found in our series of patients during secondary surgery. The regenerated nerves of 3 cases of the 12 were removed as samples during secondary surgery to detect regenerated myelinated axons. All regenerated nerves were in the submucosal connective tissue layer of the reconstructed eardrum. In the regenerated nerves, myelinated nerve fibers existed in a small fascicle or in connective tissue, but the number of myelinated axons was low compared with that in normal subjects (1,752 ± 78; n = 3), and the distribution was sparse. The total number of regenerated myelinated axons varied from 141 (8.3%) to 979 (55.9%). From a functional study using electrogustometry, incomplete recovery of electrogustation was observed in all 3 cases before secondary surgery, suggesting that chorda tympani nerves actually regenerate in the middle ear and do function.

KEY WORDS — chorda tympani nerve, electrogustometry, middle ear surgery, regeneration, transmission electron microscopy.

INTRODUCTION

The chorda tympani nerve is a mixed nerve and is known to transmit afferent sensory and efferent secretory impulses. Its sensory component is formed by afferent axons that are distributed to the taste buds of the anterior two thirds of the tongue.[1] The secretory compartment contains efferent preganglionic parasympathetic axons that innervate the sublingual and submandibular glands.[2] The chorda tympani arises from the mastoid portion of the facial nerve and crosses the tympanic cavity. Although the chorda tympani is severed in some cases of middle ear surgery,[2-4] it is still unknown whether the chorda tympani in humans regenerates after being severed. Functional studies by other researchers have demonstrated recovery of taste 1 to 2 years after the nerve has been severed.[2,3] Clinical observation of the facial nerve shows that immediate reconstruction of sharp transectional facial nerve injuries by primary direct end-to-end anastomosis of the neural stumps produces the best functional results.[5,6] Because the chorda tympani runs across the air cavity, however, direct anastomosis is considered difficult, and transected nerves are separated by a wide gap in many instances. In studies in rabbits, facial nerve regeneration in transectional injuries of the buccal division of the facial nerve was possible with autologous nerve grafts and silicone chamber implants, besides direct end-to-end anastomosis.[5,7,8] However, complete neural transections of human and rabbit facial nerves with wide gap separation of the neural stumps produced variable functional results.[5]

What conditions are necessary for regeneration, and how do the chorda tympani nerves regenerate after being severed in the middle ear cavity? To date, we have detected 12 cases of reinnervated chorda tympani nerves in the submucosal connective tissue layer of the eardrum during secondary surgery (unpublished data). In 3 of these cases, regenerated chorda tympani nerves were removed as samples to check for regenerated axons. In this report, the surgical and morphological findings of the regenerated nerves and the functional results from electrogustometry (EGM) were evaluated.

MATERIALS AND METHODS

So far, 12 regenerated chorda tympani nerves have been detected among 45 patients with chronic otitis media with or without cholesteatoma, in whom the chorda tympani was cut during primary surgery and who underwent a staged tympanoplasty or reoperation in our clinic. In 3 of the 12 patients with regenerated nerves, a segment of 2 to 3 mm in length distal from the cut end was resected as a sample for morphological observation. In all cases, the temporalis muscle fascia was used with an underlay method to cover and reconstruct the defect of the eardrum during primary surgery, and the distal and proximal

---

From the Department of Otolaryngology, Fukui Medical University, Fukui, Japan.

CORRESPONDENCE — Takehisa Saito, MD, Dept of Otolaryngology, Fukui Medical University, Matsuoka-cho, Yoshida-gun, Fukui 910-1193, Japan.

stumps of the chorda tympani were anastomosed or approximated on the fascia with fibrin glue. Direct end-to-end anastomoses were performed at the midpoint of the tympanic segment of the chorda tympani after it was severed in 2 cases (cases 4 and 5), whereas a defect of 5 to 6 mm remained in the midportion of the tympanic segment in 1 case (case 1).

The resected nerve segments were immersed in a fixative solution (2% paraformaldehyde and 0.5% glutaraldehyde in 0.1-mol/L phosphate-buffered solution [PBS], pH 7.4) for more than 2 days, embedded in gelatin (20% in PBS), and submerged in a 20% sucrose solution in PBS (pH 7.4) at 4°C for 24 hours. Transverse frozen sections of 65-μm thickness were made with a cryostat and postfixed for 2 hours with 1% osmium tetroxide at 4°C, dehydrated with a series of graded alcohol, and embedded in Epon 812. Ultrathin sections were cut and mounted on a Formvar-coated single-hole grid and observed with a transmission electron microscope (Hitachi H-7000) at magnifications ranging from ×1,000 to ×2,000 of the entire cross-sectional area. Myelinated fibers were counted on photographic montages, and histograms were obtained after the diameters of all myelinated fibers were measured.

As controls, 3 chorda tympani nerves were taken from patients with chronic otitis media with cholesteatoma. Before surgery, EGM showed a normal threshold in 2 adult cases. The nerves were severed for transmission electron microscopic observation, and fiber counts and histograms were made in the same way as for the regenerated nerves.

Functional observation by EGM was performed before and after the operation. The electrical stimulus was delivered via an electrogustometer (EG-IIB, Nagashima Medical Instruments Co, Japan) with a single, flat, circular stimulus probe (5 mm diameter) of stainless steel. The stimulus rod was placed on the tongue with the stimulus probe resting 2 cm from the anterior midline and 2 cm from the tip of the tongue. An ascending threshold procedure was then used. A 500-ms anodal stimulation was presented unilaterally, beginning at –8 dB and proceeding to 34 dB (4 to 400 mA) in 2-dB steps. The differences in thresholds between the surgical and nonsurgical sides were recorded. The normal range of the EGM threshold obtained from normal volunteers (n = 10) was ±4 dB.

RESULTS

During secondary surgery, performed 1 to 4 years after the primary surgery, regenerated chorda tympani nerves were detected after elevating the eardrum. All regenerated nerves existed as funicular structures in the submucosal connective tissue layer of the reconstructed eardrum, and they were easily exposed by a fine needle. The diameter of the regenerated nerves was almost the same as that of normal nerves by visual inspection, although it was unclear how many axons were contained in the regenerated nerves. The course of the regenerated nerves was similar to that of normal nerves, except that they did not run in the aerated tympanic cavity, but inside the reconstructed eardrum.

In 3 normal nerves, the total number of myelinated fibers ranged from 1,693 to 1,840 (1,752 ± 78). The mean was used as the control number.

In the regenerated nerves of cases 4 and 5, myelinated nerve fibers regenerated in a small fascicle or the connective tissue, but the number of myelinated fibers was low compared with that in normal nerves, and their distribution was sparse (Figs 1 and 2). The total numbers of myelinated fibers were 979 and 903 (55.9% and 51.5% of the control number) in cases 4 and 5, in which end-to-end anastomoses were performed, whereas in case 1, in which a nerve defect of 5 to 6 mm remained, the number was 141 (8.3% of the total number of the patient's own chorda tympani nerve severed during primary surgery; see Table). In the section of case 1, regenerated myelinated fibers were observed in 2 peripheral areas of the funicular connective tissue. On the histograms of the control and regenerated nerves, the diameters of the regenerated myelinated fibers are seen to be smaller than those of the control nerves (Fig 2). However, there are few fibers with a diameter below 1 μm.

The Table shows the profile of 5 cases in which transmission electron microscopic observation was performed in this study. The thresholds of EGM in 2 adults with regenerated nerves (cases 4 and 5) went beyond the scale 1 month after primary surgery, then recovered to +12 to +28 dB before secondary surgery, which was performed 1 and 4 years after the first surgery, respectively. After the secondary surgery, the EGM thresholds in cases 4 and 5 did not recover (beyond the scale) until 2 years later. One child with a regenerated nerve (case 1) had a threshold of +12 dB before secondary surgery. Subsequently, the threshold went beyond the scale 1 month after the secondary surgery and re-recovered to +14 dB 1 year later.

DISCUSSION

It was reported that 28% to 80% of patients whose chordae tympani were severed during middle ear surgery such as stapes surgery complained of taste disorders.[2,3] Taste disorders in half of these patients, however, improved within 1 to 2 years, although it

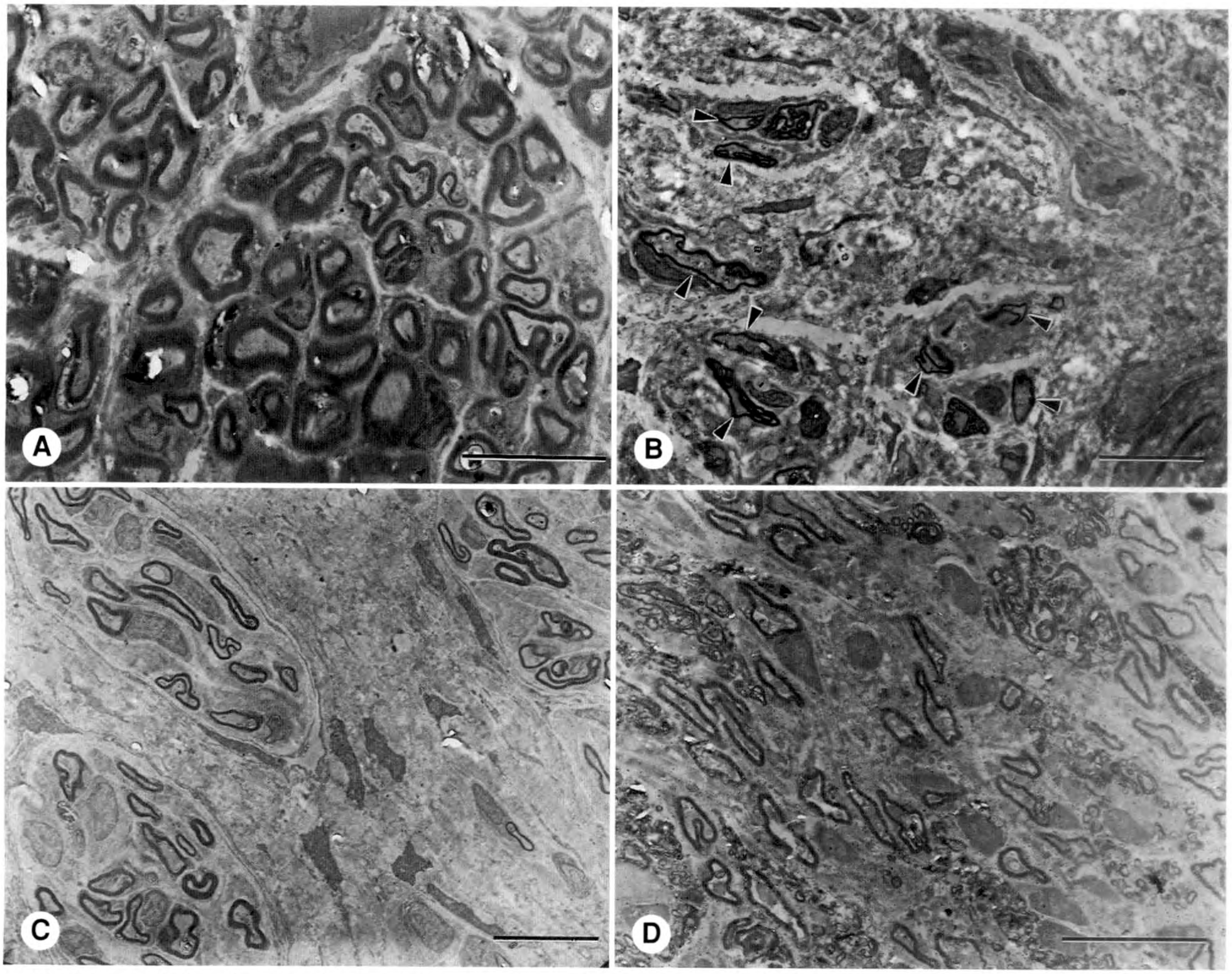

Fig 1. Transmission electron microscopic findings of normal and regenerated chorda tympani nerves. Bars — 10 μm. A) (Case 1) Normal chorda tympani. B) (Case 1) Regenerated chorda tympani. Arrowheads — regenerated myelinated fibers. C) (Case 4) Regenerated chorda tympani. D) (Case 5) Regenerated chorda tympani.

was not clear whether the chorda tympani had regenerated. Two adult patients in the present study complained of a taste disorder after primary surgery, but did not complain of it after 1 year. One child patient did not complain of any taste disorder throughout the follow-up period. Children do not usually complain of any taste disorder after their unilateral chorda tympani nerves are severed (unpublished data). Electrogustation is one of the quantitative analyses of taste, and its reliability and validity have been verified by clinical study.[9,10] Two adult patients in this study demonstrated normal EGM thresholds before primary surgery, and the thresholds of the transected sides of the tongue 1 month after surgery went beyond the scale. One to 4 years after primary surgery, their EGM thresholds had incompletely recovered and then went beyond the scale again after re-severing of the nerve during secondary surgery. The EGM threshold of one child (case 1) also showed incomplete recovery before secondary surgery, although a preoperative EGM was not performed. One month after secondary surgery, his EGM threshold went beyond the scale and then showed re-recovery 1 year later, suggesting that his severed nerve might regenerate again after secondary surgery. These findings suggest the reliability of EGM, and it may be possible to predict the incidence of regeneration of the chorda tympani by EGM alone. Such a study is under way in our clinic.

There are numerous experimental animal studies concerning the regeneration of the chorda tympani nerves. In most reports, the chorda tympani or chorda-lingual nerves were severed near the tongue and electrophysiological recovery and morphological regeneration of the nerves and taste buds were observed after the nerves were severed.[11,12] However, it is very important and useful to evaluate whether and how the severed chorda tympani regenerates in the aerated cavity, because the chorda tympani nerves in humans run across the aerated cavity (tympanic cavity), and there are no reports on the regeneration of

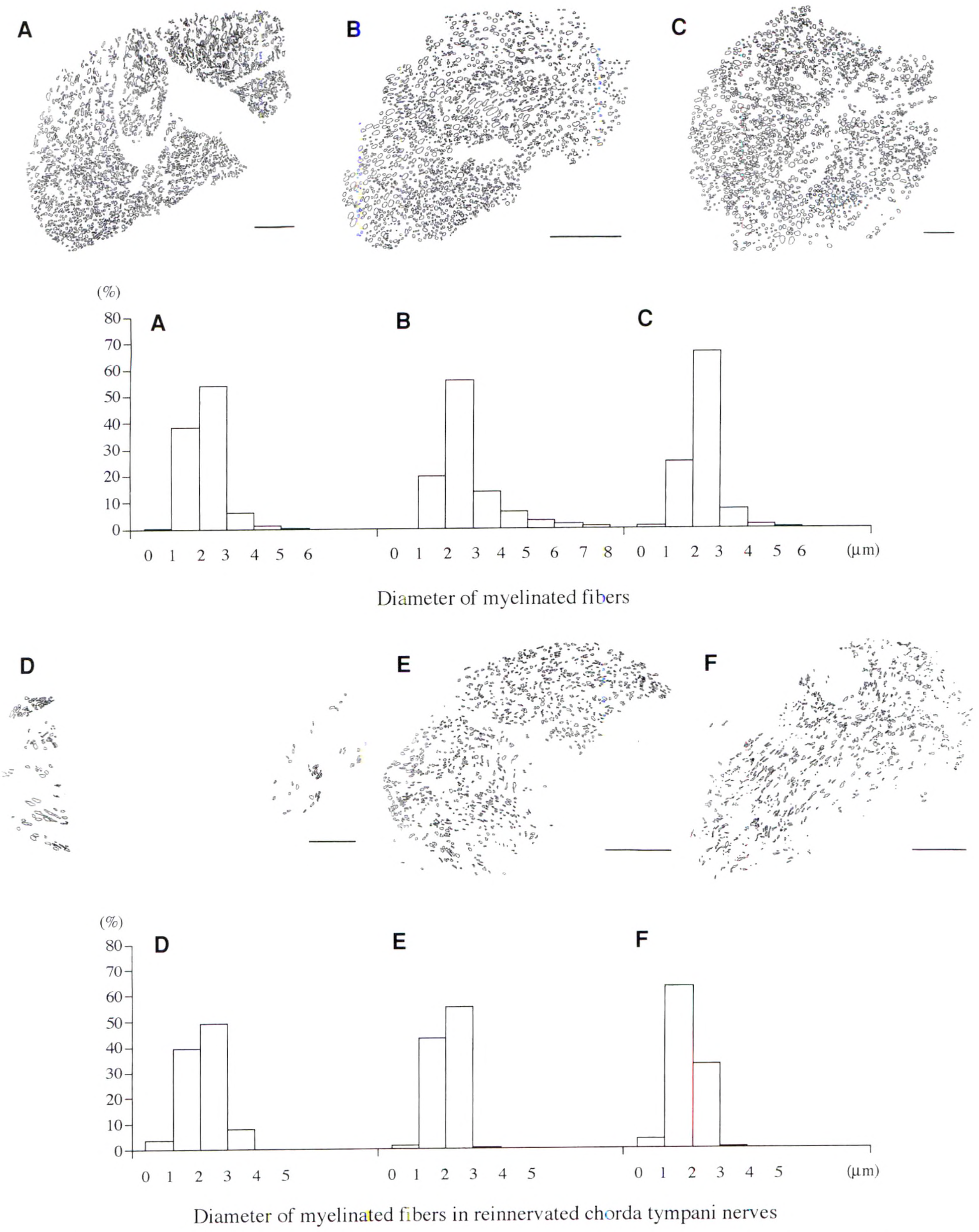

Fig 2. Complete features and histograms of myelinated fibers of normal chorda tympani (A — case 1; B — case 2; C — case 3) and regenerated nerves (D — case 1; E — case 4; F — case 5) made from photographic montage with transmission electron microscopy. Bars — 50 µm.

the tympanic segment of the chorda tympani nerve. In some experimental studies using hamsters, the chorda tympani nerves were severed or crushed in the middle ear.[13,14] Morphological observation of the

PROFILE OF PATIENTS; TOTAL NUMBER OF NORMAL AND REGENERATED MYELINATED FIBERS OF CHORDA TYMPANI NERVES; MAXIMAL DIAMETER OF NERVES AND TIME COURSE OF ELECTROGUSTATION BEFORE AND AFTER SEVERING NERVE

								*Electrogustometry**			
Normal Nerves	*Age*	*No. of Myelinated Fibers*	*Diameter of Nerves (µm)*	*Regenerated Nerves*	*Age*	*No. of Regenerated Fibers (% of Controls)*	*Diameter of Nerves (µm)*	*Before Primary Surgery*	*After Primary Surgery*	*Before Secondary Surgery*	*After Secondary Surgery*
Case 1	6	1,693	380	Case 1	7	141 (8.3)	387	NP	NP	+12 dB	SO (1 mo) +14 dB (1 y)
Case 2	51	1,840	223	Case 4	29	979 (55.9)	245	0 dB	SO	+28 dB	SO (1 mo) SO (2 y)
Case 3	54	1,723	500	Case 5	48	903 (51.5)	293	0 dB	SO	+12 dB	SO (1 mo) SO (2 y)
Mean ± SD		1,752 ± 78	368 ± 139			674 ± 463	308 ± 72				

NP — not performed, SO — scaled out (beyond scale).

*Values indicate differences in thresholds between surgical and nonsurgical sides.

regenerated chorda tympani nerves, 4 months after cutting of the nerves in the middle ear, found regeneration of the nerves near the tongue, but 67% fewer myelinated fibers than in controls were observed on transmission electron microscopy.[14] These fibers were sufficient to record the recovery of electrophysiological taste responses and to support normal taste bud sizes and numbers.

In the present study, it was demonstrated that the chorda tympani nerve may regenerate in some patients in whom the chorda tympani has been cut in the middle ear. The mean total number of myelinated fibers in a normal chorda tympani in humans varies from 1,555[15] to 3,525,[16] according to different reports. In this study, it was 1,752 in 3 patients (2 adults and 1 child), but it is unclear whether these differences depend on race. As shown in this report, the fact that the regenerated nerves did not run across the aerated cavity, but inside the reconstructed eardrum, was considered reasonable. There are no reports detailing regenerated chorda tympani nerves in the tympanic cavity in humans. This is because the regenerated nerves can be found only through secondary surgery. Further, it is difficult for surgeons to notice and detect the regenerated nerves in the eardrum if they do not recognize the existence of such regenerated nerves. Microscopically, the total number of myelinated nerve fibers in regenerated nerves showed a decrease in comparison with those of normal chorda tympani nerves in this study. The distribution of regenerated myelinated fibers was sparse. This is in agreement with the findings of experimental studies in hamster chorda tympani nerves[14] and rabbit facial nerves.[7]

Unmyelinated fibers were not counted, because of the technical problems involved. On the basis of a previous report that afferent fibers included 79% of all myelinated, but only 30% of all unmyelinated fibers in the rat chorda tympani nerve,[17] Ylikoski et al[16] reported that it would appear that the efferent function (secretory) was represented mainly by unmyelinated nerve fibers and that most of the afferents (sensory function) are myelinated in humans, if the human chorda tympani has a relationship similar to that in the rat. Thus, it is considered that myelinated fibers mainly contained afferent gustatory fibers distributing to the anterior two thirds of the tongue. In this study, the diameter of the myelinated fibers of the chorda tympani in humans ranged between 1 and 8 µm, with a peak between 2 and 3 µm. This is in good agreement with the previous report.[16] The diameters of the regenerated myelinated fibers, however, ranged from 1 to 4 µm, and the mean value decreased compared with that of the control nerve. This indicates that there is a possibility that some of the regenerated fibers were efferent parasympathetic neurons serving submaxillary and sublingual gland functions. However, there were few fibers with a diameter below 1 µm. Although it remains obscure whether the regenerated fibers should be classified as efferent or afferent, even after the morphological analyses, we think that the regenerated myelinated fibers were mostly afferent, considering that incomplete recovery of electrogustation was observed in patients with regenerated chorda tympani nerves, whereas electrogustation did not recover in patients with nonregenerated nerves in our series.

It was reported that the minimum number of regenerating facial nerve myelinated motor axons required to innervate and activate the mimetic musculature in rabbits was 12% of the original motor axon population.[8] Regeneration of facial nerve motor axons to achieve normal physiological mimetic activity requires 2 factors. First, the facial nerve must regenerate a sufficient number of myelinated motor axons to activate the affected target muscles that have been denervated. Second, the regenerating motor axons must precisely innervate their specific muscle groups (target end organs) to achieve precise behavioral and evoked integrated activity. In the regeneration of sensory afferent fibers, such as the chorda tympani nerves, it remains obscure what number of regenerating myelinated axons is required to achieve electrogustation. In a pediatric case in the present study, regeneration of only 8% of the sensory afferent axons was satisfactory for achieving electrogustation 1 year after severing of the chorda tympani, suggesting that only a small percentage of regenerating axons is required to achieve electrogustation.

Regarding factors that are necessary for reinnervation of the chorda tympani, certain conditions are considered contributory. One is the direction of the remaining part of the nerve and the distance between its proximal and distal ends. In an experimental study using a sciatic nerve, little or no regeneration was evident when the gap between the nerve segments was left empty.[18] Furthermore, complete neural transections of human and rabbit facial nerves, with wide gap separation of the neural stumps, produced variable functional results.[5] When silicone chambers prefilled with saline solution were implanted into the buccal division of the facial nerve after removal of a portion of the buccal branch in the rabbit, regenerated motor axons were observed. However, the number of total regenerated axons was smaller than that found after direct end-to-end anastomosis.[8] Although direct end-to-end anastomoses were possible in 2 cases of our 3 series, a nerve defect of 5 to 6 mm remained in the third case, and the number of regenerated axons of that case was smaller than that of the 2 cases of end-to-end anastomosis. This finding suggests that the length of the nerve gap might correlate with the incidence of nerve regeneration. Statistically, however, there was no significant difference between the length of the nerve gap and the incidence of nerve regeneration detected during secondary surgery (unpublished data).

Temporalis muscle fascia is usually applied by an underlay method to reconstruct the eardrum in our clinic. From the finding that all the regenerated chorda tympani nerves were found in the submucosal layer of the reconstructed eardrums, it appears that temporalis muscle fascia may play an important role as a contact guide for reinnervation. Thickening of the reconstructed eardrum by means of the temporalis muscle fascia and regrowth of connective tissue, such as granulation or scar tissue around the tympanic isthmus where the chorda tympani passes, are also considered important, especially immediately after the reconstruction of the nerve. If the chorda tympani is severed during middle ear surgery, therefore, it is recommended that the temporalis muscle fascia be used under the eardrum and the cut ends of the nerves be approximated to each other on the fascia with fibrin glue to promote regeneration of the nerve fibers.

Besides these factors, neurotrophic factors, such as nerve growth factor and neuropromotive factor, may be important, as reported in an experimental study on reinnervation of the sciatic nerve.[17] From the present study, it was impossible to determine the existence of these factors. Further study will be needed to clarify the role of neurotrophic and neuropromotive factors.

In conclusion, this is the first report to count the number of regenerated axons of chorda tympani nerves in humans. Regenerated chorda tympani nerves in 3 patients, which were detected during secondary surgery or reoperation, were evaluated morphologically and functionally. Electrogustometry showed recovery of the threshold before secondary surgery. Regenerated axons were observed by transmission electron microscopy, and the number of regenerated axons was 8% to 56% of that of the control subjects, suggesting that the chorda tympani in the tympanic segment regenerates in the submucosal layer of the reconstructed eardrum after being severed.

ACKNOWLEDGMENTS — We thank Takahiro Saito and Kiyofumi Saito for their assistance in making the photographic montages and histograms of the chorda tympani nerves.

REFERENCES

1. Lewis D, Dandy WE. The course of the nerve fibers transmitting sensation of taste. Arch Surg 1930;21:249-88.

2. Bull TR. Taste and the chorda tympani. J Laryngol Otol 1965;79:479-93.

3. Moon CN, Pullen EW. Effects of chorda tympani section during middle ear surgery. Laryngoscope 1963;73:392-405.

4. House HP. Early and late complications of stapes surgery. Arch Otolaryngol 1963;78:606-13.

5. Spector JG, Lee P, Peterein J, Roufa D. Facial nerve regeneration through autologous nerve grafts: a clinical and experimental study. Laryngoscope 1991;101:537-54.

6. Spector JG. Neural repair in facial paralysis: clinical and experimental studies. Eur Arch Otorhinolaryngol Suppl 1997; 254(suppl 1):S68-S75.

7. Spector JG, Lee P, Derby A, Roufa DG. Comparison of rabbit facial nerve regeneration in nerve growth factor–containing silicone tubes to that in autologous neural grafts. Ann Otol Rhinol Laryngol 1995;104:875-85.

8. Spector JG, Lee P. Axonal regeneration in severed peripheral facial nerve of the rabbit: relation of the number of axonal regenerates to behavioral and evoked muscle activity.

Ann Otol Rhinol Laryngol 1998;107:141-8.

9. Murphy C, Quinonez C, Nordin S. Reliability and validity of electrogustometry and its application to young and elderly persons. Chem Senses 1995;20:499-503.

10. Yaginuma Y, Kobayashi T, Sai Y, Takasaka T. Predictive value of electrogustometry in the preoperative diagnosis of severity of middle ear pathology. J Otolaryngol Jpn 1996;99:1635-40.

11. Oakley B, Lawton A, Riddle DR, Wu LH. Morphometric and immunocytochemical assessment of fungiform taste buds after interruption of the chorda-lingual nerve. Microsc Res Tech 1993;26:187-95.

12. Montavon P, Hellekant G, Farbman A. Immunohistochemical, electrophysiological, and electron microscopical study of rat fungiform taste buds after regeneration of chorda tympani through the non-gustatory lingual nerve. J Comp Neurol 1996; 367:491-502.

13. Whitehead MC, McGlathery ST, Manion BG. Transganglionic degeneration in the gustatory system consequent to chorda tympani damage. Exp Neurol 1995;132:239-50.

14. Cain P, Frank ME, Barry MA. Recovery of chorda tympani nerve function following injury. Exp Neurol 1996;141:337-46.

15. Naito M. Development of the chorda tympani nerve in humans. Pract Otol (Kyoto) 1996;89:749-60.

16. Ylikoski J, Gamoletti R, Galey F. Chorda tympani nerve fibers in man. Acta Otolaryngol (Stockh) 1983;95:291-6.

17. Farbman AI, Hellekant G. Quantitative analyses of the fiber population in rat chorda tympani nerves and fungiform papillae. Am J Anat 1978;153:509-21.

18. Lundborg G, Dahlin LB, Danielsen N, et al. Nerve regeneration across an extended gap: a neurobiological view of nerve repair and the possible involvement of neurotrophic factors. J Hand Surg [Am] 1982;7:580-7.

≈

NEW FRONTIERS IN THE AMELIORATION OF HEARING LOSS

The international conference New Frontiers in the Amelioration of Hearing Loss will be held in St Louis, Missouri, March 22-25, 2001. For information, contact Sarah Uffman, Central Institute for the Deaf, Department of Research, 4560 Clayton Ave, St Louis, MO 63110; telephone (314) 977-0278; fax (314) 977-0030; e-mail: suffman@cid.wustl.edu.

Ann Otol Rhinol Laryngol 109:2000

USE OF METHOTREXATE FOR AUTOIMMUNE HEARING LOSS

ERIC L. MATTESON, MD, MPH
ROCHESTER, MINNESOTA

OLTITA TIRZAMAN, MD
WORCESTER, MASSACHUSETTS

GEORGE W. FACER, MD
ROCHESTER, MINNESOTA

DAVID A. FABRY, PHD
ROCHESTER, MINNESOTA

JAN KASPERBAUER, MD
ROCHESTER, MINNESOTA

CHARLES W. BEATTY, MD
ROCHESTER, MINNESOTA

THOMAS J. MCDONALD, MD
ROCHESTER, MINNESOTA

To assess the efficacy of low-dose methotrexate (MTX) given long-term for the treatment of autoimmune hearing loss, we performed a prospective open-label study of 11 patients with treatment-refractory autoimmune hearing loss. All patients had ongoing episodic worsening of hearing in 1 or both ears before enrollment despite traditional medical therapy. The MTX dose was 7.5 to 17.5 mg/wk. Hearing loss and vertigo were evaluated at baseline and at completion of the study. Hearing improvement was defined as an improvement in the pure tone threshold (PT) average of >10 dB or an increase in speech discrimination (SD) of >15%, whereas worsening was defined as a worsening of >10 dB in PT or a decrease of >15% in SD in at least 1 ear. The MTX was well tolerated. Among the 6 patients with Meniere's disease, 4 had improvement or resolution of vertigo, while 2 had no improvement. Disequilibrium improved in all 3 patients with Cogan's syndrome. According to the parameters defined above, hearing improved in 9 patients (82%), was unchanged in 1 patient (9%), and worsened in 1 patient (9%). Long-term low-dose MTX therapy may be a useful therapy for some patients who have hearing loss with a presumptively autoimmune-mediated component that is refractory to traditional therapies.

KEY WORDS — autoimmune hearing loss, Cogan's syndrome, Meniere's disease, methotrexate.

INTRODUCTION

Autoimmune inner ear disease is a clinical syndrome of uncertain pathogenesis. It is often associated with rapidly progressive hearing loss that, especially early in the disease course, may be unilateral, but is most commonly bilateral, presenting as sudden deafness or a rapidly progressive sensorineural hearing loss.[1,2] The hearing loss may be associated with vestibular disease in idiopathic diseases, as well as when due to better-defined conditions such as Meniere's disease and Cogan's syndrome.

Autoimmunity has been proposed as the pathogenesis of sudden sensorineural hearing loss, although the mechanism of disease is poorly understood. Clinically, sudden sensorineural hearing loss has been seen in association with other autoimmune diseases such as rheumatoid arthritis, inflammatory bowel disease, and polyarteritis nodosa.[1,3,4] Cogan's syndrome is accepted as an autoimmune disease, and it is likely that Meniere's disease has an autoimmune diathesis.[5-8] Circulating autoantibodies against inner ear antigens have been reported, although the sensitivity, specificity, and role of these antibodies in the disease process are poorly defined.[9] The improvement in hearing after corticosteroid and immunosuppressive therapy, as well as plasmapheresis, further suggests an autoimmune response as the cause of the hearing loss in these conditions.[9,10] It has also been suggested that disturbance of the microcirculation in the inner ear by thrombosis associated with antiphospholipid antibodies may lead to sudden deafness.[2,11]

High doses of corticosteroids, often 40 to 80 g/d, may be useful in the initial management of autoimmune-mediated sensorineural hearing loss. Unfortunately, the improvement in hearing is rarely sustained, and unacceptable side effects from the corticosteroid therapy soon follow. To improve the outcome of autoimmune inner ear disease, the use of cytotoxic therapy with cyclophosphamide has been proposed.[9,10] Although some success has been reported with this therapy in slowing or arresting the hearing loss, cyclophosphamide use is associated with significant toxicities, including increased risk of infection, malignancy, and death.[12] Another chemotherapeutic agent, methotrexate, has been successfully used in low doses for the management of a number of autoimmune diseases, including rheumatoid arthritis, inflammatory bowel disease, and Wegener's granulomatosis, with favorable experience from both standpoints of efficacy and toxicity.[13] On the basis of this experience, methotrexate has also been used as treatment for autoimmune inner ear diseases, including

---

From the Division of Rheumatology (Matteson, Tirzaman) and the Department of Otorhinolaryngology (Facer, Fabry, Kasperbauer, Beatty, McDonald), Mayo Clinic and Foundation, Rochester, Minnesota.

CORRESPONDENCE — Eric L. Matteson, MD, MPH, Mayo Clinic and Mayo Graduate School of Medicine, 200 First St SW, Rochester, MN 55905.

Meniere's disease and Cogan's syndrome.[14,15]

We conducted a 1-year prospective study of low-dose methotrexate to evaluate the long-term efficacy of this therapy in the management of autoimmune hearing loss.

MATERIALS AND METHODS

This was an open-label prospective study of oral methotrexate for the treatment of refractory autoimmune hearing loss with a planned duration of 12 months. Patients were eligible for enrollment on the basis of the following criteria: 1) the presence of unilateral or bilateral progressive sensorineural hearing loss, symptoms of bilateral Meniere's disease, or sensorineural hearing loss associated with Cogan's syndrome; and 2) a positive response in hearing to prednisone (1 mg/kg per day).

Over a period of 15 months, 11 patients were enrolled. All patients had ongoing episodic and/or progressive worsening of hearing in 1 or both ears before enrollment despite traditional medical therapy. These therapies included the use of a low-salt diet, diuretics, and vestibular suppressants in patients with Meniere's disease, as well as oral corticosteroids. No patients had received chemotherapeutic agents for treatment of hearing loss before enrollment.

Before initiation of the study drug, methotrexate, 17 patients were given a challenge of oral prednisone at an initial dose of 1 mg/kg per day, tapering off over 3 weeks. Of these, 12 had partial improvement in hearing in at least 1 ear; 11 patients gave informed consent and were enrolled into the trial.

Oral methotrexate was administered at an initial dose of 7.5 mg/wk, increasing to 17.5 mg/wk over the ensuing 4 to 8 weeks. A laboratory evaluation, including a complete blood count and liver enzyme testing, was performed every 4 to 8 weeks to assess for methotrexate toxicity. To minimize the potential toxicity, folic acid was prescribed for each patient at a dose of 1 mg/d.

The patients returned to the clinic every 3 months for a general health assessment and evaluation of hearing and vertigo. A formal audiometric evaluation was performed before the oral prednisone challenge (pretreatment), at baseline (after the prednisone challenge, and at the time treatment with methotrexate was begun), and at completion of the study (month 12). In addition, patients were asked for a subjective assessment of hearing and, if applicable, disequilibrium or vertigo (whether improved, worse, or unchanged).

Improvement in hearing was defined as an improvement in pure tone threshold (PT) average of >10 dB or an increase in speech discrimination (SD) of >15%, whereas worsening was defined as a worsening of >10 dB in PT or a decrease of >15% in SD in at least 1 ear. These parameters of outcome were selected on the basis of the likelihood of finding true differences in hearing based on test-retest performance characteristics of audiometry.[16,17] Data from all enrolled patients were considered, including patients who did not continue methotrexate therapy for the full 12 months of the study.

The parameters of improvement were assessed by audiometry performed at baseline and at the completion of the study. We chose this statistically conservative approach to avoid possibly overestimating the treatment effect of methotrexate, as could occur if the response of patients to the initial, pretreatment prednisone challenge were compared to the audiogram done at study termination.

RESULTS

A total of 11 patients (3 women, 8 men) were enrolled into this study. The mean age at enrollment was 49.8 years (range, 19.9 to 71.1 years). The patients had had hearing loss for an average of 4.2 years (range, 3 months to 13.1 years). The hearing loss was due to Meniere's disease in 6 patients, was due to Cogan's syndrome in 3, and was idiopathic in 2. There were 4 patients who had smoked in the past; none were smokers at enrollment.

The hearing loss was bilateral in 10 patients, including 3 patients who were functionally deaf in 1 ear at enrollment (2 with Meniere's disease and 1 with Cogan's syndrome). The hearing loss was unilateral in 1 patient with idiopathic disease. Before enrollment, all patients had ongoing episodic worsening of hearing in 1 or both ears despite traditional medical therapy, including glucocorticoids in all patients and diuretic therapy in patients with Meniere's disease. Disequilibrium or vertigo was present in 10 of the 11 patients at baseline.

Before enrollment, 17 patients with putative autoimmune hearing loss were given a challenge of oral prednisone at an initial dose of 1 mg/kg per day, tapering off over 3 weeks. All 11 patients enrolled into the study had at least partial improvement of hearing as defined above in at least 1 ear. At baseline, only the 3 patients with Cogan's syndrome were on chronic daily prednisone therapy, which was continued through and following the taper of the prednisone challenge. The baseline prednisone dose was further adjusted in these patients during the active treatment period with methotrexate according to clinical symptoms.

The baseline laboratory assessment included a negative or normal complete blood count, serum aspar-

THERAPEUTIC EFFICACY OF LOW-DOSE METHOTREXATE GIVEN FOR AUTOIMMUNE HEARING LOSS IN ELEVEN PATIENTS

		PT		*SD*			*Both PT and SD*		*Patient Assessment*	
Patient	*Disease*	*Right*	*Left*	*Right*	*Left*	*Either PT or SD*	*One Ear*	*Both Ears*	*Hearing*	*Disequilibrium or Vertigo*
1	Cogan's	↑	CNT	→	CNT	Yes	No	No	Yes	Yes
2	Cogan's	→	↑	↑	↑	Yes	Yes	No	No change	Yes
3	Cogan's	→	↑	CNT	→	Yes	No	No	No change	Yes
4	Meniere's	CNT	↑	CNT	→	Yes	No	No	Yes	Yes
5	Meniere's	↑	→	↑	→	Yes	Yes	No	No change	Yes
6	Meniere's	↑	↓	↑	CNT	Yes	Yes	No	No change	Yes
7	Meniere's	↓	↓	↓	↓	No	No	No	Worse	No change
8	Meniere's	→	→	→	→	No	No	No	No change	Yes
9	Meniere's	→	→	→	↑	Yes	No	No	No change	No change
10	Idiopathic	↑	→	→	→	Yes	No	No	No change	No change
11	Idiopathic	→	→	↑	↓	Yes	No	No	No change	Not applicable
Patients improved*		7/11		5/11		9/11	3/11	0/11	2/11	7/10

↑ — improvement in pure tone threshold (PT) average by >10 dB or in speech discrimination (SD) by >15%; ↓ — worsening in PT by >10 dB or in SD by >15%; → — change in PT of ≤10 dB or in SD of ≤15%; CNT — could not test because of profound hearing loss; "yes," "no," etc, refer to patient's response to question of whether he or she felt improvement.

*In 1 or both ears.

tate aminotransferase, Westergren sedimentation rate, syphilis serology, rheumatoid factor, and antinuclear antibody. Perinuclear antineutrophil cytoplasmic antibody (p-ANCA) was present in 1 patient with Cogan's syndrome; p- and c-ANCA were negative in the remainder of the patients. Antiphospholipid IgM antibodies were present in low titer (1:32 and 1:64) in 2 patients with Meniere's disease and were negative in the other patients. Serum protein electrophoresis revealed a slight polyclonal increase in gamma immunoglobulin in 1 patient and was negative in the remaining patients. Computed tomography (4 patients) and magnetic resonance imaging (7 patients) of the brain were nondiagnostic in 9 of the 9 patients in whom the studies were performed; both studies were obtained for 2 patients.

During the course of 1 year of follow-up on methotrexate therapy, an improvement in hearing as defined in Materials and Methods (improvement in PT average of >10 dB or increase in SD of >15% in at least 1 ear) was seen in 9 of the 11 patients (82%), whereas hearing was worse in 1 patient (9%) and unchanged in 1 patient (9%). Improvement in the PT in 1 ear was seen in 7 of the 11 patients (63.6%), and SD was improved in 1 ear in 5 of the 11 patients (45.5%). In only 1 patient was SD improved in both ears, and no patients had improvement in the PT in both ears. Both the PT and SD were improved in at least 1 ear in only 3 of the 11 patients (27.8%); no patient had improvement in both the PT and SD in both ears. The Table contains a summary of these results.

The patients were asked to keep a diary of the occurrence and severity of hearing fluctuation during the course of the study. All were asked to use this information, and their overall impression of their hearing, to make a subjective assessment of their hearing at completion of the 12-month study. Only 2 of the 11 patients (18.9%) felt their hearing had actually improved by the end of the study. At month 3, 4 of the 11 felt that their hearing was improved; at month 6, this figure was 4 of the 11; and at month 9, 3 of the 11. There was discordance between the patient assessment and the audiometric assessment of hearing, as the PT results (hearing improved, unchanged, or worse) agreed with the patient assessment in 6 of the 11 cases, and the SD results agreed with the patient assessment in 4 of the 11 cases.

Hearing remained stable in all patients with Cogan's syndrome. In these patients, the average prednisone dose at enrollment was 28 mg/d; at completion of the study, the average dose was 12 mg/d, and 1 of the 3 patients discontinued steroids completely while maintaining stable hearing. None of the patients with Cogan's syndrome had active ocular or systemic disease at enrollment, and none of these patients developed these disease manifestations during the study.

All patients also kept a diary to assess the frequency and severity of disequilibrium or vertigo during the study. At baseline, this symptom was experienced to some degree by 10 patients. Improvement in disequilibrium or vertigo (reduced number and/or severity of episodes) was noted by 7 of the 10 patients, including 3 of the 3 with Cogan's syndrome and 4 of the 6 with Meniere's disease.

The methotrexate therapy was well tolerated. Low-grade elevation of serum aspartate aminotransferase occurred in 1 patient, necessitating a reduction in the weekly methotrexate dose from 17.5 mg to 12.5 mg. Two patients discontinued methotrexate prematurely, 1 (patient 5) at week 36 and 1 (patient 9) at week 28, because of their concern about possible side effects in view of their perception of a lack of therapeutic efficacy. Both patients are included in the analysis of the results.

DISCUSSION

Autoimmune inner ear disease is an uncommon condition, the cause of which is uncertain. The response to treatment, usually with glucocorticoids and/or immunosuppressive drugs, is uncertain, and many patients eventually develop some degree of permanent hearing loss.

The present study examined the 1-year outcome of patients with autoimmune hearing loss treated with low-dose oral methotrexate at doses commonly used in treatment of another immune-mediated disorder, rheumatoid arthritis. To ascertain whether the therapy could be beneficial in the studied patients, we first administered a short course of prednisone, enrolling patients who had improvement after the glucocorticoid challenge. At the outset of the study, success was defined as an improvement in the audiometric parameters in at least 1 ear: of the PT by >10 dB or of SD by >15%. These parameters were chosen because they represent true differences in hearing based on test-retest audiometrics.[16,17]

According to the audiometric criteria, improvement was seen in 9 of the 11 treated patients. It is encouraging that the PT improved in 7 of the 11 patients in at least 1 ear and SD improved in almost half of the patients. However, there was little concordance in findings, as improvement in both the PT and SD in at least 1 ear occurred in only 3 of the 11 patients. It could not be expected that both PT and SD would improve in both ears, as 3 patients were functionally deaf in 1 ear at the study outset; nevertheless, no patient had improvement in both of these parameters in both ears. This certainly was due in part to the fact that most patients had some degree of fixed hearing loss in 1 ear at enrollment.

The view of the patients was rather different. Only 2 of the 11 patients felt that their hearing had improved during the study. This discordance with the audiometric findings is of considerable clinical importance, as the final arbiter of success of a therapy must be the favorable outcome in the opinion of the patient who must take the medication and cope with the side effects. Despite an apparent improvement in the audiometric parameters, 2 patients discontinued the drug before completion of the 52-week study because they did not feel that their hearing had improved and did not wish to have the expense, inconvenience, and potential side effects of methotrexate therapy. However, in the post-study follow-up, 5 of the 11 patients, including the 3 with Cogan's syndrome, continue to take methotrexate and have had stable hearing by audiometric and subjective assessment for 2 years since the study initiation.

Although not the primary outcome of interest, disequilibrium or vertigo was improved in 7 of the 10 patients with this symptom by the end of the study. The assessment of this symptom was entirely patient-derived, and formal testing was not included as a parameter of outcome. Whether this improvement represents a true treatment effect, the natural course of the symptom and the accommodation of the patient to it, or a placebo effect remains unknown.

This study was of an exploratory nature and has all the shortcomings of all open-label trials. The outcome may simply reflect the usual course of autoimmune hearing loss rather than the result of treatment. Although 9 of the 11 patients were improved by audiometric criteria, only 2 of the 11 patients felt improved; hence, the audiometric parameters chosen may be clinically inadequate in defining success. However, only 1 of the 11 patients felt that his hearing had worsened, and no patient had worsening of disequilibrium or vertigo during the trial. If improved or stable hearing is viewed as the criterion of success, 10 of the 11 patients did well from both audiometric and subjective standpoints. Whether the improved or stabilized symptoms are due to the treatment or to the methotrexate therapy remains uncertain. A randomized, controlled trial would be required to establish the role of methotrexate in the treatment of this disease.

Future studies may need to require an even larger degree of improvement in audiometric parameters than that used in this study, including, perhaps, improvement in both ears, and perhaps a different method for patient-derived assessment. We believe that the patient assessment must be a cornerstone for any claims of success in any study, because it is the patient who must finally decide whether the treatment is of value to him or her.

Patients with Cogan's syndrome appeared to do the best, and were most willing to continue with methotrexate therapy after completion of the trial. The daily prednisone dose could be reduced by >50% during the course of the study, and 1 patient with Cogan's syndrome discontinued prednisone altogether without worsening of hearing — a factor that contributed to patient satisfaction. The number of patients was too small to permit meaningful conclusions about the ultimate role of methotrexate as adjuvant therapy for Cogan's syndrome, but this and other reports suggest that it may be useful.[15]

Three syndromes of autoimmune hearing loss were examined in this study. Patients were enrolled on the basis of diagnosis and improvement in audiometric parameters after a challenge of prednisone given before initiation of therapy with methotrexate. It is clear that these clinical syndromes are different in their course, and future studies should examine them separately.

Methotrexate may offer an additional treatment option for the treatment of some patients with autoimmune hearing loss, including some subsets of patients with Meniere's disease or Cogan's syndrome. The results of this and other studies suggest that future randomized, controlled trials of this therapy should be considered for patients with Meniere's disease and actively fluctuating hearing loss. An improved understanding of the pathogenesis of these disorders will also greatly contribute to improved therapies.

REFERENCES

1. McCabe BF. Autoimmune sensorineural hearing loss. Ann Otol Rhinol Laryngol 1979;88:585-9.
2. Toubi E, Ben-David J, Kessel A, Podoshin L, Golan TD. Autoimmune aberration in sudden sensorineural hearing loss: association with anticardiolipin antibodies. Lupus 1997;6:540-2.
3. Veldman JE, Roord JJ, O'Connor AF, Shea JJ. Autoimmunity and inner ear disorder: an immune complex mediated sensorineural hearing loss. Laryngoscope 1984;94:501-7.
4. Summers RW, Harker L. Ulcerative colitis and sensorineural hearing loss: is there a relationship? J Clin Gastroenterol 1982;4:251-2.
5. Alleman AM, Dornhoffer JL, Arenberg IK, Walker PD. Demonstration of autoantibodies to the endolymphatic sac in Meniere's disease. Laryngoscope 1997;107:211-5.
6. Hughes GB, Kinney SE, Barna BP, Calabrese LH. Autoimmune reactivity in Meniere's disease: a preliminary report. Laryngoscope 1983;93:410-7.
7. Hughes GB, Kinney SE, Barna BP. Autoimmune reactivity in Cogan's syndrome: a preliminary report. Otolaryngol Head Neck Surg 1983;91:24-32.
8. Haynes BF, Pikus A, Kaiser-Kupfer MI, Fauci AS. Successful treatment of sudden hearing loss in Cogan's syndrome with corticosteroids. Arthritis Rheum 1981;24:501-3.
9. Hughes GB, Kinney SE, Barna BP, Calabrese LH. Practical versus theoretical management of autoimmune inner ear disease. Laryngoscope 1984;94:758-67.
10. McCabe BF. Autoimmune inner ear disease: therapy. Am J Otol 1989;10:196-7.
11. Casoli P, Tumiati B. Cogan's syndrome: a new possible complication of antiphospholipid antibodies? Clin Rheumatol 1995;14:197-8.
12. Clements PJ. Alkylating agents. In: Dixon J, Furst DE, eds. Second line agents in the treatment of rheumatic diseases. New York, NY: Marcel Dekker, 1991:335-61.
13. Songsiridey N, Furst DE. Methotrexate: the rapidly acting drug. Clin Rheumatol 1990;4:575-94.
14. Sismanis A, Wise CM, Johnson GD. Methotrexate management of immune-mediated cochleovestibular disorders. Otolaryngol Head Neck Surg 1997;116:146-52.
15. Richardson B. Methotrexate therapy for hearing loss in Cogan's syndrome. Arthritis Rheum 1994;37:1559-61.
16. Thornton AR, Raffin MJM. Speech discrimination scores modeled as a binomial variable. J Speech Hear Res 1978;21:507-18.
17. Raffin MJM, Thornton AR. Confidence levels for differences between speech-discrimination scores: a research note. J Speech Hear Res 1980;23:5-18.

Ann Otol Rhinol Laryngol 109:2000

EFFECT OF 7-NITROINDAZOLE UPON COCHLEAR DYSFUNCTION INDUCED BY TRANSIENT LOCAL ANOXIA

KEIJI TABUCHI, MD ZENYA ITO, MD TETSURO WADA, MD
KAZUHIKO TAKAHASHI, MD AKIRA HARA, MD JUN KUSAKARI, MD
TSUKUBA, JAPAN

The purpose of the present study was to further elucidate how nitric oxide (NO) is involved in cochlear anoxia-reperfusion injury. Transient local anoxia of the cochlea was induced in albino guinea pigs for 15, 30, or 60 minutes by transiently compressing the labyrinthine artery through a skull base approach. 7-Nitroindazole (7NI), a relatively selective neuronal nitric oxide synthase (nNOS) inhibitor, was intraperitoneally administered to the guinea pigs 30 minutes before the onset of local anoxia. The compound action potential (CAP) thresholds were measured before the administration of 7NI and 4 hours after the onset of reperfusion. A statistically significant reduction in the postanoxic CAP threshold shift from the preadministration value was observed in the 7NI-administered animals as compared with the control animals after 15- and 30-minute periods of anoxia. These results confirm the involvement of NO and nNOS in the cochlear injury induced by transient local anoxia.

KEY WORDS — cochlea, compound action potential, local anoxia, nitric oxide, 7-nitroindazole.

INTRODUCTION

The physiological role of nitric oxide (NO) is currently of considerable interest with regard to modulation of cochlear blood flow (CoBF) and auditory neurotransmission.[1,2] In addition, it has been suggested that excessive generation of NO is cytotoxic to the cochlea.[3] In a previous study,[4] we showed that N^{ω}-nitro-L-arginine, an inhibitor of nitric oxide synthase (NOS), ameliorates cochlear dysfunction induced by transient local anoxia, and this result suggested the involvement of NO in anoxia-reperfusion injury of the cochlea. 7-Nitroindazole (7NI) is another potent NOS inhibitor. Differing from N^{ω}-nitro-L-arginine, it is derived from indazole and is reported to be a relatively selective neuronal NOS (nNOS) inhibitor.[5-7] In order to ascertain the role of NO in anoxia-reperfusion injury of the cochlea, we examined the effect of 7NI on the compound action potential (CAP) threshold shift induced by transient local anoxia.

MATERIALS AND METHODS

Albino guinea pigs (300 to 400 g) with a normal Preyer pinna reflex were anesthetized with pentobarbital sodium (28 mg/kg intraperitoneally, Nembutal, Abbott), tracheostomized, paralyzed with suxamethonium chloride (Relaxin, Kyorin), and artificially ventilated with room air. Two catheters were used for each animal: one in the external jugular vein for fluid replacement, and the other in the right carotid artery for monitoring blood pressure. Body temperature was maintained at 37°C ± 1°C with a heating pad. Electrocardiography and mean arterial pressure were monitored throughout the experiment. All experimental procedures were performed in accordance with the guidelines of the Animal Experiment Committee at the University of Tsukuba.

The methods used for measuring CAP and inducing transient local anoxia of the cochlea were the same as described in our previous study.[8] Briefly, the left tympanic bulla was opened by the ventrolateral approach. The CAP was recorded with a silver–silver chloride electrode placed on the bony edge of the round window, and the indifferent electrode was placed on the neck muscles. The sound stimuli were tone bursts of 2-, 4-, 6-, 8-, 12-, or 16-kHz pure tones (10-ms duration with 1-ms rise-fall time, delivered every 200 ms in an open-field system). Thirty-two, 64, or 128 consecutive potentials were averaged by a signal processor (Synax 2100, NEC Medical Systems), and the sound pressure level (SPL) needed to evoke 10 µV of CAP was defined as the threshold. When the sound of 110 dB SPL failed to evoke a potential of 10 µV, the threshold was defined to be 115 dB SPL to simplify the calculations.

Local anoxia of the cochlea was induced via the skull base approach.[9] The CoBF was monitored with a laser-Doppler flowmeter (BRL-100, Bio Research Center). Its needle probe was held in a micromanipulator and positioned on the lateral wall of the cochlear second turn. The CoBF was plotted as a per-

---

From the Department of Otolaryngology, Institute of Clinical Medicine, University of Tsukuba, Tsukuba, Japan. This study was supported by a grant from the Ministry of Education, Science and Culture (Grant-in-Aid for Scientific Research A(2) 09307039).

CORRESPONDENCE — Jun Kusakari, MD, Dept of Otolaryngology, Institute of Clinical Medicine, University of Tsukuba, 1-1-1 Tennodai, Tsukuba, 305-8575, Japan.

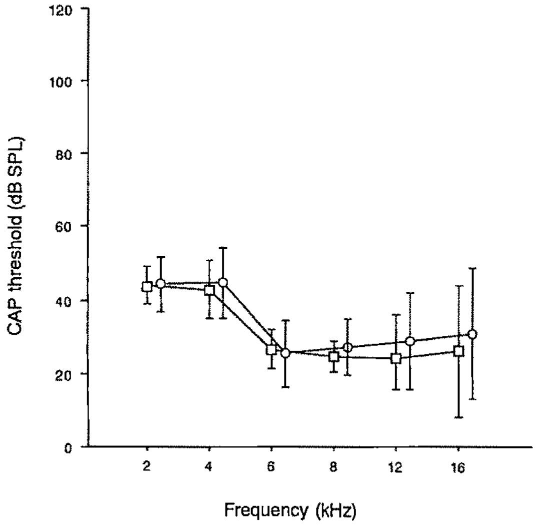

Fig 1. Compound action potential (CAP) thresholds before and 4 hours after administration of 7-nitroindazole (7NI; n = 5; mean ± SD). Preadministration and postadministration values are indicated with squares and circles, respectively. CAP thresholds were not affected significantly by 7NI administration (2-way analysis of variance).

centage relative to the value measured just before the drug administration, with the postmortem value set at 0%.

The 7NI-administered control group consisted of 5 guinea pigs. In order to examine whether administration of 7NI itself might affect the CAP thresholds, 50 mg/kg of 7NI (sonicated in 2 mL/kg of peanut oil) was intraperitoneally administered, and the CAP thresholds were measured before and 4 hours after administration.

The peanut oil–administered anoxia group consisted of 15 guinea pigs. Each animal in this group was intraperitoneally administered 2 mL/kg of peanut oil 30 minutes before the onset of anoxia and was subjected to 15-, 30-, or 60-minute anoxia (n = 5 in each subgroup).

The 7NI-administered anoxia group consisted of 25 guinea pigs. Each animal in this group was intraperitoneally administered 7NI sonicated in 2 mL/kg of peanut oil, 30 minutes before the onset of anoxia. The animals in this group were further divided into the following 3 subgroups according to the anoxic period: 1) the 15-minute anoxia group (n = 5), in which each animal was administered 50 mg/kg of 7NI; 2) the 30-minute anoxia group (n = 15), in which each animal was administered 1 (n = 5), 10 (n = 5), or 50 (n = 5) mg/kg of 7NI; and 3) the 60-minute anoxia group (n = 5), in which each animal was administered 50 mg/kg of 7NI.

The CAP thresholds were measured before the administration of peanut oil or 7NI and 4 hours after the onset of reperfusion. In order to evaluate the effect of 7NI on postanoxic cochlear dysfunction, we compared the CAP threshold shifts from the preanoxic values at 4 hours after the onset of reperfusion between the peanut oil– and the 7NI-given anoxia groups.

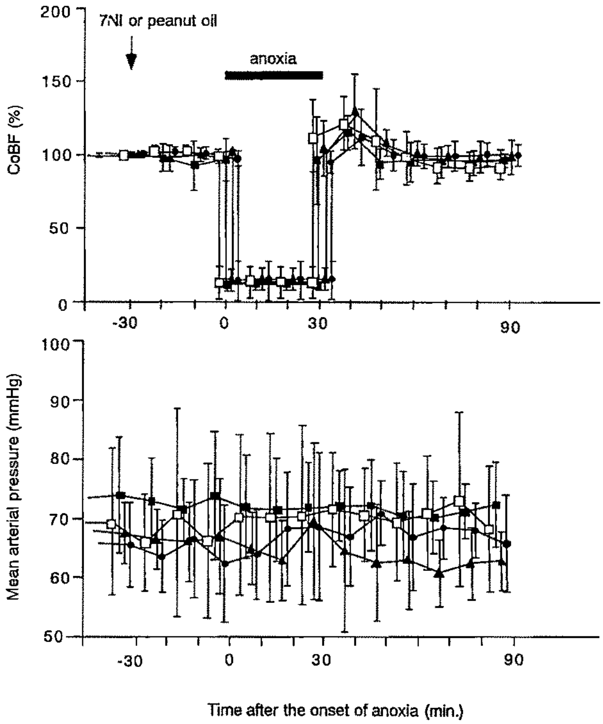

Fig 2. Cochlear blood flow (CoBF; percent) and mean arterial pressure (millimeters of mercury) before, during, and after onset of anoxia (mean ± SD) in 30-minute anoxia group. Open squares, closed squares, triangles, and circles indicate peanut oil–administered anoxia group and 50, 10, and 1 mg/kg 7NI–administered anoxia groups, respectively. 7NI did not affect CoBF or mean arterial pressure as compared with peanut oil–given control group (1-way analysis of variance).

RESULTS

Figure 1 shows the CAP thresholds before and 4 hours after the administration of 7NI (mean ± SD, n = 5). Administration of 7NI (50 mg/kg) did not significantly affect the CAP thresholds (2-way analysis of variance [ANOVA], F = 0.61, $p > .05$).

Figure 2 illustrates changes in CoBF and mean arterial pressure before, during, and after transient local anoxia of 30 minutes' duration. As the Figure indicates, the CoBF did not change for 30 minutes before anoxia. As expected from the previous study,[8] the CoBF decreased rapidly when the labyrinthine artery was compressed and remained steady during anoxia. When the artery was unclamped, the CoBF immediately increased with a transient overshoot and then gradually regained a stable value close to the preanoxic value. The 7NI did not significantly affect the CoBF or the mean arterial pressure (1-way

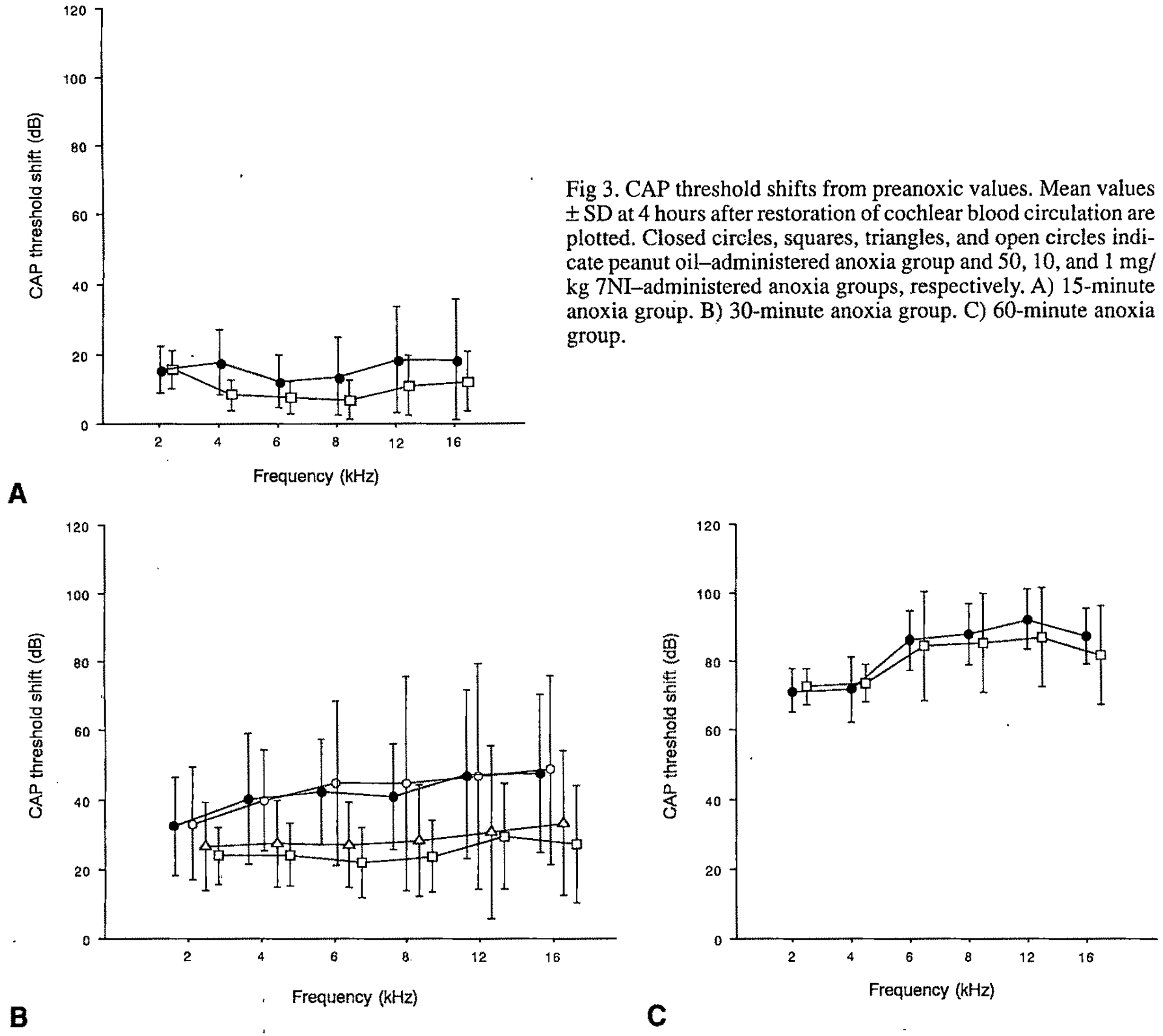

Fig 3. CAP threshold shifts from preanoxic values. Mean values ± SD at 4 hours after restoration of cochlear blood circulation are plotted. Closed circles, squares, triangles, and open circles indicate peanut oil–administered anoxia group and 50, 10, and 1 mg/kg 7NI–administered anoxia groups, respectively. A) 15-minute anoxia group. B) 30-minute anoxia group. C) 60-minute anoxia group.

ANOVA, $p > .05$).

Figure 3 shows the postanoxic CAP threshold shifts occurring 4 hours after the onset of reperfusion. In the 30-minute anoxia group (Fig 3B), intraperitoneal administration of 10 or 50 mg/kg of 7NI significantly improved the CAP threshold shifts (2-way ANOVA, $F = 6.22$, $p < .01$; Fisher test, $p < .01$ in the 50-mg/kg subgroup and $p < .05$ in the 10-mg/kg subgroup), whereas no improvement was observed after 1-mg/kg administration (Fisher test, $p > .05$). Further, 50 mg/kg of 7NI showed statistically significant protection against 15-minute anoxia (Fig 3A; 2-way ANOVA, $F = 4.19$, $p < .05$). In contrast to the protective effect observed in 15- and 30-minute anoxia, intraperitoneal administration of 50 mg/kg of 7NI did not significantly reduce the postanoxic CAP threshold shift in 60-minute anoxia (Fig 3C; 2-way ANOVA, $F = 2.00$, $p > .05$).

DISCUSSION

The present study has clearly demonstrated the significant protective effect of 7NI against transient local anoxia of the cochlea, and this finding is consistent with our previous study using another NOS inhibitor, N^{ω}-nitro-L-arginine.[4] These results strongly indicate that NO generated within the cochlea plays an important role in injury-producing processes induced by anoxia and reperfusion.

To date, NOS is divided into 3 isozymes: neuronal NOS (nNOS), endothelial NOS (eNOS), and inducible NOS (iNOS). Several investigators have demonstrated that 7NI acts as a relatively selective inhibitor of nNOS in in vivo studies.[5-7] Further, it was reported that 7NI neither elevated arterial blood pressure[5] nor inhibited acetylcholine-induced relaxation of aortic rings.[10] In addition, 7NI was known to be approximately 50 times more potent in inhibiting nNOS than in inhibiting iNOS in spleen homogenates of endotoxin-pretreated rats.[10] These results support the view that the main action of 7NI is the inhibition of nNOS.

In contrast to the selective inhibitory action of 7NI,

N^{ω}-nitro-L-arginine is known to strongly inhibit nNOS and eNOS activity, whereas it is less potent as an iNOS inhibitor.[11] We have previously shown that 1 mg/kg or more of N^{ω}-nitro-L-arginine elevates mean arterial pressure and ameliorates postanoxic cochlear dysfunction.[4] In the present study, intraperitoneal administration of 7NI (up to 50 mg/kg) did not significantly affect mean arterial blood pressure or CoBF. These findings support the assumption that 7NI did not inhibit the eNOS activity in the cochlea. Gosepath et al[12] showed immunohistochemically that iNOS was not detected in the normal cochlea, and it is well known that expression of iNOS messenger RNA and elevation of iNOS activity are delayed by several hours after exposure to stimuli such as lipopolysaccharide, cytokines, and anoxia-reperfusion in various organs.[13-15] Therefore, the observation time (4 hours) used to evaluate the effect of 7NI in the present study was too short to determine the effect of iNOS. Consequently, it seems reasonable to speculate that the results obtained in the present study are mainly due to the inhibition of nNOS activity by 7NI. Further, because the inhibitory activity of N^{ω}-nitro-L-arginine for nNOS has been reported to be stronger than that of 7NI, with 50% inhibitory concentration values of 0.05 μmol/L for N^{ω}-nitro-L-arginine versus 0.47 μmol/L for 7NI,[11,16] the present finding that 10 mg/kg or more of 7NI was needed to achieve cochlear protection against transient anoxia is quite in agreement with the known potency of these inhibitors.

In recent years, there has been an interest in determining the role of NOS isozymes in the development of ischemic injury, but it is still controversial as to which one is the most contributory to its generation. It was reported that in cerebral anoxia, neuronal and inducible NO production contributed to the development of ischemic injury,[17,18] whereas endothelial NO production protected the brain tissue by increasing regional cerebral blood flow.[19] In contrast to the results obtained in cerebral anoxia, it was reported that inhibition of nNOS activity with 7NI or aminoethyl-isothiourea did not protect the heart from anoxia-reperfusion injury.[20] In the present study, 7NI, an indazole-derived NOS inhibitor, exerted a protective effect on the cochlear injury induced by transient local anoxia of 15 or 30 minutes' duration. This result indicates that an enhanced formation of NO by nNOS contributes to cell injury during and after transient anoxia, as far as the cochlea is concerned.

In conclusion, the present finding has further confirmed the deleterious role of NO in anoxia-reperfusion injury of the cochlea and supports the hypothesis that neuronal NO production mainly contributes to this injury.

REFERENCES

1. Brechtelsbauer PB, Nuttall AL, Miller JM. Basal nitric oxide production in regulation of cochlear blood flow. Hear Res 1994;77:28-42.

2. Dais CGD, Prazma J, Ball SS, Carlton Z, Carrasco V, Pillsbury HC. Effect of nitroprusside on compound action potential thresholds in the gerbil cochlea. Hear Res 1996;99:1-6.

3. Ruan RS, Leong SK, Yeoh KH. Ototoxicity of sodium nitroprusside. Hear Res 1997;114:169-78.

4. Tabuchi K, Kusakari J, Ito Z, Wada T, Takahashi K, Hara A. Effect of nitric oxide synthase inhibitor upon cochlear dysfunction induced by transient local anoxia. Acta Otolaryngol (Stockh) 1999;119:179-84.

5. Moore PK, Wallace Z, Hart SL, Babbedge RC. Characterization of the novel nitric oxide synthase inhibitor 7-nitro indazole and related indazoles: antinociceptive and cardiovascular effects. Br J Pharmacol 1993;110:219-24.

6. Moore PK, Bland-Ward PA. 7-Nitroindazole: an inhibitor of nitric oxide synthase. Methods Enzymol 1996;268:393-8.

7. Southan GJ, Szabo C. Selective pharmacological inhibition of distinct nitric oxide synthase isoforms. Biochem Pharmacol 1996;51:383-94.

8. Tabuchi K, Ito Z, Wada T, Hara A, Kusakari J. The effect of mannitol upon cochlear dysfunction induced by transient local anoxia. Hear Res 1998;126:28-36.

9. Kusakari J, Kambayashi J, Kobayashi T, et al. The effect of transient anoxia upon the cochlear potentials. Auris Nasus Larynx 1981;8:55-64.

10. Babbedge RC, Bland-Ward SL, Moore PK. Inhibition of rat cerebellar nitric oxide synthase by 7-nitro indazole and related substituted indazoles. Br J Pharmacol 1993;110:225-8.

11. Lambert LE, Whitten JP, Baron BM, Cheng HC, Doherty NS, McDonald IA. Nitric oxide synthesis in the CNS, endothelium and macrophages differs in its sensitivity to inhibition by arginine analogues. Life Sci 1991;48:69-75.

12. Gosepath K, Gath I, Maurer J, et al. Characterization of nitric oxide synthase isoforms expressed in different structures of the guinea pig cochlea. Brain Res 1997;747:26-33.

13. Stuehr D, Marletta MA. Induction of nitrite/nitrate synthesis in murine macrophages by BCG infection, lymphokines, or interferon-γ. J Immunol 1987;139:518-25.

14. Sato K, Miyakawa K, Takeya M, et al. Immunohistochemical expression of inducible nitric oxide synthase (iNOS) in reversible endotoxic shock studied by a novel monoclonal antibody against rat iNOS. J Leukoc Biol 1995;57:36-44.

15. Iadecola C, Zhang F, Xu X. Inducible nitric oxide synthase gene expression in vascular cells after transient focal cerebral ischemia. Stroke 1996;27:1373-80.

16. Moore PK, Babbedge RC, Wallace P, Gaffen ZA, Hart SL. 7-Nitro indazole, an inhibitor of nitric oxide synthase, exhibits anti-nociceptive activity in the mouse without increasing blood pressure. Br J Pharmacol 1993;108:296-7.

17. Huang Z, Huang PL, Panahian N, Dalkara T, Fishman MC, Moskowitz MA. Effects of cerebral ischemia in mice de-

ficient in neuronal nitric oxide synthase. Science 1994;265:1883-5.

18. Iadecola C, Zhang F, Xu X. Inhibition of inducible nitric oxide synthase ameliorates cerebral ischemic damage. Am J Physiol 1995;268:R286-R292.

19. Huang Z, Huang PL, Ma J, et al. Enlarged infarcts in endothelial nitric oxide synthase knockout mice are attenuated by nitro-L-arginine. J Cereb Blood Flow Metab 1996;16:981-7.

20. Thiemermann C, Bowes J, Myint FP, Vane JR. Inhibition of the activity of poly(ADP ribose) synthetase reduces ischemia-reperfusion injury in the heart and skeletal muscle. Proc Natl Acad Sci U S A 1997;94:679-83.

≈

EIGHTH SYMPOSIUM ON COCHLEAR IMPLANTS IN CHILDREN

The Eighth Symposium on Cochlear Implants in Children will be held in Los Angeles, California, February 28 to March 3, 2001. For information, visit the web site www.hei.org/ci2001; telephone Caroline Sakai at (213) 353-7001; or write to House Ear Institute/CI2001, 2100 W Third St, Los Angeles, CA 90057.

Ann Otol Rhinol Laryngol 109:2000

OLFACTORY MUCOSAL FINDINGS IN PATIENTS WITH PERSISTENT ANOSMIA AFTER ENDOSCOPIC SINUS SURGERY

SANG HAG LEE, MD
HYUN HO LIM, MD
HEUNG MAN LEE, MD
HYO JIN PARK, MD
JONG OUCK CHOI, MD
SEOUL, KOREA

Sixty-three biopsy specimens were obtained from the olfactory region of 15 patients with persistent anosmia and 6 patients with normosmia after sinus surgery. Immunohistochemical examination of all specimens with microtubule-associated protein 5 (MAP5) antisera demonstrated olfactory epithelium in 11 of 18 specimens from normosmic patients and in 12 of 45 samples from anosmic patients. There was a significant difference in the proportion of specimens containing olfactory epithelium between the two groups of patients. In normosmic patients, most of the biopsy samples contained normal-appearing olfactory tissue. However, 2 main patterns of histologic findings were noted in the olfactory mucosa of anosmic patients. First, the olfactory receptor cells were remarkably decreased in number. Second, the orderly arrangement of cells characteristic of normal olfactory epithelium was lost, demonstrating a degenerative appearance. These data suggest that olfactory epithelium can be degenerated even in chronic sinusitis and thereafter extensively replaced with respiratory epithelium, resulting in increased sampling error. Moreover, an unimproved olfactory deficit after sinus surgery may be due to the abnormalities observed at the olfactory epithelium level.

KEY WORDS — anosmia, endoscopic sinus surgery, MAP5, olfactory mucosa.

INTRODUCTION

Biopsy of the olfactory mucosa has been used to study various human olfactory disorders, and morphological examination has been performed with both light and electron microscopy and immunohistochemistry. From these studies, researchers have suggested that dysfunction was associated with histopathologic change and that the specific type of change correlated with the cause of the dysfunction. These observations served as a guide to diagnoses and therapy, allowing improvement in the care of patients.[1-5]

Chronic sinusitis is frequently accompanied by various degrees of olfactory disturbance. This type of olfactory loss is thought to be predominantly a result of mucosal obstruction to airflow through the superior nasal meatus. Several studies have demonstrated well-preserved olfactory epithelium in chronic rhinosinusitis, suggesting that olfactory function is reversible and that chronic inflammation has no deleterious effect on the olfactory mucosa.[1,3] Endoscopic sinus surgery is usually indicated for relief of obstruction, relieving the sinusitis, with relief of anosmia or hyposmia, and actually improves the sense of smell in most patients with chronic sinusitis. Although it is thus expected that olfactory dysfunction in chronic sinusitis recovers to a normal level after surgical treatment, a considerable number of patients remain anosmic despite endoscopic sinus surgery and long-term maximal medical therapy. This type of olfactory disorder has been noted clinically by several authors.[6-9] However, its pathogenesis is not fully understood to date.

The present study was undertaken to examine the histopathologic findings of the olfactory mucosa in patients with persistent anosmia after endoscopic sinus surgery.

MATERIALS AND METHODS

Among patients with chronic polypoid sinusitis who underwent endoscopic sinus surgery between September 1995 and April 1996, 39 patients with both subjective and objective anosmia before surgery were included in this study and followed up for at least 2 years until September 1998. All patients were treated after surgery with a combination of oral macrolide antibiotics and nasal steroid spray for 3 to 6 months. For this study, each patient was regularly seen for the duration of the follow-up period to determine a subjective estimation of olfaction by the patient, to administer objective olfactory testing, and to obtain a concurrent endoscopic examination of the sinonasal bed.

From the Department of Otorhinolaryngology–Head and Neck Surgery, College of Medicine, Korea University (S. H. Lee, Lim, H. M. Lee, Choi), and the Department of Otorhinolaryngology, College of Medicine, SungKyunKwan University (Park), Seoul, Korea. This work was supported by a grant from Institute of Communication Disorders, Korea University, Seoul, Korea.

CORRESPONDENCE — Sang Hag Lee, MD, Dept of Otorhinolaryngology–Head and Neck Surgery, College of Medicine, Korea University, 126-1, 5 Ka, Anam-Dong, SungBuk-Ku, Seoul, 136-705, Korea.

CHARACTERISTICS OF BIOPSY CASES

Case No.	Sex	Age	Olfactory Function After Surgery	Average Detection Threshold/ Average Recognition Threshold*	Olfactory Samples†	No. of Receptor Cells
1	M	30	Normosmic	−1/0	2	(+++) (+++)
2	F	47	Normosmic	0/1	1	(+++)
3	M	61	Normosmic	0/1	2	(+++) (+++)
4	F	42	Normosmic	−0.8/0.2	2	(+++) (+++)
5	M	16	Normosmic	−0.6/0.2	2	(+++) (+++)
6	M	25	Normosmic	0/1	2	(+++) (+++)
7	M	51	Anosmic	5.8/5.8	1	(+)
8	F	35	Anosmic	5.8/5.8	1	(+)
9	M	37	Anosmic	5.8/5.8	1	(+)
10	M	28	Anosmic	5.8/5.8	0	(−)
11	F	33	Anosmic	5.8/5.8	2	(++) (+)
12	F	24	Anosmic	5.8/5.8	0	(−)
13	F	47	Anosmic	5.8/5.8	0	(−)
14	F	60	Anosmic	5.8/5.8	2	(++) (+)
15	M	38	Anosmic	5.8/5.8	2	(+) (+)
16	F	37	Anosmic	5.8/5.8	0	(−)
17	F	52	Anosmic	5.8/5.8	0	(−)
18	F	47	Anosmic	5.8/5.8	0	(−)
19	M	42	Anosmic	5.8/5.8	1	(+)
20	M	45	Anosmic	5.8/5.8	1	(+)
21	M	45	Anosmic	5.8/5.8	1	(+)

*Normosmic — −1.0 to 2.5; moderately hyposmic — 2.6 to 4.0; severely hyposmic — 4.1 to 5.5; anosmic — ≥5.6.

†Number of samples containing olfactory epithelium among 3 samples obtained from upper septal mucosa and nasal septum adjacent to cribriform plate.

Fifteen of these patients showed a grossly normal ethmoid sinus cavity and olfactory cleft area during the follow-up period after surgery. However, they had persistent subjective anosmia and showed anosmia on an objective olfaction test. They did not have any specific events that could be considered as possible causes of olfactory loss, such as head trauma, allergy, congenital anosmia, exposure to toxins, or neurodegenerative disorders, and no contiguity was found between an episode of viral infection and recognition of olfactory impairment. Biopsy was performed on those patients between April 1998 and September 1998. The patients consisted of 7 men and 8 women, 24 to 60 years of age (mean age, 41.4 years).

To compare the histologic pattern, 6 patients with normosmia after surgery were also included in this study and used as a control for the present series of specimens. Details of all patients are shown in the Table. The remaining 18 patients were excluded from the analysis regardless of their subjective sense of smell, because they refused the olfactory mucosa biopsy and/or had grossly edematous olfactory cleft mucosa with or without an ethmoid sinus lesion. All biopsy tissues were obtained with the informed consent of the patients, and the studies were carried out in accordance with the guidelines of the Medical Research Council of Korea University.

Olfactory Testing. Objective olfactory testing was performed by an odor threshold and identification test (T & T olfactometry). This form of olfactometry uses 5 odorants, ie, β-phenylethylalcohol, methylcyclopentenolone, isovaleric acid, γ-undecalactone, and skatole. Each odorant was prepared in 8 concentrations except for methylcyclopentenolone, which was prepared in 7 concentrations through 1:10 serial dilutions. Each odorant was given in increasing concentrations to identify each patient's threshold. If a patient could not detect the highest concentration, a score of 6 was given. According to the average values for the detection threshold and the recognition threshold, patients were classified as normosmic, moderately hyposmic, severely hyposmic, or anosmic (see Table).

Tissue Collection and Processing. In all cases, a self-retaining nasal speculum with a long blade was inserted carefully for the direct inspection of the olfactory cleft with a microscope and/or endoscope. Upon identification of the olfactory cleft, the presumptive olfactory mucosa was incised, undermined, and elevated from the underlying bone with a sickle knife, and then the elevated mucosa was removed by a small Blakesley forceps. In each case, 3 samples were obtained from the following areas: the dorsomedial and dorsoposterior areas of the left nasal septum,

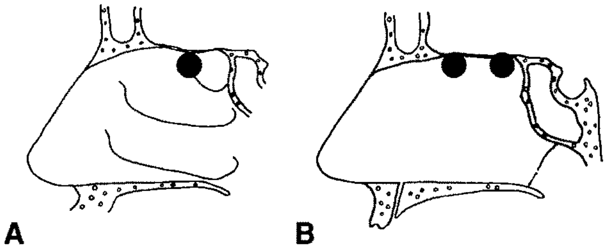

Fig 1. Schematic representations of human nasal cavity. Positions of 3 biopsy samples obtained from olfactory cleft are indicated by black circles. A) Lateral wall of nasal cavity. B) Medial wall of nasal cavity.

and the dorsomedial area of the superior turbinate adjacent to the cribriform plate (Fig 1). They were immediately immersed in Zamboni solution for 24 hours, rinsed in 30% sucrose in phosphate buffered saline (PBS), and embedded in OCT compound (Tissue Tek, Miles Scientific, Naperville, Ill). Each block was serially cryosectioned 12 µm thick, mounted on a poly-L-lysine–coated slide, and then stained with hematoxylin and eosin (H & E). To identify the olfactory epithelium inside the specimens, an alternate series of adjacent sections were immunostained with microtubule-associated protein 5 antisera (MAP5; Sigma, USA) as described earlier.[10] An avidin-biotin peroxidase method was used for immunohistochemistry. Reacted specimens were exposed to diaminobenzidine.

Quantitative Assessment of Number of Receptor Cells. The number of olfactory receptor cells was counted by immunostaining for MAP5 at a magnification of 400×. The number was counted, with the aid of a calibrated eyepiece micrometer disc, along the olfactory epithelium, and the results were evaluated as the mean number of olfactory receptor cells per 0.4 mm length: – for no receptor cells; + for a few (1 to 20); ++ for moderate (21 to 50); and +++ for many (≥50). For each case analyzed in this manner, we measured 3 to 5 sections per specimen that contained olfactory mucosa.

RESULTS

Light microscopic examination revealed that in the whole population under study, olfactory tissue alone or with respiratory mucosa was found in 23 of the 63 biopsy samples (37%). Olfactory tissue was found in 61% of the samples from subjects with normosmia and in 27% from those with anosmia. There was a significant difference in the population of samples containing olfactory epithelium between normosmic and anosmic patients (Z test, $Z = 2.5651$; $p < .05$, 1-tailed test). Detailed data obtained from the immunostaining are shown in the Table.

Olfactory Mucosal Findings of Normosmic Patients. In H & E–stained preparations, olfactory epithelium found in 5 patients (cases 1, 3, 4, 5, and 6) had sufficient thickness, and the fundamental nuclear arrangement of the supporting cells, the olfactory receptor cells, and the basal cells was retained. In the middle portion of the epithelium, many olfactory receptor cells could be observed in each field examined under high magnification. Immunostaining of consecutive sections with MAP5 antibody was able to clarify the distribution of olfactory epithelium more precisely and selectively than H & E stain. In 1 patient (case 4), pure olfactory mucosa was seen in 2 samples. Many MAP5-immunoreactive olfactory receptor cells remained in the epithelium, and many nerve bundles were retained in the lamina propria (Fig 2A). In 4 patients (cases 1, 3, 5, and 6), variously sized patches of respiratory epithelium were distributed within the olfactory epithelium. The olfactory epithelium defined by immunohistochemistry showed a number of MAP5-immunoreactive multilayered receptor cells with definite areas of transition between the olfactory and respiratory epithelia (Fig 2B). In the remaining case (case 2), different patterns were seen in the same specimen: in most parts, a number of olfactory receptor cells were found, but a complete depletion of sensory receptor cells was observed in some areas (Fig 2C).

Olfactory Mucosal Findings of Anosmic Patients. Eighteen specimens from 6 patients failed to yield a single piece of olfactory epithelium. Out of these samples, biopsy samples obtained from case 17 showed squamous metaplasia of the epithelium (Fig 3A). In 15 of 27 samples obtained from the remaining anosmic patients, only normal-appearing respiratory epithelium with or without goblet cells was identified.

Although olfactory epithelium was positively identified in the biopsy samples, the orderly arrangement of cells characteristic of normal olfactory epithelium was moderately or highly abnormal in appearance. In 5 patients (cases 7, 8, 9, 19, and 21), only a single specimen of 3 samples obtained from each subject contained a few olfactory epithelial cells or a small group of olfactory epithelial cells within the widely distributed respiratory epithelium (Fig 3B). In 3 patients (cases 11, 15, and 20), the olfactory epithelium was largely atrophic and thin. Complete depletion of sensory receptor cells immunoreactive for MAP5 was observed in large areas in which the epithelium consisted of supporting and basal cells. Some parts displayed a small number of receptor cells, the dendrites of which were tortuous in their course (Fig 3C). In case 14, the epithelium was about two-thirds as thick as the normal epithelium. However, the olfactory epithelia were mostly composed of support-

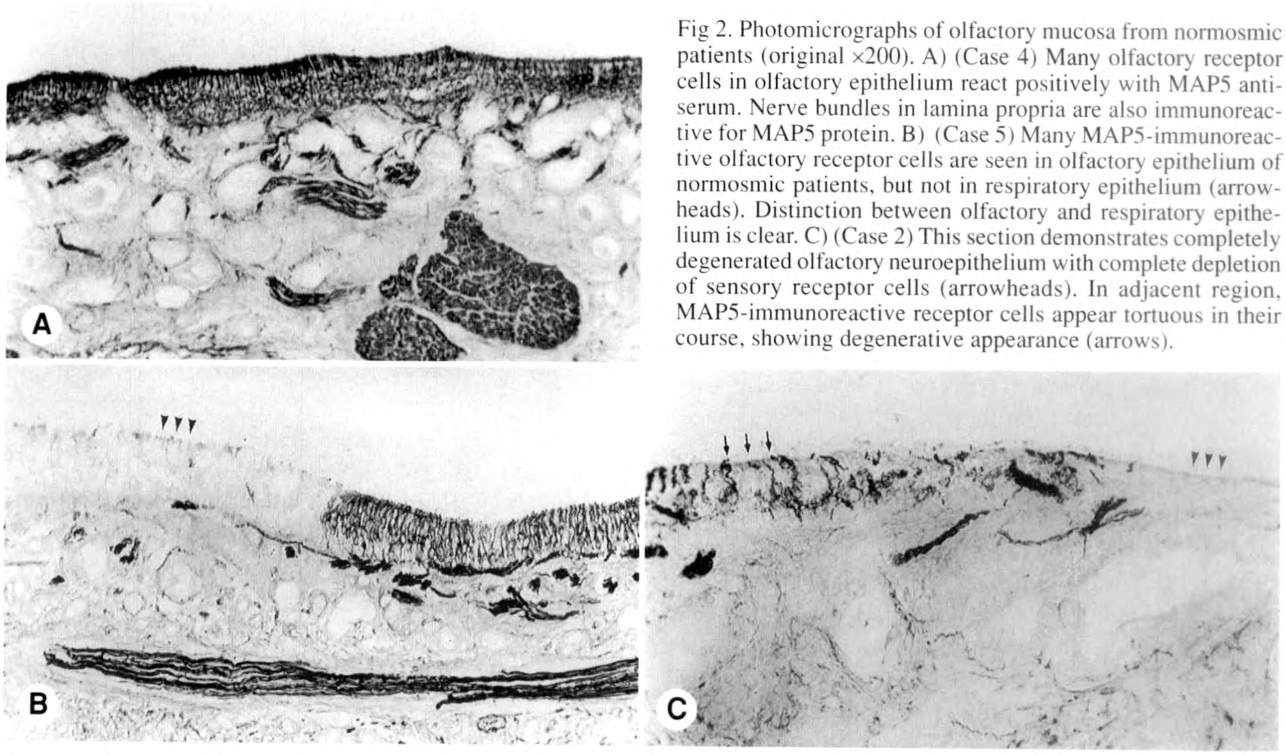

Fig 2. Photomicrographs of olfactory mucosa from normosmic patients (original ×200). A) (Case 4) Many olfactory receptor cells in olfactory epithelium react positively with MAP5 antiserum. Nerve bundles in lamina propria are also immunoreactive for MAP5 protein. B) (Case 5) Many MAP5-immunoreactive olfactory receptor cells are seen in olfactory epithelium of normosmic patients, but not in respiratory epithelium (arrowheads). Distinction between olfactory and respiratory epithelium is clear. C) (Case 2) This section demonstrates completely degenerated olfactory neuroepithelium with complete depletion of sensory receptor cells (arrowheads). In adjacent region, MAP5-immunoreactive receptor cells appear tortuous in their course, showing degenerative appearance (arrows).

ing and basal cells, with olfactory receptor cells scattered within the mucosa.

DISCUSSION

The findings of this study provide evidence that histologic changes of the olfactory mucosa are present in patients with persistent anosmia after endoscopic sinus surgery. From the results of our overall findings, the patterns of histologic changes can be summarized as follows. First, the number of fully differentiated olfactory receptor cells was remarkably reduced because of extensive replacement by respiratory epithelium within the olfactory area. Second, the orderly arrangement of cells characteristic of normal olfactory epithelia was lost, although the degree of degeneration was not equal in all patients.

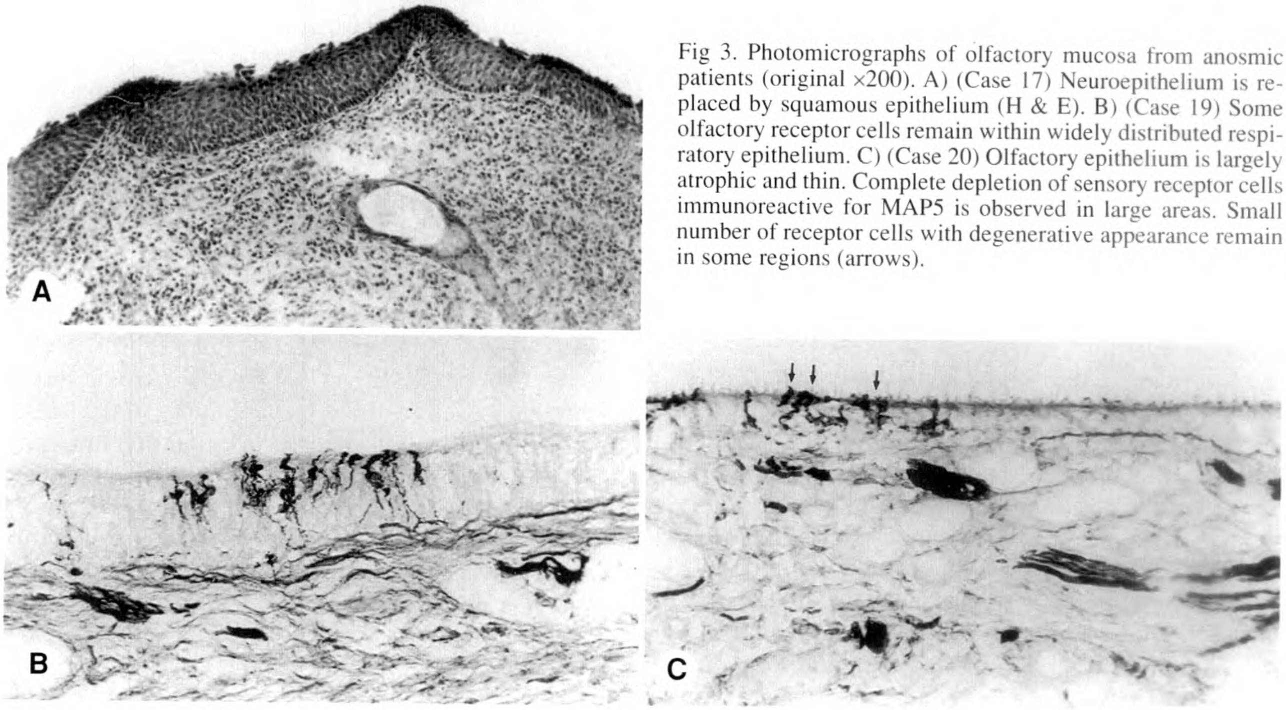

Fig 3. Photomicrographs of olfactory mucosa from anosmic patients (original ×200). A) (Case 17) Neuroepithelium is replaced by squamous epithelium (H & E). B) (Case 19) Some olfactory receptor cells remain within widely distributed respiratory epithelium. C) (Case 20) Olfactory epithelium is largely atrophic and thin. Complete depletion of sensory receptor cells immunoreactive for MAP5 is observed in large areas. Small number of receptor cells with degenerative appearance remain in some regions (arrows).

To the best of our knowledge, this is the first study to provide information regarding the olfactory mucosa in patients with persistent anosmia after sinus surgery.

The olfactory mucosa is thought to be distributed across the upper 10 mm of the nasal septum, beneath the cribriform plate, and over the medial wall of the superior turbinate, from which we obtained the specimens in this study. Nevertheless, olfactory epithelium was found in only 61% of specimens obtained from normosmic patients and was largely intermixed with various amounts of respiratory epithelium. Similar rates of successful olfactory mucosal biopsy were reported by Lanza et al[11] in 1994 and Feron et al[12] in 1998. These poor success rates may reflect an irregular and patchy distribution of the human olfactory mucosa that is possibly associated with the aging process. Other morphological studies have described age-related changes of the human olfactory mucosa. For example, Naessen[13] demonstrated that the olfactory margin in the fetus was regular, but early in life, the margin began to acquire an irregularity. The study of Paik et al[14] showed that the probability of obtaining olfactory tissue decreased significantly as the age of the subject increased, and suggested that the olfactory mucosa is gradually replaced by respiratory epithelium with aging.

An interesting finding was that the probability of obtaining olfactory tissue decreased to 27% in patients with persistent anosmia after surgery, as compared with findings from normosmic subjects. In 5 anosmic patients, a small number of fully developed olfactory receptor cells were found in a single specimen among 3 samples taken from each subject. Serial sections of all samples were required to find a few olfactory receptor cells within the widely distributed respiratory epithelium. Feron et al[12] calculated the biopsy success rate of olfactory epithelium with biopsy specimens that were collected from people with nasal abnormalities and normal individuals. They also reported that the sampling error in people with nasal abnormalities is higher than in a healthy adult population. In the presence of nasal polyps, the ratio of pure olfactory mucosa decreased substantially. Considering our results with these data, it is assumed that there may be a greater number of and more extensive respiratory patches within the olfactory area of patients with chronic sinusitis, especially in the case of persistent anosmia after sinus surgery. Also, severe degenerative changes, as well as squamous metaplasia of the olfactory epithelium, were seen in some anosmic patients presented in this study. These findings are mainly observed in the epithelium of patients with anosmia caused by head trauma or viral infection.[1,3,5] On the other hand, human olfactory neuroepithelium is believed to have a regenerative capacity.[15] It is not certain, however, that regeneration regularly takes place after degeneration of the human olfactory epithelium. On the contrary, degenerated olfactory neuroepithelium is replaced by various amounts of respiratory epithelium.[15] Immunohistochemical observation of the systemic degenerative course suggested that disrupted olfactory neuroepithelia of those cases are replaced by respiratory epithelium.[16] Jafek et al[17] performed biopsies on several patients with postviral anosmia. They reported that the olfactory epithelial region of anosmic patients contains more patches of respiratory epithelium than seen in normal patients. On the basis of these results, damaged olfactory epithelium in chronic sinusitis could, theoretically, be replaced by respiratory epithelium during the healing process if respiratory epithelial metaplasia occurs. These pathological changes may explain the loss of olfactory function in patients who describe their sense of smell as severely diminished or absent after surgery.

The available literature has described no improvement or deterioration of olfactory detection thresholds in patients with chronic sinusitis after endoscopic sinus surgery.[6-9] The underlying mechanism involving this type of olfactory dysfunction is not fully established. A blocked transport of the odor molecules to the olfactory epithelium is discussed to explain postoperative olfactory dysfunction.[6-8] Work by Downey et al[6] indicated that persistent mucosal disease in the ethmoid bed may be compatible with the concept of mucosal obstruction in the region of the olfactory epithelium as a cause of persistent postoperative anosmia. In this respect, Klossek et al[18] stressed the importance of careful surgery to prevent recurrent polyp or persistence of edema in the area medial to the middle turbinate. Min et al[7] suggested that olfactory impairment can be due to postoperative edema, granulation, scar tissue, or recurring polyps in the olfactory region. However, our data raise a possible cause related to degenerative changes of olfactory epithelium. The olfactory mucosa of patients with long-standing chronic sinusitis may be destroyed by a variety of factors that are not yet well understood. One possibility is that the recurrent epithelial damage caused by toxic inflammatory mediators or coexistent postviral olfactory dysfunction may irreversibly damage the olfactory receptors, making the olfactory dysfunction permanent. Jafek et al[19] suggested that iatrogenic endoscopic sensory olfactory injuries could occur during a heroic attempt to clean out every ethmoidal cell.

Endoscopic diagnosis and surgical intervention have enhanced our ability to control symptoms associated with chronic sinusitis. However, the underlying mechanism involving postoperative anosmia and hyposmia has not been thoroughly evaluated. The present study indicates that the lack of improvement in olfaction after surgery may be due to abnormalities observed at the olfactory epithelium level. Further, if an olfactory mucosal biopsy is performed during an initial surgical procedure, we believe that it will generally provide useful information about possible treatment and an anticipated prognosis.

REFERENCES

1. Yamagishi M, Nakamura H, Suzuki S, Hasegawa S, Nakano Y. Immunohistochemical examination of olfactory mucosa in patients with olfactory disturbance. Ann Otol Rhinol Laryngol 1990;99:205-10.
2. Moran DT, Jafek BW, Rowley C III, Eller PM. Electron microscopy of olfactory epithelia in two patients with anosmia. Arch Otolaryngol 1985;111:122-6.
3. McCaffrey TV. Rhinology and sinusology: rhinologic diagnosis and treatment. New York, NY: Thieme Medical Publishers, 1997:1-28.
4. Schwob JE, Szumowski KEM, Leopold DA, Emko P. Histopathology of olfactory mucosa in Kallmann's syndrome. Ann Otol Rhinol Laryngol 1993;102:117-22.
5. Yamagishi M, Fujiwara M, Nakamura H. Olfactory mucosal findings and clinical course in patients with olfactory disorders following upper respiratory viral infection. Rhinology 1994; 32:113-8.
6. Downey LL, Jacobs JB, Lebowitz RA. Anosmia and chronic sinus disease. Otolaryngol Head Neck Surg 1996;115: 24-8.
7. Min YG, Yun YS, Song BH, Cho YS, Lee KS. Recovery of nasal physiology after functional endoscopic sinus surgery: olfaction and mucociliary transport. ORL J Otorhinolaryngol Relat Spec 1995;57:264-8.
8. Rowe-Jones JM, Mackay IS. A prospective study of olfaction following endoscopic sinus surgery with adjuvent medical treatment. Clin Otolaryngol 1997;22:377-81.
9. Hosemann W, Goertzen W, Wohlleben R, Wolf S, Wigand ME. Olfaction after endoscopic endonasal surgery. Am J Rhinol 1993;7:11-5.
10. Trojanowski JQ, Newman PD, Hill WD, Lee VM-Y. Human olfactory epithelium in normal aging, Alzheimer's diease, and other neurodegenerative disorders. J Comp Neurol 1991; 310:365-76.
11. Lanza DC, Deems DA, Doty RL, et al. The effect of human olfactory biopsy on olfaction: a preliminary report. Laryngoscope 1994;104:837-40.
12. Feron F, Perry C, McGrath JJ, MacKay-Sim A. New techniques for biopsy and culture of human olfactory epithelial neurons. Arch Otolaryngol Head Neck Surg 1998;124:861-6.
13. Naessen R. The identification and topographical localisation of the olfactory epithelium in man and other mammals. Acta Otolaryngol (Stockh) 1970;70:51-7.
14. Paik SI, Lehman MN, Seiden AM, Duncan HJ, Smith DV. Human olfactory mucosa: the influence of age and receptor distribution. Arch Otolaryngol Head Neck Surg 1992;118: 731-8.
15. Nakashima T, Kimmelman CP, Snow JB. Immunohistopathology of human olfactory epithelium, nerve and bulb. Laryngoscope 1985;95:391-6.
16. Yamagishi M, Nakano Y. A re-evaluation of the classification of olfactory epithelia in patients with olfactory disorders. Eur Arch Otorhinolaryngol 1992;249:393-9.
17. Jafek BW, Hartman D, Eller PM, Johnson EW, Strahan RC, Moran DT. Postviral olfactory dysfunction. Am J Rhinol 1990;4:91-100.
18. Klossek J-M, Peloquin L, Friedman WH, Ferrier J-C, Fontanel J-P. Diffuse nasal polyposis: postoperative long-term results after endoscopic sinus surgery and frontal irrigation. Otolaryngol Head Neck Surg 1997;117:355-61.
19. Jafek BW, Murrow B, Johnson BW. Olfaction and endoscopic sinus surgery. Ear Nose Throat J 1994;73:548-52.

Ann Otol Rhinol Laryngol 109:2000

ULTRASTRUCTURAL CHANGES IN PLATELET ACTIVATING FACTOR–INDUCED EPITHELIAL DAMAGE IN RABBIT MAXILLARY SINUS MUCOSA

SEA-YUONG JEON, MD
CHINJU, KOREA
CHUNG-KU RHEE, MD
CHEONAN, KOREA
PIL-SEUB JEONG, MD
CHEONAN, KOREA
YANG-GI MIN, MD
SEOUL, KOREA

Platelet activating factor (PAF), a potent chemical mediator in inflammation and allergic reaction, has been thought to induce mucociliary inhibition and epithelial damage in the airway mucosa. However, several recent papers have reported that PAF may not readily damage the airway epithelium. The aim of this study was to elucidate the pathogenesis of PAF-induced epithelial damage in terms of ultrastructural changes. Sixteen micrograms of PAF (1 mL of 16 μg/mL) was administered into the maxillary sinuses of rabbits. The rabbits were divided into 2 groups according to time intervals, and the antral mucosa was taken 1 and 3 days after administration of PAF. The tissue was processed for routine transmission electron microscopy. No epithelial degeneration was observed other than platelet aggregation, red blood cell stasis, and swelling of the endothelial cells 1 day after administration of PAF. Migration of inflammatory cells into the perivascular connective tissue, infiltration of eosinophils into the subepithelial and intraepithelial spaces, and vacuolar degeneration of the epithelial cells with focal loss of cilia were seen 3 days after administration of PAF. In conclusion, PAF induced infiltration of eosinophils into the epithelium, and resulted in epithelial degeneration that varied according to the time interval. Our findings suggest that PAF may cause epithelial damage through a series of secondary events, probably due to cytotoxicity of eosinophils infiltrating the epithelium.

KEY WORDS — eosinophil, epithelial damage, platelet activating factor, sinus mucosa, transmission electron microscopy.

INTRODUCTION

Although histamine and mast cells have been proposed as playing a major role in allergic reaction, it becomes apparent that no single mediator or inflammatory cell can account for allergic inflammation. Increasing attention has been paid to platelet activating factor (PAF), a highly potent inflammatory mediator formed by the action of phospholipase A2 on membrane phospholipids such as prostaglandins and leukotrienes, as a mediator of allergic inflammation. Platelet activating factor constricts the airway smooth muscle, induces microvascular leakage in several tissues, and causes the aggregation of inflammatory cells, including eosinophils. It also reduces mucociliary transport and causes epithelial damage in the airways.[1]

It is evident that PAF induces a significant decrease in ciliary activity and mucociliary transport velocity. However, PAF-induced epithelial damage has become controversial recently. A dose-dependent acute pulmonary inflammation, characterized by degenerative and necrotic changes of the alveolar and bronchial epithelium after the intratracheal instillation of PAF in rabbits,[2] and PAF-induced ciliostasis, edema, and exfoliation of the epithelial cells of the human sinus mucosa[3,4] have been reported. It has been thought that the cytotoxicity of PAF may cause ciliary dysfunction and epithelial damage directly. In contrast to previous reports, recent studies demonstrated no evidence of epithelial shedding in the trachea after PAF inhalation in rabbits[5] or guinea pigs,[6] and suggested that PAF may not readily damage the airway epithelium.

The aim of this study was to investigate the ultrastructural changes in order to elucidate the pathogenesis of PAF-induced epithelial damage in the airways. We administered PAF to the rabbit maxillary sinuses in vivo and investigated the ultrastructural findings in the sinus mucosa, especially in the cilia, epithelial cells, intraepithelial and subepithelial spaces, inflammatory cells, and capillaries.

MATERIALS AND METHODS

Nine New Zealand White rabbits, weighing 2.5 kg on average and showing no evidence of upper respiratory tract infection, were used in this study. The rabbits were anesthetized with intramuscular administration of ketamine hydrochloride (30 mg/kg)

From the Department of Otolaryngology, GyeongSang National University, Chinju (Jeon), the Department of Otolaryngology, Dankook University, Cheonan (Jeong, Rhee), and the Department of Otolaryngology, Seoul National University, Seoul (Min), Korea.

CORRESPONDENCE — Sea-Yuong Jeon, MD, Dept of Otolaryngology, GyeongSang National University, Chilamdong 90, Chinju, 660-702, Korea.

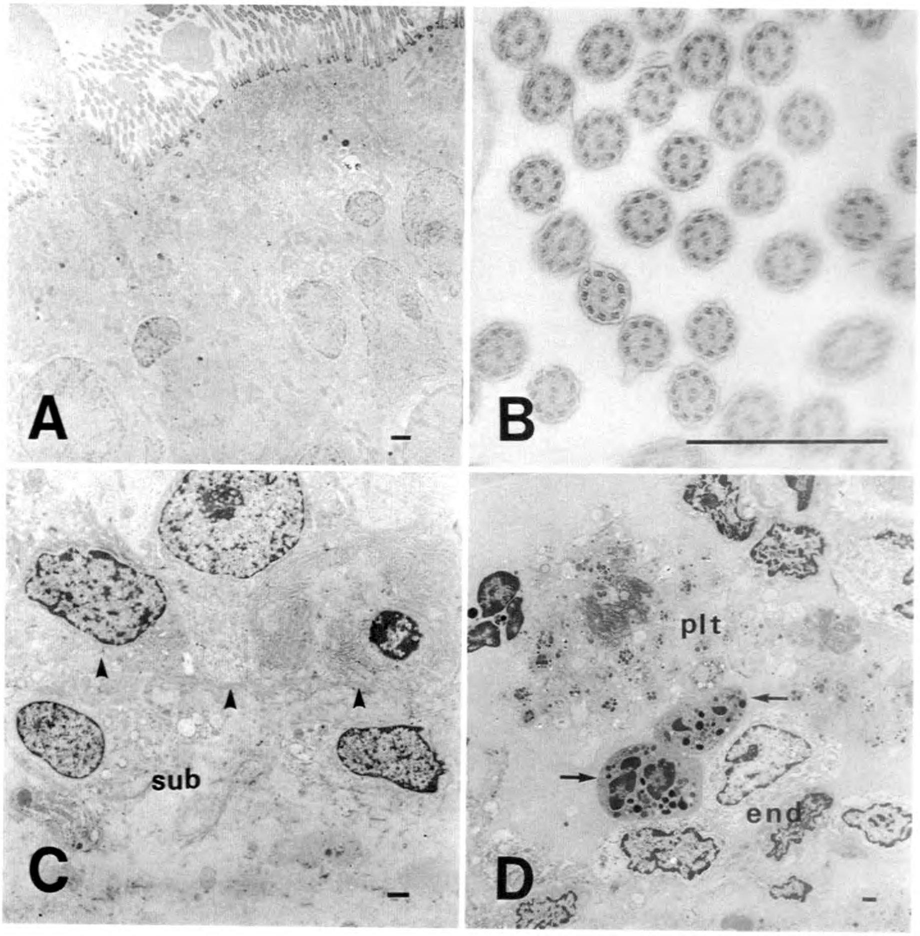

Fig 1. Electron micrographs of rabbit sinus mucosa 1 day after administration of platelet activating factor (PAF). Bars — 1 μm. A,B) Epithelial cells and cilia show no ultrastructural changes. C) Subepithelial space (sub) shows no evidence of infiltration of inflammatory cells. Arrowheads — basement membrane. D) Platelet (plt) aggregation, red blood cell stasis, and swelling of endothelial cells (end) are observed. Arrows — eosinophils.

and xylazine hydrochloride (30 mg/kg). Skin and periosteal incisions were made on the cheek, and the anterior wall of the maxillary sinus was punctured with a sterile needle. Sixteen micrograms of PAF (1 mL of 16 μg/mL) was administered into the antrum, and the skin incision was closed. Platelet activating factor (Sigma Chemical Co, St Louis, Mo) was dissolved in ethanol to make a stock solution (1 mg/mL) and diluted in normal saline solution with 0.25% bovine serum albumin to a final dose. One antrum in each rabbit was examined. The rabbits were painlessly sacrificed 1 day (n = 3) and 3 days (n = 3) after administration of PAF, and the antral mucosa was removed. One milliliter of normal saline solution was administered to the antrum of control rabbits (n = 3). The control rabbits were painlessly sacrificed 3 days after administration of normal saline solution. Tissue samples, cut into 2 × 3-mm pieces, were fixed in 2.5% glutaraldehyde (0.1 mol/L phosphate buffer, pH 7.4) at 4°C for 2 hours. The tissue was washed with buffer, postfixed in 2% osmium tetroxide for 1 hour, dehydrated in alcohol, and embedded in Epon. The epithelial layer was localized on semithin sections stained with toluidine blue. Ultrathin sections were made, stained with uranyl acetate and lead citrate, and examined by transmission electron microscopy (Hitachi H-600, Tokyo, Japan).

RESULTS

One day after administration of PAF, platelet aggregation, red blood cell stasis, and swelling of the endothelial cells were observed. However, there was no evidence of infiltration of inflammatory cells in the subepithelial space. The epithelial cells and cilia showed no ultrastructural changes or epithelial shedding (Fig 1). Three days after the administration of PAF, the swelling of the endothelial cells persisted, and migration of inflammatory cells into the perivascular connective tissue and infiltration of eosinophils into the subepithelial and intraepithelial spaces were observed. The epithelial cells had vacuolar degeneration with fusion and focal loss of cilia (Fig 2). No abnormal findings were observed in the control rabbits (Fig 3).

DISCUSSION

The principal role of the airway epithelium is as a protective barrier against the invasion of noxious materials. However, epithelial damage, or shedding of the epithelium, is often regarded as a hallmark of airway hyperreactivity such as asthma or a late allergic reaction.[7,8] Given by aerosol, PAF causes bronchial

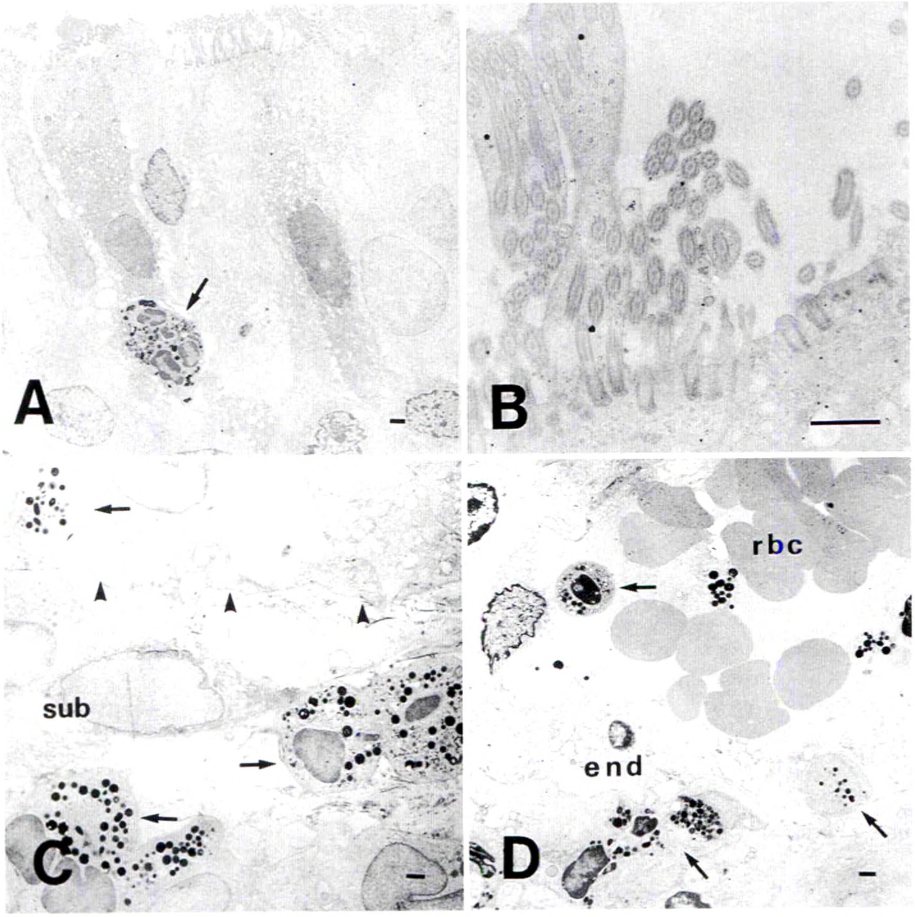

Fig 2. Electron micrographs of rabbit sinus mucosa 3 days after administration of PAF. Bars — 1 μm. A,B) Epithelial cells show vacuolar degeneration with fusion and focal loss of cilia. Eosinophil (arrow) that has infiltrated into intraepithelial space is observed. C) Eosinophils (arrows) have infiltrated into subepithelial space (sub). Arrowheads — basement membrane. D) Swelling of endothelial cells (end) and migration of eosinophils (arrows) into perivascular connective tissue are observed. rbc — red blood cell.

hyperreactivity in normal subjects and asthmatics.[9,10] It has been believed to cause airway epithelial damage by its cytotoxicity.[2-4]

In this study, PAF induced infiltration of eosinophils in the epithelium and caused epithelial degeneration according to the time interval studied. We observed no evidence of epithelial degeneration 1 day after administration of PAF. However, we found evident degeneration of the epithelial cells with infiltration of eosinophils into the subepithelial and intraepithelial spaces 3 days after administration of PAF. Our findings according to time intervals suggest that PAF may cause epithelial damage through a series of secondary events, probably through the cytotoxicity of the eosinophils that have migrated into the epithelium.

Several in vitro studies reported direct cytotoxicity of PAF to the airway epithelium.[2-4] In vivo studies,[3,4] reporting no cytotoxicity of PAF, did not perform observations more than 1 day after administration of PAF. The differences between the organs and the time intervals and the possibility of tissue lysis

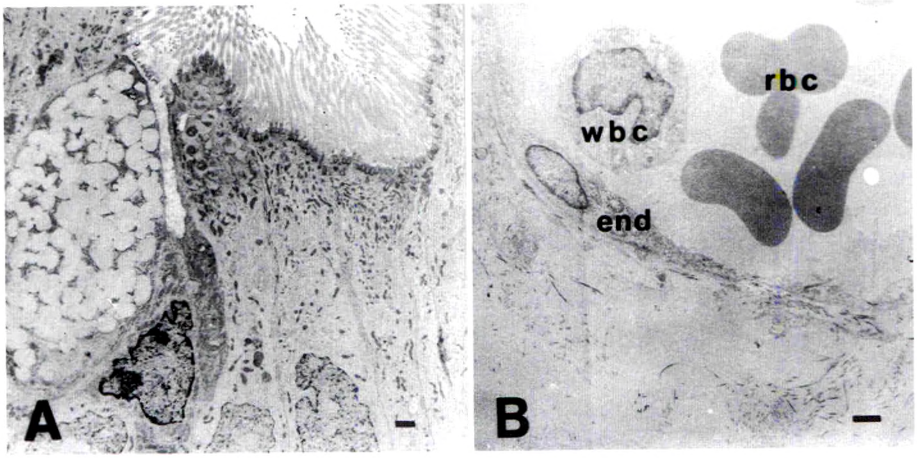

Fig 3. Electron micrographs of control rabbit sinus mucosa 3 days after administration of normal saline solution. Bars — 1 μm. A) Epithelial cells and cilia show no ultrastructural changes. B) No abnormal findings in vascular space, no ultrastructural changes in endothelial cells (end), and no evidence of infiltration of inflammatory cells in perivascular space are observed. wbc — white blood cell, rbc — red blood cell.

by protease activity in the in vitro studies may explain the discrepancy in the results.

Platelet activating factor is one of the chemotactic mediators for various inflammatory cells, including platelets, neutrophils, macrophages, and eosinophils. Of particular interest is the potent chemotaxis of PAF for eosinophils.[1] It is likely that PAF may play a crucial role in the induction and maintenance of eosinophilic infiltration in allergic diseases, and eosinophilic infiltration may be closely related to epithelial damage.[1,11] It has been reported that PAF-activated eosinophils disrupt the guinea pig tracheal epithelium after 14 hours' incubation in vitro, whereas PAF alone has no significant effect.[12] It has been suggested that PAF-activated eosinophils may release cytotoxic mediators that disrupt the epithelium.[13] This epithelial disruption may then result in increased airway responsiveness due to loss of a putative protective relaxant factor (epithelium-derived relaxing factor),[14] release of chemotactic mediators, and/or exposure of sensory nerves.[1]

Changes in the capillaries, such as platelet aggregation, red blood cell stasis, and swelling of the endothelial cells, were observed 1 day after administration of PAF. The swelling of the endothelial cells persisted 3 days after the administration of PAF, and transendothelial migration of eosinophils was observed. It has been reported that intravascular injection of PAF causes platelet aggregation, edematous degeneration of the endothelial cells, and dissociation of the basement membrane in the alveolar capillaries.[15] Our findings in the capillaries are similar to those of previous reports. It appears that the endothelial cells may play an important role in PAF-induced eosinophil transendothelial migration.[16] Swelling of the endothelial cells may be morphological evidence of a dynamic role of the endothelium in PAF-induced eosinophil transendothelial migration.

In this study, the concentration of PAF (16 μg/mL) was decided on after a preliminary functional study on the amount of serially diluted PAF that would completely inhibit the mucociliary transport of the antral mucosa. We decided to observe the sustained reaction of PAF in the antral mucosa, instead of the nasal cavity or trachea, because the PAF was retained in the antrum after the cessation of mucociliary transport. We knew that time intervals might be critical in elucidating the pathogenesis of PAF-induced epithelial damage. It has been reported that inhaled PAF causes increased bronchial responsiveness in normal subjects, and that the maximal increase in responsiveness occurs 3 days after exposure.[9] We decided on time intervals of 1 and 3 days after administration of PAF for the study.

In conclusion, PAF induced infiltration of eosinophils in the epithelium and resulted in time-dependent epithelial degeneration. Our findings suggest that PAF may cause epithelial damage through a series of secondary events, probably caused by cytotoxicity of eosinophils infiltrating the epithelium.

ACKNOWLEDGMENT — The authors acknowledge the technical assistance of Ja-Hyang Cho, MSc, in transmission electron microscopy.

REFERENCES

1. Barnes PJ, Chung KF, Page CP. Platelet-activating factor as a mediator of allergic disease. J Allergy Clin Immunol 1988;81:919-34.
2. Camussi G, Pawlowski I, Tetta C, et al. Acute lung inflammation induced in the rabbit by local instillation of 1-0-octadecyl-2-acetyl-sn-glyceryl-3-phosphorylcholine of native platelet-activating factor. Am J Pathol 1983;112:78-88.
3. Ganbo T, Hisamatsu K. Mucosal dysfunction and damage induced by platelet activating factor (PAF). Acta Otolaryngol (Stockh) 1990;110:427-36.
4. Hisamatsu K, Ganbo T, Nakazawa T, Murakami Y. Platelet activating factor induced respiratory mucosal damage. Lipids 1991;26:1287-91.
5. Ohashi Y, Nakai Y, Morimoto K, et al. Platelet activating factor compromises airway epithelial defense functions. J Allergy Clin Immunol 1997;100:520-6.
6. Greiff L, Erjefalt JS, Wollmer P, Sundler F, Persson CG. Effects of topical platelet activating factor on the guinea-pig tracheobronchial mucosa in vivo. Acta Physiol Scand 1997;106: 387-91.
7. Laitinen LA, Heino M, Laitinen A, Kava T, Hauhetela T. Damage to the airway epithelium and bronchial reactivity in patients with asthma. Am Rev Respir Dis 1985;131:599-606.
8. Nazer RM, Tellez RM, D'Ottavio TE, Bassan AE, David N. Ultrastructural changes in the human nasal respiratory epithelium in hypersensitivity reactions. Allergol Immunopathol (Madr) 1986;14:619-26.
9. Cuss FM, Dixon CMS, Barnes PJ. Effects of inhaled platelet activating factor on pulmonary function and bronchial responsiveness in man. Lancet 1986;2:189-92.
10. Chung KF, Barnes PJ. Role for platelet-activating factor in asthma. Lipids 1991;26:1277-9.
11. Frigas E, Motojima S, Gleich GJ. The eosinophilic injury to the mucosa of the airways in the pathogenesis of bronchial asthma. Eur Respir J Suppl 1991;4(suppl 13):123-35.
12. Yukawa T, Read RC, Kroegel C, et al. The effect of activated eosinophils and neutrophils on guinea pig airway epithelium in vitro. Am J Respir Cell Mol Biol 1990;2:341-53.
13. Barnes PJ. PAF, eosinophils and asthma. J Lipid Mediat 1992;5:155-8.
14. Barnes PJ, Cuss FM, Palmer JB. The effect of airway epithelium on smooth muscle contractility in bovine trachea. Br J Pharmacol 1985;86:685-91.
15. Lellouch-Tubiana A, Lefort J, Pirotzky E, Vargaftig BB,

Pfister A. Ultrastructural evidence for extravascular platelet recruitment in the lung upon intravenous injection of platelet-activating factor (PAF-acether) to guinea-pigs. Br J Exp Pathol 1985;66:345-55.

16. Casale TB, Erger RA, Little MM. Platelet-activating factor–induced human eosinophil transendothelial migration: evidence for a dynamic role of the endothelium. Am J Respir Cell Mol Biol 1993;8:77-82.

* * *

EUROPEAN ACADEMY OF FACIAL PLASTIC SURGERY

The annual meeting of the European Academy of Facial Plastic Surgery will be held September 15-17, 2000, in Thessaloniki, Greece. For information, contact Prof Dr J. Daniilidis, ENT Dept, Aristotelian University of Thessaloniki–AHEPA Hospital, 540 06 Thessaloniki, Greece; telephone 0030/31/994.761-2; fax 0030/31/994.916.

Ann Otol Rhinol Laryngol 109:2000

ACQUIRED TRACHEOESOPHAGEAL FISTULA IN CRITICALLY ILL PATIENTS

MICHAEL WOLF, MD
ERAN SEGAL, MD
ALON YELLIN, MD
MEIR FAIBEL, MD
YOAV P. TALMI, MD
JONA KRONENBERG, MD
TEL HASHOMER, ISRAEL

Acquired benign tracheoesophageal fistula (TEF) is an infrequent complication of prolonged intubation and tracheostomy. Not infrequently, it is associated with severe circumferential malacia of the trachea and a need for concomitant correction of both. Controversy exists as to whether this should be performed in a single-stage or a 2-stage procedure. Four patients with acquired TEF underwent operation in a tertiary referral medical center between 1995 and 1997. The operations were performed through either an anterior (3) or a lateral (1) neck approach. Three patients underwent closure of the fistula with tracheal resection and anastomosis in a single stage and are doing well. One patient with complete subglottic stenosis underwent closure of the TEF and was planned for tracheal reconstruction in a second stage. This patient died in the early postoperative period. The complications included aspiration of blood leading to pneumonia (2), spontaneously resolving pneumomediastinum (1), subcutaneous emphysema (2), and cardiac arrhythmia (1). Residual fistula, noted in 1 patient, was treated conservatively and resolved spontaneously within several weeks. We conclude that acquired TEF is amenable to repair through a cervical approach. A single-stage correction of the TEF with reconstruction of the trachea is suitable and successful in most patients. Several stages seem justified when concurrent laryngotracheal reconstruction is needed.

KEY WORDS — prolonged intubation, tracheal surgery, tracheoesophageal fistula, tracheomalacia.

Acquired nonmalignant tracheoesophageal fistula (TEF) is an uncommon complication of prolonged endotracheal intubation or tracheostomy. In 1972, Harley[1] reviewed the reports on 5,865 tracheotomized patients and found an acquired TEF among 0.5% of patients who were assisted by intermittent positive pressure ventilation, with a range of 0% to 4%.[1,2] High-volume, low-pressure cuffs have substantially reduced, but have not completely eliminated, the incidence of tracheal damage after prolonged intubation. Currently, about 0.5% to 5% of TEFs still arise from mechanical ventilation, especially in the presence of an indwelling nasogastric tube.[3,4]

Tracheoesophageal fistula most commonly presents with cough associated with food ingestion.[1,5] This presentation may be lacking in intubated or tracheotomized patients and may manifest itself after deflation or removal of the cuff.[6] A sudden increase in tracheal secretions, presence of gastric contents in the trachea, peritubal air leak, or sudden gastric distention by air may disclose the existence of a TEF.[7] Harley[1] also noted that abundant tracheal secretions might appear in the mouth when coughed through the fistula to the esophagus. Postintubation fistulae are quite commonly accompanied by significant circumferential tracheal damage due to the pressure effect exerted by the cuff, and often, the extent of tracheal destruction is considerably greater than that of the esophagus.[8] A significant number of fistulae involve segments above the level of the second thoracic vertebra, at the level of the cuff, and are, therefore, amenable to a cervical approach.[7,9]

Contrast studies and endoscopy[3,5,10] may establish the diagnosis of TEF. However, Gerzic et al[5] failed to reveal the fistula in nearly one third of patients undergoing endoscopic evaluation, while Couraud et al[10] found that barium swallowing showed the fistula in 70% of cases, only. Endoscopy was found to be superior, particularly among patients who are either confined to bed or are ventilatory support–dependent or unable to swallow. Bronchoscopy was more productive than esophagoscopy, because esophagoscopy may not discover a small fistula hidden behind a mucosal fold, and the tracheal orifice is generally easier to identify.[10]

Green et al[6] summarized their work by stating that head and neck surgeons should be "well versed" in the diagnosis and management of TEF. Nevertheless, we could find only a small number of related reports in the otolaryngology literature.[6,8,11,12]

This report summarizes our experience with 4 recent patients who acquired TEFs, emphasizing the need for precautions to be taken for their prevention.

From the Department of Otorhinolaryngology–Head and Neck Surgery (Wolf, Talmi, Kronenberg), the Department of Thoracic Surgery (Yellin), the Intensive Care Unit (Segal), and the Department of Radiology (Faibel), Sheba Medical Center, Tel Hashomer, and Sackler School of Medicine, Tel Aviv University, Tel Aviv, Israel.

CORRESPONDENCE — Michael Wolf, MD, Dept of Otorhinolaryngology, Sheba Medical Center, Tel Hashomer, 52621, Israel.

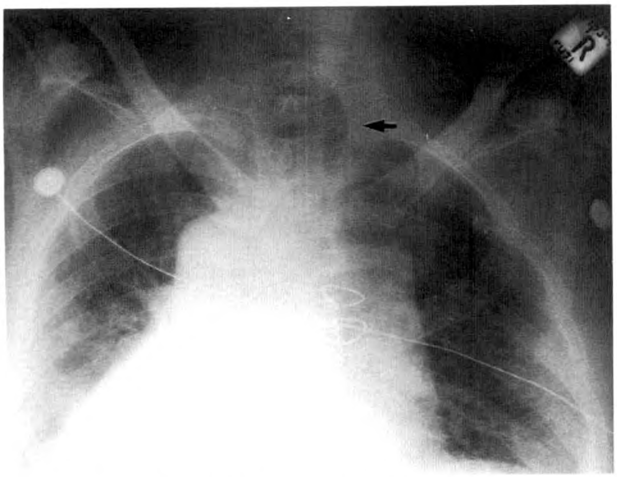

Fig 1. (Case 1) Chest x-ray. Overinflated cuff presents as rounded shadow (arrow).

MATERIALS AND METHODS

Four consecutive cases of adult patients with benign, acquired high TEFs have undergone operation through an anterior neck approach. Brief summaries of the clinical courses and operative techniques are detailed.

Case 1. A 61-year-old man underwent right lung transplantation for idiopathic interstitial pulmonary fibrosis. He was treated with azathioprine and cyclosporine, and was maintained on mechanical ventilation because of refractory pneumonia. Tracheostomy, performed on the 20th postoperative day, discovered an overinflated cuff with 25 mL of air (Fig 1), widening of the trachea up to 3.5 cm in diameter, and a 4-cm-length TEF (tracheal side) starting just below the cricoid cartilage. The cannula was secured distal to the fistula, and gastrostomy and jejunostomy were then performed.

A single-stage correction of the fistula and the trachea was postponed for 6 weeks until the patient was weaned off ventilatory support. A cervical collar skin flap was raised, and the fistula was reached anteriorly by transverse separation of the trachea at the subcricoid level. A planar dissection between the esophagus and the trachea enabled clear definition of the fistula margins. These were then trimmed and closed by continuous 4/0 polyglycolic sutures for the mucosal layer and interrupted 3/0 silk sutures for the second layer, ie, the esophageal musculature. An inferiorly based sternohyoid muscle flap was transferred to cover the fistulous bed, and an end-to-end anastomosis was performed between the cricoid and the fifth tracheal rings after suprahyoid release of the larynx. A chin-to-chest suture prevented hyperextension. Extubation was immediately performed in the recovery room, and oral intake was allowed after exclusion of residual fistula by a barium swallow study on the 8th postoperative day. Nine months after surgery, the patient is doing well. A similar technique was applied for patients 2 and 3.

Case 2. A 60-year-old woman underwent a successful cardiopulmonary resuscitation for an extensive acute myocardial infarction and was maintained on mechanical ventilation for several weeks. Tracheostomy was performed after 2 weeks of intubation. A TEF was suspected 3 weeks later, when abundant amounts of saliva appeared through the stoma and aspiration pneumonia developed. Esophageal fluoroscopy and endoscopy verified its existence. A tracheostomy tube was secured distal to the fistula; gastrostomy and jejunostomy were also performed. Because the patient gained control of aspirations and was weaned off respiratory support, surgery was postponed until her general condition improved. Her main concern, though, was embarrassing belching. Correction of the fistula and closure of the tracheal stoma was planned as a single stage. The fistula (2 cm in size at the trachea and 1 cm at the esophagus) was located 1 cm distal to the cricoid cartilage. A peristomal necrotic segment of the trachea was removed, and an anastomosis was done between the second and fifth tracheal rings. The postoperative course was notable for 2 events of ventricular arrhythmia, 1 early in the recovery room and 1 on the 19th postoperative day, both necessitating a short-term intubation. Esophageal fluoroscopy performed on the 10th day still demonstrated a small leak into the trachea, which healed spontaneously. At the 1-year follow-up, there were no complaints related to the trachea or esophagus.

Case 3. A 60-year-old man underwent an emergent 4-vessel coronary artery bypass graft procedure after an extensive myocardial infarction. His medical history was significant for non–insulin-dependent diabetes mellitus, hypertension, schizophrenia, and former withdrawal from drug abuse. The patient was maintained on mechanical ventilation, and on the second week of intubation, an air leak was noted around the cuff, requiring its further inflation in order to maintain the required tidal volumes. Gastric secretions suctioned from the tube raised the possibility of a TEF. Fiberoptic endoscopy revealed a defect of the posterior tracheal wall. A tracheotomy was performed, together with gastrostomy and jejunostomy, allowing the pneumonia to resolve, and the patient was weaned from ventilation on the 9th week after surgery. Closure of the TEF was performed in a single stage. At surgery, the trachea was found to be severely traumatized. Its outer diameter measured 4.5 cm, and severe suprastomal malacia was also evident. A fistula, 2 cm on its esophageal side and 5 cm on its tra-

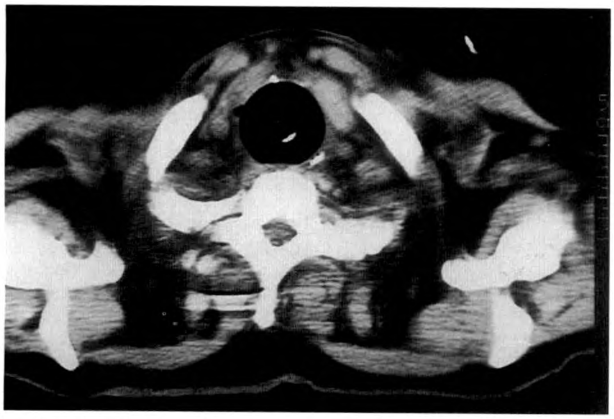

Fig 2. (Case 4) Computed tomogram of neck demonstrates widening of trachea by overinflated cuff, and nasogastric tube in esophagus.

cheal side, was located immediately distal to the cricoid cartilage. The upper 4 tracheal rings were found to be necrotic and were removed. A suprahyoid laryngeal release enabled a tensionless anastomosis between the cricoid and the fifth tracheal rings. The recovery course was uneventful, and the patient was transferred to a rehabilitation facility and was doing well. Four months later, the patient was found at night dead of an unknown cause, in his bed. An autopsy was not performed.

Case 4. A 50-year-old man underwent a 4-vessel coronary artery bypass graft procedure followed by a revision procedure due to thrombosis of the 4 grafts. His medical history was significant for recurrent thrombotic events with positive anticardiolipin antibodies. A left frontoparietal brain infarction and severe pneumonia complicated his early recovery period. Despite an extensive antibiotic regimen, the patient remained febrile and was maintained on mechanical ventilatory support. A computed tomographic scan of the neck (Fig 2) revealed widening of the tracheal lumen. Tracheostomy performed on the 24th day of intubation revealed severe malacia of the tracheal circumference at the level of the tube's cuff, and the cannula was secured distal to the necrotic segment. The patient seemed to improve, but had recurrent pulmonary infections. Three weeks later, on the 45th postoperative day, copious secretions appeared around the cannula. Endoscopy performed through the tracheostomy revealed a TEF, 2 cm in length, at the level of the stoma. Complete subglottic obstruction was also noted then, about 1 cm distal to the vocal cords. Gastrostomy and feeding jejunostomy were performed, and the patient gradually recovered. The plan was to close the TEF and reconstruct the larynx separately. The fistula was approached through a left lateral neck incision and was identified 1.5 cm below the cricoid cartilage. The esophageal side was closed in 2 layers, and an inferiorly based sternocleidomastoid myoperiosteal flap was interpositioned. The early recovery course was uneventful. The patient used a metal, Jackson-type cannula, 10 mm in size, and maintained a 94% to 95% oxygen saturation at room air. On the 8th postoperative day, the patient suddenly fell in the shower, and all attempts at immediate cardiopulmonary resuscitation failed. An autopsy was denied.

DISCUSSION

Acquired nonmalignant TEF is a potentially life-threatening complication. In 1973, Thomas[13] summarized 46 cases of TEF and found that all patients who were not surgically managed died of their disease. The high mortality rate is also expressed in other case reports and small series.[4,11,14] Mathisen et al,[9] Marzelle et al,[15] and Couraud et al[10] rated the concurrent existence of TEF with significant tracheal damage requiring reconstruction to be 75%, 35%, and 29%, respectively. Grillo et al[8] claimed that circumferential tracheal necrosis in the area of the cuff necessitates tracheal reconstruction in most cases, as was the case in all our patients.

The reported risk factors for tracheal damage in intubated patients include high cuff pressure, high airway pressure, excessive motion of an endotracheal tube, prolonged duration of intubation, respiratory infections, presence of a nasogastric tube, esophageal infection, hypotension, age, female gender, and concomitant immunosuppression or diabetes.[16] Perhaps the most important risk factor is high cuff pressure, especially in the presence of a rigid nasogastric tube.[1,13] A direct correlation between the duration of intubation and the incidence or the extent of tracheal damage is well recognized.[17] In our 4 patients, low-pressure, high-volume cuffs were used, but a rigid nasogastric tube was present.

A routine cuff pressure control has already been recommended in the era of high-pressure cuffs. Infrequent subsequent monitoring and insufficient awareness may lead to undiagnosed or overlooked catastrophes (patients 1 and 3). The necessity to use increasing volumes of air to inflate the cuff in an attempt to prevent peritubal air leak has already been considered a warning sign for impending tracheal damage.[1] This warning sign cannot be overemphasized, even when the use of high-volume, low-pressure cuffs is standard practice.

Clinical experience concerning acquired benign TEF has been summarized in significant case series[5,8-10] and in smaller numbers and isolated cases.[11,12,18,19] The management of acquired benign TEF among adults is still a matter of debate. The timing of surgical correction seems crucial: Thomas[13,14] urged immediate intervention for correcting both the fistula and the tracheal defect, thereby preventing repeated pulmonary infections, especially in low, intrathoracic lesions. However, it seems better to postpone surgical intervention until the patient is weaned off ventilation.[4] Conservative measures to control aspirations include repositioning of the tracheal tube (and cuff) to seal the trachea distal to the TEF along with a draining gastrostomy tube and a separate feeding jejunostomy. Failure has been mainly noted in distal supracarinal fistulae.[9]

In patients who no longer need ventilatory support, Grillo et al[8] and others[3,10] recommend correction of the TEF and the trachea in 1 stage. Failure and complications are related to the patient's preexisting condition, commonly aggravated by aspirations and poor nutrition.[7] The complications associated with single-stage procedures include, most commonly, recurrent tracheal stenosis and tracheal granulations, followed by aspirations and pneumonia and recurrent fistulae, and there is a 3% to 10% rate of mortality.[9,14,16,17] Therefore, others[6,7,19,20] have recommended a 2-stage procedure for correction of TEF. The advantage of a 2-stage procedure is complete separation between the airway and the digestive tracts. It was assumed that a strong, uncompromised closure of the TEF could then be achieved, as well as an ability to fully rehabilitate the patient outside the hospital before the more major definite procedure is undertaken. The general principles of staged tracheal repair are to close the fistula, repair the esophageal defect, and delay tracheal reconstruction until the fistula is closed and local infection is controlled. Nevertheless, in our experience, under proper local conditions and with general care of infection and nutrition, a single-stage reconstruction has been successful, even in an immunosuppressed patient after a lung transplant.

Whenever weaning from ventilation is not possible and the fistula remains uncontrolled, several stages are recommended: correction of the fistula with esophageal exclusion with proximal cervical esophagostomy and temporary closure of the distal esophagus, followed by esophageal anastomosis performed in a second stage. Once the patient is stable, tracheal repair is accomplished by resection and anastomosis or by various plastic techniques.[7,17,21,22] The anterior cervical approach described by Grillo et al[8] in 1976 was used in 3 of our patients in whom a single stage was planned. This technique offers exposure of the fistula bilaterally and minimizes damage to the recurrent laryngeal nerves.

It is the site rather than the size of the fistula that makes the difference.[8] Still, large TEFs are regarded as more difficult to manage, and a 2-stage procedure may be preferable.[19,23] Freeman et al[19] also suggested the use of an esophageal segment adhered to the trachea to gain more tissue for the correction of the tracheal defect. A lateral approach[9] may be used when the trachea is not involved or when only primary control of aspiration is sought. The sternohyoid or sternocleidomastoid muscles can be used for interposition and fixation. A full-thickness intercostal muscle layer has been suggested for correction of low esophageal fistulae.[18] A single sternocleidomastoid myoperiosteal flap was used in 1 of our patients for patching the tracheal defect and separating the trachea from the esophagus.

In conclusion, significant circumferential tracheal damage was evident in all our patients with TEF. Correction was possible through a cervical approach. A single-stage procedure was beneficial in 3 of our 4 cases. A 2-stage procedure may be required when laryngotracheal reconstruction is needed. The complications were related mainly to constitutional factors rather than the surgical technique. Avoidance of an indwelling nasogastric tube should be attempted when prolonged ventilatory assistance is expected. The pressure of the tube's cuff should be routinely monitored.

REFERENCES

1. Harley HRS. Ulcerative tracheo-oesophageal fistula during treatment by tracheostomy and intermittent positive pressure ventilation. Thorax 1972;72:338-52.

2. Crosby WM. Automatic intermittent inflation by tracheostomy-tube cuff. Lancet 1964;2:509.

3. Gudovsky LM, Koroleva NS, Biryukov YB, Vhernousov AF, Perelman MI. Tracheoesophageal fistulas. Ann Thorac Surg 1993;55:868-75.

4. Hilgenberg AD, Grillo MD. Acquired nonmalignant tracheoesophageal fistula. J Thorac Cardiovasc Surg 1983;85:492-8.

5. Gerzic Z, Rakic S, Randjelovic T. Acquired benign esophagorespiratory fistula: report of 16 consecutive cases. Ann Thorac Surg 1990;50:724-7.

6. Green RP, Biller HF, Sicular A, Wright M. Cervical tracheoesophageal fistula. Laryngoscope 1983;93:364-9.

7. Shaari CM, Biller HF. Staged repair of cervical tracheoesophageal fistulae. Laryngoscope 1996;106:1398-402.

8. Grillo HC, Moncure AC, McEnany MT. Repair of inflammatory tracheoesophageal fistula. Ann Thorac Surg 1976;22:112-9.

9. Mathisen DJ, Grillo HC, Wain JC, Hilgenberg AD. Management of acquired nonmalignant tracheoesophageal fistula. Ann Thorac Surg 1991;52:759-65.

10. Couraud L, Ballester MJ, Delaisement C. Acquired tracheoesophageal fistula and its management. Semin Thorac Cardiovasc Surg 1996;8:392-9.

11. Camilleri AE. Management of acquired tracheo-oesophageal fistula following intubation. J Laryngol Otol 1990;104:267-9.

12. Gerhardt HJ. Transtracheal microsurgical closure of tracheo-oesophageal fistulas. Head Neck Surg 1981;3:64-8.

13. Thomas AN. The diagnosis and treatment of tracheoesophageal fistula caused by cuffed tracheal tube. J Thorac Cardiovasc Surg 1973;65:612-9.

14. Thomas AN. Management of tracheoesophageal fistula caused by cuffed tracheal tubes. Am J Surg 1972;124:181-7.

15. Marzelle J, Dartevelle P, Khalife J, Rojas-Miranda A, Chapelier A, Levasseur P. Surgical management of acquired postintubation tracheo-oesophageal fistula: 27 patients. Eur J Cardiothorac Surg 1989;3:499-503.

16. Payne DK, Anderson WM, Romero MD, Wissing DR, Fowler M. Tracheoesophageal fistula formation in intubated patients. Risk factors and treatment with high-frequency jet ventilation. Chest 1990;98:161-4.

17. Muldur DS, Rubush JL. Complications of tracheostomy: relationship to long term ventilatory assistance. J Trauma 1969;9:389-402.

18. Bugge-Asperheim B, Birkland S, Storen G. Tracheoesophageal fistula caused by cuffed tracheal tubes. Scand J Thorac Cardiovasc Surg 1981;15:315-9.

19. Freeman MS, Livingstone AS, Goodwin WJ. Giant acquired tracheoesophageal fistulas: strategy for successful management. Head Neck Surg 1986;8:463-5.

20. Thomas AN. Discussion. J Thorac Cardiovasc Surg 1983;85:497-8.

21. Biller HF, Lawson W, Weisberg V. Staged repair of extensive tracheal and laryngotracheal stenoses. Ann Otol Rhinol Laryngol 1986;95:586-9.

22. Couraud L, Bercovici D, Zanotti L, Clerc P, Velly JF, Dubrez J. Treatment of oesophago-tracheal fistulae secondary to respiratory intensive care. Report of seventy cases [in French]. Ann Chir 1989;43:677-81.

23. Utley JR, Dillon ML, Todd EP, Griffen MO, Zeok JV. Giant tracheoesophageal fistula — management by esophageal diversion. J Thorac Cardiovasc Surg 1978;75:373-7.

≈

SAN FRANCISCO OTOLOGY & NEUROTOLOGY UPDATE 2000

The San Francisco Otology & Neurotology Update 2000 will be held October 26-28, 2000, in San Francisco, California. For information, contact University of California, San Francisco, Office of Continuing Medical Education, Room LH-450, San Francisco, CA 94143-0742; telephone (415) 476-4251; fax (415) 476-0318; e-mail: palmerk@ocme.ucsf.edu.

Ann Otol Rhinol Laryngol 109:2000

POSTINTUBATION INTERARYTENOID ADHESION

XAVIER CARRAT, MD JACQUES VERHULST, MD STEPHANE DUROUX, MD
PIERRE PESCIO, MD FRANÇOIS DEVARS, MD LOUIS TRAISSAC, MD
BORDEAUX, FRANCE

Interarytenoid fibrous adhesion is a poorly recognized complication of intubation and is frequently confused with bilateral vocal cord paralysis. Early diagnosis and treatment is essential for optimal management. Otolaryngologists should constantly remain alert for interarytenoid fibrous scar to establish the diagnosis as early as possible, optimizing the probability of restoring normal breathing and quality of life and avoiding an unnecessary tracheotomy. Surgical laser reduction is appropriate in all cases when other miscellaneous laryngeal injury lesions are eliminated. Direct laryngoscopy with careful examination of the posterior commissure and laryngeal electromyography are the 2 main clinical diagnostic aids contributing to establish the diagnosis.

KEY WORDS — arytenoid cartilage, dyspnea, intubation, larynx.

INTRODUCTION

This study reports a group of 4 patients who developed isolated interarytenoid adhesion (IAA) following intubation and received a mistaken diagnosis of bilateral abductor vocal cord paralysis. Laryngeal trauma following prolonged endotracheal intubation is now a well-recognized and common complication of this procedure. Systematic evaluation at the time of extubation shows that 94% of patients suffered from laryngeal damage due to prolonged intubation, while 5% to 6% of these patients presented a chronic airway stenosis.[1] Voice disorders following tracheal intubation are frequently seen in clinical practice, but isolated delayed dyspnea due to progressive bilateral vocal cord immobility is less usual. The incidence of short-term intubation in association with vocal cord immobility is reported to be 6% to 30% in the literature.[2] In our practice, laryngeal immobility occurred in 16% (64 cases) of 398 systematic endoscopic controls conducted after intubation procedures. In these cases, 23 cases of laryngeal immobility were bilateral, 28 were on the left side, and 13 were on the right side.[3]

Previous reports of systematic evaluation of the postintubated larynx revealed that most sequelae involve the area of the tube-tissue interface in the posterior larynx. More frequently, mucosal ulceration along the posteromedial aspects of both vocal cords has been noticed. Posterior glottic scarring frequently occurs in the severely damaged larynx and may be associated with other injuries, such as subglottic or laryngotracheal stenosis. Early differential diagnosis and management of vocal cord immobility is particularly desirable for the best management and prognosis. Globally, vocal cord immobility may be divided into true vocal cord paralysis and pseudolaryngeal paralysis, as encountered, for example, during cricoarytenoid dislocation and posterior glottic stenosis with arytenoid fixation.

However, few reports have emphasized the responsibility of IAA as a possible mechanism for bilateral vocal cord immobility and a cause of dyspnea. Most cases previously reported are isolated, and only a few publications describe more than 1 case. In 1972, Holinger and Schild[4] reported in a child a case of postintubation synechia between the arytenoids, but without any breathing problems. In 1981, Cohen[5] described a case of interarytenoid and intercordal web in a 6-year-old child, which resolved after local incision. Four cases were noted by Laccourreye et al[6] in a report of 14 cases of laryngeal immobility. Thorough knowledge and understanding of all the mechanisms leading to IAA were well analyzed by Benjamin[7] in a large survey of laryngeal injuries occurring after prolonged intubation. We report our experience with 4 new cases of IAA, emphasizing the predisposing factors leading to arytenoid fixation.

CASE REPORTS

Case 1. A 3-year-old child was admitted to the intensive care unit in a comatose state after a car crash in which he suffered a head injury. Endotracheal intubation was required for $3^1/2$ months, after which he displayed severe neurologic injury with cerebellar sequelae and problems with walking, but the major complaint was dyspnea. The examination showed a bilateral vocal cord immobility that was regarded

---

From the Department of Otolaryngology–Head and Neck Surgery, Pellegrin Hospital, University II, Bordeaux, France.

CORRESPONDENCE — Xavier Carrat, MD, Clinique Universitaire ORL, 11A2 Tripode, Hopital Pellegrin, Place Amelie Raba Leon, 33076 Bordeaux Cedex, France.

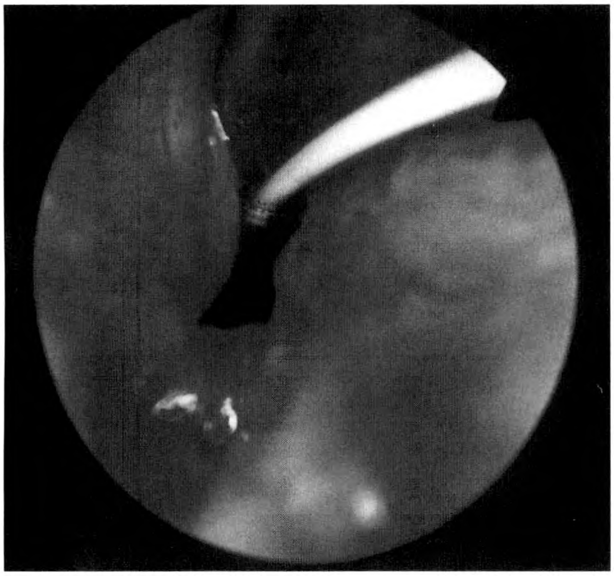

Fig 1. (Case 3) Endotracheal tube in place. Endoscopic view shows interarytenoid fibrous band hidden in posterior glottic mucosa.

for 10 years as a bilateral "true" laryngeal paralysis. Because of the poor breathing tolerance, a tracheotomy was suggested repeatedly, but the parents always rejected it. He was seen for the first time by one of us (J.V.) at the age of 13 years with still-persistent dyspnea that increased during effort. Indirect laryngoscopic examination was difficult because of laryngeal spasms. To assess the diagnosis, we performed electromyography (EMG), which showed normal innervation associated with spasmodic-like movements of the larynx of both neurologic and central origin. A direct laryngoscopy revealed a slight interarytenoid scar (1 mm wide) between the 2 vocal processes with an intact posterior interarytenoid mucosa and no posterior subglottic stenosis. Transection performed at the same time with scissors led to immediate mobilization of the 2 arytenoids. Complete vocal cord mobility was observed with still-persisting vocal cord myoclonia with a slight functional effect on laryngeal motion.

Case 2. A 72-year-old patient was continuously intubated for a month in the neurosurgical intensive care unit because of subdural hematoma. At that point, his general medical and laryngeal condition stabilized sufficiently to allow extubation. During the next 2 years, he was quite well until he experienced 2 months of progressively increasing dyspnea. He underwent an emergency tracheotomy for acute respiratory failure, and direct laryngoscopy yielded findings consistent with a bilateral vocal cord paralysis in adduction. A few days later, a reexamination with EMG revealed normal innervation of both the thyroarytenoid muscles associated with some signs of constant denervation of the posticus. Careful palpation of the posterior commissure revealed an IAA between the vocal processes, which was severed with a laser at the same time. A dramatic improvement of breathing allowed definitive decannulation and recovery of the vocal cord motion.

Case 3. A 25-year-old man was involved in a motor vehicle accident and was in a comatose state following a head injury and multiple facial fractures. He was continuously intubated for 1 month in the intensive care unit. The head injury progressively resolved, and he was able to be extubated without any side effects. He was well until 5 months later, when he complained of progressive dyspnea occurring mainly during effort. Examination by fiberoptic endoscopy revealed the vocal cords to be in the midline and immobile in association with residual bilateral vocal cord granulomas. Only some slight motion of both arytenoid tips during phonation could be observed on fiberoptic examination. No additional glottic or subglottic abnormality was obvious radiographically on computed tomography or magnetic resonance imaging. To demonstrate and confirm a mechanical laryngeal disorder, we performed EMG, and it showed normal innervation of both vocal cords. Direct laryngoscopy revealed an IAA hidden in the posterior commissure, which was resected under laser use (Fig 1). Reexamination 3 months later revealed bilateral recovered vocal cord mobility but slightly reduced abduction on the left side, consistent with a partial arytenoid ankylosis.

Case 4. A 1-year-old boy was admitted to the intensive care unit for diffuse external cutaneous and endolaryngeal burns. Because of laryngeal edema with dyspnea, he was immediately intubated. He underwent systematic endoscopic examination every week, showing progressive local recovery and favorable local evolution of the primary lesions. Interarytenoid scar was nevertheless discovered 1 month after intubation and was cured at the same time with a laser. Conversion from nasotracheal intubation to tracheotomy was then performed. No recurrence was observed during a follow-up of 8 months.

DISCUSSION

The complication of interarytenoid synechia following tracheal intubation is rarely reported in the literature. Substantial work has been performed addressing the effects of long-term endotracheal intubation on the subglottic larynx and trachea. The postintubation complications of ulcerated trough, arytenoid dislocation, subglottic edema, granuloma, and recurrent laryngeal nerve paresis are now well-recognized entities and are thoroughly researched.[7-10] All of these

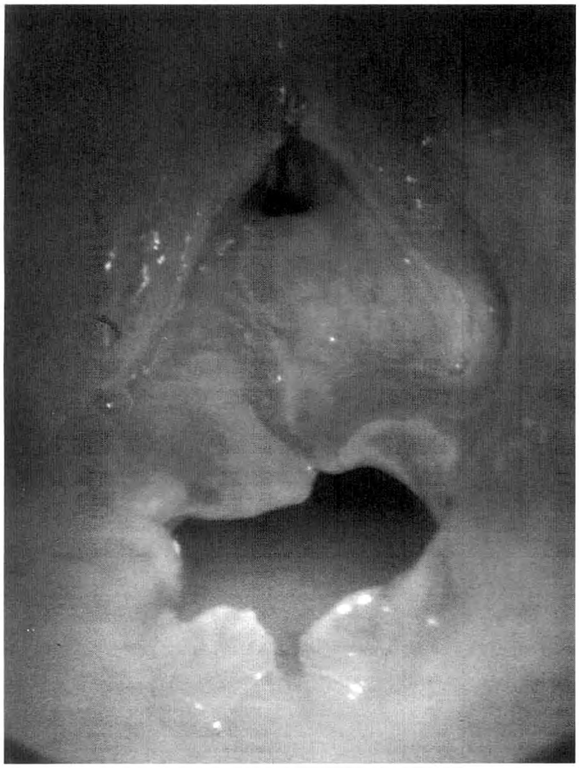

Fig 2. (Case 2) "Keyhole"-like larynx observed when nasotracheal tube is removed. Fusion of granulomas easily explains creation of interarytenoid adhesion.

lesions can be attributed to traumatic endotracheal tube insertion in the glottis, with irritation of the posterior glottis and arytenoids from tube motion during breathing and swallowing. Laryngeal joint dislocation may also represent a not-uncommon cause of vocal cord immobility and mainly follows multiple reintubations during the intensive care unit stay. Moreover, intubation may result not only in injury of laryngeal joints, but also in resultant pathophysiological changes of the thyroarytenoid muscle and its nerve branches. Previous studies have proved that laryngeal intubation may cause edema or inflammation of the cricoarytenoid area with decreased microcirculation of the posterior subglottis.

When discussing possible mechanisms for IAA, we have to consider several factors. Laryngeal damage is more likely to be found after prolonged intubation with an overlarge endotracheal tube. That may be why more than 90% of the cases of laryngeal damage were observed in female patients, who have a shorter glottic lumen. Permanent pressure of the endotracheal tube against the arytenoid leading to local ischemia and ulceration results in a progressive and extensive scarring process of various degrees of seriousness. In 1953, Chevalier Jackson[11] showed quite well that the areas most exposed to such ulceration are the anterior parts of the vocal processes of the arytenoids. Exposure of the perichondrium occurs in a short time because of the thin mucosa overlying it. The interarytenoid area, posterior commissure, and vocal process may be involved together or in an isolated fashion. Previous studies have demonstrated that ulceration of the perichondrium of the vocal process is observed after 48 hours of permanent tube contact, and ischemic necrosis occurred in all the larynges intubated more than 96 hours.[12] The same remarks were made by Lindholm[13] in a review of 267 adult larynges observed after 24 to 48 hours of intubation. Of these patients, 33% were said to have acute ulceration and granulomas at the vocal process of the arytenoid, and there was 1 formation of a posterior glottic web.

The duration of intubation represents an important cofactor and influences complications. Maximal airway injury seems to occur within the first 7 days of intubation, but it has been demonstrated previously that early lesions may arise in the first hours. Hilding[14] documented early ulceration of the vocal process after only 3 hours of intubation in calves, and the first area damaged by the endotracheal tube was the vocal process. A systematic evaluation of laryngeal lesions was conducted by Lacau St Guily et al[15] on 11 larynges from patients who died during an intensive care unit stay. Constant ulceration of the vocal process with an underlying chondritis was noticed in all cases, whatever the duration of intubation (from 3 to 10 days). It was associated in 3 cases with a coexisting cartilaginous necrosis of the vocal process. Secondary ingrowth of granulation tissue forming on the margins of granulomas or on preexisting ulceration plays a major part in the genesis of lesions like IAA.

Fusion, then fibrosis, of these granulomas creates an interarytenoid bridge that pulls the arytenoid cartilages together when the endotracheal tube is removed. At first, disappearance of the stenting effect given by the tube leaves a glottic region like a "keyhole" with a still-comfortable laryngeal lumen (Fig 2). Then, scar contracture occurs in the posterior commissure region in a progressive manner that explains the delayed symptoms presented by all the patients. The delay in development of a postintubation posterior web probably accounts for the varied time intervals to reporting of this complication in the world literature.[16]

Bilateral vocal cord immobility in adduction may result in acute respiratory failure, and a tracheotomy is sometimes required. Indeed, this complication is characterized by breathiness more than hoarseness. The dyspnea is characteristically accompanied by a good conservation of voice quality. All of our first 3 patients gave a chief symptom of dyspnea or breathiness and have never complained of vocal fatigue, dysphonia, or dysphagia. Respiratory distress requiring preservation of airway patency by a tracheotomy was encountered only once (case 2). It has to be differentiated from the tracheotomy performed in the intensive care unit to relieve nasotracheal intubation for prolonged ventilation, as in case 4. As a majority of these cases were, at the beginning, in comatose patients with head injuries, the conversion from intubation to tracheotomy was done when the necessity of continuous ventilation exceeding 7 days was obvious.

Because the IAA lesion is frequently hidden on the nasoendoscopic view, an erroneous diagnosis of bilateral abductor paralysis is usually made. Routine examination often fails to discover any posterior mucosal abnormalities, and careful examination must be conducted on the subglottis and posterior glottic commissure to rule out paralysis. The differential diagnosis may include bilateral arytenoid subluxation or cricoarytenoid fixation, scarring processes like posterior commissure synechia, or true bilateral laryngeal paralysis. In cases of long-term intubation, IAA may be accompanied by varying degrees of cricoarytenoid fixation or ankylosis in the same patient. We must separate these disorders because of the treatment often given in these cases: total arytenoidectomy or subtotal laser arytenoidectomy as described by Remacle et al.[17] Subglottic scarring with a normal glottis represents another complication occurring after long-term intubation. It has to be diagnosed with a close examination of the subglottic area during direct laryngoscopy, and specific management is needed. True bilateral recurrent laryngeal nerve paresis appears to be extremely rare and was related by Cavo[18] to local compression of the anterior branch of the recurrent nerve by the endotracheal cuff in the subglottic region 6 to 10 mm below the true vocal cords. However, when this disorder is the only condition involved, the true vocal cords will be found in the intermediate position because of the still-persisting cricothyroid muscle motion.[19] Again, for Laccourreye et al,[6] unilateral or bilateral true vocal cord paresis was exceptional, and laryngeal immobility was constantly related in their experience to an unsuspected or mistaken mechanical posterior laryngeal disorder.

Indirect mirror evaluation and flexible nasopharyngolaryngoscopy easily revealed decreased vocal cord mobility and bilateral adduction. However, certainty in the IAA diagnosis is still not possible with this simple examination alone, and the differentiation between true and "pseudo" laryngeal paralysis is difficult. In these cases, laryngeal EMG appears to be a useful clinical aid in confirming normal innervation of the larynx and in determining the nature of vocal cord immobility and the site of the lesion.[20-22] Electromyography is shown to assist in the diagnosis of IAA and differentiate it from recurrent laryngeal nerve paralysis by recording adequate function of the recurrent laryngeal nerve. Laryngeal EMG was performed in 3 of our cases and revealed normal innervation to the true vocal cord musculature. By identifying the real cause of immobility, it avoids such unnecessary and destructive surgical processes as arytenoidectomy and posterior cordectomy. Moreover, it is difficult to identify any associated damage involving the muscles and/or nerves without EMG information. Normal patterns of EMG findings provide indirect evidence of arytenoid fixation without any neurologic complication. Yin et al[20] have emphasized the necessity of performing EMG in cases of arytenoid dislocation to rule out possible associated laryngeal muscle myopathy. In case 1, coincidental myoclonia of central origin was diagnosed. Strobovideolaryngoscopy may define subtle changes in arytenoid motion and may be useful in the diagnosis of IAA. A very slight movement of the arytenoid head may be detected on phonation, as seen in case 3. Direct laryngoscopy appears to be essential, but careful evaluation of both posterior glottic and subglottic areas is required. Since IAA is often hidden by pleats of the mucosa, close and complete examination with systematic palpation of the posterior mucosa is advocated. Computed tomography and magnetic resonance imaging of the larynx failed to diagnose the fibrous scar in case 3; insufficient evaluation of the posterior glottis made the diagnosis of IAA difficult, if not impossible. However, these scans may be useful in eliminating associated complications such as subglottic stenosis before direct laryngoscopy.

Scar excision with either a laser or a microsurgical procedure is the best surgical method and provides — even performed late — a dramatic improvement in breathing and quality of life. Direct laryngoscopy is the best option and was used in most reported cases, including ours. Laryngofissure has to be done when extensive posterior lesions or subglottic stenosis exists or when the exact pathological mechanism is uncertain, as suggested by Laccourreye et al.[6] This represents a minority of the cases, IAA being mainly isolated. However, when posterior glottic stenosis is associated with IAA, increased difficulties in correcting the airway obstruction will be encountered and an external approach could be necessary.[5] Complete healing was observed in all our cases at a follow-up of 3 months after treatment, without any tendency toward recurrence, confirming the validity of this simple procedure.

ACKNOWLEDGMENT — The authors thank Jean-Michel Suzanne for his help in the preparation of the manuscript.

REFERENCES

1. Whited RE. A prospective study of laryngotracheal sequelae in long-term intubation. Laryngoscope 1984;94:367-77.
2. Yin SS, Qiu WW, Stucker FJ. Value of electromyography in differential diagnosis of laryngeal joint injuries after intubation. Ann Otol Rhinol Laryngol 1996;105:446-51.
3. Verhulst J, Duprat A, Urtasun A, Gioux M, Erny P, Traissac L. Trouble de la mobilité laryngée après intubation prolongée. Rev Laryngol Otol Rhinol (Bord) 1994;115:289-91.
4. Holinger PH, Schild JA. Pharyngeal, laryngeal and tracheal injuries in the pediatric age group. Ann Otol Rhinol Laryngol 1972;81:538-45.
5. Cohen SR. Pseudolaryngeal paralysis: a postintubation complication. Ann Otol Rhinol Laryngol 1981;90:483-8.
6. Laccourreye H, Chabolle F, Brasnu D, Lacau Saint-Guily J. Les immobilités laryngées après intubation. Ann Otolaryngol (Paris) 1984;101:253-9.
7. Benjamin B. Prolonged intubation injuries of the larynx: endoscopic diagnosis, classification, and treatment. Ann Otol Rhinol Laryngol Suppl 1993;102(suppl 160).
8. Kambic V, Radsel Z. Intubation lesions of the larynx. Br J Anaesth 1978;50:587-90.
9. Thomas R, Kumar EV, Kameswaran M, et al. Post-intubation laryngeal sequelae in an intensive care unit. J Laryngol Otol 1995;109:313-6.
10. Ward PH, Zwitman D, Hanson D, Berci G. Contact ulcers and granulomas of the larynx: new insights into their etiology as a basis for more rational treatment. Otolaryngol Head Neck Surg 1980;88:262-9.
11. Jackson C. Contact ulcer granuloma and other laryngeal complications of endotracheal anaesthesia. Anesthesiology 1953; 14:425-36.
12. Donelly WH. Histopathology of endotracheal intubation. Arch Pathol 1969;88:511-20.
13. Lindholm CE. Prolonged endotracheal intubation. Acta Anaesthesiol Scand Suppl 1969(suppl 33).
14. Hilding AC. Laryngotracheal damage during intratracheal anesthesia. Demonstration by staining the unfixed specimen with methylene blue. Ann Otol Rhinol Laryngol 1971;80:565-81.
15. Lacau St Guily J, Brasnu D, Fabre A, et al. Lésions laryngées après intubation prolongée. Etude anatomo-pathologique. Ann Otolaryngol (Paris) 1986;103:179-84.
16. Kastanos N, Miro RE, Perez AM, Xaubet Mir A, Agusti-Vidal A. Laryngotracheal injury due to endotracheal intubation. Incidence, evolution and predisposing factors. A prospective long-term study. Crit Care Med 1983;11:362-7.
17. Remacle M, Lawson G, Mayné A, Jamart J. Subtotal carbon dioxide laser arytenoidectomy by endoscopic approach for treatment of bilateral cord immobility in adduction. Ann Otol Rhinol Laryngol 1996;105:438-45.
18. Cavo JW. True vocal cord paralysis following intubation. Laryngoscope 1985;95:1352-9.
19. Nuutinen J, Karja J. Bilateral vocal cord paralysis following general anesthesia. Laryngoscope 1981;91:83-6.
20. Yin SS, Qiu WW, Stucker FJ. Major patterns of laryngeal electromyography and their clinical application. Laryngoscope 1997;107:126-36.
21. Verhulst J, Gioux M, Castro E, Quintero R, Traissac L. Intérêt et rôle de l'électromyographie dans l'évaluation d'un trouble de la mobilité laryngée et son pronostic. Rev Laryngol Otol Rhinol (Bord) 1995;116:289-92.
22. Rontal E, Rontal M, Silverman B, Kileny PR. The clinical differentiation between vocal cord paralysis and vocal cord fixation using electromyography. Laryngoscope 1993;103:133-7.

Ann Otol Rhinol Laryngol 109:2000

PERCEPTUAL CHARACTERISTICS OF ADDUCTOR SPASMODIC DYSPHONIA

TON P. M. LANGEVELD, MD
HARM A. DROST, PHD
JOHAN H. M. FRIJNS, MD, PHD
AEILKO H. ZWINDERMAN, PHD
ROBERT J. BAATENBURG DE JONG, MD, PHD
LEIDEN, THE NETHERLANDS

The evaluation of perceptual symptoms is one of the mainstays in the diagnostic workup of adductor spasmodic dysphonia (ADSD). The most widely used perceptual rating system is the GRBAS scale. However, with this system, not all audible features of ADSD can be described. Therefore, we extended the GRBAS system by 6 parameters. The aim of this study was assessment of the perceptual characteristics of ADSD with the "extended" GRBAS system and evaluation of its reproducibility. Seventy-seven patients were scored independently by 3 experienced observers quantifying the voice sound profile. Cluster analysis distinguished 4 different voice types. Intraobserver and interobserver agreement among 8 less-experienced observers appeared fair-to-good. This study demonstrates that the "extended" GRBAS system is suitable for perceptual characterization of ADSD. On the grounds of the fair-to-good interobserver variability, it is appropriate for clinical use. Moreover, 4 different voice clusters of ADSD were identified, with significant differences in voice and demographic parameters.

KEY WORDS — GRBAS scale, perceptual assessment, rating scale, spasmodic dysphonia, voice quality.

INTRODUCTION

Adductor spasmodic dysphonia (ADSD) is a voice disorder that is probably due to laryngeal dystonia. Dystonia is a neurologic disorder of central motor processing, probably related to basal ganglia dysfunction, and is characterized by abnormal, often action-induced, involuntary movements or uncontrolled spasms. Spasmodic dysphonia can be associated with other focal (blepharospasm, oromandibular dystonia [Meige syndrome], torticollis, and writer's cramp) or generalized dystonias or involuntary movements, such as myoclonus and tremor.[1] The cause of dystonia is usually idiopathic, but it can be secondary to other disorders.

Aronson[2] defined 2 main types of spasmodic dysphonia: the adductor and abductor types. The former is characterized by difficulty with voice initiation, a strained-strangled, effortful phonation with voice breaks, and glottal fry.[3] The abductor type, less common, is characterized by intermittent hyperabduction of the vocal cords leading to a whispering voice, hypophonia, and possible aphonic breaks.

A number of difficulties are encountered in the diagnostic workup of patients with spasmodic dysphonia. Objective "gold standard" tests are lacking. Dystonic symptoms vary considerably over time, during different tasks and in different situations. Patients may whisper or speak in falsetto in an attempt to escape from the strained-strangled, staccato voice, thus masking their dystonia and hampering diagnosis. Finally, spasmodic dysphonia is a relatively rare voice disorder that is not familiar to many clinicians.

For adequate evaluation of patients with spasmodic dysphonia, a team consisting of an otolaryngologist, a neurologist, and a speech-language pathologist is necessary. The diagnosis is based on history, physical examination, perceptual evaluation of speech, and laryngological and general neurologic examination. The analysis of perceptual symptoms is one of the mainstays in the diagnostic workup of spasmodic dysphonia.

Much research has been done to find acoustic parameters of voice quality. Although acoustic analysis of the voice provides objective measures of phonation, there are no specific parameters that can acoustically characterize ADSD. In 1997, Leinonen et al stated, "The correspondence of the current acoustic measures with what is perceived by the ear is still too poor to allow the substitution of acoustic tests for perceptual ones."[4(p10)]

Several perceptual systems have been developed for evaluation of voice disorders in general.[5-9] Some of these not only describe perceptual characteristics of voice quality, but also include nonlaryngeal param-

---

From the Departments of Otorhinolaryngology–Head and Neck Surgery (Langeveld, Drost, Frijns, Baatenburg de Jong) and Biostatistics (Zwinderman), Leiden University Medical Center, Leiden, the Netherlands.

CORRESPONDENCE — Ton P. M. Langeveld, MD, Dept of Otorhinolaryngology–Head and Neck Surgery, Leiden University Medical Center, Albinusdreef 2, PO Box 9600, 2300 RC Leiden, the Netherlands.

TABLE 1. VOICE QUALITY PARAMETERS AND DEFINITIONS OF EXTENDED GRBAS SYSTEM

GRBAS	
Grade	Overall degree of impairment
Roughness	Low-frequency aperiodic noise; random fluctuations of glottal pulse
Breathiness	Audible turbulent noise generated at glottis
Asthenia	Weak, powerless voice; no carrying power
Strain	Excessive tension in vocal cords
Extension	
Aphonia	Voice lacking in phonation; whispering voice
Diplophonia	Two different pitches that can be simultaneously perceived
Staccato	Abrupt voice initiation and arrest; irregular interruption of voice
Tremor	Rapidly occurring fluctuations in pitch and/or loudness; quavering voice
Falsetto	Mode of phonation
Vocal fry	Low-frequency periodic vibration

eters.[5,9] The complexity of these systems could be the reason they were not widely introduced. Perhaps another reason for the lack of a universally acceptable system is that there is not one that has shown itself to be broad enough to effectively capture the categories necessary for all pathological voices.

The GRBAS system, based on the work of Isshiki et al,[6] was originally designed for quantifying the auditory impression of hoarseness for early detection of laryngeal cancer. It contains 5 well-defined parameters of the voice: "G" (overall grade of hoarseness); "R" (roughness); "B" (breathiness); "A" (asthenia); and "S" (strained quality). A 4-point scale, from 0 to 3, was used to quantify each parameter.[10] In a multicenter study on perceptual evaluation of dysphonia, the GRBAS system appeared to be reliable and of clinical relevance, based on low intraobserver and interobserver variability. Moreover, the GRBAS profiles could discriminate quite well between different pathological groups.[11]

In the past 10 years, we routinely used the GRBAS system and found that not all pathological voices could be described with it. Therefore, in the course of time, we extended the GRBAS system (Table 1), appending the parameters aphonia (eg, psychogenic whispering), diplophonia (eg, nodules, cyst), staccato (eg, spasmodic dysphonia), tremor (eg, essential voice tremor), falsetto (eg, mutational voice disorder), and vocal fry (eg, spasmodic dysphonia). We feel that these characteristics of voice quality add relevant information to the original GRBAS system.

The "extended" GRBAS system highly agrees with the voice quality parameters proposed for perceptual evaluation of pathological voices by the Swedish authors Hammarberg and Gauffin.[8] Their system was based on the results of perceptual-acoustic correlations and on consensual validations of defining terminology. These voice quality parameters were suggested as clinically relevant and were proposed for routine voice evaluation. However, indicators for overall grade ("G" in GRBAS) and tremor ("extended" GRBAS) are lacking in the "Hammarberg system." Grade is a common description of overall severity of a voice disorder, and it reflects a global measure of voice production.[12] Voice tremor is present in several neurologic voice disorders, and cannot be described in the Hammarberg system. However, in contrast to the GRBAS scale, the Swedish system has not been widely adopted in the English-language literature.

Until the work of Stewart et al[13] (1997), there were no studies in which the perceptual characteristics of ADSD were systematically investigated. Most studies dealing with this subject only used some general descriptions of the "typical" ADSD voice, eg, strained, groaning, staccato, effortful voice.[2] Perceptual ratings, defined or otherwise, such as overall grade, strained-strangled voice quality, overpressure, vocal spasms, phonatory effort, aperiodicity, breathiness, and tremor, were mostly used for evaluation of therapy outcome after recurrent laryngeal nerve section or Botox injections and/or for determination of the relationship with acoustic features of spasmodic dysphonia. Moreover, just a few studies subjected the ratings to statistical analysis for evaluating intraobserver and interobserver reliability.[12,14-16] In general, good reliability was obtained. However, comparing the results among these studies seems unjustified, because different symptoms were investigated and/or different statistics were used. Stewart et al[13] designed the Unified Spasmodic Dysphonia Rating Scale (USDRS), a standardized measure for evaluation of symptoms and severity of ADSD. This was the first study in which the signs and symptoms of ADSD were investigated systematically. The voices of patients with ADSD were quantified with good reliability for 14 perceptual symptoms in conversational speech and 6 voice tasks that improve or worsen perceptual symptoms.

Whereas the USDRS was designed purely for ADSD, the "extended" GRBAS system was designed for voice disorders in general. The aim of the present study was assessment of the perceptual characteristics of ADSD with the extended GRBAS system and evaluation of its reproducibility.

PATIENTS AND METHODS

Between 1993 and 1997, we evaluated 77 patients with a clinical diagnosis of ADSD. Among them were

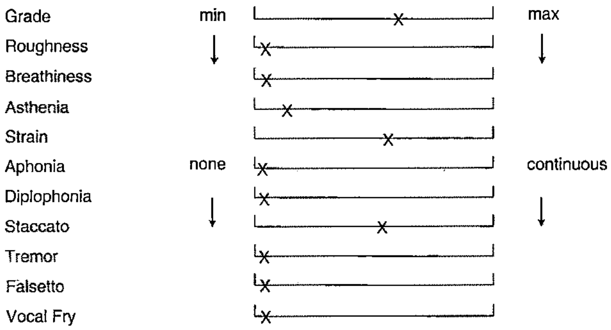

Fig 1. Example of perceptual evaluation of patient with adductor spasmodic dysphonia using our "extended" GRBAS system on visual analog scale.

61 women with a mean age of 56.2 years (19 to 87 years) and 16 men with a mean age of 55.5 years (31 to 74 years). The average durations of symptoms were 8 and 7.6 years, respectively. The diagnosis of ADSD was made independently by a speech-language pathologist (H.A.D.) and an otolaryngologist (T.P.M.L.). In addition, the patients had no history of psychiatric or neurologic disorders, particularly, no other dystonias or familial tremors. All patients had had symptoms of ADSD for more than 1 year and had undergone no previous treatment with botulinum toxin. The diagnosis was corroborated in all patients by improvement of voice quality after treatment with local injections of botulinum toxin.

All voice samples were taken before treatment and recorded in a sound-treated room with a Sony Hi-8 videocassette camera recorder and a JVC HiFi stereo videocassette recorder. The patients were seated comfortably on a chair with the microphone (Kennet ET 2100) positioned approximately 30 cm in front of the patient's mouth. Because symptoms of ADSD are markedly manifest in the habitual pitch range of the speaking voice during normal speech, spontaneous speech was used for perceptual evaluation. Spontaneous speech was recorded during history-taking, and the entire recording (on average, 3 minutes) was evaluated.

The voice quality parameters and their definitions are listed in Table 1. The ratings were performed on a visual analog (VA) scale using the extended GRBAS system. A VA scale is an undifferentiated line on which listeners rate voices by making a mark on the line to indicate the extent to which a voice possesses a given characteristic. On the score form, each parameter was scored on a continuous horizontal line of 10 cm from normal or minimal or none on the left side to extremely pathological or maximal or continuous on the right side. The distance in centimeters from the left side measured the score. Originally, in the GRBAS system, a 4-point equal-appearing interval (EAI) scale was used for each parameter. "0" equaled normal, "1" slight, "2" moderate, and "3" severe. However, we preferred the VA scale, because pilot studies suggested it was more reliable than the EAI scale (G. B. Kempster, unpublished observations, 1987). Kreiman et al[17] found that EAI ratings drifted significantly in a consistent direction within a listening session, in contrast to the VA ratings. Figure 1 shows an example of the perceptual evaluation of a patient with ADSD using the extended GRBAS system and the VA scales.

All patients were scored independently by 3 experienced observers (1 speech-language pathologist and 2 otolaryngologists) familiar with both spasmodic dysphonia and the extended GRBAS system. The voice sound profile of ADSD was quantified with the mean scores, the standard deviations, and the associated 95% confidence intervals of the different voice characteristics. For each patient, the scores of the 3

TABLE 2. VISUAL ANALOG SCORES OF THREE EXPERIENCED OBSERVERS, WITH INTEROBSERVER AGREEMENT AND DISTRIBUTION

	Visual Analog Scores (cm; mean ± SD)					*Distribution of Scores*							
						0 cm		*0-3 cm*		*3-7 cm*		*>7 cm*	
	Observer 1	*Observer 2*	*Observer 3*	*Average*	r_{ic}	*No.*	*%*	*No.*	*%*	*No.*	*%*	*No.*	*%*
Grade	6.6 ± 1.9	5.9 ± 1.7	6.6 ± 1.8	6.3 ± 1.7	.79	0	0	4	5	34	44	39	51
Roughness	0.2 ± 0.7	0.2 ± 0.7	0.2 ± 0.6	0.2 ± 0.7	.96	69	90	7	9	1	1		
Breathiness	1.0 ± 1.9	0.8 ± 1.4	0.9 ± 1.5	0.9 ± 1.6	.93	51	66	16	21	10	13		
Asthenia	3.4 ± 2.1	3.0 ± 1.9	3.4 ± 2.1	3.3 ± 1.9	.82	11	14	23	30	42	55	1	1
Strain	5.2 ± 2.7	4.7 ± 2.4	4.7 ± 2.3	4.9 ± 2.4	.90	3	4	17	22	35	45	22	29
Aphonia	0.8 ± 2.1	0.6 ± 1.8	0.7 ± 1.8	0.7 ± 1.9	.96	63	81	6	8	5	7	3	4
Diplophonia	0 ± 0	0 ± 0	0 ± 0	0 ± 0		77	100						
Staccato	3.4 ± 2.9	3.1 ± 2.8	3.4 ± 2.7	3.3 ± 2.7	.91	16	21	23	30	26	34	12	15
Tremor	1.8 ± 2.9	1.8 ± 2.7	1.6 ± 2.4	1.7 ± 2.7	.95	44	57	17	22	9	12	7	9
Falsetto	0.1 ± 0.4	0.1 ± 0.3	0.1 ± 0.5	0.1 ± 0.4	.88	74	96	3	4				
Vocal fry	2.3 ± 3.6	2.2 ± 3.4	2.0 ± 3.2	2.2 ± 3.4	.97	47	61	10	13	7	9	13	17

r_{ic} — intraclass correlation.

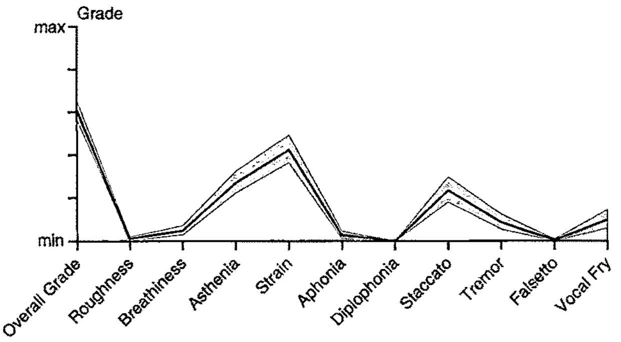

Fig 2. Voice sound profile of adductor spasmodic dysphonia. Black line — mean; shaded area — 95% confidence interval.

observers were averaged, and these patient means were averaged to obtain the voice sound profile. The observer agreement was quantified with the intraclass correlations. Because the distributions of most scales were skewed, we also calculated the geometric means. The association between the different voice characteristics was quantified with correlation coefficients. The association between the overall grade and the different voice characteristics was quantified with correlation coefficients as well, and modeled with multiple regression analysis. The results of these analyses were reported with the estimated regression coefficients (b) and their standard errors (SE). To assess whether in our sample different voice types of ADSD existed, we performed cluster analysis.

To assess the reproducibility[18] of the extended GRBAS system for ADSD, 8 less-experienced listeners scored the voices of a random subset of 58 patients. The listening procedure was performed twice (with a 4-week interval) by each listener to obtain test-retest reliability for each of the listeners on each perceptual parameter. The group consisted of 4 speech therapists and 4 otolaryngologists. To improve the interobserver rating, a training session was held with presentations of taped reference voice samples of the different parameters of the extended GRBAS system. The data were analyzed with a mixed-model ANOVA to estimate the different variance components involved. Throughout, a p value of .05 or less was considered statistically significant.

RESULTS

Voice Sound Profile of ADSD. The mean scores and standard deviations of each experienced observer are given in Table 2. The distribution of the scores was skewed. For example, on the VA tremor scale, 44 patients were scored 0, 17 patients lower than 3 cm, 9 patients between 3 and 7 cm, and 7 patients above 7 cm. Because of the skewed distribution, the geometric means and their associated 95% confidence intervals were calculated as well. The geometric means were comparable with the mean scores. Therefore, only the latter were used for analysis. The mean overall grade was 6.3. The prevalent characteristics were strain (mean, 4.9), staccato (mean, 3.3), asthenia (mean, 3.3), vocal fry (mean, 2.2), and tremor (mean, 1.7). Diplophonia was not encountered whereas roughness, breathiness, aphonia, and falsetto were rarely scored. The averages and 95% confidence intervals of the 3 observers are depicted in Fig 2. The 3 experienced observers agreed quite well: the intraclass correlations varied from .79 for the overall grade to .97 for vocal fry.

Intercorrelations. To assess whether the parameters that are not in the original GRBAS system (aphonia, staccato, diplophonia, tremor, falsetto, and vocal fry) were independent voice characteristics, we calculated the correlation coefficients between these parameters (Table 3). Although aphonia and asthenia had a correlation of .56, and tremor correlated negatively (–.52) with strain, all other correlations were .3 or less, indicating that the appended perceptual characteristics were independent parameters.

Determinants of Overall Grade. The correlations between the 10 voice characteristics and the overall

TABLE 3. INTERCORRELATIONS BETWEEN TEN VOICE PARAMETERS

	Roughness	*Breathiness*	*Asthenia*	*Strain*	*Aphonia*	*Diplophonia*	*Staccato*	*Tremor*	*Falsetto*	*Vocal Fry*
Roughness	1.00									
Breathiness	0.02	1.00								
Asthenia	–0.01	0.23	1.00							
Strain	0.15	0.06	0.17	1.00						
Aphonia	0.04	0.23	0.56	0.14	1.00					
Diplophonia						1.00				
Staccato	0.11	–0.21	–0.21	0.31	–0.11		1.00			
Tremor	–0.15	–0.10	–0.05	–0.52	–0.08		0.03	1.00		
Falsetto	–0.06	0.04	0.20	0.16	0.12		–0.04	–0.12	1.00	
Vocal fry	–0.17	–0.16	–0.08	0.18	–0.20		–0.31	–0.32	0.11	1.00
Grade	0.13	0.03	0.23	0.74	0.26		0.41	0.02	0.13	0.02

TABLE 4. VISUAL ANALOG SCORES OF VOICE PARAMETERS IN FOUR CLUSTERS OF ADDUCTOR SPASMODIC DYSPHONIA

	Cluster 1 (*n* = *17*)	*Cluster 2* (*n* = *15*)	*Cluster 3* (*n* = *23*)	*Cluster 4* (*n* = *22*)	*p**
Grade	6.6 ± 1.4	6.9 ± 1.2	7.1 ± 1.6	5.0 ± 1.7	<.001
Roughness	0.1 ± 0.2	0.5 ± 1.0	0.3 ± 0.8	0.1 ± 0.3	.23
Breathiness	0.6 ± 1.4	2.6 ± 2.2	0.6 ± 1.0	0.4 ± 1.0	<.001
Asthenia	3.2 ± 1.4	5.1 ± 1.4	2.3 ± 2.0	3.1 ± 1.7	<.001
Strain	5.9 ± 1.9	6.1 ± 1.6	6.0 ± 1.7	2.0 ± 1.2	<.001
Aphonia	0 ± 0	2.8 ± 3.0	0.2 ± 0.9	0.3 ± 1.2	<.001
Diplophonia	0 ± 0	0 ± 0	0 ± 0	0 ± 0	
Staccato	1.9 ± 2.1	2.0 ± 2.0	6.2 ± 2.1	2.2 ± 1.7	<.001
Tremor	0.3 ± 0.8	0.3 ± 0.6	1.1 ± 1.7	4.4 ± 3.3	<.001
Falsetto	0.2 ± 0.5	0.2 ± 0.7	0 ± 0	0 ± 0	0.27
Vocal fry	8.1 ± 1.3	0.2 ± 0.6	0.5 ± 1.1	0.7 ± 1.1	<.001
Number of men	4 (24%)	5 (33%)	4 (17%)	3 (14%)	.50
Age (years; mean ± SD)	45 ± 10	54 ± 15	59 ± 14	63 ± 19	<.005
Median duration of spasmodic dysphonia in months (range)	24 (3-144)	96 (8-216)	120 (7-372)	90 (8-240)	<.0001

Data are mean ± SD in centimeters, except as indicated.

*p value of 1-way analysis of variance, χ^2 test, or Kruskal-Wallis test, where appropriate.

grade are also depicted in Table 3. The most important determinant of the overall grade was strain (r = .74), followed by staccato (r = .41), aphonia (r = .26), and asthenia (r = .23). Analyzing the independent effects of each voice parameter on the overall grade, with backward stepwise multiple regression analysis, we confirmed that strain was the most important determinant of overall grade (b = 0.660, SE = 0.047, p < .0001). In addition, it was found that the other characteristics of the extended GRBAS system — staccato (b = 0.116, SE = 0.038, p = .0032), aphonia (b = 0.201, SE = 0.050, p = .0001), tremor (b = 0.355, SE = 0.040, p < .0001), and vocal fry (b = 0.069, SE = 0.030, p = .0258) — were independent determinants of overall grade.

Different Voice Types of ADSD. Cluster analysis of the 10 voice characteristics revealed 4 different voice types of ADSD. The averages of the voice characteristics in the 4 clusters are given in Table 4 (see also Fig 3). Cluster 1 consisted of 17 patients and was mainly characterized by vocal fry and strain with some asthenia and staccato. Cluster 2 consisted of 15 patients and was mainly characterized by strain and asthenia with some breathiness, aphonia, and staccato. Cluster 3 consisted of 23 patients and was mainly characterized by strain and staccato with some asthenia and tremor. Finally, cluster 4 consisted of 22 patients and was primarily characterized by tremor with some asthenia, strain, and staccato. On average, the overall grade was most severe in cluster 3 (mean, 7.1) and least severe in cluster 4 (mean, 5.0).

Men and women were equally distributed among the 4 different clusters. However, the patient's age and duration of the spasmodic dysphonic symptoms differed significantly (p values of .005 and .0001, respectively). Cluster 1 consisted of the youngest patients (45 years), with the shortest median duration of symptoms (2 years). The patients with the longest duration of symptoms (10 years) were grouped in cluster 3. Cluster 2 represented an intermediate group with respect to age and duration of symptoms. The oldest patients were found in cluster 4, in which vocal tremor was the most dominant feature. Strain was considerably less in cluster 4 compared to the other clusters.

Intraobserver and Interobserver Agreement in Eight Less-Experienced Observers. Intraobserver and interobserver agreement between the 2 observations of the 8 less-experienced observers for the subgroup of 58 patients is summarized in Table 5. On average, the differences between the first and second judgments of these observers were quite small (Table 5, "mean δ"). The intraobserver agreement calculated by means of the intraclass coefficients was acceptable, except for the roughness, diplophonia, and falsetto scales (0.36, 0.07, and 0.43, respectively). However, these scales showed almost no variation between patients, and because the intraclass coefficient is proportional to the variance between patients, the intraclass coefficients are expected to be low.

The main source of variance of the judgments was the difference between the patients: the interobserver intraclass correlations of the overall grade, strain, aphonia, staccato, and vocal fry scales were above

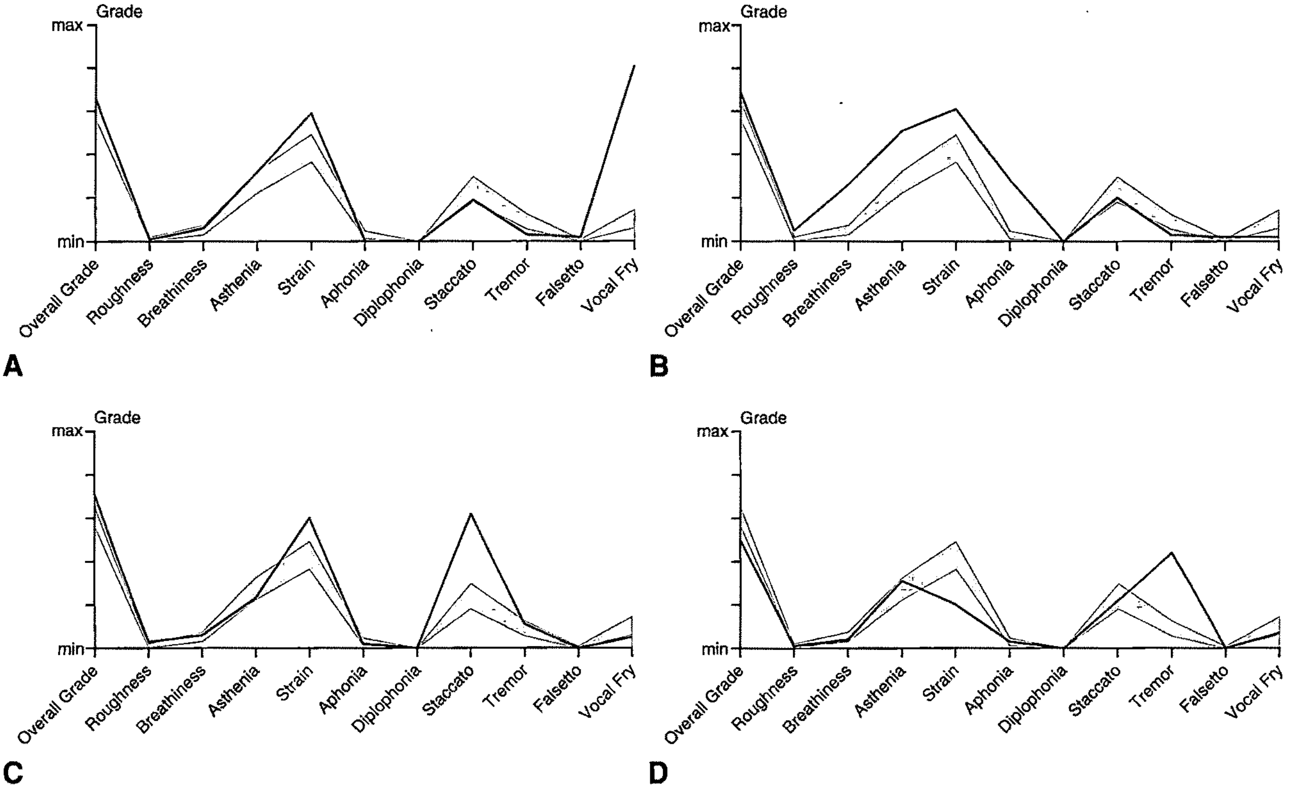

Fig 3. Voice sound profile of particular clusters (black line) and general profile of adductor spasmodic dysphonia (shaded area). A) Cluster 1. B) Cluster 2. C) Cluster 3. D) Cluster 4.

.5. For the other scales, the correlation coefficients were less than .5. Again, it must be stressed that these scales had little variance.

DISCUSSION

Perceptual evaluation of the voice is a reliable tool in the hands of experienced judges (high intraobserver and interobserver agreement). After training and with the use of anchor stimuli, good reliability for less-experienced listeners can be obtained as well.

TABLE 5. VARIANCE COMPONENTS IN JUDGMENTS OF EIGHT LESS-EXPERIENCED OBSERVERS

	Intraobserver Agreement	*Intraclass Correlation*	
	Mean δ^* ± SD	*Intraobserver Agreement*	*Interobserver Agreement*
Grade	0.1 ± 1.3	0.77	0.58
Roughness	0.0 ± 0.8	0.36	0.30
Breathiness	0.3 ± 1.4	0.52	0.41
Asthenia	0.1 ± 1.9	0.59	0.41
Strain	0.2 ± 1.9	0.75	0.52
Aphonia	0.3 ± 1.3	0.76	0.72
Diplophonia	0.1 ± 0.5	0.07	0.07
Staccato	0.7 ± 2.1	0.72	0.56
Tremor	0.2 ± 1.9	0.64	0.41
Falsetto	0.1 ± 0.6	0.43	0.30
Vocal fry	0.5 ± 2.1	0.69	0.65

*Mean δ was defined as first judgment minus second judgment averaged over observers and patients.

Nevertheless, there are several drawbacks to perceptual scaling. Numerous scales have been developed, but there is still no uniformity or standardization, and validity testing is not always performed. However, voice perception is a complex process and is probably determined by more acoustic information than we are capable of analyzing. As pointed out by Kreiman et al,[17] perceptual evaluation is the standard against which other measures are evaluated. Moreover, as long as the relationship between the perceived voice and acoustic analysis is unclear, we have to depend on our ears.

One of the best-investigated perceptual rating scales is the GRBAS system. In a multicenter study on perceptual evaluation of dysphonia, the GRBAS system appeared to be reliable and of clinical relevance, on the basis of low intraobserver and interobserver variability. In addition, the GRBAS profiles could significantly discriminate between the different pathological groups.[4,11] Compared to other systems, De Bodt et al[10] recommended the use of the GRBAS scale for clinical practice, because of its simplicity, and because it enables a relatively consistent description of voice quality, making it an effective tool for communication between disciplines.

However, not all features of pathological voices can be described with the GRBAS system. Therefore, we appended 6 parameters (aphonia, diplopho-

TABLE 6. RESEMBLANCES BETWEEN USDRS AND EXTENDED GRBAS SYSTEM

USDRS	*Extended GRBAS System*
Overall severity	Grade
Rough voice quality	Roughness
Breathy voice quality	Breathiness
Strained-strangled voice quality	Strain
Abrupt voice initiation	≈Staccato
Voice arrest	≈Staccato
Aphonia	Aphonia
Voice loudness	Asthenia
Burst of loudness	≈Staccato
Voice tremor	Tremor
Expiratory effort	≈Strain
Speech rate*	
Speech intelligibility reduced*	
Related movements and grimaces†	

USDRS — Unified Spasmodic Dysphonia Rating Scale[13]: ≈ — approximately equivalent to; * — not specific to laryngeal function; † — not applicable to laryngeal function.

nia, staccato, tremor, falsetto, and vocal fry) that were partly based on our own experience and partly derived from Hammarberg and Gauffin.[8] In contrast to other scaling methods of voice disorders,[5,9] the extended GRBAS system only describes vocal quality or laryngeal (dys)function. As no other features of the voice or speech tract are determined, clinical usefulness is enhanced.

Stewart et al[13] were the first who systematically investigated the signs and symptoms of ADSD and designed the USDRS. The perceptual parameters or voice characteristics of the USDRS highly correspond with the extended GRBAS system. In Table 6,[13] the resemblances between the rating scales are depicted. Falsetto and diplophonia were not described in the USDRS. Indeed, these perceptual parameters were not significant in our study.

The main aim of the present study was to assess the perceptual characteristics of ADSD with the extended GRBAS system. The most prevalent characteristics of ADSD were strain, staccato, asthenia, vocal fry, and tremor. The most important parameter of the overall grade was strain ($r = .74$). This is in line with the findings of Zwirner et al.[12] They found that the strained-strangled voice quality correlated significantly with the more global parameter of overall severity, so that this specific perceptual parameter is indeed suitable for the perceptual characterization of the severity of ADSD. They concluded that this parameter could provide the initial cue as to the presence of this disorder in clinical situations.

In the present study, there was high agreement among the experienced observers: the mean intraclass correlation was .91 (SD, .06; minimum, .79; maximum, .97). The correlations between the scores of the 10 voice characteristics demonstrated that all parameters were independent voice characteristics, the extension of the GRBAS system included.

Interestingly, cluster analysis of the 10 voice characteristics revealed 4 different voice types of ADSD (Table 4 and Fig 3). The sexes were equally distributed among the 4 clusters. However, the patients' ages and durations of symptoms differed significantly. The meaning of these findings is not clear. One can hypothesize that the 4 clusters represent different manifestations of the same disease related to the age of onset, or reflect compensatory strategies. On the other hand, these data could also suggest a shift in symptoms that occurs as the disease progresses. However, this could only be proven in a longitudinal study. Clusters 1, 2, and 3 all have strain as the dominant feature in combination with another characteristic voice quality parameter (vocal fry, asthenia-aphonia, and staccato, respectively). On the other hand, patients having a vocal tremor as the most dominant feature combined with a little strain possibly represent a different type of spasmodic dysphonia, which was already described by Aronson in 1981.[19] According to Aronson and Lagerlund,[20] essential voice tremor and dystonia are the 2 extrapyramidal neurologic syndromes that are responsible for most neurologic forms of spasmodic dysphonia. With respect to our study, dystonia appeared to be responsible for the perceptual characteristics of clusters 1, 2, and 3, and essential voice tremor for cluster 4.

In regard to the intraobserver and interobserver agreements in the 8 less-experienced observers, it can be concluded that the differences between the first and second judgments of these observers were quite small. The interobserver agreement can be considered fair-to-good,[21] if we take into account that the main source of variance of the judgments was the difference between the patients. The main determinants of ADSD (overall grade, strain, aphonia, staccato, and vocal fry) all showed intraclass correlations above .5. This means that even less-trained listeners are able to describe the ADSD voice with the extended GRBAS system.

CONCLUSIONS

The findings of this study demonstrate that the extended GRBAS system can be used for accurate and reproducible perceptual characterization of ADSD. Moreover, this system identified 4 voice clusters of ADSD with significant differences in voice and demographic characteristics. The relevance of this finding is not clear and requires further investigation.

ACKNOWLEDGMENTS — We gratefully acknowledge the assistance of the 8 judges. Without their cooperation, this study could not have been accomplished. We thank Robert P. Takes, MD, for his continued assistance and comments.

REFERENCES

1. Fahn S. The varied clinical expressions of dystonia. Neurol Clin 1984;2:541-54.

2. Aronson AE. Adductor spastic dysphonia; abductor spastic dysphonia. In: Aronson AE, ed. Clinical voice disorders, an interdisciplinary approach. 2nd ed. New York, NY: Thieme, 1985:157-98.

3. Davidson BJ, Ludlow CL. Long-term effects of botulinum toxin injections in spasmodic dysphonia. Ann Otol Rhinol Laryngol 1996;105:33-42.

4. Leinonen L, Hiltunen T, Laakso M, Rihkanen H, Poppius H. Categorization of voice disorders with six perceptual dimensions. Folia Phoniatr Logop 1997;49:9-20.

5. Laver J. The phonetic description of voice quality. London, England: Cambridge University Press, 1980.

6. Isshiki N, Okamura H, Tanabe M, Morimoto M. Differential diagnosis of hoarseness. Folia Phoniatr (Basel) 1969;21:9-19.

7. Hirano M. Psycho-acoustic evaluation of voice. In: Hirano M, ed. Clinical examination of voice. New York, NY: Springer-Verlag, 1981:81-4.

8. Hammarberg B, Gauffin J. Perceptual and acoustic characteristics of quality differences in pathological voices related to physiological aspects. In: Fujimura O, Hirano M, eds. Vocal fold physiology. San Diego, Calif: Singular Publishing Group, 1995:283-303.

9. Wilson DK. Voice problems of children. Baltimore, Md: Williams and Wilkins, 1987.

10. De Bodt MS, Van de Heyning PH, Wuyts FL, Lambrechts L. The perceptual evaluation of voice disorders. Acta Otorhinolaryngol Belg 1996;50:283-91.

11. Dejonckere PH, Obbens C, De Moor GM, Wieneke GH. Perceptual evaluation of dysphonia: reliability and relevance. Folia Phoniatr (Basel) 1993;45:76-83.

12. Zwirner P, Murry T, Woodson GE. Perceptual-acoustic relationships in spasmodic dysphonia. J Voice 1993;7:165-71.

13. Stewart CF, Allen EL, Tureen P, Diamond BE, Blitzer A, Brin MF. Adductor spasmodic dysphonia: standard evaluation of symptoms and severity. J Voice 1997;11:95-103.

14. Sapir S, Aronson AE, Thomas JE. Judgment of voice improvement after recurrent laryngeal nerve section for spastic dysphonia: clinicians versus patients. Ann Otol Rhinol Laryngol 1986;95:137-41.

15. Sapir S, Aronson AE. Clinician reliability in rating voice improvement after laryngeal nerve section for spastic dysphonia. Laryngoscope 1985;95:200-2.

16. Izdebski K, Dedo HH, Shipp T, Flower RM. Postoperative and follow-up studies of spastic dysphonia patients treated by recurrent laryngeal nerve section. Otolaryngol Head Neck Surg 1981;89:96-101.

17. Kreiman J, Gerratt BR, Kempster GB, Erman A, Berke GS. Perceptual evaluation of voice quality: review, tutorial, and a framework for future research. J Speech Hear Res 1993;36:21-40.

18. Bland JM, Altman DG. Statistical methods for assessing agreement between two methods of clinical measurement. Lancet 1986;1:307-10.

19. Aronson AE. Adductor spastic dysphonia as a sign of essential (voice) tremor. J Speech Hear Res 1981;46:52-8.

20. Aronson AE, Lagerlund TD. Neuroimaging studies do not prove the existence of brain abnormalities in spastic (spasmodic) dysphonia. J Speech Hear Res 1991;34:801-5.

21. Fleiss JL. Statistical methods for rates and proportions. 2nd ed. New York, NY: John Wiley and Sons, 1981.

Ann Otol Rhinol Laryngol 109:2000

CD34+ IMMUNE SUPPRESSIVE CELLS IN THE PERIPHERAL BLOOD OF PATIENTS WITH HEAD AND NECK CANCER

RAJIV PANDIT, MD
MAYWOOD, ILLINOIS
DEANNE M. R. LATHERS, PHD
MAYWOOD, ILLINOIS
NICOLE M. BEAL
MAYWOOD, ILLINOIS
THOMAS GARRITY, MD
MAYWOOD, ILLINOIS
M. RITA I. YOUNG, PHD
HINES, ILLINOIS

Patients with head and neck squamous cell carcinoma (HNSCC) have profound defects in their immune defenses. Using immunofluorescent staining and flow cytometric analysis, we found that most patients with HNSCC have increased levels of CD34+ cells within their peripheral blood. These circulating CD34+ cells contribute to the depressed functional competence of the peripheral blood T-lymphocytes. This was demonstrated by the increased level of proliferative responsiveness to interleukin-2 by the patients' peripheral blood T-cells after depletion of CD34+ cells. These results show the importance of CD34+ cells in contributing to the depression of T-lymphocyte function in patients with HNSCC and suggest that strategies designed to reduce the levels of circulating CD34+ cells may enhance the immune reactivity of the patients' circulating T-lymphocytes against the HNSCC.

KEY WORDS — cancer, CD34+ cells, head and neck squamous cell carcinoma, immune suppression, immune suppressor cells.

INTRODUCTION

Cancers are susceptible to immune-mediated destruction.[1-3] Patients with head and neck squamous cell carcinoma (HNSCC) have demonstrated defects in their cellular immunity, including dysfunction of their T-lymphocytes.[4-9] Studies with various tumors have shown that some of this immune suppression is directly mediated by soluble immune suppressive factors produced by the cancers.[5,10-12] However, cancers can also cause immune suppression indirectly, by stimulating immune suppressor cells.[13-19] The immune suppressor cells that may be induced by human HNSCC have not been extensively studied or described, although prostaglandin-producing monocytes have been among the immune suppressor cells suggested to be present in patients with HNSCC.[18] In one study with a small number of patients, patients with HNSCC were treated with low-dose cyclophosphamide to reduce suppressor T-cells and with indomethacin to block the inhibitory activity of monocytes.[4] In several of the patients whose suppressor cell levels had been reduced, treatment with immune stimulatory therapy resulted in increased immune cell infiltration into the HNSCCs and cancer regression. In other studies, a reduction in immune competence was correlated with a reduced survival rate of patients with HNSCC.[20] Such results suggest the clinical significance of immune suppressor cells in limiting immune reactivity toward HNSCC.

Studies with experimental animal tumors have indicated that some tumors stimulate immune suppressor cells that are neither suppressor T-cells nor macrophages, and whose presence is induced by tumor production of granulocyte-macrophage colony-stimulating factor (GM-CSF).[21-23] Our studies have shown that such cells mediating immune suppression can be detected within HNSCC tissue.[24-26] These immune suppressor cells were identified to be progenitor cells expressing the CD34 surface antigen and having the capacity to grow in soft agar into colonies composed of granulocytes and macrophages.[24] The HNSCCs that contained the CD34+ immune suppressor cells were those that secreted high levels of GM-CSF. More than 65% of human HNSCCs produced high levels of GM-CSF and contained immune suppressive CD34+ cells within the HNSCC. The importance of these immune suppressor cells in inhibiting immune antitumor activity in vivo was suggested in an analysis of more than 200 human HNSCC specimens that showed that cancers with a high frequency of CD34+ cells had functional defects in their intratumoral T-cells.[26] In addition, the CD34+ cell content was higher in surgically excised primary tumors that subsequently recurred or metastasized within 2 years than it was in primary tumors that remained in remission for at least 2 years after excision.[25]

From the Departments of Otolaryngology–Head and Neck Surgery (Pandit, Garrity, Young) and Pathology (Lathers, Beal, Young), Loyola University Stritch School of Medicine, Maywood, and the Department of Research Service, Hines Veterans Administration Hospital, Hines (Young), Illinois. Supported in part by the Medical Research Service of the Department of Veterans Affairs, and by grants CA-45080, CA-48080, CA-77208, and CA-78262 from the National Institutes of Health (Young).

CORRESPONDENCE — M. Rita I. Young, PhD, Research Service (151-Z2), Hines Veterans Administration Hospital, Hines, IL 60141.

PROFILE OF PATIENTS WITH HEAD AND NECK SQUAMOUS CELL CARCINOMA AND THEIR CIRCULATING LEVELS OF CD34$^+$ CELLS

Subject	*TNM*	*Site*	*CD34$^+$ (%)*
High CD34$^+$ cell content (mean, 4.8%; SD, 1.4%)			
1	T2N2b	Tongue	4.6
2	T2N1	Larynx	4.6
3	T2N0	Larynx	4.5
4	T1N0	Oral cavity	3.5
5	T1N0	Right retromolar trigone	4.5
6	T2N2b	Larynx	6.8
7	T1Nx	Right floor of mouth	4.6
8	T3N2b	Tongue	8.3
9	T1N1	Soft palate	3.9
10	T1N0	Oral cavity	4.7
11	T1N2b	Right pyriform sinus	6.2
12	T3N0	Vocal fold	5.4
13	T3N0	Vocal fold	3.4
14	T3N1	Base of tongue	3.0
15	T3N2b	Floor of mouth	4.3
16	T2N0	Tongue	4.3
17	T3N2b	Larynx	3.3
18	T4N1	Right tonsil	6.7
19	T1N0	Right base of tongue	4.9
Low CD34$^+$ cell content (mean, 1.0%; SD, 0.7%)			
20	T2N2	Floor of mouth	1.2
21	T4N0	Larynx, pharynx	1.3
22	T2N0	Tongue	0.4
23	T2N1	Larynx	1.3
24	T4N2b	Base of tongue	1.8
25	T2N0	Lateral tongue	0.0
26	T1N1	Floor of mouth	1.2
27	T4N3	Pharynx	1.1
Controls (mean, 0.5% CD34$^+$ cells; SD, 0.6%)			
1	N/A	N/A	1.3
2	N/A	N/A	1.5
3	N/A	N/A	0.3
4	N/A	N/A	0.0
5	N/A	N/A	0.2
6	N/A	N/A	0.0
7	N/A	N/A	0.1
8	N/A	N/A	0.6

Proportion of CD34$^+$ cells in peripheral blood of cancer patients and controls is expressed as percentage of positive cells from flow cytometric analysis of immunostained cells.

N/A — not applicable.

Although our previous studies focused on CD34$^+$ suppressor cells within HNSCCs that produced GM-CSF,[24-26] the possibility that CD34$^+$ cells may be mediating immune suppression within the peripheral blood of patients with HNSCC has not been previously assessed. The purpose of this study was to determine whether HNSCCs mobilize CD34$^+$ cells into the peripheral blood and whether these blood CD34$^+$ cells contribute to the immune dysfunction of patients with HNSCC. The results showed a prominent presence of CD34$^+$ cells in the blood of most of the patients with HNSCC studied. Further, these studies showed that the CD34$^+$ cells in the peripheral blood are inhibiting the functional competence of the patients' T-lymphocytes.

MATERIALS AND METHODS

Peripheral Blood Lymphocytes. Ten milliliters of peripheral blood was obtained from 27 patients with HNSCC. The peripheral blood mononuclear cells (PBMCs) were obtained by centrifuging blood in a Ficoll-Hypaque gradient (1.077 g/L), recovering cells from the interface, and washing. Blood samples were also obtained from Veterans Administration Hospital patients from whom blood was being collected for other clinical laboratory purposes, but who did not have a cancer diagnosis. These samples were used as controls.

Flow Cytometric Analysis. To quantitate the frequency of CD34$^+$ cells in the peripheral blood, we stained the PBMCs by direct immunofluorescence using a fluorescein isothiocyanate (FITC)–conjugated CD34 antibody (QBEND/10 clone; BioSource, Camarillo, Calif) or a FITC-conjugated isotype control antibody. After 30 minutes of staining on ice in the dark, the cells were washed, and the percentage of positive-staining cells was measured with a FACS 420 (Becton Dickinson, Sunnyvale, Calif). Controls included cells that were incubated with the isotype control antibody. The data shown are the percent positive-staining cells among the analyzed PBMCs.

Immunomagnetic Depletion of CD34$^+$ Cells From PBMCs. The CD34$^+$ cells within the PBMCs of patients with HNSCC were immunomagnetically depleted by a procedure previously described.[24] Briefly, PBMCs were mixed with CD34 antibody–coated magnetic beads (Advanced Magnetics, Cambridge, Mass) on ice for 15 to 20 minutes. The cells that complexed with the beads were separated with a magnetic plate at an angle perpendicular to gravity. After 3 to 5 minutes, the cells remaining in suspension were carefully removed by pipetting. These cells were then washed and used as the CD34$^+$ cell–depleted PBMC population. Magnetic beads that were not coated with antibody were used as a control and showed that the physical manipulations with the beads had no effect on PBMC function.

T-Lymphocyte Proliferation. Whether the CD34$^+$ cells in the PBMCs of patients with HNSCC had immune suppressive activity was measured by determining whether the proliferative response of PBMCs to interleukin (IL)–2 would increase on immunomag-

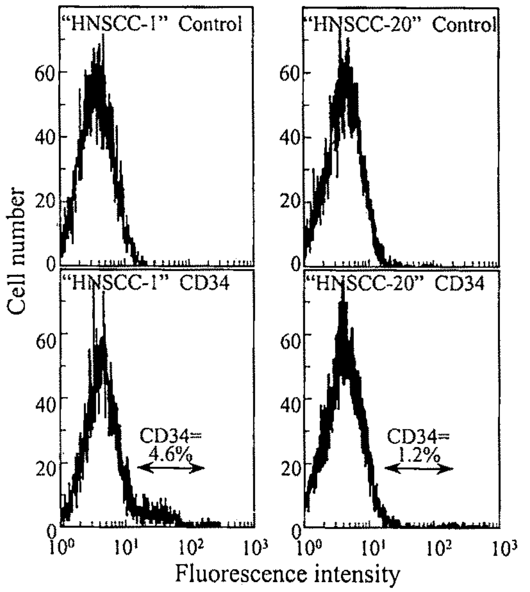

Fig 1. Histograms for CD34$^+$ cells within peripheral blood of 2 patients with head and neck squamous cell carcinoma (HNSCC): patient with 4.6% CD34$^+$ cells (left panels) and patient with 1.2% CD34$^+$ cells (right panels) within isolated peripheral blood mononuclear cells (PBMCs). Shown for each patient are FACS histograms made after staining PBMCs with either isotype control antibody (top panels) or CD34 antibody (bottom panels).

netic depletion of CD34$^+$ cells as compared with the unfractionated PBMCs. Unfractionated and CD34$^+$ cell–depleted PBMCs were seeded into microtiter wells containing 100 U/mL, 10 U/mL, or 1 U/mL of IL-2, or media without IL-2. The cells were cultured for 5 days at 37°C. Proliferation was measured with a tetrazolium-based colorimetric assay in which the colored formazan product is directly proportional to the number of cells (CellTiter96 AQ assay; Promega Corp, Madison, Wis).

Statistical Analysis of Data. All T-lymphocyte proliferative analyses were performed in triplicate. Student's *t*-test was used to analyze the significance of differences between the mean values for the proliferative responses of unfractionated PBMCs versus CD34$^+$ cell–depleted PBMCs.

RESULTS

Patient Profile and CD34$^+$ Cell Content. Because our prior studies with human head and neck cancers showed that GM-CSF–producing tumors induce an intratumoral influx of CD34$^+$ immune suppressor cells,[24,25] the blood of patients with HNSCC was analyzed by flow cytometry for the presence of these same suppressor cells expressing the CD34 antigen. Peripheral blood of 27 patients with HNSCC was obtained immediately before the surgical resection of the tumors. Shown in the Table is the CD34$^+$ cell content within the PBMCs of these patients. Most of the patients with HNSCC (19 of 27 patients) contained a readily detectable percentage of CD34$^+$ cells (average of 5%) within the peripheral blood. The peripheral blood of 8 patients with HNSCC contained only a minimal percentage of CD34$^+$ cells (1%), which tended to be slightly more than the levels of control subjects (<1%). Examples of histograms for 1 patient from the group that had a high CD34$^+$ cell content and 1 patient that had a low CD34$^+$ cell content are shown in Fig 1.

The Table also summarizes the cancer sites and stages of the patients with HNSCC whose peripheral blood CD34$^+$ cell levels were measured. These profiles do not suggest any association between either the tumor stage or site and the levels of peripheral blood CD34$^+$ cells in these patients with HNSCC. Instead, this proportion (70%) of patients with increased peripheral blood CD34$^+$ cell levels is similar to the proportion of HNSCCs that we previously showed to produce GM-CSF and contain CD34$^+$ cells within the HNSCC tissue.[24]

Removal of CD34$^+$ Cells Increases Reactivity of Peripheral Blood T-Cells. Our prior studies had shown that the CD34$^+$ cells within HNSCCs were inhibitory to the functional competence of the intratumoral T-cells.[24] Therefore, the possibility was considered that the CD34$^+$ cells within the peripheral blood of patients with HNSCC might be suppressing the functional competence of the peripheral blood T-cells. This possibility was assessed by determining whether depleting the CD34$^+$ cells from the PBMCs of patients with HNSCC would enhance the responsiveness of their peripheral blood T-cells to IL-2. Shown in Fig 2 are examples of the proliferative responses of T-cells from 2 patients with HNSCC, one of whom contained a low level of CD34$^+$ cells in the blood, whereas the other contained a high level of CD34$^+$ cells. Immunomagnetically depleting the CD34$^+$ cells from the blood containing the high CD34$^+$ cell content resulted in a significantly greater proliferative response to IL-2 as compared to the response by unfractionated PBMCs (Fig 2, left panel; $p < .001$ for each IL-2 concentration). This finding suggests that the CD34$^+$ cells within the peripheral blood of this patient with HNSCC were contributing to his suppressed T-cell activity. Similarly treating PBMCs of the patient with HNSCC who had a low CD34$^+$ cell content had no effect on the T-cell proliferative capability (Fig 2, right panel); hence, the technical manipulation of immunomagnetic fractionation did not alter T-cell activities.

A total of 12 patients with HNSCC were analyzed for the effect of CD34$^+$ cell depletion on the peripheral blood T-cell responsiveness to IL-2. Of these 12

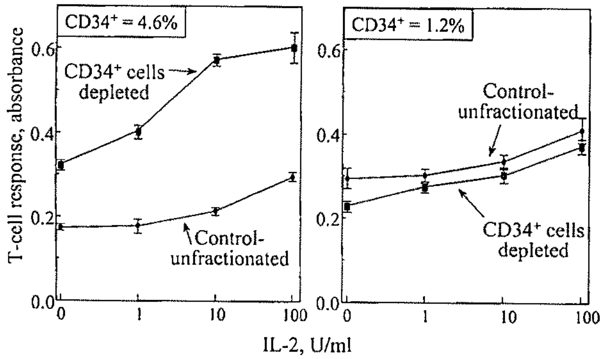

Fig 2. Immunomagnetic depletion of CD34^{+} cells from PBMCs of patients with HNSCC with high CD34^{+} cell content enhanced their T-lymphocyte proliferative responsiveness to interleukin (IL)–2. Magnetic beads that were conjugated to anti-CD34 antibody were used to remove CD34^{+} cells from half of PBMCs prepared from patients with HNSCC. Proliferative response to IL-2 by unfractionated and CD34^{+} cell–depleted PBMCs was then measured. Depicted are proliferative responses of cells from patients with HNSCC and high CD34^{+} cell content (left panel) or low CD34^{+} cell content (right panel). Data are shown as mean absorbances ± SD of triplicate determinations from which values for media only (without PBMC) were subtracted.

patients, 8 had a high CD34^{+} cell content (5.1% ± 1.6%) and 4 had a low CD34^{+} cell content (1.3% ± 0.1%). The results of these studies confirmed those shown above for 2 representative patients and are summarized in Fig 3. Specifically, removal of CD34^{+} cells from the PBMCs with a high CD34^{+} cell content allowed for a greater response to IL-2 than what could be attained in the presence of CD34^{+} cells. The IL-2 responsiveness of the PBMCs that contained the low CD34^{+} cell content was not significantly affected by immunomagnetic fractionation procedures. Overall, the CD34^{+}-depleted PBMCs from the group of patients with a high CD34^{+} cell content were at least as responsive to IL-2 as were the PBMCs from patients with a low CD34^{+} cell content. These analyses of 12 patients with HNSCC provide strong support for the conclusion that the CD34^{+} cells within the peripheral blood of patients with HNSCC are suppressing the functional competence of the peripheral blood T-cells and that the removal of these cells allows for increased T-cell responsiveness to IL-2.

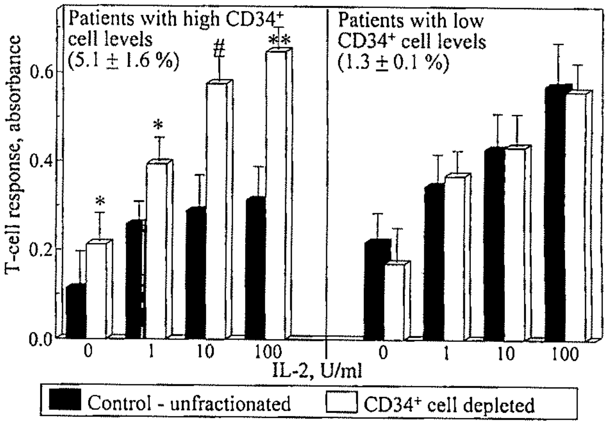

Fig 3. Summary of effect of immunomagnetically depleting CD34^{+} cells from PBMCs of patients with HNSCC and high versus low CD34^{+} cell content on their T-lymphocyte proliferative responses to IL-2. Shown are mean absorbance values ± SEM for 8 patients with HNSCC and high CD34^{+} cell content (left) and for 4 patients with HNSCC and low CD34^{+} cell content (right). Significance of effect of depleting CD34^{+} cells on T-cell proliferative response to IL-2: * — $p < .05$; # — $p < .02$; ** — $p < .01$.

DISCUSSION

This study showed that a high proportion of patients with HNSCC have an increased frequency of peripheral blood CD34^{+} cells that contributes to the suppressed T-cell functional competence of these patients. Of the 27 HNSCC patients analyzed, 19 had an increased percentage of CD34^{+} suppressor cells, and 8 had low levels that were within the range found in normal controls. This proportion (70%) of patients with increased levels of CD34^{+} cells in their peripheral blood is comparable to that which we previously reported for the frequency of HNSCCs that secrete GM-CSF and, in turn, induce the presence of CD34^{+} cells within the HNSCC tissue.[24,25] We hypothesize that the patient group with high peripheral blood CD34^{+} cell levels also have GM-CSF–secreting HNSCCs with a high intratumoral CD34^{+} cell content, but it was not possible to test this idea in this study, because cancerous tissue was not available from many of the patients from whom peripheral blood was collected.

Of significance was our demonstration that the CD34^{+} cells within the peripheral blood were inhibiting the reactivity of blood T-lymphocytes. This was shown by the increased proliferative responsiveness to IL-2 by peripheral blood T-cells on depletion of the CD34^{+} cells. The mechanisms by which the CD34^{+} cells in HNSCC patients suppress T-cell function have not yet been investigated. However, studies of similar suppressor cells in animal tumor models have shown that the majority of the suppression is mediated through their production of the immune suppressive cytokine transforming growth factor–β.[23]

The importance of antitumor immune reactivity and the potential consequences of immune impairment have been suggested through several studies. Cancers, including HNSCC, are vulnerable to immune effector cells such as natural killer cells, lymphokine-activated killer cells, and tumor-specific cytotoxic T-lymphocytes.[1-3] Immune responses to lung cancers have been suggested to be important in maintaining cancer dormancy.[27] These anticancer immune defenses have been shown to be defective in animal tumor models and cancer patients.[4-9,15,17] Clinically, patients with HNSCC have been recognized to have profound suppression of their immune functions.[6,28] Despite this, there have been minimal attempts thus far to define the cellular basis for the immune dysfunction in patients with HNSCC or the consequences of the immune impairment. In contrast, other cancers have been more extensively studied for the mechanisms by which they subvert host antitumor immune defenses. In some instances, this immune deficiency has been attributed to tumor induction of immune-suppressive monocytes.[13,29] In other studies, the tumors have been shown to induce immune-suppressive T-lymphocytes.[30] In addition, a null population of immune suppressor cells that are neither T-cells nor monocytes has been described.[15,21-23]

Our studies have shown the presence of a non–T-cell, non-monocytic suppressor cell population that expresses CD34 in a high frequency of patients with HNSCC.[24] These $CD34^+$ suppressor cells were shown in the present study to be limiting the functional capabilities of the peripheral blood T-cells and were shown in prior studies to be inhibiting the activities of the immune infiltrate within HNSCCs.[24] This does not exclude the existence of other suppressor mechanisms in these patients with HNSCC. In fact, our results that show that patients with low levels of $CD34^+$ cells also had low levels of T-cell proliferation in response to IL-2 suggest that mechanisms other than $CD34^+$ cells might be inhibiting T-cell reactivity in patients with HNSCC. Also, we had previously shown multiple immune-suppressive factors to be released from these cancers.[26] Nevertheless, the significance of our demonstration that peripheral blood $CD34^+$ cells in patients with HNSCC are limiting the activities of peripheral blood T-lymphocytes is that it identifies a mechanism that contributes to the immune defects that are characteristic of patients with HNSCC. In light of these findings, it is reasonable to raise the possibility that the $CD34^+$ suppressor cells may contribute to the failure of immunotherapeutic strategies for elevating the antitumor immune responses in patients with cancer and that such efforts may become effective if the $CD34^+$ suppressor cell levels could first be diminished.

ACKNOWLEDGMENTS — We thank Rosann Grahovac for her excellent help in the preparation of this manuscript. We also thankfully acknowledge the contributions to these studies by Drs Sharon L. Collins, Guy J. Petruzzelli, and Robert Bastian.

REFERENCES

1. Rabinowich H, Vitolo D, Altarac S, Herberman RB, Whiteside TL. Role of cytokines in the adoptive immunotherapy of an experimental model of human head and neck cancer by human IL-2–activated natural killer cells. J Immunol 1992;149: 340-9.

2. McGrath PC, Hamby LS, Freeman JW. Phorbol dibutyrate plus ionomycin improves the generation of cytotoxic T cells from draining lymph nodes of patients with advanced head and neck cancer. Am J Surg 1992;164:610-4.

3. Chikamatsu K, Eura M, Nakano K, Masuyama K, Ishikawa T. Functional and T cell receptor gene usage analysis of cytotoxic T lymphocytes in fresh tumor-infiltrating lymphocytes from human head and neck cancer. Jpn J Cancer Res 1995;86: 477-83.

4. Hadden JW, Endicott J, Baekey P, Skipper P, Hadden EM. Interleukins and contrasuppression induce immune regression of head and neck cancer. Arch Otolaryngol Head Neck Surg 1994;120:395-403.

5. Clayman GL, Taylor DL, Liu FJ, Lavedan P, Savage HE, Schantz SP. Serum and acute phase protein modulation of the effector phase of lymphokine-activated killer cells. Laryngoscope 1993;103:299-307.

6. Katz AE. Update on immunology of head and neck cancer. Med Clin North Am 1993;77:625-31.

7. Vlock DR. Immunobiologic aspects of head and neck cancer. Hematol Oncol Clin North Am 1991;5:797-820.

8. Kerrebijn JD, Simons PJ, Tas M, Balm AJ, Drexhage HA. In vivo effects of thymostimulin treatment on monocyte polarization, dendritic cell clustering and serum p15E-like transmembrane factors in operable head and neck squamous cell carcinoma patients. Eur Arch Otorhinolaryngol 1995;252:409-16.

9. Gooding R, Riches P, Dadian G, Moore J, Gore M. Increased soluble interleukin-2 receptor concentration in plasma predicts a decreased cellular response to IL-2. Br J Cancer 1995; 72:452-5.

10. O'Mahony AM, O'Sullivan GC, O'Connell J, Cotter TG, Collins JK. An immune suppressive factor derived from esophageal squamous carcinoma induces apoptosis in normal and transformed cells of lymphoid lineage. J Immunol 1993;151: 4847-56.

11. Lapointe H, Lampe H, Banerjee D. Head and neck squamous cell carcinoma cell line–induced suppression of in vitro lymphocyte proliferative responses. Otolaryngology 1992;106: 149-58.

12. Rice SQ, Crane IJ, Scully C, Prime SS. Production of a suppressor of lymphocyte proliferation by two human oral carcinoma cell lines. Scand J Immunol 1992;36:443-52.

13. Jaffe ML, Arai H, Nabel GJ. Mechanisms of tumor-induced immunosuppression: evidence for contact-dependent T cell suppression by monocytes. Mol Med 1996;2:692-701.

14. Chakraborty NG, Ergin MT, Mukherji B. Suppressor function of lymphocytes activated in in vitro co-culture against autologous tumor cells and expanded in interleukin-2. In Vivo 1991;5:631-5.

15. Koyama S, Fukao K. Phenotypic analysis of nylon-wool-adherent suppressor cells that inhibit the effector process of tumour cell lysis by lymphokine-activated killer cells in patients with advanced gastric carcinoma. J Cancer Res Clin Oncol 1994; 120:240-7.

16. Alleva DG, Burger CJ, Elgert KD. Tumour growth causes suppression of autoreactive T-cell proliferation by disrupting macrophage responsiveness to interferon-γ. Scand J Immunol 1994;39:31-8.

17. Maeda N, Sagara Y. Analysis of immunosuppressive mechanism to cytotoxic T lymphocyte generation in patients with advanced cancer. Asia Oceana J Obstet Gynaecol 1993; 19:309-18.

18. Wanebo HJ, Riley T, Karz D, Pace RC, Johns ME, Cantrell RW. Indomethacin sensitive suppressor-cell activity in head and neck cancer patients: the role of the adherent mononuclear cell. Cancer 1988;61:462-74.

19. Farinas MC, Rodriguez-Valverde V, Zarrabeitia MT, Parra-Blanco JA, Sanz-Ortiz J. Contribution of monocytes to the decreased lymphoproliferative response to phytohemagglutinin in patients with lung cancer. Cancer 1991;68:1279-84.

20. Kaffenberger W, Holzer-Muller L, Auberger T, Clasen BP, Hohlmeier G, van Beuningen D. An immunological outcome predictive score for head and neck carcinoma patients. Strahlenther Onkol 1995;171:444-53.

21. Young MRI, Wright MA. Myelopoiesis-associated immune suppressor cells in mice bearing metastatic Lewis lung carcinoma tumors: interferon-γ plus tumor necrosis factor–α synergistically reduce immune suppressor and tumor growth-promoting activities of bone marrow cells, and diminish tumor recurrence and metastasis. Cancer Res 1992;52:6335-40.

22. Oghiso Y, Yamada Y, Ando K, Ishihara H, Shibata Y. Differential induction of prostaglandin E_2-dependent and -independent immune suppressor cells by tumor-derived GM-CSF and M-CSF. J Leukoc Biol 1993;53:86-92.

23. Young MRI, Wright MA, Matthews JP, Malik I, Prechel M. Suppression of T cell proliferation by tumor-induced granulocyte-macrophage progenitor cells producing transforming growth factor–β and nitric oxide. J Immunol 1996;156:1916-22.

24. Young MRI, Schmidt-Pak A, Wright MA, Matthews JP, Collins SL, Petruzzelli G. Mechanisms of immune suppression in patients with head and neck cancer: presence of immune suppressive CD34+ cells in cancers that secrete granulocyte-macrophage colony-stimulating factor. Clin Cancer Res 1995;1:95-103.

25. Young MRI, Wright MA, Lozano Y, et al. Increased recurrence and metastasis in patients whose primary head and neck squamous cell carcinomas secreted granulocyte-macrophage colony-stimulating factor and contained CD34+ natural suppressor cells. Int J Cancer 1997;74:69-74.

26. Young MRI, Wright MA, Lozano Y, Matthews JP, Benefield J, Prechel MM. Mechanisms of immune suppression in patients with head and neck cancer: influence on the immune infiltrate of the cancer. Int J Cancer 1996;67:333-8.

27. Stewart TH, Hollinshead AC, Raman S. Tumour dormancy: initiation, maintenance and termination in animals and humans. Can J Surg 1991;34:321-5.

28. Wanebo HJ, Blackinton D, Kouttab N, Mehta S. Contribution of serum inhibitory factors and immune cellular defects to the depressed cell-mediated immunity in patients with head and neck cancer. Am J Surg 1993;166:389-94.

29. Alleva DG, Burger CJ, Elgert KD. Tumor-induced regulation of suppressor macrophage nitric oxide and TNF-α production. Role of tumor-derived IL-10, TGF-β, and prostaglandin E_2. J Immunol 1994;153:1674-86.

30. Gelber C, Eisenbach L, Feldman M, Goodenow RS. T-cell subset analysis of Lewis lung carcinoma tumor rejection: heterogeneity of effectors and evidence for negative regulatory lymphocytes correlating with metastasis. Cancer Res 1992;52:6507-15.

Ann Otol Rhinol Laryngol 109:2000

USE OF A COINCIDENCE GAMMA CAMERA TO DETECT PRIMARY TUMOR WITH ^{18}FLUORO-2-DEOXY-GLUCOSE IN CERVICAL LYMPH NODE METASTASES FROM AN UNKNOWN ORIGIN

SOPHIE PÉRIÉ, MD
JEAN-NOËL TALBOT, MD
GUY MONCEAUX, MD
DANY GRAHEK, MD
KHALDOUN KERROU, MD
FRANÇOISE MONTRAVERS, MD
JEAN LACAU ST GUILY, MD
PARIS, FRANCE

This study was performed to evaluate the ability of a dual-head gamma camera with ^{18}fluoro-2-deoxy-glucose coincidence detection emission tomography (FDG-CDET) to detect primary tumors in patients with cervical lymph node metastases of head and neck squamous cell carcinoma from an unknown origin. From 60 patients with untreated head and neck squamous cell carcinoma, we selected 4 in whom no evidence of the primary's origin was found by the conventional methods used for the evaluation of head and neck tumors. In addition to the panendoscopy, chest radiography, a computed tomography (CT) scan, and FDG-CDET were performed. Both FDG-CDET and the CT scan located cervical lymph node metastases. In addition, FDG-CDET located the primary tumor in 3 of the 4 patients, and the tumors were confirmed with histopathologic findings. In contrast, the CT scan detected the primary tumor in none of them. FDG tomography performed on a coincidence gamma camera appears to be a successful new tool in detecting occult primary tumors in head and neck carcinoma, and is useful in guiding endoscopic biopsies. It has, further, the important potential ability to detect distant metastases on whole body images.

KEY WORDS — cervical lymph node metastases, coincidence detection emission tomography, head and neck carcinoma, unknown primary tumor.

INTRODUCTION

Preoperative assessment of tumor extent, including cervical lymph node involvement and distant metastases, is mandatory for both staging and planning the best and most accurate therapy in patients with head and neck squamous cell carcinoma. In addition to endoscopic examination, computed tomography (CT) and magnetic resonance imaging (MRI) have significantly improved the detection of cervical nodes, as well as the assessment of primary tumors. Unfortunately, some patients (3% to 9%) who exhibit cervical metastases of squamous cell carcinoma have an unknown primary site, in spite of the standard methods used for the evaluation of head and neck tumors.[1] In addition to neck dissection, the necessity of tonsillectomy or elective irradiation of putative pharyngeal primary sites remains controversial in such patients.[2-8]

^{18}Fluoro-2-deoxy-glucose (FDG) is a glucose analog that is more intensely incorporated and retained by neoplastic cells than by normal tissues[9]; therefore, an increased uptake is associated with malignancy.[9] Performed with a dedicated machine, ^{18}fluoro-2-deoxy-glucose positron emission tomography (FDG-PET) is now used to detect several types of malignancies, including primary head and neck tumors and metastases, as well as recurrent tumors.[10-18] Only a few preliminary results have been obtained in cervical lymph node metastases from an unknown primary.[5,19-22] However, dedicated PET machines and cyclotrons for PET radiopharmaceutical production are expensive and not available everywhere, namely, far less available than CT or MRI. In contrast, dual-head gamma cameras are now present in almost all nuclear medicine departments. The conventional dual-head gamma camera of our Nuclear Medicine Department has been modified in order to be able to image FDG by coincidence detection emission tomography (CDET) of the two 511-keV photons resulting from each disintegration.

The purpose of the current study was to evaluate prospectively the ability of FDG-CDET in detecting the occult primary tumor of the head and neck when only a cervical lymph node metastasis from squamous cell carcinoma is exhibited.

PATIENTS AND METHODS

Four of 60 patients with untreated head and neck squamous cell carcinoma, included in a prospective study of FDG from March through October 1998,

---

From the Service d'Oto-Rhino-Laryngologie et Chirurgie de la Face et du Cou (Périé, Monceaux, Lacau St Guily), the Service de Médecine Nucléaire (Talbot, Grahek, Kerrou, Montravers), Faculté de Médecine Saint Antoine, Université Paris VI, Hôpital Tenon, Paris, France.

CORRESPONDENCE — Sophie Périé, MD, Service d'Oto-Rhino-Laryngologie et Chirurgie de la Face et du Cou, Hôpital Tenon, 4, rue de la Chine, 75020 Paris, France.

TABLE 1. PATIENTS AND CLINICAL, CT, FDG-CDET, AND HISTOPATHOLOGIC FINDINGS

Patient	*Age*	*TNM*	*Results of CT*	*Results of FDG-CDET*	*Histopathology of Neck Dissection*	*Primary Site Assessed by Histopathology*	*Final T Staging*
1	42	T0N1M0; N1 jugular (history of abscess)	T$^-$; 1N$^+$	T$^+$ oropharynx (tonsillar area); 2N$^+$	RND: DSCC 2N$^+$C$^+$ (1 and 1.5 cm)	DSCC, posterior tonsillar region	T1
2	54	T0N3M0; N3 digastric	T$^-$; 3-4N$^+$	T$^+$ oropharynx (base of tongue); 3N$^+$	RND: DSCC 12N$^+$C$^-$ (1 to 4 cm) FNDc: N$^-$	DSCC, valleculae	T1
3	44	T0N2aM0; N2a jugular	T$^-$; 1N$^+$	T$^+$ hypopharynx; 2N$^+$	RND: DSCC 3N$^+$C$^-$ (0.5, 1, and 3.5 cm)	DSCC, pyriform sinus	T1
4	72	T0N2aM0; N2a digastric	T$^-$; 1N$^+$	T$^-$; 1N$^+$	FND: UCC 2N$^+$C$^-$ (0.5 and 3.5 cm)	None	T0

FDG-CDET — ^{18}fluoro-2-deoxy-glucose coincidence detection emission tomography, CT — computed tomography, T — primary tumor, N — cervical node, RND — radical neck dissection, DSCC — differentiated squamous cell carcinoma, C — extracapsular invasion, FNDc — contralateral functional neck dissection, FND — functional neck dissection, UCC — undifferentiated cell carcinoma.

were selected because they exhibited a cervical metastasis from an unknown primary. This prospective study was performed to evaluate the ability of FDG-CDET in detecting primary tumors, as well as cervical or distant metastases. They were enrolled in an approved clinical trial, and each patient gave a written informed consent. These 4 patients were male, and their mean age was 53 years (ages 42, 44, 54, and 72 years). Tobacco and alcohol abuse was reported in all of them. None of them had been previously treated for a cancer. One patient had a history of a cervical abscess, incised 2 months before, located at the site of the lymph node metastasis.

In addition to physical examination of the awake patient and panendoscopy under anesthesia, we performed chest radiography, a CT scan, and FDG-CDET on a Picker Prism 2000XP gamma camera equipped with thick detection crystals and a coincidence detection system. The FDG-CDET examination started 45 minutes after the patient, who had fasted for 6 hours or more, was injected with 150 to 250 MBq of FDG. One tomoscintigraphic acquisition and 1 image of the whole body by scanning were obtained, without attenuation correction. The duration of each acquisition was approximately 40 minutes. Tomoscintigraphic images were reconstructed with an iterative algorithm and displayed on a computer either as slices in 3 orthogonal planes or as 3-dimensional volume rendering. The FDG-CDET procedure, as well as the CT scan, was performed on all patients before endoscopy.

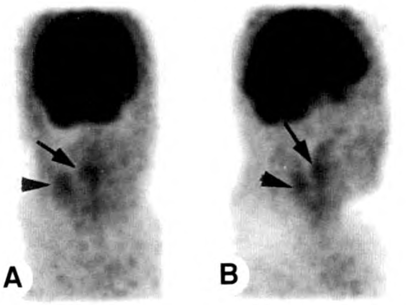

Fig 1. (Patient 1) ^{18}Fluoro-2-deoxy-glucose coincidence detection emission tomography (FDG-CDET) from 42-year-old man shows 2 cervical jugular metastases on right side (arrowheads) and primary tumor localized in ipsilateral tonsillar region (arrows). A,B) Three-dimensional (3-D) reconstruction images.

According to the classification system of the 1992 American Joint Committee on Cancer,[23] 1 patient was staged as T0N1M0 (middle jugular lymph node), 2 patients as T0N2aM0 (middle jugular lymph node in 1 patient, digastric lymph node in the other), and 1 patient as T0N3M0 (unilateral digastric lymph nodes), on the basis of the physical examination during panendoscopy and the results of CT scanning and routine chest radiography. No patient had evidence of distant metastases at diagnosis.

RESULTS

Cervical node involvement was detected by FDG-CDET in all patients, and in 3 patients, another focus was suspected to be the primary tumor (of the oropharynx and hypopharynx; Table 1). In contrast, the primary tumor was not localized on the CT scan. Distant metastasis was not detected on chest radiography or on FDG-CDET.

In 2 of the 3 patients in whom the FDG-CDET detected a primary tumor ipsilateral to the cervical lymph node involvement (Figs 1 and 2), endoscopic biopsies were performed at the suspicious site, which exhibited only inflammation. Cervicotomy was performed, followed by immediate radical neck dissection, because a cervical metastasis from a squamous cell carcinoma was assessed by the immediate histopathologic examination of the lymph node. The definitive histopathologic findings of each neck dissection showed positive cervical lymph node metastases of a differentiated squamous cell carcinoma, with ex-

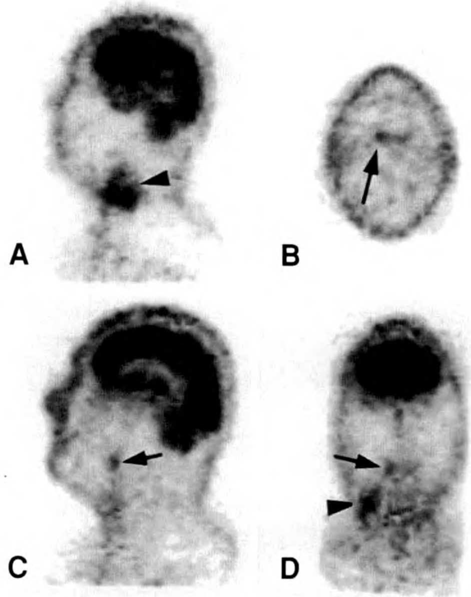

Fig 2. (Patient 2) FDG-CDET from 54-year-old man shows digastric lymph node metastases on right cervical side (arrowheads). Primary tumor was detected at base of tongue (arrows). A) Three cervical lymph nodes on 3-D reconstruction image. B,C) Primary tumor on transverse and sagittal sections. D) Both primary tumor and cervical metastases on coronal section.

tracapsular invasion in 1 patient. Contralateral neck dissection performed in 1 patient showed no invasion. In addition, from the 2 biopsies performed during endoscopy, a squamous cell carcinoma of the oropharynx (posterior tonsillar region) was found in 1 patient (42 years), and a squamous cell carcinoma of the valleculae was found in the other (54 years; both staged as T1 after results of biopsies were obtained).

In the third patient (44 years), in contrast to the FDG-CDET findings (Fig 3), no evidence of pyriform sinus involvement was found during endoscopy, and a radical neck dissection was performed. The definitive histopathologic results showed a lymph node metastasis of a differentiated squamous cell carcinoma, but random and oriented endoscopic biopsies were all negative. Therefore, a second FDG-CDET was performed 1 month later, before the scheduled radiotherapy. Because it demonstrated persistence of the hypopharyngeal focus, endoscopy under anesthesia was performed for the second time. It revealed a small tumor (less than 1 cm, staged as T1) of the pyriform sinus, ipsilateral to the lymph node previously evidenced. The histopathologic data confirmed the existence of a differentiated squamous cell carcinoma.

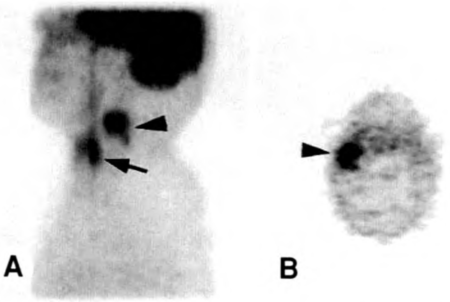

Fig 3. (Patient 3) FDG-CDET from 44-year-old man. Cervical metastases are observed on right side (arrowheads) associated with primary tumor in hypopharynx (arrow). A) Jugular lymph nodes and primary site on 3-D reconstruction. B) Cervical metastases on transverse section.

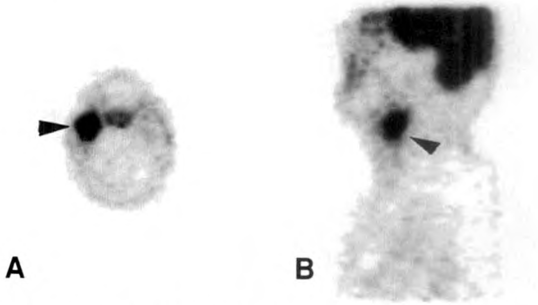

Fig 4. (Patient 4) FDG-CDET from 72-year-old man does not detect primary tumor. It shows cervical metastasis on right cervical side (arrowheads). A) Transverse section. B) Sagittal section.

In the fourth patient (72 years), no primary tumor was detected on CT scanning, endoscopy, or FDG-CDET (Fig 4). Biopsies of the most likely primary sites, such as the tonsillar region and nasopharynx, were free of tumor. A functional neck dissection was performed, and histologic examination showed 2 cervical metastases (1 digastric lymph node and 1 occult positive lymph node in the low jugular area) of an undifferentiated cell carcinoma of the nasopharynx with no extracapsular invasion.

Postoperative adjuvant radiotherapy was performed in all patients, combined with chemotherapy (cisplatin) in 3 of them. In the 3 patients in whom the primary tumor was localized, in addition to the irradiation of the node areas, elective radiotherapy was performed on the tumor site. Radiotherapy on the primary tumor site was preferred to surgical removal of the discovered tumor: in 1 patient because supraglottic laryngectomy was contraindicated, in 1 other because the primary tumor (posterior tonsillar region) was not well delineated, and in the third because the tumor measured less than 1 cm and was excised for biopsy. In the last patient, in whom no primary tumor was found, irradiation of the whole pharyngeal axis and the node areas in combination with chemotherapy was performed. The follow-ups varied from 3 to 10 months.

DISCUSSION

The standard evaluation of head and neck cancer

TABLE 2. COMPARISON OF PRESENT RESULTS WITH THOSE OF OTHER AUTHORS ON ABILITY OF FDG TO DETECT PRIMARY OF CERVICAL METASTASES OF UNKNOWN ORIGIN AFTER UNSUCCESSFUL CONVENTIONAL DIAGNOSTIC WORKUP (PANENDOSCOPY, CT OR MRI, CHEST RADIOGRAPHY)

Authors	*Year*	*Methods and Sites of Primary Tumor*	*Results*
Mukherji et al[21]	1996	FDG-SPECT; head and neck tumors	10/18 positive biopsies; 8/10 correlated with FDG+
Braams et al[19]	1997	FDG-PET; head and neck tumors; lung tumor	4/13 positive biopsies; 4/4 correlated with FDG+ (1/9 positive biopsy in later phase despite negative initial FDG)
Mendenhall et al[5]	1998	FDG-SPECT; head and neck tumors	1/5 positive biopsy; 1/1 correlated with FDG+
Kole et al[20]	1998	FDG-PET; head and neck tumors; lung tumor; breast tumors; colonic tumor	4/16 positive biopsies; 4/4 correlated with FDG+ (3/12 positive biopsies in later phase despite negative initial FDG)
Scheidhauer et al[22]	1998	FDG-PET; head and neck tumors; lung tumors	16/477 positive biopsies; 16/16 correlated with FDG+
Present study		FDG-CDET; head and neck tumors	3/4 positive biopsies; 3/3 correlated with FDG+

FDG — ^{18}fluoro-2-deoxy-glucose, CT — computed tomography, MRI — magnetic resonance imaging, SPECT — single photon emission computed tomography, PET — positron emission tomography, CDET — coincidence detection emission tomography.

includes physical and panendoscopic examinations with biopsies, as well as conventional images from CT scanning or MRI, for delineating the tumor limits and for detecting lymph node involvement, as well as bone destruction. These examinations are required for staging and for managing accurate, individualized treatment, essential for a successful therapy and a long-term remission. However, in approximately 3% to 9% of head and neck cancers, the primary cancer of the lymph node metastases remains unknown,[1] despite modern methods of conventional imaging, ie, CT and MRI. For example, CT and MRI are not contributory in detecting microscopic and superficial lesions or in discriminating tumor-infiltrated nodes from reactive enlargement of lymph nodes (inflammation). Because a subclinical primary tumor of the tonsil may be present in these patients with cervical metastases of squamous cell carcinoma of unknown origin, many otolaryngologists recommend tonsillectomy associated with a cervical lymph node dissection.[3,5,7,8] In cases of malignant occult tumor of the tonsillar fossa found on histopathologic examination, irradiation can be focused on the tonsillar fossa, avoiding irradiation of a normal larynx and hypopharynx.[3,7]

Scanning for FDG is a new noninvasive imaging method used to detect malignancy. Unlike conventional imaging methods, FDG scanning provides information on the functional consequences of a malignancy, allowing metabolic imaging of tumor tissues based upon increased uptake of glucose in neoplastic cells.[9] The FDG uptake appears strongly related to the number of viable tumor cells.[9] This procedure should precede biopsy that traumatizes tissues, creating inflammation that can lead to nonspecific FDG uptake,[16] or an interval of at least 1 week should be observed between biopsy and FDG scanning. The applicability of FDG-PET has been significantly demonstrated in detecting head and neck carcinomas and cervical lymph node involvement.[10-13,15-17] In comparison to CT, which is able to localize lymph nodes larger than 1 cm in diameter, FDG scanning is able to detect smaller lymph node metastases, down to about 0.6 cm, not only with dedicated PET machines,[10,15] but also with CDET machines.[24]

The clinical utility of FDG has been demonstrated in head and neck tumors on dedicated PET machines, and FDG has recently been registered in France for use in oropharyngeal tumors. However, the relatively high cost and limited availability of FDG-PET led us to evaluate other techniques of FDG detection, such as single photon emission computed tomography (SPECT) and, more recently, CDET.[5,18,21,24-26] The ability of FDG to detect the primary of cervical metastases of unknown head and neck tumors has been reported only in small series (Table 2[5,19-22]). The first study, published in 1996, used an ordinary gamma camera and SPECT detection with ultrahigh energy collimators, considering FDG as a monoenergetic emitter.[21] In 18 patients in whom the results of CT scanning or MRI were negative (12 patients) or suspicious (6 patients), FDG-SPECT detected 13 primary sites that were correlated with positive biopsies in 8 patients (sensitivity of 80%, specificity of 37%).[21] In contrast, CT or MRI results that suspected the primary site in 6 patients correlated with a positive biopsy in 3 patients (sensitivity of 30%, specificity of 62%).[21] These results are surprising, because this detection technique has been shown to have a low sensitivity in other cancers.[25] However, the authors considered suspicious results of CT or MRI as negative. In fact, in 12 patients in whom CT or MRI was negative, FDG-SPECT identified the primary site in 6 of 7 positive biopsies (sensitivity of 85%

and specificity of 20%). In a more recent study, FDG-SPECT detected 35% of primary sites among 24 patients exhibiting cervical lymph nodes from an unknown primary, but just 1 tumor unidentified by CT or MRI was detected with FDG-SPECT.[5] Using dedicated PET machines, one study detected primary tumor in approximatively 30% of cases[19]; in another report, the procedure identified 7 primary occult tumors among 29 patients with an unknown primary, including 4 tumors among 16 patients with metastatic cervical lymph nodes (metastases were extracervical in 13 patients).[20] However, primary tumors of the head and neck unidentified by FDG-PET were identified in a later phase in 3 patients.[20] To the best of our knowledge, the performance of the FDG-CDET in detecting occult primary tumors of head and neck carcinoma has not been evaluated yet. The current preliminary study demonstrated that FDG-CDET may be useful in such cases, because it detected the primary cancer in 3 of 4 patients. Although no evidence of tumor was present during endoscopy, directed biopsies of suspicious primary sites involved at FDG scanning were of benefit for histopathologic examinations.[19,21] The present study also suggests that endoscopy and biopsies have to be repeated, in the case of a first negative biopsy in patients with signs of primary cancer on FDG-CDET. In addition, as also demonstrated by others,[24] FDG-CDET was capable of detecting a primary lesion smaller than 1 cm. When the primary tumor was localized in 3 patients, it led to a modification of the patients' medical management: elective radiotherapy was performed on the primary site identified in the 3 patients, in addition to irradiation of the node areas.

One of the main limitations of FDG imaging is its lack of anatomic detail: a precise localization and extent of tumor is, to date, not obtainable.[4,15,16] Increased uptake of FDG by saliva pools in some areas (oral cavity, valleculae, and pyriform sinuses), giving artifacts, is also a problem.[15] Improved performance of PET and/or CDET imaging is expected with attenuation correction and new detectors leading to higher resolution, with development of tracers with less salivary excretion, and with image fusion of FDG and conventional methods. In addition, the cost of FDG limited its routine use, but further, larger studies may demonstrate an improved cost-benefit ratio for this imaging, especially if a change of medical management improves the outcome of patients exhibiting an unknown primary after an unsuccessful conventional diagnostic workup (panendoscopy, CT, or MRI).

In conclusion, FDG scanning is a new procedure for evaluating carcinomas of the head and neck, and its effectiveness has been demonstrated in detecting primary tumors, as well as cervical nodes and distant involvement, with dedicated PET cameras. This preliminary study also showed the ability of FDG with a CDET camera to detect the primary tumor in carcinomas of the head and neck of an unknown origin. The role of FDG-CDET in prospectively detecting primary tumors in head and neck carcinoma, as well as cervical and distant metastases, in comparison with conventional methods is now under investigation in our department. Such studies are necessary because CDET cameras will be more available than PET cameras, at least in the near future.

ACKNOWLEDGMENT — We are grateful to Nassima Younsi, MD (Service de Médecine Nucléaire, Hôpital Tenon, Paris, France), for her helpful participation during the preparation of the clinical trial.

REFERENCES

1. Kirschner MJ, Fietkau R, Waldfahrer F, Iro H, Sauer R. Therapy of cervical lymph node metastases of unknown primary tumor. Strahlenther Onkol 1997;173:362-8.

2. Colletier PJ, Garden AS, Morrisson WH, Goepfert H, Geara F, Ang KK. Post-operative radiation for squamous cell carcinoma metastatic to cervical lymph nodes from an unknown primary site: outcomes and patterns of failure. Head Neck 1998; 20:674-81.

3. Lapeyre M, Malissard L, Peiffert D, et al. Cervical lymph node metastasis from an unknown primary: is a tonsillectomy necessary? Int J Radiat Oncol Biol Phys 1997;39:291-6.

4. Medini E, Medini AM, Lee CK, Gapany M, Levitt SH. The management of metastatic squamous cell carcinoma in cervical lymph nodes from an unknown primary. Am J Clin Oncol 1998;21:121-5.

5. Mendenhall WM, Mancuso AA, Parsons JT, Stringer SP, Cassisi NJ. Diagnostic evaluation of squamous cell carcinoma metastatic to cervical lymph nodes from an unknown head and neck primary site. Head Neck 1998;20:739-44.

6. Sinnathamby K, Peters LJ, Laidlaw C, Hughes PG. The occult head and neck primary: to treat or not to treat? Clin Oncol R Coll Radiol 1997;9:322-9.

7. Righi PD, Sofferman RA. Screening unilateral tonsillectomy in the unknown primary. Laryngoscope 1995;105:548-50.

8. Gluckman JL, Robbins KT, Fried MP. Cervical metastatic squamous carcinoma of unknown or occult primary source. Head Neck 1990;12:440-3.

9. Minn H, Joensuu H, Ahonen A, Klemi P. Fluorodeoxyglucose imaging: a method to assess the proliferative activity of human cancer in vivo. Cancer 1988;61:1776-81.

10. Adams F, Baum RP, Stuckensen T, Bitter K, Hor G. Prospective comparison of ^{18}F-FDG PET with conventional imaging modalities (CT, MRI, US) in lymph node staging of head and neck cancer. Eur J Nucl Med 1998;25:1255-60.

11. Bailet JW, Abemayor E, Jabour BA, Hawkins RA, Ho C, Ward PH. Positron emission tomography: a new, precise imaging modality for detection of primary head and neck tumors and assessment of cervical adenopathy. Laryngoscope 1992;

102:281-8.

12. Braams JW, Pruim J, Freling NJM, et al. Detection of lymph node metastases of squamous cell cancer of the head and neck with FDG-PET and MRI. J Nucl Med 1995;36:211-6.

13. Laubenbacher C, Saumweber D, Wagner-Manslau C, et al. Comparison of fluorine-18-fluorodeoxyglucose PET, MRI, and endoscopy for staging head and neck squamous cell carcinomas. J Nucl Med 1995;36:1747-57.

14. McGuirt WF, Greven KM, Williams DW III, et al. PET scanning in head and neck oncology: a review. Head Neck 1998; 20:208-15.

15. McGuirt WF, Greven KM, Keyes JW Jr, et al. Positron emission tomography in the evaluation of laryngeal carcinoma. Ann Otol Rhinol Laryngol 1995;104:274-8.

16. Paulus P, Sambon A, Vivegnis D, et al. ^{18}FDG-PET for the assessment of primary head and neck tumors: clinical, computed tomography, and histopathological correlation in 38 patients. Laryngoscope 1998;108:1578-83.

17. Rege S, Maas A, Chaiken L, et al. Use of positron emission tomography with fluorodeoxyglucose in patients with extracranial head and neck cancers. Cancer 1994;73:3047-58.

18. Stokkel MP, Terhaard CH, Mertens IJ, Hordijk GJ, van Rijk PP. Fluorine-18-FDG detection of laryngeal cancer post-radiotherapy using dual-head coincidence imaging. J Nucl Med 1998;39:1385-7.

19. Braams JW, Pruim J, Kole AC, et al. Detection of unknown primary head and neck tumors by positron emission tomography. Int J Oral Maxillofac Surg 1997;26:112-5.

20. Kole AC, Nieweg OE, Pruim J, et al. Detection of unknown primary tumors using positron emission tomography. Cancer 1998;82:1160-6.

21. Mukherji SK, Drane WE, Mancuso AA, Parsons JT, Mendenhall WM, Stringer S. Occult primary tumors of the head and neck: detection with 2-[F-18]fluoro-2-deoxy-D-glucose SPECT. Radiology 1996;199:761-6.

22. Scheidhauer K, Jungehülsing M, Pietrzyk U, Theissen P, Stennert E, Schicha H. FDG-PET patients with CUP-syndrome [Abstract]. Eur J Nucl Med 1998;25:1021.

23. American Joint Committee on Cancer. Manual for staging of cancer. 4th ed. Philadelphia, Pa: JB Lippincott, 1992:33-44.

24. Stokkel MPM, van Isselt JW, Hoekstra A, Van Rijk PP. Lesion of 4 mm and 5 mm detected with 18F-FDG using a dual head coincidence camera [Abstract]. Eur J Nucl Med 1998;25: 1032.

25. Martin WH, Delbeke D, Patton JA, et al. FDG-SPECT: correlation with FDG-PET. J Nucl Med 1995;36:988-95.

26. Lonneux M, Delval D, Bausart R, et al. Can dual-headed 18F-FDG SPECT imaging reliably supersede PET in clinical oncology? A comparative study in lung and gastrointestinal tract cancer. Nucl Med Commun 1998;19:1047-54.

Ann Otol Rhinol Laryngol 109:2000

OBJECTIVE COMPARISON OF SHOULDER DYSFUNCTION AFTER THREE NECK DISSECTION TECHNIQUES

PAO-TSAI CHENG, MD
YANG-HUA LIN, MS
SHENG-PO HAO, MD
ALBERT RE-MING YEH, MD
TAO-YUAN, TAIWAN

A prospective study with subjective evaluation of shoulder pain and objective evaluation of shoulder muscle strength by isokinetic testing and electromyographic and electroneurographic studies of spinal accessory nerve function was performed on patients who had undergone neck dissection procedures. Twenty-one patients with head and neck cancer were enrolled in this study. Three types of neck dissection were performed: 7 selective neck dissections, 9 modified radical neck dissections, and 5 radical neck dissections. All patients who underwent radical neck dissection had shoulder pain, and 80% of them had shoulder droop after the operation. In the patients who underwent selective neck dissection, the electromyographic findings of the spinal accessory nerve were relatively normal. Their shoulder strength was sometimes decreased at 1 month after operation, but it had returned to preoperative strength by the 6-month follow-up visit. These findings suggested that patients who underwent selective neck dissection had the least damage to spinal accessory nerve function and the least shoulder disability after neck dissection.

KEY WORDS — electromyography, isokinetic muscle strength, neck dissection, spinal accessory nerve.

INTRODUCTION

Neck dissection is a valuable method for treating cervical metastasis from cancer of the head and neck. One of the most common complications of neck dissection is injury to the spinal accessory nerve (SAN). Injury of the SAN results in atrophy of the trapezius muscle and shoulder dysfunction. The ultimate goal of cancer surgery is to cure the patient and eradicate the tumor while preserving function and preventing complications. Therefore, steps should be taken to preserve the SAN whenever possible. There are 3 main types of neck dissection procedures for head and neck cancer. In radical neck dissection (RND), all 5 levels of nodal groups are removed, and the SAN, internal jugular vein, and sternocleidomastoid muscle are sacrificed. In modified radical neck dissection (MND), all 5 levels of nodes are removed, but the SAN is preserved. In selective neck dissection (SND), only the group of nodes at the highest risk of metastasis are removed, and the SAN is minimally manipulated during dissection. In MND, the SAN is preserved and dissected free from the jugular foramen to the trapezius muscle. In SND, however, the SAN is dissected free only from the jugular foramen to the posterior edge of the sternocleidomastoid muscle. The SAN is always in danger in neck dissection. Classic RND causes the SAN to be severed, causing denervation of the trapezius muscle. This results in shoulder droop, pain, weakness, and limited range of motion (ROM).[1,2] Preservation of the SAN during neck dissection might lessen shoulder morbidity after operation.[3-5] In any case, from a functional standpoint, most surgeons agree that the sacrifice of the SAN is disabling. Therefore, the importance of curing the patient but preserving as much function as possible cannot be overemphasized.

In this prospective study, we attempted to use objective techniques to measure shoulder disability and compare the differences in shoulder disability that occurred in patients who underwent different neck dissection procedures. Patients are compared on the basis of preoperative and postoperative isokinetic evaluation of shoulder function and electromyographic (EMG) assessment of SAN function.

MATERIALS AND METHODS

Subjects. A prospective evaluation of shoulder dysfunction after neck dissections in patients with head and neck cancer was undertaken from July 1993 to June 1998. Exclusion criteria included recurrences, failure to complete the isokinetic or EMG examinations, and postoperative irradiation. Twenty-one patients (18 men and 3 women) completed the study and formed the basis of the evaluation. Their ages ranged from 39 to 70 years, with a mean age of 50 years. Of these patients, 5 underwent RND, 9 underwent MND, and 7 underwent SND. None of the patients had shoulder problems or neuropathy before operation.

From the Departments of Physical Medicine and Rehabilitation (Cheng, Lin) and Otolaryngology (Hao, Yeh), Chang Gung Memorial Hospital, Chang Gung University, Tao-Yuan, Taiwan.

CORRESPONDENCE — Pao-Tsai Cheng, MD, Dept of Physical Medicine and Rehabilitation, Chang Gung Memorial Hospital, 5 Fu-Hsing St, Kuei-Shan Hsiang, Tao-Yuan, Taiwan.

TABLE 1. CLINICAL CHARACTERISTICS BY GROUP

	SND Group (n = 7)	*MND Group (n = 9)*	*RND Group (n = 5)*
Age (y; mean ± SD)	46.8 ± 5.6	54.0 ± 9.7	47.0 ± 4.0
Sex (M:F)	6:1	7:2	5:0
Operation site			
Right	4	4	2
Left	3	5	3
Significant shoulder ROM limitation			
Presence	0	2	3
Absence	7	7	2
Shoulder pain			
Presence	2	5	5
Absence	5	4	0
Shoulder weakness			
Presence	0	4	4
Absence	7	5	1

SND — selective neck dissection, MND — modified radical neck dissection, RND — radical neck dissection, ROM — range of motion.

Before surgery each patient was evaluated in the rehabilitation department to establish baseline data for ROM, strength, and shoulder posture. All patients were evaluated again at their 1- and 6-month follow-up visits. The presence or absence of shoulder pain, ROM limitation, shoulder droop, and the physical strength of the shoulder were carefully evaluated and recorded.

Physical Strength Evaluation. The physical strength of the shoulder was evaluated with a Cybex isokinetic system (Cybex 340, Lumex, New York, NY). Both shoulders of each subject were tested at flexion-extension, abduction-adduction, and external rotation–internal rotation. Because most of our patients were unable to produce torque at the speed of 240°/s with the operated arm, our testing speed was set at a slow contractive velocity of 60°/s and a medium contractive velocity of 180°/s. The uninvolved side was tested first to establish a control. The patient was allowed 3 submaximal practice attempts and 1 maximal practice attempt before the test at each testing speed to familiarize himself or herself with the machine. Verbal encouragement was consistent to each subject. Five reciprocal contractions were recorded in each test. The mean value and standard deviation of the absolute peak torque at each speed and direction were measured and calculated. The Cybex 340 dynamometer measured the torque in foot-pounds.

Electroneurography and Electromyography. Electroneurographic (ENoG) examination of the SAN and EMG examination of the trapezius muscle were performed 5 weeks after operation with a Nicolet Viking IIe EMG machine. The same examiner performed the test on all subjects. The examiner had no knowledge of which type of procedure each patient had undergone. The testing sequence began with the subject in the sitting position. The ENoG examination was performed by placing the active surface electrode at the upper trapezius muscle, halfway between the acromion and the spinal process of C7. The reference electrode was placed at the acromion. The ground electrode was placed between the active and reference electrodes. The SAN was stimulated at a point 7 cm above the active electrode, in the line between the active electrode and the mandibular angle. Each patient underwent ENoG examination of both SANs, with the normal, unoperated side serving as a control. The latency, peak-to-peak amplitude, duration, and negative phase response area of the compound muscle action potential were recorded for comparison.

The EMG examination of the involved trapezius muscle was performed with standard procedures. The EMG examination recorded resting potentials as well as active motor unit potentials. Each EMG result was rated as being normal, slightly abnormal, or severely abnormal according to the presence of fibrillation potentials, positive sharp waves, and recruitment patterns.

Data Analysis. Muscle strength data of the involved and uninvolved shoulders of patients taken before and after operation were collected into Excel software and analyzed by the SPSS software package (SPSS Inc, Chicago, Ill) with a paired *t*-test. Proportions were compared with a χ^2 test. The significance of differences was set at the level of $p < .05$.

RESULTS

The clinical characteristics of the 7 patients who underwent SND, the 9 patients who underwent MND, and the 5 patients who underwent RND are shown in Table 1. Most of our patients were men. There were no significant differences in age or side operated between the 3 groups. Patients who underwent RND were prone to postoperative shoulder pain, shoulder ROM limitation, and shoulder weakness. Their shoulder pain on the operated side was most often described as a dull ache. Only 1 patient in the RND group described the pain as a severe, sharp pain and needed medication for pain relief. Eight of the 21 patients (4 in the RND group and 4 in the MND group) believed that the surgery weakened their shoulder and resulted in shoulder droop. Five patients (2 in the MND group and 3 in the RND group) had shoulder ROM limitation in their operated shoulder, and pain was the limiting factor.

Isokinetic Shoulder Muscle Strength. A compari-

TABLE 2. COMPARISON OF ISOKINETIC PEAK TORQUE OF SHOULDER MOVEMENT BEFORE AND AFTER SELECTIVE NECK DISSECTION (N = 7)

		Lesion Side (ft-lb)		
	Sound Side (ft-lb)	*Before Surgery*	*1 mo After Surgery*	*6 mo After Surgery*
60°/s				
Flexion	20.5 ± 6.1	20.8 ± 4.8	14.7 ± 6.1*	17.7 ± 4.5
Extension	31.2 ± 9.8	32.4 ± 7.8	24.8 ± 7.6*	28.0 ± 7.1
Abduction	20.3 ± 6.1	20.7 ± 6.4	17.1 ± 4.6	17.8 ± 4.6
Adduction	33.2 ± 6.5	36.5 ± 6.9	27.2 ± 6.1*	32.5 ± 5.1
Internal rotation	16.1 ± 7.0	17.2 ± 7.5	14.0 ± 4.5	15.7 ± 5.3
External rotation	12.5 ± 4.5	11.8 ± 4.3	10.5 ± 4.2	11.2 ± 4.8
180°/s				
Flexion	13.6 ± 6.4	14.0 ± 3.9	10.3 ± 2.9*	12.3 ± 2.5
Extension	17.3 ± 5.9	17.1 ± 5.3	14.8 ± 5.7	17.8 ± 5.2
Abduction	15.6 ± 5.1	16.4 ± 5.3	10.7 ± 3.5*	13.8 ± 4.3
Adduction	26.7 ± 5.3	28.7 ± 5.9	22.4 ± 6.2*	26.5 ± 5.8
Internal rotation	11.9 ± 4.3	11.3 ± 5.1	9.8 ± 4.1	10.7 ± 2.5
External rotation	8.6 ± 3.5	8.3 ± 3.1	8.2 ± 2.8	8.8 ± 3.3

*p < .05 versus before surgery.

son of the peak torque (foot-pounds) of shoulder flexion-extension, external-internal rotation, and abduction-adduction between the initial and postoperative evaluations for the patients who underwent SND is shown in Table 2. The peak torques of shoulder flexion-extension and abduction-adduction 1 month after operation were significantly lower than those in the sound shoulder and those in the affected shoulder before operation. However, 6 months after operation, the peak torque of the operated shoulder had returned to its preoperative value.

Table 3 shows the peak preoperative and postoperative torques of shoulder movement in the patients who underwent MND. The affected shoulder showed peak torques that were significantly lower 1 month after operation than they were before operation, and they were significantly lower than those of the sound side. Six months after operation, the peak torques of the affected shoulder were still lower than those seen before the operation, although statistical significance was only seen in shoulder flexion-extension at 60°/s. The peak torques of shoulder movement in the patients who underwent RND are shown in Table 4. The peak torques of the operated shoulder in all directions were significantly lower both 1 month and 6 months after operation compared with the preoperative peak torque (p < .05).

Electroneurographic and Electromyographic Findings. The ENoG findings of the SAN are shown in Table 5. There were no significant differences between

TABLE 3. COMPARISON OF ISOKINETIC PEAK TORQUE OF SHOULDER MOVEMENT BEFORE AND AFTER MODIFIED NECK DISSECTION (N = 9)

		Lesion Side (ft-lb)		
	Sound Side (ft-lb)	*Before Surgery*	*1 mo After Surgery*	*6 mo After Surgery*
60°/s				
Flexion	24.6 ± 6.7	23.4 ± 6.0	16.5 ± 6.4*	17.7 ± 5.8*
Extension	33.5 ± 9.8	31.5 ± 8.7	23.7 ± 8.0*	24.1 ± 8.2*
Abduction	20.6 ± 7.1	19.3 ± 7.0	11.1 ± 5.7*	16.1 ± 6.8
Adduction	30.7 ± 8.1	29.6 ± 7.8	20.6 ± 6.7*	27.1 ± 7.5
Internal rotation	21.7 ± 5.3	20.8 ± 5.8	14.4 ± 5.1*	15.3 ± 6.1
External rotation	15.5 ± 5.1	16.1 ± 5.4	9.6 ± 3.5*	11.2 ± 4.8
180°/s				
Flexion	14.8 ± 6.2	13.8 ± 5.9	8.3 ± 4.8*	10.7 ± 6.3
Extension	19.8 ± 7.1	18.2 ± 5.9	13.0 ± 4.7*	14.8 ± 6.2
Abduction	14.5 ± 4.3	12.7 ± 5.2	6.9 ± 3.0*	8.8 ± 3.5
Adduction	20.3 ± 5.4	21.6 ± 6.2	10.6 ± 3.2*	18.3 ± 4.1
Internal rotation	13.8 ± 4.1	14.8 ± 5.3	10.1 ± 4.3*	11.1 ± 4.8
External rotation	11.6 ± 3.8	11.0 ± 4.2	6.8 ± 3.0*	8.4 ± 4.1

*p < .05 versus before surgery.

TABLE 4. COMPARISON OF ISOKINETIC PEAK TORQUE OF SHOULDER MOVEMENT BEFORE AND AFTER RADICAL NECK DISSECTION (N = 5)

		Lesion Side (ft-lb)		
	Sound Side (ft-lb)	*Before Surgery*	*1 mo After Surgery*	*6 mo After Surgery*
60°/s				
Flexion	22.3 ± 4.3	22.2 ± 2.5	11.6 ± 2.1*	12.0 ± 2.8*
Extension	30.8 ± 6.8	31.2 ± 6.7	16.0 ± 2.5*	19.5 ± 5.3*
Abduction	19.8 ± 5.3	19.0 ± 4.5	7.6 ± 1.2*	10.6 ± 2.8*
Adduction	35.9 ± 5.8	37.4 ± 5.4	22.8 ± 4.0*	28.1 ± 1.7*
Internal rotation	18.8 ± 4.0	19.5 ± 3.1	11.4 ± 3.2*	11.0 ± 1.4*
External rotation	14.2 ± 3.5	14.7 ± 0.9	8.5 ± 1.2*	7.8 ± 1.5*
180°/s				
Flexion	17.1 ± 3.8	17.5 ± 3.5	8.6 ± 2.8*	7.6 ± 2.5*
Extension	21.6 ± 2.8	22.0 ± 4.8	14.8 ± 4.2*	11.2 ± 4.3*
Abduction	14.5 ± 3.2	12.0 ± 1.8	5.8 ± 0.9*	8.5 ± 1.3*
Adduction	29.3 ± 5.8	28.9 ± 4.2	15.3 ± 2.0*	17.2 ± 2.3*
Internal rotation	15.2 ± 4.2	15.8 ± 2.5	10.0 ± 1.8*	7.8 ± 1.1*
External rotation	11.9 ± 2.9	12.0 ± 2.1	7.1 ± 1.2*	6.5 ± 0.5*

*p < .05 versus before surgery.

the operated side and the sound side in the SND group. The amplitude and response area were significantly lower in patients who underwent MND than in those who underwent SND. However, no latency difference was noted in these 2 groups. No ENoG findings could be detected in 3 of the 5 patients who underwent RND. The ENoG findings of the other 2 patients who underwent RND showed a very low amplitude of evoked ENoG potential. Therefore, we did not put the ENoG data of the RND group in Table 5.

Of the 3 groups, those patients who underwent RND showed the worst disturbance on EMG examination 5 weeks after operation. As shown in Table 6, all 5 patients who underwent RND had abnormal EMG findings on their operated side. Four (80%) showed a diffuse denervation pattern with a severely reduced recruitment pattern. Two patients underwent a second EMG examination 6 months after operation, and the results remained severely abnormal. The SND group was found to have the least damage to the SAN as demonstrated by the postoperative EMG findings. Their EMG findings of the trapezius muscle were relatively normal; only 3 patients showed slightly abnormal EMG findings.

TABLE 5. COMPARISON OF ELECTRONEUROGRAM OF SPINAL ACCESSORY NERVE BETWEEN LESION SIDE AND SOUND SIDE

		SND (n = 7)	*MND (n = 9)*
Latency (ms)	Lesion side	2.5 ± 0.5	2.6 ± 0.7
	Sound side	2.1 ± 0.3	2.1 ± 0.4
Amplitude (mV)	Lesion side	8.9 ± 3.5^a	4.6 ± 2.7^b
	Sound side	10.6 ± 2.2	10.3 ± 3.0^c
Duration (ms)	Lesion side	13.9 ± 2.6	14.2 ± 2.9
	Sound side	14.0 ± 2.2	13.0 ± 1.6
Response area (ms × mV)	Lesion side	72.7 ± 20.9^d	38.7 ± 10.1^e
	Sound side	86.6 ± 15.6	86.8 ± 17.0^f

p < .025 for a versus b and d versus e.
p < .005 for b versus c and e versus f.

DISCUSSION

In the normal shoulder, scapular rotation is achieved by the balance between the trapezius muscle and the serratus anterior muscle. Without the trapezius muscle to counteract it, the serratus anterior muscle pulls the scapula inferiorly and laterally, interfering with shoulder movement. Further, the failure of scapula fixation causes the deltoid to contract early during abduction; therefore, it is unable to achieve a full ROM. The SAN is the main nerve that innervates the trapezius muscle. In the classic RND procedure, the SAN is resected. This in turn limits the ability of the shoulder to move in a full active ROM and droops the shoulder.

Hillel et al[6] reported that nearly all patients who undergo RND suffer from pain, weakness, shoulder droop, and disability as a result of sacrificing the SAN. Leipzig et al[7] reported that classic RND caused shoulder disability in as many as 60% of patients, whereas

TABLE 6. DISTRIBUTION OF ELECTROMYOGRAPHY ABNORMALITIES BY GROUP

Electromyography Findings	*SND Group (n = 7)*	*MND Group (n = 9)*	*RND Group (n = 5)*
Normal	4	2	0
Slightly abnormal	3	3	1
Severely abnormal	0	4	4

in those patients whose SAN was preserved, the jugular vein and sternocleidomastoid muscle had the lowest incidence (30%) of shoulder disability. In their series, 40% of patients who underwent RND had minimal disability, perhaps because the trapezius muscle has a dual nerve supply. Jones and Stell[8] and Krause et al[9] identified several small branches arising from the third and fourth cervical nerves that pass across the floor of the posterior triangle to supply the trapezius. In our study, all 5 patients in the RND group had shoulder pain after operation, but 1 (20%) had no shoulder weakness or ROM limitation clinically. Therefore, the incidence of shoulder disability after RND may depend on the alternative motor innervation of the trapezius muscle.[10]

In theory, the MND procedure, in which the SAN is spared, should result in less shoulder dysfunction and less pain. Some authors[11,12] have reported that their patients had no postoperative shoulder pain and no loss of shoulder movement or power after MND. However, as reported by Sobol et al,[3] despite attempts to preserve the SAN in the MND and SND procedures, patients still had shoulder complications. About half of our patients who underwent MND also had shoulder pain and weakness. Two of the 7 patients who underwent SND in our study did have shoulder pain, even when their SAN was only minimally manipulated.

Cybex evaluation is an objective technique for measuring shoulder disability after neck dissection. Hillel et al[6] reported that after RND the peak torque for the affected side ranged from 0% to 85% of the peak torque for the normal shoulder. In our study, all patients underwent Cybex evaluation for their shoulder muscle strength before operation and 1 month and 6 months afterward. In patients who underwent SND, the peak torques of shoulder flexion-extension and abduction-adduction were significantly lowered 1 month after operation and had returned to the preoperative values 6 months after operation. In patients who underwent MND, the peak torques for the affected shoulder were significantly lower 1 month after operation and gradually improved; the difference was insignificant 6 months later. This finding indicates regeneration of the SAN. In patients who underwent RND, the peak torques remained significantly lower at the 6-month follow-up visit.

In ENoG examination of the SAN, the peak-to-peak values from the right and left shoulders in the same subject had been shown to vary relatively little.[13] Therefore, the unaffected shoulder might be used as a control. In neck dissection, EMG and ENoG examination could be useful for postoperative monitoring of the SAN to predict recovery in patients with postoperative paralysis. Abnormal EMG and ENoG findings might correlate with the shoulder disability and be of clinical value. In this study, the ENoG findings of the SAN were relatively normal in our SND group, whereas in the MND group the amplitude and response area of the evoked potential were significantly lower in the affected side than in the unaffected side. No evoked potential was found in the RND group. As for the EMG findings of the trapezius muscle, King et al[14] reported no voluntary EMG activity after sectioning the SAN. Our results showed normal or only slightly abnormal EMG findings in the SND group and the most abnormal EMG findings in the RND group.

Nahum et al[1] found several abnormal EMG tracings on the trapezius muscle that showed only partial denervation. Other authors[3,15] stated that the severity of shoulder dysfunction did not correlate closely with the degree of denervation of the trapezius muscle. In agreement with their findings, 4 patients in our MND group showed severely abnormal EMG findings in the trapezius muscle, but they did not have as great a degree of shoulder dysfunction as would be expected.

Sobol et al[3] reported that the EMG findings of the MND group were significantly better 16 weeks after operation, indicating a potential for recovery in this group. Three patients in our study underwent a second EMG study 6 months after operation. One was in the RND group, and the result remained severely abnormal. The other 2 were in the MND group; their repeated EMG findings revealed improvement, and the amplitude of the SAN in the ENoG findings became nearly normal.

In conclusion, the SND group was found to have the least damage to the SAN, as demonstrated by postoperative ENoG, EMG, and isokinetic evaluation. Preservation of the SAN, accompanied by rehabilitation, may lessen the development of shoulder disability after neck dissection. Unfortunately, the sample size of this study was too small to give a convincing result. More research in a larger population will be needed.

REFERENCES

1. Nahum AM, Mullally W, Marmor L. A syndrome resulting from radical neck dissection. Arch Otolaryngol 1961;74:82-6.

2. Nanning M, Stell PM. The shoulder after radical neck dissection. Clin Otolaryngol 1989;14:381-4.

3. Sobol S, Jensen C, Sawyer W, Costiloe P, Thong N. Objective comparison of physical dysfunction after neck dissection. Am J Surg 1985;150:503-9.

4. Weisberger EC. The efferent supply of the trapezius muscle: a neuroanatomic basis for the preservation of shoulder function during neck dissection. Laryngoscope 1987;97:435-45.

5. Weisberger EC, Lingeman RE. Cable grafting of the spinal accessory nerve for rehabilitation of shoulder function after radical neck dissection. Laryngoscope 1987;97:915-8.

6. Hillel AD, Kroll H, Dorman J, Medieros J. Radical neck dissection: a subjective and objective evaluation of postoperative disability. J Otolaryngol 1989;18:53-61.

7. Leipzig B, Suen JY, English JL, Barnes J, Hooper H. Functional evaluation of the spinal accessory nerve after neck dissection. Am J Surg 1983;146:526-30.

8. Jones TA, Stell PM. The preservation of shoulder function after radical neck dissection. Clin Otolaryngol 1985;10: 89-92.

9. Krause HR, Bremerich A, Herrmann M. The innervation of the trapezius muscle in connection with radical neck dissection. J Craniomaxillofac Surg 1991;19:87-9.

10. Krause HR. Shoulder-arm syndrome after radical neck dissection: its relation with the innervation of the trapezius muscle. Int J Oral Maxillofac Surg 1992;21:276-9.

11. Stearns MP, Shaheen OH. Preservation of the accessory nerve in block dissection of the neck. J Laryngol Otol 1981;95: 1141-8.

12. Pearlman NW, Myers AD, Sullivan WG. Modified radical neck dissection for squamous cell carcinoma. Surg Gynecol Obstet 1982;154:214-6.

13. Hillel AD, Dobie R, Little J. Evoked electromyography of the eleventh nerve and trapezius muscle. Head Neck Surg 1988;10:387-95.

14. King PS, Lewis FR, Weddle JL, Fowlks EW. Effect of radical neck dissection on total rehabilitation of the laryngectomee. Am J Phys Med Rehabil 1973;52:1-17.

15. Zibordi F, Baiocco F, Bascelli C, Bini A, Canepa A. Spinal accessory nerve function following neck dissection. Ann Otol Rhinol Laryngol 1988;97:83-6.

Ann Otol Rhinol Laryngol 109:2000

TIMING OF SWALLOWING EVENTS AFTER SINGLE-MODALITY TREATMENT OF HEAD AND NECK CARCINOMAS WITH RADIOTHERAPY

KATHERINE A. KENDALL, MD
SUSAN W. MCKENZIE, MS
REBECCA J. LEONARD, PHD
CHRISTOPHER U. JONES, MD
SACRAMENTO, CALIFORNIA

This paper reports the results of a preliminary study designed to evaluate swallowing function in 20 patients 1 year after successful treatment of head and neck carcinomas with radiotherapy. The timing of swallowing events was evaluated by videofluoroscopy. The mean values for each measure were compared to the normative data from 60 control subjects. The radiotherapy patients demonstrated prolonged pharyngeal bolus transit and a delay of laryngeal closure. Hyoid bone elevation began late relative to the onset of bolus movement. A strong trend toward a delay in hyoid elevation relative to bolus movement was demonstrated. The time required for the hyoid bone to reach maximal elevation did not differ from that in normals, but the hyoid was held in an elevated position for a longer period of time. As a result of changes in hyoid movement, the upper esophageal sphincter tended to open early relative to the arrival of the bolus. In conclusion, changes in deglutition occur after radiotherapy, presumably as an adaptation to changes in tissue compliance.

KEY WORDS — deglutition, radiotherapy, swallowing, videofluoroscopy.

INTRODUCTION

The effect of head and neck radiotherapy on swallowing remains poorly understood, despite many reports on the late tissue effects of irradiation for the treatment of cancer.[1-3] Normal deglutition requires the mobility of oral and pharyngeal structures to prepare the bolus, propel the bolus into the pharynx, open the upper esophageal sphincter (UES), and protect the airway. Tissue fibrosis secondary to radiotherapy may decrease the mobility of these vital structures and therefore alter bolus transit. In addition, radiation-induced xerostomia causes decreased bolus lubrication and, therefore, greater resistance to bolus movement. The recent advance of altered-fractionation radiotherapy schedules does not seem to improve the late radiation sequelae in head and neck cancer patients.[4,5] Patients complain of dysphagia after head and neck radiotherapy, but the nature of the dysfunction has never been evaluated prospectively. Previous studies and multiple case reports have shown that the sequelae of radiotherapy include fibrosis of involved structures; however, no objective evaluation of the timing of bolus transit has been done.[1-3] In particular, an evaluation of bolus movement relative to the timing of swallowing gestures reveals information concerning swallow efficiency and the risk of aspiration.[6,7] An understanding of the pathophysiology of dysphagia secondary to radiotherapy and the identification of successful strategies for dealing with altered swallowing function are needed to form a basis for rehabilitation efforts in this patient population.

Reported in this paper are the results of a study in 20 patients of the effects of head and neck radiotherapy on swallowing. The study subjects were limited to patients who underwent only irradiation to the head and neck region without surgical resection. The findings from this study will form the basis for more extensive studies. We plan to evaluate the combined treatment of surgery and radiotherapy to predict the effects of radiation on swallowing function and to separate those aspects of swallowing abnormality caused by the radiation from those caused by the surgical resection of oropharyngeal structures.

RESEARCH DESIGN AND METHODS

Twenty patients at least 1 year after successful external beam radiotherapy to the head and neck region, regardless of symptoms, were approached to enroll in the study. The 1-year delay after therapy took into account the observations that acute radiation effects such as mucositis have resolved by 3 months after therapy and that late sequelae are usually present by 8 months after the completion of the treatment.[4] All subjects were eating orally and maintaining nutritional requirements and pulmonary health at the

---

From the Department of Otolaryngology, University of California, Davis, Sacramento, California (Kendall, McKenzie, Leonard). This work was supported by a grant from the American Cancer Society (#IRG 205, Allocation No. 3-444977-58012-3).

Presented at the Sixth Annual Dysphagia Research Society Meeting, Toronto, Canada, October 16-18, 1997.

CORRESPONDENCE — Katherine A. Kendall, MD, Dept of Otolaryngology, University of California, Davis Medical Center, 2521 Stockton Blvd, Suite 7200, Sacramento, CA 95817.

time of evaluation. None of the subjects had sought treatment for dysphagia. All patients had undergone therapy at an institution different from the study facility, and all but 2 were enrolled by the radiation oncologist at the outside institution. The study protocol was reviewed and approved by the University of California, Davis (UCD), Institutional Review Board. Informed consent was obtained from each study participant. Once enrolled and studied, the patients were categorized on the basis of the location of the primary tumor into the following categories: laryngeal (n = 10), base of tongue (n = 3), and oropharynx (n = 7). The tumor site categories were not defined by the traditional clinical staging methods, which are based on the anatomic location of the tumor, but rather, by how the location of the tumor was expected to impact swallowing function. The base-of-tongue tumor patients were separated from the other oropharyngeal tumor patients, such as tonsillar fossa tumor patients, because the anticipated loss of tongue bulk in these cases was expected to have distinct effects on swallowing. The base-of-tongue tumor patients were analyzed separately from the patients whose tumor was located adjacent to the pharyngeal constrictor muscles. The incidence of these tumors and their treatment by radiotherapy is variable; thus, we anticipated unequal numbers of patients in each category.

Swallow function was assessed by a dynamic videofluoroscopic swallow evaluation. The radiographic studies were conducted in the Radiology Suite at UCD Medical Center in accordance with the routine radiographic protocols used by the UCD Otolaryngology Department and approved by the Institutional Review Board. The equipment used included a properly collimated Phillips fluoroscopic unit that provides a 63-kV, 1.2-mA type output for the full-field-of-view mode (9-inch input phosphor diameter). The fluoroscopy studies were recorded on high-quality videotape for playback and analysis on a Sony model 1380 videocassette VHS recorder-player. A graphic time display provided by an RCA character generator and JVC AC adaptor model C412 was included on the videotape so that timing information at 0.01-second intervals was recorded. The swallow studies were recorded at 30 frames per second.

All radiographic studies were performed under the supervision of a radiologist, with a speech pathologist largely responsible for the order and content of the patient tasks recorded. The measures were made sequentially during the swallowing of thin liquid boluses of 3 sizes (1 mL, 3 mL, and 20 mL) delivered by cup to the subject. A 5-cm^3 paste bolus swallow presented by spoon was also evaluated. The order of the swallow types followed the protocol used at the institution in the evaluation of dysphagic patients, which presents swallowing tasks in an order of increasing volume and, therefore, increasing potential danger in the case of aspiration. The presence or absence of tracheal aspiration and of reflux of bolus material into the nose of the study subjects was noted.

The findings from each patient were analyzed independently by the first author in a blinded fashion without knowledge of patient complaints or the location of the primary tumor. Interobserver measurement reliability was established among 4 judges with a 2-way analysis of variance on swallow studies from 60 normal control subjects without a history of dysphagia. The interobserver reliability was found to be greater than 90% for each measurement parameter.

The timing measures were made to 0.01 second and included pharyngeal transit time, defined as the time between the onset and the completion of bolus pharyngeal transit. The onset of pharyngeal transit was defined as the moment the head of the bolus passed the posterior nasal spine (B1). The completion of pharyngeal transit was defined as the moment the UES had closed and the bolus had fully entered the esophagus (Pcl). Pharyngeal transit time was divided into an oropharyngeal phase and a hypopharyngeal phase by the arrival of the bolus in the vallecula (BV). The duration of soft palate elevation and the time required for aryepiglottic fold elevation and supraglottic closure were measured. The onset of hyoid elevation relative to the onset of pharyngeal transit and the duration of hyoid elevation were also determined. The onset of UES opening relative to the onset of pharyngeal transit and the duration of UES opening were the final parameters measured.

The measured data were averaged across all subjects according to bolus size and consistency. The mean value for each measure was then compared to the mean value for that parameter derived from the evaluation of the 60 normal control subjects. The normative values were collected from studies of 30 female and 30 male volunteers with no history of dysphagia and no condition likely to cause dysphagia. The study patient mean values were compared to the normal control subject means with a 1-way analysis of variance. As 40 different comparisons were made, an alpha correction was applied to the analysis that set the significant p value at .00125. Once the measurements were completed, the patient data were averaged in groups defined by the tumor location, and the means from each group were compared in an attempt to define differences based on the location of the primary tumor.

RESULTS AND DISCUSSION

The findings for each measured parameter and a discussion of the relevance of each are reported together in this section to clarify the findings. The mean value for each parameter is reported along with the standard deviation for that parameter (see Figure). The study subjects demonstrated remarkable variability. An abnormal swallow was defined as one demonstrating a value of greater than 2 standard deviations from the normal mean on at least 1 timing measurement. None of the study patients demonstrated a completely normal swallow.

Two of the radiotherapy subjects aspirated during the dynamic swallowing study (10%). The episodes of aspiration were seen in the 2 patients with tongue base tumors and occurred on the smallest liquid bolus size of 1 mL. Both patients had significant difficulty with pharyngeal contraction, and the small bolus remained in the pharynx as residue and was aspirated at the end of the swallow when the vocal folds reopened. Both patients successfully swallowed larger bolus sizes. Aspiration was not seen in any of the normal control subjects.

Pharyngeal Transit Time. Bolus pharyngeal transit time is considered to reflect the appropriate coordination of complex events leading to a successful swallow. A pharyngeal transit of the bolus prolonged by greater than 2 standard deviations beyond the mean has already been correlated with a significant risk of aspiration pneumonia in stroke victims.[6,7] In the study subjects, the duration of pharyngeal transit was prolonged for all bolus sizes, potentially placing these patients at greater risk for aspiration. A trend toward prolongation of pharyngeal transit was demonstrated during a swallow of a paste bolus (Table 1). Pharyngeal transit time is normally constant across bolus size and consistency changes.[8,9] This was also true for the radiotherapy patients in this study.

Pharyngeal transit time was divided into oropharyngeal and hypopharyngeal transit components to determine whether the delay in overall pharyngeal transit was specific to the oropharynx or the hypopharynx (Table 1). Oropharyngeal transit (defined as the time required for the bolus to travel from the nasal spine to the apex of the vallecula) was prolonged in the study group for the 1-mL liquid and the paste bolus swallows. The 3-mL liquid bolus demonstrated a marked trend toward prolongation. Hypopharyngeal transit (defined as the time required for the bolus to travel from the apex of the vallecula completely past the UES) was also prolonged in the study group for the 3-mL and the 20-mL liquid bolus swallows. The 1-mL liquid bolus swallows tended to be prolonged in the study group. Therefore, a global slowing of pharyngeal transit was observed.

Soft Palate Elevation. Coordinated closure of the soft palate prevents reflux of a bolus into the nasopharynx and prevents loss of bolus driving pressure into the nose. Thus, the timing parameters associated with velopharyngeal competence and palatal elevation were analyzed. The onset of palatal elevation and the time required for the palate to reach its maximum elevation did not differ between the radiotherapy group and the control group. Nasopharyngeal reflux was not identified in any of the study patients or normal control subjects.

Aryepiglottic Fold Closure. As the bolus enters the oropharynx, the aryepiglottic folds begin to rock forward and elevate until they contact the downfolding laryngeal surface of the epiglottis. This action is an important mechanism of airway protection during deglutition. The supraglottic structures must close in a timely fashion so that the bolus cannot penetrate the glottis. In order to evaluate this function in our study patients, we measured the time at which the aryepiglottic folds first began to elevate and the time at which they contacted the epiglottis relative to the start time of the swallow (B1), relative to the arrival of the bolus in the vallecula (BV), relative to the timing of the hyoid's first movement anteriorly (H1), and relative to the hyoid's arrival at a point of maximum excursion (H2).

In the radiotherapy group, the onset of aryepiglottic fold closure relative to the onset of the swallow was found to be delayed except for the 20-mL bolus swallow (Table 2). The fact that aryepiglottic fold closure was also delayed relative to the arrival of the bolus into the vallecula indicates that the delay in aryepiglottic fold closure relative to the onset of the swallow cannot be accounted for by the delay in oropharyngeal bolus transit alone. The timing relationships of aryepiglottic fold and hyoid movement from onset to maximum displacement did not differ between the radiotherapy patients and the normal control group. Similarly, the time needed to complete supraglottic closure did not differ between the groups. In conclusion, the radiotherapy patients allow the bolus to travel closer to the glottis before they start gestures needed to protect the airway.

Timing of Hyoid Displacement. Elevation of the hyoid-larynx complex is a necessary event in decreasing the hypopharyngeal pressure and opening the UES.[10] In the study patients, the onset of hyoid elevation relative to the start of pharyngeal transit was delayed and a strong trend toward a delay in hyoid elevation relative to the arrival of the bolus in the vallecula was demonstrated (Table 3). This finding indicates a change in the coordination of bolus transit with swallow gestures. The interpretation of this finding must also take into account the finding that

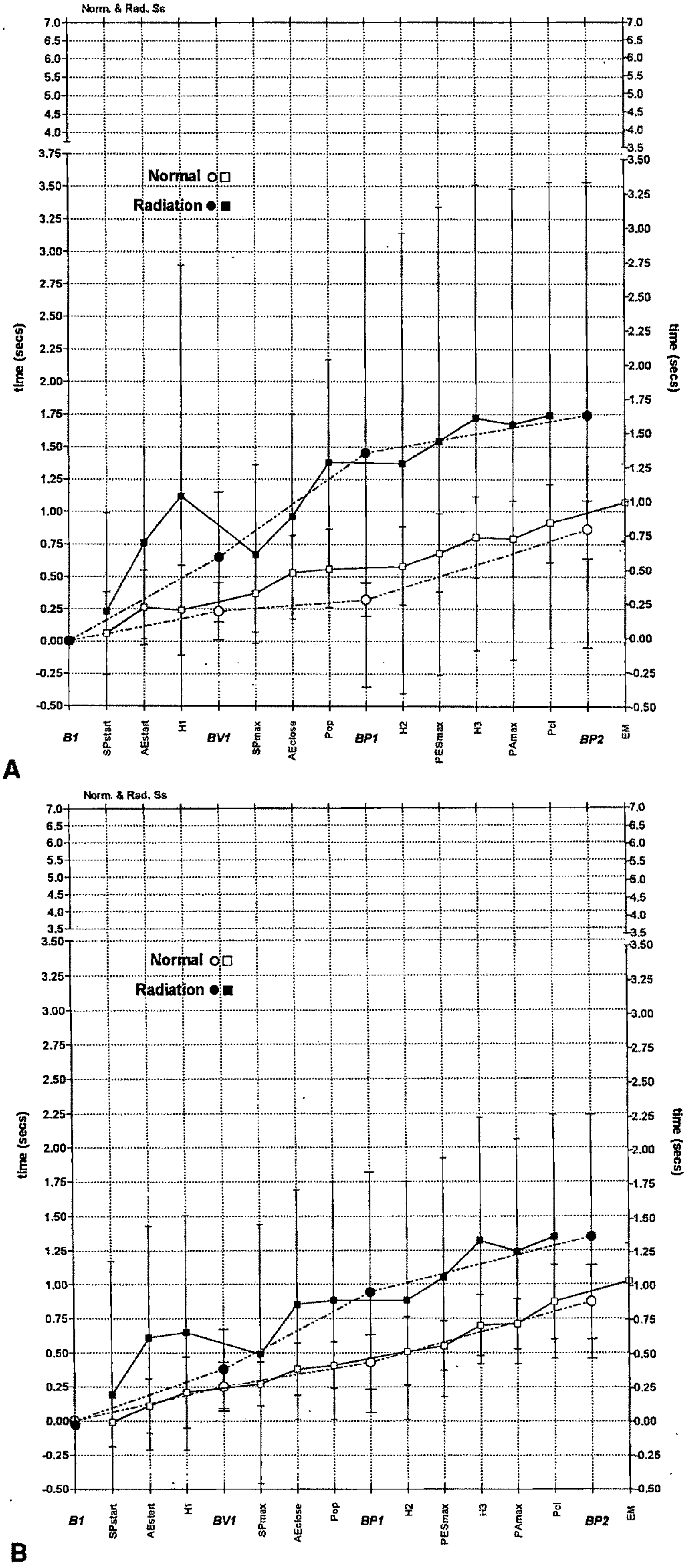

Swallow events by time. A) One-milliliter bolus. B) Three-milliliter bolus. Circles are bolus movements; squares are swallowing gestures. Means are centered on error bars. B1 — bolus head passes posterior nasal spine; BV1 — bolus enters valleculae; BP1 — bolus enters pharyngoesophageal sphincter (PES); BP2 — bolus clears PES; SPstart — soft palate starts elevation; AEstart — aryepiglottic fold elevation (larynx close) start; H1 — first hyoid displacement; SPmax — soft palate reaches maximum elevation; AEclose — maximum aryepiglottic fold closure; Pop — PES opens; H2 — hyoid maximum displacement; PESmax — maximum PES opening; H3 — hyoid begins return; PAmax — pharyngeal maximum constriction; Pcl — PES closes; EM — epiglottis returns to upright position. (Continued on next page.)

(Continued.) Swallow events by time. C) Paste bolus. D) Twenty-milliliter bolus. Circles are bolus movements; squares are swallowing gestures. Means are centered on error bars. Abbreviations as on facing page.

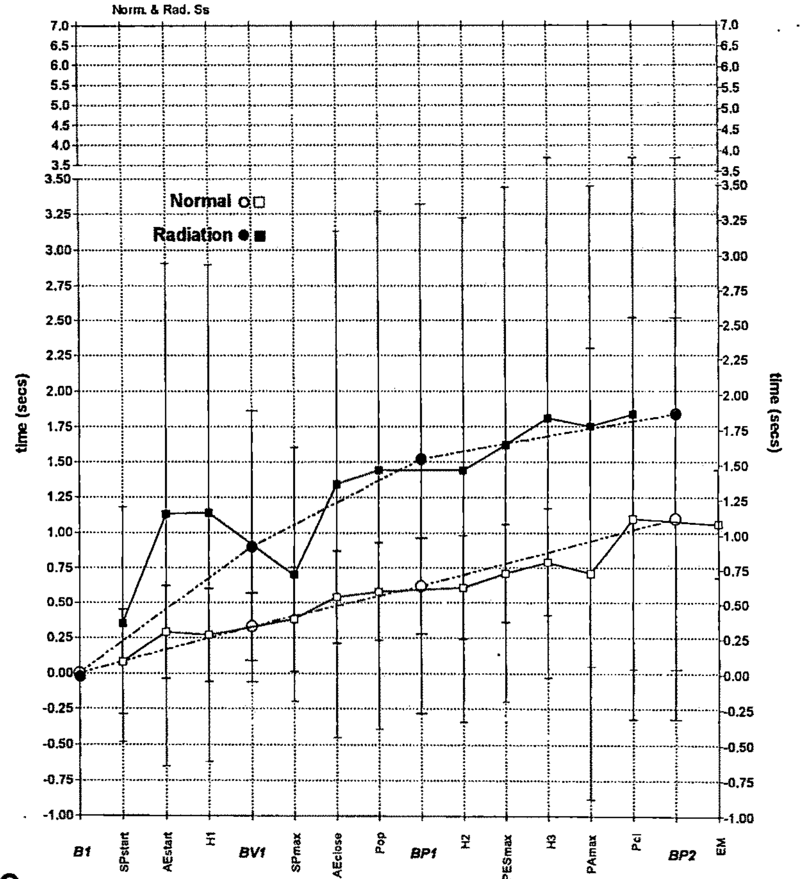

C

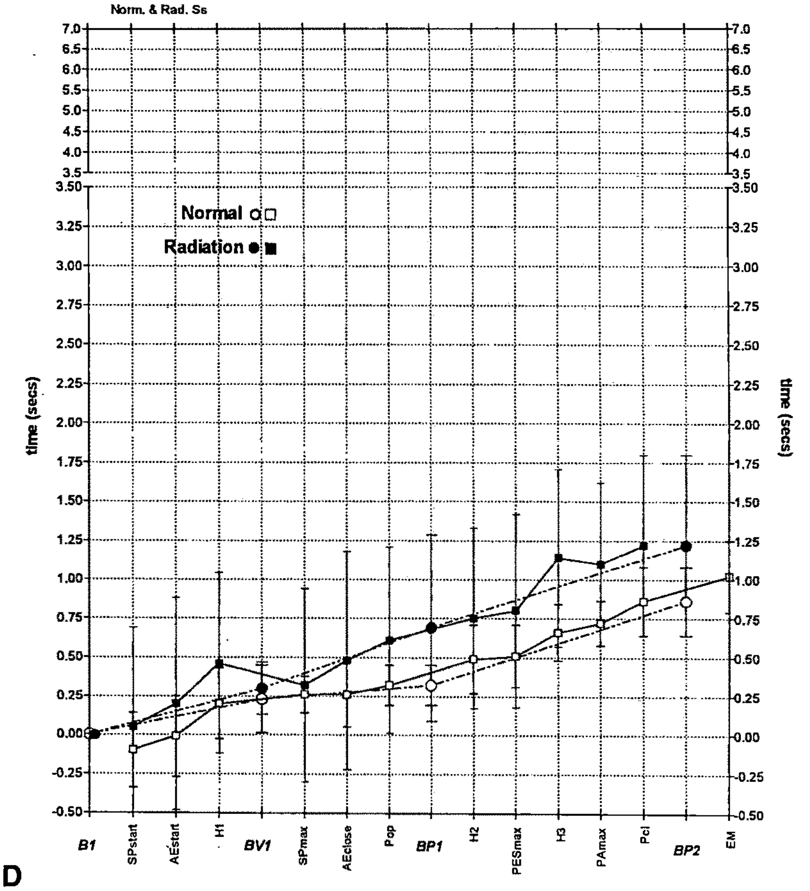

D

TABLE 1. TRANSIT TIME IN SECONDS

	1 mL	*3 mL*	*Paste*	*20 mL*
Pharynx	1.74 ± 1.79	1.35 ± 0.89	1.84 ± 1.81	1.22 ± 0.58
Norms	0.91 ± 0.3	0.87 ± 0.27	1.06 ± 1.29	0.86 ± 0.22
p	.0007*	<.0001*	.04	<.0001*
Oropharynx	0.65 ± 0.50	0.38 ± 0.29	0.90 ± 0.96	0.30 ± 0.17
Norms	0.29 ± 0.19	0.23 ± 0.16	0.33 ± 0.26	0.23 ± 0.15
p	<.0001*	.0047	<.0001*	.09
Hypopharynx	1.12 ± 1.56	0.97 ± 0.72	0.95 ± 1.38	0.92 ± 0.47
Norms	0.61 ± 0.27	0.61 ± 0.19	0.73 ± 1.29	0.68 ± 0.15
p	.01	.0006*	.52	.0008*

Data are mean ± SD.
*Significant.

oropharyngeal bolus transit was slow in the radiotherapy patients and likely influenced the timing of subsequent swallow gestures.

The time required for the hyoid to reach its point of maximum excursion in the study subjects, once started, did not differ from that in normal controls. However, the time the hyoid remained elevated was significantly longer in the radiotherapy patients. We interpret the prolonged elevation of the hyoid bone as a strategy developed by the patients to ensure adequate opening of the UES. Changes in bolus size or consistency did not alter the duration of hyoid elevation in either the radiotherapy group or the normal control group (Table 3).

Upper Esophageal Sphincter Opening. Hyoid and laryngeal elevation, along with cricopharyngeal muscle relaxation, opens the UES, creating a vacuum that aids in propulsion of a bolus into the upper esophagus.[10] The duration of UES opening did not vary between the study group and the normal controls. The duration of UES opening increased in the radiotherapy patients with increasing size of the bolus, as it did in normal subjects (p = .0003).

The UES typically opened just before the arrival of the bolus at the sphincter in the control subjects. The radiotherapy patients, however, demonstrated a trend for the UES to open earlier relative to the arrival of the bolus at the sphincter. The smallest difference in UES opening and arrival of the bolus between the patient group and the normal control subjects was found for the paste bolus swallow. This is likely because the normal control subjects also opened the UES earlier for the paste swallow than for liquid swallows (Table 4).

In the normal subjects, the arrival of the bolus at the UES corresponded closely to the time that the hyoid bone reached maximum elevation. In the study subjects, however, the hyoid bone tended to reach its maximum elevation before the bolus arrived at the sphincter, although statistical significance with a p value of .00125 was only found during the 3-mL liquid bolus swallow. The paste bolus demonstrated a similar trend in the study subjects, but was the least different when compared to the norms. Even in the normal subjects, the movement of the paste bolus tended to be slower and more variable, so that a difference was more difficult to demonstrate (Table 4).

In summary, in the radiotherapy patients, the hyoid bone began to elevate and reached its point of maximal elevation early relative to bolus location in the oropharynx. The time required for the hyoid bone to reach this point did not differ from that in normals, but the hyoid bone was held in an elevated position for a longer period of time. The overall effect was that the UES opened early relative to the arrival of the bolus. The duration of UES opening did not differ between the radiotherapy patients and the normal control subjects. The radiotherapy patients appear to be making adaptations for swallowing a liquid bolus similar to those made in normal controls to aid in the swallowing of paste boluses. This may reflect the effects of xerostomia.

Effect of Tumor Location. As a consequence of the small number of subjects studied and the diffi-

TABLE 2. ONSET OF ARYEPIGLOTTIC FOLD CLOSURE IN SECONDS

	1 mL	*3 mL*	*Paste*	*20 mL*
Subjects	0.76 ± 0.74	0.61 ± 0.82	1.13 ± 1.78	0.20 ± 0.68
Norms	0.25 ± 0.29	0.13 ± 0.24	0.26 ± 0.35	−0.01 ± 0.26
p	<.0001*	.0001*	.0005*	.06

Data are mean ± SD.
*Significant.

TABLE 3. TIMING OF HYOID DISPLACEMENT IN SECONDS

	1 mL	*3 mL*	*Paste*	*20 mL*
OHE vs SPT	1.12 ± 1.78	0.65 ± 0.86	1.14 ± 1.76	0.46 ± 0.58
Norms	0.26 ± 0.29	0.20 ± 0.23	0.26 ± 0.33	0.16 ± 0.15
p	.0005*	.0004*	.0004*	.0012*
OHE vs BAV	–0.50 ± 1.56	–0.27 ± 0.71	–0.24 ± 1.36	–0.17 ± 0.45
Norms	0.03 ± 0.30	0.03 ± 0.18	0.07 ± 0.30	0.06 ± 0.15
p	.015	.003	.09	.0025
HED	0.35 ± 0.11	0.41 ± 0.13	0.36 ± 0.18	0.40 ± 0.22
Norms	0.21 ± 0.10	0.21 ± 0.10	0.18 ± 0.14	0.20 ± 0.13
p	<.0001*	<.0001*	<.0001*	<.0001*

Data are mean ± SD.

OHE — onset of hyoid elevation; SPT — start of pharyngeal transit; BAV — bolus arrival in vallecula; HED — hyoid elevation duration.

*Significant.

culty in delineating the effects of previous tumor bulk from the effects of radiotherapy, the conclusions that can be drawn from the analysis of tumor location are limited. However, specific trends can be identified. The tongue base tumor group was small, and 2 of the 3 subjects aspirated and could not successfully complete a 1-mL bolus swallow. Therefore, statistical analysis was not possible for parameters concerning this patient group or this bolus size. The finding is nonetheless significant, as the tongue base tumor group was severely impaired when attempting to swallow the small bolus. Poor pharyngeal constriction appeared to prevent the tongue base subjects from effectively propelling the bolus into the esophagus. Both patients who aspirated improved with larger bolus sizes, perhaps because the larger size enabled some bolus contact with the enlarged pharynx. None of the other tumor location groups demonstrated aspiration.

The tongue base tumor patients were the most delayed in pharyngeal transit time, onset of aryepiglottic fold movement, onset of hyoid bone elevation, and maximum UES opening timing in swallowing a paste bolus. This may be because a paste bolus swallow may be more affected by xerostomia and may rely more on the action of the tongue base to move it into the esophagus. A liquid bolus swallow can substitute gravity in the absence of tongue base movement. The pharyngeal tumor patients were the most delayed for the same parameters during a 20-mL liquid bolus swallow (Table 5). There was no difference identified among the tumor location groups for hypopharyngeal transit duration. The bolus transit delays occurred primarily during oropharyngeal transit, so that events occurring later in the course of a swallow revealed the same pattern of differences among the tumor location groups relative to the onset of the pharyngeal transit time.

The laryngeal tumor patients demonstrated normal timing of aryepiglottic fold movement and hyoid bone elevation. A delay, however, was seen in the oropharyngeal transit times of laryngeal tumor patients for the 1-mL liquid bolus (p = .02). Also, the onset of hyoid bone elevation was early relative to bolus arrival in the vallecula for the 1-mL liquid bolus (p = .02). This early hyoid elevation may have been a strategy developed by these patients to compensate for the delay in oropharyngeal transit with this bolus size. Despite the normal transit times for most of the bolus categories, the laryngeal tumor group demonstrated a prolonged duration of hyoid bone elevation compared to that of normal controls. In addition, the UES opened early relative to the arrival of the bolus, although, unlike in the other tumor location categories, the hyoid bone did not reach

TABLE 4. RELATIONSHIPS BETWEEN SPHINCTER OPENING, BOLUS ARRIVAL, AND MAXIMUM HYOID ELEVATION

	1 mL	*3 mL*	*Paste*	*20 mL*
UES opening vs BA	0.07 ± 0.09	0.06 ± 0.09	0.08 ± 0.10	0.07 ± 0.20
Norms	0.02 ± 0.05	0.02 ± 0.03	0.05 ± 0.05	0 ± 0.01
p	.04	.04	.08	.01
BA vs MHE	0.07 ± 0.11	0.06 ± 0.13	0.08 ± 0.11	–0.06 ± 0.13
Norms	0.01 ± 0.07	–0.04 ± 0.07	0.02 ± 0.15	–0.13 ± 0.08
p	.008	<.0001*	.1	.008

Data are mean ± SD in seconds.

UES — upper esophageal sphincter; BA — bolus arrival; MHE — maximum hyoid elevation.

*Significant.

TABLE 5. PHARYNGEAL TRANSIT RELATIVE TO TUMOR LOCATION

Tumor Location	*Paste*	*20 mL*
Pharynx	2.33 ± 1.37	1.68 ± 0.78*
Tongue base	3.97 ± 3.52*	1.15 ± 0.14
Larynx	0.86 ± 0.38	0.92 ± 0.17
p	.013	.006

Data are mean ± SD in seconds.
*Significantly different from other tumor locations.

its point of maximal elevation early relative to the arrival of the bolus at the UES.

No differences among the groups were found in the time required for aryepiglottic fold closure or the time required for the hyoid bone to reach its point of maximal elevation. No differences in aryepiglottic fold closure relative to hyoid elevation or in the duration of hyoid elevation were found among the tumor location groups.

SUMMARY AND CONCLUSIONS

This study evaluated the effects of radiotherapy on deglutition with quantitative measures from videofluoroscopic x-ray studies. Even with a relatively small number of patients, statistically significant differences in a number of swallowing parameters were demonstrated in radiotherapy patients as compared to normal controls (see Figure). The radiotherapy patients were, in addition, extremely variable in terms of bolus transit timing, the onset of various swallowing gestures, and gesture timing relative to the movement of the bolus early in the course of the swallow. However, strategies used late in the swallow, such as the prolongation of hyoid elevation and the early opening of the UES relative to bolus arrival, were not variable across the patient population.

First, the pharyngeal transit time was prolonged in the radiotherapy patients. The slowing seen in the oropharyngeal phase of the swallow may be secondary to poor bolus lubrication brought on by postirradiation xerostomia. The slowing in the hypopharyngeal phase is probably due to tissue fibrosis and poor pharyngeal contraction.[11] A smaller bolus size was associated with increasing delays in pharyngeal transit. The patients with laryngeal tumors were found to demonstrate normal pharyngeal transit times, in both the oropharyngeal and hypopharyngeal phases of transport, except for the smallest liquid bolus size, which was delayed in the oropharynx. The patients with tongue base tumors also had significant trouble with the smallest bolus size. In patients with a risk of aspiration as defined by the prolongation of pharyngeal transit, it is often assumed that a smaller bolus volume is safer and minimizes the amount of bolus aspirated. The radiotherapy patients, however, demonstrated more difficulty with the smaller bolus size.

Second, the timing of hyoid bone elevation relative to the onset of the pharyngeal phase of the swallow and relative to the arrival of the bolus in the vallecula was delayed in the radiotherapy patients. It is possible that poor pharyngeal sensation contributes to a delay in the onset of swallow gestures relative to the position of the bolus in the pharynx. The late onset of hyoid bone elevation was offset by early maximal hyoid elevation resulting in opening of the UES before the arrival of the bolus at the sphincter. Previous studies have demonstrated a negative pressure created by the opening of the sphincter that draws the bolus into the upper esophagus.[10] It appears that the radiotherapy patients in this study may have used this strategy to aid in bolus transfer and, further, used it early in the course of the swallow. Alternatively, these patients may have been unable to completely adjust to the slow bolus movement or adequately coordinate sphincter opening to correspond to the delayed time of the bolus arrival. In addition to the early maximal hyoid elevation relative to bolus movement, the hyoid bone remained maximally elevated for a longer time in the radiotherapy patients than in the normal subjects.

This study defines clear abnormalities in patients who have adequate function in terms of nutritional requirements and pulmonary hygiene. The patients who had undergone radiotherapy for laryngeal cancers did not experience changes relative to the speed of pharyngeal bolus transit, but they did demonstrate abnormal hyoid movement timing. Both base-of-tongue and pharyngeal tumor patients demonstrated more severe effects, resulting in slowed pharyngeal transit of the bolus. Future study of patients with complaints of dysphagia after radiotherapy will evaluate qualitative and quantitative differences in swallow timing with respect to the nonsymptomatic patients in this study.

REFERENCES

1. Lazarus CL, Logemann JA, Kahrilas PJ, Mittal BB. Swallow recovery in an oral cancer patient following surgery, radiotherapy, and hyperthermia. Head Neck 1994;16:259-65.

2. Dejaeger E, Goethals P. Deglutition disorder as a late sequel of radiotherapy for a pharyngeal tumor. Am J Gastroenterol 1994;90:493-5.

3. Eisele DW, Koch DG, Tarazi AE, Jones B. Aspiration from delayed radiation fibrosis of the neck. Dysphagia 1990;6: 120-2.

4. Olmi P, Celai E, Chiavacci A, Fallai C. Accelerated fractionation in advanced head and neck cancer: results and analysis of late sequelae. Radiother Oncol 1990;17:199-207.

5. Fallai C, Olmi P. Altered fractionation schedules in radiotherapy of head and neck cancer. A review. Tumori 1992;78:311-25.

6. Johnson ER, McKenzie SW, Sievers A. Aspiration in stroke. Arch Phys Med Rehabil 1993;74:1-4.

7. Johnson ER, McKenzie SW, Rosenquist CJ, Lieberman JS, Sievers A. Dysphagia following stroke: quantitative evaluation of pharyngeal transit times. Arch Phys Med Rehabil 1992; 73:419-23.

8. Kendall KA, McKenzie S, Leonard RS, Gonçalves MI, Walker A. Timing of events in normal swallowing: a videofluoroscopic study. Dysphagia 2000;15:74-83.

9. Kendall KA, McKenzie SW, Leonard RJ, Gonçalves MI, Walker A. Timing of events in normal swallowing: a videofluoroscopic study. Dysphagia 2000;15:74-84.

10. McConnel FMS. Analysis of pressure generation and bolus transit during pharyngeal swallowing. Laryngoscope 1988; 96:71-8.

11. Kendall KA, McKenzie SW, Leonard RJ, Jones C. Structural mobility in deglutition after single modality treatment of head and neck carcinomas with radiation therapy. Head Neck 1998;20:720-5.

≈

INTERNATIONAL CONFERENCE ON NEWBORN HEARING SCREENING DIAGNOSIS AND INTERVENTION

The International Conference on Newborn Hearing Screening Diagnosis and Intervention will be held in Milan, Italy, October 12-14, 2000. In Europe, contact Dr Ferdinando Grandori, Center of Biomedical Engineering, Polytechnic of Milan, piazza Leonardo da Vinci 32, I-20133 Milan, Italy; fax +39.02.2399.3360; e-mail NHS2000@biomed.polimi.it. In the United States, contact Dr Deborah Hayes, The Children's Hospital, 1056 E 19th Ave, B030, Denver, CO 80218; telephone (303) 861-6424; fax (303) 764-8220; e-mail: Hayes.deborah@tchden.org.

Ann Otol Rhinol Laryngol 109:2000

CLINICAL NOTE

MASSIVE EPISTAXIS AFTER RUPTURE OF INTRACAVERNOUS CAROTID ARTERY ANEURYSM

CASE REPORT

HOLGER SUDHOFF, MD
THOMAS STARK, MD
HORST LUCKHAUPT, MD
SIEGFRIED KNORZ, MD
GERD BORKOWSKI, MD
BOCHUM, GERMANY

We present a case of massive epistaxis caused by an internal carotid artery aneurysm. The initial treatment with endovascular balloon embolization failed as a result of balloon displacement. After rebleeding, the intracavernous aneurysm was treated with an endovascular detachable balloon embolization technique, which resulted in cessation of epistaxis. The different treatment options for interventional radiology and management of ruptured carotid artery aneurysms are discussed.

KEY WORDS — carotid artery aneurysm, embolization, epistaxis.

INTRODUCTION

Epistaxis is a common symptom that is easy to control in 90% of cases. However, in certain circumstances and in the presence of various conditions, life itself may be at risk.[1] Aneurysms of the internal carotid artery are rarely mentioned as a cause of epistaxis. This condition is quite rare, but it is important to consider aneurysms in determining the cause of epistaxis because of their high rate of mortality. In addition, they require quite different management from that of epistaxis due to other causes.[2] We present a nontraumatic case of an internal carotid artery aneurysm causing massive epistaxis that was finally managed with coil embolization.

CASE REPORT

A 52-year-old woman presented having had several periods of mild anterior epistaxis for 2 weeks before admission. There was no recent or remote history of head or facial trauma. A complete otolaryngological examination did not reveal any local abnormality. The results of a motor and sensory examination were normal. There was no hypertension or abnormality of blood clotting, and no medication that would affect blood clotting. On the first day after hospitalization, the patient had another interval of epistaxis that was managed by nasal packing. Two days later, the packing was removed, and 5 days later, the patient was discharged from the hospital. Five days after discharge, the patient was admitted again with massive pulsatile epistaxis on the right side and cardiovascular shock. After anterior and posterior nasal

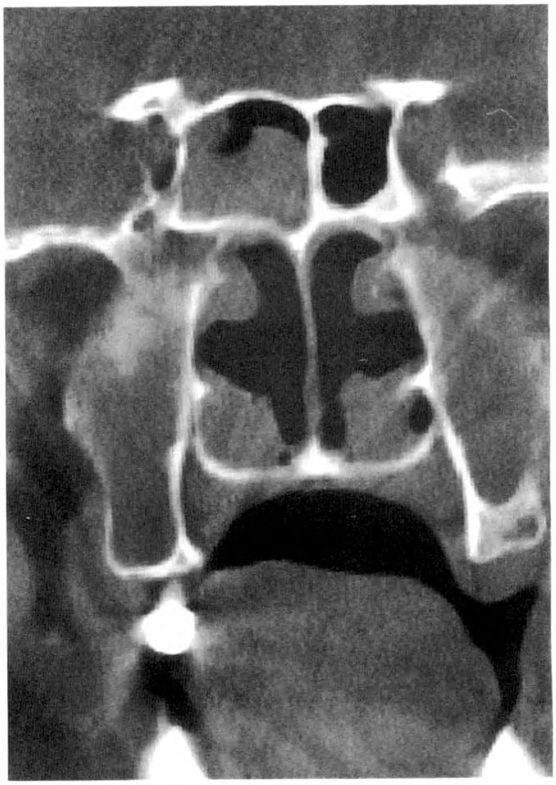

Fig 1. Initial coronal computed tomographic scan of paranasal sinuses reveals blood within right sphenoid sinus.

From the Departments of Otorhinolaryngology–Head and Neck Surgery (Sudhoff, Stark, Luckhaupt, Borkowski) and Radiology and Nuclear Medicine (Knorz), St Elisabeth Hospital, University of Bochum, Bochum, Germany.

CORRESPONDENCE — Holger Sudhoff, MD, Dept of Otorhinolaryngology–Head and Neck Surgery, St Elisabeth Hospital, Bleichstr 15, 44787 Bochum, Germany.

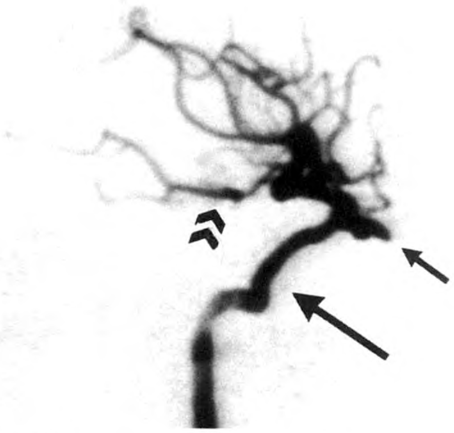

Fig 2. Right anterior oblique view of right carotid artery angiogram demonstrates intracavernous carotid artery aneurysm. Small arrow — aneurysm; double arrowhead — anterior choroid artery; large arrow — internal carotid artery.

packing, she was transferred to the intensive care unit. Because of a hemoglobin level of 6.0 mg/dL and continuous intervals of epistaxis, the patient required transfusion of 14 units of blood and 5 units of fresh frozen plasma. A computed tomographic scan of the brain revealed no abnormalities, but a scan of the paranasal sinuses after removal of the packing showed blood within the right sphenoid sinus without any bony defect (Fig 1). Endonasal coagulation of the anterior ethmoid artery and exploration of the ethmoid sinus was performed the next day with the patient under general anesthesia. However, another episode of severe epistaxis occurred, and a cerebral angiogram obtained after transfemoral catheterization demonstrated bilateral intracavernous carotid artery aneurysms, ruptured on the right side and intact on the left side (Fig 2). The ruptured intracavernous aneurysm was treated with an endovascular detachable balloon embolization technique, but 2 weeks later, another interval of severe epistaxis occurred in a rehabilitation clinic. An angiogram confirmed a reentry of blood into the ruptured intracavernous aneurysm of the right carotid artery, which was treated with electrolytically detachable platinum coils after nasal packing (Fig 3). After this episode, the patient remained free from further epistaxis.

DISCUSSION

Arteriosclerosis is known to be the most frequent cause of internal carotid artery aneurysm, followed by closed or penetrating craniofacial traumatic injury.[3] The cavernous portion of the carotid artery is the most frequent site of localization.[2] There, the aneurysm has a close anatomic relationship with the wall of the sphenoid sinus, as well as the nasal fossae. In our patient, an intracranial carotid artery disorder was suspected because of the recurrent massive epistaxis. It is an unusual feature in these patients, and when present, it is nearly always associated with a traumatic aneurysm.[3-6] There are only a few reported cases of nontraumatic intracavernous carotid aneurysms presenting with epistaxis and diagnosed during the lifetime of the patient.[7] We present such a case with bilateral aneurysms. Emergency control of massive epistaxis is critical because of the high mortality rate associated with this entity.[4] This may be achieved by nasal packing or an epistaxis balloon catheter, which provides time for invasive neuroradiological intervention with detachable balloons or electrolytically detachable coils. In our opinion, emergency carotid artery ligation is not an adequate treatment option.[8] In our case, endovascular balloon embolization of the aneurysm was unsuccessful be-

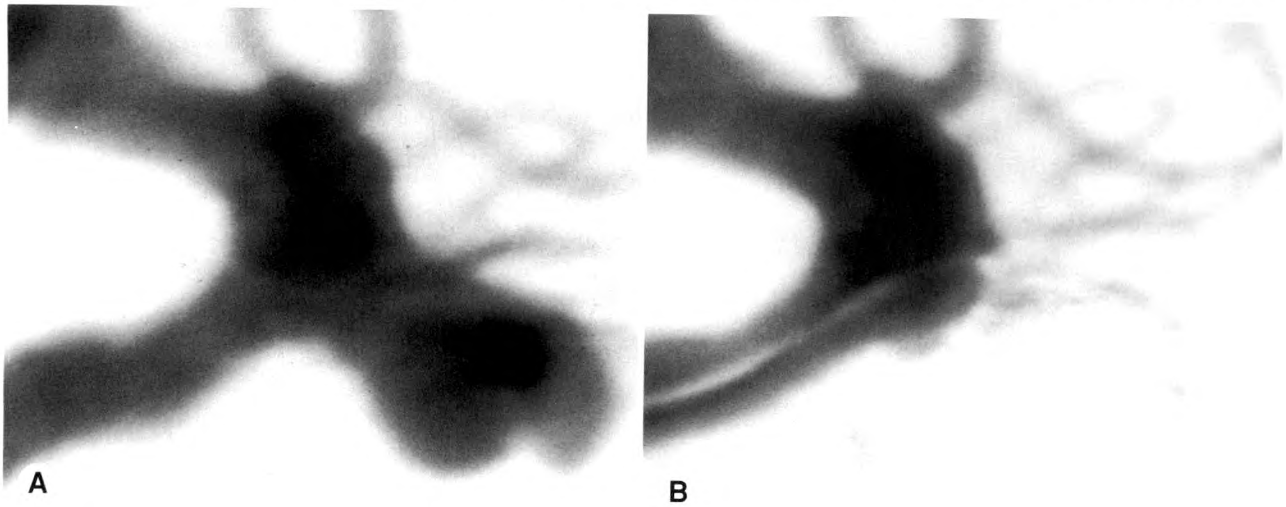

Fig 3. Higher magnification of intracavernous carotid artery aneurysm A) before embolization and B) after embolization of aneurysm cavity with platinum coils. Aneurysm appears occluded, and internal carotid artery remains patent.

cause of dislocation of the balloon into the right sphenoid sinus.[9] However, electrolytically detachable coils offered an excellent treatment method that permitted aneurysm closure with the preservation of flow in the carotid artery.[10] Our case emphasizes the importance of considering aneurysm in the differential diagnosis of massive epistaxis. It must be kept in mind even if there is no history of severe head injury, transsphenoidal surgery for pituitary adenoma, or infection.[5,11,12]

REFERENCES

1. Schreiner L. Complications and errors in the management of nose bleeding. Laryngol Rhinol Otol (Stuttg) 1976;4: 257-63.

2. Mahmoud NA. Traumatic aneurysm of the internal artery and epistaxis: review of the literature and report of a case. J Laryngol Otol 1979;93:629-56.

3. Bhatoe HS, Suryanarayana KV, Gill HS. Recurrent massive epistaxis due to traumatic intracavernous internal carotid artery aneurysm. J Laryngol Otol 1995;109:650-2.

4. Ildan F, Uzuneyupoglu Z, Boyar B, Bagdatoglu H, Cetinalp E, Karadayi AI. Traumatic giant aneurysm of the intracavernous internal carotid artery causing fatal epistaxis: case report. J Trauma 1994;36:565-7.

5. Mauerer MY, Mills M, German WJ. Triad of unilateral blindness, orbital fracture and massive epistaxis in head injury. J Neurosurg 1961;18:837-46.

6. Liu MY, Shih CJ, Wang YC, Tsai SH. Traumatic intracavernous carotid aneurysm with massive epistaxis. Neurosurgery 1985;17:569-73.

7. Chandy MJ, Rajshekhar V. Nontraumatic intracavernous carotid artery aneurysm presenting with epistaxis. J Laryngol Otol 1989;103:425-6.

8. Shallat RF, Tackamm MS, Nagle RC. Delayed complications of craniocerebral trauma: a case report. Neurosurgery 1981;8:569-73.

9. Higashida RT, Halbach VV, Dowd C, et al. Endovascular detachable balloon embolization therapy of cavernous carotid artery aneurysms: results in 87 cases. J Neurosurg 1990;72:857-63.

10. Teitelbaum GP, Halbach VV, Larsen DW, et al. Treatment of massive posterior epistaxis by detachable coil embolization of a cavernous internal carotid artery aneurysm. Neuroradiology 1995;37:334-6.

11. Raymond J, Hardy J, Czepko R, Roy D. Arterial injuries in transsphenoidal surgery for pituitary adenoma: the role of angiography and endovascular treatment. AJNR Am J Neuroradiol 1997;18:655-65.

12. Takahashi Y, Sugita Y, Maruiwa H, Hirohata M, Tokutomi T, Shigemori M. Fatal hemorrhage from rupture of the intracranial internal carotid artery caused by aspergillus arteritis. Neurosurg Rev 1998;21:198-201.

Ann Otol Rhinol Laryngol 109:2000

CLINICAL NOTE

EPIGLOTTIC HYPOPLASIA ASSOCIATED WITH LACRIMO-AURICULO-DENTAL-DIGITAL SYNDROME

TARANEH AZAR, MD
JAMES E. ARNOLD, MD
JENNIFER A. SCOTT, MS
NATHANIEL H. ROBIN, MD
CLEVELAND, OHIO

We present a case of a young boy with clinical manifestations of lacrimo-auriculo-dental-digital syndrome (LADD) with the additional finding of a hypoplastic epiglottis that caused airway obstruction at birth. We also reviewed the 30 cases of LADD that have been reported since 1967. It is a rare syndrome that includes lacrimal system, aural, digital, and dental anomalies. Our patient has lacrimal duct obstruction, deficient tissue in the inferior portion of the ear pinnae, and a hypoplastic epiglottis with collapse of the supraglottic tissue. Many findings of LADD are recognizable at birth. The clinical spectrum has widened with more case reports. Our patient adds a life-threatening airway abnormality, a hypoplastic epiglottis, to the clinical spectrum of LADD.

KEY WORDS — hypoplastic epiglottis, lacrimo-auriculo-dental-digital syndrome, LADD, Levy-Hollister syndrome.

INTRODUCTION

In 1967, Levy[1] first reported a case of bilateral absence of the lacrimal system, cup-shaped ears, dry mouth, and dental, arm, and digit abnormalities. Hollister et al[2] reported on a family with similar anomalies and used the term lacrimo-auriculo-dental-digital syndrome (LADD). The syndrome is also referred to as Levy-Hollister syndrome.[3] Thirty cases of LADD have been reported to date, showing an autosomal dominant inheritance with variable expression. Renal anomalies, absent salivary glands, congenital hip dislocation, congenital hiatal hernia, and diaphragmatic hernia[4] have been also reported with this syndrome. Here we present a case of a young boy with clinical manifestations of LADD and with the additional finding of a hypoplastic epiglottis that caused life-threatening airway obstruction at birth.

CASE REPORT

Our patient was born at term by spontaneous vaginal delivery. Immediately after birth, he had respiratory distress and required intubation, which was successful after multiple attempts with difficult visualization because of an anterior and deviated larynx. Physical examination findings at that time were significant for micrognathia with a normal palate, deficient tissue in the inferior portion of the ear pinnae, eye drainage, and a right undescended testicle. On day of life 6, he underwent direct laryngoscopy that showed a remnant of an epiglottis (Fig 1) with no true vallecula and with collapse of the supraglottic tissue on inspiration. A tracheotomy was performed. He also required a gastrostomy tube, as his glottic abnormalities caused aspiration.

Otologic examination revealed a shortened angled handle of the malleus with a blunted anterior sulcus bilaterally. A temporal bone computed tomography scan showed bilateral semicircular canal dysplasia. He has an associated bilateral mild conductive hearing loss. An ophthalmologic evaluation revealed right epiblepharon and left entropion. He had been treated

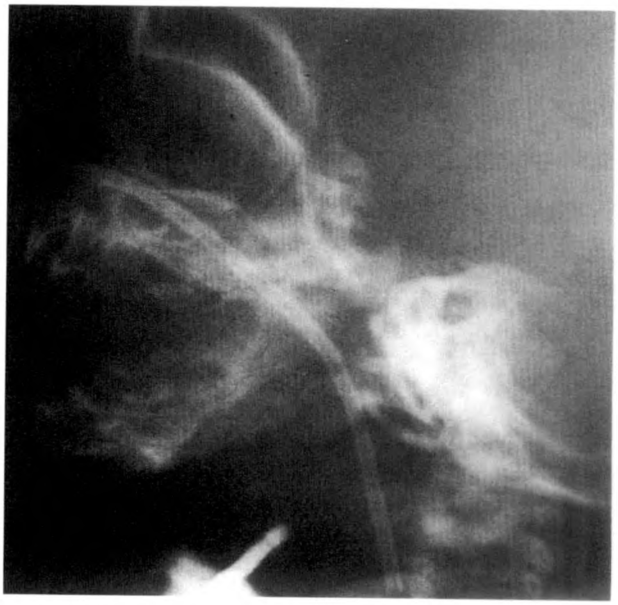

Fig 1. Epiglottic remnant as seen on direct laryngoscopy.

From the Departments of Otolaryngology–Head and Neck Surgery (Azar, Arnold), Genetics (Scott, Robin), and Pediatrics (Arnold, Robin), Case Western Reserve University School of Medicine, University Hospitals of Cleveland, Cleveland, Ohio.

CORRESPONDENCE — Nathaniel H. Robin, MD, University Hospitals of Cleveland, Center for Human Genetics, 11100 Euclid Ave, Cleveland, OH 44106.

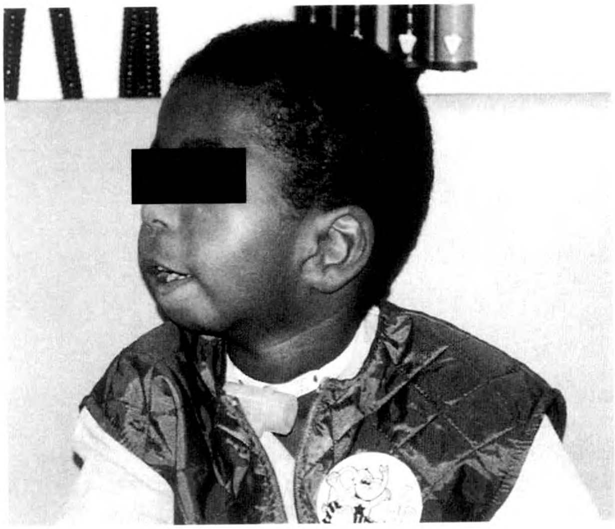

Fig 2. Patient at 5 years of age.

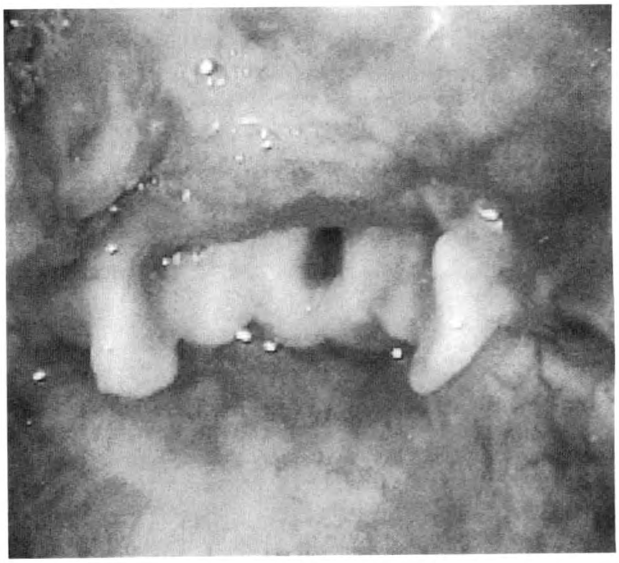

Fig 3. Peg-shaped teeth seen on radiograph.

for pseudomonas conjunctivitis before he underwent surgical repair of his nasolacrimal duct system. Orthopedic examination revealed an abnormally shaped talus bone bilaterally, which has been of no consequence. Urologic examination included a renal ultrasound scan that showed bilateral hydronephrosis with normal renal vasculature. His voiding cystourethrogram was normal. Serial ultrasound showed slow resolution of his hydronephrosis by 4 years of age. At 2½ years of age, he had an orchiopexy.

At 5 years old, the patient remains dependent on a gastrostomy tube and a tracheostomy tube because of upper airway obstruction (Fig 2). He is being evaluated for mandibular advancement and is receiving occupational therapy to learn how to eat. He has normal muscle tone and range of motion. His speech, fine and gross motor skills, and social skills are delayed.

DISCUSSION

We report on a male child with many classic manifestations of LADD who has the previously unreported associated finding of a hypoplastic epiglottis. A rare disorder, LADD includes lacrimal system, aural, dental, digital, and radial anomalies. Most cases are sporadic, although parent-to-child transmission has been observed, suggesting that LADD is an autosomal dominant disorder with variable expression.[2,5,6] Also reported are associated renal, salivary gland, and lower extremity abnormalities. Here we present the first case that has an associated congenital airway anomaly, a hypoplastic epiglottis that caused life-threatening respiratory distress and aspiration in the neonatal period. The only previously described airway abnormality is a bifid uvula[6] without any associated cleft palate or lip. Isolated epiglottic abnormalities have included a hypoplastic, absent, or bifid epiglottis. Bifid epiglottis has been associated with several skeletal anomalies in the autosomal recessive short rib polydactyly syndrome type II (Majewski syndrome).[7-9]

The purpose of the epiglottis has been debated since Aristotle proposed that is served to protect the glottis when eating.[9] Absence of the epiglottis, whether congenital or from surgical excision for supraglottic airway obstruction from neoplasm or an inflammatory process, has been reported to cause problems with speech, breathing, and swallowing and even death.[9-11] Other studies have shown that people[11] and dogs[9] breathe and eat well after having the epiglottis surgically removed. Our patient has a hypoplastic epiglottis with an otherwise normal glottis, compounded by micrognathia that may have contributed to his neonatal respiratory distress and persistent aspiration.

The lacrimal system abnormalities can be either unilateral or bilateral and include hypoplasia or aplasia of the nasolacrimal duct and absent superior and/or inferior puncta. These anomalies cause the patients to have chronic conjunctivitis, chronic epiphora, dacryocystitis, keratoconjunctivitis, tear deficiency, photophobia, and corneal ulcerations.[6] Associated deep-set eyes, telecanthus,[5] and nasal lacrimal duct fistulae have also been reported.[3]

The most common auricular finding is a small ear with an absent or underdeveloped antihelix, referred to as a "cup-shaped ear" as first described by Potter.[12] The ears in LADD have also been described as hypoplastic or dysplastic and low-set. Our patient has deficient lobules. Fifty percent of the patients with this syndrome have an associated hearing loss that can be unilateral or bilateral, sensorineural, conductive, or mixed.[13] Most have a mild to severe sensorineural hearing loss.[13] Our patient had a mild bilateral conductive hearing loss. Most syndromes with cup-shaped ears and associated middle ear anomalies causing hearing loss have autosomal recessive inheritance patterns.[13]

Most patients with LADD have enamel dysplasia that causes the teeth to show early excessive wear and darkening.[14] Often, the patients lose their teeth to decay as adolescents or young adults.[3,14] Although the absence of salivary glands and/or Stensen's ducts is not considered a primary manifestation of the syndrome, it has been reported, and the absence of saliva contributes to the rapid decay of teeth. Other associated dental findings are hypodontia and peg-shaped incisors (Fig 3).

A variety of limb defects have been reported in LADD, the most common being bilateral clinodactyly of the fifth digit.[14] Other abnormalities include digitalization of the thumb, duplication of a distal phalanx, syndactyly, and an absent digit or radius. Our patient has bilateral talus abnormalities. There has been no consistent dermatoglyphic pattern described with LADD; however, "abnormal" dermal ridge patterns have been reported.[3]

Hypospadias, nephrosclerosis, and renal agenesis have been seen in patients with LADD.[15] Our patient had an undescended testicle, which has not previously been reported. Although urogenital and renal anomalies are not commonly seen with LADD, they are commonly seen in patients who have otologic abnormalities (eg, branchio-oto-renal syndrome). Therefore, all patients in whom LADD is suspected should undergo renal ultrasound as part of the evaluation.

Although many of the findings of LADD are evident at birth, the clinical variability can make the diagnosis difficult. Further, each of the major anomalies of LADD can be seen as an isolated finding in otherwise normal persons, and each is independently autosomal dominant in transmission. However, if more than 2 of them appear together, LADD should be considered in the differential diagnosis. The evaluation should include an audiogram, a renal ultrasound scan, and otolaryngological and ophthalmologic examinations. If there is hearing loss, a computed tomography scan of the temporal bones should be performed. It is important to begin the workup early in the hope that the hearing loss and lacrimal abnormalities can be surgically corrected.[3] If the hearing loss is permanent, the patient can be fitted with a hearing aid to allow normal speech and language development.

REFERENCES

1. Levy WJ. Mesoectodermal dysplasia. Am J Ophthalmol 1967;63:978-82.
2. Hollister DW, Klein SH, De Jager HJ, Lachman RS, Rimoin DL. The lacrimo-auriculo-dento-digital syndrome. J Pediatr 1973;83:438-44.
3. Kreutz JM, Hoyme HE. Levy-Hollister syndrome. Pediatrics 1988;82:96-9.
4. Francannet C, Vanlieferinghen P, Dechelotte P, Urbain MF, Campagne D, Malpuech G. LADD syndrome in five members of a three-generation family and prenatal diagnosis. Genet Couns 1994;5:85-91.
5. Ostuni PÁ, Modolo M, Revelli P, et al. Lacrimo-auriculo-dento-digital syndrome mimicking primary juvenile Sjogren's syndrome. Scand J Rheumatol 1995;24:55-7.
6. Wiedemann HR, Drescher J. LADD syndrome: report of new cases and review of clinical spectrum. Eur J Pediatr 1986; 144:579-82.
7. McClay JE, Wiatrak B, Proud VK. Bifid epiglottis and polydactyly: a new genetic syndrome. Otolaryngol Head Neck Surg 1997;11:129-33.
8. Sturgis EM, Howell LL. Bifid epiglottic syndrome. Int J Pediatr Otorhinolaryngol 1995;33:149-57.
9. Reyes BG, Arnold JE, Brooks LJ. Congenital absence of the epiglottis and its potential role in obstructive sleep apnea. Int J Pediatr Otorhinolaryngol 1994;30:223-6.
10. Benjamin B, Dalton C. Hypoplasia of the epiglottis: case report and review. Int J Pediatr Otorhinolaryngol 1996;38:65-9.
11. Klein AD, Wasserstrom JP, Sessions DG, Mreson R, Ogura JH. Rehabilitation of partial laryngectomy patients. Trans Am Acad Ophthalmol Otolaryngol 1977;84:324-34.
12. Potter EL. A hereditary ear malformation transmitted through five generations. J Hered 1937;28:255-8.
13. Ensink RJH, Cremers CWRJ, Brunner HG. Congenital conductive hearing loss in the lacrimoauriculodentodigital syndrome. Arch Otolaryngol Head Neck Surg 1997;123:97-9.
14. Hollister DW, Klein SH, De Jager HJ, Lachman RS, Rimoin DL. Lacrimo-auriculo-dento-digital syndrome. In: Bergsma D, ed. Limb malformations. Miami, Fla: Symposia Specialists, 1974:153-66. (Birth defects: original article series on malformation syndromes; vol 10.)
15. Shiang EL, Holmes LB. The lacrimo-auriculo-dento-digital syndrome. Pediatrics 1977;59:927-30.

Ann Otol Rhinol Laryngol 109:2000

IMAGING CASE STUDY OF THE MONTH

PARACLINOID INTERNAL CAROTID ARTERY ANEURYSM PRESENTING AS MASSIVE EPISTAXIS

JU Y. KIM, MD
BOSTON, MASSACHUSETTS

JEFFREY FARKAS, MD
NEWARK, NEW JERSEY

CHRISTOPHER M. PUTMAN, MD
BOSTON, MASSACHUSETTS

MARK VARVARES, MD
BOSTON, MASSACHUSETTS

INTRODUCTION

Epistaxis is a common occurrence that afflicts 60% of the general population during some point in their lives.[1] The majority of these individuals will be able to control their bleeding easily. Therefore, only 6% of those affected will seek or require medical attention.[1] There are several causes of epistaxis, including dryness of the nasal cavity, digital trauma to the nasal cavity, hypertension, anticoagulation, and blood dyscrasias. Conservative therapy includes local pressure, vasoconstrictors, sedation, and nasal packing, but for patients who do not respond to such measures, more invasive methods must be applied, such as surgical ligation of the internal maxillary artery, anterior ethmoid artery, posterior ethmoid artery, and/or external carotid artery, or embolization of vessels supplying the nasal cavity.

Trauma and vascular abnormalities account for less than 5% of all severe cases of epistaxis.[2] Aneurysms of the cavernous internal carotid artery (ICA) can be a source of massive and life-threatening nasal bleeding. The majority of cavernous ICA aneurysms that result in epistaxis are traumatic in origin and are therefore more appropriately termed pseudoaneurysms.[2-5] There have been a multitude of case reports published on such traumatic pseudoaneurysms presenting as massive epistaxis, but there have been no reported cases within the medical literature of paraclinoid ICA aneurysms presenting in a similar fashion.[2-5] We present a case of a nontraumatic paraclinoid ICA aneurysm presenting as massive, recurrent epistaxis and discuss the clinical presentation, diagnosis, and management of these lesions.

CASE REPORT

A 49-year-old woman with no history of head trauma and no other significant medical history was transferred to the Massachusetts Eye and Ear Infirmary after repeated, unsuccessful attempts at controlling her left-sided epistaxis episodes. She had undergone in succession a septoplasty, bilateral anterior and posterior ethmoid artery ligations, and left internal maxillary and left external carotid artery ligations, which had all failed to control her massive epistaxis episodes. She had undergone a computed tomography (CT) scan of the sinuses that showed air-fluid levels in bilateral sphenoid and maxillary sinuses but no evidence of any intracranial or nasopharyngeal lesions nor of any bony dehiscences involving the sinus walls. In addition, an angiogram obtained at an outside facility after her multiple surgical ligations showed no significant remaining vessels feeding her nasal cavity.

Upon presentation to our infirmary, the patient had a left nasal balloon packing in place with no obvious active bleeding. She was alert and oriented, and her neurological examination, including her cranial nerves, showed no abnormalities. Her hematocrit level was 32%, and the remainder of her hematologic and chemical laboratory values were within the normal range. Her left nasal balloon was removed 4 days after her left external carotid artery ligation with no active bleeding, and she was discharged home after an additional 24-hour observation period.

The patient returned 3 days later with recurrent bleeding from her left nasal cavity. She underwent angiography, which demonstrated successful surgical ligation of the left external carotid artery just distal to the origin of the facial artery. The left internal maxillary artery, which had previously been surgically ligated, showed evidence of retrograde filling via collateral blood flow from the ipsilateral ascending pharyngeal and facial branches. In addition, an 8-mm paraclinoid ICA aneurysm was noted projecting lat-

---

From the Department of Otolaryngology, Massachusetts Eye and Ear Infirmary (Kim, Varvares), and the Department of Radiology, Massachusetts General Hospital (Farkas, Putman), Harvard Medical School, Boston, Massachusetts.

CORRESPONDENCE — Mark Varvares, MD, Dept of Otolaryngology, Massachusetts Eye and Ear Infirmary, 243 Charles St, Boston, MA 02114.

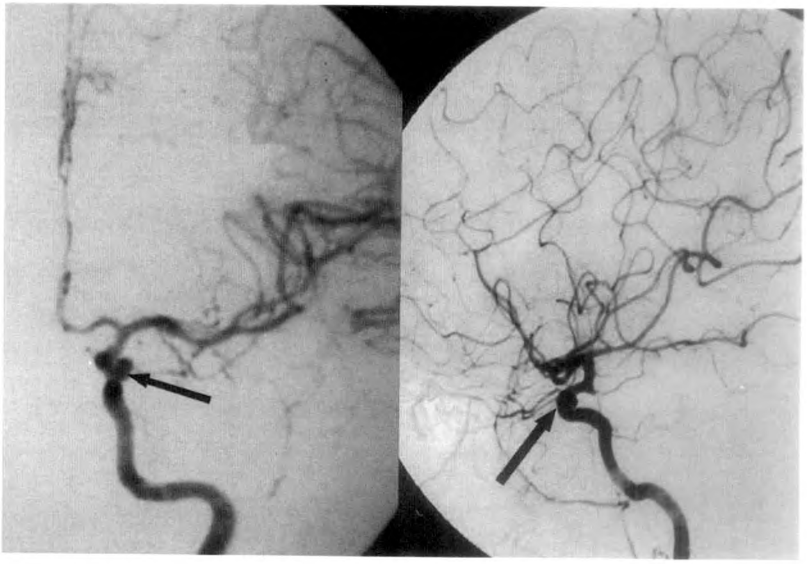

Fig 1. Anteroposterior and lateral digital subtraction angiograms demonstrate 8.5-mm aneurysm (arrows) arising from clinoidal segment of internal carotid artery. Aneurysm projects directly lateral to anterior genu of internal carotid artery.

erally and slightly superior to the ophthalmic artery (Fig 1). The patient's left ascending pharyngeal and facial arteries and the right internal maxillary artery were successfully embolized. A CT scan of the head, as well as a CT angiogram performed to further evaluate the paraclinoid ICA aneurysm, showed the aneurysm to measure 8.5 mm in maximal diameter and to be located medial to the anterior clinoid process. The aneurysm itself did not appear to communicate directly with the sphenoid or ethmoid sinus and therefore did not appear to be the cause of her recurrent bleeding episodes. The neurosurgery department was consulted and, as no immediate neurosurgical intervention was deemed necessary for the ICA aneurysm and the patient had no further bleeding episodes, she was discharged home.

The patient returned 7 days after discharge with recurrent, profuse epistaxis from her left nasal cavity. A repeat angiogram was subsequently taken and demonstrated that the left nasal cavity was fed by primary branches off the ophthalmic artery and the internal maxillary artery, which was supplied in turn by collateral branches off the middle meningeal and mandibulovidian arteries. As attempted occlusion of any of these vessels was of high risk to the patient, no additional embolizations were performed. Again, the left paraclinoid ICA aneurysm was noted and had not changed in size. The patient continued to have several episodes of profuse epistaxis lasting several minutes, preceded by a throbbing, pulsating sensation in the retro-orbital region. A repeat noncontrast CT scan of the sinuses with 1-mm sections through the sphenoid sinus was performed to further evaluate the aneurysm's relationship to the sphenoid sinus. There was evidence of dehiscence of the medial wall of the left anterior clinoid process with communication into the sphenoid sinus, which had not been appreciated on her prior CT scans (Fig 2). A closer evaluation of her prior CT angiogram showed the paraclinoid ICA aneurysm projecting into the pneumatized anterior clinoid process, thereby communicating with the sphenoid sinus and resulting in the recurrent, severe episodes of epistaxis (Fig 3). The

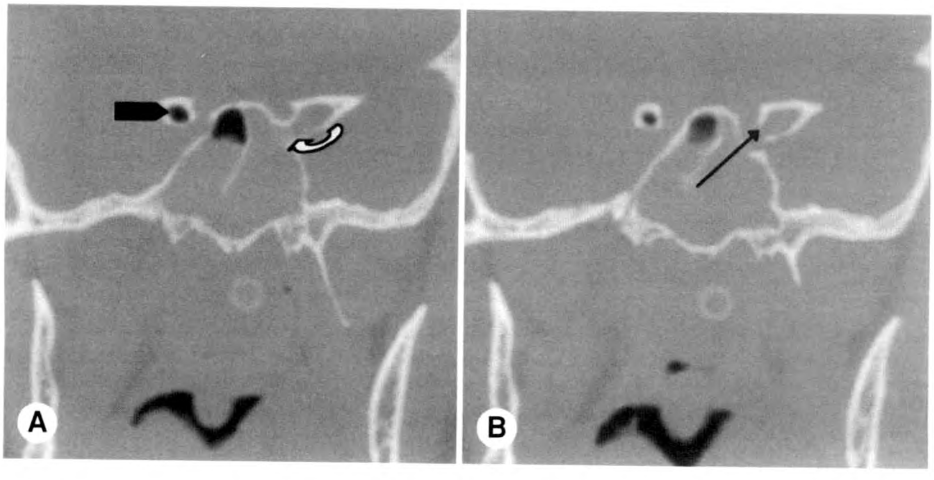

Fig 2. Serial computed tomography (CT) scans of sphenoid sinus obtained in coronal plane. A) Bone windows demonstrate right anterior clinoid process to be aerated (black arrow). Curved white arrow shows normal communication between anterior clinoid process and sphenoid sinus. B) Bony defect (arrow) is identified along medial wall of anterior clinoid process, likely secondary to pressure from adjacent aneurysm.

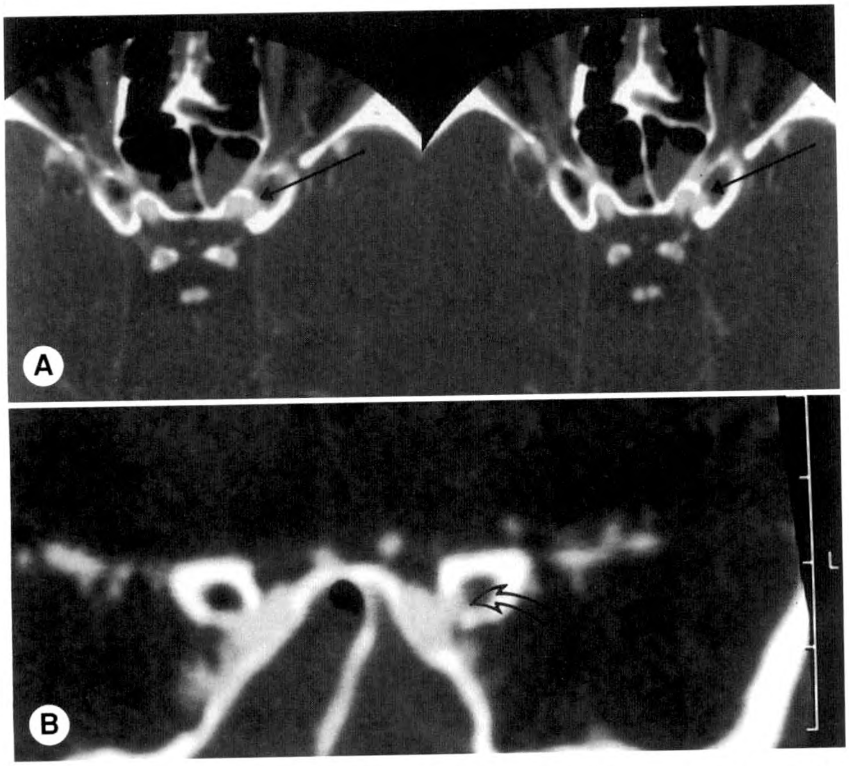

Fig 3. Relationship of aneurysm to anterior clinoid process. A) Serial contrast-enhanced axial CT scans demonstrate aneurysm projecting into bony defect (arrows). Right clinoid process is aerated. B) Coronal contrast-enhanced planar CT reconstruction shows that aneurysm is clearly burrowing into left anterior clinoid process (arrow).

left anterior clinoid process, although filled by fluid, was presumably pneumatized, as the contralateral anterior clinoid process showed aeration. The patient subsequently underwent successful embolization of her paraclinoid ICA aneurysm using 3 Guglielmi detachable coils. A postembolization angiogram showed 100% occlusion of the ICA aneurysm (Fig 4). The patient was observed, had no further bleeding episodes, and was discharged home. A 3-month follow-up angiogram showed small interval refilling of the base of the aneurysm, but 95% of the aneurysm still remained successfully occluded. The patient has had no further episodes of epistaxis to date.

DISCUSSION

Aneurysms of the clinoidal segment of the ICA are located between the emergence of the carotid artery from the roof of the cavernous sinus and the origin of the posterior communicating artery. These aneurysms are rare and account for 1.3% to 5% of all documented intracranial aneurysms.[6] In addition, paraclinoid ICA aneurysms are associated with a high female preponderance and the presence of multiple as well as symmetric intracranial aneurysms.[7]

Clinically, the majority of patients with paraclinoid ICA aneurysms present with visual disturbances or a subarachnoid hemorrhage.[8,9] The classic symptom of a subarachnoid hemorrhage is a headache of unusual severity and sudden onset. In addition, patients may present with meningeal signs, nausea, vomiting, motor deficits, and obtundation, in addition to mul-

Fig 4. Digital subtraction angiograms taken before (A) and after (B) aneurysm coiling (long arrows). There has been complete obliteration of aneurysmal filling since 3 Gugliemi detachable coils were placed into aneurysmal sac. Coils are seen in ascending pharyngeal artery, left from previous epistaxis embolization (small arrow in A). There is enlarged mandibulovidian artery (wide arrow in B); this vessel reconstitutes distal internal maxillary artery (not shown).

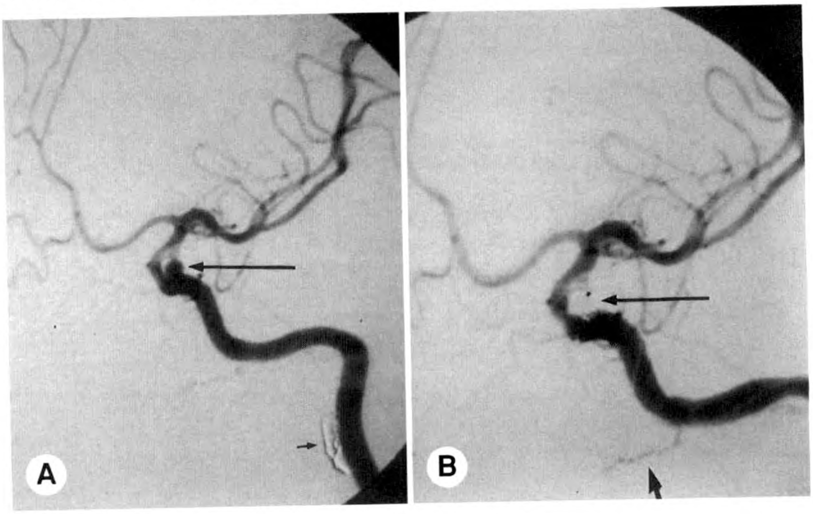

tiple other neurologic deficits.

Aneurysms of the ICA can also present with life-threatening epistaxis. The majority of such aneurysms are cavernous in origin and usually arise from a traumatic source with an associated 30% to 50% mortality rate.[10] The cavernous ICA has an intimate relationship with the sphenoid sinus, bulging into the lateral sphenoid sinus wall in 71% of cadaveric dissections.[11] In addition, Renn and Rhoton[11] found that the bony covering over the cavernous ICA within the sphenoid sinus was less than 1 mm in 66% of cases, and in 4%, there was no bony covering between the ICA and the sinus mucosa. Because of this anatomic relationship, a cavernous ICA aneurysm, upon rupture, can present with life-threatening epistaxis through a dehiscence or fracture along the sphenoid sinus wall. Paraclinoid aneurysms, unlike cavernous ICA aneurysms, are intradural in nature and therefore, upon rupture, present as a subarachnoid hemorrhage. Our patient, however, presented with massive, recurrent epistaxis because of several unique anatomic relationships. First, her aneurysm projected laterally into a pneumatized anterior clinoid process. Second, the anterior clinoid process communicated directly with the sphenoid sinus, and in this manner, the blood from the ruptured aneurysm egressed into the sinus and eventually into the nasal cavity. Our patient represents the first reported case of a paraclinoid ICA aneurysm presenting as massive, recurrent epistaxis.

The gold standard for diagnosis of these aneurysms is carotid angiography. A paraclinoid ICA aneurysm will demonstrate itself as a radiopaque outpouching of the ICA distal to the ophthalmic artery branch and proximal to the posterior communicating artery. Interestingly, the dimensions of the aneurysm may change with time in relation to the quantity of blood and thrombus within it. This may explain why the aneurysm was not appreciated on our patient's earlier angiogram performed at an outside hospital. In addition, CT and magnetic resonance imaging may provide the initial information to suggest the possibility of an ICA aneurysm. Blood in the sphenoid sinus may indicate a communication or dehiscence in the sinus wall, and any obvious fractures involving the sphenoid sinus, sella turcica, or orbital apex should alert the physician to a possible traumatic ICA pseudoaneurysm.

In the past, paraclinoid ICA aneurysms have been managed surgically by ligation of either the cervical common carotid artery or the ICA or by direct neurosurgical exposure of the paraclinoid ICA with surgical clipping. However, with the development of endovascular techniques, detachable balloons and coils have been successfully used in the treatment of these aneurysms. These balloons and coils provide distinct advantages over the traditional surgical techniques, in that areas that are either difficult to expose or inaccessible by surgery can be successfully visualized and embolized. In addition, a test occlusion of the ICA can be performed with a nondetachable balloon to determine the adequacy of collateral blood flow to the brain. If the patient fails the test occlusion, an extracranial-intracranial bypass procedure can be performed before the embolization or the patient can be adequately volume-resuscitated and another attempt made at test occlusion. Detachable balloons also allow for not merely the proximal occlusion of the ICA, but also occlusion of the segment of the ICA distal to the aneurysm. In this manner, collateral blood flow to the aneurysm can be prevented and the likelihood of a rebleed, as well as delayed embolic strokes, which can occur with isolated cervical ICA or common carotid artery ligation, can be reduced.[12] The confirmation of complete occlusion of the aneurysm can be obtained with a postembolization arteriogram. Coils can also be used for occlusion of the aneurysmal sac itself, leaving the lumen of the ICA intact. This method can be used in individuals whose aneurysms have a well-defined neck or in those who fail test occlusion but are not candidates for an extracranial-intracranial bypass procedure. Last, the complication rates associated with balloons and coils are comparable, if not superior, to those associated with surgical ligation. Most studies have reported a mortality rate of 0% to 2.5% and a morbidity rate of 1% to 5%.[13-16]

CONCLUSION

Epistaxis secondary to aneurysms of the paraclinoid ICA, although extremely rare, requires early diagnosis and treatment to prevent significant morbidity or even death. Any patient with massive, exsanguinating epistaxis episodes should be adequately evaluated for an ICA aneurysm. Magnetic resonance imaging and CT scanning may show evidence of blood in the paranasal sinuses, particularly the sphenoid sinus, but a carotid arteriogram is the diagnostic method of choice. Any ICA aneurysm can be appropriately managed with detachable balloons and coils and the potential deadly outcome successfully prevented.

REFERENCES

1. Elahi MM, Parnes LS, Fox AJ, Pelz DM, Lee DH. Therapeutic embolization in the treatment of intractable epistaxis. Arch Otolaryngol Head Neck Surg 1995;121:65-9.

2. Chen D, Concus AP, Halbach VV, Cheung SW. Epistaxis originating from traumatic pseudoaneurysm of the internal carotid artery: diagnosis and endovascular therapy. Laryngoscope

1998;108:326-31.

3. Han MH, Sung MW, Chang KH, Min YG, Han DH, Han MC. Traumatic pseudoaneurysm of the intracavernous ICA presenting with massive epistaxis: imaging diagnosis and endovascular treatment. Laryngoscope 1994;104:370-7.

4. Ghorayeb BY, Kopaniky DR, Yeakley JW. Massive posterior epistaxis. Arch Otolaryngol Head Neck Surg 1988;114: 1033-7.

5. Liu MY, Shih CJ, Wang YC, Tsai SH. Traumatic intracavernous carotid artery aneurysm with massive epistaxis. Neurosurgery 1985;17:569-73.

6. Knosp E, Muller G, Perneczky A. The paraclinoid carotid artery: anatomical aspects of microsurgical approach. Neurosurgery 1988;22:896-901.

7. Day AL. Aneurysms of the ophthalmic segment. A clinical and anatomical analysis. J Neurosurg 1990;72:677-91.

8. Batjer HH, Kopitnik TA, Giller CA, Samson DS. Surgery for paraclinoid carotid artery aneurysms. J Neurosurg 1994; 80:650-8.

9. Heros RC, Nelson PB, Ojemann RG, Crowell RM, DeBrun G. Large and giant paraclinoid aneurysms: surgical techniques, complications and results. Neurosurgery 1983;12:153-63.

10. Goleas J, Mikhael MA, Paige ML, Wolff AP. Intracavernous carotid artery aneurysm presenting as recurrent epistaxis. Ann Otol Rhinol Laryngol 1991;100:577-9.

11. Renn WH, Rhoton AL. Microsurgical anatomy of the sellar region. J Neurosurg 1975;43:288-98.

12. Higashida RT, Halbach VV, Dowd CF, Barnwell SL, Hieshima GB. Intracranial aneurysms: interventional neurovascular treatment with detachable balloons — results in 215 cases. Radiology 1991;178:663-70.

13. Fox AJ, Vinuela F, Pelz DM, et al. Use of detachable balloons for proximal artery occlusion in the treatment of unclippable cerebral aneurysms. J Neurosurg 1987;66:40-6.

14. Guglielmi G, Vinuela F, Duckwiler G, et al. Endovascular treatment of posterior circulation aneurysms by electrothrombosis using electrically detachable coils. J Neurosurg 1992;77: 515-24.

15. Guglielmi G. Embolization of intracranial aneurysms with detachable coils and electrothrombosis. In: Vinuela F, Halbach VV, Dion JE, eds. Interventional neuroradiology: endovascular therapy of the central nervous system. New York, NY: Raven Press, 1992:63-75.

16. Bavinzski G, Killer M, Ferraz-Leite H, Gruber A, Gross CE, Richling B. Endovascular therapy of idiopathic cavernous aneurysms over 11 years. Am J Neuroradiol 1998;19:559-65.

Ann Otol Rhinol Laryngol 109:2000

IMAGING CASE STUDY OF THE MONTH

SCINTIGRAPHIC MONITORING OF SWALLOWING REHABILITATION AFTER HORIZONTAL SUPRAGLOTTIC LARYNGECTOMY

JACOPO GALLI, MD
FRANCESCA REALE, MD
VENANZIO VALENZA, MD
GIOVANNI ALMADORI, MD
LUCIA D'ALATRI, MD
GAETANO PALUDETTI, MD
ROME, ITALY

INTRODUCTION

The resection of the top two sphincters of the upper airways represented by the epiglottis, the aryepiglottic folds, and the false vocal cords — better known as horizontal supraglottic laryngectomy (HSL) — is a well-established conservative surgical procedure in cases of supraglottic laryngeal cancer.[1] Along with the oncological aspects, its functional success depends on the patient's ability to resume physiologic respiration, phonation, and deglutition. However, normal respiratory and swallowing functions sometimes are hardly recovered after surgery, delaying decannulation and normal oral feeding.[2-4]

Oropharyngoesophageal scintigraphy (OPES) is a relatively simple, noninvasive technique that allows a semiquantitative and qualitative assessment of upper and lower digestive tract function. The acceptable radiation dose delivered to the patient at each scintigraphic swallowing test (0.00043 Gy and 0.011 mSv/MBq) allows the examination to be repeated in follow-up studies.[5,6]

We already demonstrated the objective effectiveness of OPES in assessing deglutition recovery after HSL[7]; the present paper demonstrates how this procedure allows monitoring of the results of rehabilitation therapy after HSL.

SCINTIGRAPHY TECHNIQUE

Based on the rapid sequential acquisition of images of each single deglutition, OPES readily detects possible tracheobronchial aspiration during the HSL procedure and allows a qualitative and semiquantitative assessment of the deglutitional function.[7-9] An initial test with plain water was performed to achieve 3 goals: to reassure the patient, to make him or her familiar with the technique, and to be sure that he or she could easily drink 10 mL of liquid in a single swallow. A 5-minute interval is necessary to discharge the ingested water from possible esophageal diverticula and to eliminate damming in the surgical area.

The patient was placed in an 80° right anterior oblique position in front of a gamma camera with a large-field, high-resolution, low-energy collimator. After requesting the patient to swallow on command only, we administered 10 mL of water containing 37 MBq of technetium 99m sulfur colloid with a straw. The initial bolus swallow was followed by dry swallows every 20 seconds. Eight 0.125-second frames were recorded every second during deglutition, for a total of 60 seconds. Three regions of interest were selected: the oral cavity, pharynx, and esophagus.

The esophagus was further divided into 3 regions of interest (superior, middle, and inferior) to thoroughly investigate this part of the digestive tract. At the end of the dynamic study, three 30-second static scintigrams were acquired to detect possible tracheobronchial aspiration.

The following semiquantitative parameters were evaluated: 1) oral transit time, ie, the time required for the bolus to leave the oral cavity after swallowing (normal value, <1.00 second)[6,7]; 2) pharyngeal transit time (PTT), ie, the time interval between the appearance and disappearance of the bolus in the pharynx (normal value, <1.20 seconds)[6,7]; 3) esophageal transit time, ie, the time required for the bolus to pass through the esophagus and enter the stomach (normal value, <10.00 seconds)[6,7]; 4) oral retention index, ie, the residual amount of radioactivity in the oral cavity after deglutition (normal oral retention index is less than 5%); 5) pharyngeal retention index (PRI), ie, the residual amount of radioactivity in the pharynx at 10 and 60 seconds after deglutition (normal PRI is less than 5%, and frequently equal to 0%);

From the Institutes of Otolaryngology (Galli, D'Alatri, Almadori, Paludetti) and Nuclear Medicine (Valenza, Reale), Università Cattolica del Sacro Cuore, Rome, Italy.

CORRESPONDENCE — Jacopo Galli, MD, Corso Vittorio Emanuele 229, 00186 Rome, Italy.

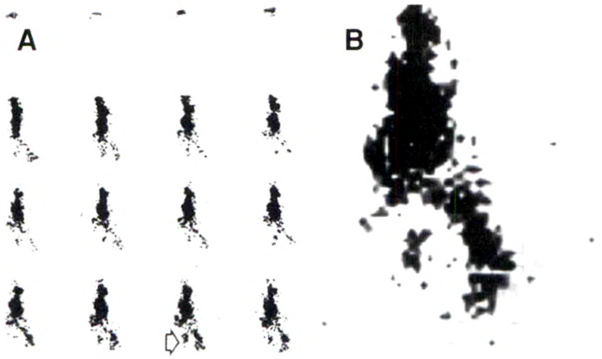

Fig 1. Oropharyngoesophageal scintigraphy (OPES). A) Dynamic images obtained 1 month after surgery. Note swallowing incoordination with marked immediate aspiration in tracheobronchial tree (aspiration percentage [AP], 90%) and elevated pharyngeal retention index (PRI) with consequent residual postswallowing aspiration. Only small fraction reaches lower esophagus at later time (arrow). B) Same study, immediate static image. Image confirms data obtained with dynamic study: tracheobronchial tree shows marked aspiration, and consequently, gastric fundus is not visualized.

and 6) aspiration percentage (AP), assessed when laryngeal or tracheobronchial aspiration was detected during visual inspection of the images. The AP was calculated as follows: $AP = (AC \times 100)/OC - OC2$ where AC is the count in the aspiration site, OC the count in the oral cavity region of interest before deglutition, and OC2 the residual count in the oral cavity after deglutition.

CASE REPORT

In October 1996, a 64-year-old man underwent HSL extended to the base of the tongue at our institution for a T4N0M0 supraglottic laryngeal squamous cell carcinoma. Because the patient presented as clinically N0 (palpation, ultrasound, and computed tomography), neck dissection was not performed, whereas postoperative radiotherapy was indicated for the presence of positive margins at the base of the tongue. Postoperative surgical healing progressed normally, but 1 month later, oral intake still had not resumed. At this time, OPES with an open tracheal cannula was performed and indicated a high PTT value (5.83 seconds; mean normal value ± 2 SD, 0.90 ± 0.30[6,7]) and a marked aspiration of liquids in the tracheobronchial tree (AP, 90%; Fig 1). For this reason, when the patient started postoperative radiotherapy 40 days after surgery, the nasogastric tube and the tracheal cannula were still in place. The radiotherapy lasted 50 days and was delivered through an anterior field and 2 lateral opposed fields for a total dosage of 60 Gy.

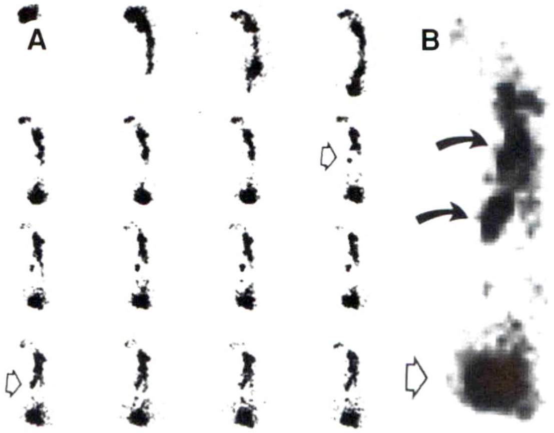

Fig 2. OPES. A) Dynamic images obtained 14 months after surgery show coordinated swallowing with immediate but partial passage of bolus in esophagus and marked pharyngeal retention of bolus (PRI, 40%) responsible for postswallowing aspiration in tracheobronchial tree, which increased by seconds as shown by first and second empty arrows (AP, 6.7%). B) Same study, static image. Image shows tracheobronchial aspiration (curved arrows), but normal esophagogastric transit, with well-evident gastric fundus (empty arrow).

After radiotherapy, the patient progressively recovered satisfactory phonatory and respiratory functions. Deglutition was still impaired by postswallowing pharyngeal stasis and minor aspiration of liquids, but function was sufficient to ensure oral nutrition and hydration and to remove the feeding tube, though not the tracheal cannula.

Fourteen months after surgery, no evidence of locoregional recurrence was present, and laryngeal motility was preserved. The patient again underwent OPES (Fig 2), which showed a persistent but limited increase in PTT (2.40 seconds) that was decreased from the baseline (5.83 seconds), and a high PRI value (40%) with consequent residual postswallowing aspiration as documented by AP data (6.7%). Videolaryngoscopy confirmed the presence of marked postswallowing pharyngeal stasis (Fig 3).

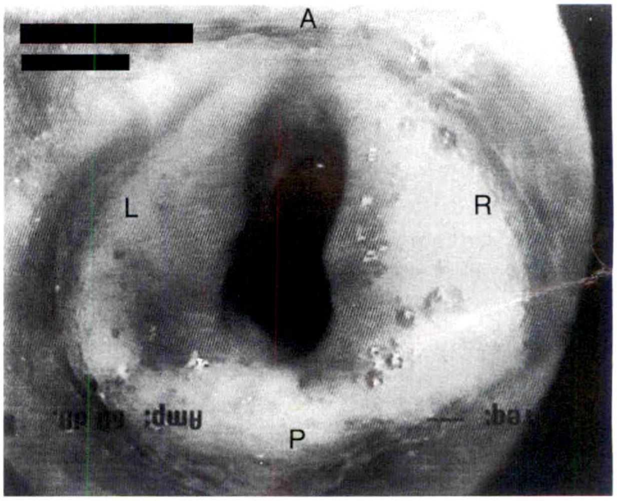
[redacted]

Fig 3. Videolaryngoscopy. Image obtained before swallowing rehabilitation shows marked postswallowing pharyngeal stasis.

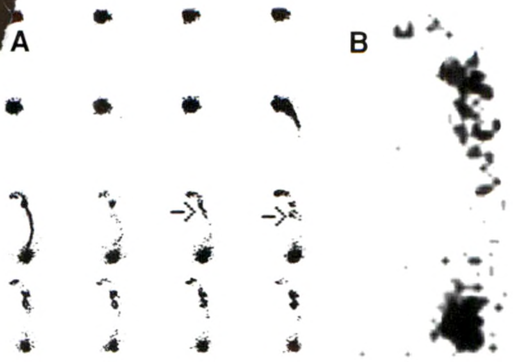

Fig 4. OPES. A) Dynamic images obtained about 2 months after swallowing rehabilitation and 16 months after surgery. Rapid and coordinated swallowing with normal oropharyngoesophageal transit (see gastric fundus) is present. Pharyngeal retention is now reduced (PRI, 20%), but still pathological (arrows), and is responsible for residual tracheobronchial aspiration (AP, 4.7%). B) Same study, static image. Note marked reduction of tracheobronchial aspiration.

To enhance deglutition, allow acceptable feeding, and remove the tracheostomy tube, supraglottic swallowing rehabilitation[10] was started on a schedule of 3 times a week. About 2 months later, the patient presented a satisfactory recovery of swallowing function as documented by a third OPES study (Fig 4); PTT normalization and a marked reduction in PRI value (20%) were also confirmed by videolaryngoscopy (Fig 5), whereas a slight residual liquid aspiration (4.7%) was still present. The tracheostomy tube was removed; 2 years after primary surgery and 7 months after closure of the tracheostomy, no recurrence was present, and respiratory, phonatory, and swallowing functions were reestablished, with an occasional slight dysphagia for liquids.

DISCUSSION

Dynamic scintigraphy was first used to assess gastric emptying and esophageal transit time.[11] Esophageal scintigraphy quantitatively determines the esophageal transit, differentiates between nonmotor disorders and some motor disorders such as scleroderma and achalasia, and detects esophageal strictures and diverticula.[12]

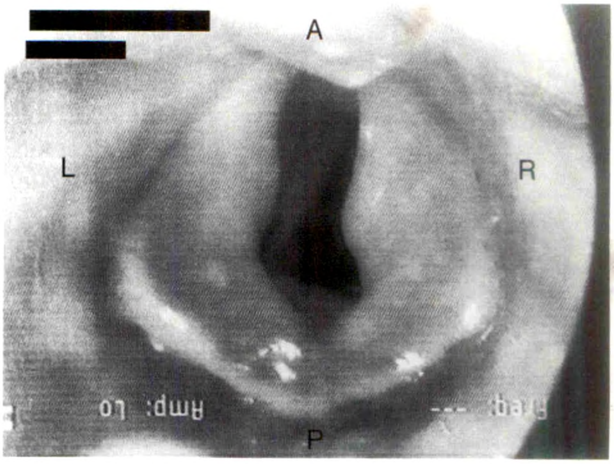
[redacted]

Fig 5. Videolaryngoscopy. Image after swallowing rehabilitation demonstrates no significant postswallowing pharyngeal stasis.

Recently, OPES has gained currency as a useful complement to routine investigations of upper aerodigestive pathways used during deglutition, such as videofluoroscopy and fiberoptic endoscopy.[13-15] The duration of oral, pharyngeal, and esophageal swallowing phases,[15,16] a semiquantitative measure of bolus transit, and the percentage of liquid that may be aspirated into the tracheobronchial tree or remain as residue in the oral and pharyngeal cavities can be assessed.[17,18]

Postoperative oropharyngoesophageal swallowing efficiency can be objectively investigated by calculating semiquantitative parameters of dynamic scintigraphy.[5-7,16] Furthermore, OPES, based on AP values, evaluates the amount of aspiration in the tracheobronchial tree at any deglutition,[17,18] alerting the clinician to the possible development of sequelae such as aspiration pneumonia. Postoperative impairment of the pharyngeal phase of swallowing, from bolus stasis at the glossolaryngeal recess to the consequent postswallowing aspiration, is scored by means of PRI and AP values.[7]

A limitation of scintigraphy is the lack of detailed anatomic images, but the oral cavity, pharynx, and esophagus are rather well delimited.

In our case, the patient underwent HSL extended to the base of the tongue, and radiotherapy was started

OROPHARYNGOESOPHAGEAL SCINTIGRAPHY FOLLOW-UP DATA

	Transit Time (s)			*Regional Retention*			
Follow-up	*OTT (NV < 1.00 s)*	*PTT (NV < 1.20 s)*	*ETT (NV < 10.0 s)*	*ORI (NV < 5%)*	*PRI 10 (NV < 5%)*	*PRI 60 (NV < 5%)*	*Aspiration (NV < 0%)*
First (1 mo after HSL)	0.80	5.83		10	50	15	90.0%
Second (14 mo after HSL)	0.68	2.40	4.20	5	40	15	6.7%
Third (16 mo after HSL and 2 mo after rehab)	0.93	1.05	5.17	3	20	10	4.7%

OTT — oral transit time, PTT — pharyngeal transit time, ETT — esophageal transit time, ORI — oral retention index, PRI 10 — pharyngeal retention index at 10 seconds, PRI 60 — pharyngeal retention index at 60 seconds, NV — normal value, HSL — horizontal supraglottic laryngectomy.

1 month later, when decannulation and oral intake were not possible, as well documented by the first OPES study (see Table). The second and third OPES studies, performed before and after complete swallowing rehabilitation, respectively, showed a progressive PTT normalization and a marked reduction in AP values for liquids (see Table).

The PRI values were definitely abnormal at the beginning of rehabilitation and slightly lower at t last scintigraphy scan, confirming the good results of rehabilitation and a satisfactory clinical recovery.

In conclusion, the present study outlines the effectiveness of OPES in objectively monitoring oropharyngeal swallowing rehabilitation after HSL and demonstrates its close correspondence with the clinical findings.

REFERENCES

1. Bocca E, Pignataro O, Oldini C. Supraglottic laryngectomy: 30 years of experience. Ann Otol Rhinol Laryngol 1983; 92:14-8.

2. Maurizi M, Ottaviani F, Rosignoli M. Le laringectomie sopraglottiche allargate. In: Chirurgia funzionale della laringe: stato attuale dell'arte. LXXX Congresso Nazionale SIO. Rome, Italy: Pacini, 1993:323-32.

3. Woisard V, Serrano E, Yardeni E, Puech M, Pessey JJ. Deglutition after supra-glottic laryngectomy. J Otolaryngol 1993;22:278-83.

4. Herranz-González J, Gavilán J, Martínez-Vidal JM, Gavilán C. Supraglottic laryngectomy: functional and oncologic results. Ann Otol Rhinol Laryngol 1996;105:18-22.

5. Hamlet SL, Muz J, Patterson R. Pharyngeal transit time: assessment with videofluoroscopic and scintigraphic techniques. Dysphagia 1989;4:4-7.

6. Galli J, Valenza V, Paludetti G, et al. An oro-pharyngeal-esophageal scintigraphic study of deglutition. Acta Otorhinolaryngol Ital 1996;16:412-9.

7. Galli J, Valenza V, Ottaviani F, et al. Scintigraphic assessment of swallowing after horizontal supraglottic laryngectomy. J Otolaryngol 1999;128:189-96.

8. Klein HA, Wald A. Computer analysis of radionuclide esophageal transit studies. J Nucl Med 1984;25:957-64.

9. Zohar Y, Grusko I, Sulkes J, Melloul MM. Oropharyngeal scintigraphy: a computerized analysis of swallowing in patients with obstructive sleep apnea. Laryngoscope 1998;108:37-41.

10. Logemann JA. Evaluation and treatment of swallowing disorders. Austin, Tex: ProEd, 1983.

11. Kazem I. Scintigraphic technique for the study of esophagus. AJR Am J Roentgenol 1972;115:681-8.

12. Jorgensen F, Hesse B, Tromholt N, Hojgaard L, Stubgaard M. Esophageal scintigraphy: reproducibility and normal ranges. J Nucl Med 1992;33:2106-9.

13. Langmore SE, Schatz K, Olson N. Endoscopic and videofluoroscopic evaluations of swallowing and aspiration. Ann Otol Rhinol Laryngol 1991;100:678-81.

14. Logemann JA. Role of the modified barium swallow in management of patients with dysphagia. Otolaryngol Head Neck Surg 1997;116:335-8.

15. Humphreys B, Mathog R, Rosen R, Miller P, Muz J, Nelson R. Videofluoroscopic and scintigraphic analysis of dysphagia in the head and neck cancer patient. Laryngoscope 1987;97: 25-32.

16. Hamlet SL, Wilson S, Stachler RJ, Salwen WA, Muz J, Heilbrun LK. Scintigraphic assessment of swallow efficiency postlaryngectomy. Laryngoscope 1994;104:1159-62.

17. Muz J, Hamlet SL, Mathog RH, et al. Scintigraphic assessment of aspiration in head and neck cancer patients with tracheostomy. Head Neck 1994;16:17-20.

18. Valenza V, Meduri G, D'Errico G, et al. Scintigraphic assessment of laryngotracheopulmonary aspiration post-laryngectomy [Abstract]. Nucl Med Commun 1996;17:294.